

Durham E-Theses

*Stability and degradation of colliery shale
embankments and properties of tailings lagoon
deposits*

A. E. Cobb

How to cite:

Cobb, A. E. (1977) Stability and degradation of colliery shale embankments and properties of tailings lagoon deposits. Doctoral thesis, Durham University.

Use policy

The full-text may be used and/or reproduced, and given to third parties in any format or medium, without prior permission or charge, for personal research or study, educational, or not-for-profit purposes provided that:

- a full bibliographic reference is made to the original source
- a <https://etheses.durham.ac.uk/id/eprint/8379/> is made to the metadata record in Durham E-Theses
- the full-text is not changed in any way

The full-text must not be sold in any format or medium without the formal permission of the copyright holders.

Please consult the [full Durham E-Theses policy](#) for further details.

The copyright of this thesis rests with the author.
No quotation from it should be published without
his prior written consent and information derived
from it should be acknowledged.

STABILITY AND DEGRADATION OF
COLLIERY SHALE EMBANKMENTS AND
PROPERTIES OF TAILINGS LAGOON DEPOSITS

by

A.E. Cobb B.Sc.

being a thesis presented in fulfilment of requirements for
the degree of Doctor of Philosophy at the Department of
Geological Sciences in Faculty of Science of the University
of Durham.



SUMMARY

The work comprises part of a continuing research programme on colliery spoil, undertaken at Durham University.

The purpose of the present work was to elucidate material constraints controlling the behaviour of spoil heaps. The extent of curvature of the failure envelope of coarse colliery discard has been investigated. Linear envelopes fitted to a range of spoils associated with bituminous coals are shown to have statistically valid cohesion intercepts. Cohesion, c' , is interpreted, however, as being a product of a curved envelope. The expression $\tau = m (\sigma')^z$ is used to describe the failure envelopes of these spoils: some properties of the curves are illustrated. It is believed that burnt and high rank materials may have linear envelopes with $c' = 0$. For discards, conventional reversing shear-boxes are unsatisfactory for residual shear strength determinations.

Two potential sources of instability, which may be present within tips, were also studied. These are, the possible occurrence and shear strength of buried layers of weathered discard, and the consolidation and shear strength behaviour of lagoon sediments (tailings).

Experiments conducted on fresh discard were compared with results acquired for older, surface waste heap materials from the same colliery.

It is deduced that compacted coarse discards are not prone to physical weakening unless they contain about 50 per cent seatearth.

Consolidation parameters obtained from Rowe Cell tests on lagoon discards show a varying rate of consolidation, being rapid near the lagoon inlet, but slow at the outlet.

SUMMARY (Cont'd.)

The amount of consolidation, however, is uniform. The promotion of consolidation by contained flocculants was also considered. Starch flocculants are shown to possess no consistent advantages in comparison with polyelectrolytes.

Finally, various factors such as curved failure envelopes and weak materials buried within and under tips are assessed, using a slope stability program developed by the writer.

ACKNOWLEDGEMENTS

I wish to thank my supervisor, Dr. R.K. Taylor for many useful discussions during this research. I also wish to thank the following technical staff of the Department of Geological Sciences for their assistance: Mr. R.G. Hardy (Senior Experimental Officer), Mr. A. Swann, Mr. B. McEleavey and Mr. P. Kay.

I am indebted to the National Coal Board for financing this work through the contract Research Grant to Dr. Taylor. Co-ordination of the Board's research into the properties of colliery discards is under the general direction of Mr.A.R. Taylor, Chief Civil Engineer. It should be stated that the views expressed in this thesis are those of the writer and not necessarily those of the Board. Of the N.C.B. staff who have offered assistance, Mr. A.R. Bacon (H.Q. Senior Soils Engineer) should be mentioned especially, for helping with the procurement of samples. Thanks are also due to Mr. L. Gould for the use of his data.

Finally, I should like to thank Mrs. Megan Phillips for typing this script.

CONTENTS

	<u>Page</u>
Summary	(i)
Acknowledgements	(iii)
Contents	(iv)
List of Tables	(vi)
List of Figures	(viii)
List of Symbols and Abbreviations	(xiii)
Chapter 1 Introduction	1
1.1 Background of research into colliery discard	1
1.2 Aims of current work	1
1.3 Methods employed	3
1.4 Failures of spoil heaps and lagoons	5
1.5 Mineralogy and weathering of colliery discards	6
1.6 Mechanical properties of coarse and fine discards	10
1.7 Published material	12
Chapter 2 Effects of weathering processes upon shear strength of coarse colliery discards	17
2.1 Introduction	17
2.2 Gedling discard	19
2.3 Kellingley discard	33
2.4 Oakdale discard	42
2.5 Burnt colliery spoils	47
2.6 Weathering effects upon shear strength of coarse colliery discards - conclusions	52
Chapter 3 Peak and residual shear strengths as a function of normal pressure	94
3.1 Effective shear strength parameters	94
3.2 Curvature of Mohr envelopes	95
3.3 Residual shear strength	110
3.4 Conclusions	113
Chapter 4 Fine discard (tailings/slurry) deposits	149
4.1 Introduction	149

CONTENTS (Cont'd.)

	<u>Page</u>
4.2 Field and laboratory investigations of lagoon deposits	153
4.3 Laboratory investigation of the effects of flocculants on tailings	198
4.4 Vane shear tests in colliery tailings	231
4.5 Colliery lagoons - conclusions	247
Chapter 5 Case history studies of the stability of shale embankments	289
5.1 Introduction	289
5.2 The slope stability program	294
5.3 Gedling spoil heaps - overtipping of lagoon	301
5.4 Gale Common pulverized fuel ash lagoon, a shale embankment on weak foundations	322
5.5 Conclusions	345
Chapter 6 General summary and conclusions	372
Bibliography	383
Appendix A - Slope stability program	392
Appendix B - Reduced major axis regression program	418
Appendix C - Excess pore water pressure program	424

LIST OF TABLES

<u>Table</u>	<u>Page</u>
1.1	8
2.1	21
2.2	22
2.3	23
2.4	24
2.5	29
2.6	37
2.7	40
2.8	45
2.9	49
3.1	97
3.2	98
3.3	102
3.4	102
3.5	103
3.6	107
3.7	108
3.8	114
3.9	115
4.1	154
4.2	158-159
4.3	160
4.4	161-162
4.5	165
4.6	168
4.7	176
4.8	179
4.9	180
4.10	181
4.11	183
4.12	188
4.13	201
4.14	203
4.15	213
4.16	220
4.17	225
4.18	225
4.19	227

LIST OF TABLES (Cont'd.)

<u>Table</u>	<u>Page</u>
5.1	304
5.2	306
5.3	320
5.4	326
5.5	327-328
5.6	333
5.7	334
5.8	339
5.9	343
6.1	374

LIST OF FIGURES

	<u>Page</u>
<u>Chapter 1</u>	
1.1 Locations of colliery spoils sampled	13
1.2 Triaxial testing apparatus	14
1.3 Rowe cell apparatus	15
1.4 Rotational gravity slide	16
1.5 Flow slide	16
<u>Chapter 2</u>	
2.1 Grading, Gedling washery and surficial tip coarse discard	55
2.2 Grading, Gedling coarse discard from trench	56
2.3 Mohr circle top point relationship	57
2.4 Deviator stress to strain diagram (D.S.S.D.), Gedling washery	57
2.5 D.S.S.D. Gedling tip U100	58
2.6 D.S.S.D. Gedling tip 6-12 months old	58
2.7 D.S.S.D. Gedling tip, 1m deep	59
2.8 D.S.S.D. Gedling tip, 3m deep	60
2.9 D.S.S.D. Gedling tip, 4m deep	61
2.10 Mohr stress diagram (M.S.D.) Gedling washery	62
2.11 M.S.D. Gedling surficial tip	63
2.12 M.S.D. Gedling tip trench, individual samples	64
2.13 M.S.D. Gedling tip trench, composite samples	65
2.14 Stress ratio to displacement diagram (S.R.D.D.) Gedling washery	66
2.15 S.R.D.D. Gedling tip 6-12 months old	66
2.16 Reorientation peaks	67
2.17 Slickensided shear plane in Gedling coarse discard from 0.3 x 0.3m shear-box	68
2.18 Grading, Kellingley coarse discard	69
2.19 D.S.S.D. Kellingley stockpile	70
2.20 D.S.S.D. Kellingley south embankment	71
2.21 D.S.S.D. Kellingley 6 years old, shale blanket	72
2.22 D.S.S.D. Kellingley 8 years old, above water table	73
2.23 D.S.S.D. Kellingley 8 years old, below water table	74
2.24 M.S.D. Kellingley stockpile	75
2.25 M.S.D. Kellingley south embankment	76
2.26 M.S.D. Kellingley 6 years old, shale blanket	77
2.27 M.S.D. Kellingley 8 years old, above water table	78
2.28 M.S.D. Kellingley 8 years old, below water table	79
2.29 S.R.D.D. Kellingley south embankment	80

LIST OF FIGURES (Cont'd.)

	<u>Page</u>
2.30 S.R.D.D. Kellingley 8 years old, above water table	81
2.31 S.R.D.D. Kellingley 8 years old, below water table	81
2.32 Grading, Oakdale coarse discard	82
2.33 D.S.S.D. Oakdale washery	83
2.34 D.S.S.D. Oakdale tip	84
2.35 M.S.D. Oakdale washery	85
2.36 M.S.D. Oakdale tip	86
2.37 S.R.D.D. Oakdale washery	87
2.38 S.R.D.D. Oakdale tip	87
2.39 Grading, Ireland burnt discard	88
2.40 Grading, Horden burnt discard	89
2.41 D.S.S.D. Ireland	90
2.42 D.S.S.D. Horden	91
2.43 M.S.D. Ireland	92
2.44 M.S.D. Horden	92
2.45 S.R.D.D. Ireland	93
<u>Chapter 3</u>	
3.1 Linear envelope, peak shear strength of 0.6 to 1.2mm size fraction samples	117
3.2 Grading after dead loading, Gedling	118
3.3 Grading after dead loading, Kellingley	118
3.4 Grading after dead loading, Oakdale	118
3.5 ϕ'_e , Kellingley and Oakdale	119
3.6 Log-log plot of Kellingley data	120
3.7 Definition of triaxial failure stress point	120
3.8 Curved envelope, Birch Coppice	121
3.9 Curved envelope, Cynheidre	121
3.10 Curved envelope, Yorkshire Main	122
3.11 Curved envelope, Isabella	123
3.12 Curved envelope, West Virginia, U.S.A.	124
3.13 Curved envelope, Denby Hall	125
3.14 Curved envelope, Gedling tip trench, individual samples	126
3.15 Curved envelope, Gedling tip trench composite	127
3.16 Curved envelope, Gedling tip, pre-1968	128
3.17 Curved envelope, 0.6 to 1.2mm size fraction samples	129
3.18 Curved envelope, Kellingley 8 years old, above water table	130
3.19 Curved envelope, Kellingley 8 years old, below water table	131

LIST OF FIGURES (Cont'd.)		<u>Page</u>
3.20	Curved envelope, Kellingley, 6 years old shale blanket	132
3.21	Curved envelope, Kellingley, south embankment	133
3.22	Curved envelope, Kellingley stockpile	134
3.23	Curved envelope, Oakdale	135
3.24	Curved envelope, Horden	136
3.25	Curved envelope, Ireland	136
3.26	Variation in shape of curves with variation in m and z	137
3.27	Residual shear strength, Ollerton (0.6 to 1.2mm)	138
3.28	S.R.R.D. Ollerton (0.6 to 1.2mm)	139
3.29	S.R.R.D. Gedling (0.6 to 1.2mm)	140
3.30	S.R.R.D. Kellingley (0.6 to 1.2mm)	141
3.31	S.R.R.D. Oakdale (0.6 to 1.2mm)	142
3.32	Final grading, Gedling	143
3.33	Final grading, Kellingley	143
3.34	Final grading, Oakdale	144
3.35	Residual shear strength, Gedling	145
3.36	Residual shear strength, Kellingley	146
3.37	Residual shear strength, Oakdale	147
3.38	Final grading, Ollerton	148
<u>Chapter 4</u>		
4.1	Typical lagoon cross-section	251
4.2	Range of lagoon gradings	252
4.3	Cadeby site plan	253
4.4	Cadeby, lagoon 8 U100	254
4.5	Cadeby Lagoon 9, sample gradings	255
4.6	Cadeby Lagoon 9, relationship between organic carbon and specific gravity	256
4.7	Cadeby Lagoon 9, shear strength	257
4.8	Cadeby Lagoon 8, shear strength	257
4.9	Cadeby Lagoon 9, log pressure to voids ratio	258
4.10	Cadeby Lagoon 9, log pressure to c_v	259
4.11	Cadeby, samples B and C	260
4.12	Cadeby Lagoon 9 excavated face	260
4.13	Cadeby Lagoon 8, log pressure to voids ratio	261
4.14	Cadeby Lagoon 9, embankment-sediment intersection	262
4.15	Grading of embankment-sediment intersection	262
4.16	Gedling Lagoon 12, central sample	263

LIST OF FIGURES (Cont'd.)		<u>Page</u>
4.17	Grading of Gedling Lagoon 12	263
4.18	Gedling Lagoon 12 outlet, Log pressure to voids ratio	264
4.19	Gedling Lagoon 12 outlet, Log pressure to c_v	265
4.20	Gedling Lagoon 12 centre, log pressure to voids ratio	266
4.21	Gedling Lagoon 12 centre, log pressure to c_v	267
4.22	Kellingley pressed tailings, stress ratio to displacement	268
4.23	Kellingley pressed tailings, shear strength	268
4.24	Sedimenting apparatus	269
4.25	Grading of Manvers tailings	270
4.26	Manvers, log pressure to voids ratio	271
4.27	Manvers, grading of top and bottom of samples	272
4.28	Grading of Morrison Busty tailings	273
4.29	Morrison Busty log pressure to voids ratio	274
4.30	Grading of Gedling tailings	275
4.31	Gedling log pressure to voids ratio	276
4.32	Vane shear strength to final voids ratio	277
4.33	Consolidated, undrained shear strength	278
4.34	Vane shear strength at simulated depth apparatus	278
4.35	Manvers laboratory vane shear strength	279
4.36	Gedling laboratory vane shear strength	280
4.37	Overconsolidated, consolidated undrained failure envelope	281
4.38	Manvers vane at calculated depths	282
4.39	Gedling vane at calculated depths	282
4.40	Gedling East tip lagoon inlet	283
4.41	Gedling East tip lagoon outlet	283
4.42	Grimethorpe lagoon	284
4.43	Blidworth lagoon	285
4.44	Kinneil lagoon	285
4.45	William thorpe lagoon	286
4.46	Cadeby lagoons 1,3,4,5 and 8	286
4.47	Cadeby lagoon 9	287
4.48	Cadeby lagoon 8, positions F1 and F2	287
4.49	Denby Hall lagoon C	288

LIST OF FIGURES (Cont'd.)

	<u>Page</u>
<u>Chapter 5</u>	
5.1 Method of slices, giving symbols	348
5.2 Definition of ϕ'_p	349
5.3 Interpolation of slice boundaries	350
5.4 Plot of Factor of Safety against the number of slices	351
5.5 Plot of Factor of Safety against the number of points on the failure surface	351
5.6 Geological sketch map of Gedling spoil heaps	352
5.7 Gedling site plan	353
5.8 Section A-A, Gedling	354
5.9 Section B-B, Gedling	355
5.10 Section C-C, Gedling	356
5.11 Section D-D, Gedling	357
5.12 Section E-E, Gedling	358
5.13 Comparison of shear strengths of materials at Gedling colliery	359
5.14 Effect on the Factor of Safety of varying \underline{m}	360
5.15 Effect on the Factor of Safety of varying \underline{z}	360
5.16 Comparison of different shear strength parameters	361
5.17 Typical 'Fir Tree' embankment profile	361
5.18 Gale Common scheme	362
5.19 Gale Common site plan	363
5.20 Gale Common main embankment	363
5.21 Comparison of shear strengths of materials at Gale Common	364
5.22 Geological sketch map of Lake Humber	365
5.23 General geology of Gale Common area	365
5.24 Cross sections of Gale Common area	366
5.25 '25 foot drift' clays	367
5.26 Plasticity properties of '25 foot drift' clays	367
5.27 Log pressure to voids ratio of '25 foot drift' clays	368
5.28 Old section of south embankment	369
5.29 Proposed new section of south embankment	370
5.30 Piezometer profile, August 1975, at Gale Common	371
<u>Chapter 6</u>	
6.1 Average curved envelope, English spoils	381
6.2 Average curved envelope, Welsh spoils	382

List of Symbols and Abbreviations

ϕ'	Effective angle of shearing resistance
ϕ'_e	Equivalent angle of shearing resistance at 350kN/m^2 normal pressure
ϕ'_p	Equivalent angle of shearing resistance at pressure p
c'	Effective cohesion
τ	Shear stress
σ_1	Major normal stress
σ_3	Minor normal stress
e	Voids ratio
C_c	Compression index
c_v	Coefficient of consolidation
m_v	Coefficient of volume change
k	Permeability

CHAPTER 1

INTRODUCTION

1.1 Background of research into colliery discard

When Tip number 7 at Aberfan failed in 1966, there was little knowledge of the behaviour of colliery discards. Spoil was disposed of as cheaply as possible, with little appreciation of the potential dangers.

After the disaster, site investigations were initiated by the National Coal Board upon other potentially dangerous tips. This answered the questions of stability of the tips concerned, but gave little information upon the long term or overall behaviour of colliery spoil. To obtain information in this respect, further research was undertaken. It is of this research programme that the current work forms a part.

1.2 Aims of current work

The current work is concerned with some of the properties of both coarse and fine colliery discards*. Investigation of coarse colliery discards has indicated that contrary to earlier belief, there is little weathering in the body of old, loosely placed tips (McKechnie Thomson and Rodin, 1972). Weathering is restricted to the outermost 3m at the maximum. However, considerable breakdown could occur during emplacement, especially with modern thin layer construction techniques. Some of the main factors relating to the extent and effects of superficial weathering

* Coarsediscard consists principally of material above 0.5mm in size separated in the washery. Fine discard constitutes fine material left in suspension after the washing process (slurry) and material normally less than 0.5mm size separated by the froth flotation process (tailings) (McKechnie Thomson and Rodin, 1972).



upon peak and residual shear strength parameters of modern compacted spoil heaps are therefore considered in the current work (Chapter 2).

Another point to emerge from past investigations was that some coarse discards apparently possessed curved Mohr failure envelopes (McKechnie Thomson and Rodin 1972, Taylor and Spears 1972). This subject has been investigated in more detail in Chapter 3, in terms of both peak and residual shear strength.

Compared to coarse colliery discards, the properties of fine discards are less well known. Sufficient data were collected for the range of the peak shear strength and permeability parameters to be reasonably well known. However, there was little data on the consolidation parameters and, with that which has been recorded, tests were carried out with small (76mm diameter) oedometers. Because there is reason to believe such parameters to be misleading (Rowe and Barden, 1966), the consolidation properties of materials from two fine discard lagoons have been investigated using large (150mm diameter and above) Rowe cells for the first time.

Largely in response to a request from the National Coal Board, an attempt has also been made to evaluate the effects of two different types of flocculant upon the consolidation parameters of tailings, since this could have a bearing on the economics of excavating lagoons.

The in situ shear strength of lagoon deposits is another factor which is important, particularly when it is necessary to excavate the deposits. In this respect an evaluation of vane shear strengths has been carried out. This part of the work has drawn attention to the high degree of variability across a lagoon, both in grain size and in the degree of consolidation.

Finally, stability analyses have been undertaken, to determine what effect, if any, the more important factors arising from the foregoing investigations have upon colliery spoil embankments. These factors are: buried weathered layers from extension of an old tip, curved shear strength

envelopes and unfavourable situations which arise when lagoons are overtipped with coarse discard.

Overtipping in excess of 3m in thickness is normally prohibited (National Coal Board 1970). This results in severe pressure on tipping space. Instead of being overtipped, many lagoons may have to be reused by excavation of the partly consolidated deposits, which will then have to be disposed of with the coarse discard elsewhere in the layered heap.

In order to perform these stability analyses, a computer program has been written by the author. It incorporates a number of options which enable it to cope with the above problems, viz: a multi-layered slope, the shear strength parameters of each layer of this can be curved or linear, with or without anisotropy. To cater for the overtipping situation, excess pore pressures in individual layers can also be specified, while analyses by both circular arc and non-circular failure surfaces may be performed.

1.3 Methods employed

To determine the weathering effects, peak and residual shear strength of ex-washery material and of superficial material from the spoil heap have been determined. The material from the spoil heap had to be at least 6 months old. Where possible, material from the body of the tip was also tested. The locations of the collieries from which material was obtained are shown in Figure 1.1.

Peak shear strengths of coarse colliery discards were determined by means of consolidated - drained (Cd) triaxial tests, following the procedure described by Bishop and Henkel (1962, pl22ff). Samples were fabricated by compacting the passing 19mm fraction to British Standard maximum density (2.5kg rammer) in a 100 mm diameter mould. In situ densities were found to be generally in accordance with those used in the tests. Previous work by McKechnie Thomson and Rodin (1972) had already shown that effective shear strength is insensitive to the initial placement density of these materials. Saturation was ensured

by using the back-saturation technique, a back-pressure of 280 kN/m^2 being employed. The triaxial test rig system used in this work is shown in Figure 1.2. As set up in this figure, a maximum effective confining pressure of 630 kN/m^2 can be obtained. Initially, however, an effective confining pressure of only 210 kN/m^2 was attainable.

For residual shear strengths, a reversing shear - box was employed. For coarse discards, a $0.3 \times 0.3 \text{ m}$ box was used, whilst a $60 \times 60 \text{ mm}$ box was employed for finer materials. In the larger box, samples were manufactured by compaction of the passing 38 mm fraction. The reversing shear - box is not particularly satisfactory for determining residual shear strengths of 'degrading' aggregates such as colliery spoils, due mainly to the sample loss that occurs. This sample loss is caused by particles working their way between the two halves of the box as they move back and forth. However, a ring shear - box, which largely overcomes this problem, was not available for the current work.

Consolidation tests were performed in two Rowe cells, one of 254 mm diameter and the other of 152 mm diameter. The operation followed the method described by Rowe and Barden (1966). The system employed is shown in Figure 1.3. In this, it can be seen that a back-pressure facility is incorporated. This assisted in saturating the samples, which, being large, would otherwise have taken many days to saturate. The Rowe cell has several advantages over the conventional 76 mm diameter oedometer, as will be demonstrated in Chapter 4. It may be mentioned here, however, that the single drainage situation, combined with the thick samples which are possible with the Rowe cell effectively slow down the rate of consolidation in a test. This is extremely useful with some fine discards which have proved free draining. The slower rate of consolidation imposed by the Rowe cell enables readings to be taken where this would have been impossible with an oedometer.

The chemical and mineralogical analyses were performed by Mr. R.G. Hardy. The major element geochemistry was determined using a Phillips PW1212 Automatic Sequential Analyser X-ray Fluorescence (XRF) machine. A Phillips PW1130 2kW X-ray diffractometer (XRD) machine was used to determine the mineralogy.

1.4 Failures of spoil heaps and lagoons

Considering the lack of rational design methods prior to 1966, it is surprising that so few of the 2000 tips which have existed in the United Kingdom have given serious trouble. The commonest kind of failure was the "plain gravity slide" of Terzaghi and Peck (1967). In this type of failure (Figure 1.4), little disturbance of the sliding mass occurs and strains are not extensive. It is not usually fatal. However, considerable damage may be caused to fixed installations. The shear plane that is formed is also a zone of weakness that may permit further failures to occur. The failure of Tip 7 at Aberfan in 1966 is believed to have been a reactivation of an earlier failure in 1963 (Bishop, Hutchinson, Penman and Evans, 1969).

The flow slide (Figure 1.5) is potentially far more destructive. In it, the sliding mass is much disturbed and extensive strains of up to 600 metres have been recorded with colliery spoil (Bishop, 1973). With coarse colliery discard this type of failure has only occurred with high (50m), loose tipped faces. It requires a substantial reduction in volume in order to take place. This is because pore pressure elevation is necessary for reduction of the effective shear strength of the material to negligible proportions (Bishop, 1973). With modern methods of construction, with low faces and compacted materials, such failures are unlikely to occur.

A failure of a lagoon bank is potentially disastrous. While the actual embankment failure may be only a plain gravity slide, the release of water and saturated, uncompacted tailings which may follow can be highly destructive. For example, the failure of a tailings

dam across Middle Fork, Buffalo Creek in West Virginia may be cited. Here some 500,000m³ of tailings, slurry and water was released after Dam No. 3 failed in 1972 (Bishop, 1973), destroying the town of Saunders. This embankment was constructed from uncompacted coarse discard, a practice which has been phased out in the United Kingdom since the publication of the National Coal Board's Technical Handbook's 2nd draft in 1970. Prior to this several breaches of lagoon banks had occurred, with associated tailings runs, but fortunately without disastrous consequences.

Tailings lagoon embankments are only raised when required. They are thus liable to contain weathered crusts. Thus, if these are weaker than the remainder of the spoil, the embankment may be weakened with potentially serious consequences.

1.5 Mineralogy and weathering of colliery discards

1.5.1. Average mineralogy of spoil heaps

British colliery spoil is an aggregate of Carboniferous Coal Measures age rocks. Generally, the discard contains mudstone/shale, seatearth, siltstone and minor sandstone fractions. The proportions of each can be highly variable, depending upon the stratigraphy at the horizons of the coal seams being worked. the proportions of "roof" to "floor" (i.e. the beds on top of the coal seam to those beneath it) will also vary from colliery to colliery, and also from seam to seam in the same colliery.

Taylor (1975) gives the average mineralogy of 74 specimens from England and Wales. This is reproduced in Table 1.1. While these averages are somewhat biased towards the South Wales coalfield (49 out of the 74 specimens), due to the preponderance of investigations in this coalfield, some interesting points can be seen. The 10⁰ micaceous clay - minerals (illite and mixed - layer clay) are dominant, amounting to 50 per cent of the total, while kaolinite is a relatively minor component. Comparisons between coalfields by Taylor

(1975) indicate that at the statistical 95 per cent confidence level, the total clay-mineral content of the English spoil samples (excluding Durham) is higher than the South Wales suite, whilst at the same confidence level quartz is more abundant in the Welsh materials.

In contrast to British spoils, spoils from the West Virginia Coalfield, U.S.A., have quartz as the dominant mineral (Busch, Backer Atkins and Kealy, 1975). Illite and kaolinite are relatively minor components. These West Virginian spoils are also considerably more carbonaceous, having on average 29 per cent coal, compared to the 13 per cent average coal content of British spoils.

According to Taylor (1975), potassium and sodium ions can largely be attributed to clay minerals (10\AA micaceous or illitic minerals in particular), since other K^+ and Na^+ bearing minerals such as sulphates and feldspars, are on average present in very small quantities, (Table 1.1). Alumina (Al_2O_3) is almost entirely a clay-minerals component. Hence, high potassium oxide to alumina (K_2O/Al_2O_3) and sodium oxide to alumina (Na_2O/Al_2O_3) ratios are indicative of shales rich in illite and mixed-layer clay (10\AA minerals), whilst low ratios imply that other clay minerals such as kaolinite are predominant (Taylor 1975).

Recently, work by Collins (1976) has shown that samples taken from 8 coalfields infer that kaolinite is the second most common mineral. This confirms earlier conclusions of Taylor and Spears (1970), that kaolinite was dominant in the northern coalfields (i.e. Scotland, Northumberland and Durham). Collins' high kaolinite samples were from Scotland. It may well be that the average order of abundance of the main clay minerals in British coalfields is: i) illite, ii) kaolinite, iii) mixed-layer clay, iv) minor chlorite.

Table 1.1
(Table 2, Taylor, 1975)

Average Mineralogy of 74 specimens considered (wt%)

Illite	31.5)
Mixed layer clay	26.0)
)— 57.5
Kaolinite	10.5
Chlorite	0.5
Quartz	17.5
Carbonates *	1.0
Organic Carbon	13.0

Trace sulphates, pyrite, felspar, rutile, phosphate (apatite) account for less than 2%.

* Dominantly siderite (FeCO_3)

1.5.2 Weathering

The clay minerals and quartz are relatively stable in a normal temperate weathering environment. The unstable (i.e. non-detrital and secondary minerals) such as carbonates, pyrite and sulphates make up a very small proportion of most spoil heaps (see Table 1.1). Investigations carried out at Yorkshire Main colliery and Littleton colliery have shown that there is little, if any, mineralogical change in the body of the tip (Taylor, 1974a). Intense oxidation was limited to the top metre in both spoil heaps, while at Yorkshire Main the soluble sulphate content only increased significantly in the top 3m of the tip.

This increase is probably a reflection of pyrite decomposition, the resulting sulphuric acid reacting with carbonates and ions in the clay minerals to form gypsum ($\text{CaSO}_4 \cdot 2\text{H}_2\text{O}$) and jarosite ($\text{KFe}_3(\text{SO}_4)_2(\text{OH})_6$). Pyrite content showed two interesting highs, one at 3m in depth and the other at 3m above the water table, which was 36.6m below the surface of the tip.

In terms of physical disintegration, desiccation followed by saturation of shale type rocks can be important. The air in the fragment is pressurised by the capillary pressures developed in the outer pores on wetting. The high air pressures then force apart the mineral skeleton of the fragment. This method of breakdown is ineffective on some rocks, and it is believed that expandable mixed-layer clay is another control on disintegration (Taylor, 1974a).

Where sodium is the dominant exchangeable cation in mixed-layer clay, disintegration can be very rapid and complete. For example, the Stafford tonstein (a mudstone) will explode when dry pieces are immersed in water. This material contains 70 per cent expandable mica-montmorillonite and has a high exchangeable sodium figure (seven times the average for colliery spoils).

With coarse colliery discards, the average content of expandable mixed-layer clay is high (Table 1.1), this is offset to some degree by a low average exchangeable Na^+ figure (Taylor, 1974a). Disintegration of the weaker rock types will also be masked to a certain extent by the more silty and stronger inert rock types which are present.

Lawrence (1972) showed that, in South Wales at least, there was a marked difference in behaviour between seatearths (i.e. floor material) and roof rocks. The former disintegrated far more rapidly upon exposure.

It should be noted that physical weathering, as with chemical weathering is restricted to the outermost 3m of a tip at the greatest extent (McKechnie Thomson and Rodin, 1972).

1.6 Mechanical properties of coarse and fine discards

1.6.1 Coarse discard

Test results from all the site investigations in England and Wales (McKechnie Thomson and Rodin, 1972) imply that the overall effective shear strength of coarse colliery discard lies in the range $\phi' = 25.5$ degrees to $\phi' = 41.5$ degrees. Spoils from Scotland have a smaller range ϕ' , from 25.5 to 39 degrees. However, spoils from West Virginia, formed from rocks of similar age to British spoils, have a ϕ' value which reaches 46 degrees (Busch, Backer and Atkins 1974). In the case of many discards the Mohr failure envelope is curved, i.e. ϕ' decreases with increasing normal stress (McKechnie Thomson and Rodin 1972).

The main mineralogical control on shear strength is the coal content (Taylor 1974b). As the coal content increases, the clay mineral content falls, while the shear strength increases. Quartz content has no statistically significant correlation with shear strength. While the coal content of the spoil may often mask

variations in the strength of the parental rock constituents, such variations can be shown to exist. Coal-free material from Cynheidre colliery in West Wales probably has a ϕ' value of around 34 degrees, while material from Birch Coppice colliery in the South Midlands area probably has a ϕ' value of 27 degrees (Taylor, 1974b).

This fundamental difference in the shear strength of the rock constituents could be caused by several factors, notably clay mineral type, particle grading and the structure of the clay particles forming individual shale fragments. It is also possibly a function of the extent of diagenesis. In this context, Price (1966) demonstrated a possible correlation between the uniaxial strength of some South Wales coalfield rocks and their probable depth of burial. The depth of burial can be qualitatively related to the rank of the associated coal seams. In terms of the actual strength of colliery spoils, however, there is no correlation between shear strength and rank (Ratsey, 1973). Other variables, such as the coal content, drown any strength variation with rank.

There is a possible correlation between shear strength and material passing the B.S. 200 sieve, ϕ' tending to decrease with increasing fines content (McKechnie Thomson and Rodin, 1972). This may be related to Taylor's (1974b) proposition that ϕ' decreases with increasing clay mineral content, in that material with a large fraction of less than B.S. 200 sieve size may well have a high clay mineral content. It should be pointed out, however, that Ratsey (1973) did not find a statistically significant correlation between particle grading and shear strength for his data.

1.6.2 Fine discard

In so far as it is known, fine discard has a lower shear strength range than does coarse colliery discard. The range of ϕ' is 21.5 to 39 degrees. However, this does not give the true picture,

as in most cases, the shear strength of the fine discard is greater than the associated coarse discard from the same colliery (McKechnie Thomson and Rodin, 1972).

Fine discards generally possess a high carbon content (35 to 40 per cent). This is probably the cause of their shear strengths being higher than that of the corresponding coarse discards, which would customarily have a much lower carbon content (mean = 13 per cent).

1.7 Published material.

The writer should mention that parts of this work have now been published in:-

- i) 'The Engineering Geology of Devensian Deposits Underlying P.F.A. Lagoons at Gale Common, Yorkshire' (Q. Jl. Engng. Geol. Vol. 9, No. 3 pp 195 - 216) by Taylor, R.K., Barton, R, Mitchell, J.E. and Cobb, A.E. (1976)
- ii) 'Mineralogical and Geotechnical controls on the storage and use of British coal-mine wastes' (9th International Conference of Soil Mechanics and Foundation Engineering, Tokyo, 1977) by Taylor, R.K. and Cobb, A.E. (in press).

FIGURE 1.1

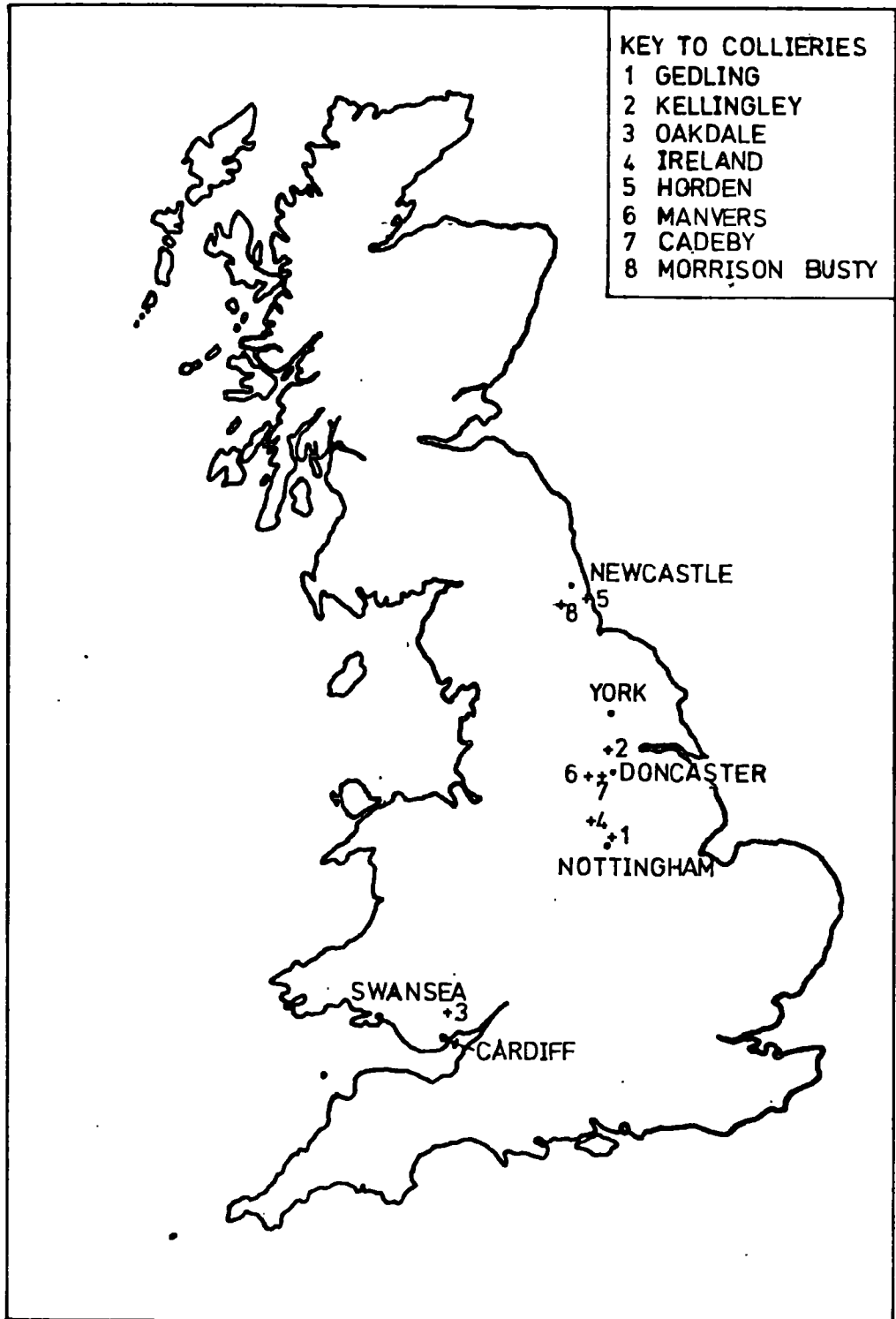


FIGURE 1.2

APPARATUS FOR TRIAXIAL SHEAR WITH SATURATION BY BACK-PRESSURE

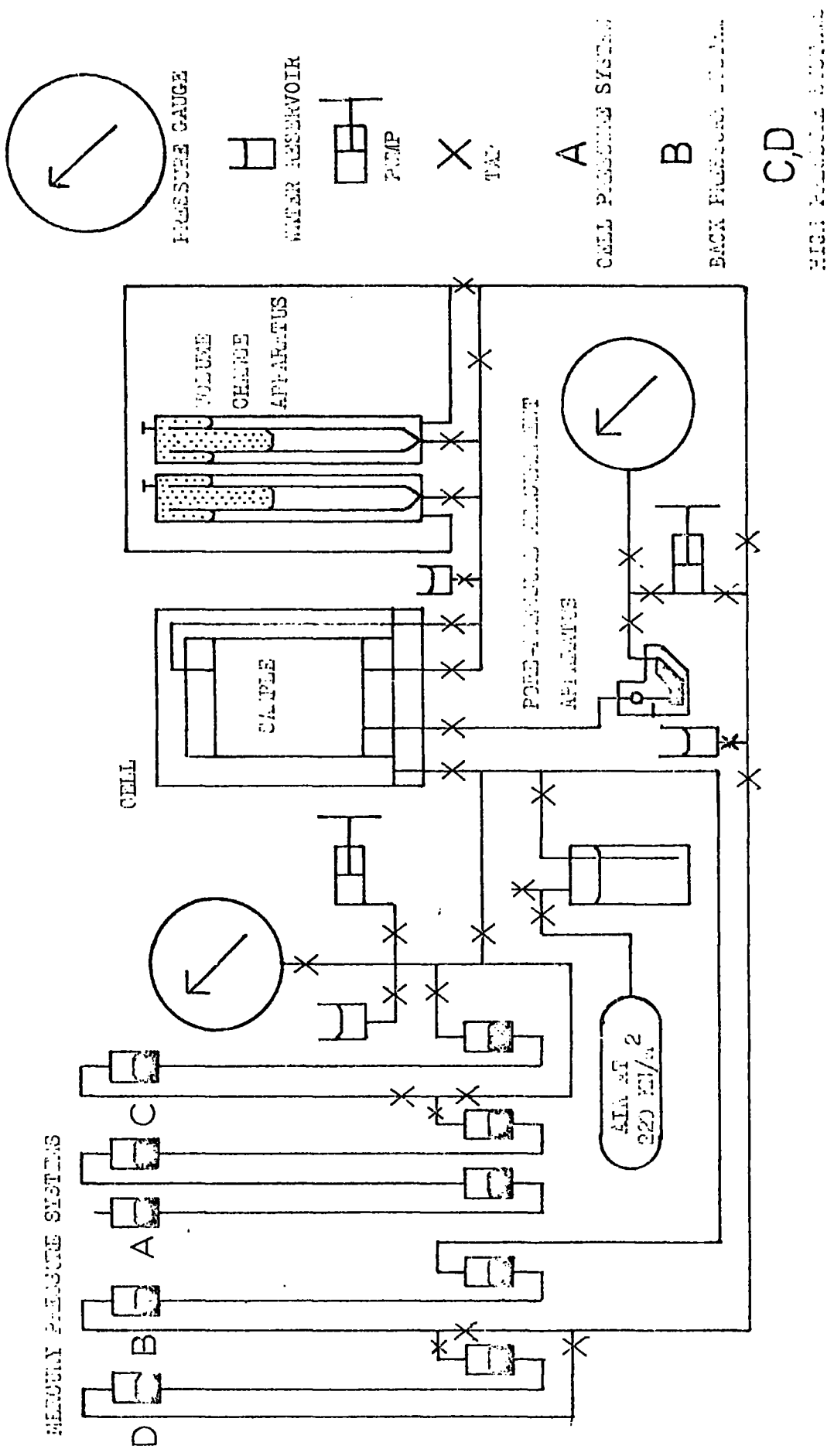
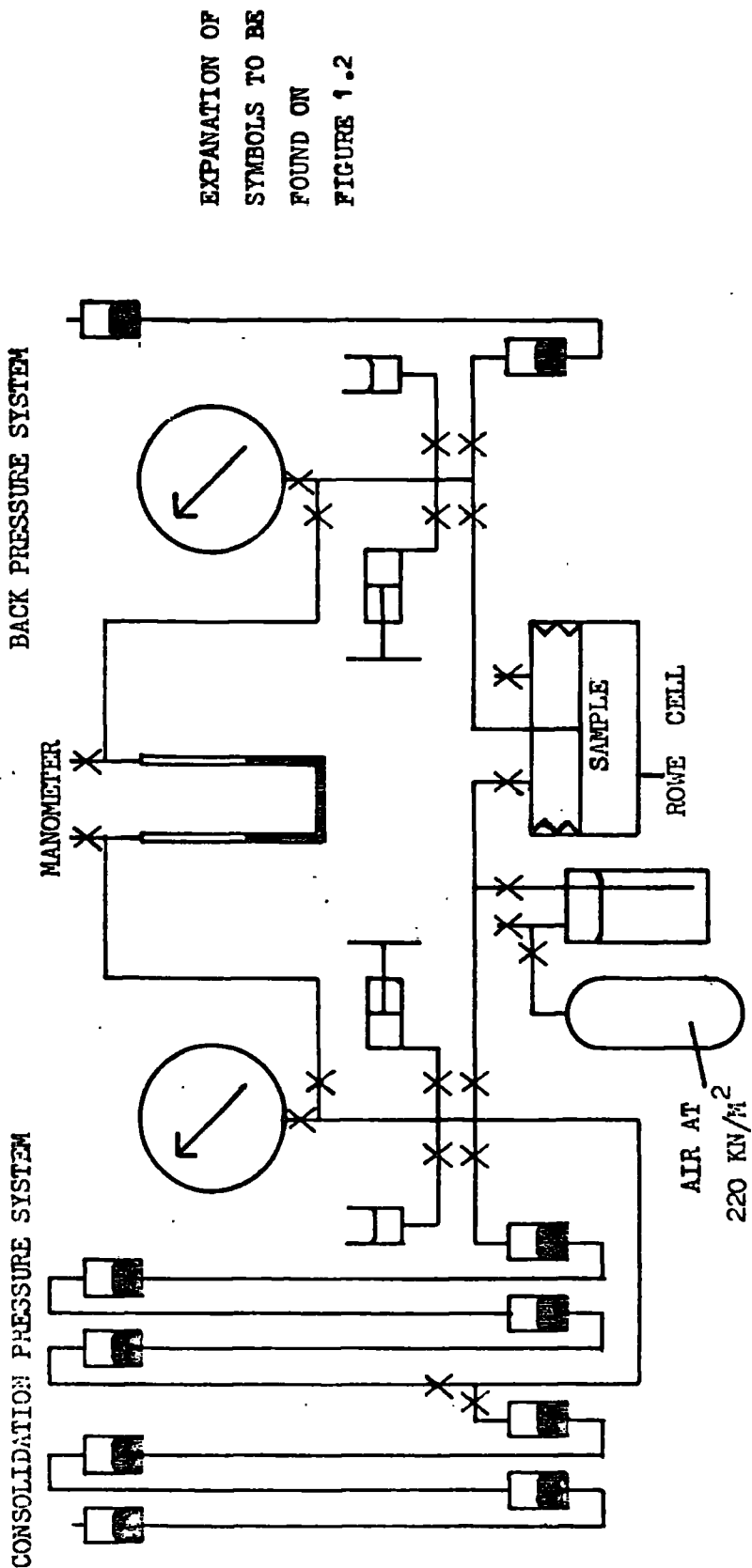
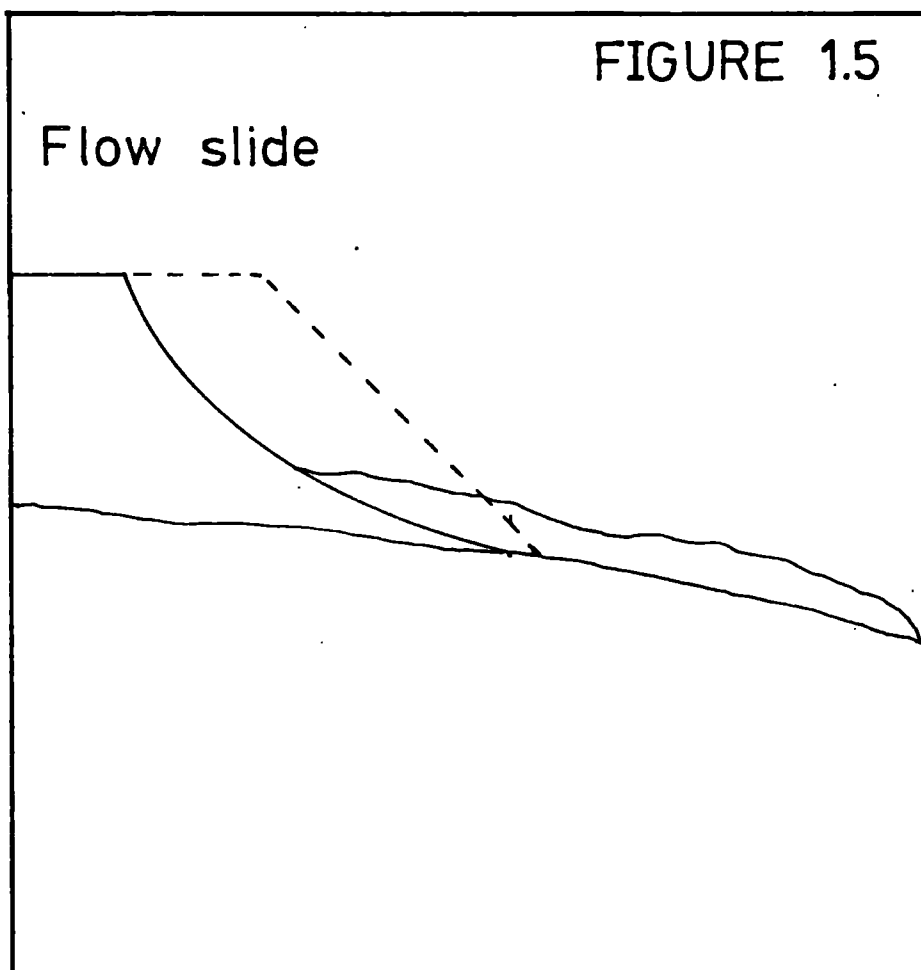
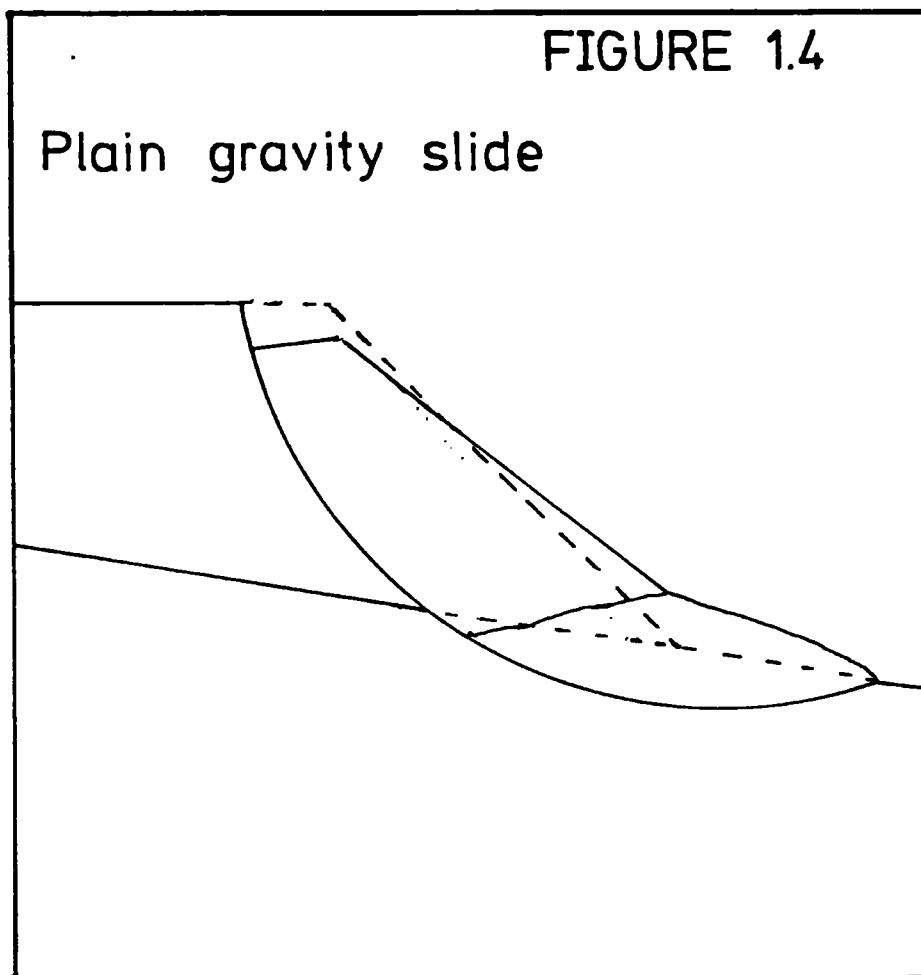


FIGURE 1.3

APPARATUS FOR ROWE CELL CONSOLIDATION TESTS WITH SATURATION BY BACK-PRESSURE





CHAPTER 2

EFFECTS OF WEATHERING PROCESSES UPON SHEAR
STRENGTH OF COARSE COLLIERY DISCARDS2.1 Introduction

Once unburnt spoil is deeply buried within a spoil heap, little change apparently takes place, either mineralogically or mechanically (Taylor, 1974a). From investigations at Yorkshire Main and Littleton collieries, it appeared that weathering was only active within the outermost 3m of a tip.

Now, while material may be stable once buried below 3m depth, present day construction techniques using thin, compacted layers, may leave surfaces exposed for considerable periods before burial under a succeeding lift. If weathering processes are rapid, it is possible that the material will be severely degraded and weakened before burial, especially upon its upper surface. Lagoon embankments which are raised to increase lagoon capacity are also liable to similar effects. With lagoon embankments the resulting weak zones would lie parallel to the external surface, an unfavourable position from a stability point of view.

While modern construction methods may permit excessive weathering to occur, they have eradicated the old problem of burning spoil banks. Spoil, deposited at its angle of repose by tipping over high faces and with the consequent low degree of compaction, was very susceptible to ignition. It is the opinion of Carr (1947/48), that the majority of old tips caught fire. The source of ignition could be either internal or external. The external cause would be hot cinders from the boiler house, which were often deposited on the tip, or some other small fire started on the surface, igniting the coaly material in the tip. The internal causes were exothermic oxidation reactions. Internal heating was the most common cause of combustion (National Coal Board,

Technical Handbook 1970). Burning can thus be considered to be an extreme weathering effect.

In investigations into a partly burnt spoil heap at Brancepeth, Co. Durham, by Taylor 1973a), there were two samples which contained red (burnt) shale. These two samples had the highest shear strengths, with ϕ' values of 40 to 41.5 degrees compared to a range of 28.5 to 37.5 degrees for the remainder of the samples. There was also evidence that the failure envelope was curved, in contrast to the unburnt Brancepeth spoil which had no determinable curvature.

While burnt colliery discard is not now being formed, there are considerable stocks of the material in old burnt and partly burnt heaps. Its mechanical behaviour is of interest in that it is used not only in collieries but elsewhere, as a strong aggregate. In old collieries which are still active there may be sufficient quantities of burnt spoil such that it cannot be ignored when designing the tip.

The mechanical behaviour of two burnt discards has been considered. One from the old (now closed) Ireland colliery in Derbyshire and the other from the also closed Horden colliery, Co. Durham. Material from the latter is currently being exploited commercially as an aggregate.

To discover how much shear strength reduction might be expected before material was buried in a tip, it was decided to compare the shear strength of material as currently produced by the washery with that of material, from the surface of the tip, which was at least 6 months old. In addition, where it proved possible, buried tip material was also tested. In all, spoils from three different collieries were investigated. These were Gedling (low rank coal), Kellingley (low rank coal) and Oakdale (high rank coal). Kellingley and Oakdale were chosen to show any difference in behaviour between spoils from collieries producing low and high rank coals. Gedling spoil indicates the behaviour of a spoil of high seatearth content.

2.2 Gedling discard (rank 802 and 902)

2.2.1 Sampling

Five bulk samples were obtained from Gedling colliery, Nottingham (Fig. 1.1). One was ex-washery, and another from the surface of a part of the tip which had been stationary for 6-12 months. The other three samples came from a trench dug in spoil which had been emplaced for 3-4 months. These three were taken at various depths, namely 1, 3 and 4 metres. In addition, a single U100 was driven into material that had been emplaced for up to 12 months in the vicinity of the major haul road on the tip.

2.2.2 Chemistry and mineralogy

The chemistry of the samples is shown in Table 2.1. There are some variations between the samples. The three samples from the body of the tip, of some 3-4 months age, are reasonably similar in composition. The other two samples, i.e. that from the washery and that of 6 months age differ slightly in that total silica (SiO_2) and alumina (Al_2O_3) are lower than the samples from the body of the tip. It is also noticeable that the washery material has a higher organic carbon content (16%) compared to the tip (9-10%). From Table 2.2 it is noticeable that the 3-4 month old samples have very low $\text{K}_2\text{O}/\text{Al}_2\text{O}_3$ ratios, considerably lower than the average of Ratsey's (1973) eight ranked samples (Table 2.3).

Considering the mineralogy which is shown in Table 2.4, differences are again noticeable. In terms of clay minerals, the washery sample contains the greatest proportion, while the 3-4 month old material contains the least. The tip materials contain more quartz than the washery sample. Ankerite is also of noticeable proportions in the tip. Considering that ankerite is a cleat mineral in coal, it is perhaps surprising that it does not appear in detectable proportions in the washery material which has the highest coal content.

One mineral which does not appear is jarosite. This indicates a lack of significant mineralogical alteration, even in the material from the tip surface.

It should be mentioned that Gedling discard contains a high proportion of seatearth. During a three week period over which the make of dirt was measured, seatearth accounted for some 54 per cent of all material placed on the tip.

TABLE 2.1

CHEMISTRY OF COARSE DISCARD SAMPLES
WEIGHT PER CENT

Components	Gedling Tip	Gedling Washery	Gedling 1m deep	Gedling 3m deep	Gedling 4m deep
S102	54.13	48.21	57.92	57.48	57.50
AL203	22.60	21.69	24.69	24.21	24.63
FE203	4.36	4.29	4.06	4.07	3.82
MGO	1.54	1.48	1.37	1.40	1.32
CAO	0.91	0.92	0.13	0.11	0.18
NA20	0.49	0.35	0.36	0.37	0.36
K20	3.55	3.62	0.77	0.76	0.73
T102	1.02	0.91	1.08	1.07	1.08
S	1.57	1.48	0.51	0.41	0.51
P205	0.71	0.67	0.05	0.02	0.03
C	9.12	16.39	9.04	10.09	9.84
	Kell- ingley	Oakdale Tip	Oakdale Washery	Ireland Tip	Horden Burnt Shale
S102	38.28	51.64	42.62	53.04	62.36
AL203	21.61	25.50	28.16	30.21	25.05
FE203	5.61	3.45	3.81	7.22	7.43
MGO	1.19	1.06	1.17	1.78	1.21
CAO	0.31	0.37	0.88	0.40	0.38
NA20	0.33	0.28	0.40	0.66	0.41
K20	1.15	2.71	3.51	4.53	0.82
T102	0.91	1.32	1.34	1.01	1.03
S	3.67	0.53	0.77	1.06	1.19
P205	0.19	0.07	0.17	0.08	0.10
C	26.75	13.07	17.17	0.00	0.00

TABLE 2.2

ELEMENT OXIDE TO ALUMINA RATIOS OF COARSE DISCARD SAMPLES

Components	Gedling Tip	Gedling Washery	Gedling 1m deep	Gedling 3m deep	Gedling 4m deep
S102	2.39	2.22	2.35	2.37	2.33
Al2O3	1.00	1.00	1.00	1.00	1.00
FE2O3	0.19	0.20	0.16	0.17	0.15
MGO	0.07	0.07	0.06	0.06	0.05
CAO	0.04	0.04	0.01	0.00	0.01
NA2O	0.02	0.02	0.01	0.02	0.01
K2O	0.16	0.17	0.03	0.03	0.03
TlO2	0.05	0.04	0.04	0.04	0.04
S	0.07	0.07	0.02	0.02	0.02
P2O5	0.03	0.03	0.00	0.00	0.00
C	0.40	0.76	0.37	0.42	0.40
	Kell-ingley	Oakdale Tip	Oakdale Washery	Ireland Tip	Horden Burnt Shale
S102	1.77	2.02	1.51	1.76	2.49
AL2O3	1.00	1.00	1.00	1.00	1.00
FE2O3	0.26	0.14	0.14	0.24	0.30
MGO	0.05	0.04	0.04	0.06	0.05
CAO	0.01	0.01	0.03	0.01	0.02
NA2O	0.02	0.01	0.01	0.02	0.02
K2O	0.05	0.11	0.12	0.15	0.03
TlO2	0.04	0.05	0.05	0.03	0.04
S	0.17	0.02	0.03	0.04	0.05
P2O5	0.01	0.00	0.01	0.00	0.00
C	1.24	0.51	0.61	0.00	0.00

TABLE 2.3

AVERAGE ALUMINA RATIOS OF 8 SAMPLES FROM RATSEY(1973)

Component Ratio	Average
$\frac{\text{SiO}_2}{\text{Al}_2\text{O}_3}$	2.01
$\frac{\text{Fe}_2\text{O}_3}{\text{Al}_2\text{O}_3}$	0.165
$\frac{\text{MgO}}{\text{Al}_2\text{O}_3}$	0.05
$\frac{\text{CaO}}{\text{Al}_2\text{O}_3}$	0.02
$\frac{\text{Na}_2\text{O}}{\text{Al}_2\text{O}_3}$	0.025
$\frac{\text{K}_2\text{O}}{\text{Al}_2\text{O}_3}$	0.14

TABLE 2.4
 MINERALOGY OF COARSE DISCARD SAMPLES
 WEIGHT PER CENT

Discard	Gedling			Kellingley			Oakdale
	Washery	Tip 6m old	Tip 4m old	Stockpile	8 yrs.old Above W.T.	8 yrs. old Below W.T.	
Quartz	15.0	22.0	26.0	6.0	8.0	15.0	7.0
Illite*	51.0	49.0	41.5	51.0	49.0	33.5	53.5
Kaolinite	17.0	15.0	11.5	14.0	6.0	13.5	23.0
Chlorite	0.0	0.0	0.0	0.0	1.5	1.5	0.0
Ankerite	0.0	5.0	11.0	0.0	3.5	4.0	1.0
Jarosite	0.0	0.0	0.0	0.0	3.5	0.0	0.0
Pyrite	0.0	0.0	1.0	3.0	1.5	5.5	1.0
Coal	16.5	9.0	9.0	26.5	26.5	26.5	14.5

* 'Illite' includes mixed-layer clay

W.T.=Water Table

2.2.3 Grading

As can be seen in Figures 2.1 and 2.2, Gedling discard is dominantly of sand and gravel size, ranging up to coarse gravel. Considering first the ex-washery material which is shown in Figure 2.1 it can be seen that the majority (56%) of the material is of gravel size, i.e. between 2 and 60mm. However, with 44 per cent smaller than 2mm size and 20 per cent smaller than 0.072mm size, it is fine grained in so far as coarse discards are concerned. None of the eight ranked samples tested by Ratsey (1973) have more than 30 per cent smaller than 2mm and 11 per cent smaller than 0.072mm (Figure 2.1).

Turning to the material which had been on the surface of the tip for some 6-12 months, this material is considerably finer grained than the ex-washery material, having 68 per cent smaller than 2mm and 35 per cent smaller than 0.072mm size. Thus in this period of 6-12 months, Gedling spoil can be degraded from a silty-sandy gravel to a silty-gravelly sand.

Of the three samples which were 3-4 months old when excavated (Figure 2.2), the sand size content of the grading curves are similar, but the gravel size section of the sample from 3m in depth is finer than the other two. This 3m deep sample has very little material coarser than 20mm. With an average of 55 per cent smaller than 0.072mm the grading of these materials lies between the ex-washery material and the 6-12 month old material, but closer to the latter than the former.

2.2.4 Shear strength

2.2.4.1 Peak shear strength

The peak shear strength of each of the samples was determined using four or more consolidated - drained triaxial tests. In the case of the 3-4 month old material these tests employed effective confining pressures (σ_3) of up to 630 kN/m². At the time when tests were performed on the other two samples (i.e. ex-washery and

6-12 months old), however, the apparatus was only capable of reaching an effective confining pressure of 210 kN/m^2 . The solitary U100 sample was tested at an effective confining pressure of 20 kN/m^2 .

The values of c' and ϕ' are determined by the K_f line relationship. A line drawn through the top points of the Mohr's circles (the K_f line) is related to c' and ϕ' in the following manner (Figure 2.3).

$$\sin \phi' = \tan \theta$$

$$c' = \frac{a}{\cos \phi'}$$

where $\tan \theta$ is the gradient of the K_f line

and a is the y-intercept of this line.

In order to obtain the best line through the top points, the statistical linear regression method known as 'reduced major axis' was employed. This method assumes a normal error distribution on the points in both x and y directions.

To carry out the necessary calculations, a computer program has been written (Appendix B). This program can also drive the Calcomp 563 plotter attached to the NUMAC IBM 370 machine. This plotter then produces a diagram (e.g. Figure 2.10) showing the shear stress to normal stress relationship. The program can also handle data obtained by shear-box tests.

Considering the results of the triaxial tests, which are shown in Figures 2.4 to 2.9, there are a number of points common to all the samples from Gedling colliery. The strain at failure is generally large, from 10 to 20 per cent, with the strain at this condition usually increasing with the effective confining pressure. The volumetric strain is small, never being greater than 2.3 per cent. It also generally increases with the confining pressure. At low pressures (70 kN/m^2) and below), while there is still an overall volume decrease at failure, the actual volumetric strain is decreasing to a slight extent, e.g. the U100 sample, Figure 2.5.

Compared with typical examples of consolidated-drained triaxial shear stress-strain data given in Part 3.4 of Bishop and Henkel(1962), the material is behaving in a manner which has similarities with both a loose sand and a normally consolidated clay. It is, however, behaving in a similar way to that commonly found for coarse colliery discard of both British and American origin. The volumetric strain is smaller than normal, though not to an abnormal degree.

The shear strength parameters of the samples are given in Table 2.5 and illustrated in Figures 2.10 to 2.13. With a statistically determined linear envelope, all the samples exhibit cohesion of varying amounts. For ease of comparison of the materials, the equivalent shearing angle, ϕ'_e is also given in Table 2.5. McKechnie Thomson and Rodin (1972) defined ϕ'_e as the angle between the normal stress axis and a line drawn from the origin of the stress axis (i.e. where $c' = 0$) to the point on the failure surface at 350 kN/m^2 normal stress.

The fresh washery discard (Figure 2.10) exhibits a peak ϕ' of 27.5° with a small cohesion (linear fit), or a ϕ'_e of 30° . This lies within the range to be expected of colliery spoils (i.e. 25.5 to 42 degrees). The material of 6-12 months age from the surface of the tip is shown in Figure 2.11, along with the solitary U100 sample result (shown by dotted line). This weathered material shows a low peak shear strength with $\phi' = 16.9^\circ$ and $c' = 33.9 \text{ kN/m}^2$ - $\phi'_e = 22^\circ$. The material of 3-4 months age (Figure 2.12) was tested at much higher effective confining pressures than the other samples. Owing to curvature of the failure envelopes, which will be discussed in detail in Chapter 3, the linear strength parameters cannot be compared meaningfully with those of the washery and 6-12 month old samples. However, the ϕ'_e values can still be compared. These lie in the range 26° to 28° i.e. between the washery and 6-12 month old samples, but closer to the former. Of the three horizons sampled in the trench,

that at 3m proved strongest, with a ϕ'_e of 28° , while that at 1m proved weakest, ϕ'_e being 26° . The 4m deep sample had a ϕ'_e of 27° . Compared to the value of 29° for ϕ'_e obtained for Gedling East spoil heap by Messrs Wimpey Central Laboratories in 1968, these results show the present material to be somewhat weaker. The possible explanations of these peak shear strength values will be considered in Section 2.2.5.

2.2.4.2 Residual shear strength

The residual shear strength was determined on two samples, the fresh washery material and the 6-12 month old material. A 0.3 x 0.3m reversing shear-box was used. The residual envelope was determined using a single specimen, the step loading technique of Ratsey (1973) being adopted. In this, the sample is subject to a stepwise increase in normal stress to a maximum value, with shearing being continued at each increment until residual is apparently attained. The sample is then unloaded in steps, residual shear strength being measured at each stage. This technique enables stress/strain behaviour at low normal stresses (i.e. equivalent to shallow depths in tips) to be observed. Lack of sufficient sample prevented individual specimens being run to residual at each normal pressure.

The residual shear strength parameters of the Gedling materials are shown in Table 2.5 and in Figures 2.10 and 2.11. They are similar to each other, ϕ'_r being 12.1° with small amounts of cohesion. This is lower than residual strength values customarily obtained for coarse colliery discard. The range of values obtained by Ratsey (1973) for 8 ranked discards lies between 15.5° and 35° for similar shear displacements.

The stress ratio/displacement curves, shown in Figures 2.14 and 2.15 show that residual was attained in under 2m displacement in both cases. They also show some other interesting points. The maximum shear strength was not mobilised until considerable displacement

TABLE 2.5
SHEAR STRENGTH PARAMETERS OF GEDLING SPOIL

Sample	Peak			Residual			Figure	
	c'_p kN/m ²	ϕ'_p *	ϕ'_e	c'_r kN/m ²	ϕ'_r *	I_b		
Ex-washery	12.2	27.5°	30°	10.2	12.1°	33%	2.10	
6-12 months on surface of tip	33.9	16.9°	22°	5.3	12.1°	46%	2.11	
3-4 months in tip	1m deep	24.7	22.0°	26.0°	n.d.	n.d.	n.d.	2.12
	3m deep	12.8	25.7°	28.1°	n.d.	n.d.	n.d.	2.12
	4m deep	31.3	22.6°	27.4°	n.d.	n.d.	n.d.	2.12
	Composite result	19.4	23.8°	27.4°	n.d.	n.d.	n.d.	2.13

N.B. ϕ'_e determined upon Gedling spoil by Wimpey (1968) is 28.7°

* c' and ϕ' determined by reduced major axis statistical fit

+ I_b = Brittleness Index (Bishop 1967), determined at 80 kN/m² normal stress

n.d. - not determined.

(0.08-0.1m) has occurred, corresponding to two to three reversals of the shear-box. This is obviously similar to the large strains encountered in the triaxial tests before peak shear strength was developed. After passing the peak strength, the stress ratio, and therefore shear strength, drops steadily, but fairly rapidly. That the material bears little resistance to degradation on shearing, even at low normal stresses, is shown by the high values of Bishop's (1967) Drained Brittleness Index (I_b) (Table 2.5). I_b is defined as:

$$I_b = \frac{(T_f - T_r)}{T_f} \times 100$$

where T_f is the peak shear stress

and T_r is the residual shear stress.

It is calculated in the current work from the shear-box data at the first normal stress increment, i.e. 80 kN/m^2 .

The tip material, with an I_b value of 46 per cent is obviously more brittle than the washery material which has an I_b value of 36 per cent. However, both are high, indicating the brittleness of Gedling spoil.

The shape of the stress-strain plots for individual runs requires some explanation. It can be seen that for each individual run, the shear stress rises rapidly initially. There is then a pronounced inflexion, after which (apart from the first few runs) the shear stress continues to rise slightly. This behaviour is characteristic of a reversing shear-box (Bishop, Green, Garga, Andresen and Brown 1971). The cause is not known with certainty, but Taylor (1973b) suggests that it is due to the interaction of the trailing edges of the two halves of the box with the sample*. That this is so is also

* Owing to these unpredictable errors, no area correction has been applied in the calculation of shear stress. The area correction, if applied, would have the effect of increasing the shear strength at the end of the run. The effect of the decreasing area of contact of the sample is obviously less than that of the other errors inherent in the apparatus.

suggested by the lack of any rise at the end of shear-box travel when the same shear-box was used to determine the shear strength of a joint plane in a sandstone block. This rock was cemented such that it was contained in the centre of the box, and there was no possibility of it coming in contact with the sides of the shear-box. As stated, the shear stress did not continue to rise with displacement; after failure it tended to remain at a constant value.

Another feature of the individual stress-strain curves is the small peak which develops at the inflection point in the curve (Figure 2.16a). This peak has been interpreted as an orientation effect (Agarwal, 1967, Bishop et al, 1971). This interpretation was verified by McWilliam (1975). The problem then arises as to what value should be taken to represent the shear strength. When the stress-displacement curve from a ring shear-box was compared to that from a reversing shear-box by Bishop et al (1971) they found that the ring shear-box curve coincided at times with the troughs, at others with the peaks and occasionally with neither (Figure 2.16a and b). They also note that there is little theoretical justification for taking the troughs as the residual strength. Normal practice is to take the value at the peak of the reorientation peak as the shear strength, and this has been followed in the current work*.

The large-scale displacement tests on Gedling spoil showed good examples of these reorientation peaks. At the end of the shear test, the top half of the box could be removed complete with the top half of the sample. This revealed a single well developed, slickensided, shear plane (Figure 2.17).

* It should be noted, however, that colliery discards in 0.3 x 0.3m shear-boxes give reorientation peaks of relatively small magnitude (compared to clays). The difference in ϕ' that would result from using the trough as opposed to the peak is only a matter of some 0.2 of a degree.

Compared to clays and sand, the strain necessary to reach residual is much greater for colliery discard (Ratsey 1973). The discard from Gedling reaches residual at a lower strain than that of other discards, requiring less than 2m. Of the eight discards tested by Ratsey (1973), only Birch Coppice spoil reached a 'true' residual after a displacement of 2.2m.

2.2.5 Discussion of the properties of Gedling spoil

There is a noticeable difference in carbon content in the samples (Table 2.1). Whilst this must cause a certain amount of the variation in peak shear strength, it cannot be the cause of it all. From Figure 5 in Taylor, 1974b, the maximum fall in ϕ'_e that can be expected for a fall in carbon content of 7 per cent (from 16 per cent to 9 per cent) is 2 degrees. Thus, this could explain the difference in ϕ'_e between the 3m deep 3-4 month old material and the ex-washery material, but not differences between the other samples. It can however, explain the difference between the ϕ'_e value of the 1968 tests and the current series. The samples from the tip in 1968 had a carbon content of about 18 per cent, some 8 per cent higher than the average of the samples taken from the tip in the current work. The difference in ϕ'_e between the 3-4 month old tip material and the 1968 tip material is some 2 degrees.

The bulk of the drop in shear strength of the tip materials must be due to the weathering (degradation) effects at the surface. The material from the tip surface is the weakest, followed by the material at 1m depth. The material 3m deep shows no shear strength reduction which cannot be accounted for by the carbon content. It should be noted that 3m is the maximum depth of mineralogical weathering noted by Spears, Taylor and Till (1970) in a 50 year old loose tip at Yorkshire Main colliery. It is perhaps surprising, then, that the material from 4m depth is weaker than that from 3m. The most likely explanation is that it is from a previous lift, and was subject to a

short period of weathering before being covered by the next lift.

The cohesion parameter which is present for all the samples is probably not real, being a result of fitting a straight line to a failure envelope which is in fact curved (see Chapter 3). There may, however, be an exception to this in the case of the superficially weathered material (see Figure 2.11). The U100 sample tested at only 20 kN/m^2 effective confining pressure had a deviator stress of 122 kN/m^2 (Figure 2.5). Because this U100 was a sample of old, superficial material of similar age to the bulk sample from the tip, it is reasonable to include it with the bulk sample results. When this is done, it reinforces the impression that material that has spent a considerable time upon the surface of this tip does possess cohesion. The cause is probably to be found in the fine grading of the material, with over 30 per cent silt size and under, of which a considerable proportion must be of clay size. On dessication, which must happen fairly frequently to the exposed crust of the tip, this clay fraction will become overconsolidated and develop cohesive forces. The amount of clay is sufficiently large to give a noticeable cohesion to the bulk of the spoil.

2.3 Kellingley discard (Rank 502 and 702)

2.3.1 Sampling

During site investigation work at Gale Common Pulverised Fuel Ash (P.F.A.) disposal site, it was possible to obtain a number of samples of the discard from Kellingley colliery (Figure 1.1) which forms some of the embankments at the site. Five samples were collected at locations shown on Figure 5.19. They comprise:

- a) Fresh material from the stockpile of only a few days age,
- b) Material, probably of some 2 months in age, from a minor haul road on the main southern embankment to Lagoon B,
- c) Material of some 6 years in age from near the surface of the shale drainage blanket,

- d) Material of some 8 years in age from 2.2m below the crest of the low, eastern embankment to emergency Lagoon D, and from above the water table in this embankment,
- e) Material from the same embankment as d), but some 2.5m below the crest and below the water table.

These samples provide a contrast between the behaviour of colliery spoil compacted to civil engineering standards (i.e. the material from the main part of the site, samples b) and c) and that of loose tipped colliery spoil as found in the embankment to the emergency Lagoon D (samples d) and e).

2.3.2 Chemistry and mineralogy

The most surprising point emerging from the chemistry (Table 2.1) is the high organic carbon content of 26.8 per cent, some 13 per cent above average. Comparing the element oxide to alumina ratios (Table 2.2) with those of Ratsey (1973) in Table 2.3, it is apparent that $\text{SiO}_2/\text{Al}_2\text{O}_3$ is lower than average as are the alkali oxide to alumina ratios.

Mineralogically (Table 2.4) it can be seen that clay minerals are well represented, while quartz is low in all but the 8 year old sample from below the water table. Quartz might be high in this sample due to the segregation which occurs during loose tipping. When material is tipped over a face which is standing at the material's angle of repose, large particles tend to roll farther down slope than do small ones, giving rise to segregation. This provides an explanation for differences in primary minerals of the two 8 year old samples from Lagoon D embankment, which, being formed in one lift might otherwise be expected to be homogenous. The larger particles tend to be formed of the stronger rock types, which contain more quartz (i.e. sandstones). There is however one other noticeable difference in these two samples in that the secondary mineral jarosite is of noticeable proportions

(3.5%) in the sample from above the water table. This indicates severe mineralogical weathering of the material above the water table but not of that below this level. It should be noted that the material from the shale blanket which was not mineralogically analysed did show considerable limonite staining. It was not, however visibly altered in any other way to any great extent.

2.3.3 Grading

The material comprises mainly sand and gravel sizes, ranging up to 80mm size particles, as shown in Figure 2.18. The shale from the main southern embankment is in fact slightly coarser than that from the stockpile, indicating some variability in the grading of the output of Kellingley colliery. This being so, the 8 year old material from the Lagoon D embankment cannot be rigorously compared to the newer material. It is noticeable, however, that this old material, from an uncompacted embankment, is finer grained than the newer material.

Of the two horizons sampled in the old embankment, that from above the water table is finer grained than that from below this level. It is impossible to ascertain how much of this is due to the segregation that occurs on loose tipping (see Section 2.3.2), and how much is due to the severe weathering experienced by the material above the water table.

Compared to the ex-washery discards given in Ratsey (1973), this material from Kellingley is fine grained, though not as fine grained as Gedling (q.v.). It is similar to material from the tip at Orgreave colliery (Ratsey, 1973) and Askern (McKechnie Thomson and Rodin, 1972). As noted by the latter authors, there is considerable breakdown during emplacement of spoil on a tip.

2.3.4 Shear strength

2.3.4.1 Peak shear strength

Some interesting points are apparent from the deviator

stress-strain diagrams, which are shown in Figures 2.19 to 2.23. The fresh material from the stockpile (Figure 2.19) fails at low strains (less than 10 per cent) in a brittle-like failure mode. Post failure reduction in shear strength is, however, small in common with other coarse colliery discards. The old materials (e.g. that from below the water table of the Lagoon D eastern embankment, Figure 2.23) behave in a slightly more plastic failure mode, strains being between 10 and 20 per cent.

At low effective confining pressures (70 kN/m^2) the fresh stockpile material is dilating at failure (a volumetric strain of +0.01 per cent). The only other sample to dilate at failure is that tested at 30 kN/m^2 from the main southern embankment to Lagoon B. This dilatant behaviour is probably due to particles riding over one another at failure rather than rupturing

The shear strength parameters are given in Table 2.6. The material from the stockpile, with a ϕ'_e value of 35.9 degrees is fairly strong. This is partly due to its high carbon content of 27 per cent. Computing from Figure 5 in Taylor 1974b, it might possess a ϕ'_e value of 32 degrees if its carbon content was at the average 13 per cent. Thus the Kellingley material is stronger than that from Gedling. Visual examination reveals that it does not contain the large quantities of seatearth that Gedling discard contains.

As can be seen from Table 2.6, the only sample with a distinct drop in shear strength is the material from above the water table in the Lagoon D embankment. The material from below this water table shows little change in ϕ'_e when compared with younger material. The 6 year old material from the shale blanket, unlike the 6-12 month old superficial material from Gedling tip, shows little fall in shear strength.

2.3.4.2 Residual shear strength

The residual shear strength has been determined for three

TABLE 2.6

SHEAR STRENGTH PARAMETERS OF KELLINGLEY DISCARD

Sample	Peak			Residual			Figure
	c'_p kN/m ²	ϕ'_p	ϕ'_e	c'_r kN/m ²	ϕ'_r	I_b	
Stockpile	29.2	31.8	35.9	0.0	16.0	5%	2.24
S. Embankment, Lagoon B	25.9	31.1	34.8	n.d.	n.d.	n.d.	2.25
6 year old shale blanket	10.6	31.7	33.2	n.d.	n.d.	n.d.	2.26
8 year old, E Embankment Lagoon D above water table	13.7	25.8	28.6	0.0	14.3	25%	2.27
8 year old, E. Embankment Lagoon D below water table	35.2	27.9	34.4	0.0	16.0	13%	2.28

n.d. - not determined.

of the samples, viz: the stockpile material and the two samples from the embankment to Lagoon D. The stress ratio-displacement curves are shown in Figures 2.29 to 2.31. As can be seen, all three samples reach residual after some 2m displacement. The material from above the water table has a lower residual (14.3°) than the other two samples which have a residual value ϕ'_r of 16° (Table 2.6). It also has a higher value of I_p (25%) than the other two samples, indicating greater brittleness at lower pressures. The stockpile material is remarkably resistant to degradation on shearing at low pressures, its I_p value being only 5 per cent (Table 2.6).

2.3.5 In situ dry densities of samples

A number of in situ density determinations were performed on Kellingley spoil at the Gale Common site. For the materials in the main southern embankment and in the Lagoon D embankment above the water table, the sand replacement method was employed. For the material below the water table, this method obviously could not be used. Instead a U100 was jacked into the material using a JCB mechanical excavator, which was also used to extract the U100. The density of the material could then be measured. While this method obviously leads to some over-compaction, it is believed to give a figure which can be compared within limits to the other figures.

The dry densities are given in Table 2.7. It can be seen that only the material from above the water table in the Lagoon D embankment is inadequately compacted, at 82 per cent of B.S. maximum density whereas the other samples are all over 95 per cent of the maximum value, i.e. an acceptable level from a civil engineering standpoint. The above water table, Lagoon D embankment material is, in fact less well compacted than the old loosely placed colliery spoil heaps for which average values of 90 per cent B.S. maximum dry density are normally recorded (Taylor, 1974a). This is probably due to the low

height of the emergency embankment which precludes any large amount of self compaction.

2.3.6 Discussion of the properties of Kellingley spoil

It is apparent from Table 2.6 that Kellingley spoil does not weaken appreciably with time, provided that the material is well compacted. In this it differs from Gedling spoil. This is probably because Kellingley spoil does not contain large quantities of seatearth. Kellingley spoil is also resistant to degradation during emplacement, the southern embankment material being little weaker than the stockpile material. This situation is reflected in the resistance of the material from the stockpile to breakdown at 79.2kN/m^2 normal stress during the large displacement shear-box experiment.

The material from the embankment to Lagoon D does show some interesting weathering effects. The sample from above the water table (i.e. 2.2m below the crest of the embankment) is much weaker than that from below the water table (i.e. 2.5m below the crest of the embankment). Furthermore, the latter is of much the same strength (in terms of σ'_e) as the younger material from the main part of the site. The material from below the water table has two main differences in environment to that from above, namely (i) it has been permanently saturated (ii) it has a higher density. Since this embankment was emplaced in one lift by end tipping and without compaction this increase in density below the water table is probably due to seepage forces generated by water flowing out of the permanently wet lagoon behind the embankment. Thus this material would have only gradually attained good compaction. Hence the continuous saturation must have contributed to the protection from chemical and physical weathering.

The material from above the water table has undergone considerable chemical degradation and has been physically weakened by it. The material from the shale blanket, which also exhibited some chemical weathering (Section 2.3.2) has, however, not been physically weakened to any great extent. Thus compaction can prevent severe weakening of Kellingley discard.

TABLE 2.7

IN SITU DRY DENSITIES OF KELLINGLEY SPOIL AT GALE COMMON

Location	Average dry density (Mg/m ³)	No. of determinations	Moisture content
Main Southern Embankment	1.72	5	9.24
Lagoon D Embankment above water table	1.41	1	9.6
Lagoon D Embankment below water table	1.98 *	1	10.9

Density determined by sand displacement except where otherwise shown.

* Determined by jacking U100 into material with a JCB.

B.S. compaction (2.5 kg rammer) gave a maximum dry density of 1.73 Mg/m³ at 7.0 per cent moisture content.

The chemical weathering would appear also to have produced a reduction in the value of the residual shearing angle (ϕ'_r). Perhaps of greater importance is the enhanced degradation that occurs when it is sheared at low normal stresses. This could give rise to severe degradation and weakening should such material ever be re-worked.

It is of interest to note the similar behaviour of the shale fill used in the Balderhead Dam. The parent rocks of this shale fill were of Carboniferous (Namurian) age and hence older than the parent rocks of colliery spoils. They were, however, similar, except that there were no discrete coal seams. It was found that only chemically weathered material from a loose tip of some 50 years age showed a marked reduction in strength. Surficial material from the nearby Burnhope Dam, some 30 years old, which was, of course, compacted, was of similar strength to the fresh Balderhead Dam material after compaction (Kennard, et al 1967).

2.4. Oakdale Discard (Rank 301)

2.4.1 Sampling

Two bulk samples of discard from Oakdale colliery (Figure 1.1) in South Wales were provided by the Scientific Department of the National Coal Board. These comprised a sample of fresh washery discard and a sample from the surface of the tip which had been exposed for some 6-12 months.

2.4.2 Chemistry and Mineralogy

From the chemistry, shown in Table 2.1, it can be seen that the two samples are not strictly compatible. The fresh washery material has higher organic carbon and Al_2O_3 contents and a lower SiO_2 content than the tip sample. The element oxide to alumina ratios (Table 2.2) show up differences between the samples and with the average values for colliery discards. Between the two samples, the main differences are in the SiO_2/Al_2O_3 (washery material lowest),

$\text{CaO}/\text{Al}_2\text{O}_3$ (tip material lowest) and $\text{K}_2\text{O}/\text{Al}_2\text{O}_3$ (tip material lowest). Compared to the average ratios (Table 2.3), all the ratios, except the $\text{SiO}_2/\text{Al}_2\text{O}_3$ ratio for the tip and the $\text{GaO}/\text{Al}_2\text{O}_3$ ratio for the washery are lower than average. The low alkali oxide alumina ratios indicate a greater proportion of kaolinite to illite than normal.

From the mineralogical results, given in Table 2.4, and by comparison with the average values shown in Table 1.1, it can be seen that while illite plus mixed-layer clays are of average concentration, kaolinite is much higher than normal (23 per cent as opposed to 10.5 per cent). This increase in kaolinite is at the expense of quartz, which, at 7 per cent is very low (17.5 per cent average). This situation is somewhat surprising, as South Wales discards in general are higher in quartz than English ones (Taylor 1975).

The mineralogical results quoted in Table 2.4 were obtained from a mixture of the two samples. Separate qualitative mineralogical analyses of the two samples indicated that the tip material was richer in quartz than the washery discard, this variation being at the expense of illite in the tip. The higher quartz in the tip is an indication that the tip sample contained some run-of-mine debris*, such as sandstones, not present in the washery discard. The lower illite content of the tip will be the cause of the lower $\text{K}_2\text{O}/\text{Al}_2\text{O}_3$ ratios of the tip material (with respect to the washery materials).

The qualitative analysis disclosed a trace of chlorite in the samples, which was not recorded in the quantitative analysis. It is noticeable that none of the minerals produced by weathering (i.e. gypsum and jarosite) showed up in the tip material.

* Run-of-mine dirt is that produced during development work at a colliery, as opposed to that produced during normal working of a coal seam. It generally by-passes the washery and is emplaced directly onto the tip.

2.4.3 Grading

The incompatibility of the two samples is also shown by the grading curves (Figure 2.32).

The tip material, ranging up to 60mm size, is much coarser than the washery material, which only reaches a maximum size of 20mm. The presence of run-of-mine dirt in the tip would account for the tip material being coarser. However, it is obvious that there has been no significant physical disintegration occurring on the tip, or during the emplacement of the material on the tip.

This material from Oakdale is a sandy gravel, and is of similar grading to other washery discards (Figure 2.32).

2.4.4 Shear strength

2.4.4.1 Peak shear strength

Triaxial shear tests could only be carried out at effective confining pressures of up to 500 kN/m^2 . This was due to the rubber membrane containing the sample repeatedly puncturing at higher pressures. These punctures were caused by the membrane being ripped by shale fragments during the shearing stage. This problem did not arise with either Gedling or Kellingley spoils, as the shale fragments in these materials were more rounded. The problem was alleviated to a certain extent by employing a double membrane, at the expense of increasing the errors due to membrane strength; 500 kN/m^2 proved to be the maximum effective confining pressure at which a test could be run.

The failure strains again increase as effective confining pressure increases. Failure strains are less than 10 per cent when the effective confining pressure is 70 kN/m^2 , increasing to 18 per cent for pressures of 500 kN/m^2 i.e. failure is more plastic in mode as pressure increases. Volumetric strains up to 4 per cent at failure are of a similar order to those commonly found with colliery discards.

TABLE 2.8

SHEAR STRENGTH PARAMETERS OF OAKDALE DISCARD

Sample	Peak			Residual*			Figure
	c'_p kN/m ²	ϕ'_p	ϕ'_e	c'_r kN/m ²	ϕ'_r	I_b	
Ex-washery	22.7	30.1	33.3	0.0	24.2	13%	2.35
6-12 months on tip surface	25.8	30.9	34.8	0.0	27.6	12%	2.36

* Apparent values only. True residual shear strength not attained.

It will be noticed that one sample from the tip that was tested at 70 kN/m^2 , was dilating at failure.

The shear strength parameters of the samples are given in Table 2.8. The tip material, with a ϕ'_e of 34.8 degrees, is, in fact, stronger than the washery discard which has a ϕ'_e of only 33.3 degrees. These values lie in the middle of the range of shear strengths applicable to colliery discards.

2.4.4.2. Residual Shear Strength

The large strain shear-box tests failed to reach the true residual shear strength. After some 2.2m displacement the tests had to be terminated due to excessive sample loss through the split in the box. An unloading cycle was performed, and the shear strength parameters derived from these are reported in Table 2.8. It can be seen that, although a strength reduction of around 20 per cent has occurred, shear strengths still fall close to the lower strength boundary for the peak strengths of colliery spoils.

The behaviour of both samples under large shear displacements is similar (Figures 2.37 and 2.38). The values of I_b (Table 2.8) are both low, at 12 to 13 per cent, i.e. strength reduction is not marked at low normal stresses. The drop in stress ratio (and hence shear strength) is accelerated at the higher normal stress levels.

2.4.5. Discussion of the properties of Oakdale Spoil

The peak shear strengths of these samples from Oakdale provide an exception to the general rules of Taylor (1974b) that organic carbon content is directly related to shear strength and that quartz has no significant influence upon shear strength. With these samples from Oakdale, the more carbonaceous washery materials are weaker than the more quartz-rich tip materials. This state of affairs is probably brought about by the tip containing run-of-mine debris in which the quartz is contained as hard sandstones, whereas in normal colliery discard, the quartz will occur as small sand grains in the shale

fragments and thus will be screened from performing an important role in the peak shear strength properties. It is relevant that Spears and Taylor (1971) note that the shear strength of the parent strata (i.e. the coal measures rocks) are influenced by the quartz content. The parent strata, will, of course contain a much larger proportion of sandstones than do colliery discards, collieries being primarily concerned with the extraction of coal and not sandstone.

With regard to superficial weathering, it is apparent that Oakdale spoil is resistant, both chemically and physically. No mineralogical products of weathering were present in detectable amounts.

It would appear that it is only materials with a high seatearth content such as Gedling, which are liable to severe short-term degradation.

2.5. Burnt colliery spoils

2.5.1 Sampling

The bulk sample of Ireland burnt spoil was provided by the Scientific Department of the National Coal Board. It is understood that it came from near the surface in a part of the tip which had recently been lowered by regrading. The bulk sample of Horden burnt discard was taken from material that had been treated for sale. It had thus been processed by a jaw-crusher and passed through a 76.2mm ring.

2.5.2 Grading

The particle size curves are shown in Figures 2.39 and 2.40. The Ireland red shale (Figure 2.39), is virtually all gravel size. Horden (Figure 2.40) is slightly finer grained, with 20 per cent smaller than 2mm size. Both have an upper limit of 76 mm in size. The particle gradings are thus very similar to many unburnt ex-washery discards. Horden is finer grained than Ireland probably

because of the treatment it received in a jaw-crusher.

2.5.3. Chemistry and Mineralogy

From the chemistry, shown in Table 2.1, the most noticeable difference to unburnt spoils is the lack of organic carbon which has been totally oxidised by ignition processes. The two burnt spoils are themselves different from each other. Since they come from different coalfields (Ireland from the East Pennine Coalfield, and Horden from the Durham Coalfield) this could well be due to original differences in composition.

Mineralogically, both materials show the effect of thorough combustion. All the clay minerals have been destroyed, leaving a mainly amorphous mass behind. Quartz is however present, this mineral being stable at high temperatures. There were also small traces of mullite, a silicate formed at high temperatures under atmospheric pressure. The presence of mullite indicates localised temperatures in the range 950°C to $1,300^{\circ}\text{C}$, this being the range over which it forms (Richardson, 1951). Kaolinite decomposes at 550°C and illite at 700°C , thus background temperatures above these values must have been sustained in the tips. This is by no means unlikely, as temperatures of well over $1,000^{\circ}\text{C}$ have been measured in burning spoil heaps and vitreous glass (analogous to volcanic glass) has been excavated as a plug in the body of a spoil heap (see Figure 2.1, National Coal Board, 1970).

2.5.4. Shear Strength

2.5.4.1 Peak shear strength

The problem of punctured sheaths was considerably more common than when encountered in the Oakdale triaxial tests. Well burnt spoil is exceedingly hard and angular. The material was sharp enough to puncture the sheath upon application of an effective confining pressure in excess of 280 kN/m^2 . Ireland spoil proved

TABLE 2.9
SHEAR STRENGTH PARAMETERS OF BURNT DISCARDS

Sample	Peak			Residual*		Figure
	c'_p kN/m ²	ϕ'_p	ϕ'_e	c'_r kN/m ²	ϕ'_r	
Ireland	58.3	43.0°	47.3°	0.0	38.3°	2.43
Horden	21.1	42.1°	44.2°	n.d.	n.d.	2.44

* Apparent values only. True residual shear strength not attained.

impossible to test at pressures over 210 kN/m^2 .

Ireland spoil exhibited a brittle mode of failure (Figure 2.41) with strains of 4 to 7 per cent at failure. At effective confining pressures of 140 kN/m^2 and below, the material was also dilating at failure. This behaviour is similar to that of the burnt parts of Brancepeth spoil heap (Taylor, 1973a).

In contrast, Horden spoil behaved in a manner more typical of unburnt spoils, with failure strains increasing from 11 to 20 per cent as effective confining pressure increases. At a confining pressure of 280 kN/m^2 , a plastic mode of failure was apparent. Volumetric strains were negative and large, reaching over 5 per cent at failure for the sample tested at 280 kN/m^2 effective confining pressure.

Considering the shear strength parameters (Table 2.9), it is apparent that the Ireland burnt spoil is stronger than Horden. Both are considerably stronger than the strongest unburnt discards, and also stronger than the partly burnt material from Brancepeth.

Both failure envelopes may well be curved. The cohesion intercept of the Horden material has a 95 per cent probability (i.e. probably significant) of being real if the failure envelope is assumed to be linear (see Chapter 3.2.1). If the presence of cohesion in an aggregate which is predominantly gravel size is not considered acceptable, then it follows that there is a 95 per cent probability that Horden has a curved failure envelope. In the case of the Ireland material, the limited number of successful tests makes it impossible to be certain of the degree of curvature. A test at 280 kN/m^2 effective confining pressure, gave a deviator stress of the same order as that obtained at 210 kN/m^2 . This would suggest an extreme amount of curvature. However, examination of the test records revealed that the volumetric strain in this test

has been exceedingly large, 8.5 per cent, and, furthermore, after 6 per cent linear strain, it increased at a constant rate until failure occurred at 16 per cent linear strain. From this, it was apparent that the rubber membrane had punctured, so the results from this test were discarded.

2.5.4.2. Residual strength

A large strain shear-box test was performed on the Ireland burnt spoil. It could not be carried to completion (i.e. true residual) due to excessive loss of sample through the gap between the two halves of the shear-box. This gap was forced open to such an extent that material of up to 20mm diameter could escape. From the stress ratio-displacement curve (Figure 2.45), it is apparent that appreciable breakdown only occurs at normal stresses above 240 kN/m^2 . It can also be seen that even after 1m displacement, the shear strength is still high. It is 38.3° (Figure 2.43 and Table 2.9), which is stronger than many unburnt spoils, although some 9 degrees lower than the peak ϕ'_e value of 47.3 degrees. However, because of the large amount of sample loss, this value of apparent residual and the shearing displacement required to reach it is probably meaningless. After this experience with Ireland material, a large strain shear test was not attempted with Horden material.

2.5.5. Discussion of properties of burnt colliery spoil

It is apparent that burnt colliery spoils are considerably stronger than unburnt ones, as was indicated by Taylor's (1973a) results from Brancepeth (also National Coal Board, 1970). Furthermore, both fully burnt shales tested were stronger than the partly burnt Brancepeth material. The burnt material was predominantly amorphous and its strength must be dependant upon different factors than unburnt spoils. The most obvious difference is, of course, the lack of dependance upon organic carbon content, except in so far as a high carbon content in the original spoil would be conducive

to total combustion. The high temperatures deduced from the mineralogy of these samples suggests that the fragmented material must have been nearing fusion.

2.6. Weathering effects upon shear strength of coarse colliery discards:- conclusions

2.6.1 Unburnt discards

In terms of physical strength, spoils of low seatearth content are resistant to short-term weathering, provided that they are well compacted. Material from South Wales (i.e. Oakdale) is resistant to mineralogical alteration for a period of at least 6-12 months. Material from the north-eastern part of the Yorkshire coal-field (i.e. Kellingley) does show a slight amount of mineralogical change in a 6 year period in the zone above the water table (this is the shale blanket material). The same material when maintained under full saturation, is, however resistant to mineralogical change. When unsaturated and uncompactd, it is prone to both physical and mineralogical degradation.

Considering that seatearths degrade more readily than roof rocks (Lawrence, 1972), it might be expected that a spoil containing large quantities of seatearth would be more prone to weathering than one which does not. Gedling spoil, which contains at least 50 per cent of seatearth does indeed show a severe decrease in physical strength upon exposure for 6-12 months. It does not show any noticeable mineralogical changes, however. A considerable quantity of degradation of this material occurs when it is emplaced on the tip (McKechnie Thomson and Rodin, 1972). However, the grading of the superficial material is finer than that obtained from the body of the tip, thus indicating further breakdown. This superficial material is considerably weaker than any material from the body of the tip. It may however, contain sufficient clay size fraction to provide a measurable cohesion. The degradation occurring during

emplacement adversely effects the shear strength, since the tip material is noticeably weaker than the ex-washery material.

From the foregoing, it is apparent that the type of spoil produced determines whether or not there will be a weathering problem with compacted spoils, i.e. high proportions of seatearth produce a spoil prone to rapid degradation. Ideally it would be desirable to limit the output of seatearth as much as possible. However, this is not strictly feasible since it is the weak seatearths which pose problems in terms of settlement of mining machinery. Consequently they are extracted and disposed of on the tip. In tips where this material occurs, the presence of potentially weak layers should be taken into account in the design of the tip.

From the mineralogical standpoint weathering is obviously slow in compacted spoil. The only samples to show pronounced alteration came from Kellingley and were over 6 years old. Both of these samples were also in a location where they would be subject to alternate wetting and drying from periodic fluctuations in the water table as well as being close to the surface. The 6 year old compacted (shale blanket) material showed much less alteration, both physically and mineralogically than the 8 year old, uncompacted (Lagoon D embankment) material. The mineralogical alteration suffered by this 8 year old material apparently caused a drop in residual shear strength as well. As shown in Chapter 3.3.1. the residual strengths obtained in a 60mm x 60mm shear-box are not reliable at normal stresses less than $300-400 \text{ kN/m}^2$. While the $0.3\text{m} \times 0.3\text{m}$ shear-box tests were run at normal pressures higher than these (up to 528 kN/m^2) there is no reason to suppose that the characteristics of the two sizes of shear-box are similar*. It can be said

* (see footnote on next page)

however, that the weathered material reaches residual far more readily than does the unweathered material. There is thus a possible difference in behaviour of mineralogically weathered to physically weathered materials, in that there was little difference in residual shear strength behaviour with the Gedling materials.

2.6.2 Burnt Discards

Where weathering (oxidation) and coal content was sufficient to cause a spoil heap to catch fire, the resulting burnt spoil is considerably stronger, in contrast to unburnt weathered spoil which is very much weaker than unweathered material. From the limited data available, it would appear that fully burnt spoils, such as Ireland and Horden are stronger than partly burnt ones such as Brancepeth. Localised temperatures possibly up to $1,300^{\circ}\text{C}$ may have occurred, sufficient to cause fusion. The bulk of the discard fragments are composed of amorphous matter. The chemical changes have produced a complete breakdown of the original minerals.

Burnt discards are also more resistant to comminution under large shear displacements than are unburnt types.

* It was not possible to check the normal pressure-residual shear strength relation in the $0.3\text{m} \times 0.3\text{m}$ box in a similar manner to that employed with the $60\text{mm} \times 60\text{mm}$ shear-box because the former can only attain a maximum normal stress of 528 kN/m^2 , which is too low to determine the stress at which true residual is attained with any accuracy.

FIGURE 2.1

GRADING CURVES FOR GEDLING DISCARD, FRESH WASHERY AND 6-12 MONTHS ON TIP MATERIAL

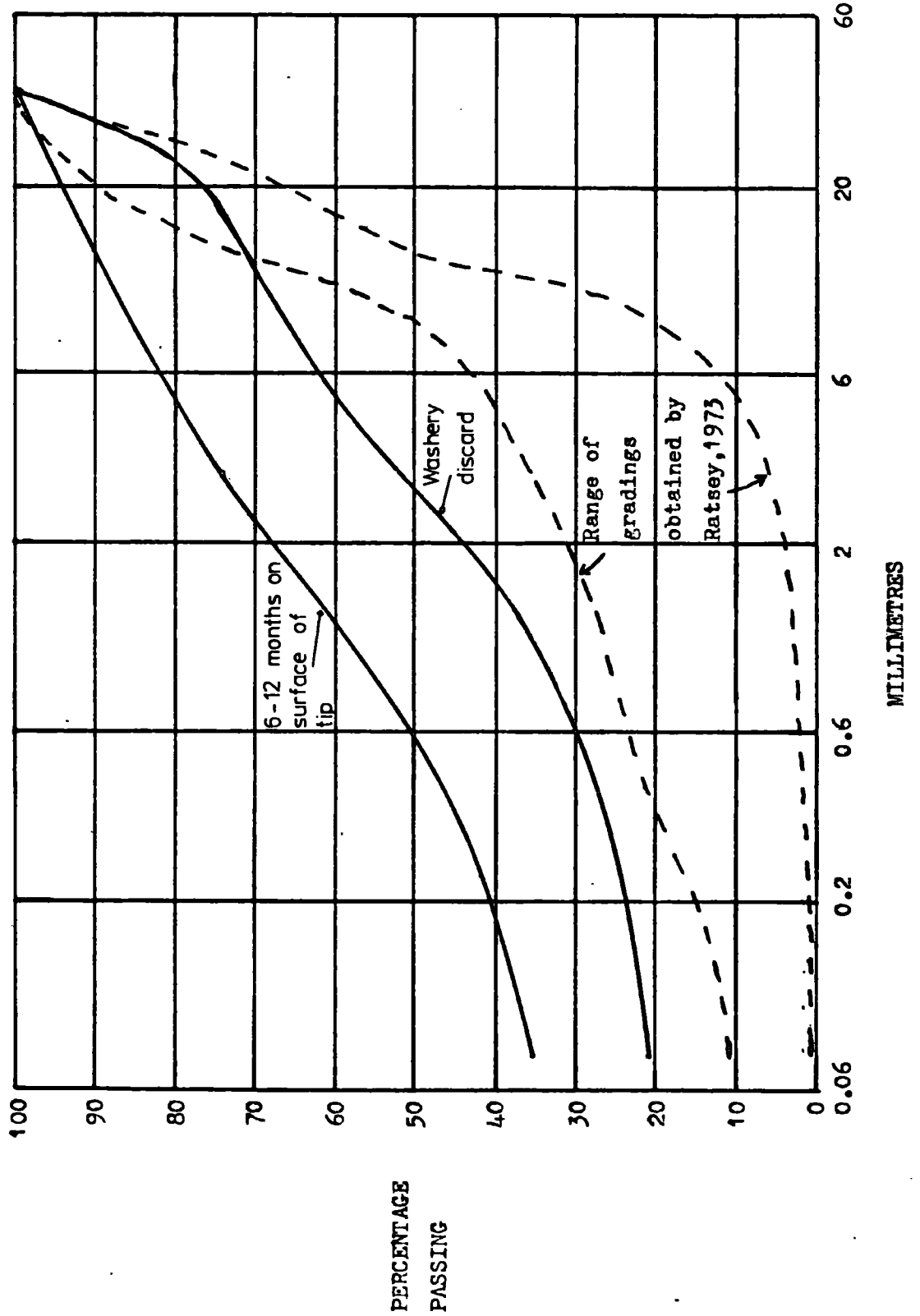


FIGURE 2.2

GRADING CURVES FOR MATERIAL BURIED IN GEDLING TIP FOR 3-6 MONTHS

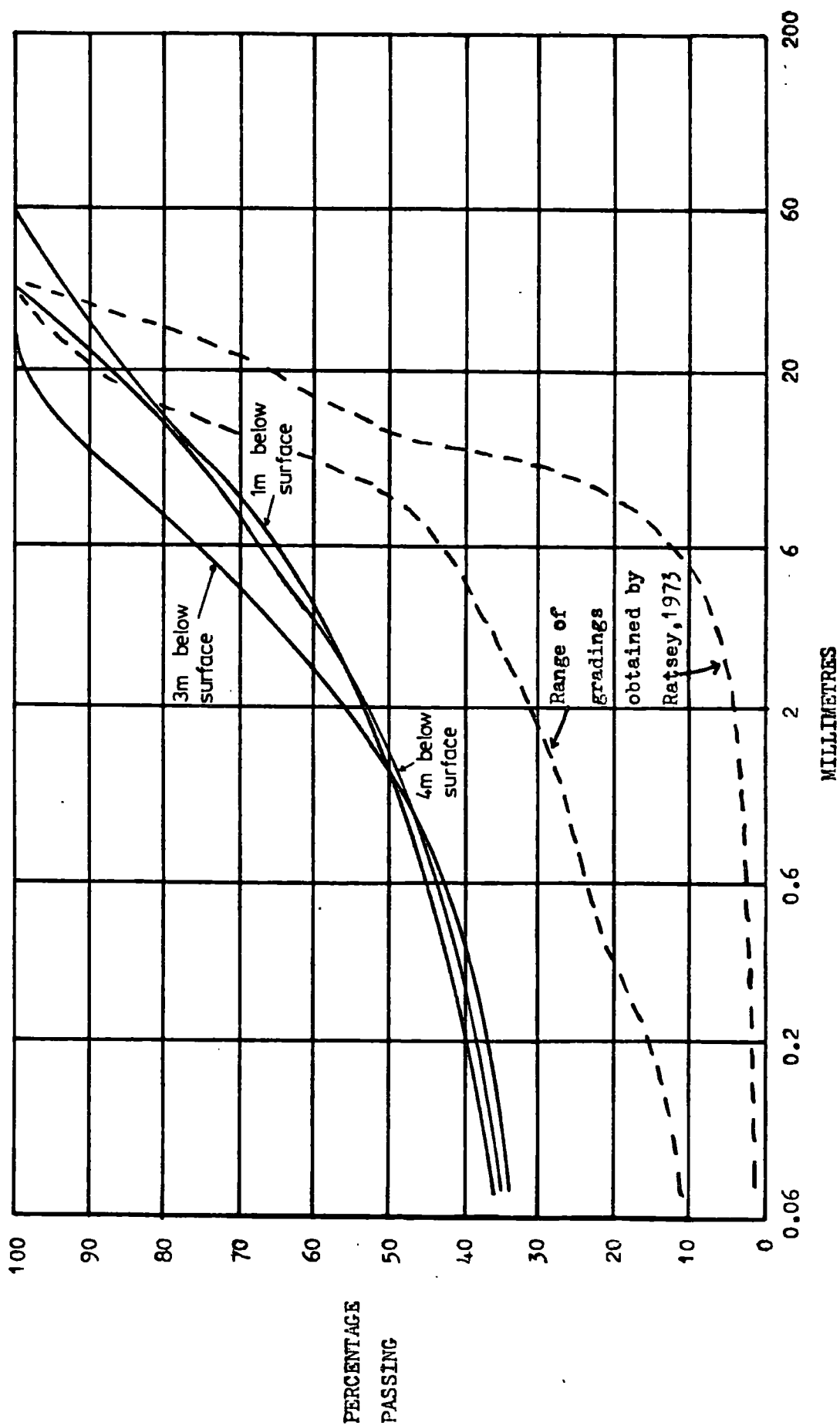
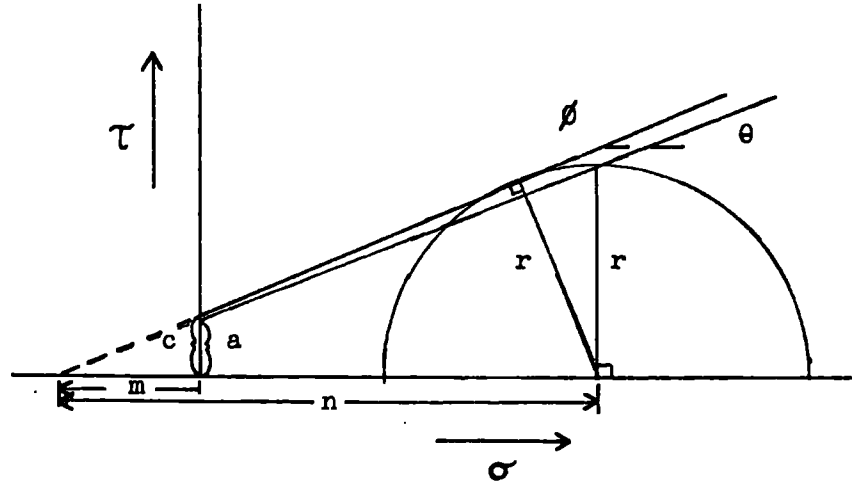


FIGURE 2.3

RELATIONSHIP BETWEEN SHEAR STRENGTH PARAMETERS AND
TOP POINT OF MOHR'S CIRCLES



$$\sin \phi = \frac{r}{h} = \tan \theta$$

$$m = \frac{c}{\tan \phi} = \frac{a}{\tan \theta}$$

$$\therefore c = \frac{a \cdot \tan \phi}{\sin \phi} = \frac{a}{\cos \phi}$$

FIGURE 2.4

GEDLING FRESH WASHERY DISCARD STRESS-STRAIN CURVES

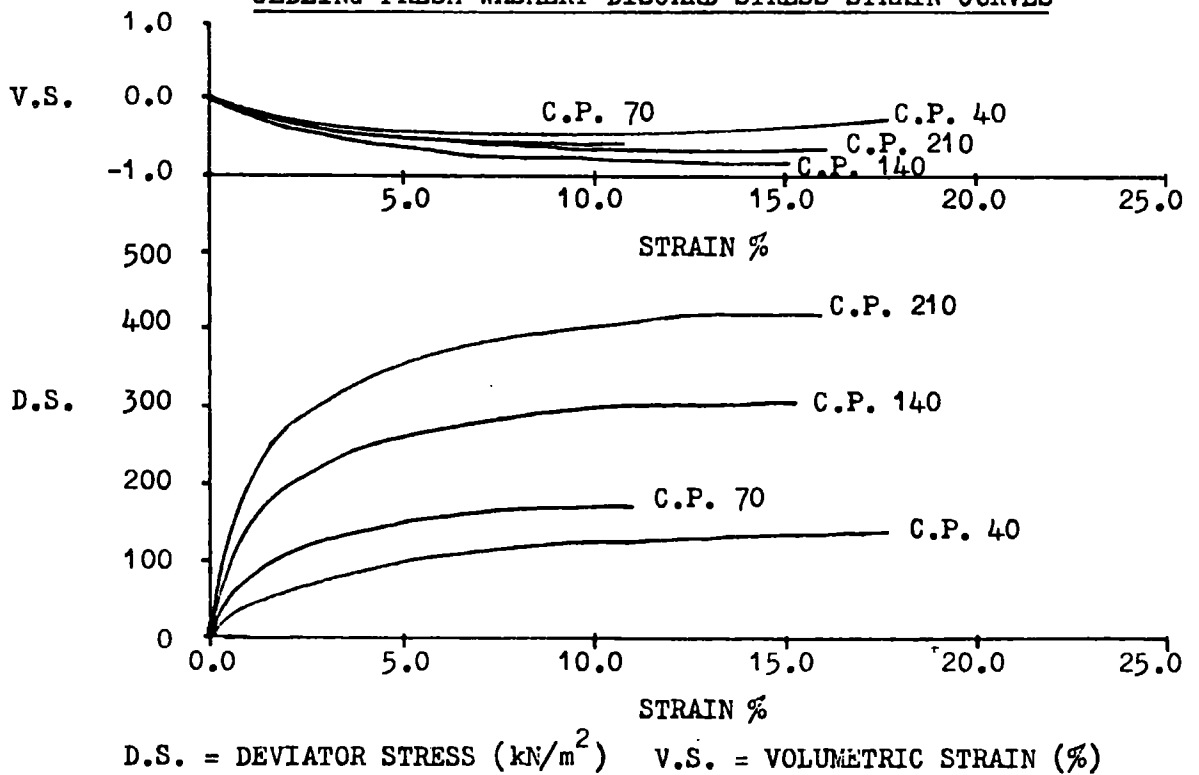


FIGURE 2.5 GEDLING TIP-U100

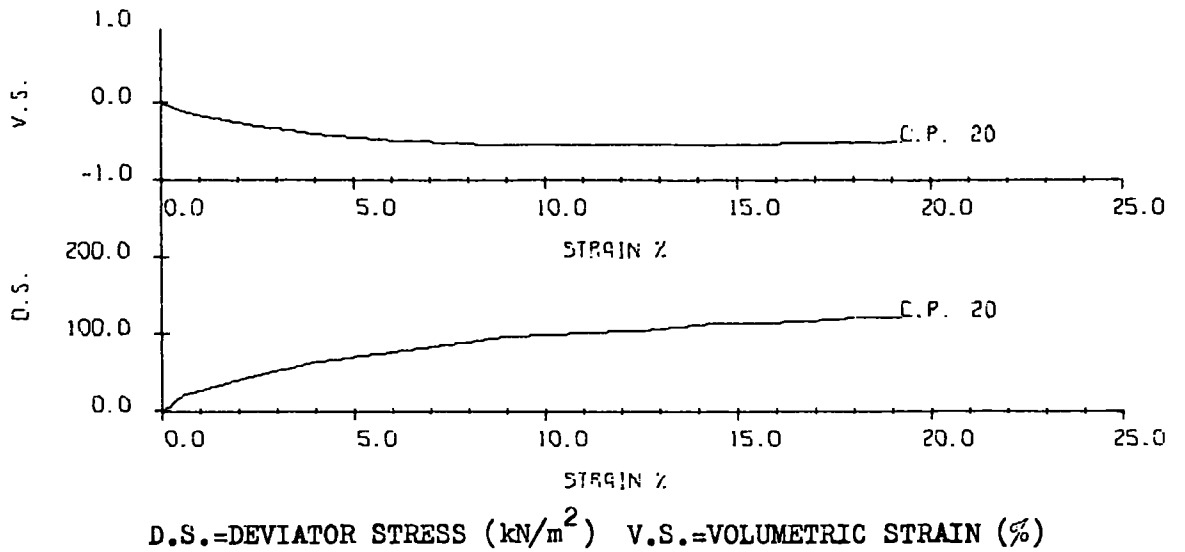
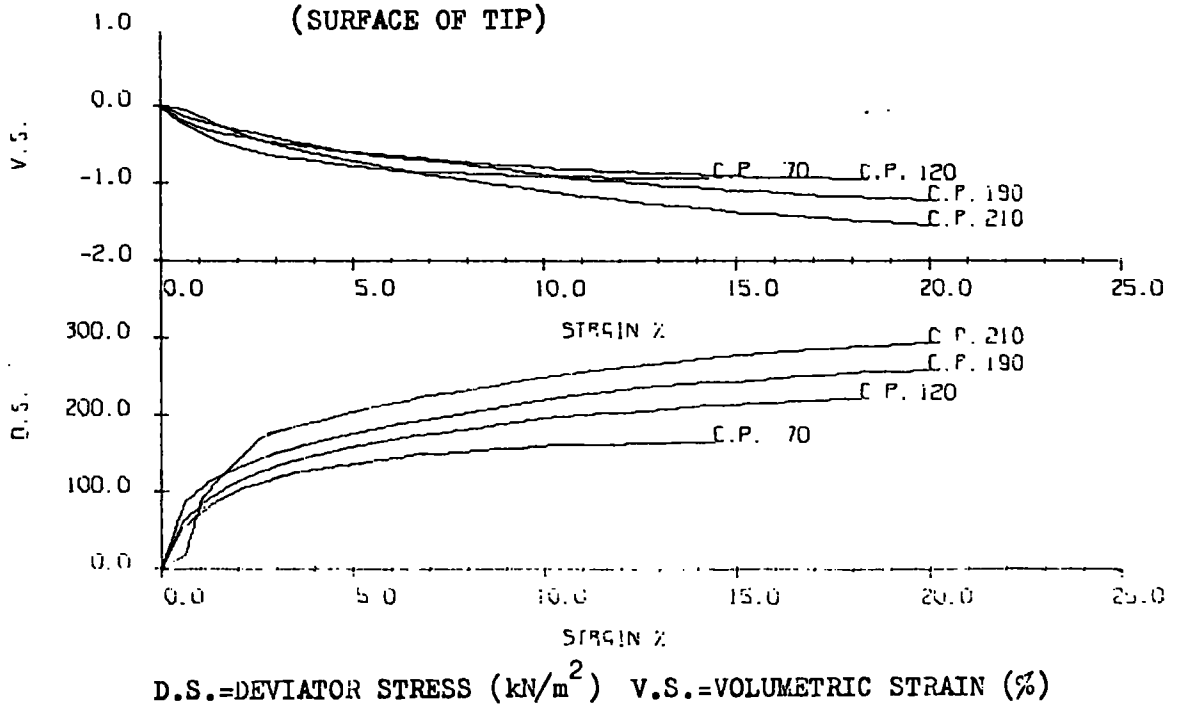
FIGURE 2.6 GEDLING-6 TO 12 MONTHS OLD
(SURFACE OF TIP)

FIGURE 2.7 GEDLING-3 TO 4 MONTHS OLD.
(1m BELOW SURFACE OF TIP)

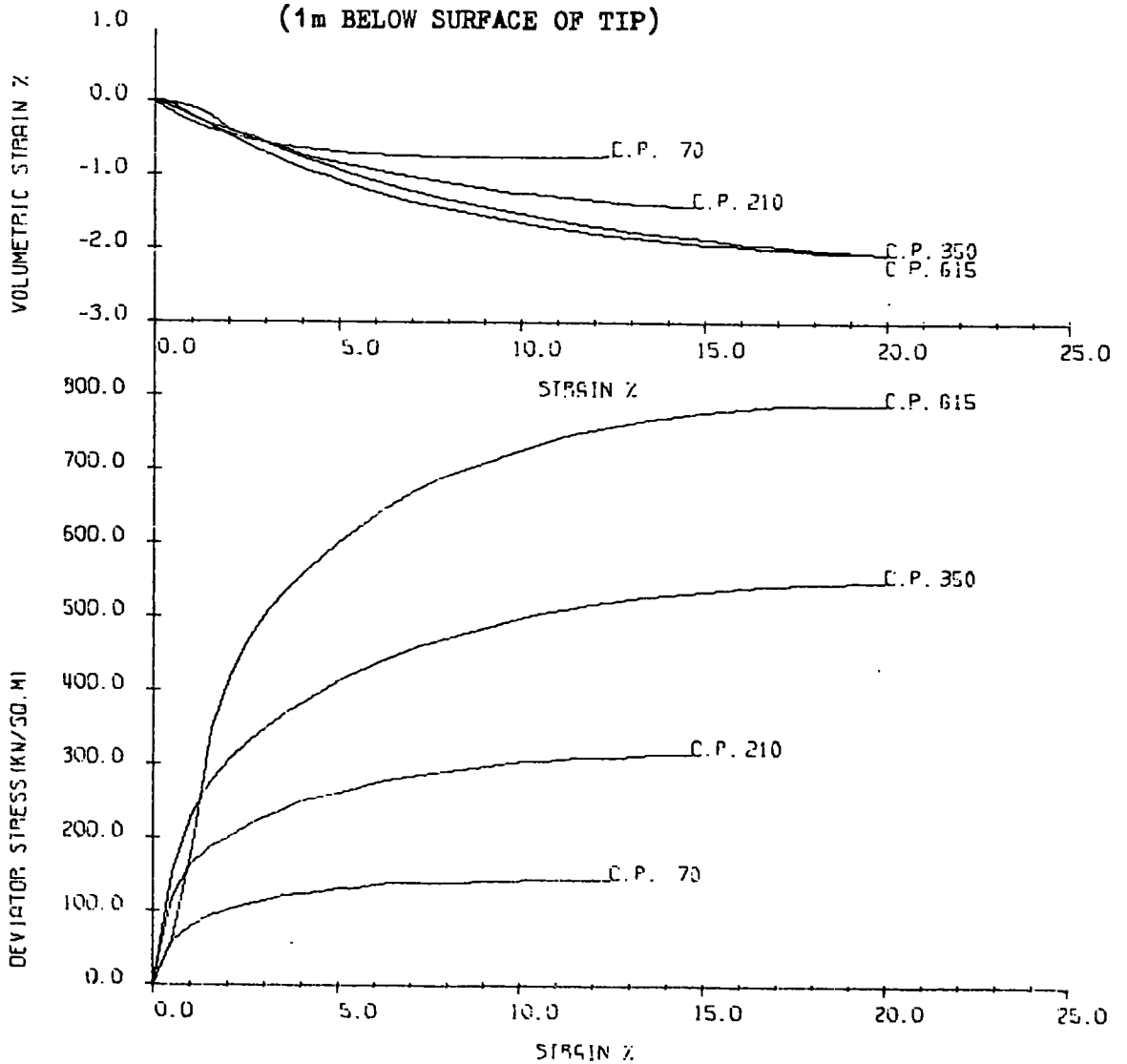


FIGURE 2.8 GEDLING-3 TO 4 MONTHS OLD,
(3m BELOW SURFACE OF TIP)

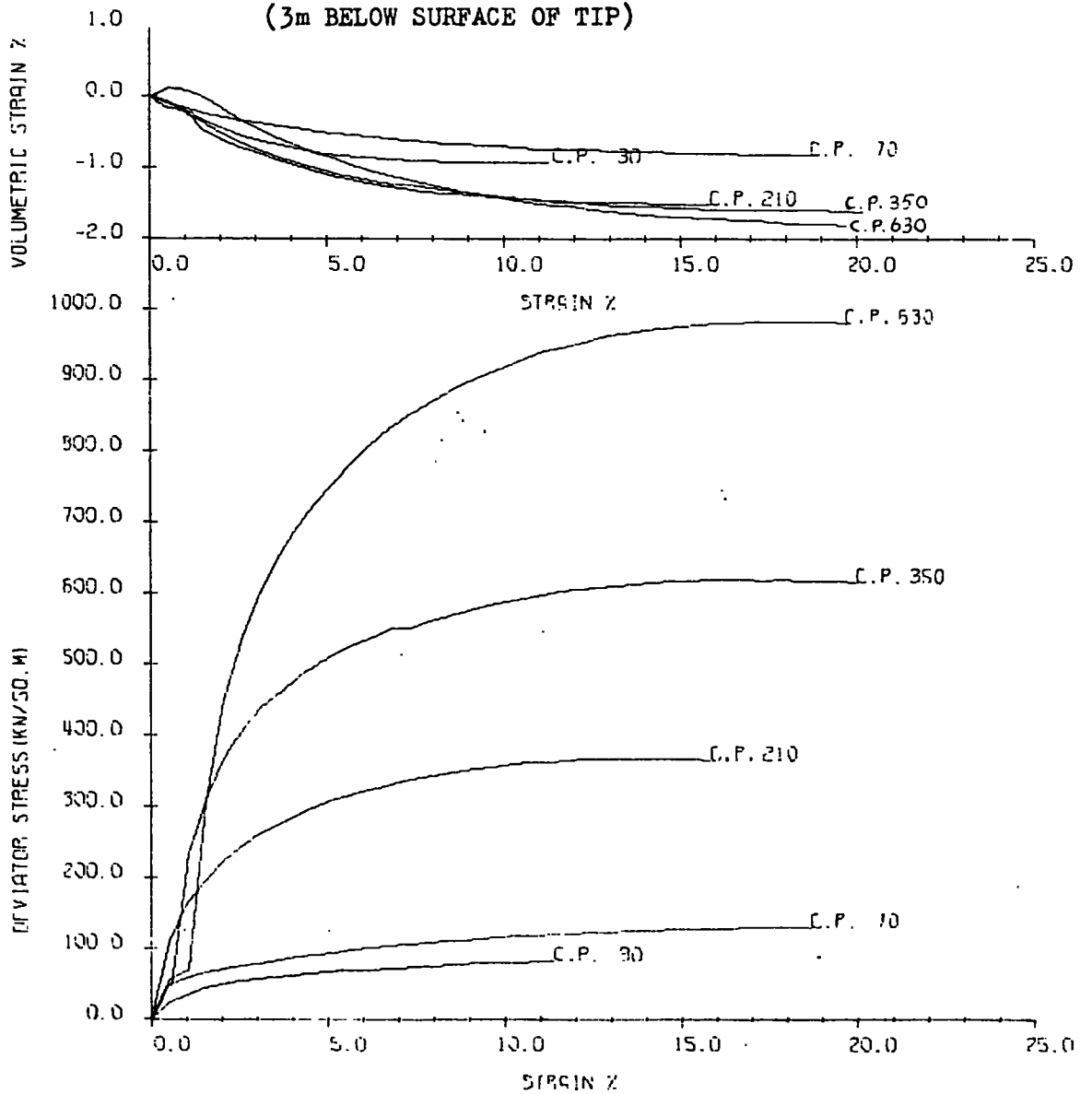


FIGURE 2.9 GEDLING-3 TO 4 MONTHS OLD,
(4m BELOW SURFACE OF TIP)

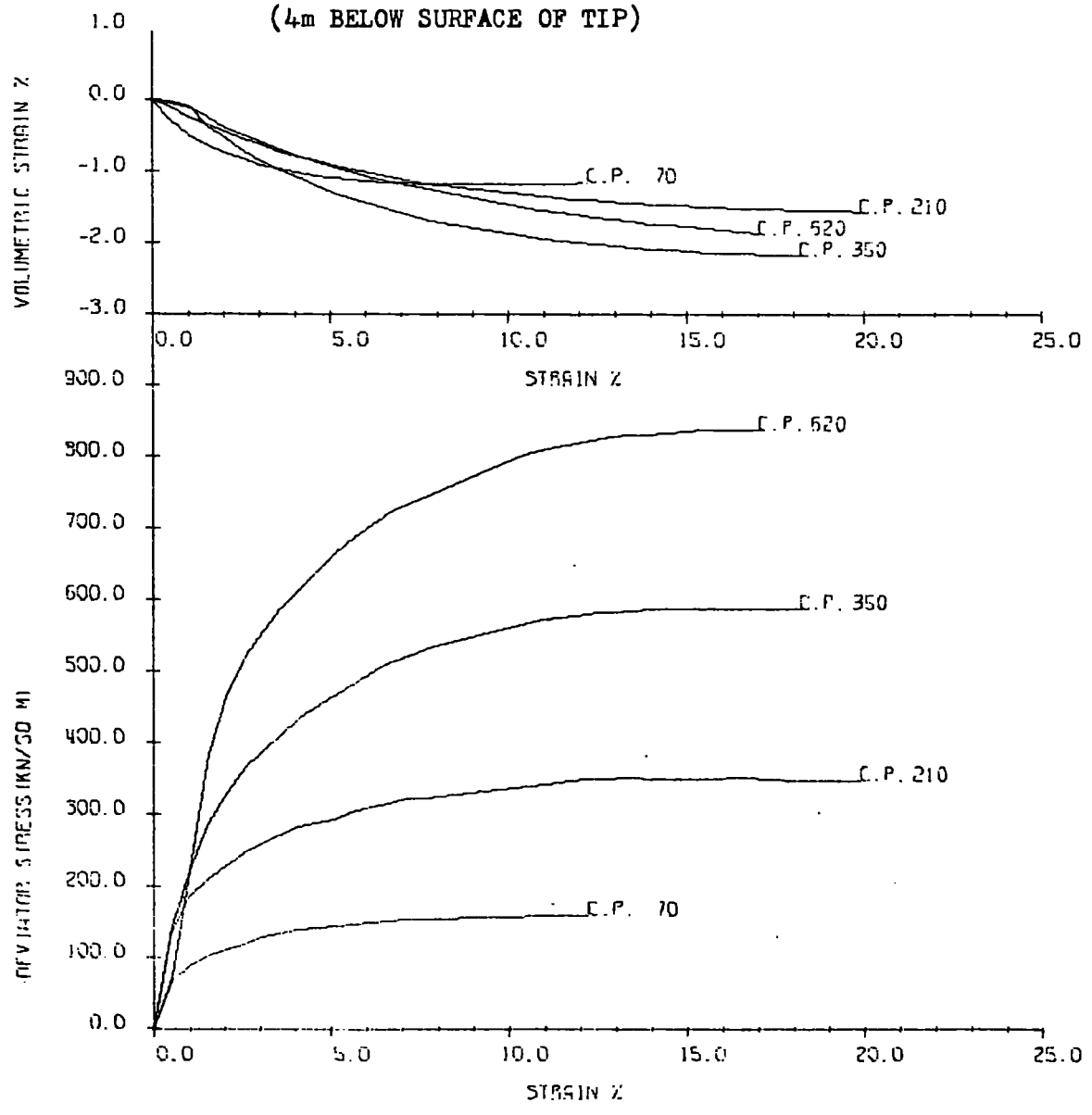
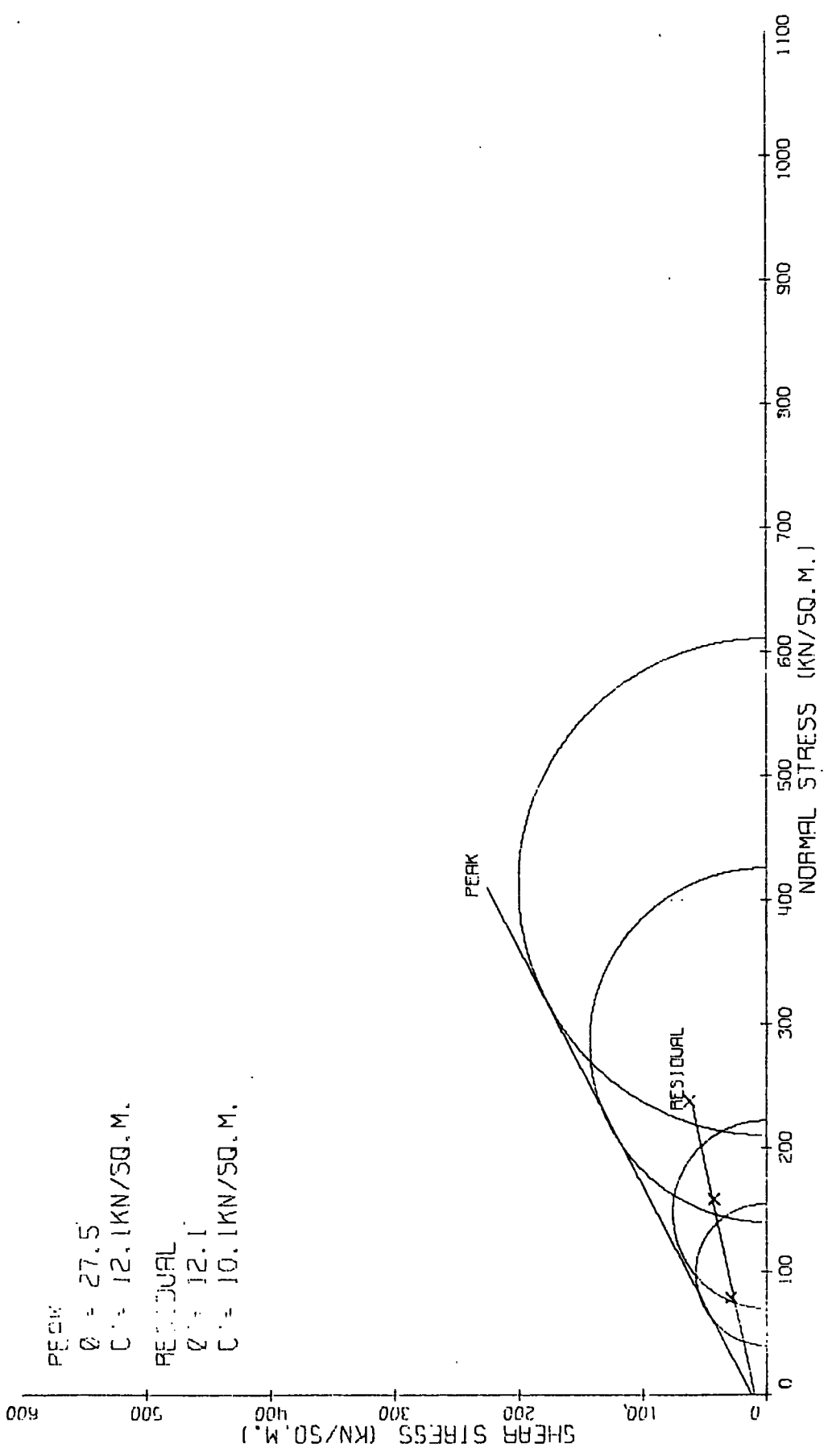


FIGURE 2.10 GEDLING--FRESH WASHERY DISCARD



PEAK
 $\phi = 27.5$
 $c = 12.1 \text{ KN/SQ.M.}$

RESIDUAL
 $\phi = 12.1$
 $c = 10.1 \text{ KN/SQ.M.}$

FIGURE 2.11 GEDLING-6 TO 12 MONTHS ON SURFACE OF TIP

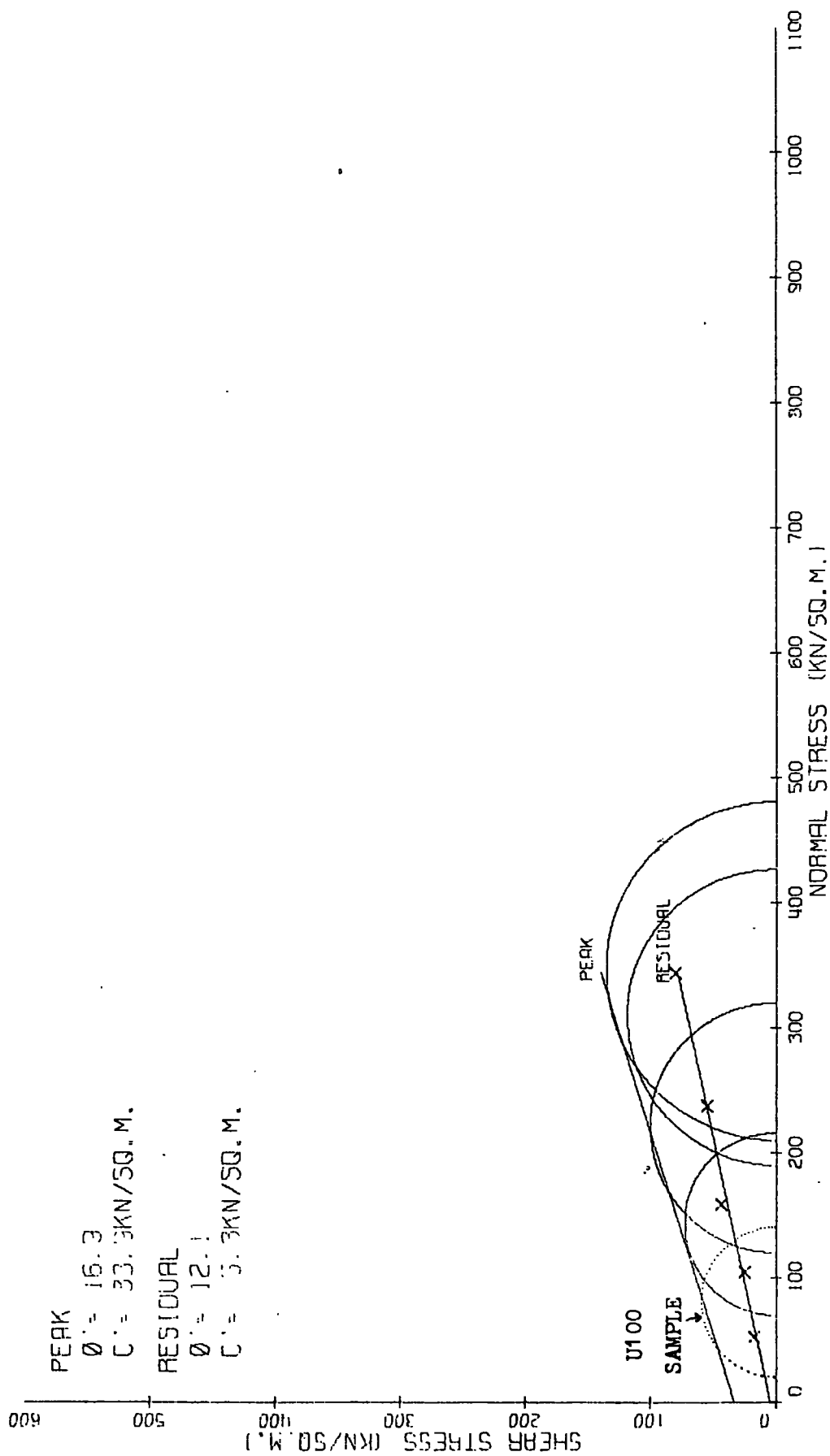


FIGURE 2.12 GEDLING TIP, 3-4 MONTHS OLD, INDIVIDUAL RESULTS

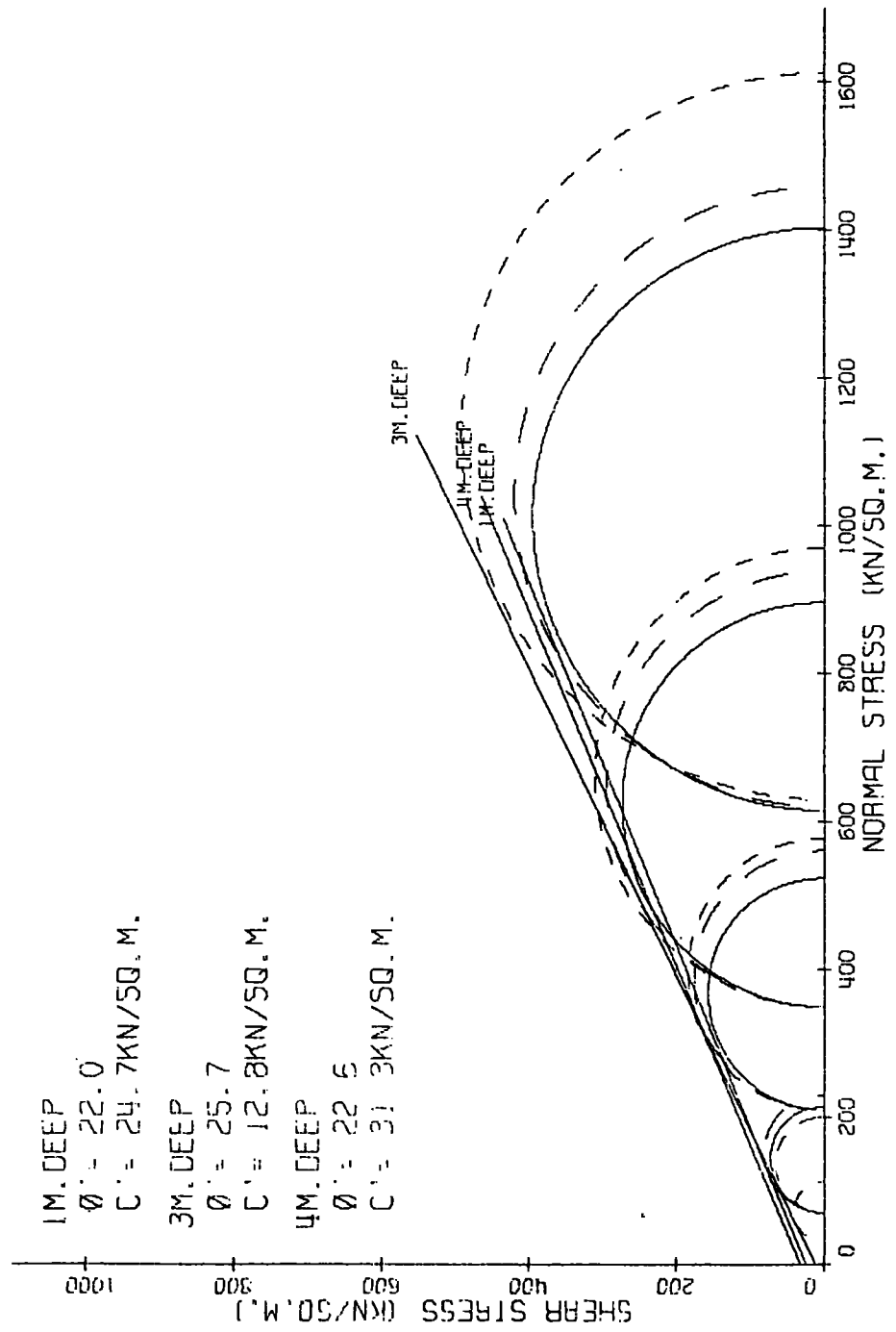


FIGURE 2.13 GEDLING TIP, 3-4 MONTHS OLD, COMPOSITE RESULT

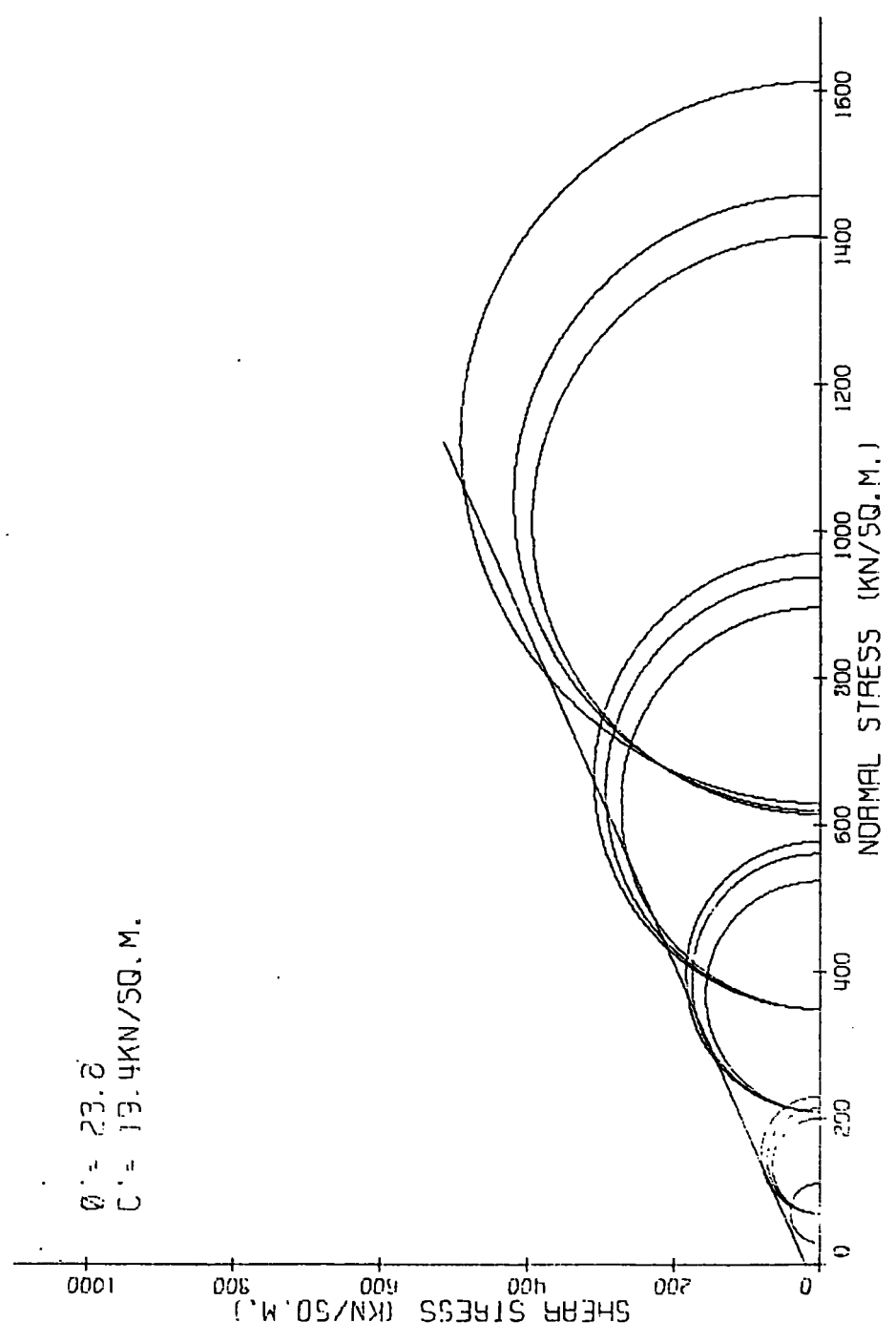


FIGURE 2.14

12 INCH SHEAR BOX TEST

GEDLING DISCARD (EX-WASHERY)

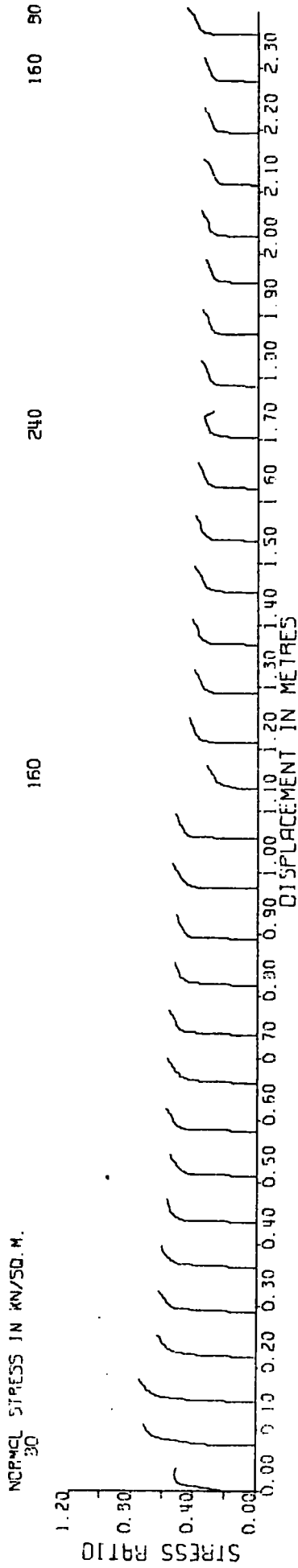


FIGURE 2.15

12 INCH SHEAR BOX TEST

GEDLING DISCARD (6 MONTHS ON TIP)

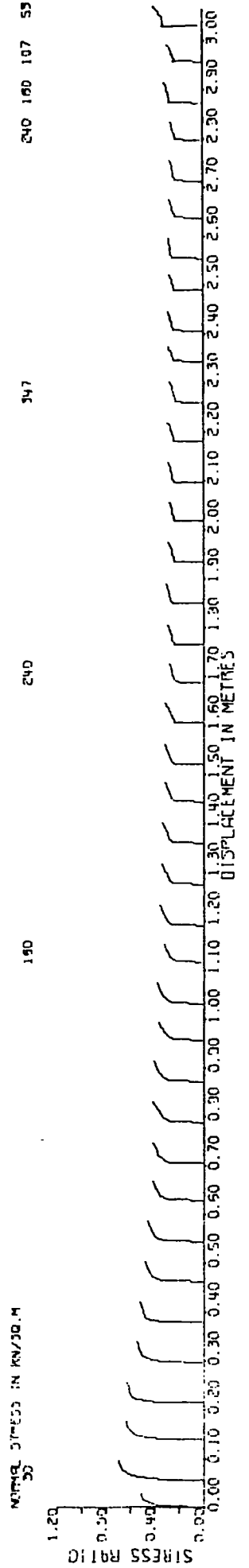
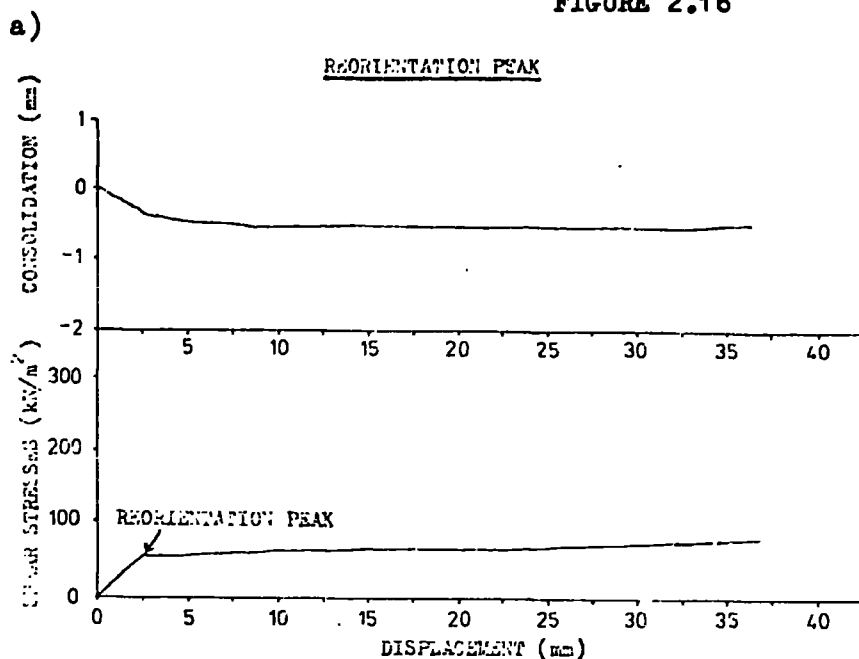


FIGURE 2.16



(b) & (c) redrawn from Figures 15 & 16 in Bishop et al(1971)

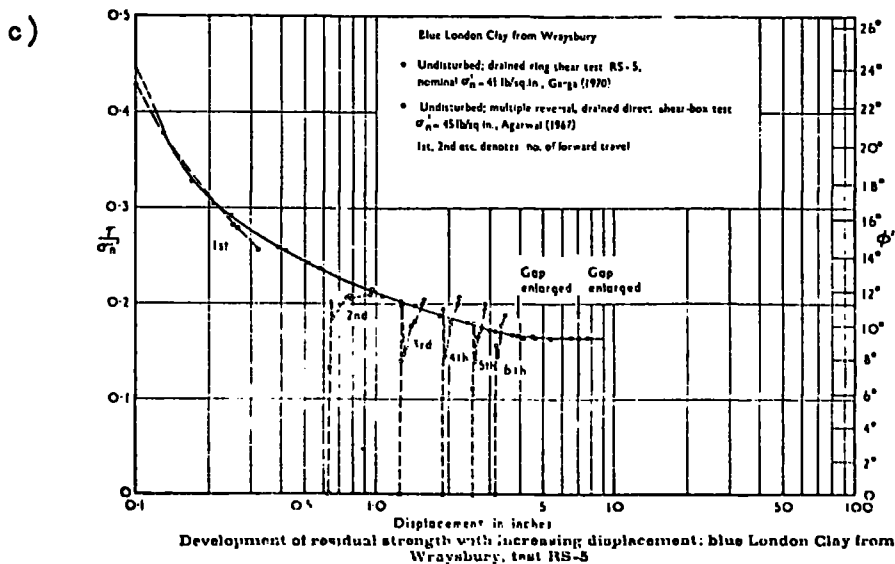
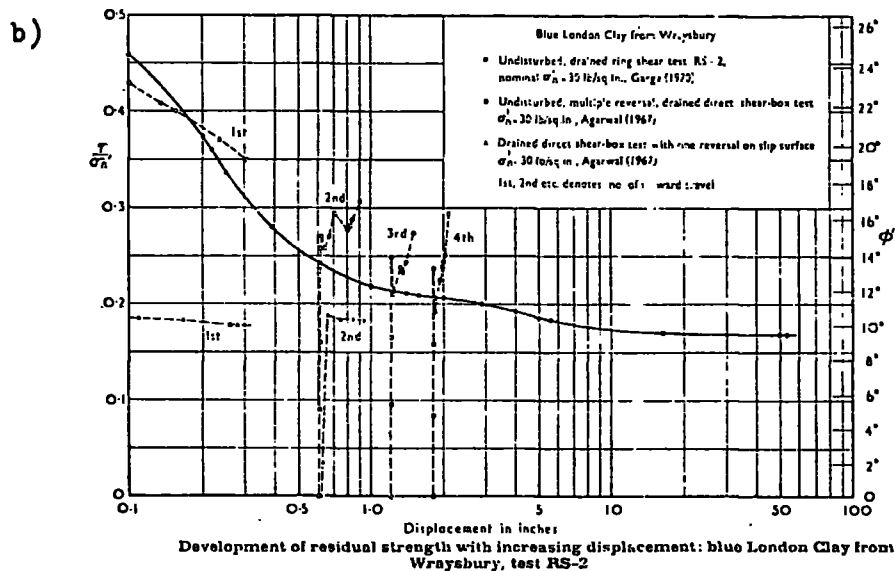


FIGURE 2.17

SLICKENSIDED SHEAR PLANE IN MATERIAL FROM GEDLING TIP
AFTER 3m DISPLACEMENT IN 0.3m x 0.3m SHEAR-BOX

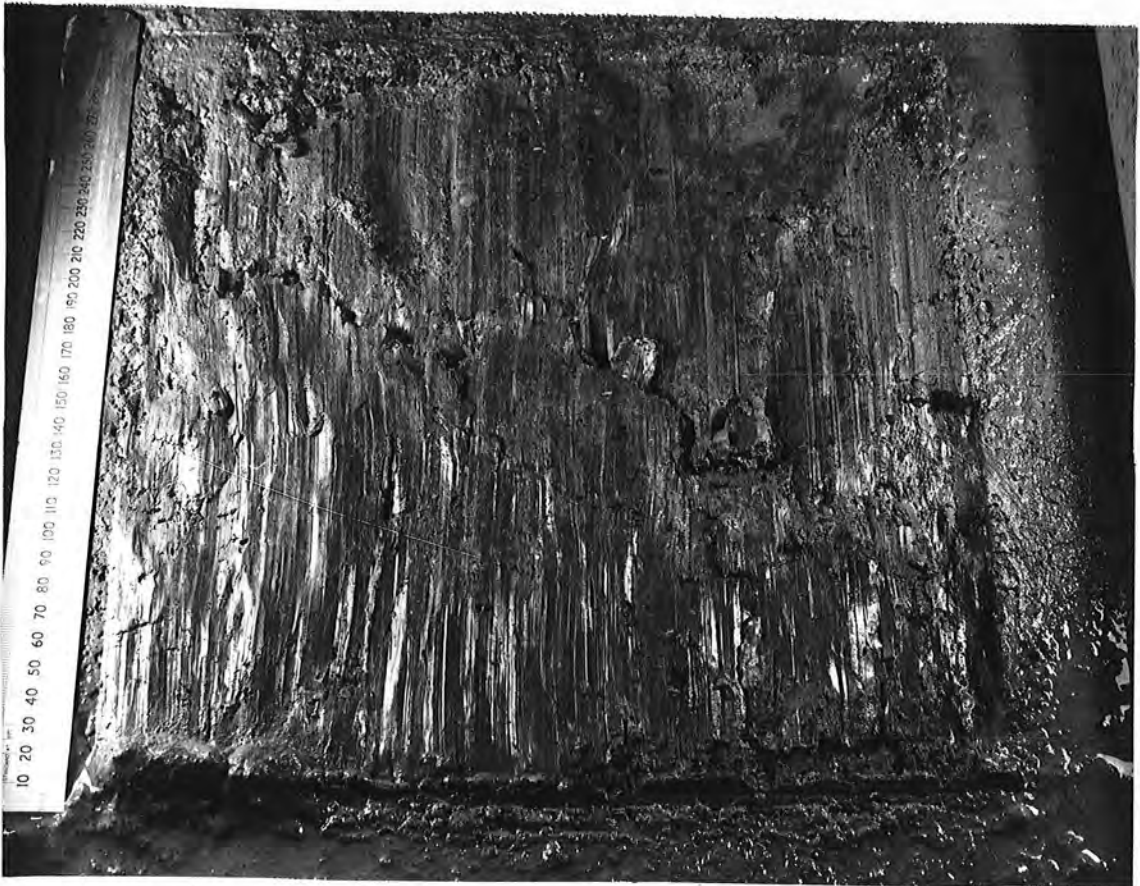


FIGURE 2.18

GRADING CURVES OF KELLINGLEY DISCARD FORMING EMBANKMENTS AT GALE COMMON

P.F.A. DISPOSAL LAGOONS

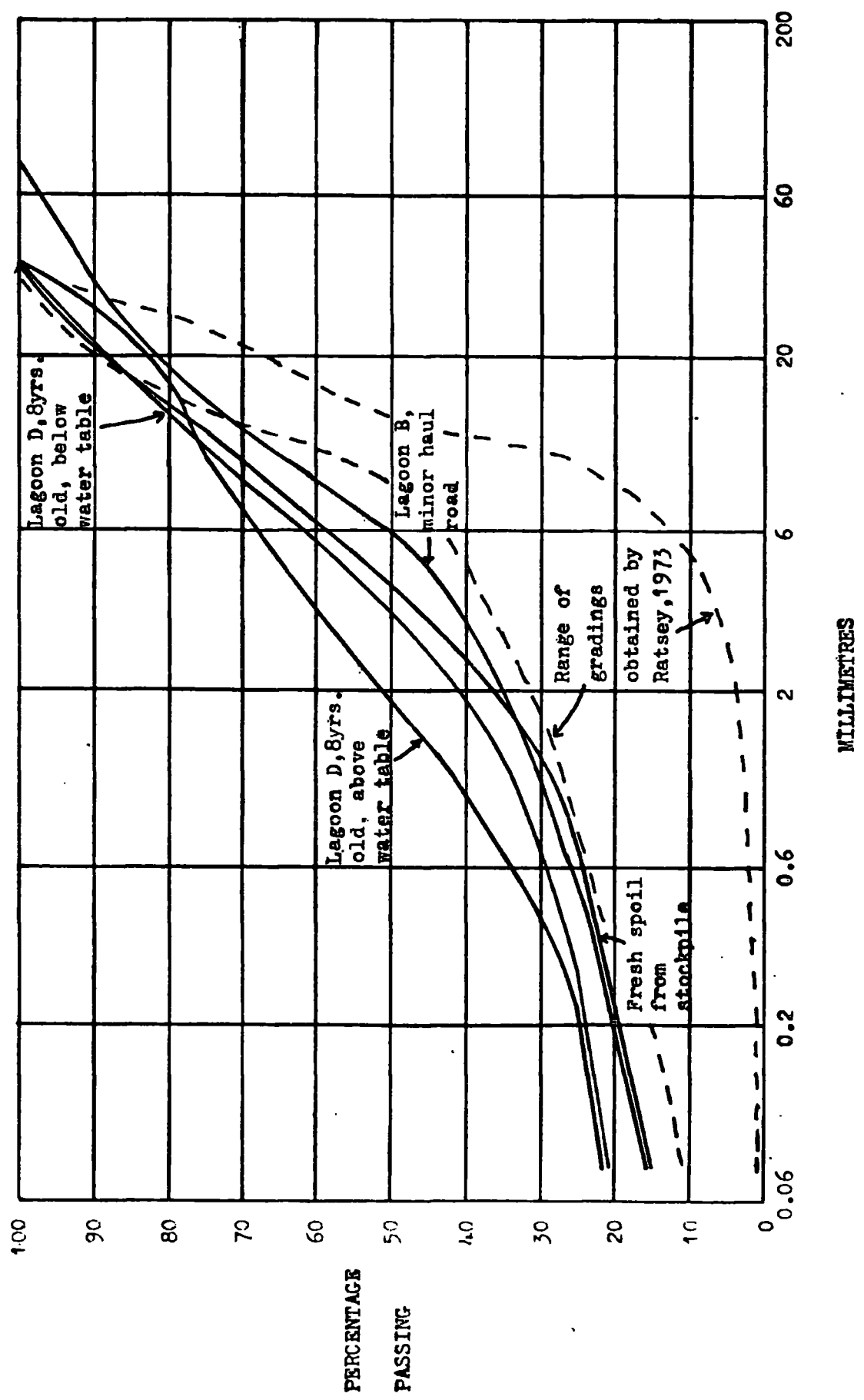


FIGURE 2.19 KELLINGLEY, SPOIL FROM STOCKPILE

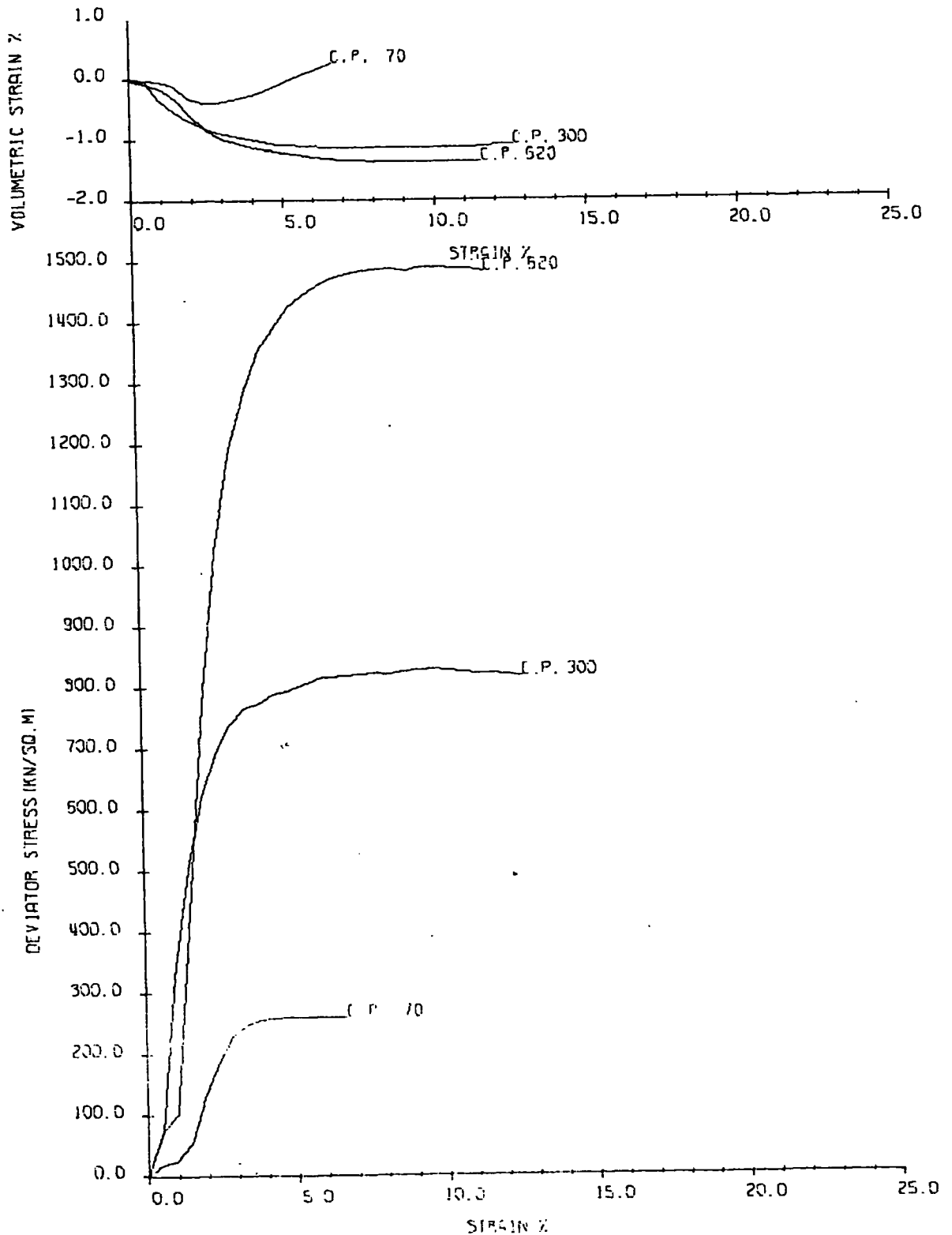


FIGURE 2.20 KELLINGLEY, GALE COMMON SOUTH EMBANKMENT

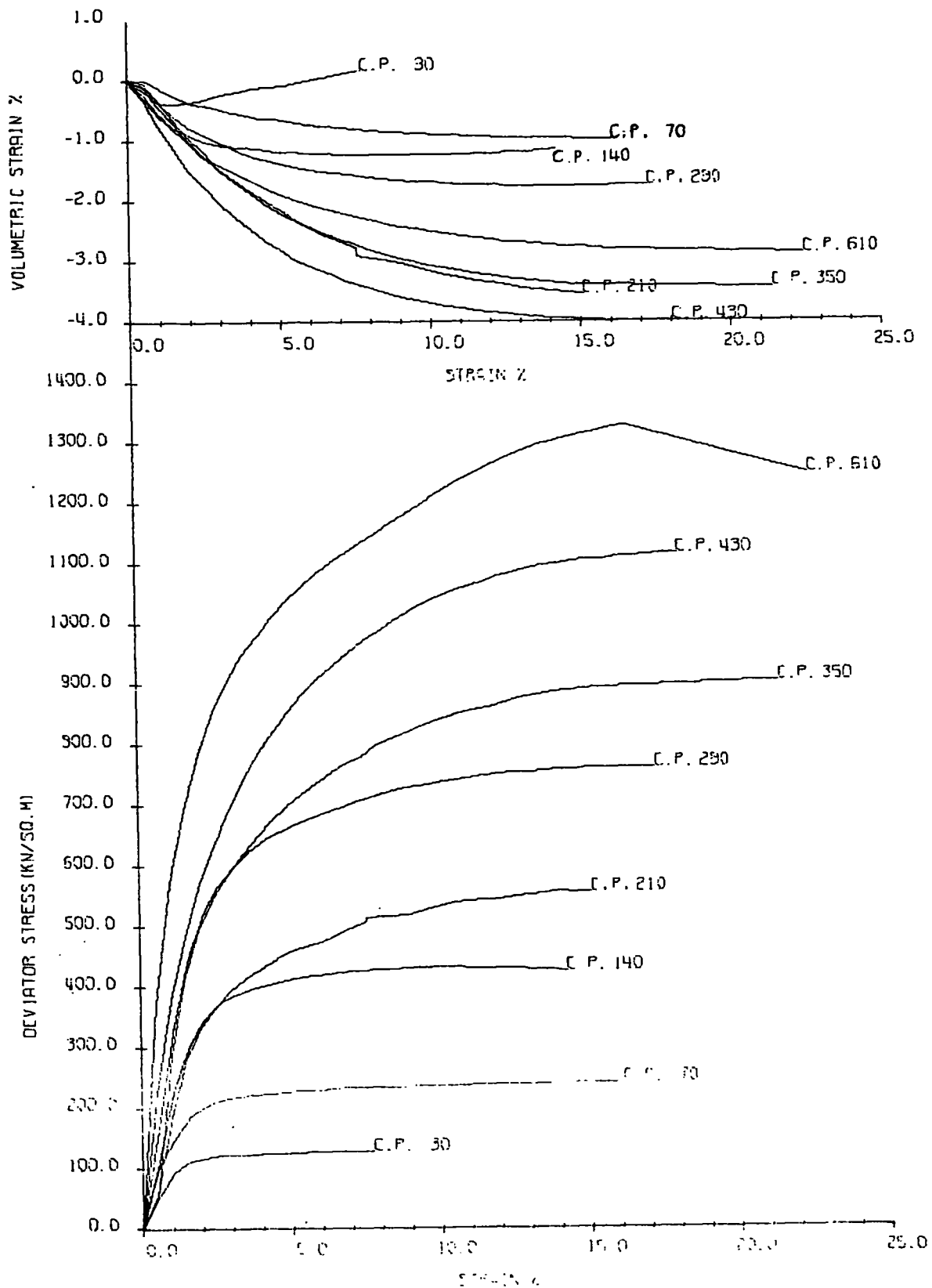


FIGURE 2.21 KELLINGLEY, 6YR. OLD SHALE BLANKET

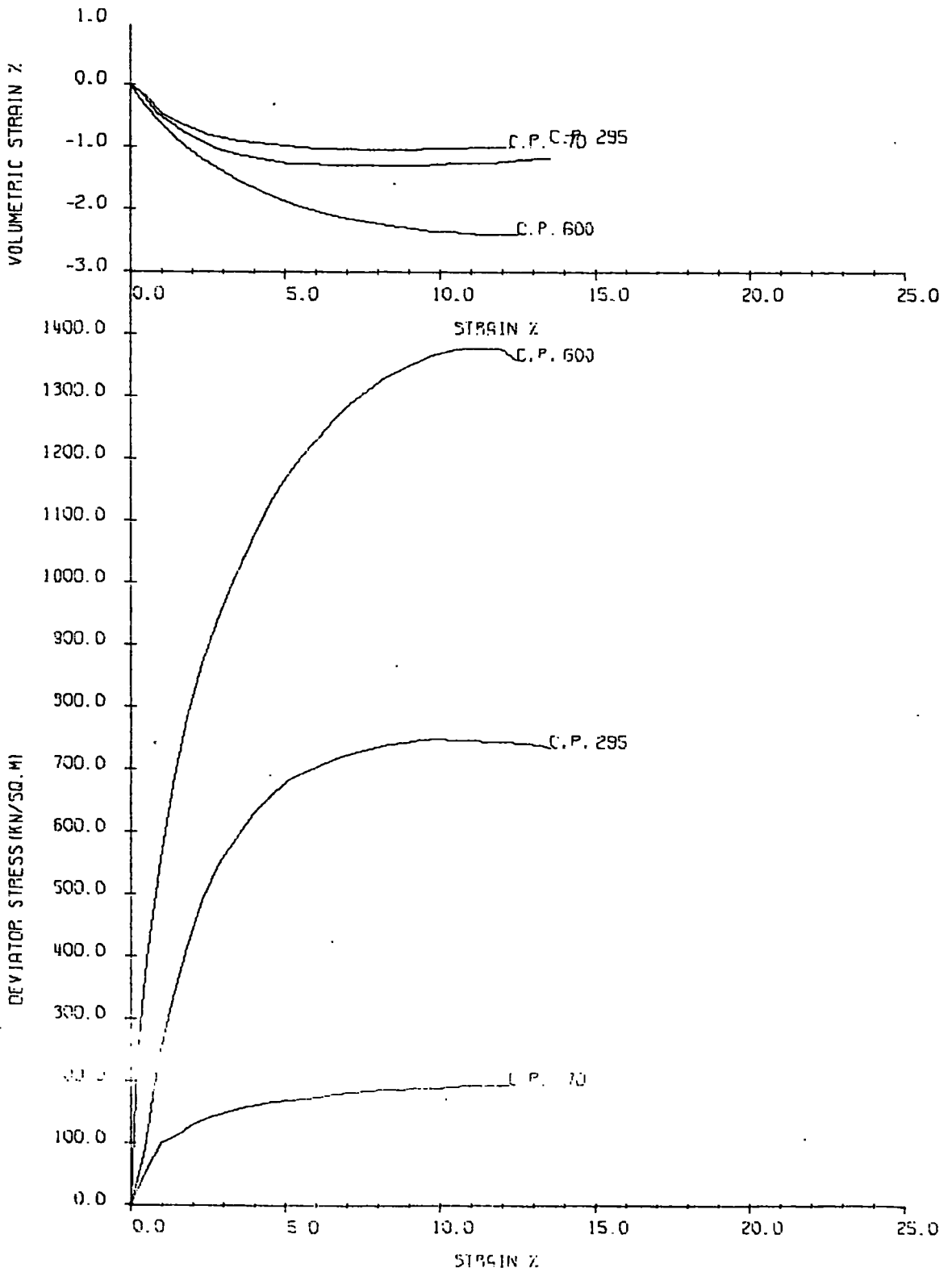


FIGURE 2.22 KELLINGLEY, 8YRS. OLD.
(ABOVE THE WATER TABLE)

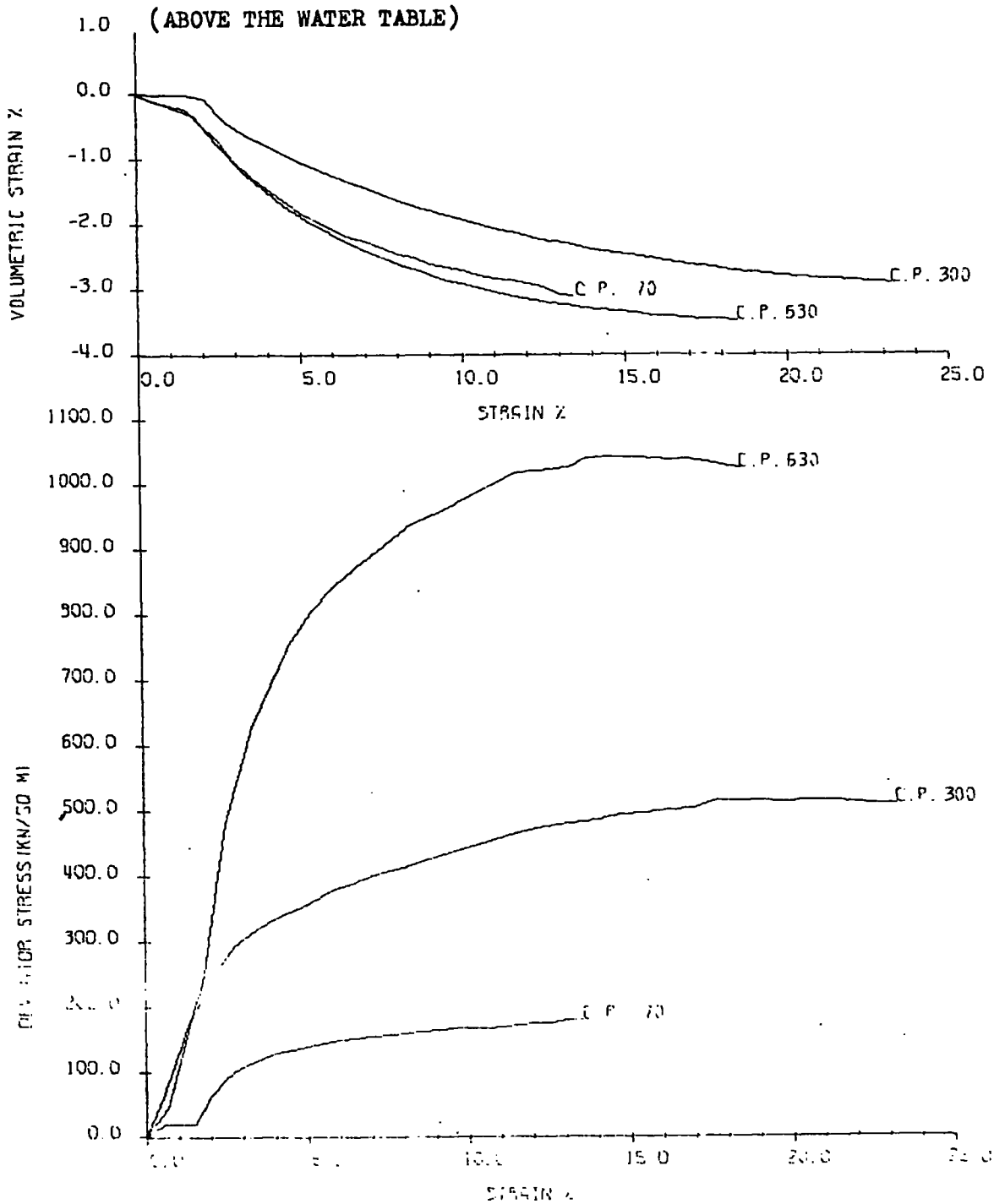


FIGURE 2.23 KELLINGLEY, 8YRS. OLD,

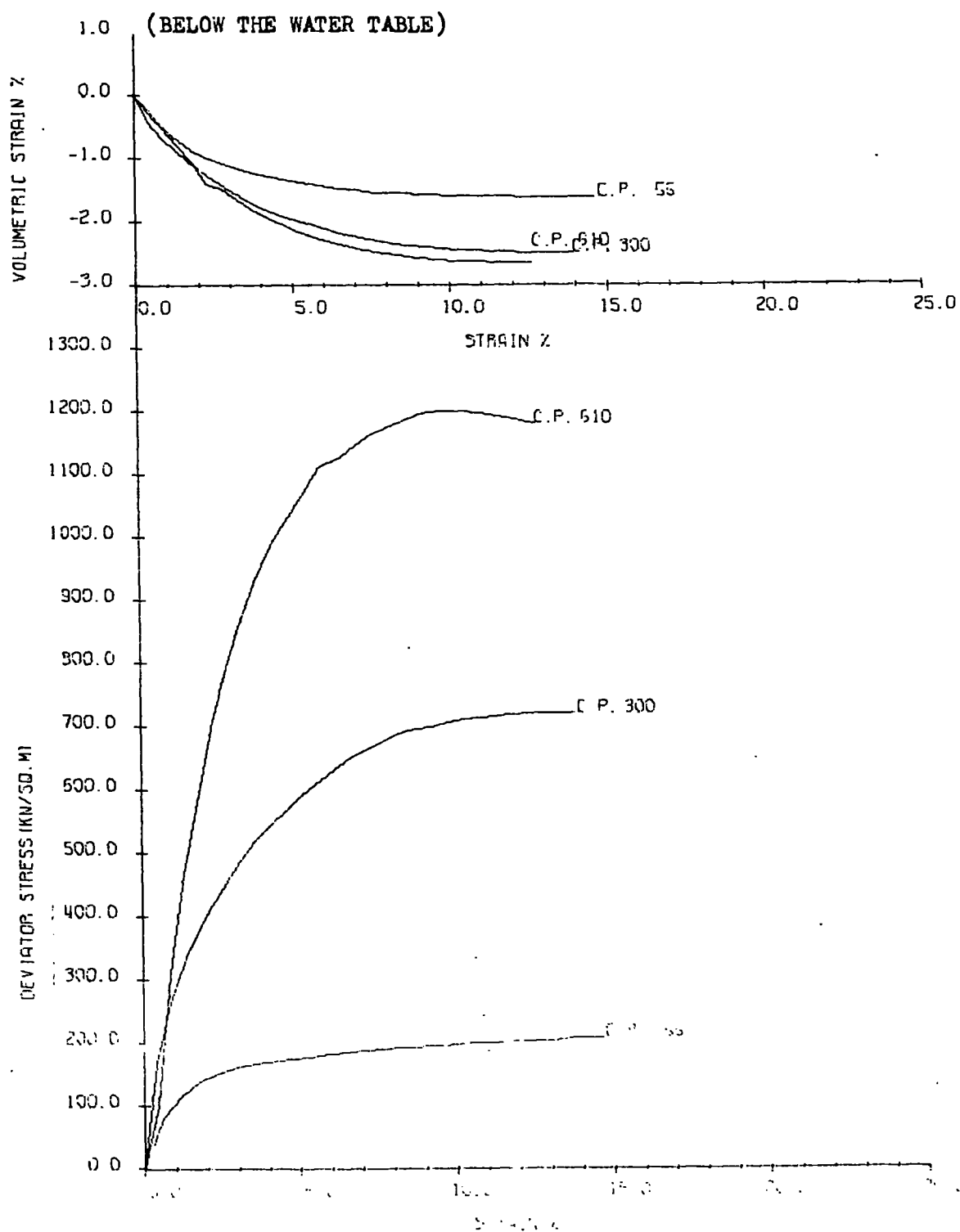


FIGURE 2.24 KELLINGLEY, SPOIL FROM STOCKPILE

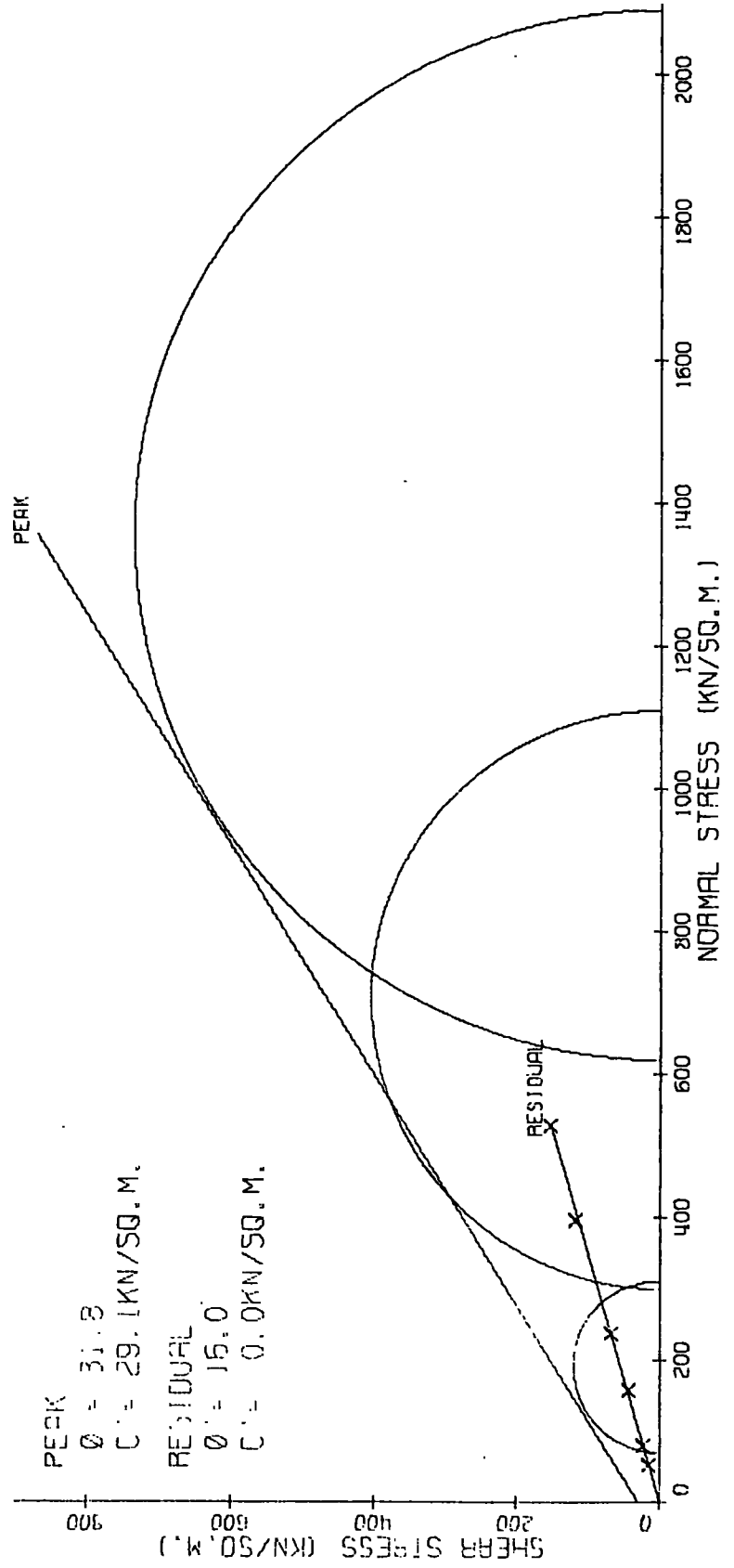


FIGURE 2.25 KELLINGLEY, MINOR HAUL ROAD, MAIN EMBANKMENT

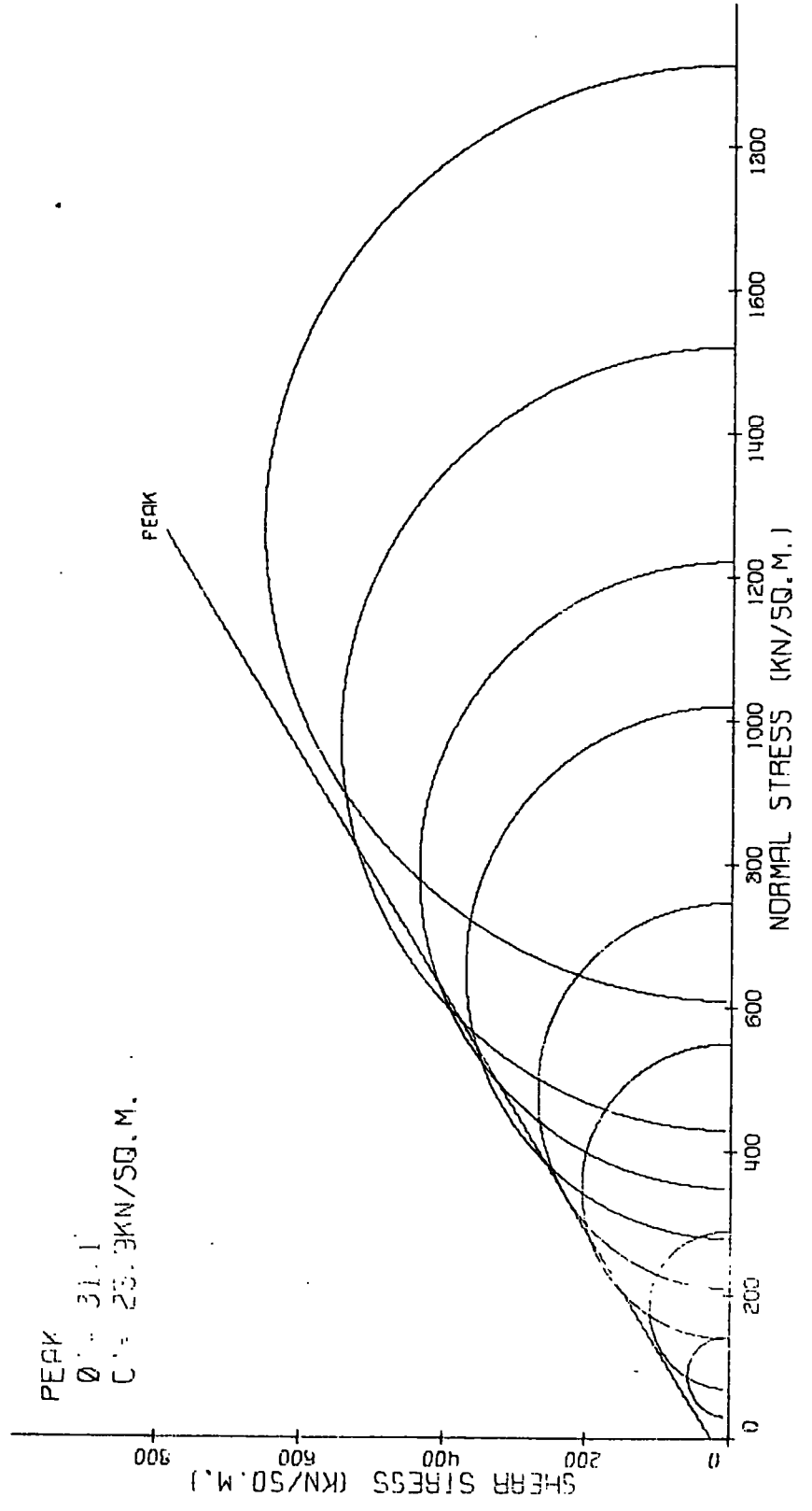


FIGURE 2.26 KELLINGLEY, 6YRS OLD, SHALE BLANKET

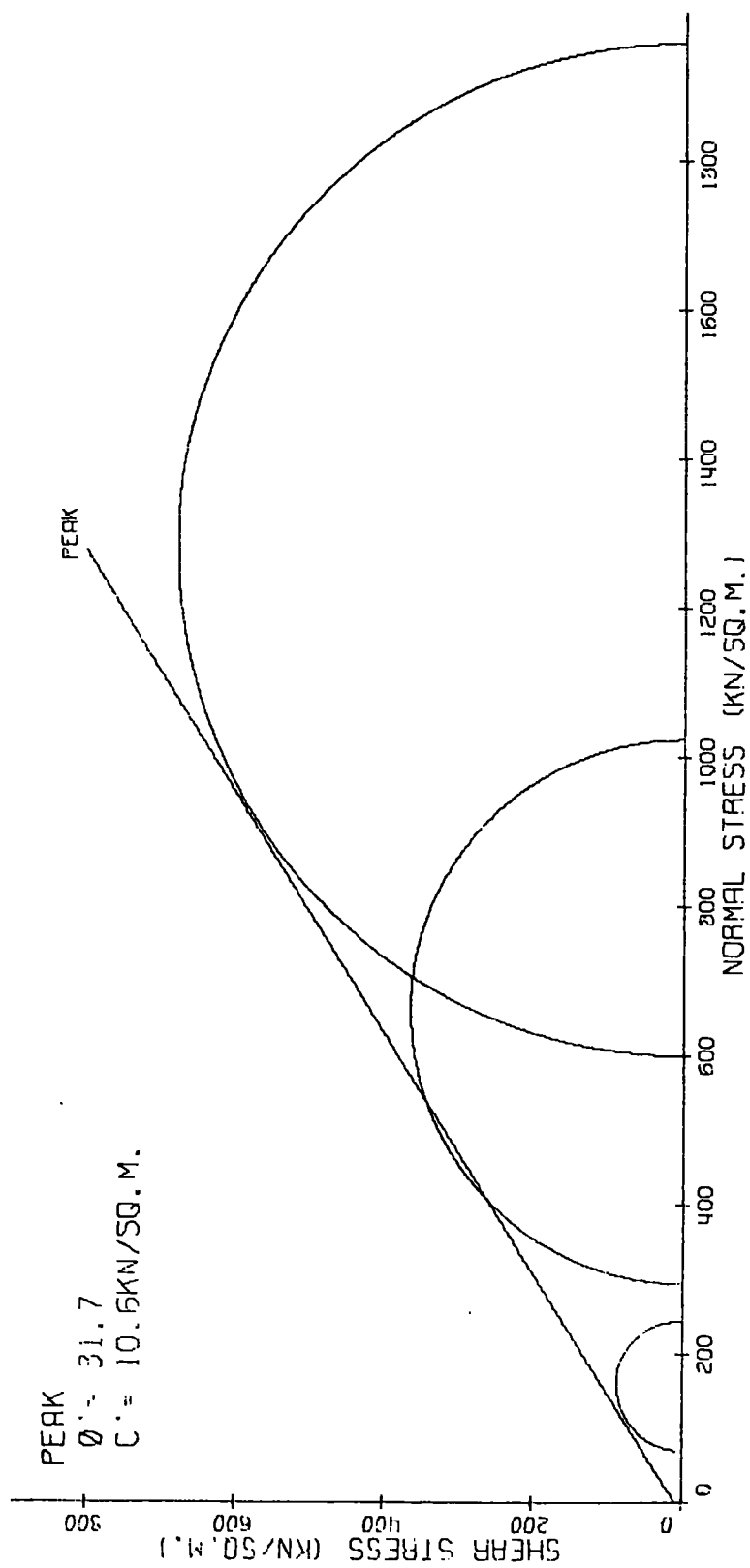


FIGURE 2.27 KELLINGLEY, 8YRS. OLD, ABOVE WATER TABLE

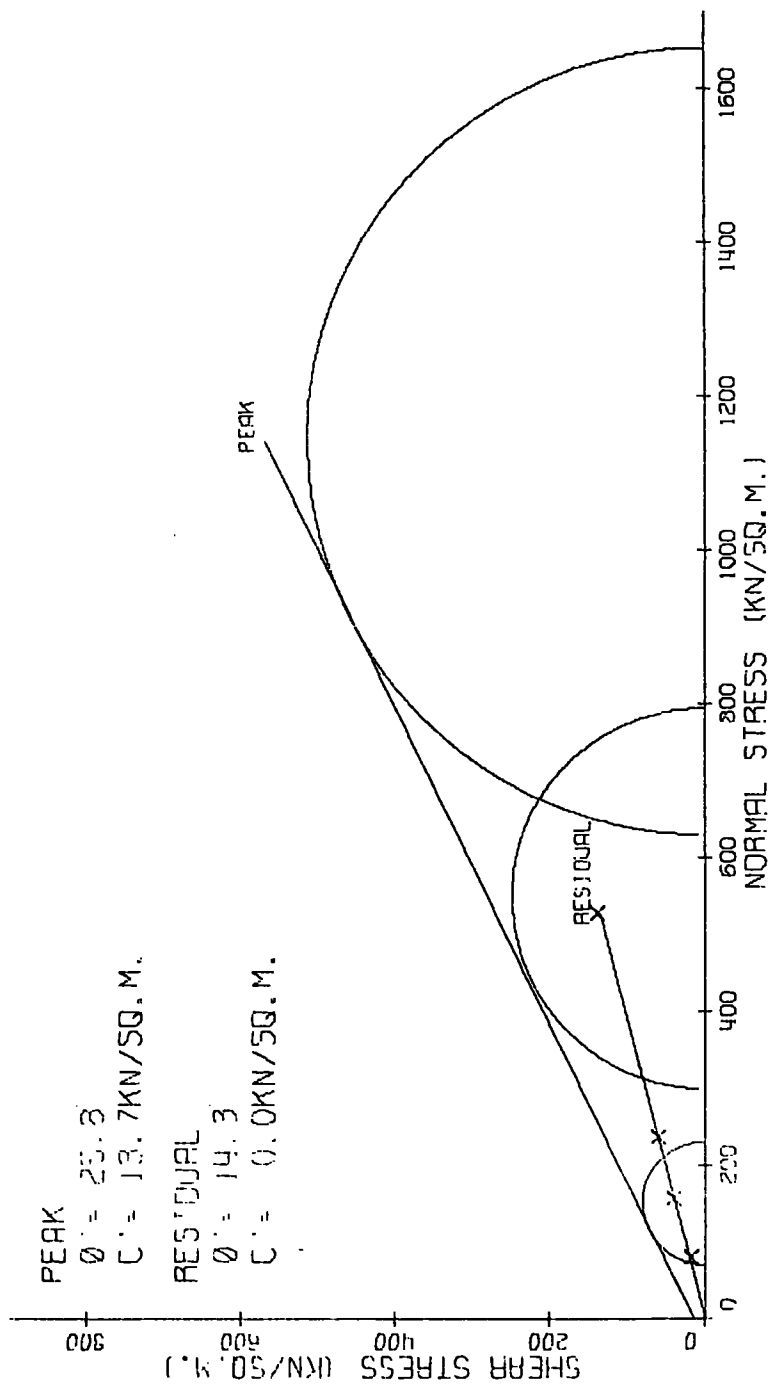


FIGURE 2.28 KELLINGLEY, 8YRS. OLD, BELOW WATER TABLE

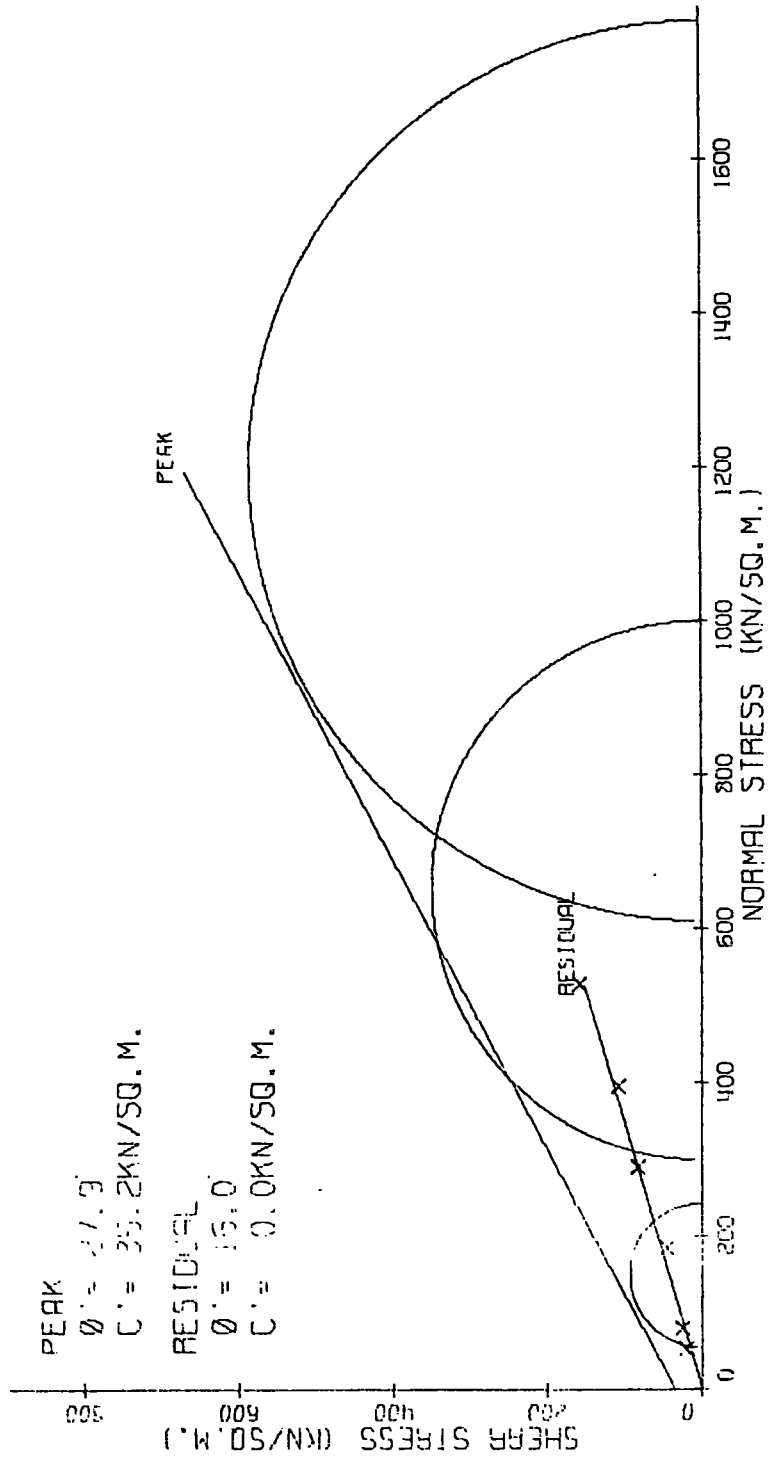
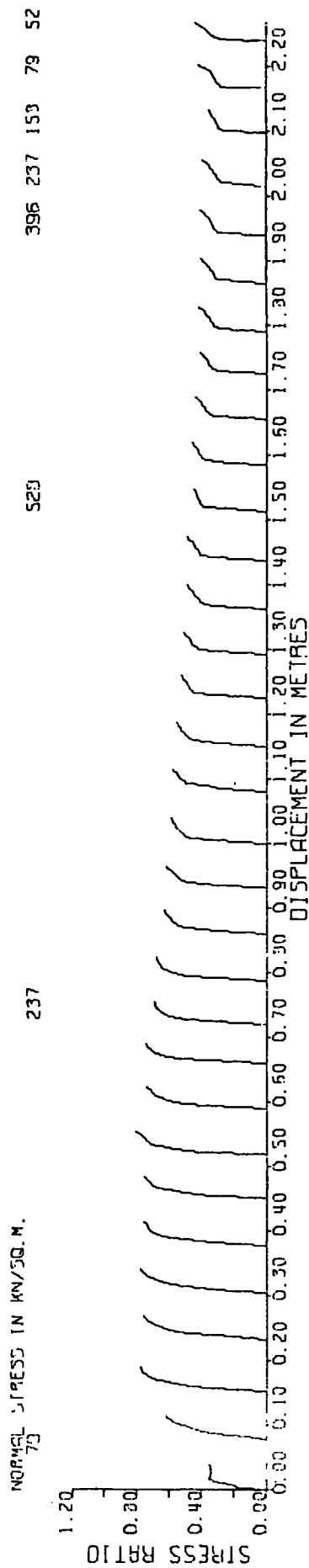


FIGURE 2.29

12 INCH SHEAR BOX TEST

GALE COMMON, FRESH SHALE FROM KELLINGLEY COLLIERY



NORMAL STRESS IN KN/50. M.

237

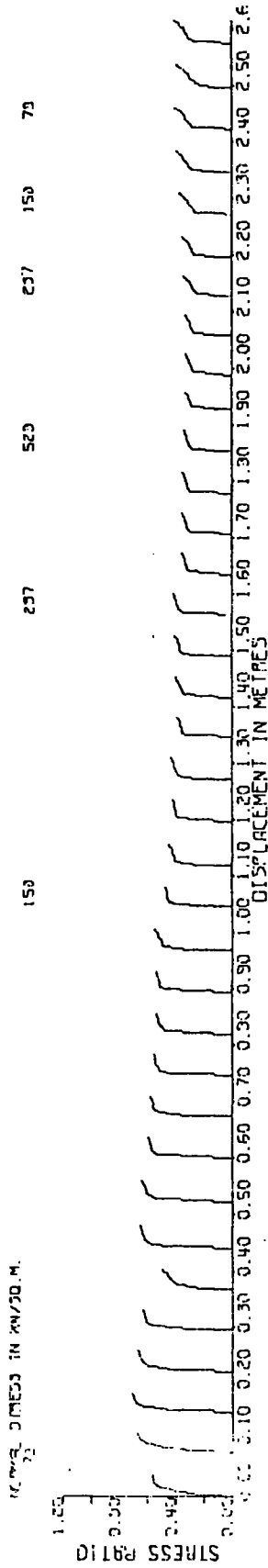
529

396 237 153 79 52

12 INCH SHEAR BOX TEST

FIGURE 2.30

GALE COMMON EMBANKMENT SHALE 37YRS. ABOVE WATER TABLE



12 INCH SHEAR BOX TEST

FIGURE 2.31

GALE COMMON EMBANKMENT SHALE 37YRS OLD, BELOW WATER TABLE

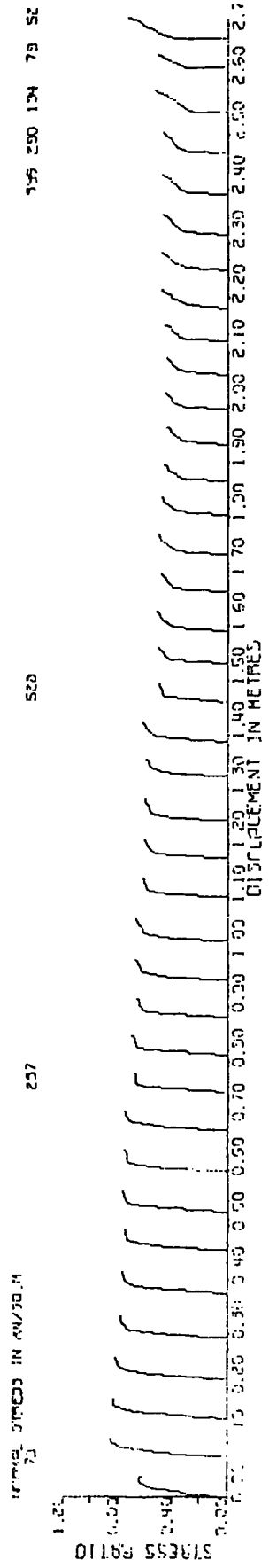


FIGURE 2.32

GRADING CURVES FOR OAKDALE DISCARD

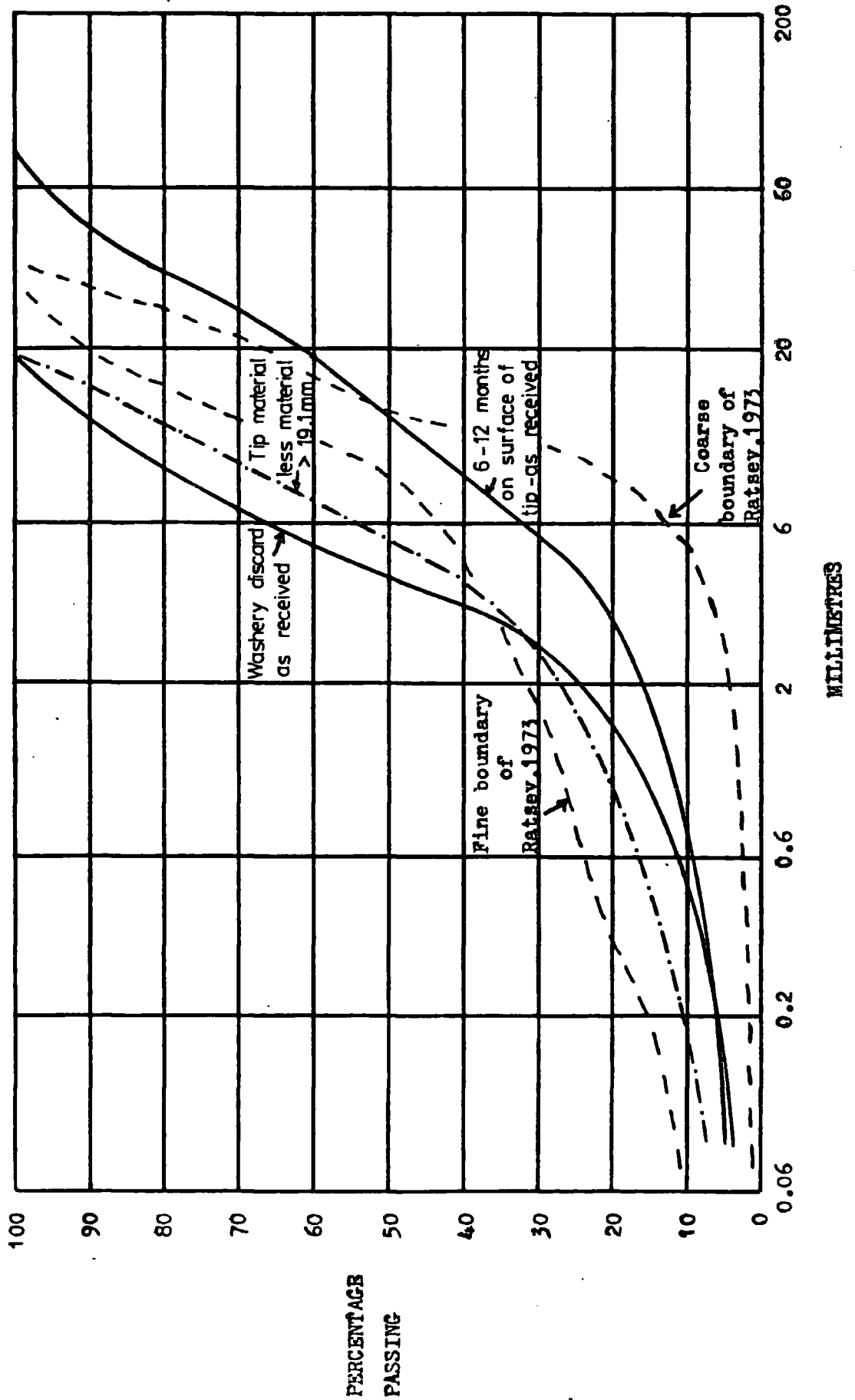


FIGURE 2.33 OAKDALE, FRESH WASHERY DISCARD

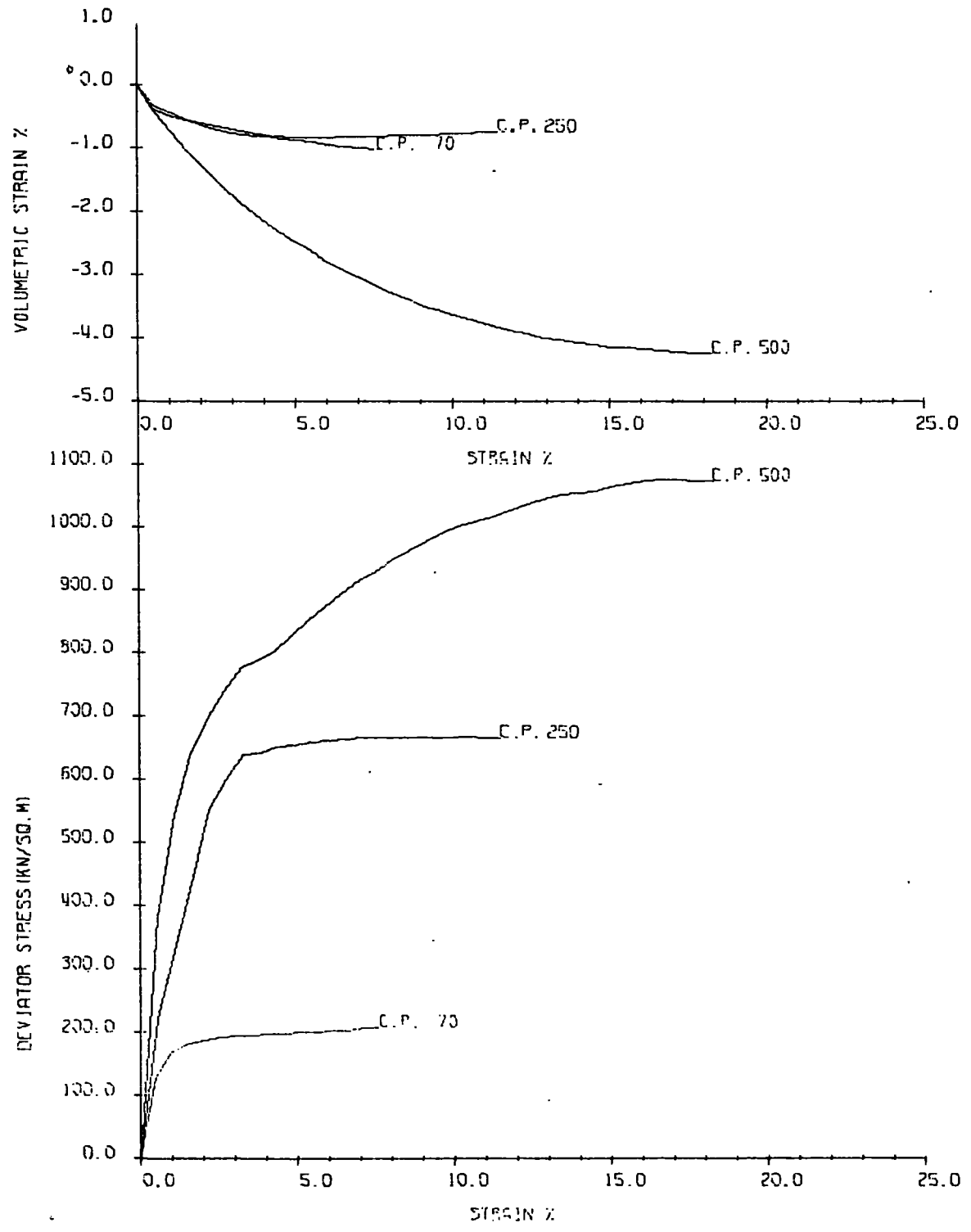


FIGURE 2.34 OAKDALE, 6 TO 12 MONTHS ON TIP

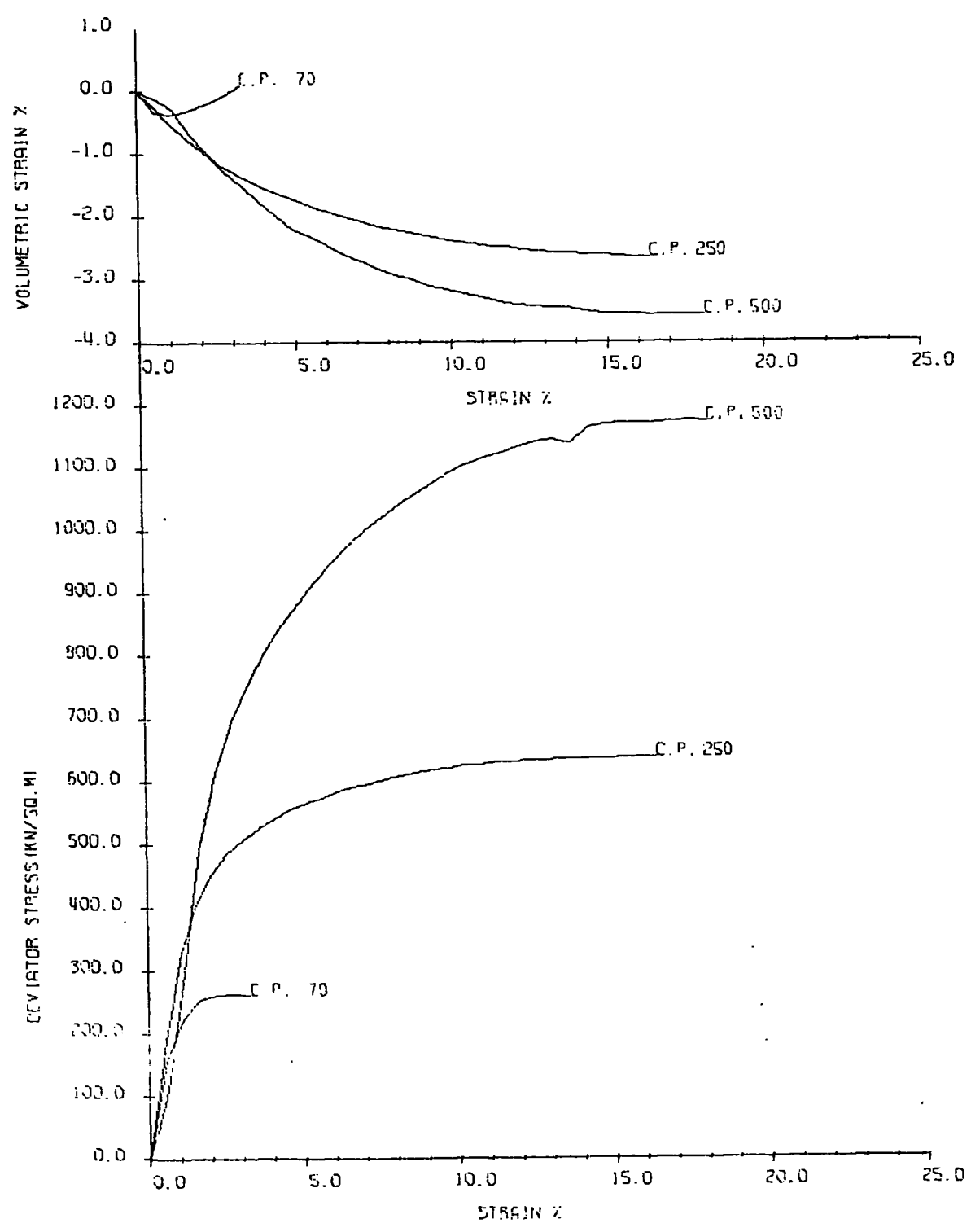


FIGURE 2.35 OAKDALE, FRESH WASHERY DISCARD

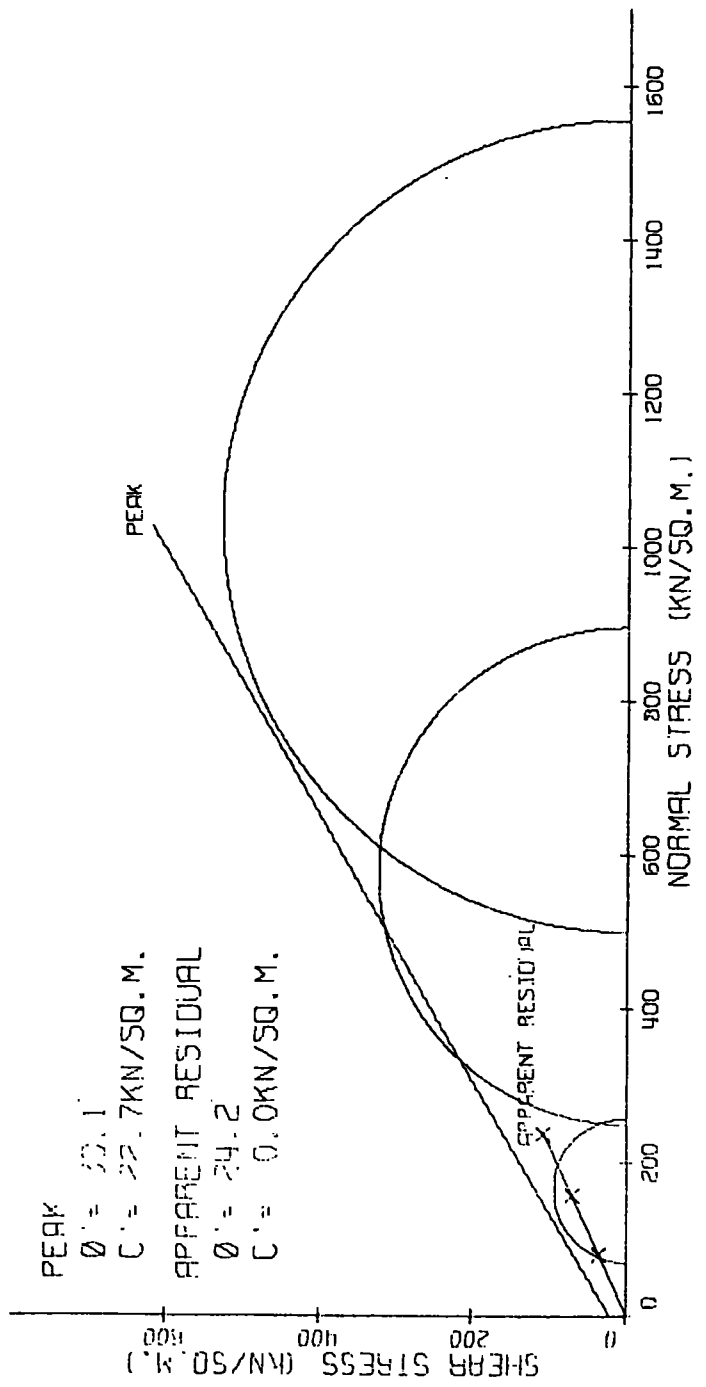
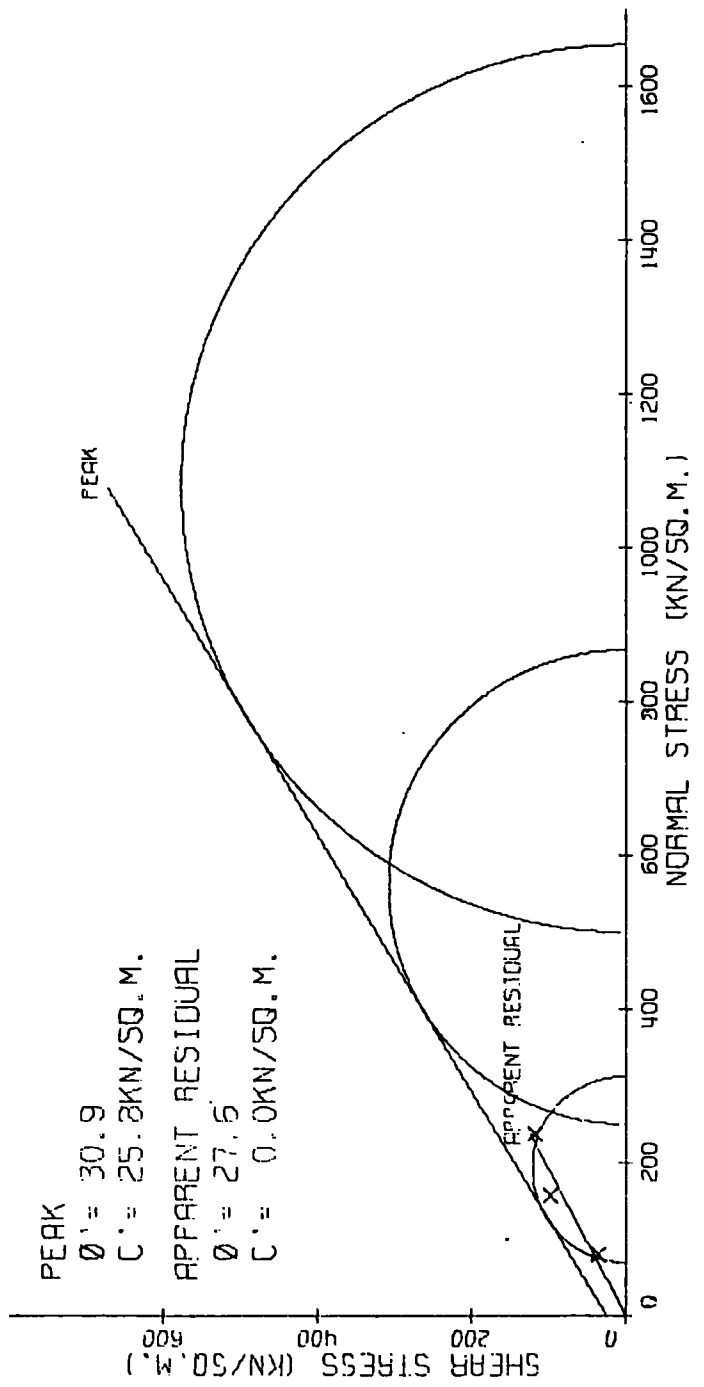


FIGURE 2.36 OAKDALE, 6 TO 12 MONTHS ON TIP



12 INCH SHEAR BOX TEST
ORKDALE WASHERY DISCARD

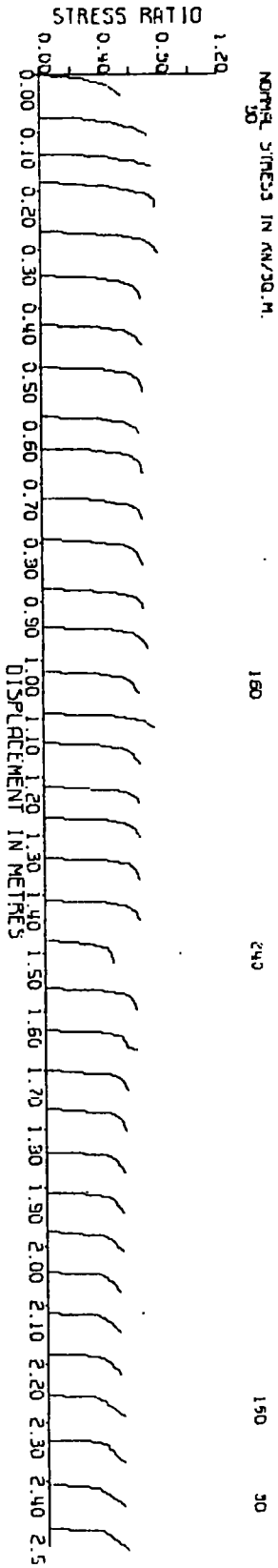


FIGURE 2.37

12 INCH SHEAR BOX TEST
ORKDALE TIP

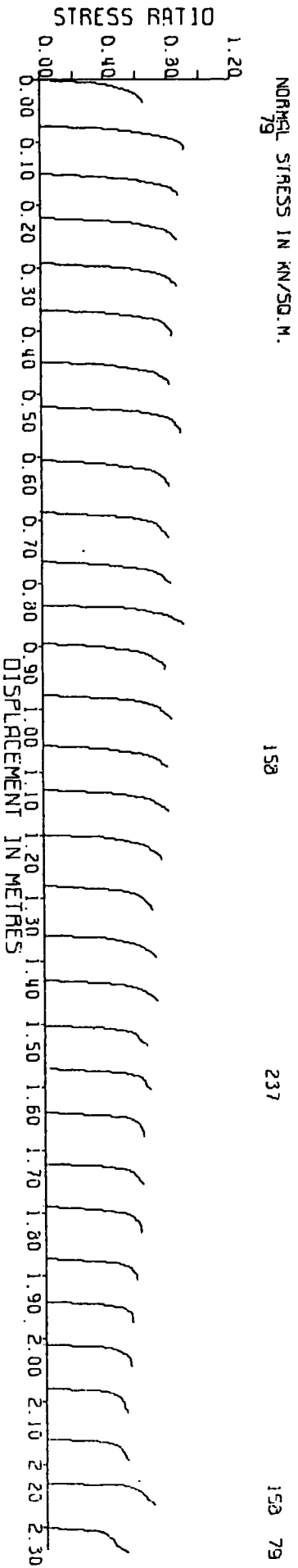


FIGURE 2.38

FIGURE 2.39

GRADING CURVE FOR IRELAND BURRT SHALE

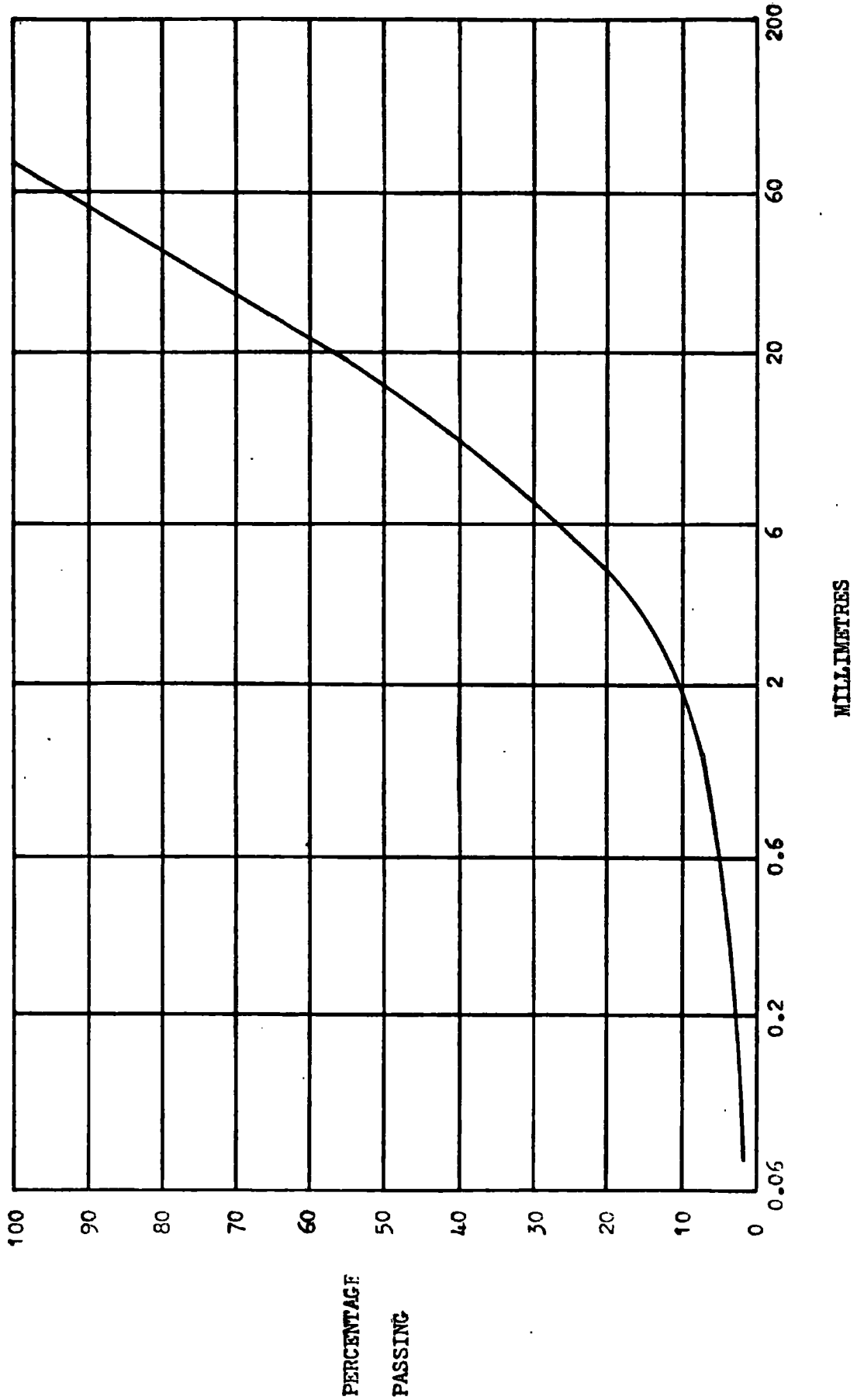


FIGURE 2.40

GRADING CURVE FOR HORDEN BURNT SHALE

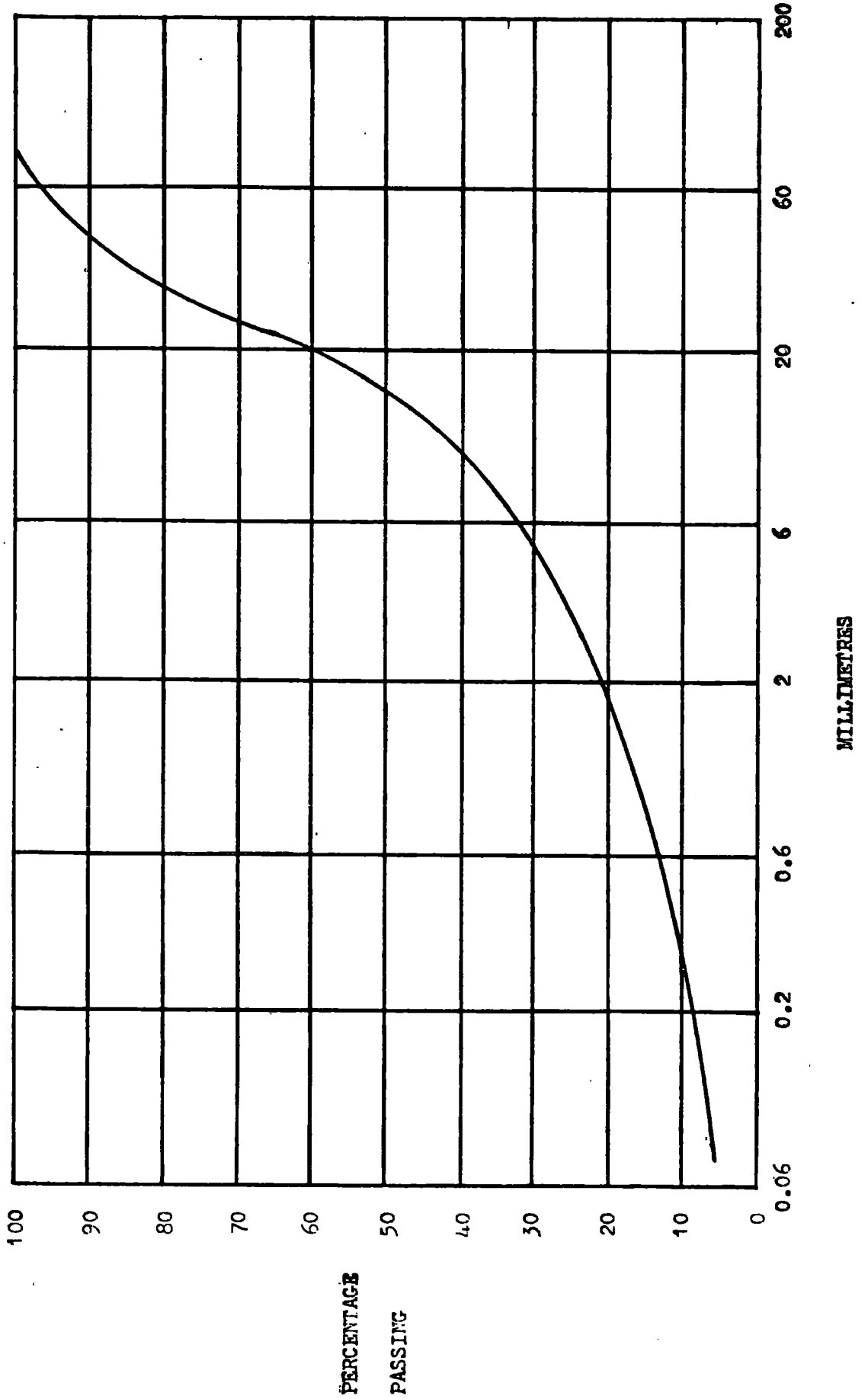


FIGURE 2.41 IRELAND, BURNT SPOIL

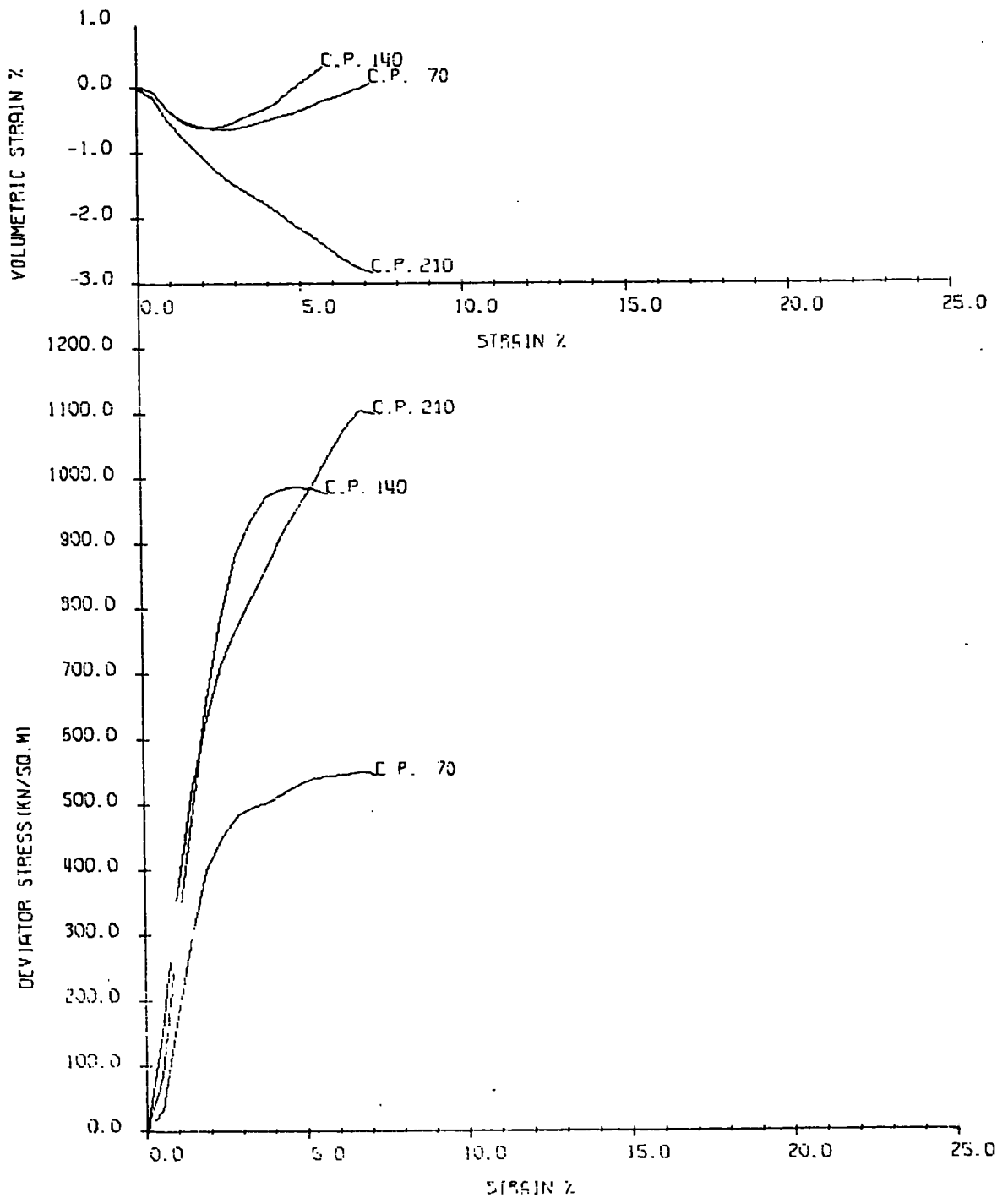


FIGURE 2.42 HORDEN, BURNT SPOIL

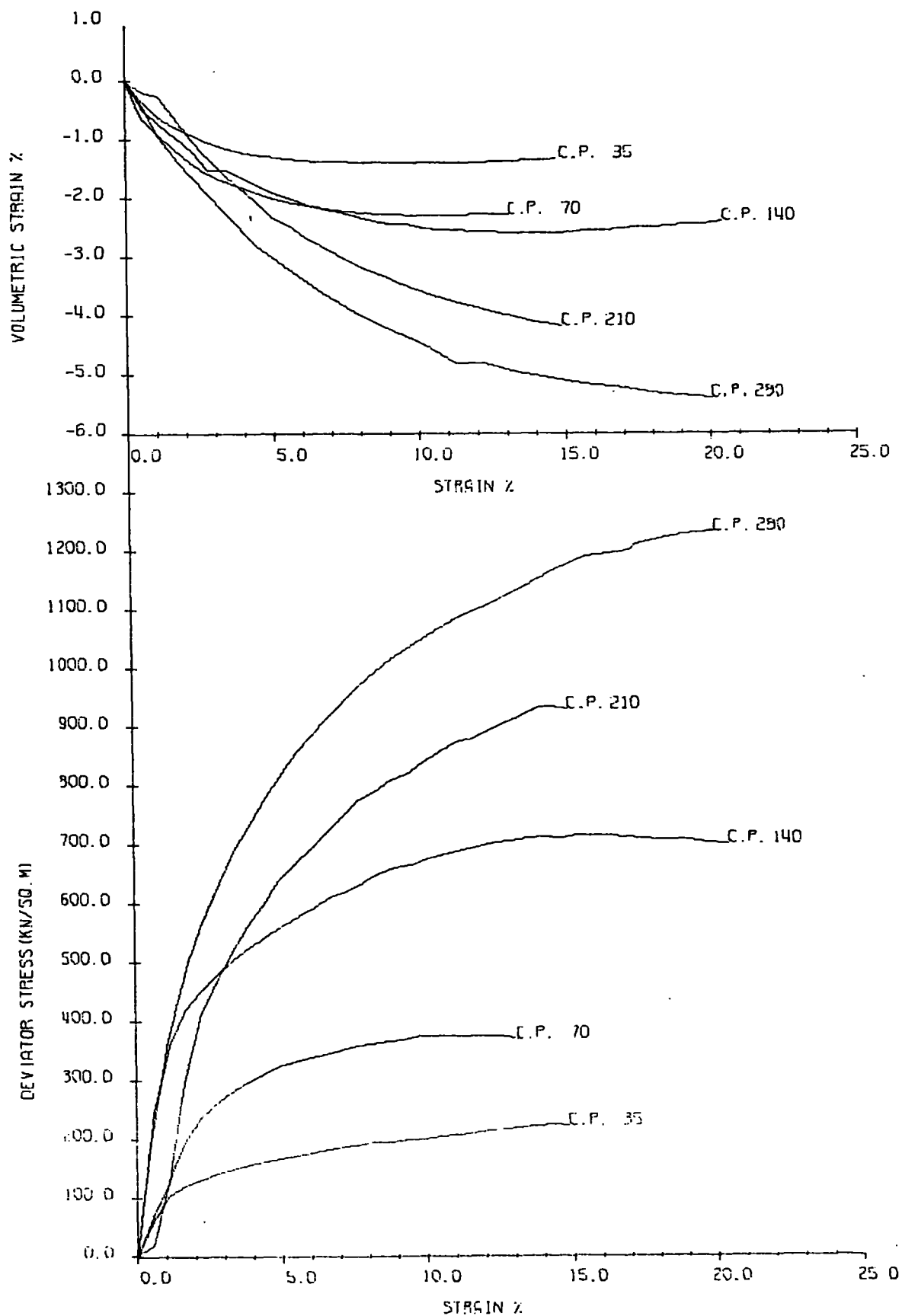


FIGURE 2.43 IRELAND, BURNT SPOIL

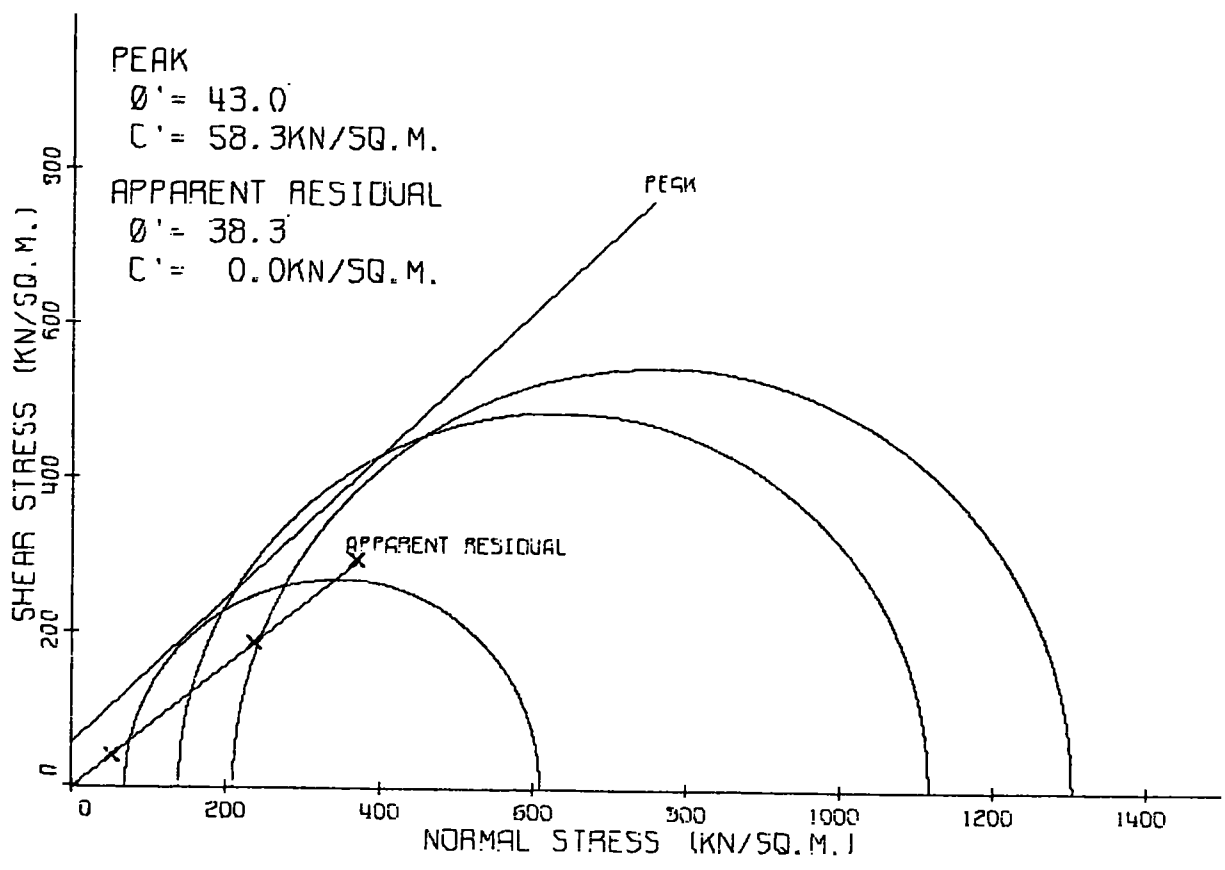


FIGURE 2.44 HORDEN, BURNT SPOIL

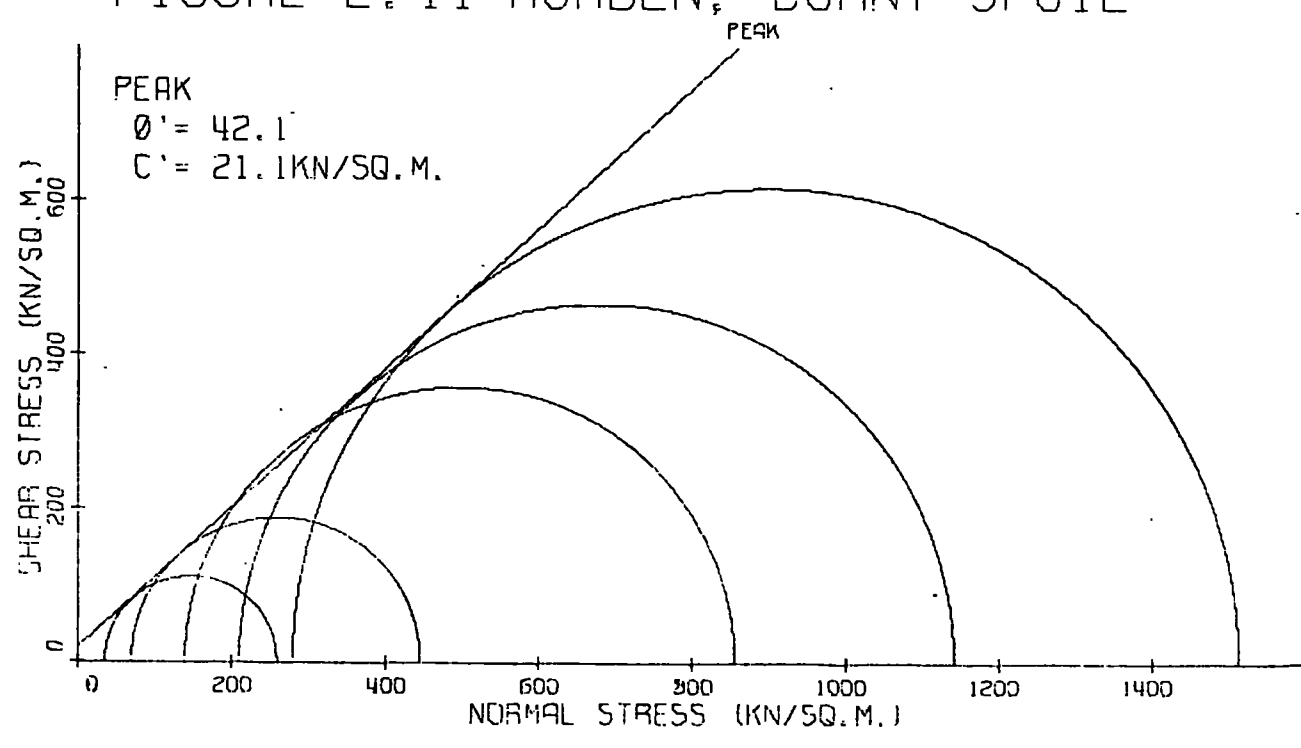
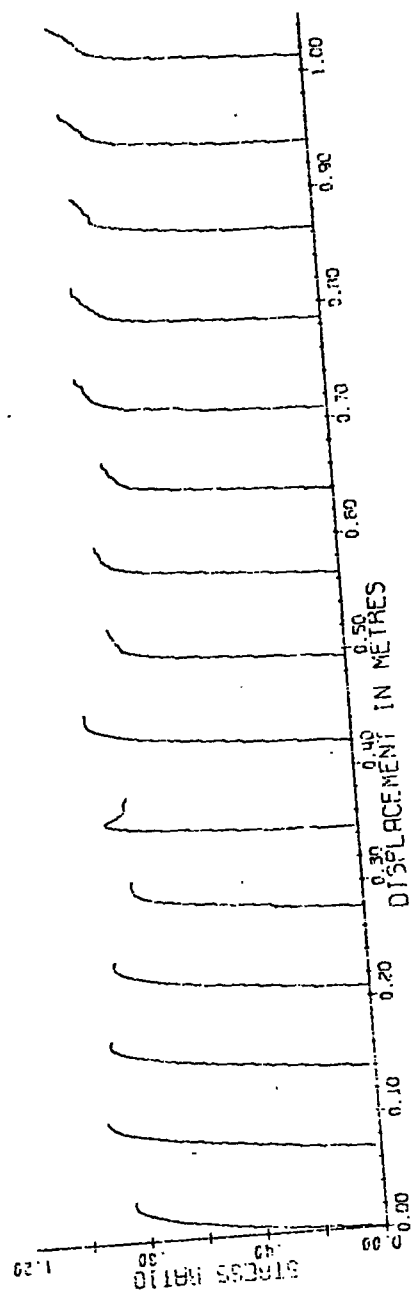


FIGURE 2.45

12 INCH SHEAR BOX TEST

IRELAND COLLIERY . BURNT SHALE



CHAPTER 3

PEAK AND RESIDUAL SHEAR STRENGTHS AS A FUNCTION OF NORMAL PRESSURE

3.1 Effective shear strength parameters

Rockfill is known to exhibit a curved Mohr failure envelope (Marsal, 1973), ascribed to the crushing of points of contact of fragments by high contact pressures. The greatest curvature occurs in the pressure range 0-2,000 kN/m². Colliery spoil, being a weak rock aggregate, might also be expected to exhibit similar properties. From a visual examination of shear strength test results, McKechnie Thomson and Rodin (1972) concluded that the Mohr failure envelope for some colliery discards were, in fact, curved. Taylor and Spears (1972) showed that when a reduced major axis regression line was fitted to the K_f line data for spoil from Yorkshire Main Colliery, the cohesion intercept was statistically significant, whilst that for Brancepeth (Taylor, 1973a) was not (i.e. $c' = 0$ in the latter case). On the basis that colliery spoil is a granular material, it should not logically possess any cohesion. It therefore follows that the Mohr failure envelope for Yorkshire Main spoil is essentially curved. In the case of weak (seatearth-rich) spoils such as Gedling it is probable that the comminuted skin of such heaps may well have a cohesion intercept. There is little evidence that this is a common phenomenon, however. Linear fits have now been considered for other spoils, the results of which are discussed in Section 3.2.

It will be appreciated that, with a curved failure envelope, the precise values for c' and ϕ' given by a linear fit will depend upon the effective stress range over which testing has been performed. To overcome this difficulty, McKechnie Thomson and Rodin (Figure 30, 1972) proposed an equivalent angle of shearing resistance, ϕ'_e (see Chapter 2.2.4.1.)

This parameter is useful for comparing spoils, although it must

be remembered that it is possible for two spoils with failure envelopes of differing curvature to have the same ϕ'_e value if they both have the same shear strength at 350 kN/m^2 normal stress. This parameter is not, however, very useful for stability computations, as will be shown later in Chapter 5.3.

3.2. Curvature of Mohr envelopes

3.2.1. Coarse colliery discard

The statistical tests for significance of cohesion mentioned in the previous section, performed by Taylor and Spears (1972) on Yorkshire Main spoil, and by Taylor (1973a) on Brancepeth spoil, have been applied here to other spoils. The significance of a value of cohesion obtained by the reduced major axis regression method depends on the Student's t distribution of the y -intercept. This can be obtained by dividing the y -intercept by its standard error. This ratio can then be compared with the Student's t distribution at $N-2$ degrees of freedom, where N is the number of points. From this, the confidence level can be deduced (Fisher and Yates, 1948).

The results of applying this technique to a number of spoils is shown in Table 3.1. The test data for Gedling, Oakdale, Kellingley and Horden are from the present work (see Chapter 2), while the remainder have been gleaned from the literature. All the test data from Gedling have been combined, with the exception of the 6-12 month old weathered material, which, as mentioned in Chapter 2.2.5 may actually possess cohesion. Similarly, the results for material from Kellingley colliery (i.e. fresh spoil, embankment spoil and shale blanket) are also combined, and so are the results for material from Oakdale colliery. Among the results taken from the literature, those for spoil from West Virginian coalmines given by Busch, et al (1974) should be mentioned. The failure criteria used in this reference are those of maximum stress ratio. This is liable to give failure envelopes with a small value

of cohesion (Bishop and Henkel, 1962). To overcome this, the failure points have been recalculated using a maximum deviator stress at failure basis (or the deviator stress at 20 per cent strain, where this is applicable).

It can be seen from Table 3.1 that all but three of the spoils show a 99 per cent probability confidence level (i.e. statistically significant), that cohesion is greater than zero for a linear reduced major axis K_f line fit. Of the exceptions, two, Horden (a burnt shale) and Oakdale (a high rank spoil) have a 95 per cent probability (i.e. probably significant) and one, Aberfan, has a 90 per cent probability (i.e. below the acceptable confidence level). In addition, Table 3.2 lists some results obtained by other authors.

The values for the rank of the associated coals, shown in Table 3.2, were supplied by the National Coal Board, with the exception of the West Virginian material. For these, no rank values are available. However, Barrabé and Feys (1965) mention that the West Virginian coalfield contains bituminous coals of 30-40 per cent volatile matter, which would imply a rank in excess of 400, but below 901.

Spoils which display a 99 per cent probability, or above, of cohesion are all of low rank (i.e. 400 to 902). For these, the most likely explanation is that the Mohr failure envelope is, in fact, curved, so that the actual failure envelope will pass through the origin (i.e. not display any cohesion). Of the spoils which show a lower statistical probability, the four which have only a 'probably significant' cohesion (i.e. 95 per cent probability) are ones for which the number of specimens tested are small, being six or less. In statistical work a large number of data points is desirable for meaningful correlations. Furthermore, with the exception of Oakdale, the tests were carried out in the lower stress range (confining pressures, σ_3^1 , of up to 280 kN/m²). The amount of apparent cohesion will, of course, increase as the effective normal stress range increases,

Table 3.1
Significance of linear parameters of 8 ranked spoils

Spoil	Number of Specimens	ϕ' degrees	c' kv/m ²	Correlation Coefficient	v+	Significance with respect to $\phi' > 0(\%)$	u*	Significance with respect to $c > 0(\%)$	Rank
Aberfan ¹	17	36.6	12.2	0.9954	42.9231	99.9	2.1027	90.0	202-205
Penby Hall ²	51	25.6	33.4	0.9930	38.8416	99.9	4.5344	92.9	702
Godling	17	23.6	24.5	0.9942	39.2277	99.9	3.7978	93.0	802-902
Forden	5	42.2	21.1	0.9938	40.2735	99.9	4.1414	95.0	Print
Isabella ³	7	31.3	34.2	0.9990	60.3453	99.9	6.2405	99.0	600-700
Kellingley	14	31.6	24.2	0.9936	59.8401	99.9	3.5115	99.0	502-702
Oskdale	6	30.6	22.6	0.9426	46.1963	92.9	3.2722	95.0	301
N. Virginia ⁴ Triaxial	12	45.0	24.9	0.9991	72.6765	99.9	4.2650	99.0	400-901
N. Virginia ⁴ Shear box	65	33.6	14.5	0.9999	56.7853	99.9	4.5700	99.9	400-501
All British spoil data	418	32.4	13.2	0.9753	92.5401	99.9	2.9560	99.0	
All English spoil data	277	29.7	23.9	0.9713	69.9655	99.9	4.6567	92.9	
All Welsh spoil data	141	34.7	15.8	0.9904	85.6343	99.9	2.6988	99.0	

+ v = Gradient of k_f line divided by its standard error

* u = y-intercept of k_f line divided by its standard error

Data from the following references : 1. Bishop et al (1969)

2. Sir Wm. Balguy and Partners (1972), Geotechnical and Concrete Services Ltd. (1968) and Alibey (1969b)
3. McWilliam (1975)
4. Busch et al (1974)

TABLE 3.2
 PROBABILITY OF COHESION INTERCEPT BEING GREATER THAN ZERO, AS
 DETERMINED BY OTHER AUTHORS

Sample	Rank	No. of Specimens	Percentage Probability that $c' > 0$	Maximum σ'_3 of test (kN/m^2)
Yorkshire Main ¹	600	49	99.0 (significant)	340
Brancepeth ²	301-401	36	80.0 (not significant)	340
Cynheidre ³	102	4	95 (probably significant)	280
Birch Coppice ³	902	4	95 (probably significant)	280

1 - Taylor and Spears, 1972

2 - Taylor, 1973a

3 - Allen, 1973

when a linear fit is applied to a curved envelope.

The two samples without significant cohesion, Aberfan and Brancepeth, are both high rank, hard, brittle materials, Brancepeth being partly burnt. It is of interest that the other two high rank spoils, Oakdale and Cynheidre, and the burnt spoil, (Horden) have only a 95 per cent probability with respect to cohesion.

From the information to date it would appear that the low rank spoils, even when strong (i.e. the West Virginian spoils), show pronounced curvature over the normal pressure range to be expected in colliery spoil heaps (i.e. 0-1,000 kN/m²), whilst the harder, high rank and burnt spoils do not show such pronounced curvature over these pressures.

This overall situation is illustrated by the last three entries in Table 3.1. Firstly, all the British spoil data available, some 418 points, were analysed statistically. This revealed that there was 99.0 per cent probability of a positive cohesion intercept for all British spoils. When split into Welsh and English collieries, an interesting point arises. For Welsh spoils, the probability of there being a positive value of cohesion is still 99.0 per cent. For English spoils, however, the probability has risen to 99.9 per cent. This difference may be an expression of the different ranks of the spoils comprising the two suites. The Welsh spoils, which are all from the South Wales coalfield, are generally of higher rank than are those from England.

3.2.2 Peak shear strength of 0.6mm to 1.2mm size fractions

A series of tests on 0.6 to 1.2mm size fraction material were carried out in a 60 x 60mm reversing shear-box to investigate the effect of normal stress on rate of particle breakdown. This effect will be discussed later in this chapter (Sections 3.3.1 and 3.3.2). The tests also help in elucidating the effects of normal stress on peak shear strength and can therefore be compared with

the results for coarse discard given in Section 3.2.1.

The tests were conducted over a pressure range from 50 to 1,000 kN/m². Each specimen was prepared by wet sieving the 0.6mm to 1.2mm fraction from a bulk sample of the material. This fraction was then sluiced into the shear-box, and the normal stress applied. If the material in the box consolidated to such an extent that the top platten encroached upon the shearing zone in the sample, the sample was unloaded, and the box topped-up with more material, after the top surface of the compressed material had been roughened. The normal stress was then re-applied. This usually only happened when a high normal stress was operative.

Each sample was then sheared until it had apparently reached residual, i.e. shear stress remained constant over several reversals. When this stage was reached, the sample was removed and wet sieved to find the extent of particle breakdown.

In addition, some specimens were not sheared. For these, the requisite normal pressure was applied and the sample was then sieved after consolidation was complete. This procedure gives an indication of the amount of particle breakdown caused by normal stress alone.

Peak shear strength results using a reduced major axis fit are illustrated in Figure 3.1 and Table 3.3. From these, it is apparent that for both Kellingley and Gedling there is a 99 per cent probability that the cohesion parameter is greater than zero.

It is, of course, improbable that a sample of coarse sand size will possess cohesion. An examination of Figure 3.1 shows that the failure envelope is, in fact, curved, passing through the origin. In the case of Oakdale, however, there is no noticeable curvature, nor is the small value of cohesion in Table 3.3 significant (only 30 per cent probability that c' is greater than zero). This reinforces the impression gained from the coarse colliery discards, namely that the low rank (high volatile) materials, show a significant amount of curvature in the pressure ranges associated with colliery

waste tips, whereas the high rank (low volatile) ones do not.

The amount of particle breakdown which occurs due to the application of normal stress alone can be seen in Figures 3.2 to 3.4, and in Table 3.4. As might be expected, the amount of degradation increases as normal stress increases. With rockfill, increasing degradation with increasing normal stress causes a reduction in ϕ' , i.e. curvature of the Mohr envelope (Marsal, 1973).

Presumably, the same situation exists with colliery spoils. Of the three spoils tested, the one showing the least particle breakdown was Oakdale, and it did not show significant curvature of its Mohr envelope, whilst the one with the greatest amount of breakdown, Gedling, shows the greatest amount of curvature (see Table 3.5).

Three normal loading tests were performed on Gedling material (Figure 3.2). It can be seen that the amount of breakdown does not increase linearly with stress increase. This could explain why the amount of curvature per unit stress becomes less as normal stress increases.



TABLE 3.3
PEAK SHEAR STRENGTH PARAMETERS - 0.6mm- 1.2mm SIZE FRACTION

Spoil	No. of specimens	ϕ' c=0	ϕ' degrees	c' kN/m ²	Correlation Coefficient	Student's t	Confidence level	u*	Significance with respect to $c' > 0\%$	Rank
Oakdale	8	29.1	28.8	3.4	0.9976	40.5728	99.9	0.5021	30	301
Kellingley	10	27.8	25.6	18.2	0.9970	41.0768	99.9	3.3736	99	502-702
Gedling	9	27.9	24.0	35.3	0.9928	25.0605	99.9	4.1464	99	802/902

* u = y-intercept of reduced major axis divided by its standard error

TABLE 3.4
SORTING COEFFICIENTS - 0.6mm-1.2mm SIZE FRACTION AFTER DEAD LOADING

Sample	Normal Stress (kN/m ²)	Uniformity Coefficient (u)	Trask Sorting Coefficient (So)	Median Diameter (p50)mm
Gedling	50	2.8	1.3	0.40
	200	Approx. 80 (> 10)	2.2	0.53
	1000	Approx. 150 (> 9)	Approx. 4.0 (> 3.4)	0.80
Kellingley	200	1.5	1.2	0.83
	1000	5.7	1.4	0.79
Oakdale	200	1.4	1.2	0.83
	1000	2.1	1.2	0.81

u - Uniformity Coefficient, if given by u = F60/P10

So - Trask Sorting Coefficient, is given by So = F75/P25

N.B. Before loading, u = 1.4 and So = 1.2 for all samples

For u, uniformity increases as u decreases

For So, uniformity increases as So decreases

TABLE 3.5

DECREASE IN ϕ' AND INCREASE IN DEGRADATION, 0.6 to 1.2mm SIZE

FRACTION SAMPLES

Sample	ϕ' at 200 kN/m ²	ϕ' at 1,000 kN/m ²	Increase in uniformity coefficient, u, at 1,000 kN/m ²	Increase in Trask sorting coefficient So, at 1,000 kN/m ²
Gedling	32.4	25.6	Approx.150 (>8)	Approx.2.8(>2.2)
Kellingley	29.6	26.4	4.3	0.2
Oakdale	29.1*	29.1*	0.7	0.0

* The angle of ϕ' given for Oakdale is calculated for a straight line fit with $c' = 0$.

3.2.3 Curve fitting

Figure 3.5 illustrates one of the problems with the ϕ'_e method of describing curved envelopes. The ϕ'_e value for Gedling is 29.9° and for Kellingley it is 28.5° . Whilst this gives a sensible interpretation for the lower stress range (up to 600 kN/m^2) - that Gedling is stronger than Kellingley - it does not highlight the fact that at higher normal stresses, Gedling is weaker than Kellingley. The materials could be described in terms of equivalent shear strength parameters by giving the value of ϕ' at several normal stresses, as has been done in Table 3.5. This is a very cumbersome method, however. Furthermore, it suffers, as does ϕ'_e , from being very subjective, depending upon the individual observers opinion of where the envelope should lie*. It is obviously easier and more desirable to represent the failure envelope by a mathematical expression which describes a curve and whose parameters can be assessed statistically.

Owing to the scatter of data points, it is not possible to know what the precise shape of the curve ought to be. Therefore an assumption has to be made. The general equation that has been chosen is of the form:

$$\tau = m(\sigma')^z$$

where τ = shear stress

σ' = normal stress

m = constant

z = constant

* In this work, the values of ϕ'_e quoted in Chapter 2 have, in fact, been calculated from the curved envelopes developed here, using the parameters shown in Table 3.6.

this has the following advantages:

- a) There are only two parameters, m and z , to define. This is important, as, with the usual number of test specimens, there is not enough data to give sensible values to a large number of parameters.
- b) The equation passes through zero, i.e. there is no cohesion, because when $\sigma' = 0$, $m(\sigma')^z$ and therefore $\tau_c = 0$.
- c) The amount of curvature is variable, being controlled by m and z .
- d) The curve can be easily fitted to a set of data points by using a reduced major axis statistical fit to a log-log transform of the points.

The theoretical basis for fitting the curve is as follows:-

Given that the curve equation is

$$\tau = m(\sigma')^z \dots \dots \dots (1)$$

taking logs of each side, this is transformed to:

$$\log \tau = \log m(\sigma')^z \dots \dots \dots (2)$$

$$\therefore \log \tau = z \log \sigma' + \log m \dots \dots \dots (3)$$

This is the equation of a straight line of gradient z and with a y axis intercept of $\log m$.

Therefore, if the shear strength results are plotted on a log-log basis, the equation of the reduced major axis line through them will give values of z and $\log m$ (see Figure 3.6)

This procedure is easily applied to shear-box results, where there is a discrete point, but for triaxial results it is more difficult. When using the curve fitting technique for triaxial results, it is necessary to select the point on each Mohr circle which represents the stress conditions at failure for that sample. This is accomplished by the construction shown in Figure 3.7, and will be known as the 'triaxial failure stress point'

The reduced major axis program (Appendix B) was modified to give estimates of m and z and to draw the curves. The curves are

drawn by calculating the values of γ at 10 kN/m² intervals on the σ axis. These points are then joined by straight lines. Using this program, curves have been fitted to several spoils. The results are shown in Figures 3.8 to 3.25 and in Table 3.6.

3.2.4. Some features of the curves

Examination of the figures shows that the value of z is controlled by the shape of the curve. Where sharp curvature is required in the low stress range, z is lowest (e.g. Birch Coppice, Figure 3.8) and where it is spread over the whole of the stress range, z is highest (e.g. Kellingley shale blanket, Figure 3.20). Where z is approximately constant, an increase in m indicates an increase in strength (e.g. Oakdale, Figure 3.23 is stronger than Gedling 3m deep specimen, Figure 3.15). These variations can also be seen in Figure 3.26, where several shapes of curve are shown. Where $z = 1$, the line is straight (e.g. Oakdale 0.6 - 1.2mm size fraction). In this case, m is equal to $\tan \phi'$ in the expression $\gamma = \sigma' \tan \phi'$.

Consideration of the values of z and the graphs of particle breakdown for 0.6 to 1.2mm size samples (Figures 3.2 to 3.4) shows that there is a positive correlation between these two. Table 3.7 shows the values of the 'Area Ratio' and z . The 'Area Ratio' is here defined as the ratio of the area under the particle size curve between 600 and 72 μm^* for a normal pressure of 200 kN/m² to a similar area at 1,000 kN/m² normal stress. This implies that the amount of curvature increases with increase in crushing of particle contacts.

* As the original particle size grading in these tests was between 600 and 1200 μm , that part of the grading curve below 600 μm in size can be regarded as being solely due to particle breakdown.

TABLE 3.6
VALUES OF m AND z FOR 11 SPOILS

Sample	Rank	m	z	Figure	
Birch Coppice	902	2.613	0.771	3.8	
Cynheidre	102	1.412	0.890	3.9	
Yorkshire Main	600	0.946	0.952	3.10	
Isabella	600-700	2.158	0.816	3.11	
West Virginia	a) Triaxial	400-901	1.404	0.902	3.12
	b) Shear-box	400-901	1.255	0.902	3.12
Denby Hall	702	1.629	0.831	3.13	
Gedling	Composite 3-4m old sample	802/902	1.189	0.858	3.14
	1m deep		1.135	0.856	3.15
	3m deep		0.972	0.898	3.15
	4m deep		1.334	0.839	3.15
	Wimpey data (old tip)		0.874	0.920	3.16
	0.6-1.2mm fraction		1.597	0.825	3.17
Kellingley	Lagoon D Embankment 8 years old, above W.T.	502-702	1.061	0.886	3.18
	Lagoon D Embankment 8 years old, below W.T.		1.957	0.821	3.19
	Shale blanket 6 years old		0.762	0.974	3.20
	Lagoon B, South Embankment		1.324	0.890	3.21
	Fresh spoil from stockpile		1.380	0.890	3.22
	0.6-1.2mm fraction		0.881	0.917	3.17
Oakdale	Composite sample	301	1.215	0.899	3.23
	0.6-1.2mm fraction		0.557	1.000	3.17
Horden	Burnt		1.811	0.894	3.24
Ireland	Burnt		3.628	0.794	3.25

TABLE 3.7

COMPARISON OF z AND AREA RATIOS FOR 0.6 to 1.2mm SIZE FRACTION SAMPLES

Sample	z	Area Ratio (see text, Chapter 3.2.4.)
Gedling	0.825	0.73
Kellingley	0.917	0.26
Oakdale	1.000	0.19

It should be noted that the value of m is dependent on the units used, whereas z is not. If the conversion factor between one set of units and another is f , and assuming the shear stress and normal stress in the first set of units to be s and p respectively and t and u in the second set, then from equation (1) above:

$$s = mp^z \quad \dots \dots \dots (4)$$

also

$$t = s.f \quad \dots \dots \dots (5)$$

and

$$u = p.f \quad \dots \dots \dots (6)$$

From (4) and (5)

$$t = m.f.p^z$$

and from (6)

$$p = \frac{u}{f}$$

$$\therefore t = m.f. \left(\frac{u}{f}\right)^z$$

$$\therefore t = \frac{m}{f^{(z-1)}} u^z$$

$$\therefore t = m.f.(1-z) u^z \quad \dots \dots \dots (7)$$

It follows from this expression that, when used with different units, z remains unaltered, while the parameter m must be multiplied by a factor of $f^{(1-z)}$ where f is the conversion factor between the two units*.

In the current work, S.I. units are used. Thus m is always a function of stresses in kN/m^2 .

* This parallels the Culomb-Navier equation $\tau = \sigma \tan \phi + C$, where ϕ is unaffected by units, but c is unit-dependent.

3.3 Residual shear strength

3.3.1 Residual shear strength of 0.6mm to 1.2mm size fraction

As mentioned in Section 3.2.2. a series of specimens of the 0.6mm to 1.2mm size fraction of material from Gedling, Kellingley and Oakdale were sheared to their residual strengths at varying normal pressures. This experiment was an extension of a single test suite performed on material from Ollerton Colliery by Ratsey (1973). This Ollerton material (Rank 802) showed (a) a markedly curved residual shear strength envelope and (b) residual shear strength was attained at considerably smaller displacements at normal stress levels of 300 kN/m^2 and greater, than at a stress level of 133.7 kN/m^2 (see Figures 3.27 and 3.28). These tests on Ollerton were slightly different from the present series in that material of the required size was obtained by crushing the larger size fractions. This practice, which was necessary due to shortage of material, may have led to samples not being of consistent composition.

Figures 3.29 to 3.31 show the stress ratio-displacement curves of the materials tested, and Figures 3.32 to 3.34 show the gradings at the end of each test. From the curves of stress ratio against displacement it is apparent that the residual stress ratio drops rapidly with increase in normal stress up to a certain normal stress level, where this decrease nearly ceases. This cut-off value, above which the residual failure envelope is virtually linear (see Figures 3.35 - 3.37) varies for different spoils, from 300 kN/m^2 (Kellingley) to 400 kN/m^2 (Gedling and Oakdale). For Ollerton it is in the region of 350 kN/m^2 (Figure 3.27). It is of interest to note that it is at these cut-off values that reorientation peaks first appear.

In a reversing shear-box, there is considerable sample loss due to material working its way through the split in the box. As this

loss chiefly affects the finer fractions, a time will arise during the test when the production of finer material by the shearing process will equal the rate of loss, and the shearing resistance will drop no further. As the angle of apparent residual shear strength drops with increase in normal stress (see Figures 3.29 to 3.31) it is obvious that the rate of supply of finer material (i.e. the rate of particle breakdown) must therefore increase with increasing normal stress. This will also have the effect of decreasing the displacement required to reach residual, as normal stress increases.

This more rapid drop to residual at high normal stresses could be the reason for the results obtained by Bishop (1973). Here, material from Aberfan Tip 2 was sheared for 270m in a ring shear-box before a near-residual shear strength was obtained, whereas in the failure of Tip 7 at Aberfan (containing similar material) a residual value of 17.5 to 18.5 degrees was achieved in about 21m displacement. The ring shear test was, however, conducted at a normal stress of only 100 kN/m^2 whereas the actual pressure on the slip plane of Tip 7 was over 350 kN/m^2 for most of its length, rising to a maximum of 440 kN/m^2 (calculated from Figure 1.28 in Bishop et al, 1969). Thus the rate of reduction in shear strength on the shear plane under field conditions would have been much greater than in the ring shear test.

While the mechanism outlined above explains the reduction in stress ratio as normal stress increases, one would not expect such a sharp break in the rate of reduction of residual shear strength as actually occurs. This change in rate could indicate a change in mechanism. At low normal stresses the particles will have the facility for limited dilation and will be able to ride over one another during shearing with breakdown being due to abrasion. At higher stresses, the particles will become locked together, and

shearing will take place through individual particles to cause breakdown. It is impossible to test this hypothesis, as the amount of sample loss during shearing masks the small amount of dilatant behaviour. However, it is of interest to note that in the triaxial tests upon coarse discard, dilation, if only on a small scale, was often occurring at low confining pressures (approx. 70 kN/m^2).

3.3.2 Particle size after residual shear

From the grading curves after the shear tests, it is apparent that generally, for each material, the amount of breakdown increases as normal stress increases. However, the breakdown is not linear, the rate of increase being greatest at the lower normal pressures.

It is of interest to note that the final grading for the different materials does not correlate with the residual shear strength of the material. The material with the highest angle of ϕ'_r , Ollerton, (18° at $1,000 \text{ kN/m}^2$) (Figure 3.28) has 30 per cent of material passing $72 \mu\text{m}$ at this pressure (Figure 3.38). It should be noted that this material was only sheared until it was approaching residual, and its true residual may well be lower (Ratsey, 1973). The material with the lowest ϕ'_r at $1,000 \text{ kN/m}^2$, Kellingley (10.5°) has only 20 per cent passing $72 \mu\text{m}$ (Figures 3.36 and 3.33). Gedling and Oakdale both have a similar residual value at $1,000 \text{ kN/m}^2$, 14° (Figures 3.35 and 3.37), but Gedling has 40 per cent passing $72 \mu\text{m}$ (Figure 3.32) whilst Oakdale only has 14 per cent passing $72 \mu\text{m}$ (Figure 3.34) at this pressure. It is obvious that the final particle size distribution does not constitute the only major control on ϕ'_r , and hence some other control must be sought.

3.3.3 Mineralogy

The mineralogy of the samples is reproduced, for convenience, in Table 3.8. That of Ollerton is taken from Ratsey (1973). As

can be seen, there is no overall control on ϕ'_r from the mineralogy either. Considering the two samples, Gedling and Kellingley, which have similar peak strengths but dissimilar residuals, the main difference in mineralogy is that Gedling has a higher quartz and lower organic carbon content. It also has the higher residual shear strength value. As carbon usually increases the peak shear strength (Taylor, 1974b), it was thought that coaly material might have been migrating from the shear plane. This was tested with three available shear plane specimens (Table 3.9) and found not to be the case. The possibility arises, therefore, that the higher quartz content of the Gedling spoil is the cause of its higher residual shear strength. Quartz did not show any correlation with peak shear strength however (Taylor, 1974b). A possible mechanism is the releasing of quartz grains from the mineral aggregates which form the shale particles during the mechanical breakdown of the latter over large shear displacements. It is noticeable that Ollerton, which also has a high residual shear strength also has a fairly high quartz content. Oakdale, on the other hand, has a low quartz content, but has a residual shear strength equal to that of Gedling. In this case, however, it will be remembered that very little particle breakdown occurred during the test.

3.4. Conclusions

In conclusion, it can be accepted that coarse colliery discards exhibit curved failure envelopes. The amount of curvature is dependent upon the amount of particle breakdown with increasing normal stress. This appears to be small with low volatile, high rank spoils, where the failure envelope is virtually straight over the 0-1000 kN/m² pressure range. Spoils associated with bituminous coals, however, which have a lower rank (400 to 902) and 30 to 50 per cent volatile matter, exhibit considerable curvature.

The shape of the Mohr failure envelope can be approximated by

TABLE 3.8

MINERALOGY OF 0.6 - 1.2mm SIZE FRACTION SAMPLES
WEIGHT PER CENT

	Gedling	Kellingley	Oakdale	Ollerton
Quartz	26.0	6.0	7.0	19.5
Illite	41.5	51.0	53.5	61.0
Kaolinite	11.5	14.0	23.0	13.5
Chlorite	0.0	0.0	0.0	2.0
Ankerite	11.0	0.0	1.0	0.0
Jarosite	0.0	0.0	0.0	0.0
Pyrite	1.0	3.0	1.0	0.0
Coal	9.0	26.5	14.5	5.0

TABLE 3.9
SHEAR PLANE CARBON CONTENT

Sample		Carbon Content (% dry weight)
Gedling	Shear plane	15.8
	Bulk	15.8
Askern	Shear plane	8.0
	Bulk	8.0
Birch Coppice	Shear plane	13.7
	Bulk	12.2

the expression:

$$\tau = m(\sigma')^z$$

The parameters in this expression, m and z , can be approximated by means of a log-log transform upon the failure stress data. $\log m$ is then the y intercept of the reduced major axis line through the transformed points, while z is the gradient of this line. The practical implications of curved Mohr failure envelopes upon stability calculations will be discussed in Chapter 5.

Turning to the residual shear strength, it has been shown that the displacement at which residual is attained is dependent upon the normal stress. As normal stress is increased, less displacement is necessary to attain residual. This is attributed to the rate of particle breakdown increasing with normal stress.

The factors influencing the actual residual strength attained are not known with certainty, and further research on this subject would be useful. It is tentatively suggested that quartz content and final grading may have a bearing on the outcome, with high quartz contents raising the residual strength, whilst a high degree of particle breakdown will lower it.

One point which also emerges from this shear-box work is that the reversing shear-box is a poor means for determining the residual shear strength of colliery spoils below a normal stress level of 400 kN/m^2 . This is due to material being lost through the split in the box. An equilibrium is attained between fines production by particle breakdown and their loss, which gives an apparent value of residual shear strength which is higher than the actual value.

FIGURE 3.1

PEAK SHEAR STRENGTH, 0.6 - 1.2mm SIZE FRACTION
(LINEAR ENVELOPES)

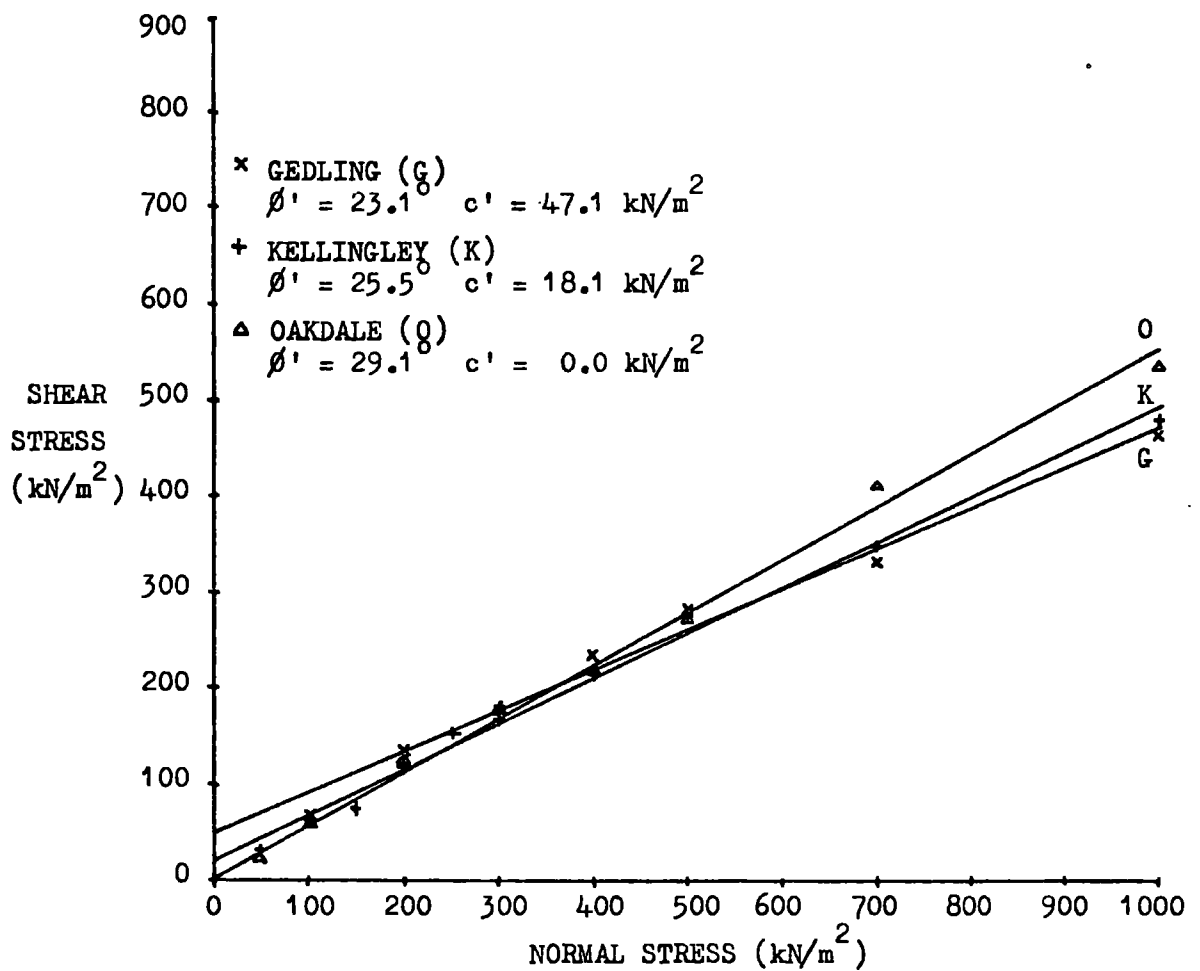


FIGURE 3.2
GEDLING, PARTICLE BREAKDOWN
ON DEAD LOADING

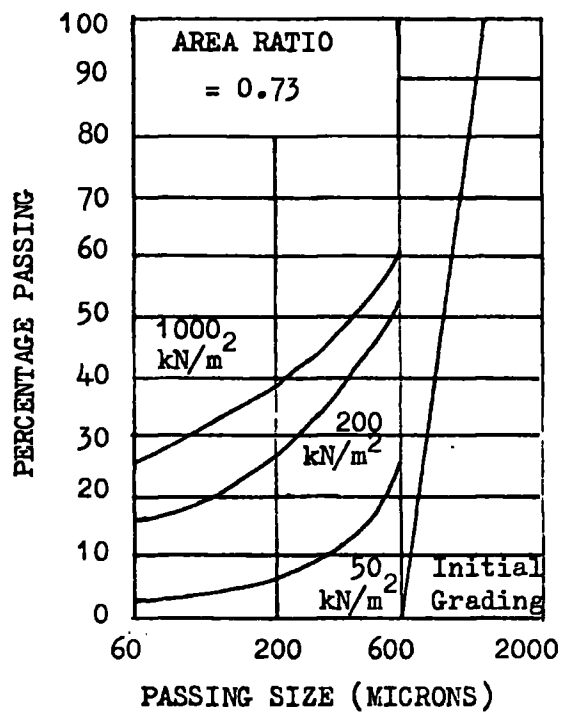


FIGURE 3.3
KELLINGLEY, PARTICLE BREAKDOWN
ON DEAD LOADING

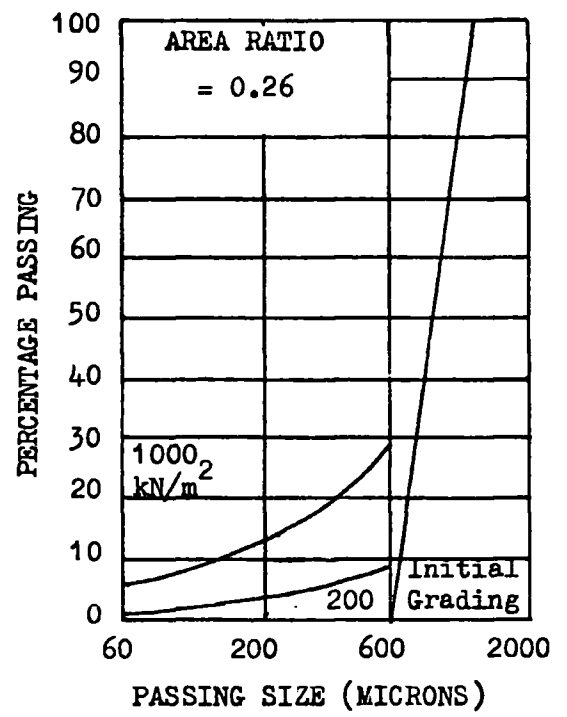


FIGURE 3.4
OAKDALE, PARTICLE BREAKDOWN ON DEAD LOADING

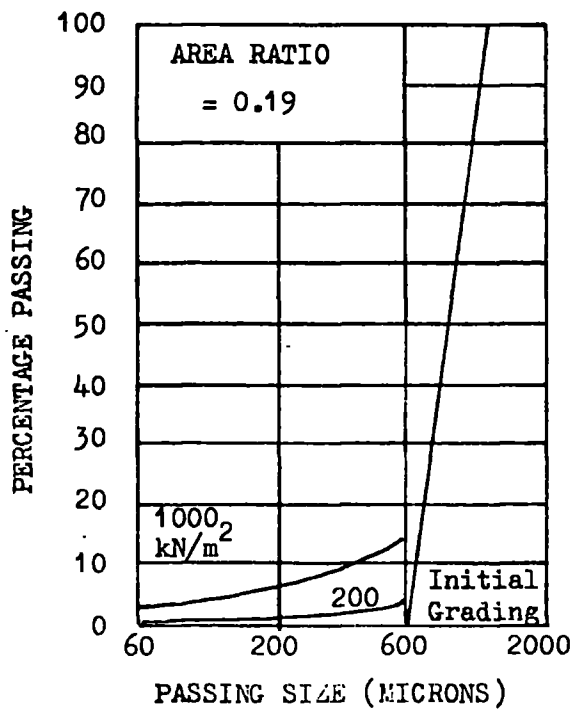


FIGURE 3.5

ϕ'_e FIT TO GEDLING AND KELLINGLEY 0.6 - 1.2mm SIZE FRACTION
SHEAR TESTS

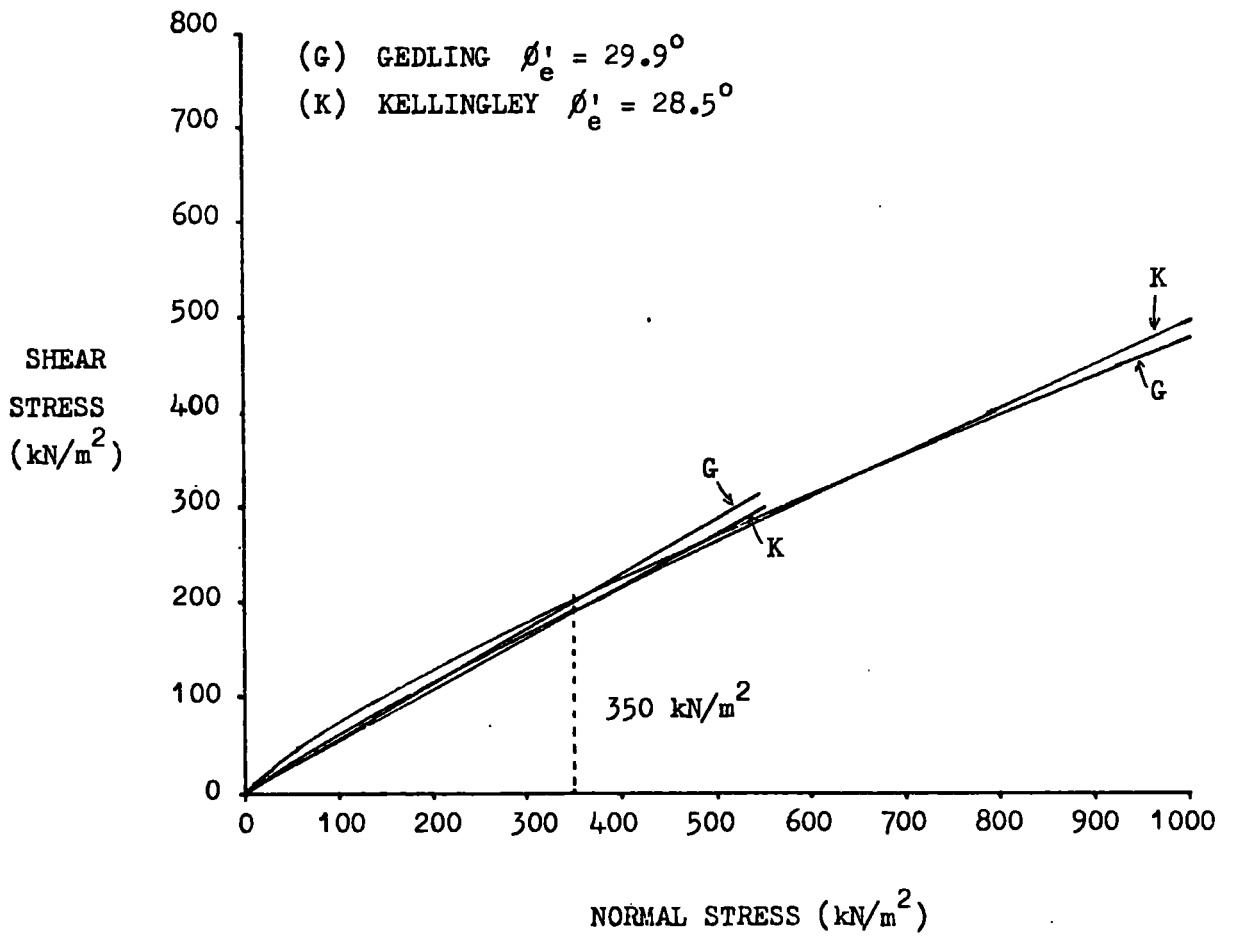


FIGURE 3.6

LOG - LOG PLOT OF KELLINGLEY 0.6 TO 1.2mm SIZE FRACTION
SHEAR TESTS

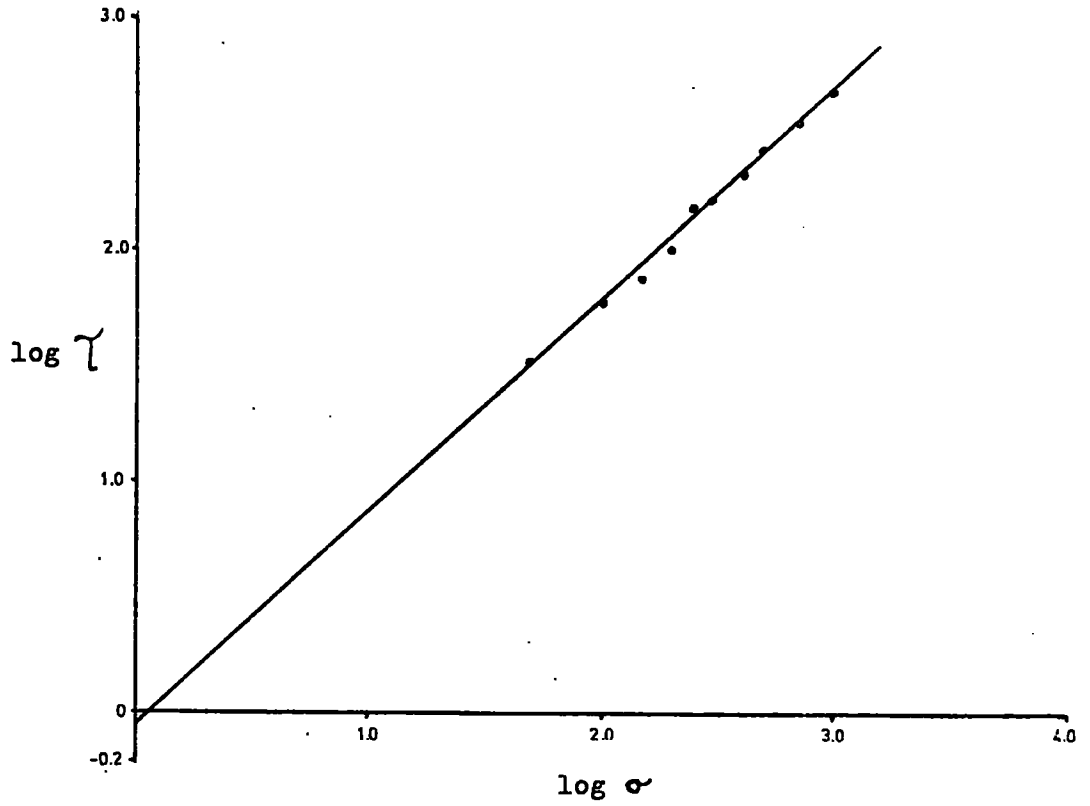


FIGURE 3.7

DEFINITION OF TRIAXIAL FAILURE STRESS POINT

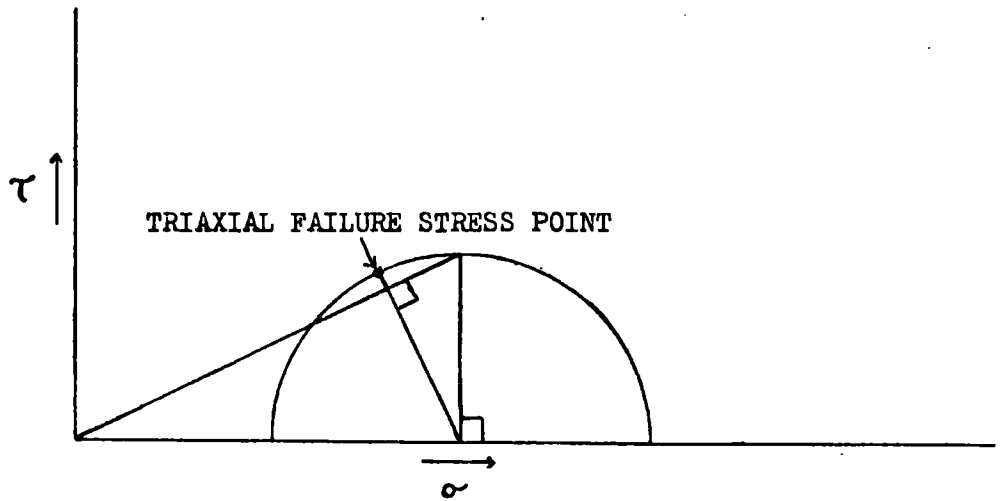


FIGURE 3.9 CYNHEIDRE (DATA, ALLEN, 1973)

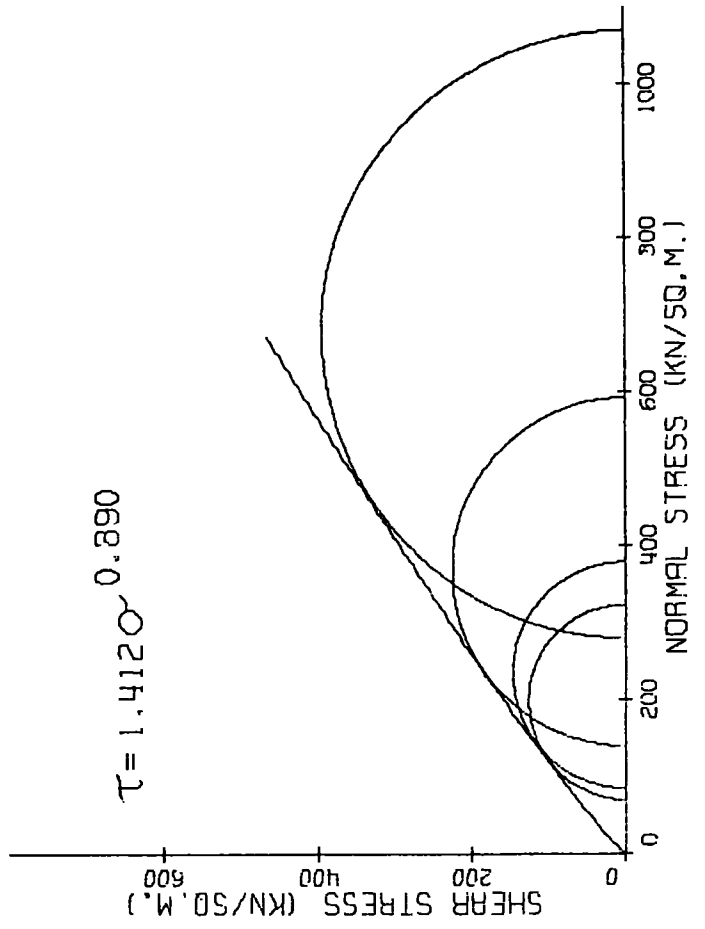


FIGURE 3.8 BIRCH COFFICE (DATA, ALLEN, 1973)

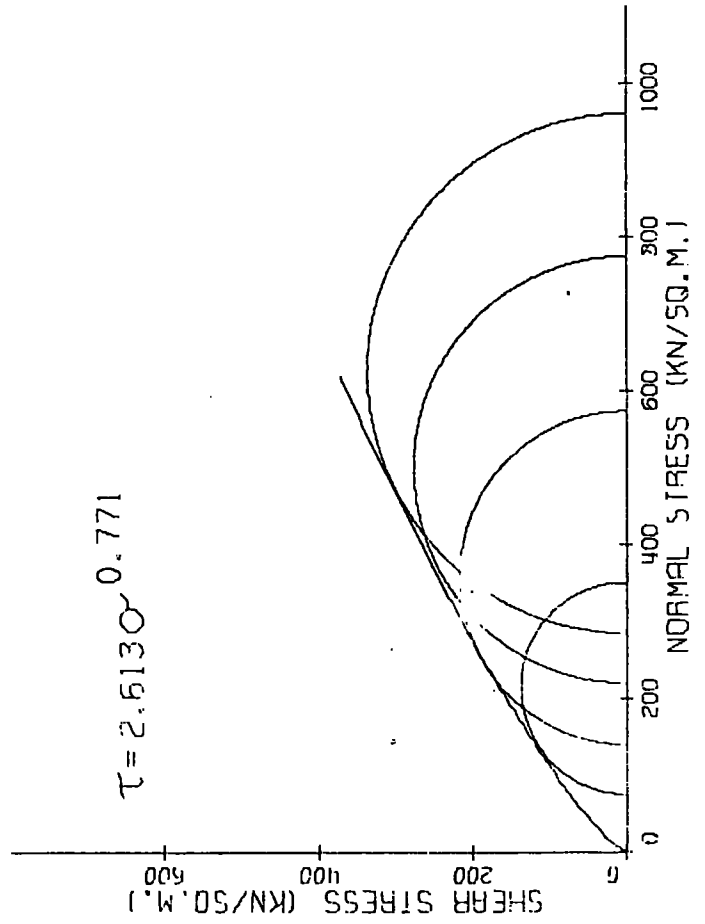
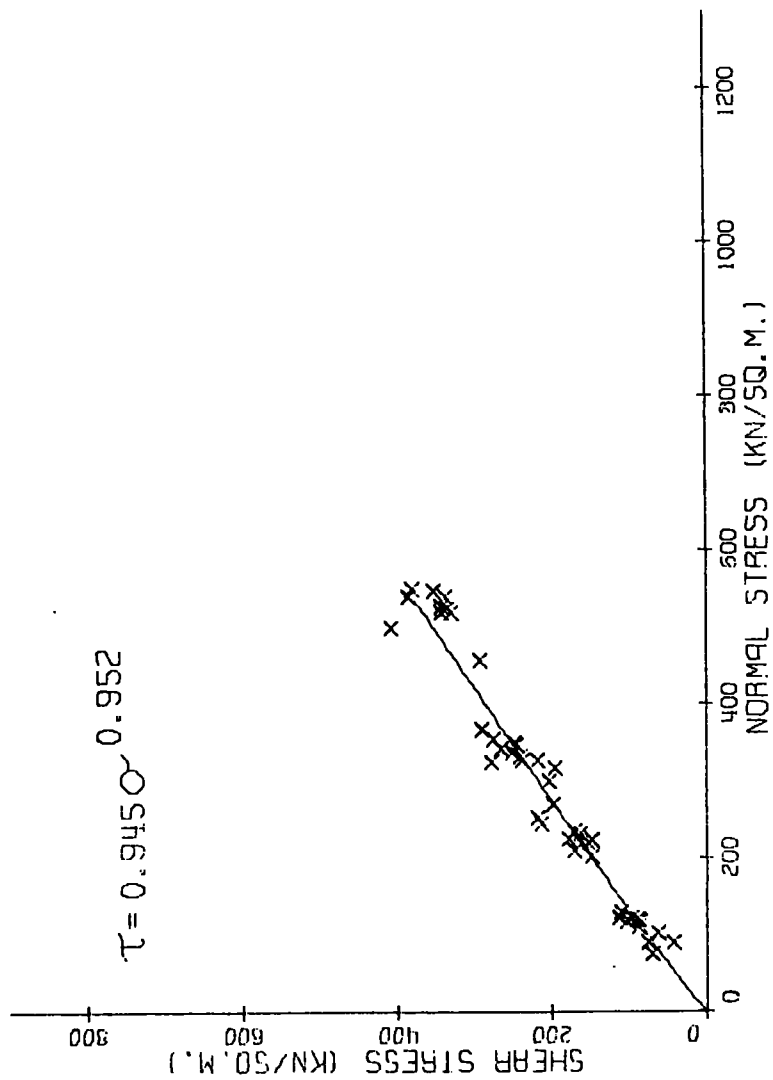


FIGURE 3.10 YORKSHIRE MAIN (DATA; TAYLOR & SPEARS, 1972)



N.B. TRIAXIAL FAILURE STRESS POINTS ONLY
HAVE BEEN PLOTTED FOR CLARITY

FIGURE 3.11 ISABELLA (DATA, MCWILLIAM, 1975)

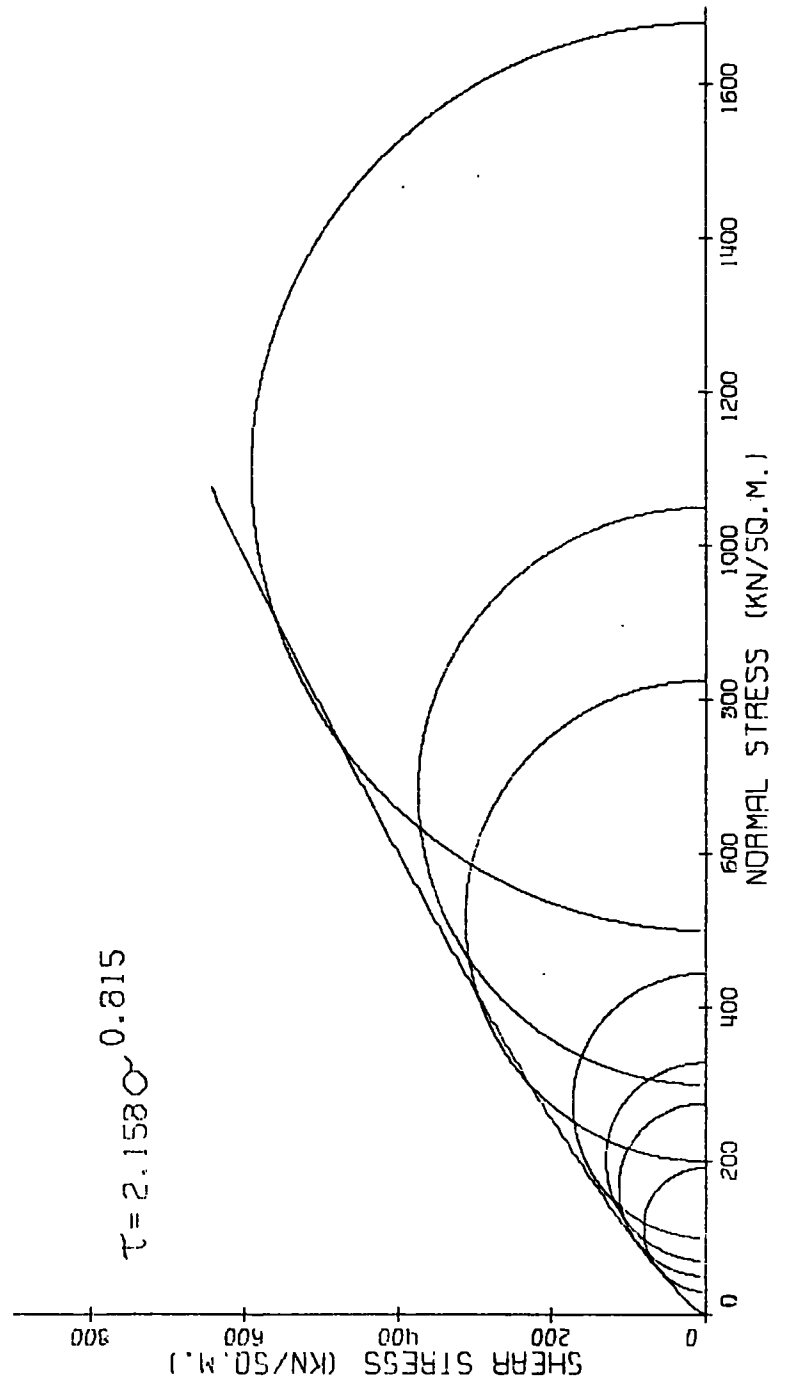


FIGURE 3.12 WEST VIRGINIA, U.S.A. (DATA, BUSCH *et al.*, 1974)

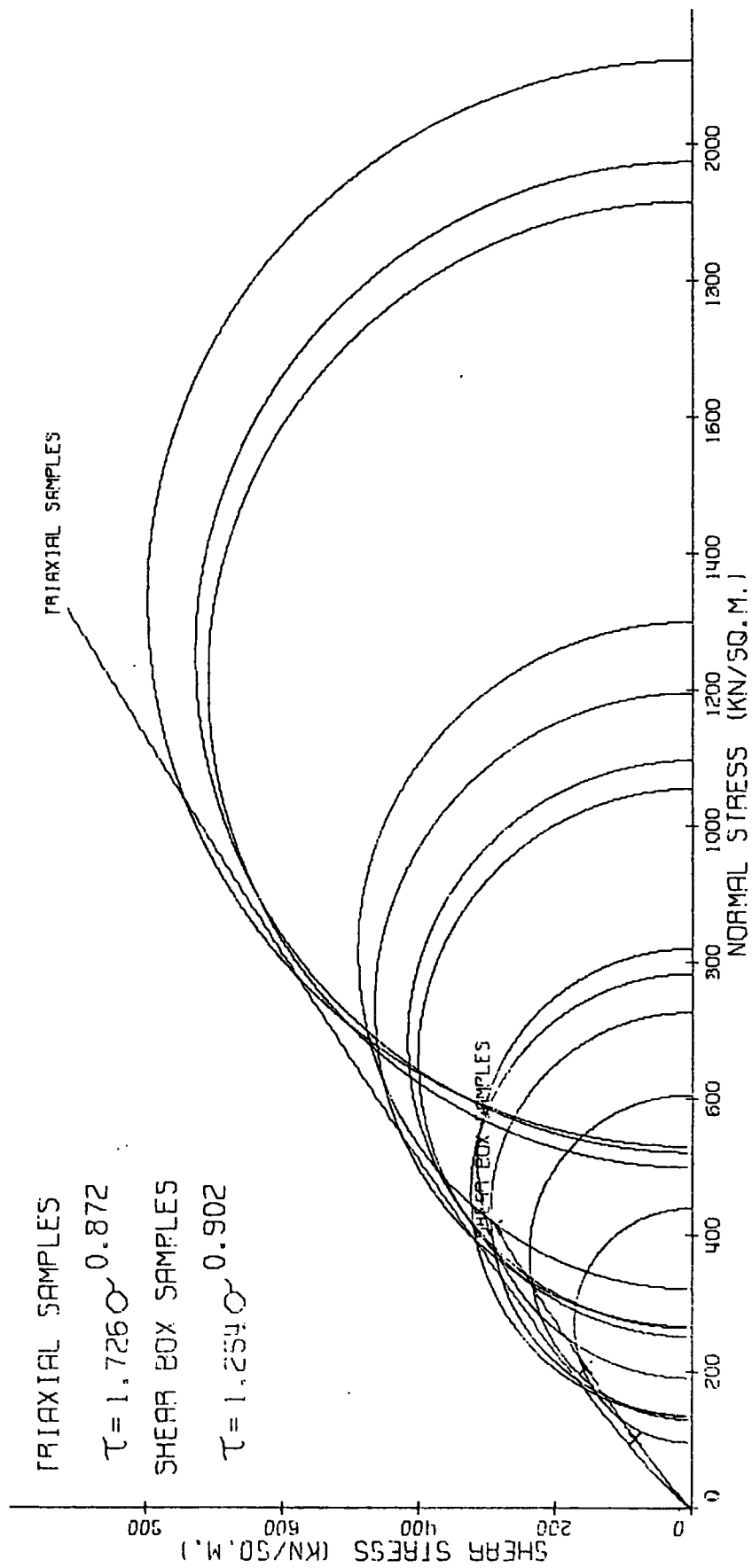
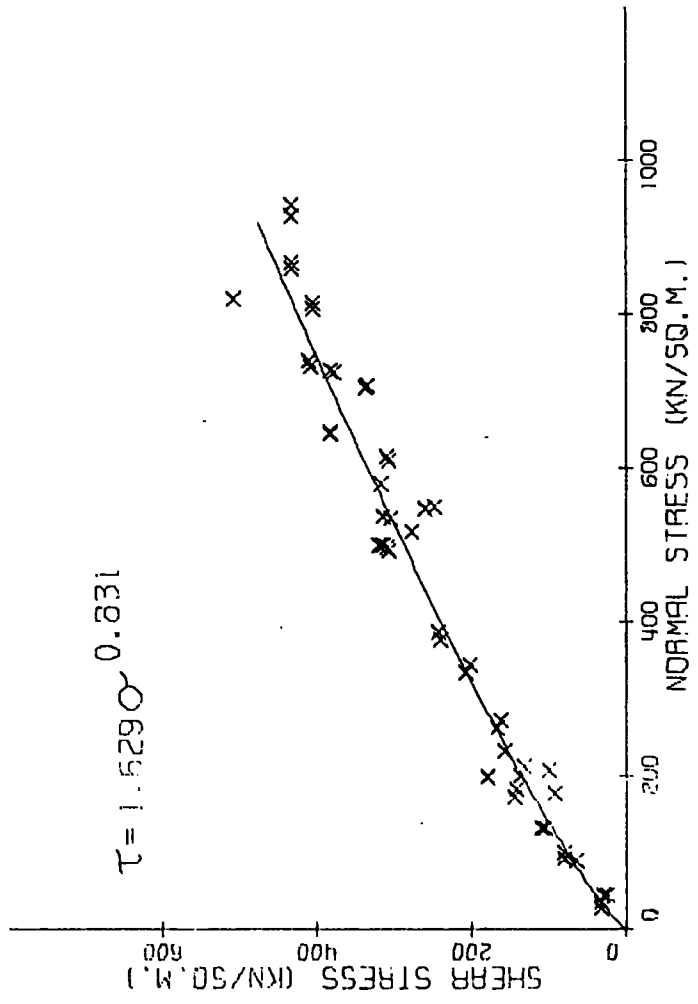


FIGURE 3.13 DENBY HALL



N.B. TRIAXIAL FAILURE STRESS POINTS ONLY
HAVE BEEN PLOTTED FOR CLARITY

FIGURE 3.14 GEDLING TIP, 3-4 MONTHS OLD, COMPOSITE RESULT

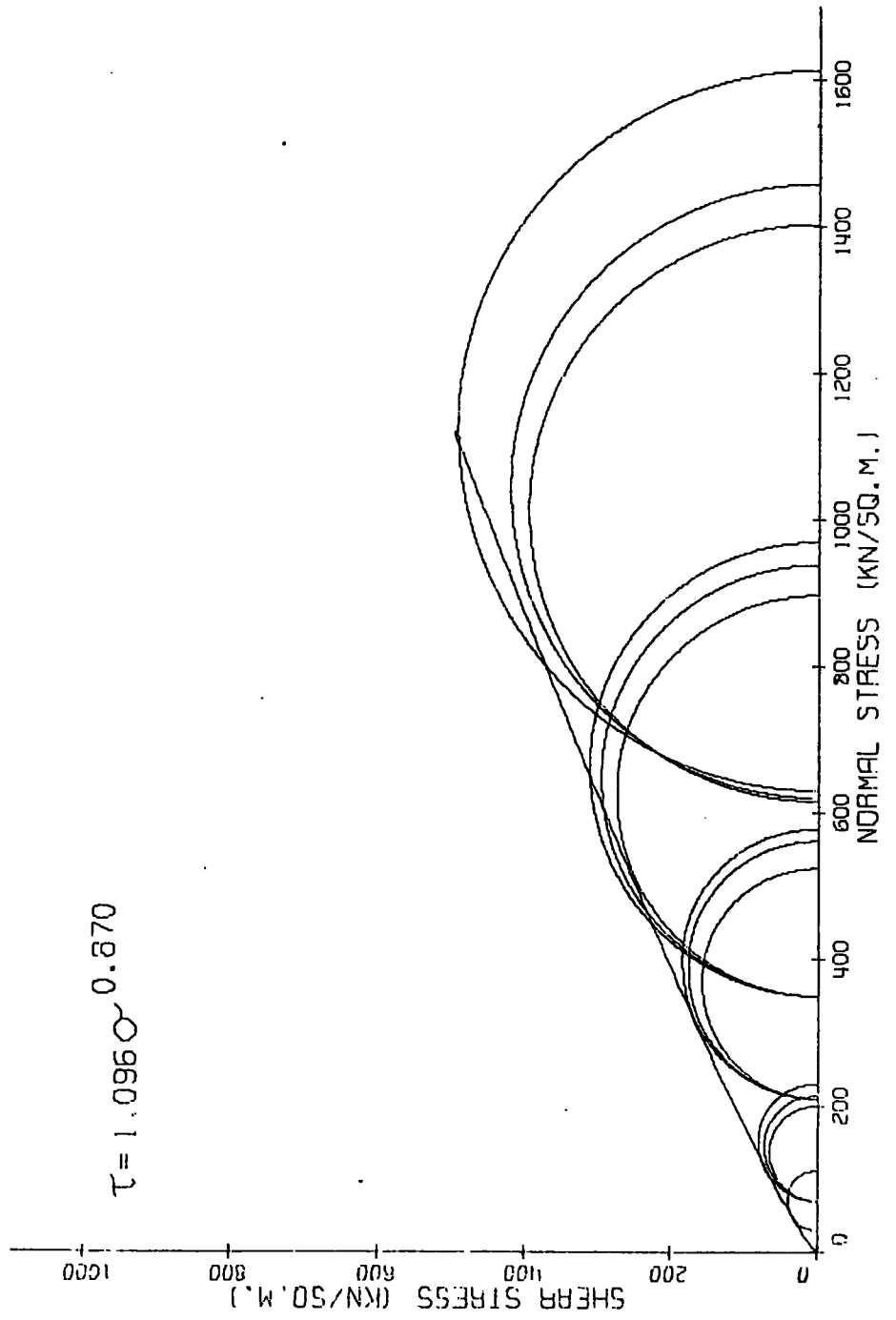


FIGURE 3.15 GEDLING TIP, 3-4 MONTHS OLD. INDIVIDUAL RESULTS

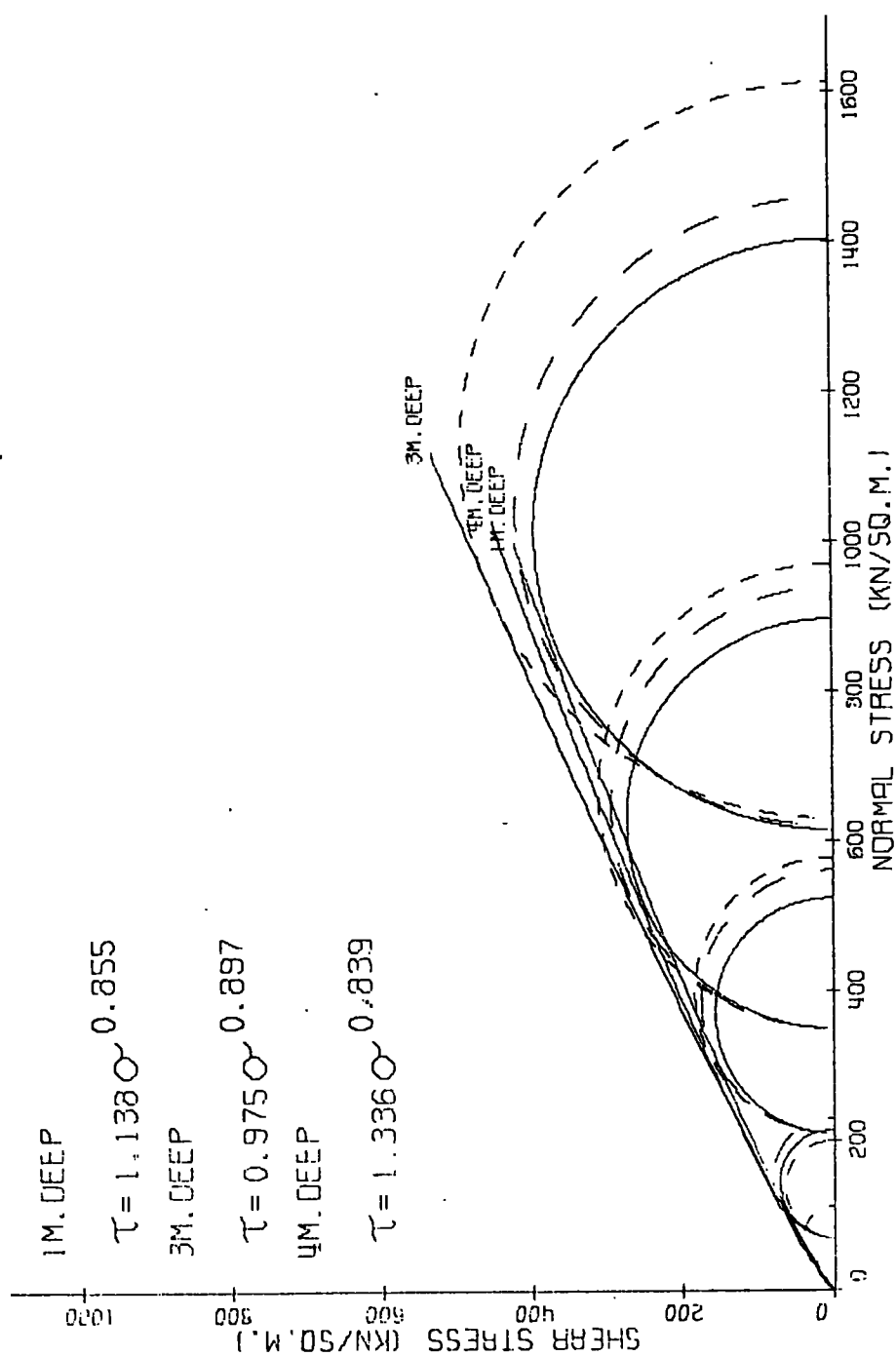


FIGURE 3.16 GEDLING TIP (DATA, WIMPEY, 1968)

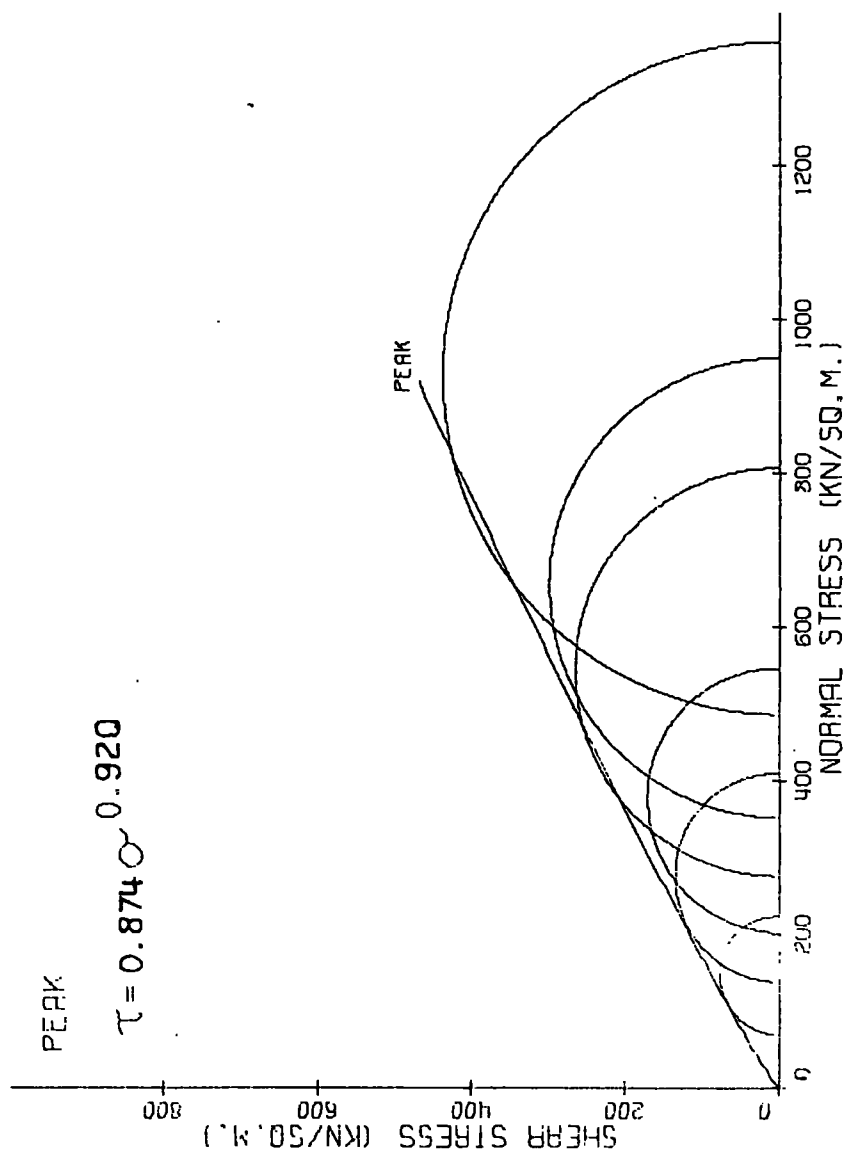


FIGURE 3.17 0.6-1.2MM. SIZE FRACTION, CURVED ENVELOPE, PEAK

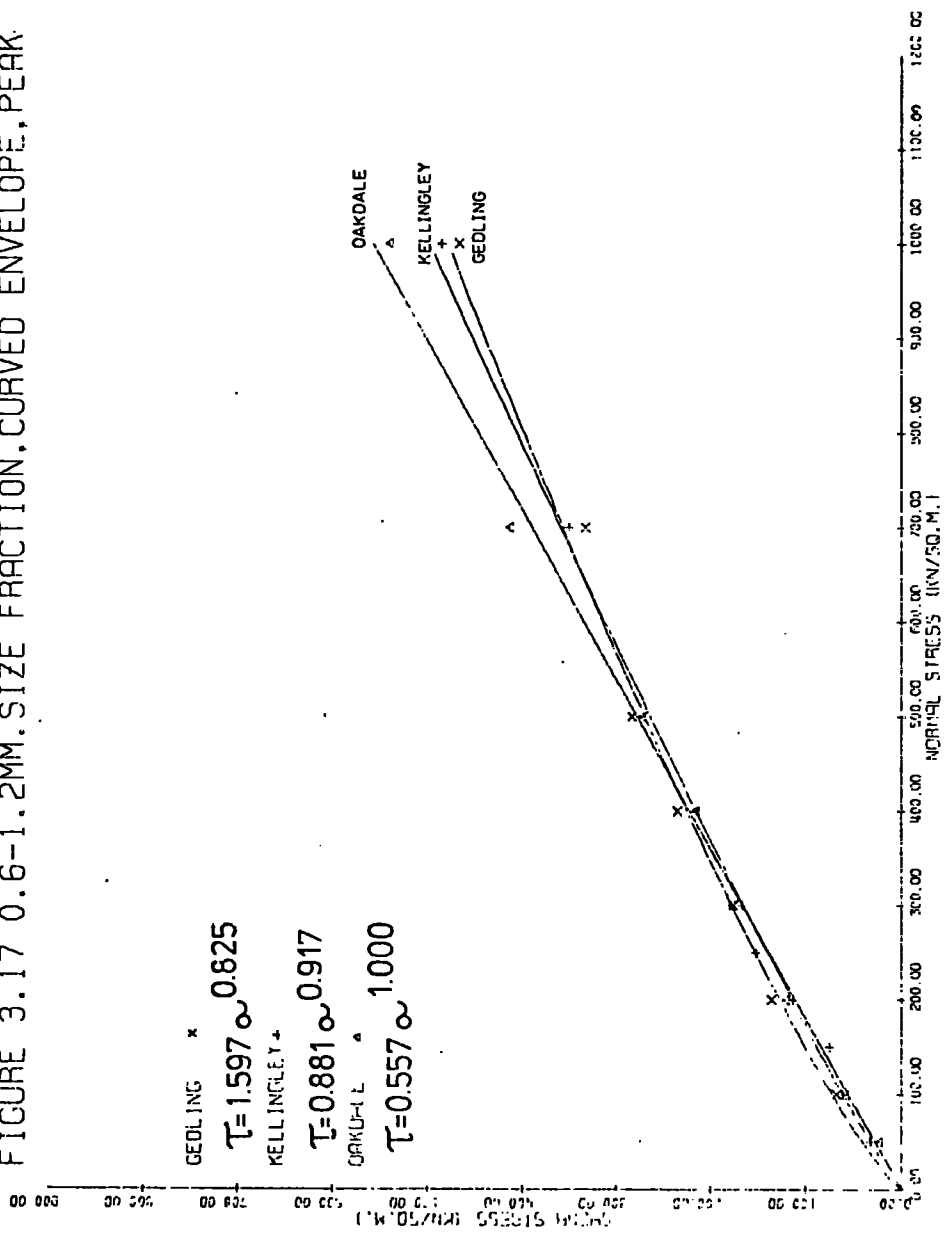


FIGURE 3.18 KELLINGLEY, 8YRS. OLD, ABOVE WATER TABLE

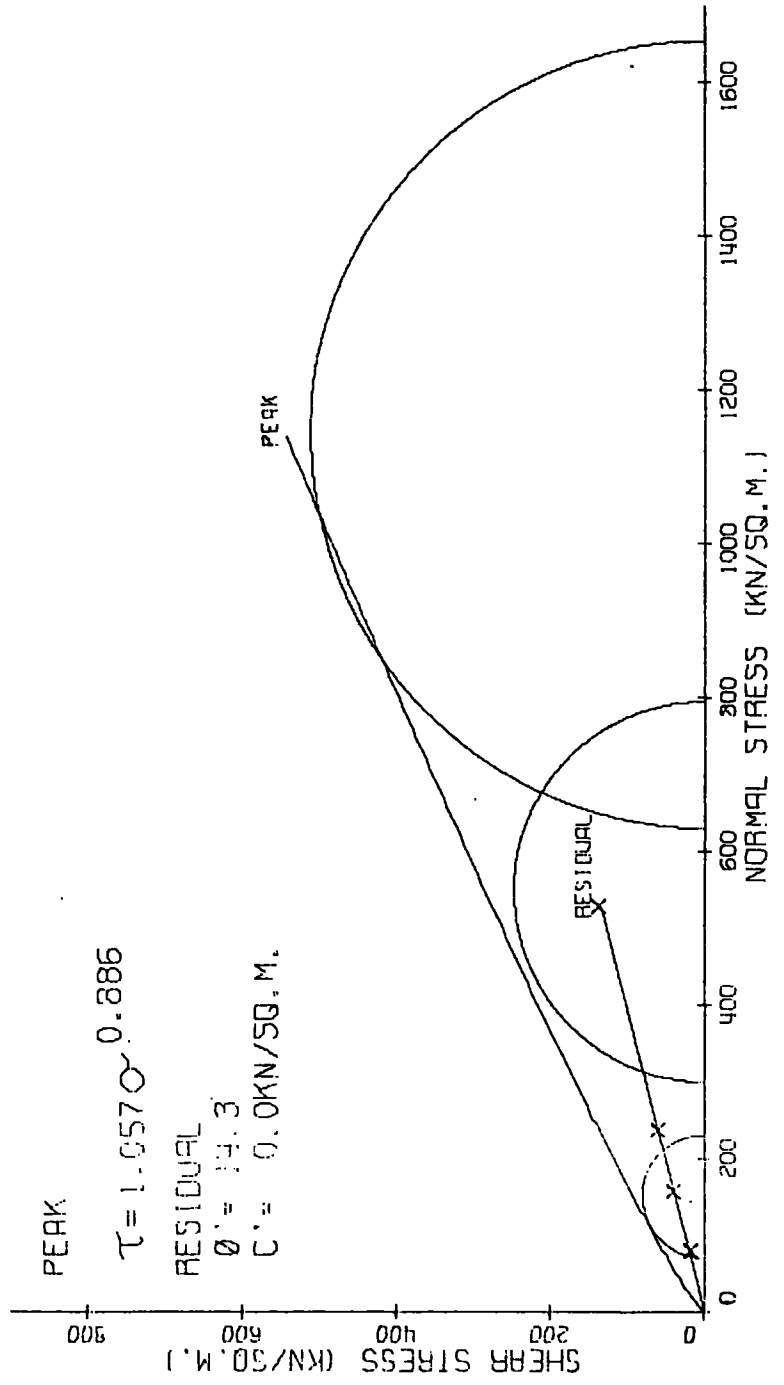


FIGURE 3.19 KELLINGLEY, 8YRS. OLD, BELOW WATER TABLE

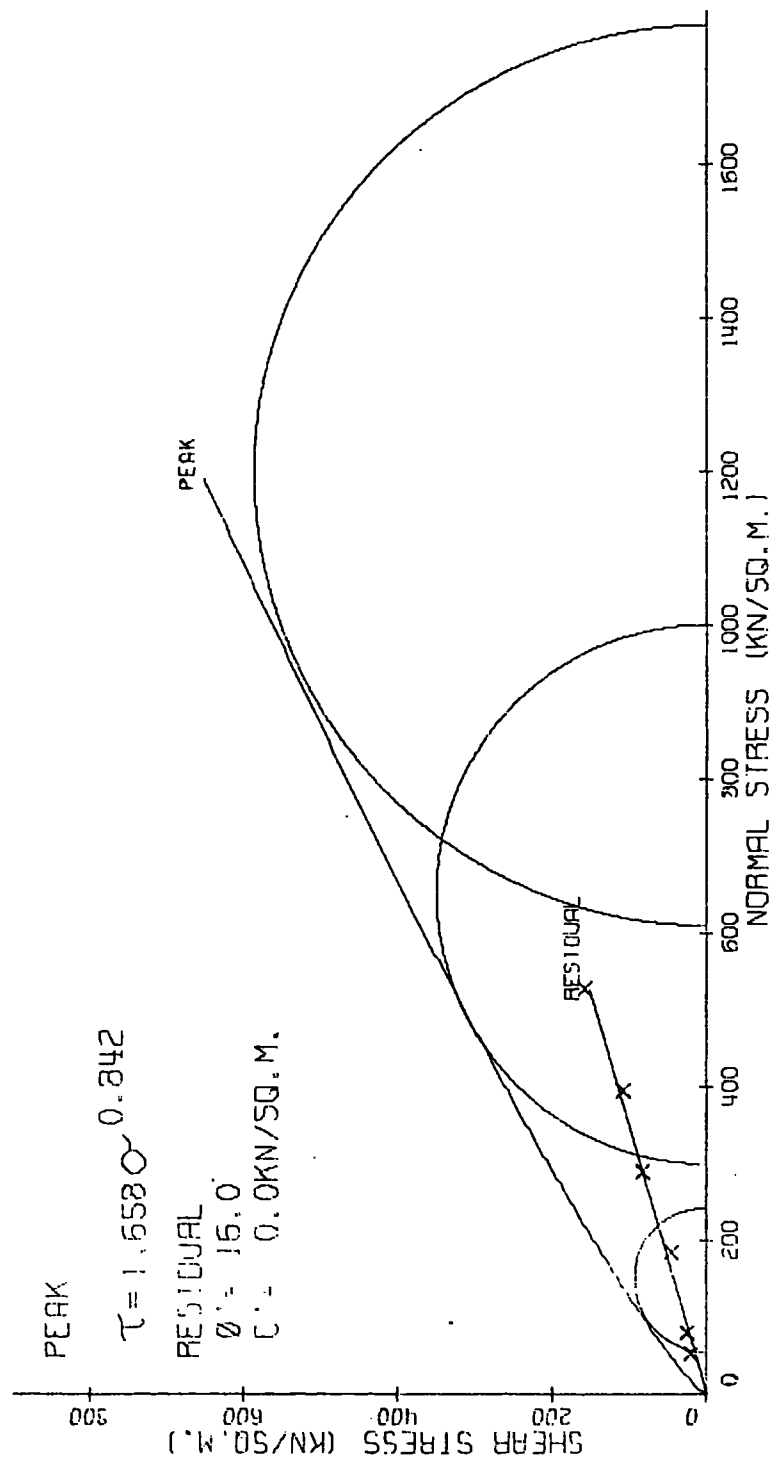


FIGURE 3.20 KELLINGLEY, 6YRS OLD, SHALE BLANKET

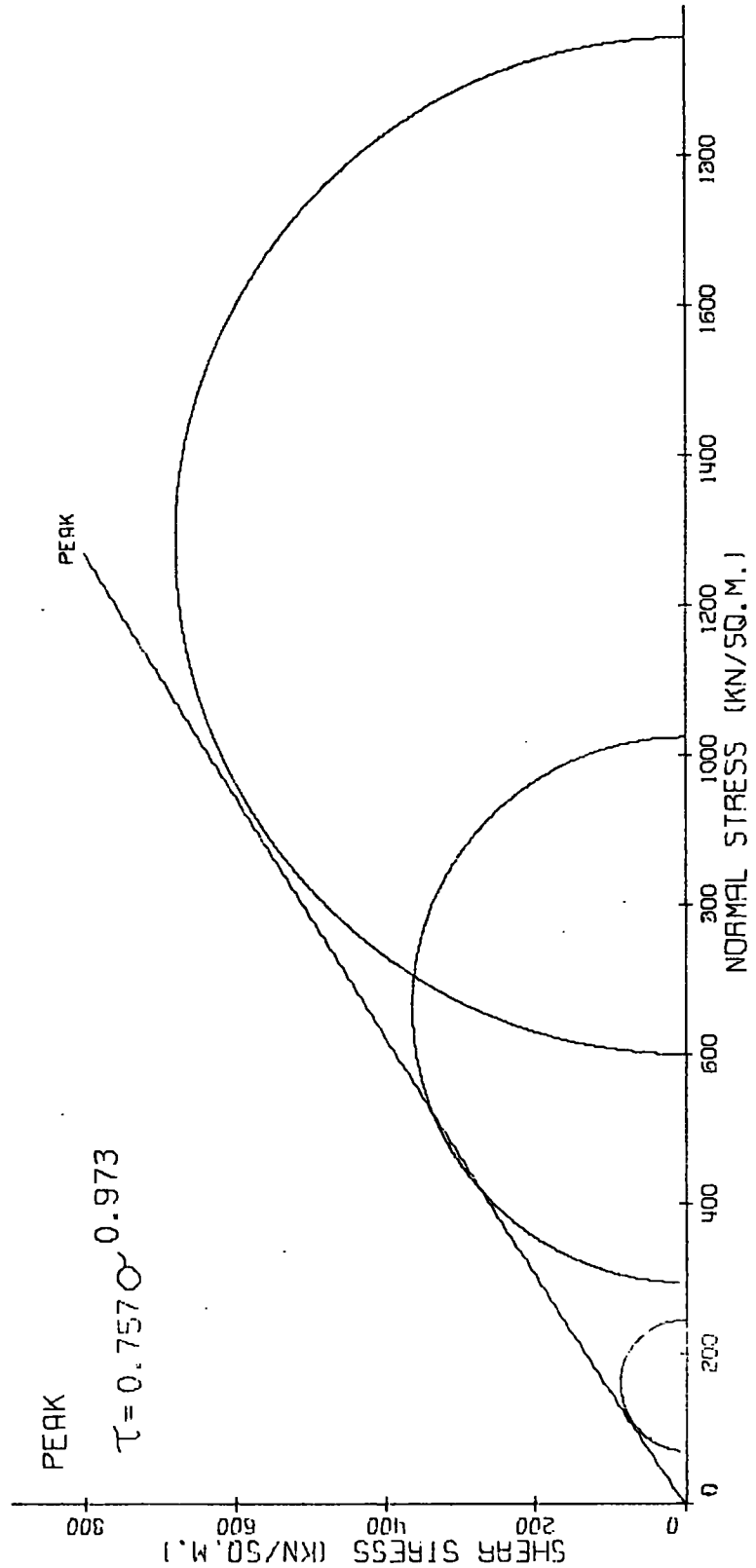


FIGURE 3.21 KELLINGLEY, MINOR HAUL ROAD, MAIN EMBANKMENT

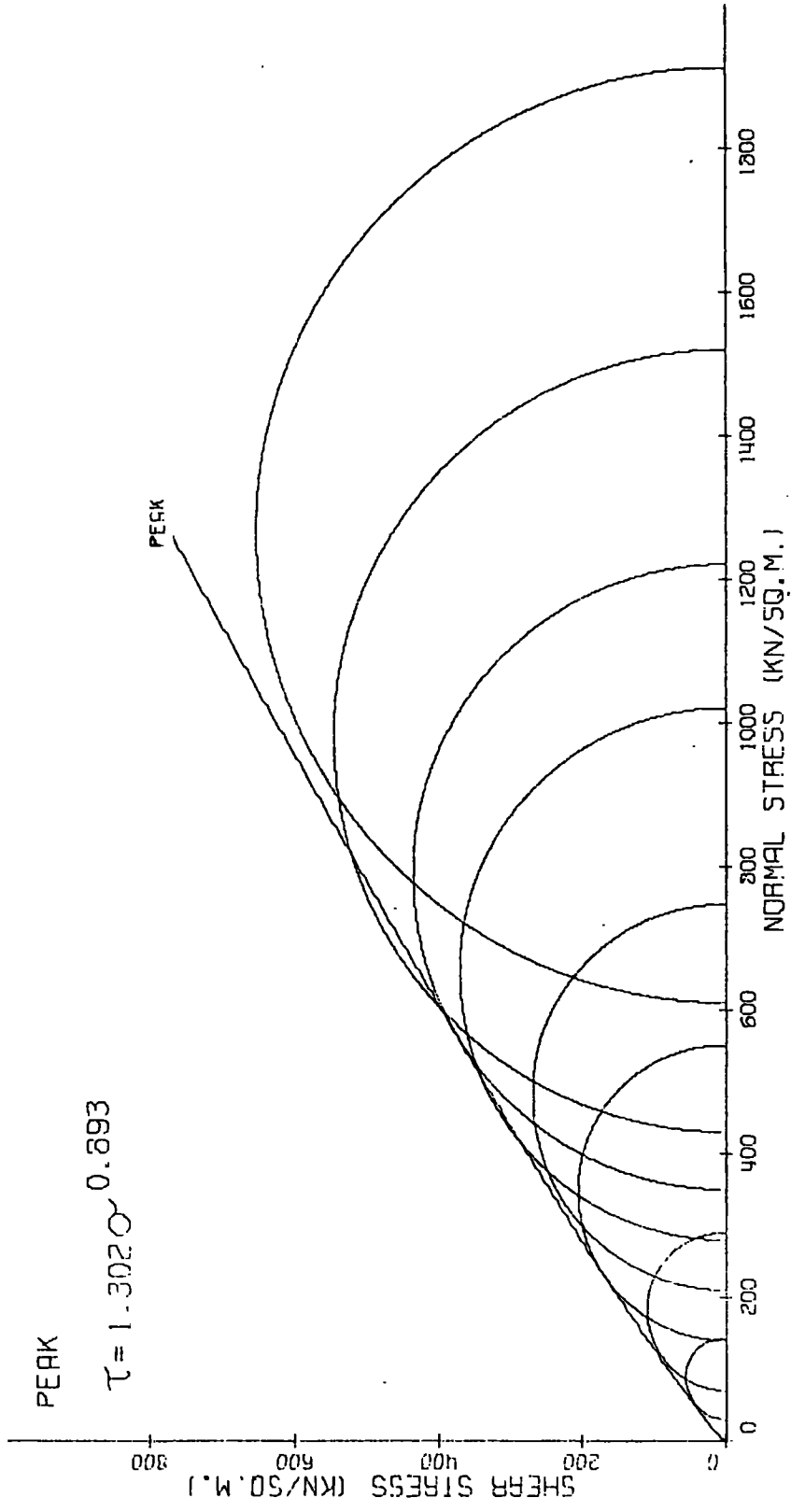


FIGURE 3.22 KELLINGLEY, SPOIL FROM STOCKPILE

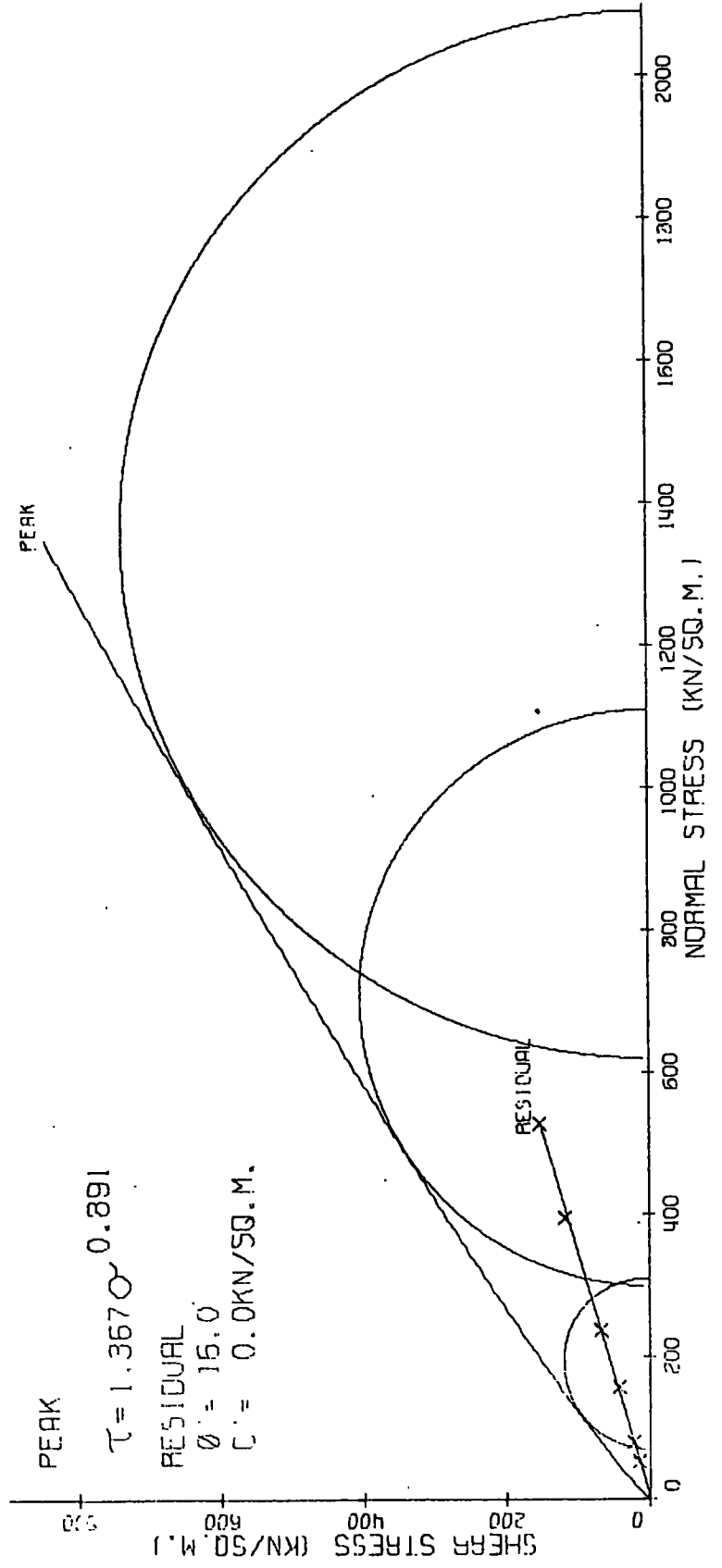


FIGURE 3.23 OAKDALE, COMPOSITE RESULT

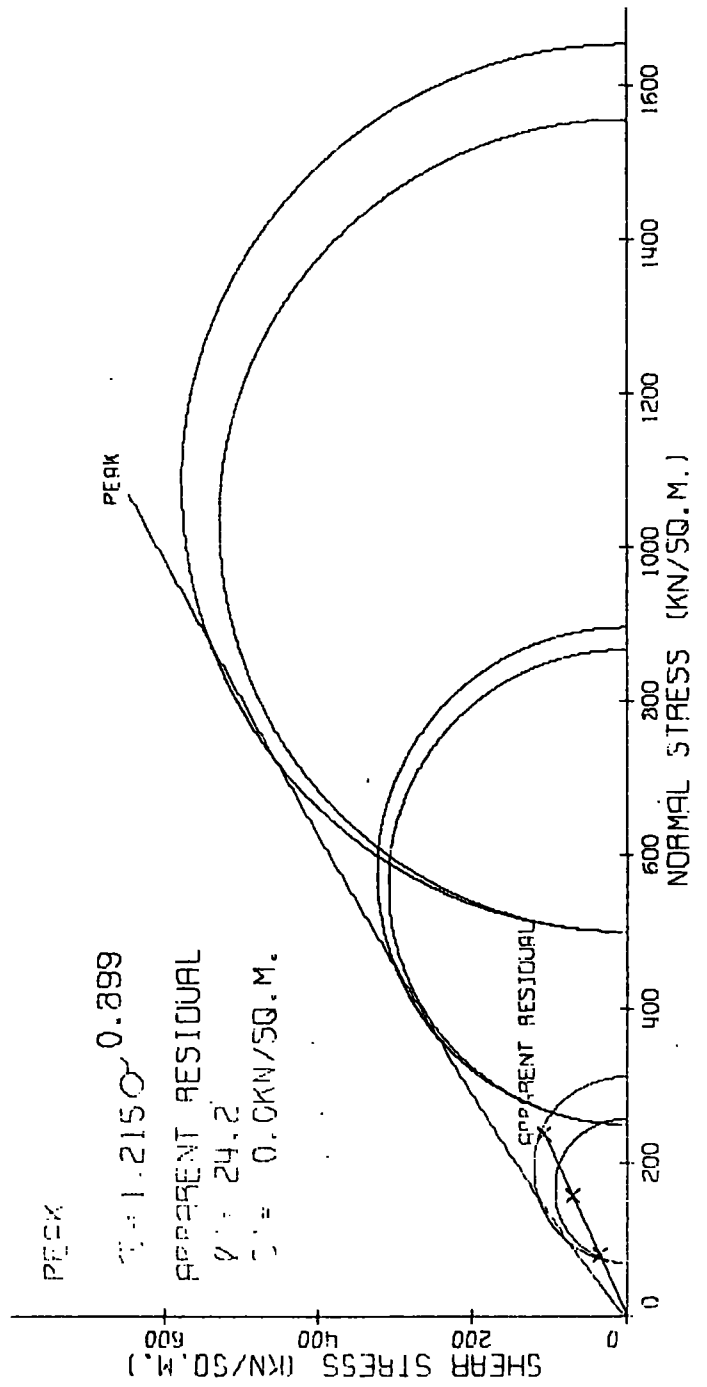


FIGURE 3.24 HORDEN, BURNT SPOIL

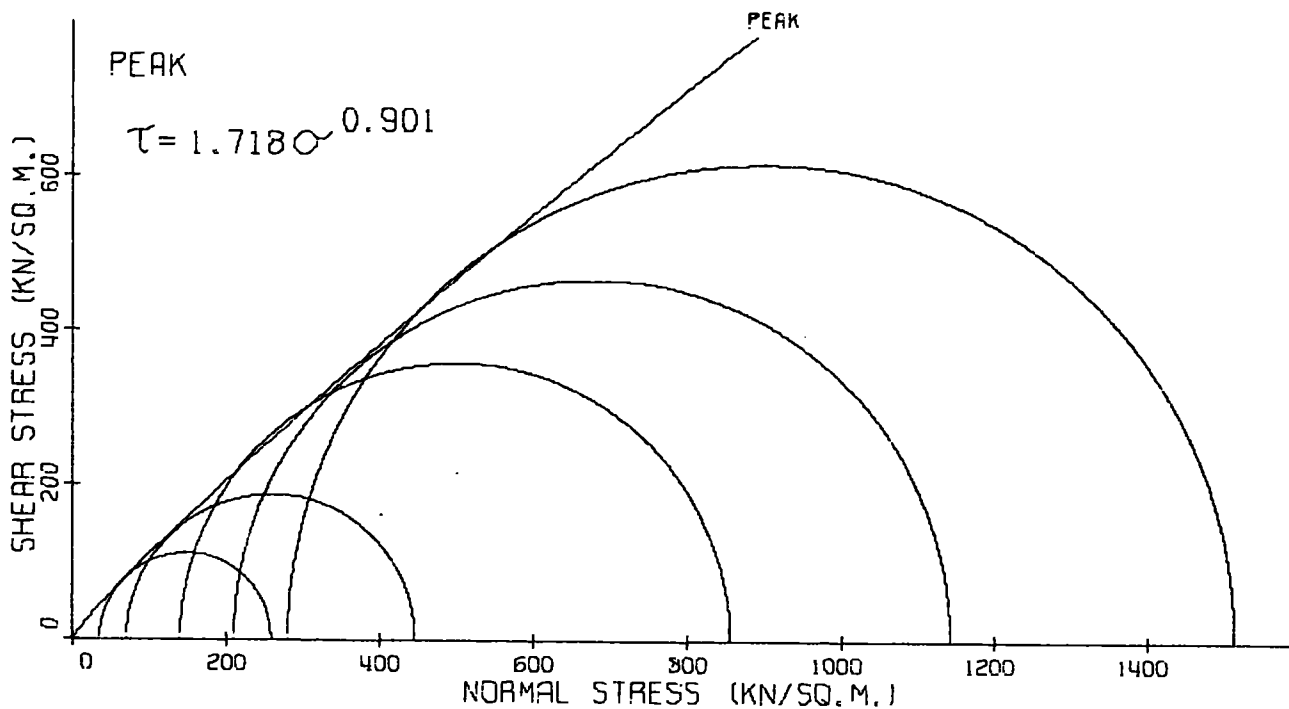


FIGURE 3.25 IRELAND, BURNT SPOIL

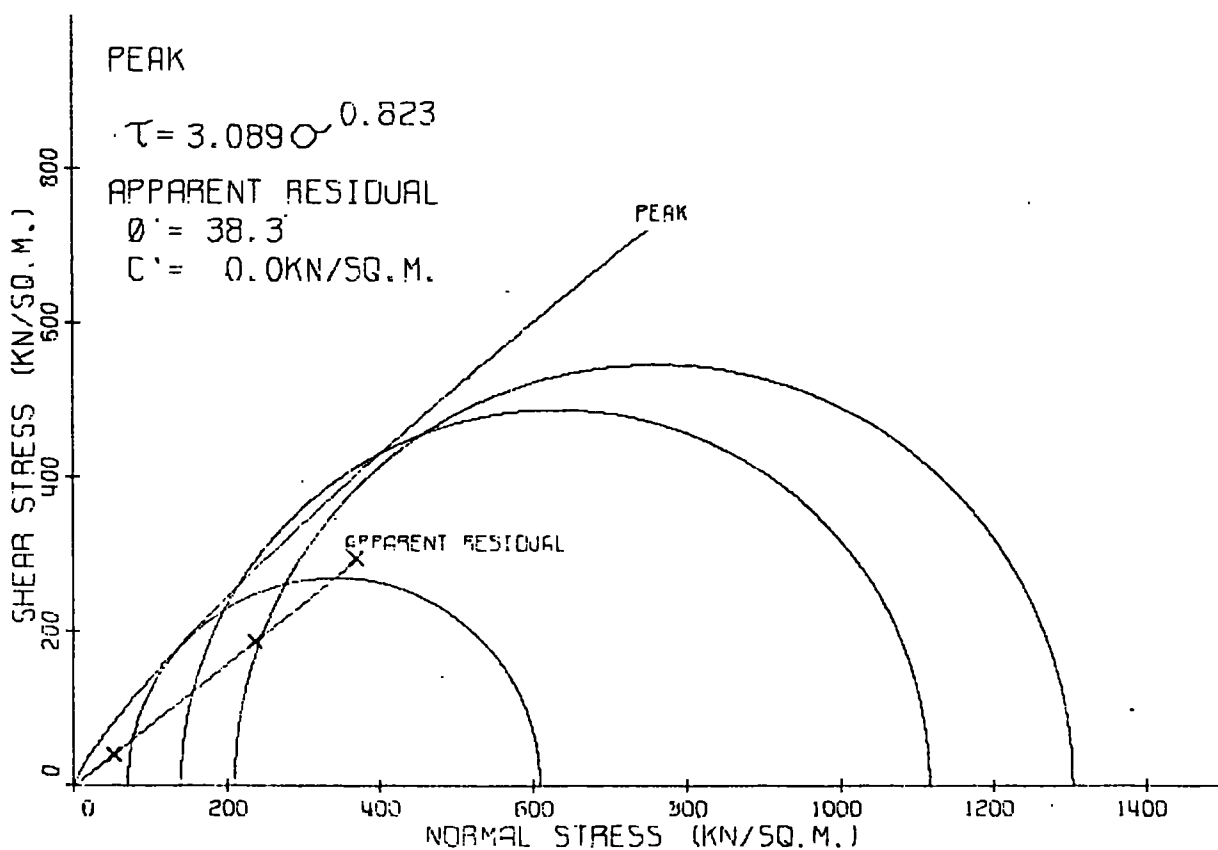


FIGURE 3.26 VARIATION IN SHAPE OF CURVE WITH VARIATION IN VALUE OF PARAMETERS m & z

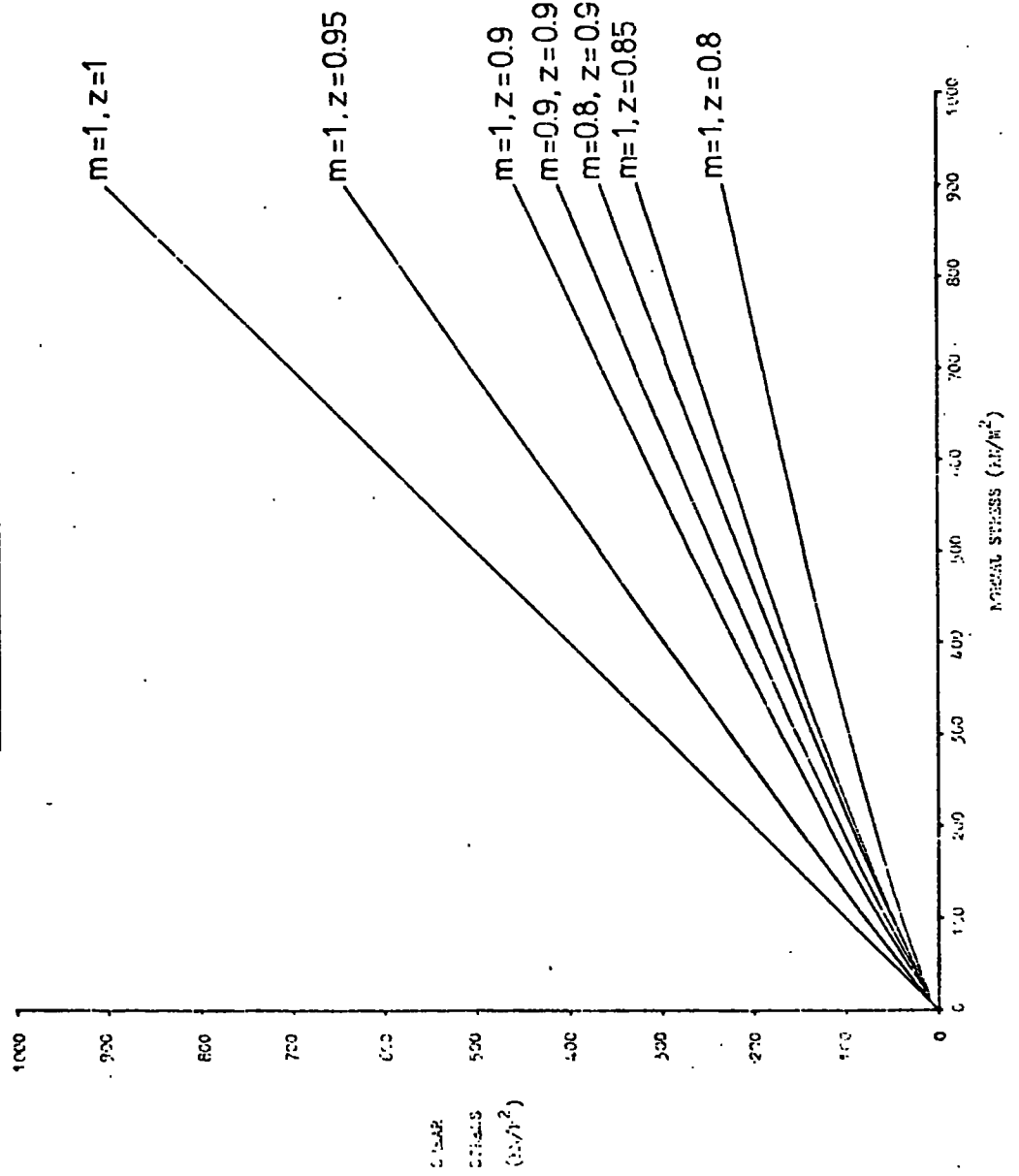


FIGURE 3.27

(FIGURE 3.41, RAJSEK, 1973)

Ollerton discard
stress displacement curves for different normal stresses

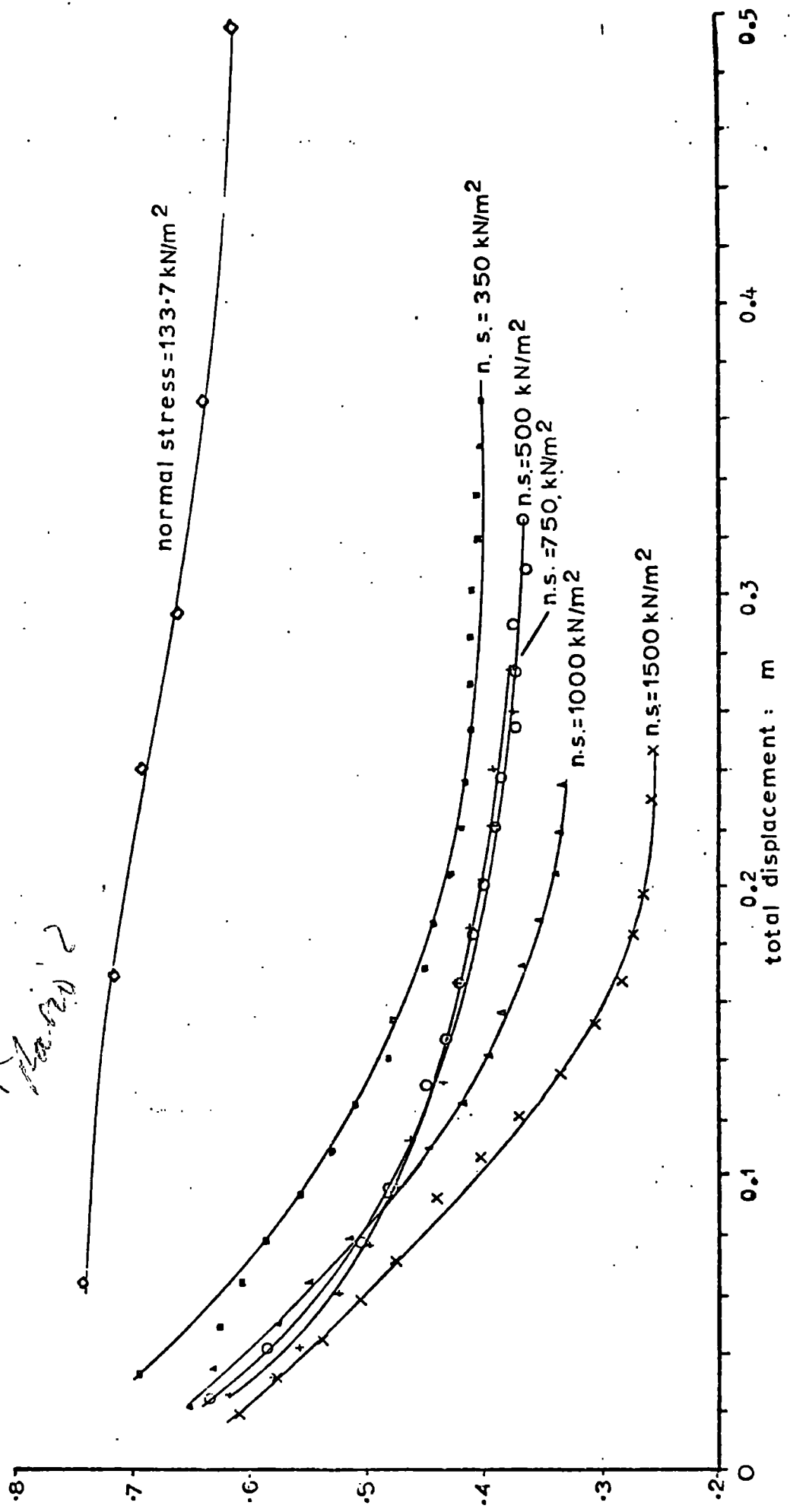


FIGURE 3.28

(FIGURE 3.42, RATSEY, 1973)

Ollerton discard, peak and residual failure envelopes, 0.6-1.2mm size fraction

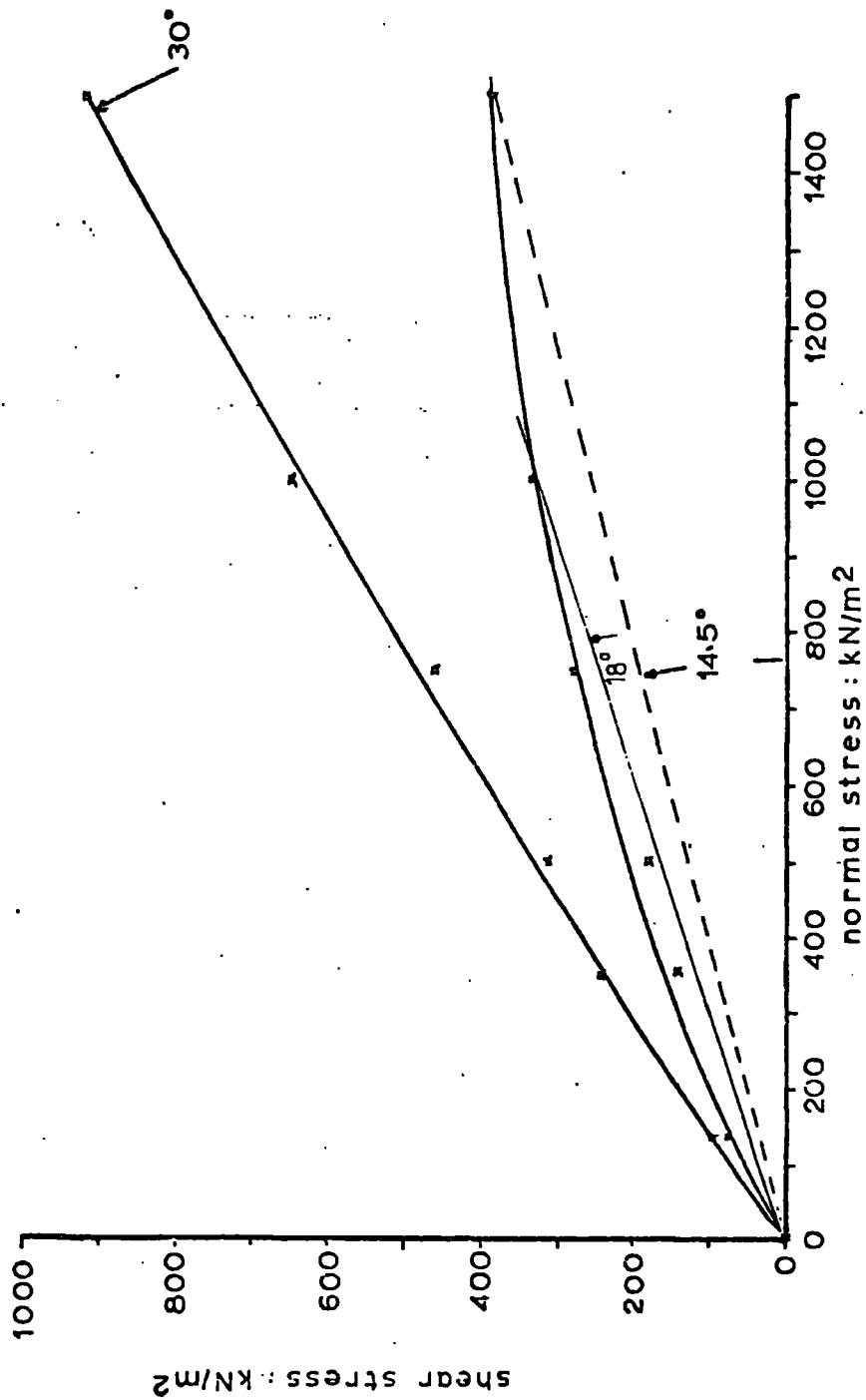


FIGURE 3.29

GEDLING 0.6-1.2mm SIZE FRACTION, STRESS RATIO - DISPLACEMENT CURVES

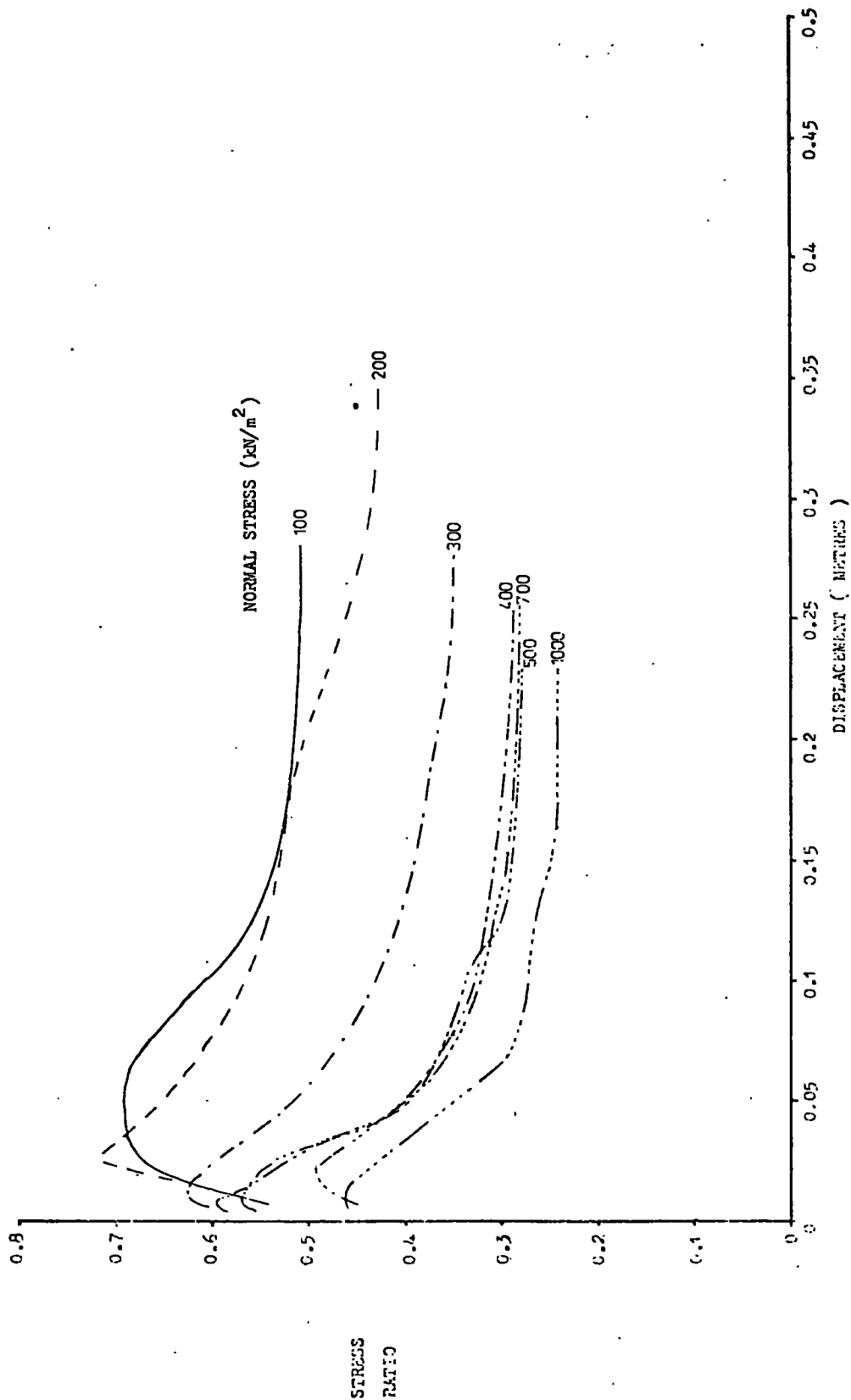


FIGURE 3.30

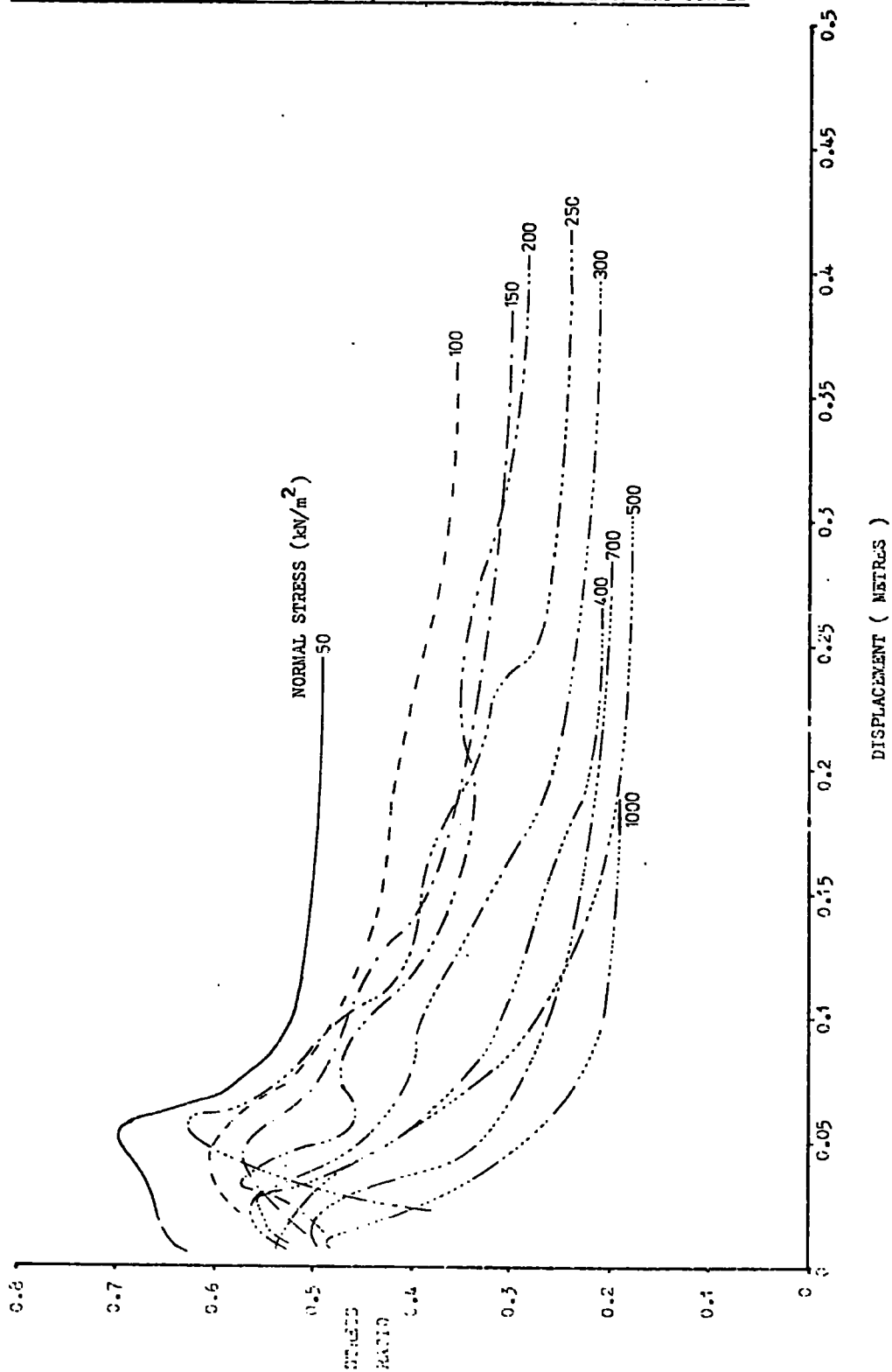
KELINGLEY 0.6-1.2mm SIZE FRACTION, STRESS RATIO - DISPLACEMENT CURVES

FIGURE 3.31

OAKDALE 0.6-1.2mm SIZE FRACTION, STRESS RATIO - DISPLACEMENT CURVES

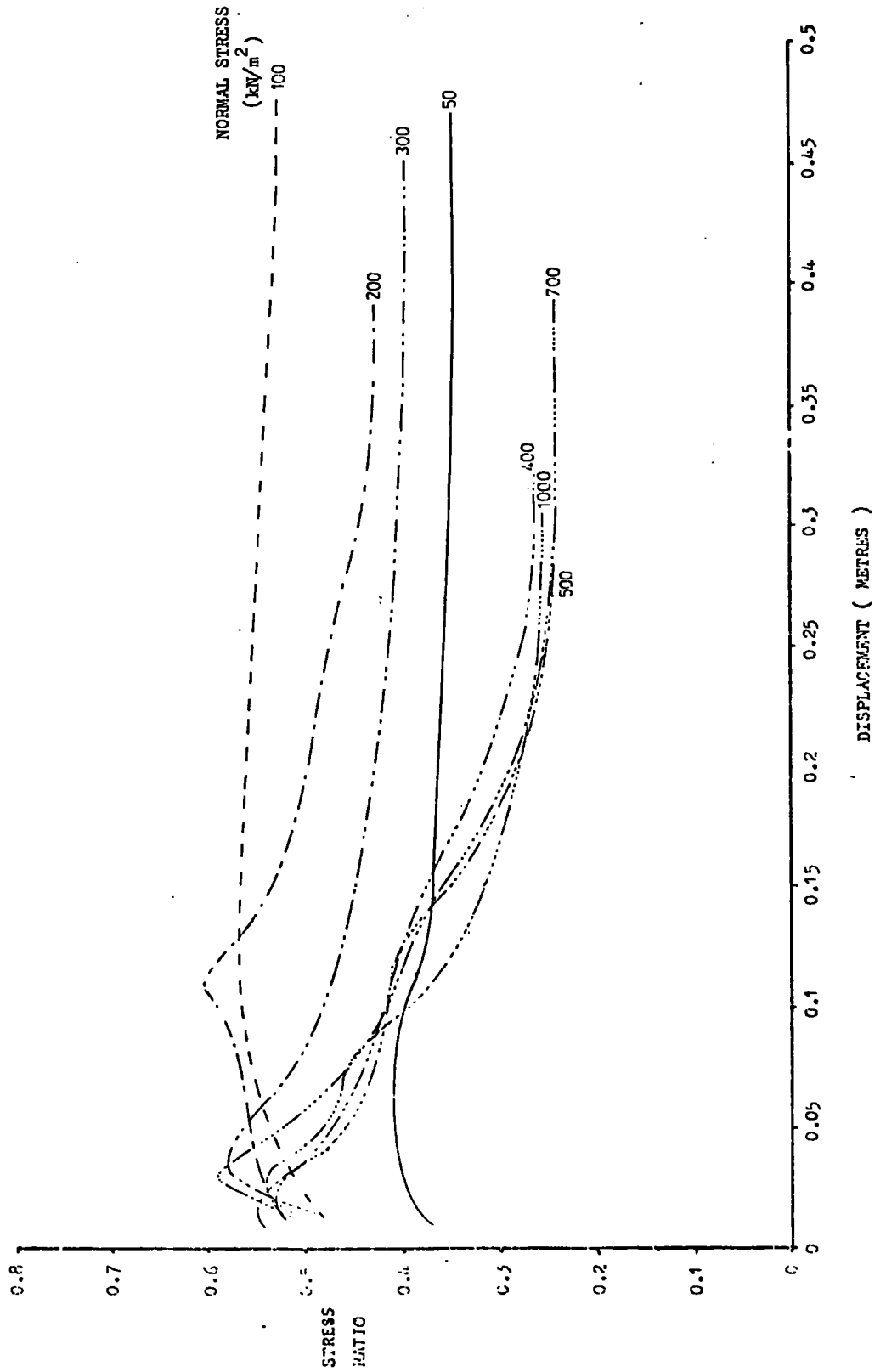


FIGURE 3.32

GEDLINT 0.6-1.2mm SIZE FRACTION, GRADING AFTER SHEARING

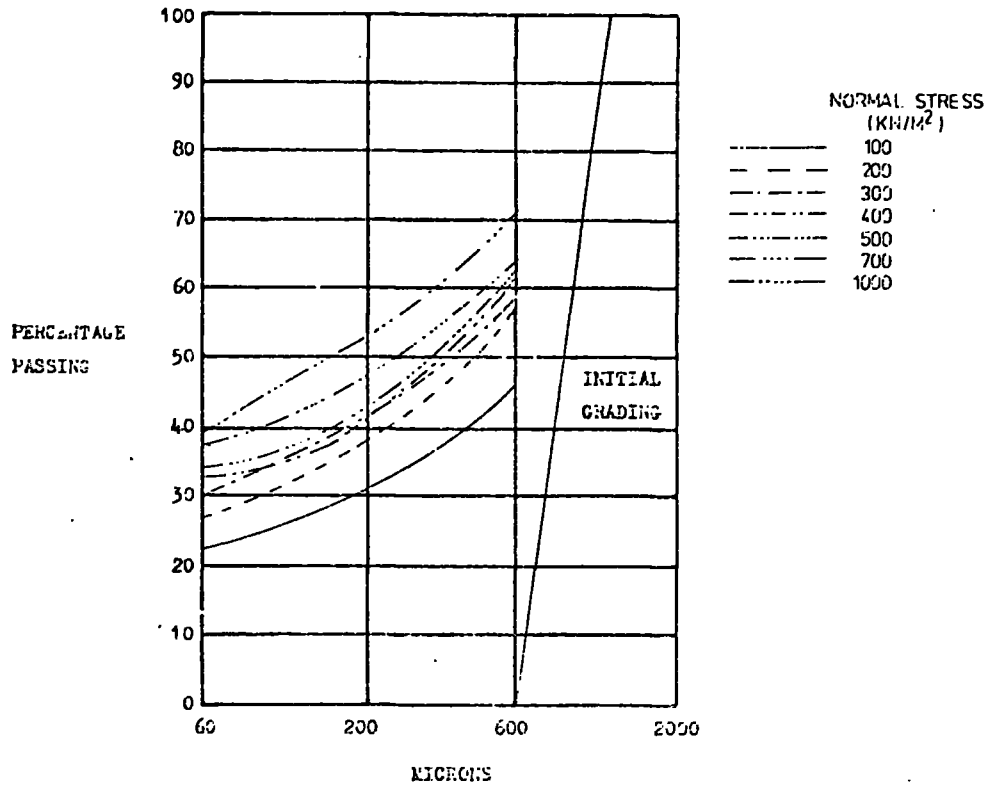


FIGURE 3.33

HELLINGLEY 0.6-1.2mm SIZE FRACTION, GRADING AFTER SHEARING

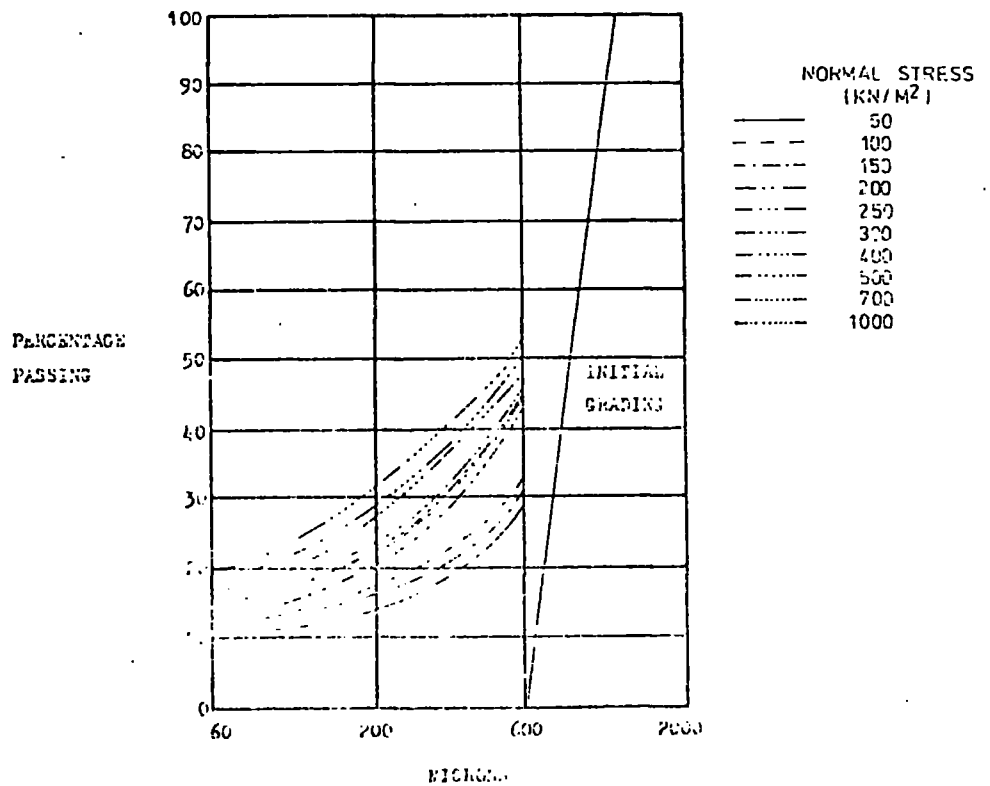


FIGURE 3.34

OSKDALE 0.6-1.2mm SIZE FRACTION, GRADING AFTER SHEARING

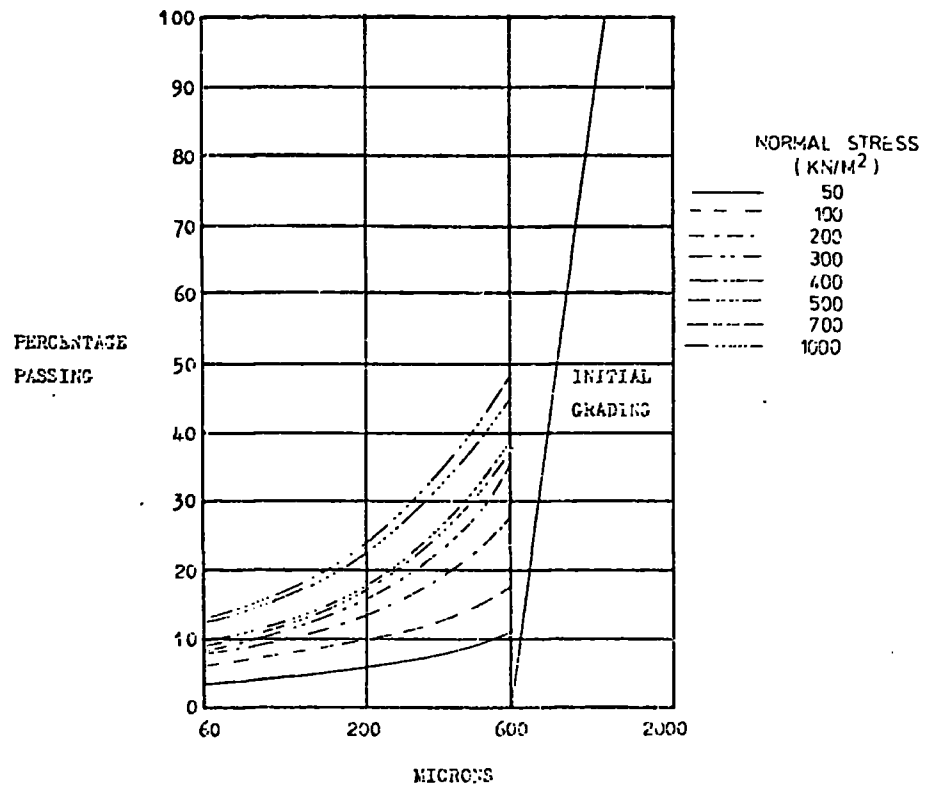


FIGURE 3.35 0.6-1.2MM SIZE FRACTION, RESIDUAL-GEDLING

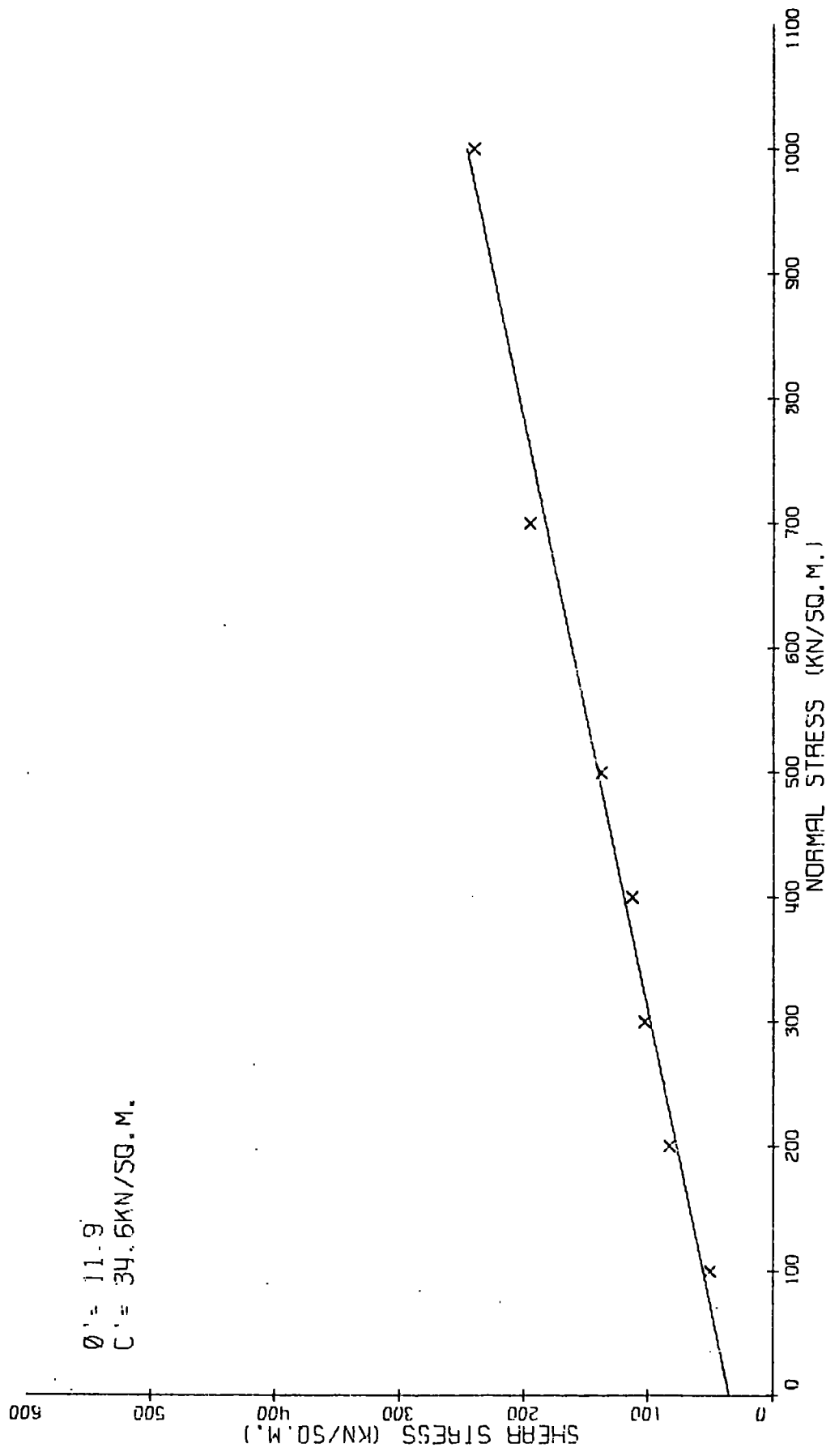


FIGURE 3.36 0.6-1.2MM SIZE FRACTION, RESIDUAL-KELLINGLEY

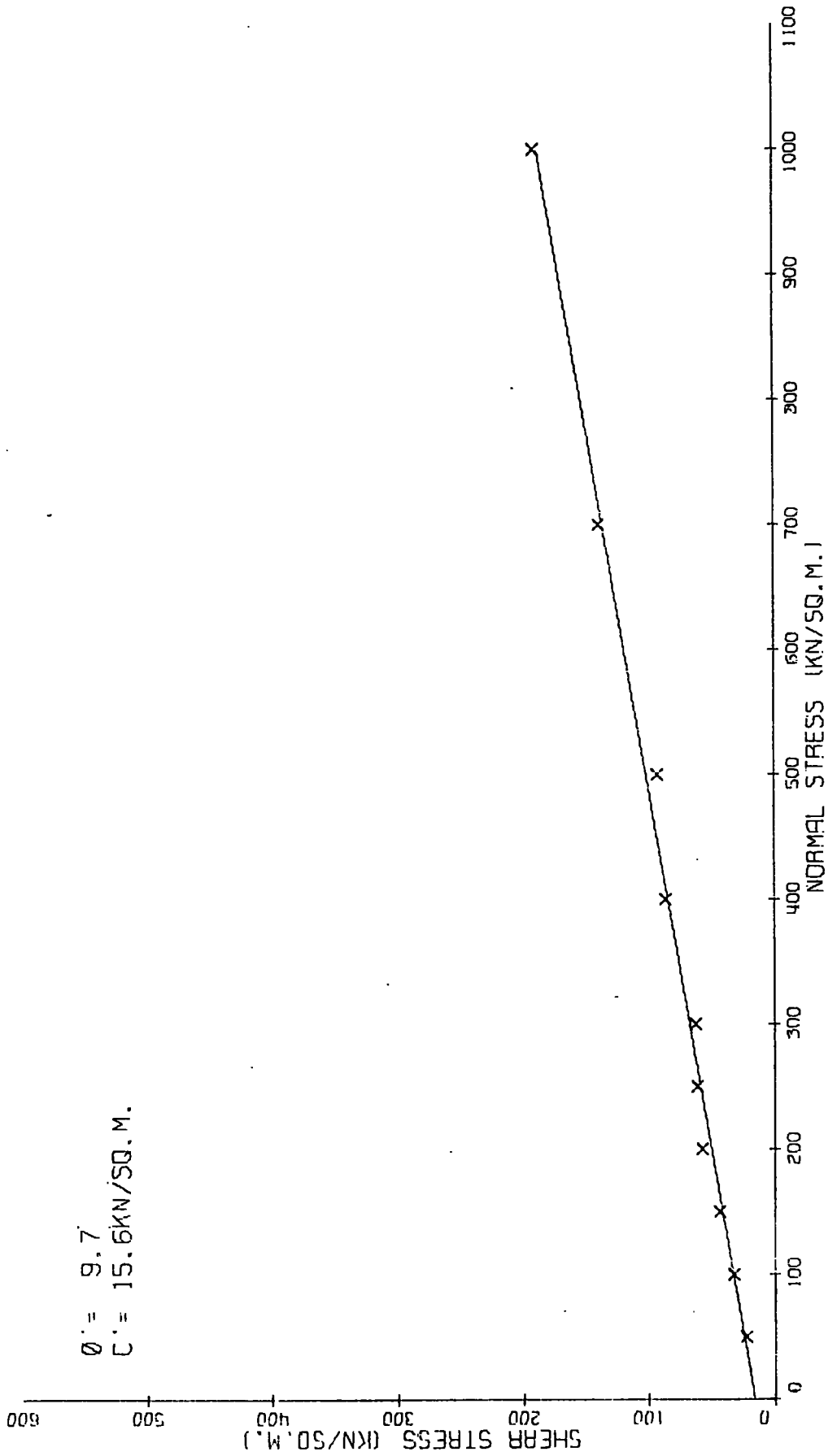


FIGURE 3.37 0.6-1.2MM SIZE FRACTION, RESIDUAL-DAKDALE

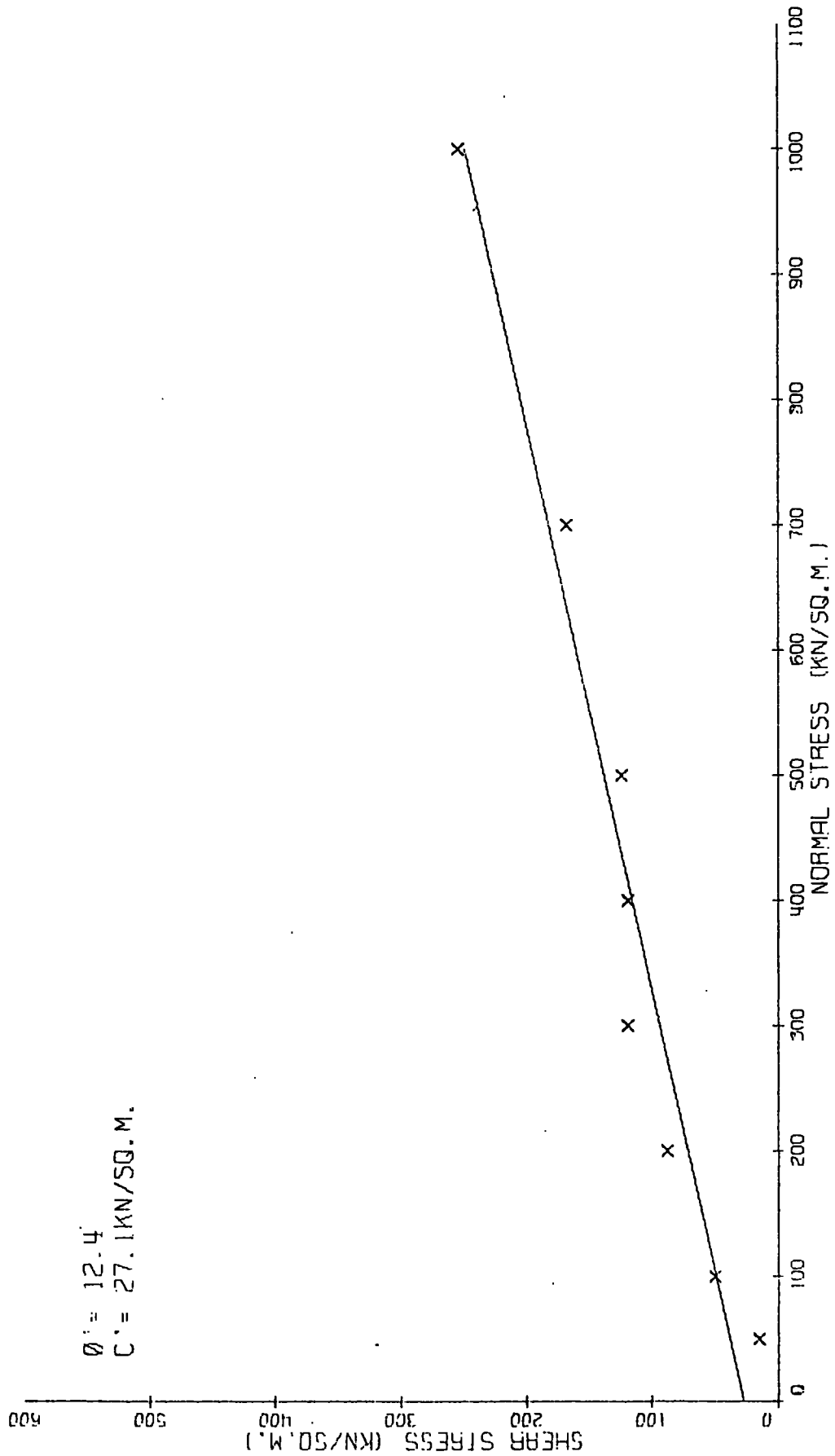
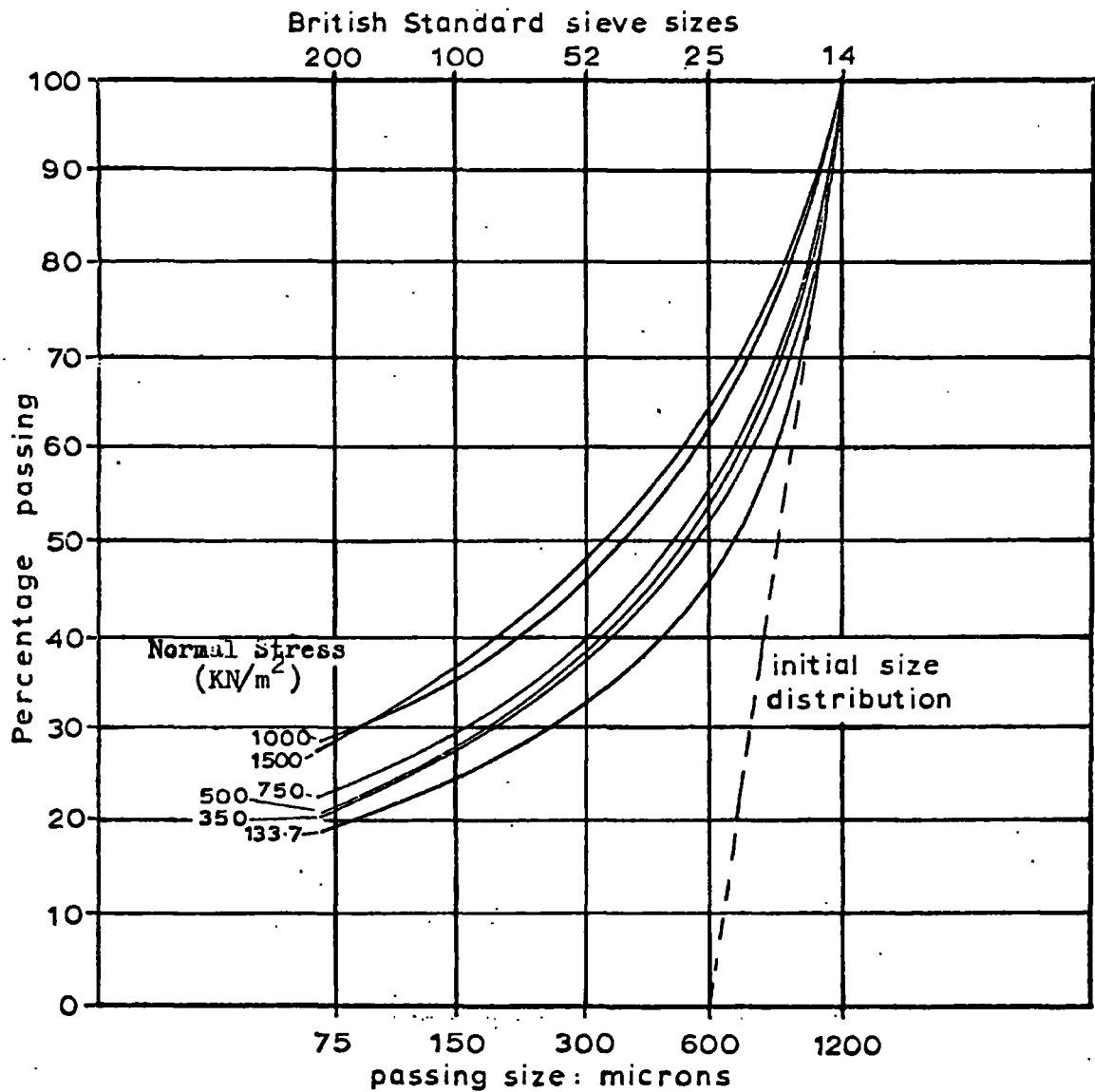


FIGURE 3.38

(FIGURE 3.44, RATSEY, 1973)

OLLERTON DISCARD, 0.6-1.2mm SIZE FRACTION, GRADING AFTER SHEARING

CHAPTER 4

FINE DISCARD (TAILINGS/SLURRY) LAGOON DEPOSITS

4.1 Introduction

During the coal preparation process, large quantities of solids charged water are produced. This water has to be treated in some manner to remove the solids before the water can be either recycled or discharged. Two methods of treatment are in common use, both involving the addition of a flocculant (usually an electrolytic polymer of some description) to aid sedimentation. In the first method a relatively small amount of flocculant is added and the water pumped to a settling pond, known as a lagoon, where the solids sediment out and the clean supernatant water can be drawn off.

In the other method, considerably more flocculant is added, and the thickened mud is press-filtered to remove excess water. The resulting blocks, known as "pressed tailings", can then be disposed of on a tip. It is with the lagoon deposits formed by the first method that this chapter is chiefly concerned.

When a lagoon is filled with sediment, there are three possible courses of action. It can be abandoned and a new lagoon built elsewhere. It could also be re-used by excavating the sediments and spreading them over the tip*. Finally, its capacity can be increased by raising the lagoon banks periodically. Lagoon banks can be raised by tipping new bank material (coarse discard normally) either upon the upstream side of the old bank (i.e. over the existing lagoon deposits) or on the downstream side. The former method gives rise to "fir-tree" banks (see Figure 5.17). This has the advantage that it uses less material than the latter method. Because of this, it is much used in the metal mining industry. However, it has a

* In some cases, notably with slurries, the coal content is sufficiently high for the sediment to be saleable.

number of defects. Saturated fine discard is in close proximity to the toe of the slope, which results in a high water table. Furthermore, as the new bank material is emplaced over the soft sediments, bearing capacity type failures are liable to occur, giving rise to zones of weakness in the embankment. Hence, in the coal mining industry this type of lagoon embankment construction has now been discontinued (McKechnie Thomson and Rodin, 1972) in favour of the downstream method in which compaction can be used efficiently. The supply of coarse discard from the colliery is generally sufficient for this form of construction.

Figure 4.1 shows a typical lagoon, with downstream construction of the banks. The coarser sediments usually settle out close to the inlet, building up a beach. The top surface of sediment tends to become dished due to differential settlement. In the centre of the lagoon there is a greater thickness of deposit than over the banks, thus the centre of the deposit can consolidate under its own weight to a greater extent than that over the banks, which are relatively incompressible (Hughes and Windle, 1976). It is considered good practice to increase this dishing effect, and to spread the inlet beach round the lagoon by periodically moving the sites of the inlet and outlet (McKechnie Thomson and Rodin, 1972). However, in the coal mining industry, this is rarely done, the results not being considered worth the extra work involved.

The dished profile results in water being trapped in the centre of the lagoon, which is consequently nearly always wet. However, the material near the banks dries out occasionally, giving rise to desiccation and increased strength. It also gives rise to perched water tables when the lagoon is reflooded (Hughes and Windle, 1976).

Owing to the restricted areas available for tipping discard near most collieries, it may well become necessary to overtip disused lagoons with coarse colliery discard. When this operation is put

into practice, it is obviously desirable to know how the fine discard sediment will behave. This involves primarily a knowledge of the consolidation and shear strength parameters. The amount of consolidation that can occur may, with deep lagoons overtipped by weak spoils (e.g. Gedling), be enough to reduce the shear strength of a volume of spoil to residual shear strength over the zone of differential settlement between relatively incompressible banks and the compressible lagoon deposits * (see Chapter 5.3.3). The rate of consolidation will depend on the permeability of the lagoon sediments, its banks and its foundation. Upon these factors will depend the degree of excess pore pressure generated, and hence the amount of shear strength mobilised by the deposits.

4.1.2. Physical and Mechanical properties of lagoons

4.1.2.1. Grading and structure

From the data given in National Coal Board, 1972, it can be seen that the overall grading of lagoon deposits is very variable, ranging from silty sands to clayey silts. This is mainly due to the segregation which often occurs in the lagoon. The slurry and tailings, as discharged, usually contain roughly equal proportions of silt and sand, and some 10-20 per cent of clay size particles. When the gradings for lagoon outlet area samples from West Virginia given by Busch et al (1975) are compared with samples from similar locations in British lagoons, the gradings can be seen to be similar, i.e. they are both clayey silts. It is of interest to compare fine colliery discard with similar waste from some other extraction industries. (Figure 4.2). Fine colliery discard proves to have a wider range of grain size than either the metaliferous mine tailings given by Pettibone and Kealy (1971) or the micaeous residue from China clay

* In this work the possible development and effects of liquefaction have not been considered to any degree.

extraction (China Clay Association, 1971). The coarser bound of the grading curves are similar in all three cases. However, the finest fine colliery discard gradings are considerably finer than the other two residues.

As stated above, particle grading can vary across a lagoon from inlet to outlet. However, this does not always occur (McKechnie Thomson and Rodin, 1972). In reservoir sedimentation, coarse particles sediment out first, becoming progressively finer towards the outlet, (Barland, 1971). Fine colliery discard sedimentation characteristics, are, however, complicated by the fact that it consists of materials of widely differing specific gravities namely coal and shale*. The nature of the deposits is also affected by the rate of inflow, its solids content and periodicity. In fact, where samples from lagoons have been taken they show considerable variation. According to McKechnie Thomson and Rodin (1972), they range from highly stratified, alternating layers of coarse and fine layers to poorly stratified, visually homogenous deposits. The layer thickness varies from 1 to over 150mm. Considering that colliery lagoons might be considered as a deltaic environment it is perhaps surprising that cross bedding, which is so common in deltas, has not been recorded. This could be due to the lack of a suitable lighter coloured bedding marker than to their actual absence.

* Specific gravity of coal is approximately 1.3

Specific gravity of shale is approximately 2.3 - 2.6

4.1.2.2. Shear Strength

The drained shear strength of lagoon deposits is variable, with ϕ' ranging from 21.5 to 39 degrees; in contrast to coarse discards, the West Virginian fine discards, with ϕ' values of 20 - 35 degrees (Busch et al 1975) are slightly weaker than the British materials. They are also considerably weaker than their coarse discards, whereas for British fine discards, four out of the six cases cited by McKechnie Thomson and Rodin (1972) were stronger than their corresponding coarse discard. In the three cases where comparisons were made, there was no significant difference in strength between inlet and outlet ends. The high coal content of lagoon deposits (commonly 30-40 per cent) is the probable cause of their high shear strength, counterbalancing their fine grading. Taylor (1974b) showed a positive correlation between coal content and peak shear strength for coarse discard, and it is probable that a similar relation holds for fine discards.

In terms of undrained strength, a large number of vane tests have been performed upon lagoon deposits. These show a wide scatter of results although strength generally increases with depth (McKechnie Thomson and Rodin 1972). Vane test results will be considered in greater detail in Section 4.4.

4.2. Field and laboratory investigations of lagoon deposits

4.2.1. Cadeby

4.2.1.1. Site sampling

At Cadeby colliery, near Doncaster (see Figure 1.1) several samples were collected from Lagoons 8 and 9 at a period when the latter lagoon was being excavated. Figure 4.3 shows the sampling positions. Nine bulk samples were taken from the 4.1m face at the position marked with a cross in Lagoon 9. These samples were extracted from a vertical section and are labelled 1 to 9 in Table 4.1. In situ peak shear strengths were also measured using a Pilcon hand

TABLE 4.1
CADEBY, LAGOON 9

a) Vertical Sampling												
<u>SAMPLE</u>	<u>DEPTH</u> <u>M</u>	<u>MOISTURE</u> <u>CONTENT</u> <u>%</u>	<u>LIQUID</u> <u>LIMIT</u>	<u>PLASTIC</u> <u>LIMIT</u>	<u>PLASTICITY</u> <u>INDEX</u>	<u>ORGANIC</u> <u>CARBON %</u> (Coal content)	<u>SPECIFIC</u> <u>GRAVITY</u>	<u>MEDIAN</u> <u>DIAMETER</u> <u>D₅₀</u> <u>MICRONS</u>	<u>LESS THAN 200</u> <u>SIEVE SIZE</u>			
1	SURFACE approx. 36m AOD	32.2	non-plastic			21.8	2,271	240	17			
2	0.6	33.4	"	"		35.6	1,866	170	32			
3	1.10	35.0	31	20	11	32.1	2,089	120	45			
4	1.60	46.8	40	23	17	42.9	1,906	20	67			
5	2.10	35.0	26	21	5	65.8	1,744	110	46			
6	2.60	22.3	non-plastic			50.2	1,651	250	31			
7	3.10	25.4	"	"		66.8	1,634	205	24			
8	3.60	15.0	"	"		35.6	1,984	400	12			
9	4.10	30.2	"	"		63.9	1,669	220	34			
b) Horizontal Vane Traverses Carried Out at 1m Distances in N.E. Direction from a)										Mean Value	Standard Deviation	
Sample 3)	HORIZON	1.4,1.4,1.4,3.5,1.4,1.4	1.4	1.4	1.4	1.4	1.4	1.4	1.4	1.75	0.86	
Sample 5)	HORIZON	24.1,10.3,13.8,20.7,6.9,6.9,5.5,5.5	6.9	6.9	6.9	5.5	5.5	5.5	5.5	12.4	7.50	
Sample 7)	HORIZON	51.7,51.7,46.9,48.3,40.0	48.3	40.0						47.7	4.80	

vane operating in the horizontal mode. Three traverses were carried out at horizons corresponding to vertical samples 3,5 and 7. The traverses were in a north-easterly direction, moving roughly along the strike of the laminations and obliquely away from the final inlet (Figure 4.3).

For the consolidation tests, four 'undisturbed' pillar samples of $0.3\text{m} \times 0.3\text{m} \times 0.3\text{m}$ (0.027m^3) were extracted from Lagoon 9. Three of these samples were from the vicinity of the final inlet position, and one (Sample D) from the outlet end of the lagoon. In addition four U100's were extracted from Lagoons 8 and 9. One of these (Number 4 on Figure 4.3) penetrated the lagoon embankment.

4.2.1.2. Stratification of Lagoon 8

Before considering the properties of the deposits from Lagoon 9 it is pertinent to refer to the complex nature of the sediments. A U100 sample from Lagoon 8 was obtained by pressing a double U100 tube into the deposit. The sample represents the bottom section of the double tube, i.e. base level approximately 0.9m below the surface of the lagoon. After extruding the sample it was cut longitudinally by means of a cheese wire. Well defined laminations enabled the specimen to be divided up into 27 sections (Figure 4.4). These laminae vary from 5 to 59 mm thick and show well marked graded bedding, i.e. the particle size of the bases of the individual laminae are coarser than their tops.

Moisture content and full major element and organic carbon determinations were carried out on all sub-samples and mineralogical analyses on a representative selection of them. Liquid and Plastic limits were then obtained for the thicker laminae, and for combinations of any two adjacent thinner laminae. The latter results, together with natural moisture content values and organic carbon contents are shown in Figure 4.4b.

The results demonstrate a number of pertinent points which are

no doubt common to many stratified lagoons, viz:

- 1) Stratification of the deposits does not exclude high organic carbon contents in apparently argillaceous layers. The range in this case is from 25.88 per cent to 75.72 per cent, with a mean of 41.01 per cent.
- 2) Natural moisture contents well in excess of the liquid limit infer that most of the layers could flow under gravity as a viscous fluid*. Wimpey results (Location F1, Lab. Report S/10190, 1974) confirm that this state pertains to depths of over 2.30m. Busch et al (1975) have shown that a similar situation is found in West Virginian tailings lagoons.
- 3) Although organic carbon contents are very high indeed (Table 4.2) it is clear that limit determinations are still feasible in most layers. This suggests that much of the carbon must be in a very finely divided state indeed. Limits that were determined by Messrs Wimpey are of the same general order.
- 4) The mineralogical composition, ignoring pyrite and coal, (Table 4.3) shows that the shale portion of the deposits does not vary greatly in composition. Kaolinite does seem to increase slightly at the expense of illite in the higher portions of the core (Layer 7 and above). This lack of large scale variation is also shown by the major element geochemistry (Table 4.2) as do the liquid and plastic limits.
- 5) The element oxide/alumina ratios are shown in Table 4.4. The higher Fe_2O_3 , CaO and MgO ratios are generally compatible with the higher organic carbon (coaly) layers. When sulphur is also high this suggests that pyrite (from the coal) is enhancing the Fe_2O_3 ratios. Pyrite was detected (up to 2%) in all the mineralogical analyses. High CaO and MgO ratios indicate that

* This was noted to be actually happening during the extraction of the U100 in the field.

carbonates and probably gypsum are also associated with the coal fraction as cleat minerals.

4.2.1.3. In situ shear strengths

In order to ascertain the lateral and vertical variation in in situ strength, three Pilcon hand vane traverses were conducted, as described in Section 4.2.1.1.

From the results in Table 4.1 two features are apparent, a) there is an increase in strength with depth and b) the lateral change in strength suggests that strength is decreasing in a north easterly direction i.e. away from the final inlet position.

While it is possible that the relative strength differences are functions of moisture content and grain size, there is probably sufficient similarity in moisture content and consistency limits between layers 3 and 5 to accept that the increase in strength with depth is a real one. The subject of vane shear strengths in lagoons will be discussed in greater detail in Section 4.4.

4.2.1.4. The vertical bulk sample sequence

The nine bulk samples from the exposed face (Figure 4.3) were analysed for natural moisture content, particle size distribution, consistency limits, organic carbon (coaly materials) and specific gravity.

The grading curves (Figure 4.5) and grading parameters (Table 4.1) show that only three samples (3,4 and 5) have appreciable silt content. Samples 3 and 4 contain more than 15 per cent clay size particles, the remaining specimens having little or no clay size fraction.

Consistency limit determinations were only feasible for the three samples mentioned above and it is of interest that these samples also have the highest natural moisture contents.

Perhaps the most striking feature of these deposits is the high organic carbon content, which shows a reasonable correlation with specific gravity (Figure 4.6). It is apparent that some of this

TABLE 4.2
 CHEMISTRY OF UIOO SAMPLE WEIGHT PER CENT
 CADEBY LAGOON 8

Components	1	2	3	4	5	5	7	8	9	10	11	12	13
SiO ₂	7.08	34.21	30.11	35.86	33.14	37.30	21.90	21.41	37.14	27.70	31.42	39.31	28.79
Al ₂ O ₃	3.99	15.79	14.35	17.83	15.16	18.60	10.66	10.33	17.43	12.93	15.08	18.70	12.89
Fe ₂ O ₃	3.18	4.15	3.52	3.96	3.74	3.95	3.31	3.68	3.63	3.44	3.68	3.94	3.55
MgO	0.91	0.98	0.87	1.12	0.93	1.12	1.39	0.71	1.05	0.80	0.89	1.16	0.73
CaO	1.54	1.41	1.10	1.01	1.14	0.96	0.88	1.00	1.14	0.73	0.86	0.71	0.96
Ni ₂ O	0.61	0.40	0.33	0.60	0.34	0.44	0.40	0.54	0.38	0.23	0.35	0.68	0.36
K ₂ O	0.80	2.85	2.54	3.03	2.74	3.60	1.97	2.19	2.80	2.48	3.00	3.23	2.49
TiO ₂	0.32	0.66	0.57	0.65	0.62	0.69	0.50	0.56	0.59	0.59	0.66	0.69	0.60
S	5.78	3.24	2.77	2.42	2.56	2.17	3.08	3.07	2.05	2.74	2.50	1.90	2.84
P ₂ O ₅	0.07	0.11	0.10	0.09	0.09	0.09	0.07	0.07	0.09	0.09	0.06	0.08	0.10
C	75.72	36.17	43.74	33.39	39.54	31.07	55.83	56.45	33.66	48.21	41.50	29.60	46.65

Continued.....

TABLE 4.2 Cont'd.

	14	15	16	17	18	19	20	21	22	23	24	25	26	27
SI02	20.20	38.47	32.27	33.56	41.18	39.04	29.56	32.32	31.86	36.50	28.69	23.99	17.67	30.62
AL203	9.61	18.86	14.71	16.21	20.68	19.91	14.96	16.30	16.21	19.02	14.52	12.52	5.71	15.67
FE203	3.33	3.79	3.62	3.55	3.84	3.87	3.52	3.68	3.71	3.62	3.50	3.78	3.46	3.59
MGO	0.67	1.12	1.39	0.97	1.21	1.14	0.82	0.92	0.89	1.07	0.83	0.66	0.52	0.93
CAO	1.14	0.98	1.56	0.88	0.77	0.87	0.96	0.74	0.74	1.45	1.06	0.66	0.70	1.07
NA2O	1.83	0.38	0.42	0.50	0.48	0.63	0.32	0.28	0.38	0.41	1.27	0.34	0.33	0.46
K2O	1.91	3.48	2.48	2.78	3.48	3.33	2.89	3.00	3.10	3.21	2.77	2.61	1.75	2.90
Tl02	0.54	0.67	0.59	0.59	0.74	0.71	0.63	0.65	0.69	0.66	0.60	0.64	0.50	0.62
S	3.62	1.96	2.61	2.21	1.68	2.09	2.76	2.31	2.36	2.71	2.86	3.32	3.87	2.90
F205	0.10	0.10	0.09	0.14	0.08	0.09	0.11	0.06	0.06	0.06	0.06	0.07	0.06	0.06
C	56.84	30.17	40.05	38.60	25.88	28.34	43.46	39.75	39.99	31.30	43.84	51.41	61.43	41.19

TABLE 4.3
 MINERALOGY OF CADEBY LAGOON 8
 WEIGHT PER CENT

Mineral	Sample							
	2	5	7	11	15	17	21	25
Quartz	10.5	7.5	8.0	8.0	10.0	10.0	5.0	6.5
Illite*	42.0	43.5	28.0	44.0	50.0	43.5	48.5	35.0
Kaolinite	10.0	8.5	7.0	5.5	9.0	6.5	5.0	6.0
Pyrite	1.0	1.0	0.5	1.0	1.0	1.0	1.0	1.0
Coal	36.0	39.5	56.0	41.5	30.0	38.5	40.0	51.5

* Illite includes mixed layer clay

TABLE 4.4
ALUMINA RATIOS OF UICO SAMPLE
CADEBY LAGOON

COMPONENTS	1	2	3	4	5	6	7	8	9	10	11	12	13
SiO ₂	1.77	2.17	2.10	2.01	2.19	2.01	2.06	2.07	2.13	2.14	2.08	2.10	2.23
Al ₂ O ₃	1.00	1.00	1.00	1.00	1.00	1.00	1.00	1.00	1.00	1.00	1.00	1.00	1.00
Fe ₂ O ₃	0.80	0.26	0.25	0.22	0.25	0.21	0.31	0.36	0.21	0.27	0.24	0.21	0.28
MgO	0.23	0.06	0.06	0.06	0.06	0.06	0.13	0.07	0.06	0.06	0.06	0.06	0.06
CaO	0.39	0.09	0.08	0.06	0.08	0.05	0.08	0.10	0.06	0.06	0.06	0.04	0.07
Na ₂ O	0.15	0.03	0.02	0.03	0.02	0.02	0.04	0.05	0.02	0.02	0.02	0.04	0.03
K ₂ O	0.20	0.13	0.18	0.17	0.18	0.19	0.19	0.21	0.16	0.19	0.20	0.17	0.19
TiO ₂	0.08	0.04	0.04	0.04	0.04	0.04	0.05	0.05	0.03	0.05	0.04	0.04	0.05
S	1.45	0.21	0.19	0.14	0.17	0.12	0.29	0.30	0.12	0.21	0.17	0.10	0.22
P ₂ O ₅	0.02	0.01	0.01	0.01	0.01	0.00	0.01	0.01	0.00	0.01	0.00	0.00	0.01
C	18.96	2.29	3.05	1.87	2.61	1.67	5.24	5.46	1.93	3.73	2.75	1.58	3.62

Continued.....

TABLE 4.4 Cont'd.

	14	15	16	17	18	19	20	21	22	23	24	25	26	27
SI02	2.06	2.04	2.19	2.07	1.99	1.96	1.98	1.98	1.97	1.92	1.98	1.92	1.82	1.95
AL203	1.00	1.00	1.00	1.00	1.00	1.00	1.00	1.00	1.00	1.00	1.00	1.00	1.00	1.00
FE203	0.34	0.20	0.25	0.22	0.19	0.19	0.24	0.23	0.23	0.19	0.24	0.30	0.36	0.23
MGO	0.07	0.06	0.09	0.06	0.06	0.06	0.05	0.06	0.05	0.06	0.06	0.05	0.05	0.06
CAO	0.12	0.05	0.11	0.05	0.04	0.04	0.06	0.05	0.05	0.08	0.07	0.05	0.07	0.07
NA2O	0.19	0.02	0.03	0.03	0.02	0.03	0.02	0.02	0.02	0.02	0.09	0.03	0.03	0.03
K2O	0.19	0.18	0.17	0.17	0.17	0.17	0.19	0.18	0.19	0.17	0.19	0.21	0.18	0.19
TI02	0.06	0.04	0.04	0.04	0.04	0.04	0.04	0.04	0.04	0.03	0.04	0.05	0.05	0.04
S	0.37	0.10	0.19	0.14	0.08	0.10	0.18	0.14	0.15	0.14	0.20	0.27	0.40	0.19
P2O5	0.01	0.01	0.01	0.01	0.00	0.00	0.01	0.00	0.00	0.00	0.00	0.01	0.01	0.00
C	5.79	1.60	2.72	2.38	1.25	1.42	2.19	2.44	2.47	1.65	3.02	4.11	6.33	2.63

coaly material must be in a very finely divided state, as there is no correlation with the grading or limits. The correlation coefficient between carbon content and specific gravity is 0.900 however, indicating a highly significant (greater than 99.9 per cent probability) correlation between these two variables. This is not an altogether surprising result, considering the wide variation in specific gravity of the two principal constituents, coal and shale (see Section 4.1.2.1.). Using the reduced major axis fit to the data shown in Figure 4.6, an estimate of the specific gravities of the coal and shale at Cadeby may be made. Assuming a carbon content of zero, i.e. pure shale, the specific gravity would be 2.4, while with a carbon content of one hundred per cent, i.e. pure coal, the specific gravity is 1.2. These values agree reasonably well with the approximate values quoted in Section 4.1.2.1. of 2.3 to 2.6 (shale) and 1.3 (coal).

4.2.1.5. Laboratory shear strength tests

Effective shear strength parameters were determined on the following:-

- 1) Remoulded sample of material from block samples A and C (Figure 4.2). Peak and residual shear strength parameters were determined in a 0.3 x 0.3m shear-box and should provide information on the 'average' effective strength parameters.
- 2) A coaly undisturbed sample from a U100 (No. 1, Figure 4.2). Peak shear strength parameters only determined in a 60 x 60mm shear box.
- 3) Fine grained 'clayey' specimen from block sample D (Figure 4.2). Peak and residual shear strength parameters determined in a 60 x 60mm shear box.

The results (Figure 4.7) imply that the coaly material enhances shear strength (e.g. coaly specimen, $\phi' = 32.3^\circ$) whilst the 'average' shear strength is only $\phi' = 21.9$, $c' = 13.2 \text{ kN/m}^2$ over the greater part of the range, or $\phi' = 31.5^\circ$ at a normal stress of less than

100 kN/m². It is of interest to note that the shear strength had not dropped measurably after a further displacement of 2.56m.

The finer grained, undisturbed block D material gave a peak strength of $\phi' = 23.8^\circ$, $c' = 8.4 \text{ kN/m}^2$, which dropped to $\phi' = 20^\circ$ at residual (0.25m total displacement). In both cases the fact that the residual values are not markedly lower than the peak strength could be in line with the near normally-consolidated state of the lagoon deposits. However, the coal content is probably equally as important.

Wimpey tests carried out on some Lagoon 8 materials reveal some interesting features. All their triaxial test data have been processed to give a composite picture (Figure 4.8). The specimens would appear to be very similar to the laminated core of Figure 4.4a. By computing the 'best fit' to the effective Mohr circles, the shear strength parameters that emerge are not greatly different to those of Lagoon 9, i.e. $c' = 12.2 \text{ kN/m}^2$, $\phi' = 24.5^\circ$.

4.2.1.6. Rowe Cell consolidation tests

Four block (0.3 x 0.3 x 0.3m pillar) samples were extracted from close to the surface of Lagoon 9, at the locations shown in Figure 4.2. Three of the samples (A, B and C) were closer to the final inlet than the fourth (D). The samples were subjected to consolidation tests using a 254mm diameter Rowe cell under back pressured, single drainage conditions. As far as is known these were the first samples from colliery lagoons to be tested in the large size Rowe cell.

4.2.1.7. Sample composition

The three inlet zone samples, A, B and C, were all laminated though not on such a small scale as the Lagoon 8 core. Particle size distributions (Figure 4.5) show that the three specimens are similar in grading to the coarser bulk samples of the vertical section, which, of course, also came from the inlet end of the lagoon. Sample D, from near the outlet, was the finest grained

TABLE 4.5
CADEBY COLLIERY LAGOON 9

	<u>Sample Composition (Normalized to 100%)</u>							<u>Plasticity Index</u>
	<u>Illite</u>	<u>Expandable mixed-layer/clay</u>	<u>Kaolinite</u>	<u>Chlorite</u>	<u>Quartz</u>	<u>Gypsum</u>	<u>Organic Carbon</u>	
BLOCK A	32.5	15.0	8.5	tr	7.5	Present	36.5	
BLOCK B	29.0	29.0	7.5	tr	6.0	Present	28.5	
BLOCK C	22.5	14.5	6.5	tr	tr	Present	56.5	
BLOCK D	30.5	12.5	10.5	2.0	9.5	N.D.	35.5	
EXCAVATED FACE (2.6m)		39.0	8.0	N.D.	3.0	N.D.	50.0	
N.D. Not detected								
	<u>LIMITS</u>							
		<u>Liquid Limit</u>			<u>Plastic Limit</u>		<u>Plasticity Index</u>	
BLOCK A		45			24		21	
BLOCK A (coaly layer)		29			25		4	
BLOCK B		33			21		12	
BLOCK C		32			Not obtainable		Non-plastic	
BLOCK D		44			25		19	

sample taken from the lagoon with the exception of the U100 sample No. 4 from close to the bank. Both of these samples were visually homogenous.

In terms of mineralogical composition (Table 4.5) all samples are rich in micaceous minerals (illite and mixed layer clay), with block sample B having a particularly high content of the latter expandable component. All samples are again very high in organic carbon content, especially sample C. Although sample D is finer grained than the others its limits are very similar to the more silty section of sample A, which also had a coaly band incorporated in it - see limits (Table 4.5). Although the samples were taken from near the surface of the lagoon there was no evidence of weathering and it is concluded that the small gypsum component in the three 'inlet' samples originated from the included coal, it being a cleat mineral, as found in the Yorkshire Main investigation of Spears, Taylor and Till (1971).

4.2.1.8. Consolidation tests

The consolidation tests were carried out in a 254mm diameter Rowe cell with saturation by back-pressure, as stated above. The system is shown in Figure 1.3. Certain problems were experienced with the cell at low pressures, due to friction within the apparatus. This led to the log Pressure against voids ratio ($\log P - e$) curves (Figure 4.9) being kinked at low pressures in the cases of samples B, C and D.

The log Pressure-voids ratio ($\log P - e$) curves of Figure 4.9 represent samples A, C and D with laminations in the horizontal plane, whilst sample B was orientated with the laminations as near vertical as possible. Also shown is the curve for a conventional (76.2mm diameter) oedometer test on sample D, which shows good compatibility at high pressures but divergence at low pressures.

The initial voids ratio of the oedometer specimen is much lower than the Rowe cell sample. This is probably because of:-

- a) The oedometer sample came from an horizon in the pillar sample which was closer to the original lagoon surface than was the Rowe cell sample. Thus the oedometer specimen would have been desiccated to a greater extent than the Rowe cell sample.
- b) The oedometer sample is of limited thickness and very susceptible to disturbance when being prepared and placed in the oedometer.

The P-e curves demonstrate that the voids ratio of the two samples with the highest initial volumes (samples A and C) are still elevated at maximum loading. The very coaly sample (C) does not display a marked linear normal consolidation curve and it is clear that rebound is minimal for this coaly material.

It is also apparent that all the samples are over-consolidated to a certain degree, which indicates a certain amount of desiccation, because they have not been subject to any surcharge during their history.

The consolidation parameters (Table 4.6) raise a number of important questions regarding the behaviour of lagoon deposits, as well as demonstrating major differences between Rowe cell and conventional oedometer tests.

The coarse grained, laminated samples (A, B and C) gave coefficients of consolidation (c_v 's) of between 290 and $1323\text{m}^2/\text{hr}$ on the linear portions of the P-e curves. From the graphs of c_v against pressure, shown on Figure 4.10, it can be seen that, for these three samples, the value of c_v rises to a peak around 300 kN/m^2 and then falls away rapidly. A normal c_v - pressure graph (e.g. Figure 27.5, Lambe and Whitman, 1969) starts with high values of c_v which then drop rapidly but may rise slightly

TABLE 4.6a
CADEBY LAGOON 9

Block A

Horizontal bedding S.G. 1.93
Initial dry density 0.800 Mg/m³
Final dry density 0.951 Mg/m³

Pressure	Voids Ratio	$\frac{m_v}{m^2/MN}$	Cc	$\frac{C_v}{(m^2/YR)}$	K (m/sec)	
0	1.412	-	-	-	-	
30	1.299	1.558	-	390.8	1.89×10^{-7}	
55	1.258	0.717	-0.157	442.4	9.86×10^{-8}	
110	1.166	0.715	-0.306	455.7	1.05×10^{-7}	Linear Section
220	1.079	0.366	-0.289	902.4	1.03×10^{-7}	
440	0.989	0.197	-0.300	684.8	4.20×10^{-8}	
850	0.890	0.122	-0.348	366.6	1.39×10^{-8}	
200	0.919	0.024	-0.047	-	-	Un- loading cycle
100	0.933	0.071	-0.045	-	-	
0	1.029	0.502	-0.032	-	-	

TABLE 4.6b

Block B

Vertical bedding S.G. 2.10
 Initial dry density 1.092 Mg/m³
 Final dry density 1.338 Mg/m³

Pressure (kN/m ²)	Voids Ratio	m v (m ² /MN)	Cc	Cv (m ² /YR)	K (m/sec)	
0	0.923	-	-	-	-	
9.4	0.922	0.055	-	-	-	
18.75	0.860	3.472	-0.208	447.2	4.83 x 10 ⁻⁷	
37.5	0.816	1.264	-0.146	298.1	1.17 x 10 ⁻⁷	
75	0.779	0.534	-0.121	246.6	4.10 x 10 ⁻⁷	
150	0.722	0.432	-0.192	349.2	4.70 x 10 ⁻⁸	Linear Section
300	0.655	0.258	-0.221	930.2	7.47 x 10 ⁻⁸	
600	0.567	0.178	-0.293	636.0	3.52 x 10 ⁻⁸	
1200	0.483	0.089	-0.279	290.7	8.06 x 10 ⁻⁹	
120	0.510	0.017	-0.027	-	-	Un- loading cycle
12	0.543	0.202	-0.033	-	-	
0	0.570	1.443	-	-	-	

TABLE 4.6c

Block C

Horizontal Bedding S.G. 1.93
 Initial dry density 0.766 Mg/m³
 Final dry density 0.882 Mg/m³

Pressure (kN/m ²)	Voids Ratio	m_v (m ² /MN)	Cc	C_v (m ² /YR)	K (m/sec)
0	1.488	-	-	-	-
10	1.477	0.404	-	-	-
20	1.449	1.129	-0.093	185.0	6.49 x 10 ⁻⁸
37.5	1.429	0.450	-0.071	383.9	5.38 x 10 ⁻⁸
75	1.395	0.381	-0.115	375.4	4.45 x 10 ⁻⁸
150	1.347	0.212	-0.127	609.9	4.02 x 10 ⁻⁸
300	1.300	0.159	-0.186	1002.0	4.95 x 10 ⁻⁸
600	1.227	0.106	-0.242	1323.0	4.35 x 10 ⁻⁸
1200	1.126	0.075	-0.334	512.3	1.20 x 10 ⁻⁸
120	1.164	0.016	-0.037	-	-
12	1.182	0.077	-0.018	-	-
0	1.189	0.274	-	-	-

} Un-
loading
cycle

TABLE 4.6d

Block D 254mm diameter sample

Clay, Horizontal bedding S.G. 1.96

Initial dry density 0.949 Mg/m³Final dry density 1.200 Mg/m³

Pressure	Voids Ratio	m_v (m ² /MN)	Cc	Cv (m ² /YR)	K (m/sec)	
0	1.065	-	-	-	-	
9.4	1.061	0.217	-	-	-	
18.75	0.884	9.187	-0.590	27.36	7.82 x 10 ⁻⁸	
37.5	0.843	1.166	-0.137	1.43	5.20 x 10 ⁻¹⁰	Linear Section
75	0.764	1.135	-0.260	4.39	1.55 x 10 ⁻⁹	
150	0.700	0.485	-0.213	8.53	1.29 x 10 ⁻⁹	
300	0.635	0.253	-0.214	13.39	1.05 x 10 ⁻⁹	
600	0.576	0.122	-0.199	18.13	6.87 x 10 ⁻¹⁰	
1200	0.513	0.067	-0.209	41.53	8.60 x 10 ⁻¹⁰	
120	0.549	0.022	-0.36	-	-	
12	0.595	0.278	-0.047	-	-	
0	0.634	2.000	-	-	-	

Table 4.6e

Block D 76.2mm diameter sample

Specific Gravity 1.96
 Initial dry density 1.057 Mg/m³
 Final dry density 1.203 Mg/m³

Pressure (kN/m ²)	Voids Ratio	m_v (m ² /MN)	Cc	Cv (m ² /YR)	K (m/sec)
1.52	0.854	-	-	-	-
10.98	0.815	2.193	-0.037	5.21	3.55 x 10 ⁻⁹
20.45	0.790	1.470	-0.094	1.56	7.13 x 10 ⁻¹⁰
39.37	0.761	0.873	-0.104	2.51	6.83 x 10 ⁻¹⁰
77.22	0.726	0.521	-0.119	4.38	7.10 x 10 ⁻¹⁰
152.92	0.685	0.311	-0.137	3.54	3.43 x 10 ⁻¹⁰
304.31	0.637	0.189	-0.161	4.33	2.54 x 10 ⁻¹⁰
607.10	0.575	0.125	-0.206	9.11	3.54 x 10 ⁻¹⁰
1210.31	0.509	0.070	-0.222	8.100	1.83 x 10 ⁻¹⁰
1.52	0.629	0.066	-0.041	-	-

at high pressures. While the shape of the current series of c_v - p curves might be characteristic of lagoon inlet materials, it is probably a result of friction in the apparatus limiting the spread of consolidation, by which c_v is calculated, at the lower pressures.

The fine grained, homogenous, sample D material shows considerably lower c_v 's, which follow the normal pattern with increasing pressure, i.e. falling then rising again. It is noticeable that, over the range where the e values are similar (i.e. 300 - 1200 kN/m²) the c_v of the large 254mm diameter sample is from 2 to 4 times larger than the c_v of the small sample. This is due to the difference in size of the samples (Rowe and Barden, 1966).

Although it is difficult to make comparisons between samples with such different log P - e curves (except samples B and D) it is possible to make a comparison between c_v 's at approximately similar voids ratios:-

e.g. Sample A	$e = 0.89$	$c_v = 367\text{m}^2/\text{yr}$
Sample B	$e = 0.86$	$c_v = 477\text{m}^2/\text{yr}$
Sample D	$e = 0.88$	$c_v = 27\text{m}^2/\text{yr}$
Sample A	$e = 1.17$	$c_v = 456\text{m}^2/\text{yr}$
Sample C	$e = 1.13$	$c_v = 512\text{m}^2/\text{yr}$

From this it is obvious that the fine-grained, silty specimen (D) consolidates far slower than the coarser, laminated ones. This is as one would expect. Even though the finer parts of the laminated specimens may be of similar grading to sample D, their aggregate thickness is much less, thus causing less impediment to water flow. What is perhaps more surprising is the lack of significant difference in c_v 's between the samples consolidated with laminations horizontal (i.e. with water draining vertically across the laminations) and the one with vertical laminae (i.e. with water draining along the laminations). It would seem that the latter sample should drain

much more readily, since all the coarse layers could be expected to act as drains. An examination of Figures 4.11(a) and (b) provides a probable explanation. In the horizontal sample C (Figure 4.11b) the individual laminae can be seen to be lensoid in shape, so that the coarse parts of the different laminae commonly impinge on one another, thus giving an easy passage for water in a vertical as well as horizontal direction. Thus the material is effectively isotropic. In sample C, the silt/clay layers are much thinner than in sample B (Figure 4.11(a)) thus giving the former the higher c_v .

It can be seen from Figure 4.11(a) that the laminations can be very contorted. The contortion visible in Figure 4.11(a) corresponds to the "intraformational recumbent fold" type of contorted lamination of McKee et al (1962). They are very common in deltaic deposits (Coleman and Gagliano, 1965). Contorted laminations on a larger scale could be seen in the excavated face of the lagoon (Figure 4.12).

Wimpey Central Laboratories carried out five oedometer tests on Lagoon 8 materials from position F1 on Figure 4.3. (Wimpey Report S/10190, 1974). As details of the grading and structure are scanty, it is not possible to compare them precisely with the results given above. The voids ratios (see Figure 4.13) were initially in the range 0.74 - 0.84 compared to 0.92 - 1.49 for Lagoon 9. At 430 kN/m^2 these values have dropped to 0.61 to 0.73 and 0.6 to 1.26 respectively. The reduced initial voids ratios of the Lagoon 8 material (compared to Lagoon 9) might be due to disturbance during driving of U100 sampling tubes.

Average coefficients of consolidation for the Lagoon 8 tests are in the range 8 to over $80 \text{ m}^2/\text{yr}$. These values are much lower than those for samples A, B and C, but in the same order as Sample D from Lagoon 9. Coefficients of volume compressibility (m_v) in

the comparable stress range are of the order 0.084 to 1.15 m^2/MN for Lagoon 8 and 0.46 to 1.00 m^2/MN for Lagoon 9.

4.2.1.9. Permeability of the sediment-embankment interface

As mentioned in Section 4.2.1.1. a U100 (No. 4 on Figure 4.2) was driven through the sediment-embankment interface. A photograph of a section across this interface is shown in Figure 4.14. Particle size analyses were carried out upon the three sections of the sample viz: Lagoon sediments, Embankment, and Interface. The results are shown in Figure 4.15. They show some interesting points. Even though this part of the lagoon was nearer to the inlet than Sample D, it is finer grained than sample D. The embankment is very fine grained for coarse discard, even being finer than the severely degraded material from the surface of Gedling tip (Figure 2.1.). Presumably solids from the lagoon have been carried into the embankment.

Before the sample was analysed for particle size, the permeabilities of the three portions were ascertained. These are tabulated in Table 4.7. They contain some surprising results. Despite the fine grain size, the lagoon sample has a surprisingly high permeability of 10^{-6} m/s. This compares with values of 10^{-5} to 10^{-8} m/s for in situ permeabilities, as measured by McKechnie Thomson and Rodin (1972) in four lagoons. It also contrasts strongly with values of permeability of 10^{-9} m/s calculated for sample D from the tests conducted in the 254mm diameter Rowe cell (Table 4.6d). This demonstrates how seriously the consolidation test underestimates the permeability (and hence c_v), even when large size samples are used*.

* In comparisons between field performance of embankments and laboratory consolidation tests, the underestimation of c_v by laboratory consolidation tests has often been remarked upon (Murray and Symons, 1974).

TABLE 4.7
PERMEABILITY OF U100 SAMPLE NO. 4

Part of Sample	Mean Permeability m/s	Standard Deviation m/s	No. of determinations
Embankment	1.63×10^{-12}	1.02×10^{-13}	3
Lagoon	4.71×10^{-6}	1.82×10^{-6}	4
Interface	5.24×10^{-10}	1.24×10^{-10}	2

In marked contrast to the lagoon sediments, the permeability of the embankment, at 10^{-12} m/s, is very low indeed. In situ permeabilities of compacted coarse colliery discards, as measured by McKechnie Thomson and Rodin (1972) range from 10^{-4} to 10^{-9} m/s. Even allowing for the fact that laboratory measurements of permeability tend to be low compared to in situ tests, the value for the Lagoon 9 embankment is still low. Presumably the voids in the part of the embankment closest to the lagoon have been plugged with fine silt and clay brought in by the mud laden waters of the lagoon.

4.2.2. Gedling Lagoon 12

4.2.2.1. Site sampling

Lagoon 12 is a disused lagoon upon the West Tip at Gedling. At the time of sampling it had been disused for at least a year. One 0.3m x 0.3 x 0.3m pillar sample was extracted from the outlet vicinity and two cylindrical 203mm diameter samples were extracted from between the inlet and outlet, close to one of the retaining banks.

4.2.2.2. Sample composition

Structurally the central sample has poorly developed laminations, with no well marked change vertically across a lamination (Figure 4.16). The outlet sample is visually homogenous.

The bulk grading of the samples is shown in Figure 4.17. It can be seen that both samples are poorly sorted, with the outlet sample being the finer grained. This sample, with only 10 per cent sand size fraction, resembles the coarsest outlet material from Denby Hall Lagoon C (Figure 4.17). Of all the samples tested by Messrs Wimpey (National Coal Board, 1972) only some samples from the outlet of Kinneil lagoon 22/28 are finer grained. These have only 5 per cent sand size.

The Wimpey tests on materials from the old lagoon on the East Tip at Gedling produced similar gradings to the coarser sample from

Lagoon 12.

The central sample from Lagoon 12 shows a fairly marked vertical change in bulk grading. The two sub-samples which were consolidated with a radial drain came from the top of the main sample and are considerably finer grained than the remainder. Compared to Cadeby Lagoon 9 (Figure 4.5), the upper part of this central sample is similar to sample D, whilst the lower part resembles the grading of sample 3 in the vertical sequence.

In terms of consistency limits, which are given in Table 4.10 the finer grained outlet material has higher liquid and plastic limits, as might be expected. The limits are of the same order as those found at Cadeby (Figure 4.4) and at Gedling old East Tip Lagoon (National Coal Board, 1972).

In terms of chemical composition (Table 4.8), the organic carbon content at 38 per cent, is at the normal level for fine discard. The other element oxides are also present in similar amounts to the Cadeby samples. The S_iO_2/Al_2O_3 ratio (Table 4.9) is at the higher end of the range, indicating a higher quartz content than usual, while the low K_2O/Al_2O_3 ratio indicates low illite (potassium feldspars being present in very small amounts indeed in Coal Measures shales and mudstones of England). The cleat minerals would appear to be less abundant since sulphur and calcium oxide are lower than for Cadeby.

4.2.2.3. Consolidation tests

Four tests were performed on the 0.3 x 0.3 x 0.3mm pillar sample from the outlet end. In three of these a 152mm diameter Rowe cell was used, a 254mm diameter cell being used in the fourth. In these tests the sample was orientated with the bedding horizontal except in the case of one of the 152mm diameter samples, where it was orientated vertically. One of the other 152mm diameter samples was only pressurised to 300 kN/m², instead of 1200 kN/m². This sample

TABLE 4.8

CHEMISTRY OF LAGOON AND TAILINGS SAMPLES

COMPONENTS	WEIGHT PER CENT												
	CADEBY LAGOON 9	CADEBY LAGOON 9	CADEBY LAGOON 9	CADEBY LAGOON 9	CADEBY LAGOON 9	CADEBY LAGOON 9	CADEBY LAGOON 9	CADEBY LAGOON 9	CADEBY LAGOON 9	MANVERS TAIL- INGS	MORR- ISON BUSTY	GEDLING TAIL- INGS	GEDLING LAGOON 12
	BLOCK A	BLOCK B	BLOCK C	BLOCK D	1.10M	2.60M	3.60M						
SI02	32.81	38.69	15.65	34.19	36.62	20.95	33.34	35.16	44.80	34.53	36.38		
AL203	15.12	19.39	8.96	16.52	19.00	11.00	17.55	17.49	26.55	17.78	17.35		
FE203	3.81	4.25	3.55	3.78	2.46	3.21	2.78	4.76	5.53	2.18	3.73		
MGO	0.05	1.12	0.55	0.97	1.02	0.86	0.99	1.02	0.97	1.04	0.93		
CAO	1.19	1.98	1.50	0.88	0.94	2.09	1.48	0.19	1.11	0.47	0.19		
NA2O	0.25	0.17	0.30	0.19	0.41	0.34	0.17	0.14	0.12	0.31	0.21		
K2O	2.59	3.47	1.55	2.72	4.09	2.75	3.85	0.74	0.88	3.31	1.03		
TI02	0.61	0.68	0.46	0.62	0.74	0.68	0.71	0.69	1.06	0.83	0.86		
S	3.07	2.75	4.60	2.51	2.51	7.85	3.46	2.04	1.38	1.47	1.17		
P205	0.09	0.10	0.09	0.09	0.11	0.07	0.08	0.10	0.07	0.04	0.03		
C	39.50	27.40	62.79	37.53	32.10	50.20	35.60	37.67	17.53	38.04	38.13		

TABLE 4.9
ELEMENT OXIDE TO ALUMINA RATIOS OF LAGOON AND TAILINGS SAMPLES

COMPONENTS	CADEBY LAGOON 9	CADEBY LAGOON 9	CADEBY LAGOON 9	CADEBY LAGOON 9	CADEBY LAGOON 9	CADEBY LAGOON 9	CADEBY LAGOON 9	CADEBY LAGOON 9	CADEBY LAGOON 9	CADEBY LAGOON 9	MANVERS TAIL- INGS	MORR- ISON BUSTY TLGS.	GEDLING TAIL- INGS	GEDLING LAGOON 12
	BLOCK A	BLOCK B	BLOCK C	BLOCK D	1.10M	2.60M	3.60M							
SI02	2.17	2.00	1.75	2.07	1.93	1.90	1.90	1.90	1.90	2.01	1.69	1.94	1.94	2.10
AL2O3	1.00	1.00	1.00	1.00	1.00	1.00	1.00	1.00	1.00	1.00	1.00	1.00	1.00	1.00
FE2O3	0.25	0.22	0.40	0.23	0.13	0.29	0.16	0.27	0.21	0.27	0.21	0.12	0.12	0.22
MGO	0.06	0.06	0.06	0.06	0.05	0.08	0.06	0.06	0.04	0.06	0.04	0.06	0.06	0.05
CAO	0.08	0.10	0.17	0.05	0.05	0.19	0.08	0.01	0.04	0.01	0.04	0.03	0.03	0.01
NA2O	0.02	0.01	0.03	0.01	0.02	0.03	0.01	0.01	0.00	0.01	0.00	0.02	0.02	0.01
K2O	0.17	0.18	0.17	0.16	0.22	0.25	0.22	0.04	0.03	0.04	0.03	0.19	0.19	0.06
TI02	0.04	0.04	0.05	0.04	00.04	0.06	0.04	0.04	0.04	0.04	0.04	0.05	0.05	0.05
S	0.20	0.14	0.51	0.15	0.13	0.71	0.20	0.12	0.05	0.12	0.05	0.08	0.08	0.07
P2O5	0.01	0.00	0.01	0.01	0.01	0.01	0.00	0.01	0.00	0.01	0.00	0.00	0.00	0.00
C	2.61	1.41	7.01	2.27	1.69	4.57	2.03	2.15	0.66	2.15	0.66	2.14	2.14	2.20

TABLE 4.10

GEDLING LAGOON 12 - CONSISTENCY LIMITS

Sample	Liquid Limit	Plastic Limit	Plasticity Index
Outlet	51	32	19
Central	43	27	16

was vane tested to determine its shear strength after being loaded to 300 kN/m^2 . This was for purposes of correlation with the flocculant/tailings tests which will be described later. The consolidation results for these outlet samples are given in Table 4.11.(A-D).

The six tests carried out on the 203mm diameter samples from between inlet and outlet were conducted by L. Gould. They consisted of four tests in a 152mm diameter Rowe cell and two in a 76.2mm diameter oedometer. In both Rowe cell and oedometer a sample drained by a) a single vertical drain and b) a radial drain was consolidated. The other two Rowe cell samples consisted of one with both a single vertical drain plus a radial drain, and the second was similar but with a sand blanket drain as well (i.e. double drainage plus radial drainage). The results of these tests are tabulated in Table 4.12 (A-F).

The log pressure-voids ratio curves of the specimens from the outlet sample (Figure 4.18) are virtually coincident. Those for the central samples (Figure 4.20) show more scatter, but they all lie below those of the outlet specimens. That the coarser grained sample has the lower voids ratio (contrary to the case at Cadeby), is probably due to the difference in structure between the two lagoons. Gedling has only poorly developed graded bedding with the result that the voids between the coarser particles, which existed at Cadeby, are filled by finer particles.

Comparing the different sized sub-samples, in the outlet sample series, there is no difference between 254mm and 152mm diameter log P- e results except that the curve for the larger sample is kinked at low pressures. The most likely cause of this is friction within the Rowe cell apparatus between the drain spindle and its housing in the top part of the cell. In the smaller cell, there was a greater clearance between these two sections. In the case of the

TABLE 4.11a
CONSOLIDATION PARAMETERS

Sample Gedling Lagoon 12, outlet end. 254mm diameter

Specific gravity 2.02
Initial dry density 0.998 Mg/m³
Final dry density 1.169 Mg/m³

Pressure (kN/m ²)	Voids Ratio	α_v (m ² /MN)	Cc	Cv (m ² /YR)	K (m/sec)
0	1.024	-	-	-	-
9.4	1.020	0.21	-	-	-
29.2	0.898	3.06	-0.25	682.6	6.49 x 10 ⁻⁷
37.5	0.884	0.90	-0.13	4.8	1.35 x 10 ⁻⁹
75	0.838	0.64	-0.15	7.5	1.50 x 10 ⁻⁹
150	0.783	0.40	-0.18	17.1	2.14 x 10 ⁻⁹
300	0.726	0.21	-0.19	29.5	1.96 x 10 ⁻⁹
600	0.668	0.11	-0.19	33.4	1.16 x 10 ⁻⁹
1200	0.605	0.06	-0.21	41.5	8.17 x 10 ⁻¹⁰
120	0.642	0.02	-0.04	-	-
12	0.684	0.24	-0.04	-	-
0	0.729	0.22	-	-	-
Average over linear section		0.22	-0.19	30.4	1.52 x 10 ⁻⁹

} Linear
Section

TABLE 4.11b

CONSOLIDATION PARAMETERS

Sample Gedling Lagoon 12 outlet end, 152.4mm diameter, horizontal bedding

Specific gravity 2.02

Initial dry density 0.922 Mg/m³

Final dry density 1.121 Mg/m³

Pressure (kN/m ²)	Voids Ratio	m_v (m ² /MN)	Cc	Cv (m ² /YR)	K (m/sec)
0	1.191	-	-	-	-
9.4	0.951	11.63	-	64.1	2.32 x 10 ⁻⁷
18.75	0.918	1.86	-0.11	235.6	1.36 x 10 ⁻⁷
37.5	0.875	1.18	-0.14	675.3	2.47 x 10 ⁻⁷
75	0.829	0.66	-0.15	54.0	1.11 x 10 ⁻⁸
150	0.770	0.43	-0.20	22.6	3.02 x 10 ⁻⁹
300	0.707	0.24	-0.21	21.9	1.61 x 10 ⁻⁹
600	0.645	0.12	-0.21	23.6	8.86 x 10 ⁻¹⁰
1200	0.570	0.07	-0.25	25.5	6.02 x 10 ⁻¹⁰
120	0.605	0.02	-0.04	-	-
12	0.620	0.08	-0.01	-	-
0	0.801	9.32	-	-	-
Average over linear section		0.22	-0.22	23.4	1.53 x 10 ⁻⁹

Linear
Section

TABLE 4.11c

CONSOLIDATION PARAMETERS

Sample Gedling Lagoon 12 outlet end, 152.4mm diameter vertical bedding

Specific Gravity 2.02
 Initial dry density 0.860 Mg/m³
 Final dry density 1.160 Mg/m³

Pressure (kN/m ²)	Voids Ratio	m_v (m ² /MN)	Cc	Cv (m ² /YR)	K (m/sec)	
0	1.349	-	-	-	-	
9.4	0.974	17.0	-	-	-	
18.75	0.948	1.44	-0.09	576.2	2.58×10^{-7}	
37.5	0.917	0.84	-0.10	31.3	8.15×10^{-9}	
75	0.882	0.49	-0.12	28.6	4.37×10^{-9}	
150	0.826	0.40	-0.19	27.8	3.32×10^{-9}	} Linear Section
300	0.765	0.22	-0.20	30.2	2.09×10^{-9}	
600	0.698	0.13	-0.22	43.0	1.68×10^{-9}	
1200	0.630	0.07	-0.23	30.4	6.33×10^{-10}	
120	0.657	0.02	-0.03	-	-	
12	0.693	0.20	-0.04	-	-	
0	0.741	2.38	-	-	-	
Average over linear section		0.21	-0.21	32.6	1.93×10^{-9}	

TABLE 4.11d

CONSOLIDATION PARAMETERS

Sample Gedling Lagoon 12 outlet end, 152.4mm diameter sample
used for vane test

Specific gravity 2.02
Initial density 1.021 Mg/m³
Final dry density 1.094 Mg/m³

Pressure (kN/m ²)	Voids Ratio	m_v (m ² /MN)	Cc	Cv (m ² /YR)	K (m/sec)
0	0.978	-	-	-	-
9.4	0.952	1.40	-	-	-
18.75	0.923	1.56	-0.10	254.3	1.24 x 10 ⁻⁷
37.5	0.887	1.00	-0.12	568.0	1.77 x 10 ⁻⁷
75	0.847	0.57	-0.13	88.7	1.58 x 10 ⁻⁸
150	0.797	0.36	-0.17	20.4	2.29 x 10 ⁻⁹
300	0.740	0.21	-0.19	21.2	1.40 x 10 ⁻⁹
120	0.747	0.02	-0.02	-	-
12	0.781	0.18	-0.03	-	-
0	0.847	3.06	-	-	-

Average shear strength (kN/m²)

	Before consolidation		After consolidation	
	m	s	m	s
Peak	20.0	1.7	27.2	0.8
Remoulded	8.1	0.5	4.8	0.3

m = mean value

s = standard deviation

152mm and 76.2mm diameter samples, there is a large difference in one case, but not in the other. It is the radially drained oedometer sample which has the higher voids ratio (at similar pressures). As the oedometer sample is thinner than the lamination thickness in the bulk material, it is likely that an unrepresentative sample is being considered, since, although the laminations are poor, some fining upwards does occur in them (see Figure 4.16).

Convex-upwards curvature is apparent at low pressures, which is probably a function of desiccation, since these deposits have never been subject to a surcharge.

In these samples the log pressure-voids ratio curves are close enough together to make it possible to compare values of c_v . Considering first the outlet sample, graphs of c_v against log pressure are shown in Figure 4.19. It can be seen that at a pressure of 75 kN/m^2 , the small Rowe cell samples with horizontally orientated bedding have the highest value of c_v ($71 \text{ m}^2/\text{yr}$), while the large Rowe cell has the lowest value, at $8 \text{ m}^2/\text{yr}$. The small Rowe cell sample with its bedding orientated vertically (i.e. parallel to the axial stress) lies between these two at $28 \text{ m}^2/\text{yr}$. As the pressure rises, the c_v 's of the small samples fall until at about 125 kN/m^2 they are all virtually coincident at $27 \text{ m}^2/\text{yr}$. Above this pressure, the c_v 's of the horizontally orientated specimens continue to fall, reaching $22 \text{ m}^2/\text{yr}$ at 400 kN/m^2 pressure. The c_v of the vertically orientated sample rises, however, reaching $35 \text{ m}^2/\text{yr}$ at 400 kN/m^2 . Meanwhile, the c_v of the large Rowe cell sample has been steadily rising, until it reaches a value of $31 \text{ m}^2/\text{yr}$ at 400 kN/m^2 , i.e. higher than the small Rowe cell samples with bedding of a similar orientation, but less than that achieved by the small Rowe cell sample with bedding orientated vertically.

The low values of c_v in the large cell at low pressures are

TABLE 4.12a

CONSOLIDATION PARAMETERS

Sample Gedling Lagoon 12, vertical drainage 152.4mm diameter cell

Specific Gravity 1.99
 Initial dry density 1.059 Mg/m³
 Final dry density 1.217 Mg/m³

Pressure (kN/m ²)	Voids Ratio	m_v (m ² /MN)	Cc	Cv (m ² /YR)	K (m/sec)	
0	0.772	-	-	-	-	
10	0.759	0.85	-	23.1	6.11 x 10 ⁻⁹	
20	0.728	1.77	-0.10	22.6	1.29 x 10 ⁻⁸	
40	0.629	2.09	-0.22	22.8	1.41 x 10 ⁻⁸	} Linear Section
79.7	0.607	0.81	-0.17	61.1	1.53 x 10 ⁻⁸	
160	0.551	0.45	-0.18	51.4	7.07 x 10 ⁻⁹	
319.8	0.497	0.22	-0.17	36.4	2.36 x 10 ⁻⁹	
79.7	0.502	-	-0.01	-	-	
20	0.510	-	-0.01	-	-	
0	0.557	-	-	-	-	
Average (linear section)		0.89	-0.19	42.9	9.71 x 10 ⁻⁹	

Average shear strength (kN/m²)

	After loading (mean)	Standard deviation
Peak	23.5	14.5
Remoulded	3.7	2.9

TABLE 4.12b

CONSOLIDATION PARAMETERS

Sample Gedling Lagoon 12, radial drainage, 152.4mm diameter cell

Specific gravity 2.46

Initial dry density 1.060 Mg/m³Final dry density 1.159 Mg/m³

Pressure (kN/m ²)	Voids Ratio	m_v (m ² /MN)	Cc	Cv (m ² /YR)	K (m/sec)	
0	1.072	-	-	-	-	
10	0.959	6.21	-	203.8	3.92 x 10 ⁻⁷	
20	0.925	1.75	-0.09	127.7	6.91 x 10 ⁻⁸	
40	0.810	3.09	-0.30	145.6	1.39 x 10 ⁻⁷	} Linear Section
79.7	0.731	1.12	-0.20	92.8	3.22 x 10 ⁻⁸	
160	0.654	0.57	-0.20	29.2	5.14 x 10 ⁻⁹	
320	0.574	0.31	-0.20	34.0	3.24 x 10 ⁻⁹	
160	0.579	-	-0.01	-	-	
79.7	0.587	-	-0.02	-	-	
0	0.887	-	-	-	-	
Average over linear Section		1.27	-0.23	75.4	4.49 x 10 ⁻⁸	

Average shear strength (kN/m²)

	After loading (mean)	Standard deviation
Peak	16.0	4.1
Remoulded	5.0	1.4

TABLE 4.12c

CONSOLIDATION PARAMETERS

Sample Gedling Lagoon, radial and vertical drainage, 152.4mm diameter

Specific gravity 1.99

Initial dry density 1.033 Mg/m³

Final dry density 1.271 Mg/m³

Pressure (kN/m ²)	Voids Ratio	m_v (m ² /MN)	Cc	Cv (m ² /YR)	K (m/sec)	
0	0.927	-	-	-	-	
20	0.716	6.11	-	62.5	3.34 x 10 ⁻⁶	
40	0.666	1.46	-0.16	55.4	2.51 x 10 ⁻⁸	} Linear Section
79.7	0.614	0.79	-0.16	54.2	1.33 x 10 ⁻⁸	
160	0.557	0.45	-0.18	49.7	6.93 x 10 ⁻⁹	
319.9	0.498	0.24	-0.19	41.9	3.17 x 10 ⁻⁹	
40	0.521	-	-0.02	-	-	
20	0.530	-	-0.03	-	-	
0	0.566	-	-	-	-	
Average over linear section		0.62	0.17	50.3	1.21 x 10 ⁻⁸	

TABLE 4.12d

CONSOLIDATION PARAMETERS

Sample Gedling Lagoon 12, vertical and radial drainage with
blanket, 152.4mm diameter

Specific gravity 1.99
Initial dry density 1.095 Mg/m³
Final dry density 1.258 Mg/m³

Pressure (kN/m ²)	Voids Ratio	m_v (m ² /MN)	Cc	Cv (m ² /YR)	K (m/sec)	
0	0.818	-	-	-	-	
20	0.754	1.87	-	27.1	1.57 x 10 ⁻⁸	
40	0.712	1.20	-0.13	30.5	1.14 x 10 ⁻⁸	} Linear Section
79.7	0.665	0.70	-0.15	37.3	8.09 x 10 ⁻⁹	
160	0.610	0.43	-0.18	56.7	7.52 x 10 ⁻⁹	
319.8	0.557	0.21	-0.17	55.9	3.60 x 10 ⁻⁹	
40	0.562	-	-0.01	-	-	
20	0.568	-	-0.02	-	-	
0	0.583	-	-	-	-	
Average over linear section		0.64	0.16	45.1	7.65 x 10 ⁻⁹	

TABLE 4.12e

CONSOLIDATION PARAMETERS

Sample Gedling lagoon, vertical drainage, 76.2mm diameter cell

Specific gravity 1.99

Initial dry density 1.058 Mg/m³Final dry density 1.327 Mg/m³

Pressure (kN/m ²)	Voids Ratio	m_v (m ² /MN)	Cc	Cv (m ² /YR)	K (m/sec)
1.8	0.731	-	-	-	-
24.9	0.698	0.84	-0.03	5.7	1.47 x 10 ⁻⁹
47.1	0.673	0.64	-0.08	7.7	1.53 x 10 ⁻⁹
91.5	0.634	0.51	-0.12	10.3	1.64 x 10 ⁻⁹
180.3	0.596	0.28	-0.13	22.2	1.91 x 10 ⁻⁹
357.8	0.540	0.20	-0.18	20.9	1.31 x 10 ⁻⁹
713.0	0.485	0.10	-0.17	26.9	8.47 x 10 ⁻¹⁰
1423.4	0.429	0.05	-0.18	25.0	4.20 x 10 ⁻¹⁰
180.3	0.459	-	-0.03	-	-
47.1	0.478	-	-0.03	-	-
1.8	0.481	-	-0.01	-	-
Average over linear section		0.16	-0.17	23.8	1.12 x 10 ⁻⁹
Average over 47 to 358 kN/m ²		0.41	-0.13	15.3	1.60 x 10 ⁻⁹

Linear
Section

TABLE 4.12f

CONSOLIDATION PARAMETERS

Sample Gedling lagoon 12, radial drainage, 76.2mm diameter cell

Specific gravity 2.46

Initial dry density 1.060 Mg/m³Final dry density 1.447 Mg/m³

Pressure (kN/m ²)	Voids Ratio	m_v (m ² /MN)	Cc	Cv (m ² /YR)	K (m/sec)
2.7	0.945	-	-	-	-
13.8	0.922	1.09	-0.03	7.1	2.38 x 10 ⁻⁹
24.9	0.902	0.93	-0.06	8.2	2.38 x 10 ⁻⁹
47.1	0.871	0.75	-0.09	7.1	1.65 x 10 ⁻⁹
91.5	0.845	0.31	-0.07	9.9	9.53 x 10 ⁻¹⁰
180.3	0.798	0.29	-0.12	9.9	8.85 x 10 ⁻¹⁰
357.8	0.741	0.18	-0.15	16.4	9.22 x 10 ⁻¹⁰
713.0	0.677	0.11	-0.17	24.8	8.17 x 10 ⁻¹⁰
1423.4	0.608	0.06	-0.18	41.3	7.58 x 10 ⁻¹⁰
712.0	0.618	-	-0.02	-	-
357.8	0.625	-	-0.03	-	-
2.7	0.678	-	-0.02	-	-
Average over linear section		0.16	-0.16	23.1	8.46 x 10 ⁻¹⁰
Average 47 to 358 kN/m ²		0.38	-0.11	10.8	1.10 x 10 ⁻⁹

Linear
Section

probably due to the friction in the apparatus mentioned earlier. At the higher pressures, where these effects are not so important, the improved cylindrical surface area to cross sectional area ratio of the larger sample causes it to give a value of c_v nearer to the true one (Rowe and Barden, 1966).

The difference in c_v between the vertically and horizontally orientated samples of similar size seems to indicate some anisotropy of the sample. Considering the sedimentary character of the deposit one would expect a higher horizontal to vertical permeability (the particles tending to settle with their short axes vertical) thus giving a higher c_v for the sample with vertically orientated bedding*. This would appear to be the case with pressures in excess of 150 kN/m^2 . Below this pressure, however, the horizontally orientated samples have higher c_v 's. This could be due to vertical desiccation cracks, acting as drains initially, but becoming sealed as the pressure increases.

Turning to the central sample, the graphs of c_v against log pressure are shown in Figure 4.21. Unfortunately, it is not possible to make a direct comparison between the sub-sample with a radial drain, and the one with a single vertical drain. This is due to the differences between the two sub-samples mentioned previously. It should be possible, however, to compare sub-samples with vertical drainage and sub-samples with composite vertical and radial drains so long as the voids ratios are similar.

Examination of the results of the three samples concerned show considerable scatter. The sample with radial and vertical drains has an opposite trend to that of the sample with the same drainage facilities, but with the addition of a sand blanket. There does not appear to be any consistent variation which could be attributed

* The drain in the apparatus only allows water to flow vertically upwards.

to anisotropy. This being so, it must be assumed that other factors, such as desiccation cracks and structure must be of equal importance in determining the permeability and hence the coefficient of consolidation. This, it will be recalled, was also the case at Cadeby.

The major observable difference is between the small and large samples. This shows the superiority of a Rowe cell to the common oedometer, especially with materials such as these where individual beds can be considerably thicker than the oedometer sample.

Comparing the central and outlet samples of similar size, above 100 kN/m^2 pressure, all the central samples have higher c_v 's than the outlet samples. This might be expected as the central sample is coarser grained than the outlet sample. Below 100 kN/m^2 the position is not so clear. The values of c_v of both sets of samples become very scattered, and no useful conclusions can be drawn.

In contrast, the coefficient of volume change, m_v , and the compression index, C_c , are similar for all the samples. The former (m_v) shows an exponential drop in value from $3-10 \text{ m}^2/\text{MN}$ to $0.2 \text{ m}^2/\text{MN}$ at 300 kN/m^2 and to $0.05 \text{ m}^2/\text{MN}$ (approximately) at 1200 kN/m^2 . C_c shows a slight fall in value.

4.2.2.4. Vane strength

The vane shear strengths determined on the samples are listed in Tables 4.11d, 4.12a and 4.12b. It can be seen that the finest grained material is the strongest. This is to be expected, when no normal stress is applied, since the component of strength due to ϕ will not be mobilised. The greater amount of clay particles in the outlet sample ensures it a higher strength due to cohesive forces. With the two samples from the central part of the lagoon this does not appear to apply, however, as the coarsest specimen is strongest. It will be noticed, however,

that the coarsest grained specimen also has the lowest voids ratio, and this may be responsible for the increase in shear strength.

As would be expected, the shear strength of the sample tested before and after loading shows an increase after the loading cycle (Table 4.11d).

4.2.3. Kellingley pressed tailings

During the investigation of the southern embankment at Gale Common some pressed tailings from Kellingley Colliery were tested in a 60 x 60mm shear-box. The results, Figures 4.22 and 4.23, show a peak ϕ' of 27° and a residual of 13.2° . It is noticeable that both are lower than the corresponding values for Kellingley coarse discard (i.e. 31.8° and 16° respectively, Figure 2.24). The peak shear strength of the coarse discard is highest, in contrast to the usual situation, probably because of its high carbon content (26%).

It is of importance to note that this material reached residual after a displacement of 0.2 metres (Figure 4.22). Whilst this might be expected, because tailings contain a large amount of fine material in which a shear plane is more easily formed, such behaviour could cause problems on tips during handling.

4.2.4. Summary of properties of fine discard deposits

The characteristics of the two lagoons at Cadeby and Gedling showed some marked lateral variation in lithology from inlet to outlet. Where it could be seen, Cadeby Lagoon 9 showed no overall vertical change. On a smaller scale, both lagoons showed stratifications which were no longer visible as the outlet was approached. The development of the laminae was, however, different in the two lagoons. At Cadeby they were well marked, with a high order of graded bedding, while at Gedling they were but poorly developed. Observations at Cadeby showed that these laminations

could become distorted during filling of the lagoon.

Disturbance of the laminations could be the cause of the coarser samples from the lagoons behaving in an apparently isotropic manner. The visually homogenous, fine grained outlet sample at Gedling was the only one to show distinct anisotropy (Cadeby outlet was not tested in this manner).

The actual amount of consolidation as measured by the coefficient of volume change, m_v , shows little change across the lagoons. The rate at which this consolidation takes place, however, differs markedly. The inlet end, with the coarse sediments consolidates rapidly, while the fine grained outlet sediments consolidate at a much slower rate. A permeability test has shown that the rate of consolidation recorded in the consolidation test is logically an underestimate. However, it is feasible to compare them, one to another on a relative basis.

Compared to the Cadeby Lagoon 9 sediments, the permeability of the embankment face adjacent to the lagoon is very low (10^{-12} m/s for the embankment face, 10^{-6} m/s for the lagoon, Table 4.7). The permeability is such that drainage from the lagoon must be virtually non-existent through the embankment. It follows that, if drainage is required from the lagoon sediments via the embankment, properly designed, filter-protected, drainage blankets on the upstream face are necessary.

In terms of shear strength, the parameters found for Cadeby Lagoon 9 and Kellingley pressed tailings are within the range of values (21.5 to 39°) found by McKechnie Thomson and Rodin (1972). At Cadeby, Lagoon 9, there is a marked difference between the peak shear strengths of coarse layers of inlet material ($\phi' = 32^\circ$) and the fine outlet material ($\phi' = 24^\circ$). A remoulded sample of inlet material, however, was only as strong as the outlet material.

4.3. Laboratory investigation of the effects of flocculants on tailings

As mentioned in Section 4.1.1. flocculant is added to the solids suspension in the washery to promote sedimentation. Two types are in use, polyelectrolyte (Polymer) and starch, with the former being more common. Polyelectrolytes give the higher rate of settling but are about five times more expensive than starch, kilogram for kilogram. There is a suspicion in some N.C.B. areas, notably with reference to the lagoons at Gedling, that polyelectrolyte results in poor drainage of lagoons with consequent lower consolidation rates and lower shear strength.

Jowett and Chopra (1974) conducted experiments on 88mm diameter specimens sedimented from tailings/flocculant mixtures. After removal of supernatant water, the samples were then subjected to up to 25 kN/m^2 suction, the permeability and amount of consolidation being measured. Samples 50mm diameter by 19mm thick were also tested up to pressures of 200 kN/m^2 .

They concluded that:-

- a) Faster settling rates are obtained with polyelectrolyte than with starch.
- b) In systems dosed to give the same settling rate, there is not a significant difference in permeability.
- c) Polyelectrolyte flocculant systems produce a sediment with lower moisture content (i.e. they have lower voids ratios, since the samples were saturated).

Furthermore, with polyelectrolyte (polymer) as flocculant, two peaks in permeability were observed, at concentrations of 0.02 kg/Mg and 1.0 kg/Mg.

While these results give interesting information on the permeability with respect to flocculant dosage it was felt that the consolidation characteristics should be investigated to see

whether there is any advantage in using either starch or poly-electrolyte. To this end the following experiment was designed.

The top of the 254mm Rowe cell was removed and a 203mm diameter alkathene tube was bolted upright in its place (Figure 4.24). (N.B. A tube 254mm in diameter would have been preferable, but one could not be obtained). The requisite amount of flocculant was then added to 18 litres of tailings suspension and vigorously stirred to a) mix the flocculant, and b) to simulate travel along the pipe from thickener to lagoon. The suspension was then poured into the alkathene tube and allowed to settle for two to three days. After this time the tailings had all sedimented out into the Rowe cell. The water in the alkathene tube could then be drawn off via the tap shown in Figure 4.24. The tube was then removed and a 254mm diameter by 0.32mm thick, saturated, sintered bronze plate was allowed to sink slowly onto the upper surface of the sediment. Sufficient water was now siphoned off from above this plate to enable the top of the cell to be assembled in the usual manner. A conventional* Rowe consolidation test could then be carried out, with the consolidation pressure being taken up to a maximum of 300 kN/m^2 .

After the consolidation test, the central ring of the Rowe cell was removed, complete with sample, and inverted into a water bath. A spacer was placed between the porous plate and the base of the bath to keep the sample in place. The shear strength of the sample was then found using a laboratory vane. While the vane does not give a very satisfactory value for shear strength, as will be explained in Section 4.4, it is the only method available which does not destroy the sample. The results are of use on a relative basis.

* It was not necessary to employ back-pressure for saturation in these tests as the material was obviously fully-saturated initially.

The sample, still in the ring, was then submerged and stored in its correct orientation for up to 30 days under an effective stress of 300 kN/m^2 . This was accomplished by using the water bath of a $0.3 \times 0.3 \text{ m}$ shear-box (with the box removed), the load being applied via the lever system of the shear box (See Figure 4.34). At the end of the 30 days, the shear strength was determined as previously. After this, the sample could be dried and weighed.

This method enabled a large size tailings sample to be tested with the minimum of external disturbance. In all, tailings samples from three different sources were tested in this manner. The results will be discussed in the succeeding sections.

4.3.2.1. Manvers tailings

155 litres of raw tailings suspension was supplied by the Scientific Branch of the N.C.B. It is possible that the tailings already contained a small amount of polyelectrolyte, because water is recycled in the Manvers preparation plant. The amount, however is negligible. The initial moisture content was of the order of 2,000 per cent.

4.3.2.2. Sample composition

The grading of the sample is shown in Figure 4.25. It can be seen that it is of non-uniform grading with a uniformity coefficient in excess of 70. It contains 19 per cent clay size and 44 per cent silt size particles with a mean of 22 microns (i.e. coarse silt size). It is very similar to sample 4 in the vertical sequence from Cadeby Lagoon 9 (Figure 4.5).

In terms of consistency limits, the material is an inorganic clay of medium plasticity (Casagrande Plasticity Chart). The limits (see Table 4.13) are similar to Cadeby samples, although the liquid limit and plasticity index are slightly lower than the sample with similar grading.

TABLE 4.13

CONSISTENCY LIMITS OF TAILINGS SAMPLES

Sample	Liquid Limit	Plastic Limit	Plasticity Index
Manvers	35	23	12
Morrison Busty	34	19	15
Gedling	43	29	14

The chemistry (Table 4.8) shows the high carbon content (37.65%) common to most tailings samples. Iron and sulphur are both high, probably combined as pyrite, which is a mineral found in coal. The element oxide ratios are similar to Cadeby (Table 4.9).

4.3.2.3. Consolidation tests

Five consolidation tests were carried out, the results being tabulated in Table 4.14A - E. the five tests were based on the following flocculant concentrations:

- A Unflocculated control sample
- B 1.25 kg/Mg starch (Flocyel)*
- C 0.014 kg/Mg Polymer (Polyfloc 93APA)
- D 0.135 kg/Mg Polymer (Polyfloc 93APA)
- E 0.26 kg/Mg Polymer (Polyfloc 93APA)

The dosage of Polymer initially used, 0.014 kg/Mg (sample C) was taken from Jowett and Chopra (1974) since their work indicated that permeability was enhanced in this dosage region. The starch figure, which was communicated by Mr. A.R. Bacon (N.C.B.) appears to be a 'consensus' value used in coal preparation plants. He pointed out, however, that as starch was added by hand, the actual values used were liable to vary widely. It was also inferred that over-dosing with polyelectrolyte commonly occurs in practice so further tests were carried out at higher dosages. No tests were conducted at the other Jowett and Chopra permeability peak of 1.0kg/Mg since this dosage would be uneconomic in practice.

4.3.2.4. Pressure/voids ratio

The P-e curves are shown in Figure 4.26. It is apparent that large drops in voids ratios occur up to pressures of 40 kN/m² from initial values of 2.2 to 4.8. Above 40 kN/m², the P-e curve is linear up to at least 300 kN/m². The high initial voids ratios are due to the finer material forming a dense suspension at the sediment

* This stands for 1.25kg of Flocgel per Megagram of dry tailings.

TABLE 4.14A

CONSOLIDATION PARAMETERS

Sample Manvers tailings, unflocculated

Specific Gravity 2.05

Initial dry density 0.599 Mg/m³Final dry density 0.951 Mg/m³

Pressure (kN/m ²)	Voids Ratio	m_v (m ² /MN)	Cc	Cv (m ² /YR)	K (m/sec)
0	2.42	-	-	-	-
9.4	2.42	-	-	-	-
18.75	1.58	2.61	-2.79	127.5	1.04 x 10 ⁻⁶
37.5	1.35	4.93	-0.79	1019.6	1.56 x 10 ⁻⁶
75	1.26	0.97	-0.28	52.7	1.59 x 10 ⁻⁸
150	1.17	0.50	-0.28	79.5	1.24 x 10 ⁻⁸
300	1.09	0.25	-0.27	154.9	1.18 x 10 ⁻⁸
120	1.11	0.03	-0.03	-	-
12	1.14	0.14	-0.03	-	-
0	1.16	-	-	-	-
Average (75-300)kN/m ²		0.57	-0.28	95.7	1.34 x 10 ⁻⁸

Average shear strength (kN/m²)

	0 days		30 days		Increase ratio
	m	s	m	s	
Peak	3.9	0.8	6.3	4.0	1.61
Remoulded	3.4	0.0	3.8	1.3	1.12
Sensitivity	1.15		1.66		

m = mean

s = standard deviation

TABLE 4.14B

CONSOLIDATION PARAMETERS

Sample Manvers tailings, 0.014 kg /Mg Polyfloc 93APA

Specific gravity 2.05

Initial dry density 0.642 Mg/m³Final dry density 0.941 Mg/m³

Pressure (kN/m ²)	Voids Ratio	m_v (m ² /MN)	Cc	Cv (m ² /YR)	K (m/sec)
0	2.19	-	-	-	-
9.4	1.66	17.92	-	-	-
18.75	1.50	6.31	-0.52	5.8	1.14 x 10 ⁻⁸
37.5	1.39	2.31	-0.36	22.7	1.63 x 10 ⁻⁸
75	1.29	1.08	-0.32	104.3	3.49 x 10 ⁻⁸
150	1.18	0.66	-0.38	114.4	2.35 x 10 ⁻⁸
300	1.07	0.34	-0.37	248.1	2.61 x 10 ⁻⁸
120	1.09	0.06	-0.06	-	-
12	1.16	0.29	-0.06	-	-
0	1.18	0.8	-	-	-
Average 75-300)kN/m ²		0.69	-0.36	155.6	2.82 x 10 ⁻⁸

Average shear strength (kN/m²)

	0 days		30 days		Increased Ratio
	m	s	m	s	
Peak	5.6	1.4	10.5	2.6	1.88
Remoulded	3.6	0.1	3.6	0.0	1.00
Sensitivity	1.56		2.9		

m = mean

s = standard deviation

TABLE 4.14C

CONSOLIDATION PARAMETERS

Sample Manvers tailings 0.135 kg /Mg Polyfloc 93APA

Specific gravity 2.05

Initial dry density 0.353 Mg/m³Final dry density 0.934 Mg/m³

Pressure (kN/m ²)	Voids Ratio	m_v (m ² /MN)	Cc	Cv (m ² /YR)	K (m/sec)
0	4.81	-	-	-	-
9.4	1.89	53.54	-	-	-
18.75	1.61	10.56	-0.95	824.6	2.71 x 10 ⁻⁶
37.5	1.44	3.52	-0.57	7.3	7.98 x 10 ⁻⁹
75	1.30	1.51	-0.46	152.6	7.18 x 10 ⁻⁸
150	1.19	0.60	-0.34	858.7	1.61 x 10 ⁻⁷
300	1.12	0.24	-0.26	351.4	2.59 x 10 ⁻⁸
120	1.12	0.02	-0.02	-	-
12	1.15	0.12	-0.03	-	-
0	1.19	1.63	-	-	-
Average (75-300 kN/m ²)		0.78	-0.35	454.2	8.62 x 10 ⁻⁸

TABLE 4.14D

CONSOLIDATION PARAMETERS

Sample Manvers tailings 0.26 kg/Mg Polyfloc 93APA

Specific gravity 2.05

Initial dry density 0.374 Mg/m³Final dry density 1.137 Mg/m³

Pressure (kN/m ²)	Voids Ratio	m_v (m ² /MN)	Cc	Cv (m ² /YR)	K (m/sec)
0	4.49	-	-	-	-
9.4	2.18	44.73	-	-	-
18.75	1.59	19.74	-1.96	12.4	7.60 x 10 ⁻⁸
37.5	1.01	12.07	-1.95	92.1	3.46 x 10 ⁻⁷
75	0.89	1.59	-0.40	6.6	3.27 x 10 ⁻⁹
150	0.76	0.90	-0.42	7.8	2.18 x 10 ⁻⁹
300	0.64	0.46	-0.40	8.83	1.26 x 10 ⁻⁹
120	0.66	0.07	-0.05	-	-
12	0.71	0.30	-0.05	-	-
0	0.80	4.37	-	-	-
Average (75-300)kN/m ²		0.98	-0.41	7.7	2.24 x 10 ⁻⁹

Average shear strength (kN/m²)

	0 days		30 days		Increased Ratio
	m	s	m	s	
Peak	10.1	2.5	16.0	2.7	1.58
Remoulded	6.2	3.1	5.3	2.1	0.85
Sensitivity	1.63		3.02		

m = mean

s = standard deviation

TABLE 4.15E

CONSOLIDATION PARAMETERS

Sample Manvers tailings, 1.25 kg/Mg Flocgel (starch)

Specific gravity 2.05

Initial dry density 0.363 Mg/m³Final dry density 1.080 Mg/m³

Pressure (kN/m ²)	Voids Ratio	m _v (m ² /MN)	Cc	Cv (m ² /YR)	K (m/sec)
0	4.64	-	-	-	-
9.4	2.27	44.71	-	-	-
18.75	1.62	21.28	-2.16	518.8	3.43 x 10 ⁻⁶
37.5	1.14	9.67	-1.58	96.6	2.90 x 10 ⁻⁷
75	0.99	1.97	-0.53	89.6	5.50 x 10 ⁻⁸
150	0.85	0.89	-0.44	62.7	1.74 x 10 ⁻⁸
300	0.73	0.43	-0.39	62.9	8.35 x 10 ⁻⁹
120	0.76	0.07	-0.06	-	-
12	0.82	0.35	-0.07	-	-
0	0.90	3.4	-	-	-
Average (75-300)kN/m ²		1.10	-0.95	71.7	2.69 x 10 ⁻⁸

Average shear strength (kN/m²)

	0 days		30 days		Increased Ratio
	m	s	m	s	
Peak	7.3	0.5	15.0	1.6	2.05
Remoulded	3.5	0.1	5.6	1.8	1.6
Sensitivity	2.09		2.68		

m = mean

s = standard deviation

water interface. This suspension dewateres rapidly on application of pressure.

The P-e curves for the unflocculated sample and the two samples with the lowest concentration of Polyfloc 93APA are virtually coincident. However, it should be pointed out that the voids ratios of the 0.13 kg/Mg sample (D) are slightly suspect. This sample was used to compare vane/shear strength with shear-box strength and its total mass had to be calculated from a sub-sample.

On addition of a high dose of Polyfloc 93APA, the voids ratio drops to the lowest value attained with this material i.e. 0.64 at 300 kN/m². With the sample dosed with starch, the voids ratio decreased to only 0.73. Thus a starch concentration of at least five times that of polyfloc is required to attain the same order of consolidation. This cancels out its cost advantage*.

The gradient of the linear portion of the log P-e curve is steeper in the case of the starch treated material, and that with a high polyfloc concentration, than that of the remainder of the samples, i.e. the higher the pressure, the more divergent the values of e become. An analysis of the grading of the fines of the top and bottom halves of the different samples (Figure 4.27 a-d) provides a probable mechanism. The gradings fall into two groups, between which there is a large difference in grading. One group contains the unflocculated and the sample with low polyfloc concentration. The other contains the sample with the high polyfloc concentration and the starch treated sample. The obvious cause is that with effective doses of flocculant, the clay particles will sediment at a similar rate to the silt

* The cost of polyelectrolyte is £1,200 to £1,500 per tonne (Megagram) while the cost of starch is £400 per Megagram (A.R. Bacon, personal communication).

and sand sized particles, thus giving a sample with poorly developed or non-existent graded bedding. This also would account for the lower voids ratios of these samples after consolidation, since the voids between large particles will be filled with clay.

As Figure 4.26 shows, only the sample with a high polyfloc dose actually has a moisture content that is lower than the liquid limit. This may, however, be a false impression, as the voids ratio is the average value of a stratified material. Hence the clay layer at the top may have a lower voids ratio, and therefore be below the liquid limit, even in the other samples.

4.3.2.5. Consolidation parameters

In order to compare consolidation characteristics, averages have been calculated for the most linear sections of the log P-e curves i.e. 70 - 300 kN/m² (Tables 4.14 A - E)

Permeabilities (K) do not show any systematic variation with flocculant or voids ratio. They are of the order of 10⁻⁸ m/s with the exception of the sample with the high polyfloc dose (E), where K is 10⁻⁹ m/s. Below a pressure of 70 kN/m², the permeabilities are usually higher. These values compare to 10⁻⁸ to 10⁻¹⁰ m/s for normal oedometer tests and 10⁻⁵ to 10⁻⁷ measured in the field (McKechnie Thomson and Rodin, 1972). The Rowe cell would appear to be giving an intermediate value.

The values of c_v are similarly higher than those measured in oedometers. Compared to the values obtained from lagoon deposits in the current work, they lie about and above the values obtained for the centrally placed lagoon sample. The sample with a high polyfloc concentration is highlighted by its low values of c_v (only 7.7 m²/yr).

Both m_v and C_c show some correlation with flocculant concentration. The values of m_v increase from 0.57 to 0.98 m²/MN as flocculant

increases. This indicates a steeper log P-e curve, as flocculant concentration increases. Values of C_c decrease from -0.28 to -0.41) as flocculant concentration increases.

4.3.2.6. Vane shear strength

The peak and remoulded vane shear strengths, before and after storage, are shown in Tables 4.14 A,B,D and E. The sample with 0.135 kg/Mg polyfloc 93APA was not tested in this manner because it was used to correlate the vane at simulated depths with the shear strength as measured in a shear-box. This will be considered in Section 4.4.

Examination of the vane strengths shows that shear strengths increase with decreasing voids ratio, and hence also with flocculant concentration. All samples show an increase in strength upon storage, the ratio varying from 1.6 to 2.05, with the starch flocculated material increasing by the greatest amount.

Sensitivities also increase with storage, as remoulded strengths show little, if any, increase with time. The initial sensitivities range from 1.15 to 2.09, increasing to 1.66 to 3.02 after 30 days. It is interesting that initially, the starch flocculated specimen was the most sensitive, but after storage the position was reversed and the specimen dosed with a high concentration of polyfloc has the highest sensitivity. These two specimens do, however, have the highest remoulded strengths after storage.

4.3.3.1. Morrison Busty tailings

Three tests were performed on 90 litres of tailings suspension from Morrison Busty Washery, Co. Durham (see Figure 1.1). The tailings had a moisture content of approximately 2,000 per cent. At this washery, the tailings are pressed into a cake rather than being pumped into lagoons. The discard that is treated is gathered from several collieries in the western part of the Durham coalfield.

4.3.3.2. Sample composition

Figure 4.28 shows the particle size distribution. The tailings are poorly sorted, ranging in size from clay to coarse sand. The material is coarser than the Manvers tailings sample, with only 13 per cent clay and 25 per cent silt size fractions. It has a median diameter of 150 micrometers (i.e. in the fine sand size).

In view of its coarser nature, it is perhaps surprising that the sample has a lower plastic limit than Manvers, and a similar liquid limit (see Table 4.13). The element oxide ratios (Table 4.9) show that the $\text{SiO}_2/\text{Al}_2\text{O}_3$ ratio is substantially lower for Morrison Busty, however, indicating that it contains less free quartz. This lower quartz content probably gives rise to the increase in plasticity.

These tailings also have a surprisingly low carbon content of 17.52 per cent. This is reflected by the specific gravity of 2.42 which is higher than for more normal tailings samples. It is possible that the low organic carbon content may also affect the plastic limit since the statistical analysis of spoil heap materials (Taylor, 1975) showed an unusual feature in this respect i.e. plastic limit increased with increasing coal content.

4.3.3.3. Consolidation tests

The results of the three tests are given in Table 4.15 A-C. The samples were treated with the following amounts of flocculant.

- A - Unflocculated control sample
- B - 1.13 kg/Mg starch (Flocgel)
- C - 0.177 kg/Mg Polymer (Polyfloc 93APA)

The flocculant doses that were added were as close as was possible to those used for the Manvers tailings (i.e. for the high polymer and starch dosages). The differences are due to the water/

tailings suspension not being of constant concentration.

4.3.3.4. Pressure-voids ratio

The pressure-voids ratio relationships are like those of the Manvers tailings (Figure 4.29), with similar voids ratios being attained. As the voids ratio at the liquid limit (assuming saturation) is higher than that of Manvers, both the starch and polymer flocculated specimens are seen to consolidate to below the liquid limit. It is noticeable that although the voids ratios of these two tailings samples are similar, the moisture contents of Morrison Busty are lower. This is because of the higher specific gravity of the latter material.

With the one sample flocculated with starch (Table 4.15B), the voids ratio was measured (at 300 kN/m^2) after the thirty day storage period. As can be seen from Figure 4.29, the voids ratio had dropped by 0.24, from 0.77 to 0.53. This large decrease in voids ratio indicates that a large amount of secondary consolidation must be taking place and it is probably this feature which results in the increased vane shear strength after storage.

4.3.3.5. Consolidation parameters

The consolidation parameters are slightly different to those of Manvers.

The permeability of the unflocculated sample is lower, at $8.63 \times 10^{-9} \text{ m/s}$, than the corresponding Manvers specimen ($1.34 \times 10^{-8} \text{ m/s}$). However, the flocculated samples exhibit higher permeabilities. In the case of the starch sample, this increase is minimal, with a k value of $3.16 \times 10^{-8} \text{ m/s}$ compared with $2.69 \times 10^{-8} \text{ m/s}$ for Manvers. The polyfloc sample has a k value of $3.02 \times 10^{-8} \text{ m/s}$, similar to the starch dosed sample. This is an order of magnitude greater than the Manvers value of $2.24 \times 10^{-9} \text{ m/s}$.

TABLE 4.15A

CONSOLIDATION PARAMETERS

Sample Morrison Busty tailings, unflocculated

Specific Gravity 2.42

Initial dry density 0.557 Mg/m^3 Final dry density 1.103 Mg/m^3

Pressure (kN/m^2)	Voids Ratio	m_v (m^2/MN)	C_c	C_v (m^2/YR)	K (m/sec)
0	3.34	-	-	-	-
9.4	2.18	28.50	-	-	-
18.75	1.61	19.20	-1.90	126.9	7.58×10^{-7}
37.5	1.38	4.61	-0.75	611.4	8.76×10^{-7}
75	1.30	0.92	-0.27	20.8	5.93×10^{-9}
150	1.22	0.48	-0.27	10.5	1.55×10^{-9}
300	1.12	0.31	-0.34	193.2	1.84×10^{-8}
120	1.13	0.04	-0.04	-	-
12	1.16	0.13	-0.03	-	-
0	1.19	1.23	-	-	-
Average (75-300) kN/m^2		0.57	-0.29	74.8	8.63×10^{-9}

Average shear strength (kN/m^2)

	0 days		30 days		Increased Ratio
	m	s	m	s	
Peak	3.7	0.8	4.8	0.0	1.30
Remoulded	2.5	0.3	2.5	0.3	1.00
Sensitivity	1.48		1.92		

m = mean

s = standard deviation

TABLE 4.15B

CONSOLIDATION PARAMETERS

Sample Morrison Busty tailings, 0.177 kg/Mg Polyfloc 93APA

Specific gravity 2.42

Initian dry density 0.579 Mg/m³Final dry density 1.422 Mg/m³

Pressure (kN/m ²)	Voids Ratio	m_v (m ² /MN)	Cc	Cv (m ² /YR)	K (m/sec)
0	3.12	-	-	-	-
9.4	1.27	48.73	-	-	-
18.75	1.00	12.50	-0.88	175.9	6.84 x 10 ⁻⁷
37.5	0.93	2.00	-0.25	5.7	3.58 x 10 ⁻⁹
75	0.84	1.20	-0.29	98.0	3.67 x 10 ⁻⁸
150	0.75	0.69	-0.32	123.9	2.67 x 10 ⁻⁸
300	0.64	0.42	-0.36	208.2	2.71 x 10 ⁻⁸
120	0.65	0.04	-0.03	-	-
12	0.68	0.19	-0.03	-	-
0	0.70	1.02	-	-	-
Average (75-300)kN/m ²		0.77	-0.32	143.4	3.02 x 10 ⁻⁸

Average shear strength (kN/m²)

	0 days		30 days		Increased Ratio
	m	s	m	s	
Peak	6.2	1.6	9.6	1.0	1.54
Remoulded	2.5	0.3	3.6	0.0	1.44
Sensitivity	2.48		2.67		

m = mean

s = Standard deviation

TABLE 4.15C

CONSOLIDATION PARAMETERS

Sample Morrison Busty tailings 1.13kg/Mg Flocgel (starch)

Specific gravity 2.42

Initial dry density 0.669 Mg/m³Final dry density 1.332 Mg/m³

Pressure (kN/m ²)	Voids Ratio	m_v (m ² /MN)	Cc	Cv (m ² /YR)	K (m/sec)
0	2.62	-	-	-	-
9.4	1.12	44.20	-	-	-
18.75	1.07	2.46	-0.16	6.1	4.63 x 10 ⁻⁹
37.5	1.00	1.79	-0.23	113.6	6.33 x 10 ⁻⁸
75	0.92	1.00	-0.25	105.7	3.28 x 10 ⁻⁸
150	0.85	0.52	-0.25	131.1	2.12 x 10 ⁻⁸
300	0.77	0.27	-0.25	483.3	4.09 x 10 ⁻⁸
120	0.78	0.02	-0.02	-	-
12	0.81	0.14	-0.03	-	-
0	0.82	0.52	-	-	-
After one month at 300 kN/m ²	0.53	-	-	-	-
Average (75-300kN/m ²)		0.60	-0.25	240.0	3.16 x 10 ⁻⁸

Average Shear Strength (kN/m²) (overleaf)

Continued.../

TABLE 4.15C (Continued)

		0 days		30 days		Increase Ratio
		m	s	m	s	
	Peak	8.7	-	14.8	-	1.70
	Remoulded	4.1	-	5.0	-	1.22
	Sensitivity	2.1	-	3.0	-	-
Lower (Coarse) Part	(Peak	6.6	2.1	8.6	1.7	1.30
	(Remoulded	3.4	0.5	3.8	0.0	1.12
	(Sensitivity	1.9	-	2.3	-	-
Upper (fine) Part	(Peak	10.7	1.2	20.9	1.7	1.95
	(Remoulded	4.8	0.5	6.2	0.4	1.29
	(Sensitivity	2.2	-	3.4	-	-

m = mean

s = standard deviation

The values of c_v follow the same pattern as the values of k . Thus, with Morrison Busty tailings, there is no difference between polyfloc 93APA and starch flocculants for these parameters.

For the unflocculated samples, there is no significant difference between the corresponding values of m_v and C_c . With the flocculated samples, the Morrison Busty tailings have lower m_v 's and higher C_c 's. Unlike Manvers, the Morrison Busty sample dosed with polyfloc has the higher m_v and lower C_c . The positions are reversed in the case of Manvers.

4.3.3.6. Vane shear strength

Similar to the Manvers tailings, the flocculated specimens show higher vane shear strengths than do unflocculated specimens. Surprisingly, the sample dosed with starch has a higher strength than the sample dosed with polyfloc. This would seem to indicate that vane shear strength is not entirely a function of voids ratio.

With the starch flocculated sample, the shear strength was measured at two different horizons (Table 4.15B). The lower part was considerably weaker than the upper part, also showing less increase in strength with time and lower sensitivity. This is a function of grain size, i.e. the difference in grain size between the bottom and the top of the sample. The coarser grained lower part is weaker because, with the normal stress being zero, the vane does not mobilize the frictional component of the material. The frictional strength of 'granular' tailings is considered further in Section 4.4.

As with Manvers, the strength and sensitivity of the Morrison Busty materials increases with time. It has been mentioned previously (Section 4.3.3.4) that the strength increase is probably caused by the decrease in voids ratio accompanying secondary consolidation. It is pertinent to note that the polyfloc dosed specimen has similar remoulded strengths to the unflocculated one, whereas

in the Manvers sample containing polyfloc the remoulded strength was considerably higher.

4.3.4.1. Gedling tailings

Three tests were performed on 70 litres of reject wet fines suspension (washery underflow) from Gedling Colliery, Nottingham (see Figure 1.1). The tailings had a moisture content of approximately 1,000 per cent, and may have had a small starch content due to recycling of water in Gedling washery (starch is used as a flocculant at Gedling).

4.3.4.2. Sample composition

The grading (Figure 4.30) is similar to Manvers tailings (Figure 4.25), with 20 per cent clay size, 40 per cent silt size and a very non-uniform grading from clay to coarse sand size. It lies between the particle size distributions for the central sample from Lagoon 12 at Gedling (Figure 4.17).

Consistency limits are similar to the central sample from Lagoon 12, although the plastic limit is slightly higher, and hence the plasticity index is rather smaller (Table 4.13). Both liquid and plastic limits are, however, considerably higher than those of the tailings sample from Manvers Colliery.

The sample has a carbon content of 38 per cent (Table 4.8), which is a typical value for tailings. In chemical composition, it is very similar to other tailings and lagoon samples, although Fe_2O_3 and sulphur are on the low side, inferring a low pyrite content.

A comparison of the 'raw' tailings with the coarse discard chemistry (Table 2.1) shows the major difference to be one of carbon content - 38 per cent for the tailings and an average of 10.9 per cent for the coarse discard. In the element oxide ratio the $\text{SiO}_2/\text{Al}_2\text{O}_3$ and $\text{Fe}_2\text{O}_3/\text{Al}_2\text{O}_3$ values are lower for the tailings.

With the other element oxides, the ratios for the tailings lie within the range of ratios for the coarse discard. There would appear to be less quartz (SiO_2) and iron in the tailings than in the coarse discard. As the $\text{S}/\text{Al}_2\text{O}_3$ ratio for the two materials is similar, suggesting that the pyrite content is similar, the higher iron content of the coarse discard is probably contained in siderite (clay ironstone).

4.3.4.3. Consolidation tests

The results of the three consolidation tests carried out are given in Table 4.16 (A-C). The three tests were slightly different to the usual sequence and were as follows:-

- A - Unflocculated sample, with sediment disturbed prior to consolidation.
- B - 0.257 kg/Mg polyfloc 93APA with sample taken to an effective stress level of only 100 kN/m^2 .
- C - 1.109 kg/Mg flocgel (starch).

Sample A was prepared to discover what effects agitation of the dense suspension would have, following sedimentation. Such agitation might be caused in the field by vibrations from plant, waves on the lagoon (if of large enough fetch) or by currents set up by the tailings inflow. The usual method of sedimentation was followed until the stage of reassembling the Rowe cell was reached. At this stage the sample was disturbed using a 254mm diameter metal plate which was oscillated with an amplitude of 15mm in a manner such that it pivoted about a diameter. The diameter about which it pivoted was changed from time to time. After this, the cell was assembled and the test proceeded in the normal manner.

With Sample B, the pressure was taken to only 100 kN/m^2 in small increments. This sample was then vane tested at various pressures. It was necessary to check whether overconsolidation

TABLE 4.16A

CONSOLIDATION PARAMETERS

Sample Gedling tailings, unflocculated, disturbed sample

Specific gravity 1.90

Initial dry density 0.407 Mg/m^3 Final dry density 1.083 Mg/m^3

Pressure (kN/m^2)	Voids Ratio	m_v (m^2/MN)	C_c	C_v (m^2/YR)	K (m/sec)
0	3.311	-	-	-	-
9.4	1.439	46.30	-	-	-
18.75	1.044	17.26	-1.31	-	-
37.5	0.922	3.20	-0.41	-	-
75	0.823	1.37	-0.33	390.1	1.66×10^{-7}
150	0.738	0.62	-0.28	134.3	2.59×10^{-8}
300	0.660	0.30	-0.26	300.3	2.79×10^{-8}
120	0.671	0.04	-0.03	-	-
12	0.697	0.14	-0.03	-	-
0	0.754	0.28	-	-	-
Average (75-300 kN/m^2)		0.76	-0.29	274.9	7.33×10^{-8}

Average shear strength (kN/m^2)

	0 days		30 days		Increase Ratio
	m	s	m	s	
Peak	14.8	0.4	32.9	2.4	2.22
Remoulded	4.9	1.0	7.1	2.5	1.45
Sensitivity	3.0		4.6		

m = mean

s = standard deviation

TABLE 4.16B

CONSOLIDATION PARAMETERS

Sample Gedling tailings 0.257 kg/Mg Polyfloc 93APA

Specific gravity 1.90

Initial dry density 0.434 Mg/m³Final dry density 0.943 Mg/m³

Pressure (kN/m ²)	Voids Ratio	m_v (m ² /MN)	Cc	Cv (m ² /YR)	K (m/sec)
0	3.37	-	-	-	-
10.7	1.39	42.50	-	-	-
20	1.17	9.86	-0.81	231.6	7.10 x 10 ⁻⁷
30	1.10	3.11	-0.38	172.2	1.66 x 10 ⁻⁷
40	1.05	2.36	-0.40	121.0	8.87 x 10 ⁻⁸
50	1.01	1.84	-0.39	169.4	9.71 x 10 ⁻⁸
60	0.98	1.69	-0.43	290.5	1.53 x 10 ⁻⁷
70	0.96	0.84	-0.25	6.2	1.62 x 10 ⁻⁹
80	0.94	0.95	-0.32	88.0	2.60 x 10 ⁻⁸
90	0.92	1.09	-0.42	29.2	9.94 x 10 ⁻⁹
100	0.90	0.88	-0.37	1.6	4.48 x 10 ⁻¹⁰
50	0.91	0.08	-0.03	-	-
0	1.01	1.06	-	-	-
Average (40-100kN/m ²)		1.38	-0.37	100.8	5.38 x 10 ⁻⁸

Average shear strength (kN/m²)

	0 days
Peak	6.0
Remoulded	2.9

TABLE 4.16C

CONSOLIDATION PARAMETERS

Sample Gedling tailings 1.109 kg/Mg starch

Specific gravity 1.90

initial dry density 0.460 Mg/m³Final dry density 1.070 Mg/m³

Pressure (kN/m ²)	Voids Ratio	m_v (m ² /MN)	Cc	Cv (m ² /YR)	K (m/sec)
0	3.13	-	-	-	-
9.4	1.40	4.46	-	-	-
18.75	1.27	5.56	-0.42	122.7	2.12 x 10 ⁻⁶
37.5	1.01	6.06	-0.86	161.6	3.04 x 10 ⁻⁶
75	0.91	1.38	-0.35	196.6	8.43 x 10 ⁻⁸
150	0.81	0.72	-0.34	269.1	6.00 x 10 ⁻⁸
300	0.71	0.34	-0.31	527.7	5.66 x 10 ⁻⁸
120	0.72	0.04	-0.03	-	-
12	0.75	0.16	-0.03	-	-
0	0.78	0.97	-	-	-
Average (70-300kN/m ²)		0.81	-0.33	331.1	6.70 x 10 ⁻⁸

Average shear strength (kN/m²)

	0 days		30 days		Increase Ratio
	m	s	m	s	
Peak	13.2	2.9	26.4	7.7	2.0
Remoulded	5.3	0.8	10.7	3.2	2.0
Sensitivity	2.5		2.5		

m = mean s = standard deviation

Voids Ratio during storage	
Time(days)	Voids Ratio
1	0.63
5	0.61
17	0.52
30	0.52

was affecting vane shear strength and consequently a low pressure range was adopted. Consolidated-undrained triaxial tests were also carried out on the sample, in order to compare with the vane test results.

Sample C was a conventional test except that the sample was stored in a starch solution and the amount of consolidation during storage was measured.

4.3.3.4. Pressure/Voids ratio

The log pressure/voids ratio curves (Figure 4.31) show some pertinent features. The starch flocculated sample reaches a similar voids ratio at 300 kN/m^2 as the Manvers tailings. However, the gradient of the line is flatter for the Gedling material, i.e. the voids ratio of Gedling tailings is less than Manvers tailings at lower pressures. The consolidation on storage is noticeably irregular, and was complete after 17 days (Table 4.16C). The polyfloc flocculated specimen follows a similar path to the starch flocculated specimen; this is unlike either Manvers or Morrison Busty where lower voids ratios were attained.

Disturbing the suspension obviously destroys the graded bedding. The disturbed unflocculated sample produces the lowest voids ratios and visual examination showed it to be similar to the central sample from Lagoon 12 at Gedling.

The voids ratio equivalent to the liquid limit moisture content is attained by the starch flocculated specimen at 150 kN/m^2 and by the disturbed specimen at 75 kN/m^2 . If consolidation had been taken far enough, the polymer flocculated specimen would presumably have reached the liquid limit at a similar pressure to the specimen treated with starch.

It should be noted that the degree of secondary consolidation is sufficient for the moisture content equivalent to be below the

plastic limit of these tailings.

4.3.4.5. Consolidation parameters

It is possible to compare the parameters for the unflocculated and starch flocculated specimens at the 75 kN/m^2 (i.e. from 37.5 to 75 kN/m^2) loading stage with the average parameters of the polyfloc treated specimen over the range $40 - 70 \text{ kN/m}^2$ (Table 4.17). It is evident that the parameters are similar. At this loading the disturbed specimen has a higher c_v and permeability. This is only transient at best, because the averages for the $75-300 \text{ kN/m}^2$ loadings show little difference between the unflocculated disturbed sample and the starch treated sample.

When compared to the other sedimented tailings samples (Table 4.18) the m_v and C_c parameters are seen to be of the same order. The values of c_v and K lie at the higher end of the range. This is perhaps most marked with the disturbed, unflocculated specimen where c_v is approximately three times as large as the values for either Manvers or Morrison Busty. It would appear that disruption of graded bedding increases the rate of consolidation.

When compared with the results for the consolidation tests carried out on the material from the central part of Lagoon 12 at Gedling, a number of significant points arise. Firstly, the voids ratios attained by the sedimented samples are not as low as those reached by the lagoon samples at similar pressures, until the former have been stored for thirty days. Secondly, the sedimented tailings samples display a steeper gradient on the log pressure-voids ratio plot. Finally, the rate of consolidation and permeability of the sedimented samples are considerably higher (by a factor of five). The most likely reason for these differences is the desiccation to which the lagoon samples have been subjected. In other words, they are effectively overconsolidated. The question as to which samples

TABLE 4.17

Gedling tailings 37.5 - 75 kN/m² loading stage

Sample	m_v (m ² /MN)	Cc	Cv(m ² /YR)	K(m/sec)
Unfloc.	1.37	-0.33	390.1	1.66 x 10 ⁻⁷
Polyfloc 93APA(40-70) (0.26 kg/Mg)	1.68	-0.37	146.8	8.5 x 10 ⁻⁸
Flocbel(starch) (1.11kg/Mg)	1.38	-0.35	196.6	8.43 x 10 ⁻⁸

TABLE 4.18

Table of average values (70 - 300 kN/m²) of consolidation parameters for sedimented samples

Sample	m_v (m ² /MN)	Cc	Cv(m ² /YR)	K(m/sec)
Manvers Unflocculated	0.57	-0.28	95.7	1.34 x 10 ⁻⁸
0.041kg/Mg Polyfloc	0.69	-0.36	155.6	2.82 x 10 ⁻⁸
0.135kg/Mg Polyfloc	0.78	-0.35	454.2	8.62 x 10 ⁻⁸
0.26 kg/Mg Polyfloc	0.98	-0.41	7.7	2.24 x 10 ⁻⁹
1.25 kg/Mg Starch	1.10	-0.95	71.7	2.69 x 10 ⁻⁸
Morrison Busty Unfloc.	0.57	-0.29	74.8	8.63 x 10 ⁻⁹
0.177kg/Mg Polyfloc	0.77	-0.32	143.4	3.02 x 10 ⁻⁸
1.13 kg/Mg Starch	0.60	-0.25	240.0	3.16 x 10 ⁻⁸
Gedling 1.11kg/Mg starch	0.81	-0.33	331.1	6.70 x 10 ⁻⁸
Unfloc. disturbed	0.76	-0.29	274.9	7.33 x 10 ⁻⁸

are the most representative of actual lagoons will depend to a large extent upon how often the lagoon dries out during the period over which it is being filled. This will obviously depend to a large extent on the rate of filling, the climatic conditions prevailing, and the permeability of the lagoon and its containing embankments. Some evidence on the matter of desiccation during filling will be discussed in the section on vane shear strengths of lagoon deposits (Section 4.4).

4.3.4.6. Vane Shear strength

The vane strength on unloading is similar for the two samples taken to effective pressures of 300 kN/m^2 . Both increase in strength on storage, probably due to the decrease in voids ratio on secondary consolidation. It is noticeable that the flocculated specimen has a higher remoulded strength, and hence a lower sensitivity. The starch treated specimen has a noticeably higher strength than either of the other two starch flocculated tailings specimens from Manvers and Morrison Busty. The unflocculated one cannot be compared because of its mode of preparation (disturbance).

Since the starch flocculated specimen which was stored in starch solution behaved in a similar manner to the other tailings samples it is apparent that leaching effects due to supernatant precipitation are unlikely to be of any consequence in colliery lagoons.

In Table 4.19 the results of a statistical correlation analysis between voids ratio and vane shear strength is given. The voids ratio on unloading is the value used, since this is the value which is relevant to the situation upon vane testing. Three groupings of the data are considered, numbers 1, 2 and 3 in Table 4.19. In the first, all the sedimented samples and the Gedling Lagoon 12 samples are considered. Here a 95 per cent

TABLE 4.19

Correlation between vane shear strength and final voids ratio

Sample	Vane shear strength	Voids Ratio	Used in correlation number
Gedling lagoon 12/6 centre vertical drain	23.5	0.557	1
Gedling lagoon 12/6 centre radial drain	16.0	0.887	1
Gedling lagoon 12/6 outlet	27.2	0.847	1
Manvers Unfloc.	3.9	1.16	1,2,3
Polyfloc. 93APA 0.014 kg/Mg	5.6	1.18	1,2,3
0.26 kg/Mg	10.1	0.80	1,2,3
Starch 1.25 kg/Mg	7.2	0.90	1,2,3
Morrison Busty Unflocculated	3.7	1.19	1,2
Polyfloc 93APA 0.177 kg/Mg	6.2	0.70	1,2
Starch 1.13 kg/Mg	8.7	0.82	1,2
Gedling Disturbed Unflocculated	14.8	0.754	1,2,3
0.26 kg/Mg Polyfloc. (up to 100 kN/m ² only)	6.0	1.01	1,2,3
Starch 1.11 kg/Mg	13.22	0.78	1,2,3

Correlation number	No. of Points	Correlation Coefficient	Significance (%)
1	13	-0.6223	95
2	10	-0.7329	98
3	7	-0.9024	99.9

significance level is reached, i.e. a 1 in 20 chance of there being no correlation. Next, only the three sedimented samples were correlated. This gave a 98 per cent significance level, or a 1 in 50 chance of no correlation. Finally, the Manvers and Gedling sedimented samples were correlated. These gave a 99.9 per cent significance level or a 1 in 1,000 chance of no correlation.

From these tables it is apparent that there is a correlation between voids ratio and vane shear strength. However, there is considerable scatter when all samples are included, as can be seen when the points are plotted on Figure 4.32. The correlation improves when only samples of similar grading are compared (i.e. Manvers and Gedling). This infers that grading is also of importance, as was suggested in Section 4.2.2.4.

4.3.5. Comparison of the effects of flocculants upon the voids ratio of sedimented tailings

Flocculant in high doses causes the graded bed formed by normal sedimentation to be less well developed. It achieves this by causing the fine clay particles to sediment out at a rate similar to that of the coarser particles. An effect of this poorer sorting of the sediment is to produce a lower voids ratio on consolidation, the voids which would normally be present between the larger particles being filled by clay size particles. Obviously, with low flocculant doses, where the sedimentation rate is less, this effect will be less pronounced. In fact, in the one sample tested at varying flocculant dosages, (i.e. Manvers), there is little effect upon the voids ratio until a flocculant concentration of over 0.14 kg/Mg of Polyfloc 93APA is used.

The reduction in voids ratio produced by high flocculant concentrations has two beneficial effects. Firstly, it reduces

the moisture content of materials which are certain to be saturated on formation, so reducing the amount of water trapped in the lagoon sediment. Secondly, it enables more material to be contained in the lagoon, i.e. increasing the lagoon's capacity, which will decrease the area of land required for tailings disposal.

Considering the two types of flocculant employed in these experiments Polyfloc 93APA (polyelectrolyte) and Flocgel (starch), both cause a reduction in voids ratio. However, starch requires a concentration of at least five times that of polyelectrolyte to give the same voids ratio. On this basis, therefore, starch has no advantage over polyelectrolyte, as its cost per unit weight is only one third to a quarter of that of polyelectrolyte (see footnote, Section 4.3.2.3).

4.3.6. Summary, the effects of flocculants on the consolidation parameters and vane shear strength

The coefficients of consolidation (c_v) and the permeability (K) will be considered first. They show a considerable variation, (Table 4.18) with c_v ranging from 7.7 to 454.2 m²/yr (average values) and K ranging from 2.24×10^{-9} to 8.62×10^{-8} m/s (average values). In the case of two of the tailings samples, Gedling and Morrison Busty, there is no significant variation between samples flocculated with Polyfloc 93APA and those treated with starch (Tables 4.17 and 4.18). With Manvers, tailings the situation is somewhat more complicated. At a high concentration of Polyfloc (0.26kg/Mg), c_v and K are low, i.e. 7.7m²/yr and 2.24×10^{-9} m/s respectively, while with starch as flocculant, c_v and K are somewhat higher, at 71.7 m²/yr and 2.69×10^{-8} m/s respectively. At low Polyfloc concentrations (i.e. below 0.14 kg/Mg), both c_v and K are enhanced (up to 454.2m²/yr and 8.62×10^{-8} m/s) with Manvers tailings. It will be remembered

that with Manvers tailings, at these concentrations, no reduction in voids ratio (relative to an unflocculated sample) was taking place. Presumably the structure of the clay layer at the top of the sedimented sample is more permeable when formed of floccules.

With respect to the unflocculated samples, in one case, (Manvers) the high flocculant dosed samples had lower values of c_v and K whilst in the other (Morrison Busty) these parameters were higher.

Turning to the parameters m_v and C_c , with both Manvers and Morrison Busty tailings m_v increases with increase in concentration of Polyfloc 93APA. With starch as flocculant only with Manvers is there any noticeable increase in m_v (Table 4.18). Both Polyfloc and starch decrease the value of C_c compared to that of unflocculated material, for Morrison Busty there is little change.

In terms of shear strength, there is a statistically significant (99.9 per cent) correlation between final voids ratio and vane shear strength for materials with similar grading (i.e. Gedling and Manvers tailings). The coarser grained Morrison Busty material is generally weaker than Gedling or Manvers samples of similar voids ratio. This is presumably due to the smaller proportion of clay size particles in the Morrison Busty material, the clay size particles providing the cohesive forces which are being measured.

On storage under an effective stress of 300 kN/m^2 for 30 days, the unconfined vane strength increases for all the samples. The increase is greatest with the high flocculant dosed samples. The increase is probably due to the voids ratio decrease caused by the large degree of secondary consolidation. This secondary consolidation can result in a decrease of up to 30 per cent in

the voids ratio. This large decrease may be due to the breakdown of the flocculated structure and reorientation of particles under effective stress conditions during an extended time interval.

4.4. Vane shear tests in colliery tailings

4.4.1. Introduction

With soft deposits, sample disturbance during driving of the sampling tube is often excessive. In these cases, laboratory measurement of the undrained shear strength will not be reliable. In situ measurement of this parameter is therefore desirable. Of the possible techniques, the vane test is generally considered to give the best results. When used in clays, it may give values some 10 to 15 per cent higher than those measured by consolidated undrained triaxial test on the same sample (Terzaghi and Peck, 1967). When silt and sand layers occur, the strength measured by a vane increases considerably, due to partial drainage along the silt or sand layers. Thus the shear strength as measured by a vane becomes unreliable when such deposits are encountered.

A considerable number of vane tests have been carried out in lagoons. Owing to the soft nature of lagoon deposits, they are difficult to sample without disturbance (except in the desiccated crust). The vane, therefore is an attractive method for measuring undrained strength. However, lagoon deposits contain considerable quantities of silt and sand, often in well defined laminations, as has been shown in previous sections of this chapter. Vane results are not, therefore, immediately interpretable. This section constitutes an attempt to extract some useful information from the previously published vane test results.

With normally consolidated deposits, undrained shear strength increases linearly with depth. This can be shown as follows:

From Figure 4.33, which is modified from Figure 28.12 in Lambe and Whitman (1969), it can be seen that: =

$$\frac{1}{2} (\sigma_1 - \sigma_3) = \frac{\sigma_3' \sin \phi'}{1 - \sin \phi'}$$

where σ_1 = total major principal stress at failure

σ_3 = total minor principle stress at failure

σ_3' = effective minor principle stress at failure

ϕ' = effective angle of shearing resistance

The cohesion intercept (c') is taken as zero, this being the situation for normally consolidated deposits.

$$\text{let } q = \frac{1}{2} (\sigma_1 - \sigma_3)$$

$$\text{then } q = \frac{\sigma_3' \sin \phi'}{(1 - \sin \phi')}$$

With Skempton's pore pressure parameter, A , having a value A_f , the pore pressure at failure, u_f , is given by:

$$u_f = A_f (\sigma_1 - \sigma_3)$$

$$\therefore u_f = 2A_f q$$

$$\text{Now, } u_f = \sigma_3 - \sigma_3'$$

$$\therefore q = \frac{(\sigma_3 - 2A_f q) \sin \phi'}{(1 - \sin \phi')}$$

$$\therefore q = \frac{\sigma_3 \sin \phi'}{(1 + (2A_f - 1) \sin \phi')}$$

The term $\frac{\sin \phi'}{(1 + (2A_f - 1) \sin \phi')}$ is a constant

Also, σ_3 , the total pressure, is proportional to the depth, provided that bulk density is constant. Hence q is proportional to depth. Now q is the "top point" of the Mohr's circle, and, as

shown in Chapter 2.2.4.1, can be directly related to the shear strength. Therefore, undrained shear strength should increase linearly with depth.

In the case of clays, where undrained loading occurs, Skempton (1957) has shown an empirical relationship between the shear strength (c), the effective pressure (\bar{p}) and the plasticity index (PI), whereby:

$$\frac{c}{\bar{p}} = 0.11 + 0.0037 \text{ PI}$$

This, of course, cannot be expected to apply to silts and sand, where partial dissipation of pore pressures occurs during the shearing process. Blight (1968) has developed a method for using the vane to measure drained shear strength in silty soils, but this is not applicable to the current investigation, as there was no control over the method in which the vane was used. It is doubtful if the method would be of use in colliery tailings, anyway. This is because the upper, fine part of the laminae will probably fail in an undrained state, while the lower, coarser part fails in a drained mode.

Thus, to make some sense of the vane results in colliery tailings, it was decided to empirically calibrate a vane in the laboratory against alternative laboratory methods of measuring undrained shear strength. In addition, possible empirical relationships between the shear strength and the ^{overburden} pressure were investigated.

4.4.2. Laboratory calibration of a vane

4.4.2.1. Apparatus

The calibration of a vane involved measuring vane shear strength in a tailings sample under different effective normal pressures. The technique involved a modification of the apparatus

used to apply a 300 kN/m^2 load to the sedimented tailings samples during storage (Figure 4.34). A hole was drilled in a 254 mm diameter, 15mm thick, steel disc, the hole being some 40mm from the perimeter.

It was just large enough to allow passage of the vane shank. The plate, with the vane in it, was then placed on top of the sample which was loaded via the hanger and lever system of a $0.3 \times 0.3\text{m}$ shear-box to the desired stress level. The motor drive of the vane could now be mounted in place. The sample was left for one day to consolidate, after which the vane was advanced some 20mm into the specimen and the vane strength determined. Both peak and remoulded strengths were recorded. To find the vane strength at different normal pressures, the apparatus was dismantled and the sample rotated by 15-20 degrees, so that when reassembled the vane was in an undisturbed part of the sample.

With the apparatus shown in Figure 4.34, there are two points which should be explained. The vane mounting frame was erected with one end on the hanger and the other end upon the shear-box frame. Thus approximately half its weight would bear upon the sample. A certain amount of its weight would also be transmitted by friction along the sides of the vane. Calculation shows, however, that the weight of the vane frame, which was 4.16kg, is very small in terms of the stress applied to the sample.

$$\text{i.e. Weight of frame} = 4.16\text{kg}$$

$$\therefore \text{Additional weight on hanger} = \frac{4.16}{2}$$

(N.B. half of weight carried on the shear-box frame)

$$\text{Area of sample} = 0.127^2 \times \pi \text{ m}^2$$

$$\therefore \text{Pressure} = \frac{4.16 \times 9.807}{2 \times 1,000 \times 0.127^2 \times \pi} \text{ kN/m}^2$$

$$\therefore \text{Pressure} = 0.40 \text{ kN/m}^2$$

This amount was, in fact, added to the stress calculated from the lever loading system. Although it is only an approximation of the stress due to the vane frame, the errors in this figure will be of the same order as those for the lever loading system and can therefore be ignored.

The hole in the steel top plate must produce a region of 'pressure shadow' in the sample which may extend into the zone being tested by the vane. This is, however, similar to conditions in the field, where the tubing protecting the vane rods will produce a similar effect. A more aggravating effect of the hole is to produce some sample loss. A certain amount of sample is forced up through the hole as pressure is applied. The amount however, is small and can safely be ignored.

4.4.2.2. Results

Two samples were tested using the apparatus outlined above. Both were sedimented out from a flocculant/tailings suspension. The first sample, of Manvers tailings was consolidated in the Rowe cell to 300 kN/m^2 , but not stored. After the vane tests were carried out at varying normal stresses, 60 x 60mm specimens were carefully cut from the sample and placed in a 60 x 60mm shear-box with the minimum of disturbance. A normal stress was now applied, and the sample allowed to consolidate. The sample was then sheared at a rate of strain similar to that of the vane. This rate was chosen to try and ensure parity in pore pressure dissipation.

The results (Figure 4.35) show the shear strength as measured in the shear-box is considerably higher than the vane shear strength.

The second sample, of Gedling tailings was only consolidated to 100 kN/m^2 . This was to remove the possible effects of over-

consolidation at the higher pressures. This sample was subjected to a consolidated-undrained triaxial test after completion of the vane tests. The strain rate was again similar to that of the vane. Bishop and Henkel (1962) show that shear strength can vary with rate of strain. The results (Figure 4.36) imply that the consolidated-undrained triaxial results are higher than those obtained with the vane.

Considering both sets of results, it can be seen that it is the remoulded shear strength results which follow Skempton's (1957) relation:

$$\frac{c}{p} = 0.11 + 0.0037PI$$

With clays, the remoulded strength often follows the relation

$\frac{c}{p} = 0.3 + 0.01$ (Lambe and Whitman, 1969). However, with materials such as colliery tailings with low plasticity indices, Skempton's relation for peak strength gives lower values of c . In fact, as can be seen from Figures 4.35 and 4.36, the peak strength follows the $\frac{c}{p} = 0.3$ relation fairly closely.

For overconsolidated clays, the total stress failure envelope for consolidated undrained tests is of the form shown in Figure 4.37. It is not possible to discern an overconsolidated shear strength envelope for either of the two samples. Presumably the strength increase due to overconsolidation is less than the scatter in the test results.

As mentioned previously, both shear-box and triaxial testing techniques give higher shear strength than those obtained with the vane. It would appear then, that the vane underestimates the shear strength of graded laminated materials.

It is interesting that although the samples have differing

voids ratios (Tables 4.14D and 4.16B)* they both follow similar shear strength relationships with depth i.e. $\frac{c}{p} = 0.3$ (peak); $\frac{c}{p} = f$ (PI) (remoulded strength). This is due to the frictional component of the strength being mobilized as effective normal pressure is applied. (The voids ratio/vane shear strength relationship discussed in Section 4.3.4.6. is probably only operative at zero normal pressures where only cohesive forces are operative). As pointed out by Lambe and Whitman (1969), the use of 'c' to denote the shear strength of a consolidated undrained test is misleading. However, it has been used so often in the literature that it has been used here to prevent confusion.

4.4.3. Field vane results

4.4.3.1. Introduction

Field vane results for a number of lagoons have been plotted in Figures 4.40 - 4.49. These results have been taken from reports to the National Coal Board by Messrs. Wimpey Laboratories Ltd. and Sir William Halcrow and Partners. The Laboratory results for Manvers and Gedling are also shown (Figures 4.38 and 4.39) in terms of c against equivalent depth.

There are several difficulties when computing c / p lines. With the variability in the nature of lagoon deposits, the plasticity index will vary considerably. Thus, the values for a borehole in one part of a lagoon cannot be expected to apply to a different part of the same lagoon. Again, if the inlet and outlet have been in much the same position during the filling of the lagoon, the mean values of bulk density and plasticity index

* It should be remembered that the Gedling sample was not over-consolidated initially to the same degree as the Manvers sample. At higher pressures (over 100 kN/m^2), it will therefore consolidate to a greater extent than the Manvers sample. The Gedling sample will therefore have an even lower voids ratio than the Manvers Sample.

may remain constant in a vertical direction, but there will still be considerable variability in lithology and properties e.g. the U100 from Lagoon 8, Cadeby, Figure 4.3. Since lagoon deposits generally have low bulk densities, the position of the water table at the time of a vane test will be of great importance. The water table position is not always recorded. Furthermore, where piezometers are installed, piezometric water levels can often be seen to decrease with depth in the lagoon. Where this happens, either perched water tables or zones of excess pore pressure must be present.

Bearing all these factors in mind it will be appreciated that the following interpretations of field data involve some highly speculative elements. Nevertheless, it will be shown that a number of features can be resolved which help in the overall understanding of what are generally reported as "shear strength trends".

4.4.3.2. Gedling Lagoon (East Tip)

Figure 4.40 shows the results of two vane tests in two boreholes (E7 and E8) near the inlet of the old East Tip Lagoon. Results of another borehole, E15, positioned near the outlet, are shown in Figure 4.41.

Borehole E8 was at the side of the lagoon, where the depth of tailings is only 4 metres. At position E7, there was some 16 metres of tailings. Piezometers in the boreholes indicate that there is no continuous ground water table. A piezometer at 16 metres depth showed a water level of a similar depth. In comparison, one at 9.2 metres depth showed a water level 3.5 metres below ground level.

It is demonstrated on Figure 4.40 that the E7 peak shear strength results down to a depth of 8.5 metres follow the relation

$\frac{c}{p} = 0.3$ where the pressure is computed on a total stress basis. The remoulded strength follows the $\frac{c}{p} = f$ (PI) line. Below 8.5 metres, the peak strength increases beyond that predicted by the line $\frac{c}{p} = 0.3$. The water pressure at 9.2 metres depth appears to have no effect on the measured shear strength.

In borehole E8, the shear strength approximately follows a line defined by $\frac{s}{p} = \tan 31^\circ$, s being the shear strength, and 31 degrees being the drained angle of shearing resistance of the tailings at the inlet end. It would seem that with the coarse, free draining, materials at the inlet end of this lagoon, the vane is mobilizing the drained shear strength of the material. This effect will be met again at Grimethorpe Lagoon 16 (Section 4.4.3.3. That the vane can measure drained shear strength was shown by Blight (1968).

It is interesting to note that, in Borehole E7, the peak shear strength below 8.5 metres approximately follows a line which is parallel to the line $\frac{s}{p} = \tan 31^\circ$, but the values lie below it. This effect could be caused by there being a constant excess pore pressure of 4.2 metres of water, below 8.5 metres (see Figure 4.40), with the vane mobilizing a shear strength of $\frac{s}{(p-u)} = \tan 31^\circ$. This would presumably require the material below 8.5 metres to be coarser than that above this depth. Having thus postulated a change in material properties, it must be admitted that a change in a different property could also account for the increase in shear strengths, viz: that the bulk density of the material below 8.5 metres is higher than the bulk density above this depth. A higher bulk density would produce an increase in the pressure gradient. This, in turn, should lead to a more rapid rise in shear strength with depth.

At the outlet end (Figure 4.41) the situation is less well

known than at the inlet end. Neither water level or piezometer readings are available. Lines have been drawn depicting the $\frac{c}{p}$ relation in terms of $f(PI)$, 0.3 and $\tan 31^\circ$ (the angle of shearing resistance). Both total and effective stress (with water table at the surface) conditions are shown. In the absence of excess pore pressures the earlier findings would suggest that peak strength values should not lie below the $\frac{c}{p} = f(PI)$ line. although normally consolidated clays follow this relationship, it has been shown in the previous section that in the case of tailings it is the remoulded vane shear strength which agrees closely with it. Peak vane shear strengths of tailings lie above it. Considering the actual results, no points do in fact lie below the $f(PI)$ effective stress line. However, it is obvious that there is a great deal of scatter. This could indicate large variations in the lithology of the deposit or could be due to desiccation producing a higher overconsolidated shear strength. As far as is known, the position of the inlet and outlet of the lagoon did not vary considerably. Some of the results, however, give strengths above the $\tan 31^\circ$ effective shear strength line. This would necessitate coarse free draining material to be present, which is unlikely at this end of the lagoon. Thus, the high strengths are more likely to be due to desiccation. An alternative explanation is that total stress conditions apply, the values below the $f(PI)$ total stress line being a function of restricted zones of excess pore pressure.

4.4.3.3. Grimethorpe Lagoon 16

Grimethorpe No. 16 lagoon is unusual. It is constructed on a floor of impermeable clay and has a highly permeable bank at the outlet end (National Coal Board, 1972). The results of

vane tests in four positions in the lagoon are shown in Figure 4.42. Only peak strength values are available. The position of the water table is known at both the inlet and outlet testing positions.

Between the inlet and the centre of the lagoon a significant shear strength progression can be elucidated. The shear strengths which lie about a $\frac{s}{p} = \tan \phi'$ line at the inlet (with a noticeable kink at the water table) move to a line where $\frac{c}{p} = 0.3$ between inlet and centre, and to between this line and the $\frac{c}{p} = f(PI)$ line at the centre. The cause is the gradual fining of the deposits.

At the outlet, in the upper 3 metres, the values show a relationship similar to that of the central material. However, below 3 metres, the shear strengths are considerably higher. This is probably due to desiccation. It is noticeable that the deepest results for the central part are also higher than is usual.

4.4.3.4. Blidworth lagoon, outlet

The results from this lagoon are all from shallow depths near the outlet (Figure 4.43). Of the ten results, six lie close to the $\frac{c}{p} = 0.3$ line (total stresses), one lies on the $f(PI)$ line, and three about or above the $\tan \phi'$ line. It would appear that total stress conditions apply, i.e. there is no water table. The higher shear strengths that were measured are probably due to desiccation effects during periods of drying out.

4.4.3.5. Kinneil Lagoon 22/2S, outlet

The shear strengths of Kinneil lagoon 22/2S at its outlet end (Figure 4.44), lie about or above the $f(PI)$ line, where pressures are calculated on a total stress basis. The grading of this portion of the lagoon is very fine grained (for lagoon materials), with 40 per cent clay size particles, as mentioned previously (Section 4.2.2). With such a large clay fraction,

the material might be expected to follow the $\frac{c}{p} = f(\text{PI})$ ratio, as this ratio describes clays. The large number of strengths exceeding the ratio are probably a feature of considerable desiccation.

4.4.3.6. Williamthorpe Lagoon 6

This lagoon is known to comprise two major divisions. The lower one, below 9 metres depth, consists of tailings discharged from an adjacent lagoon. The upper layer, which is 9 metres thick consists of tailings deposited in the conventional manner. Figure 4.45 shows the results of vane tests in three locations near the centre of the lagoon.

By comparison with Grimethorpe, the shear strength measured at this location in the lagoon should lie between the $\frac{c}{p} = f(\text{PI})$ and $\frac{c}{p} = 0.3$ lines. They should certainly lie above the former line which describes clays or remoulded tailings shear strength values. Even when it is assumed that the water table is at the surface, Figure 4.45 shows that this situation only obtains below 10 metres in depth. This means that above this depth up to the base of the desiccated crust the material is under-consolidated i.e. excess pore pressures have not dissipated, thus preventing consolidation. Minimum values of excess pore pressure are shown in Figure 4.45 alongside the vane results. These are calculated using the difference between the effective pressure at a given depth and the effective pressure required to give the strength at that depth using the relationship

$$\frac{c}{p} = f(\text{PI}).$$

4.4.3.7. Cadeby

The vane results for several positions in Lagoons 1,3,4,5 and 8 are plotted in Figure 4.46. Values of plasticity index and

bulk density are only known for two locations in Lagoon 8. It can be seen that there is considerable scatter. As there is so little information on plasticity indices and bulk densities it is not possible to interpret these results, other than to show that the average shear strength shows a general increase with depth.

More detailed examinations are possible for Lagoon 9 and for two vane positions (F1 and F2) in Lagoon 8. In Lagoon 9, the two block samples A and B (Figure 4.2) were taken in the same locality as the vane tests. In Lagoon 8, plasticity indices and bulk densities were recorded at Locations F1 and F2 during the vane tests.

The vane results for Lagoon 9 are shown in Figure 4.47. The Pilcon handvane results in the excavated face of this lagoon (Table 4.1) are also included. Taking average values derived from block samples A and B, and calculating on a total stress basis, it can be seen that the results lie on or above the $\frac{c}{p} = f(\text{PI})$ line. As there was no visible seepage from the excavated face, it can be assumed that no water table was present in the area behind the face where the vane tests were conducted. Of the three hand vane results, the one at 1.1m depth lies on the $f(\text{PI})$ line. This was in a fine-grained layer in the face. Many of the vane results lie above the shear strength attributable to ϕ' . It would appear that considerable desiccation has taken place.

In Figure 4.48, the vane results for positions F1 and F2 in Lagoon 8 are shown. At position F1 the values of plasticity index and bulk density are known down to a depth of 3.75 metres. $\frac{c}{p}$ lines have been drawn using the values for each depth. Below 3.75 metres an average value has had to be used. For position F2

only the average values of the two variables are available. The two vane strength profiles show different trends. In F1, down to 1.5 metres depth the values follow the line $\frac{c}{p} = 0.3$, computed on an effective stress basis with a water table at the surface. Observations in this lagoon during the sinking of the U100 mentioned previously (Section 4.2.1.2) showed that it was possible that there was a water table at, or near, the surface. Below 1.5 metres the strength values drop, so that below 2.5 metres they fall below the $f(\text{PI})$ line. It would appear that excess pore pressures must be present here, in a similar manner to Williamthorpe. It is noticeable that the remoulded strengths follow the $f(\text{PI})$ line to 1.5 metres depth, before dropping below it. It will be remembered that in the laboratory tests, peak shear strength followed the $\frac{c}{p} = 0.3$ relationship and remoulded results followed the $\frac{c}{p} = f(\text{PI})$ convention.

The F2 profile is close to the relevant $\frac{c}{p} = 0.3$ line at 0.5 metres. It then falls beneath it, before rejoining this line at 4 metres depth. Because there are only average values of PI and bulk density for the top 0.95 metres, it is not possible to be precise as to where the relevant lines fall. However, it is apparent that between 1 and 3 metres depth the shear strength values lie well below their expected levels. It could be that another area of excess pore pressure exists at this horizon.

These two vane positions are on the same side of the lagoon, and suggest that excess pore pressures can be fairly localised, the excess pore pressure areas being at different depths in the two boreholes.

4.4.3.8. Denby Hall Lagoon C

Vane profiles from three locations in Lagoon C, Denby Hall, are shown in Figure 4.49. An average value of bulk density is available and an average plasticity index for some clayey bands.

It is recorded in the report (Sir William Halcrow and Partners, 1972) that the coarser bands at the northern (inlet) end of the lagoon are non-plastic. A desiccated crust of at least 0.75 m thickness occurs at the northern end of the lagoon.

Grading curves from the inlet end are similar to those for the Gedling and Manvers tailings. At the outlet some 40 per cent of clay size and 50 per cent silt size particles are present, the grading being similar to that obtained for the sample taken at the outlet of Gedling Lagoon 12.

Considering first the outlet end, the plasticity index may be taken as being close to the average clay band layer. Down to a depth of 4 metres, the values are scattered with a range which covers an area from below the effective stress $f(\text{PI})$ line to the $\frac{c}{p} = 0.3$ total stress line. Below 4 metres the strengths cluster about and below the two effective stress lines. Presumably the values below the effective stress $f(\text{PI})$ line are due to under-consolidated materials which have developed high pore pressures. The change from total stress to effective stress which appears to occur in one of the vane profiles could be due to the vane penetrating an aquifer which is connected to a water table at the surface.

Turning now to the inlet end which has a similar grading to the samples tested by the writer in the laboratory vane shear strength/normal pressure study, it might be expected that the field samples should behave in a similar manner. If a water table at 1 metre depth is postulated, it can be seen that the remoulded strengths do, in fact, follow the $\frac{c}{p} = f(\text{PI})$ relation which is compatible with the laboratory experiment. If a plasticity index of 13 is employed, i.e. allowing for the non-plastic layers in this part of the lagoon, the fit is improved.

The peak shear strengths however, are much higher than the values predicted by the relation $\frac{c}{p} = 0.3$. This could again be due to desiccation. Considering the vane shear strength profiles in the central part of the lagoon, they are seen to be very similar to those at the inlet. They can presumably be accounted for in a similar manner, i.e. a water table at 1 metre depth, with desiccation of the lagoon during filling.

4.4.4. Summary of Laboratory and field vane shear strengths of Lagoon deposits.

It has been shown that, in the laboratory, the vane shear strength of two tailings samples increased with increasing pressure. The peak shear strengths could be approximated by the relation $\frac{c}{p} = 0.3$, while the remoulded strengths followed a line defined by $\frac{c}{p} = 0.11 + 0.0037 \text{ PI}$. Compared to other methods of determining shear strength, (i.e. consolidated undrained triaxial and shear-box tests, run at rates similar to that of the vane), the vane underestimates the shear strength of the tailings. This is in contrast to the situation in clays, where the vane gives a higher value of shear strength.

In the field, the vane strengths followed the relationships found in the laboratory only in some of the cases. At the inlet of a few lagoons, where the tailings are coarsest, the vane may be mobilizing the strength due to the drained angle of shearing resistance (ϕ'), whilst at the outlet end, where the tailings are finest, the vane shear strength tends to lie between the two relations $\frac{c}{p} = 0.3$ and $\frac{c}{p} = f(\text{PI})$.

With such a variation in possible shear strength values, it is obviously not possible to interpret the vane shear strengths precisely. Further difficulties arise if values of plasticity index, bulk density or the water table position are unknown in

the vicinity of the vane test. However, provided an approximation for these values can be made it is possible to conclude that the shear strength should not lie below a value predicted by the relation $\frac{c}{p} = f(\text{PI})$ or above the value predicted by the relation $\frac{s}{p} = \tan \phi'$. If the shear strength does lie outside these values, it is probable that, in the former case, the material is subject to excess pore pressures which may be due to under-consolidation. In the latter case, desiccation may be suspected, i.e. the material will be over-consolidated.

4.5. Colliery Lagoons - conclusions

It has been shown that lagoon deposits can be very variable indeed, especially in a lateral direction. Large-scale disturbances are possible in the sediments, which may vary from distinctly laminated beds with good graded bedding to visually homogenous deposits. On the scale of the consolidation tests, i.e. up to 254mm by 40mm there is no marked anisotropy in consolidation parameters. However, on a larger scale, there is some evidence for aquifers and aquicludes being developed, with the aquifers being lensoid in places. This feature would point to large-scale anisotropy. These features of lagoon materials are due to the deltaic regime under which they are deposited.

Considerable variation in some consolidation parameters occurs laterally in a lagoon. Progressing from inlet to outlet, the coefficient of volume compressibility, m_v , shows little change, whilst the coefficient of consolidation, c_v , decreases. The decrease in the latter is very marked. At the inlet end it generally ranges from 400 - 600 m^2/yr dropping to 10 - 40 m^2/yr at the outlet end. These variations are evident from the Rowe cell work, but are not highlighted by the conventional oedometer used for routine investigations, mainly because the oedometer

sample (10mm thick at the most) is thinner than the laminations prevalent in lagoons.

Flocculants have been shown to produce a reduction in voids ratio, when their concentration is sufficiently high. The reduction is attributable to the poorer graded bedding (compared to unflocculated materials) which is produced by the increased rate of sedimentation of the silt/clay particles. A similar reduction in voids ratio can be induced by disturbing recently sedimented, unflocculated material.

The effect of flocculants upon the consolidation parameters is somewhat variable. The polymer flocculant Polyfloc 93APA shows a positive statistical correlation between its concentration and m_v . Starch does not appear to show any consistent variation with m_v .

Neither flocculant type produces a consistent change in C_c . In terms of coefficient of consolidation (c_v), and the closely related permeability (K), it appears that, at high doses, polymer gives values which are in one case (Manvers) smaller than those obtaining with starch while in the remaining case (Morrison Busty) there is no significant difference. In some cases unflocculated materials have smaller values, in others, greater. In the case of the one specimen (Manvers) which was tested with varying polymer concentrations, c_v and K increase to a peak near 0.14kg of flocculant to 1Mg of dry tailings, and then rapidly drops away. Jowett and Chopra (1974) noted a permeability peak at 0.02kg/Mg with Gedling tailings. The position of this peak would thus appear to vary.

Another point arising from the flocculant work is the long period and large amount of secondary consolidation that freshly deposited tailings are subject to. It masks any effect there may

be due to ageing of the flocculant.

In general there is no evidence for polyelectrolyte type flocculants producing either weaker or poorer draining deposits than starch type flocculants. It is possible that there may be a difference with some tailings. Apart from the deposits themselves, the only other possible cause of poor drainage is the lagoon/embankment interface. It might be that polyelectrolyte flocculants produce a less permeable interface than starch flocculants, although this seems a somewhat unlikely situation. As far as the results from Cadeby Lagoon 9 are concerned, it would appear that the embankment is far less permeable than the lagoon deposits. This being so, it is obviously desirable that more attention be paid to producing permeable banks, if free draining lagoons are required (e.g. for over-tipping).

Vane shear strengths can be used to give useful information despite the sand and silt content of tailings. At zero normal pressure, tailings of similar grading show a strong negative correlation between voids ratio and vane shear strength. When the grading becomes coarser, the vane shear strength drops.

This relationship appears to be only operative at zero normal pressure, however. When flocculated samples of differing voids ratio and containing 20 per cent clay size, 40 per cent silt size and 40 per cent sand size particles are vane tested at increasing pressures, they show a relation between peak shear strength and pressure, whereby $c = 0.3 \bar{p}$. Their remoulded strengths follow the relation due to Skempton (1957), $c = (0.11 + 0.0037PI)\bar{p}$, where c undrained shear strength, PI = plasticity index and \bar{p} = effective pressure. Comparison with triaxial and shear-box tests indicates that the true undrained shear strength is some 40-50 per cent higher than the values given by the vane.

Hughes and Windle (1976) have pointed out the usefulness of the vane in locating areas of high sensitivity which would be susceptible to liquefaction. It is shown here that, with detailed analysis, it is possible to extract additional information knowing that clays follow Skempton's (1957) shear strength/depth relationship, and that an average tailings sample shear strength will lie above it. It is possible to infer the position of the water table and even zones of high pore pressure provided that sufficient information exists concerning relevant bulk densities and plasticity indices in the vicinity of the vane test position.

TYPICAL LAGOON WITH DOWNSTREAM EMBANKMENT CONSTRUCTION
FIGURE 4.1

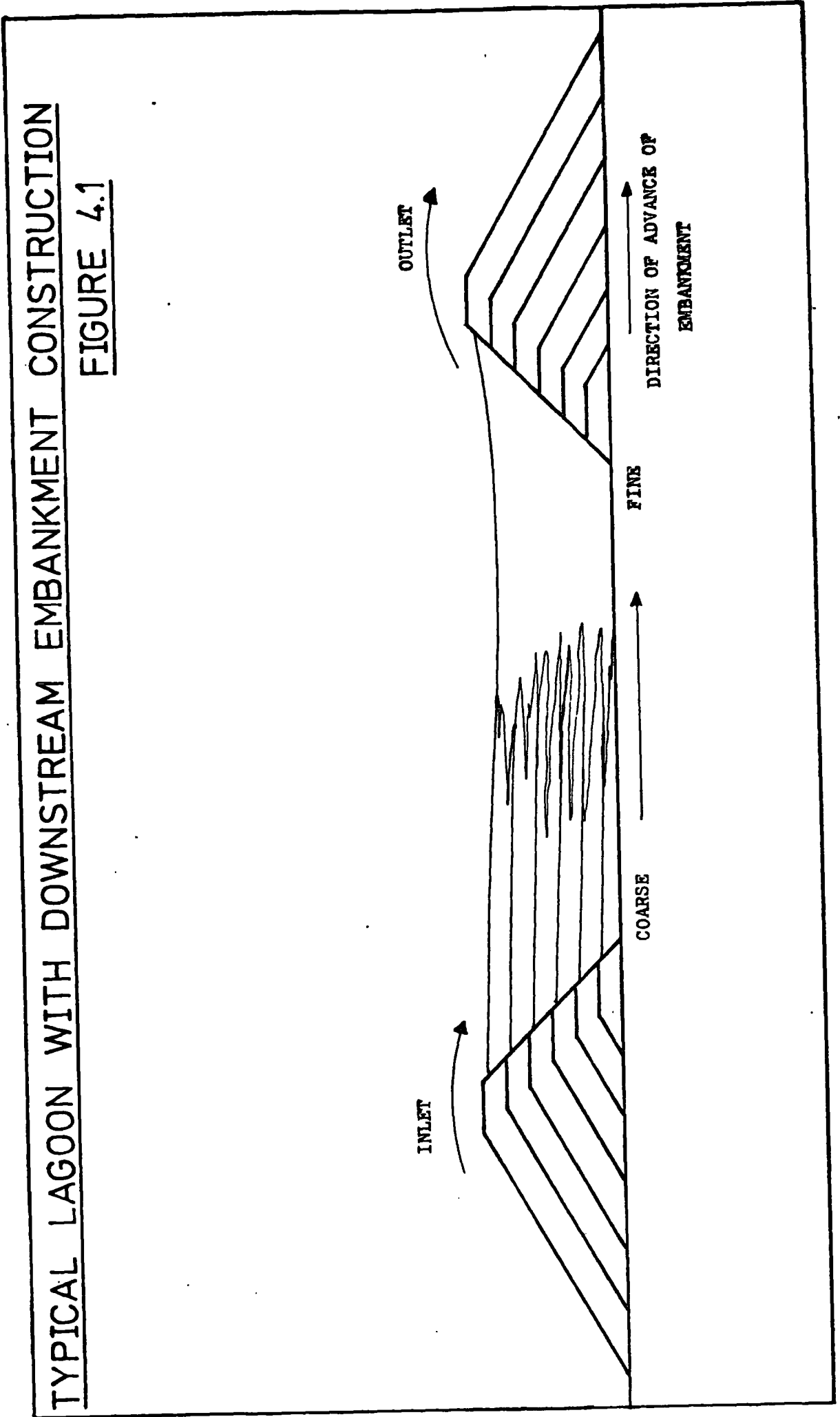
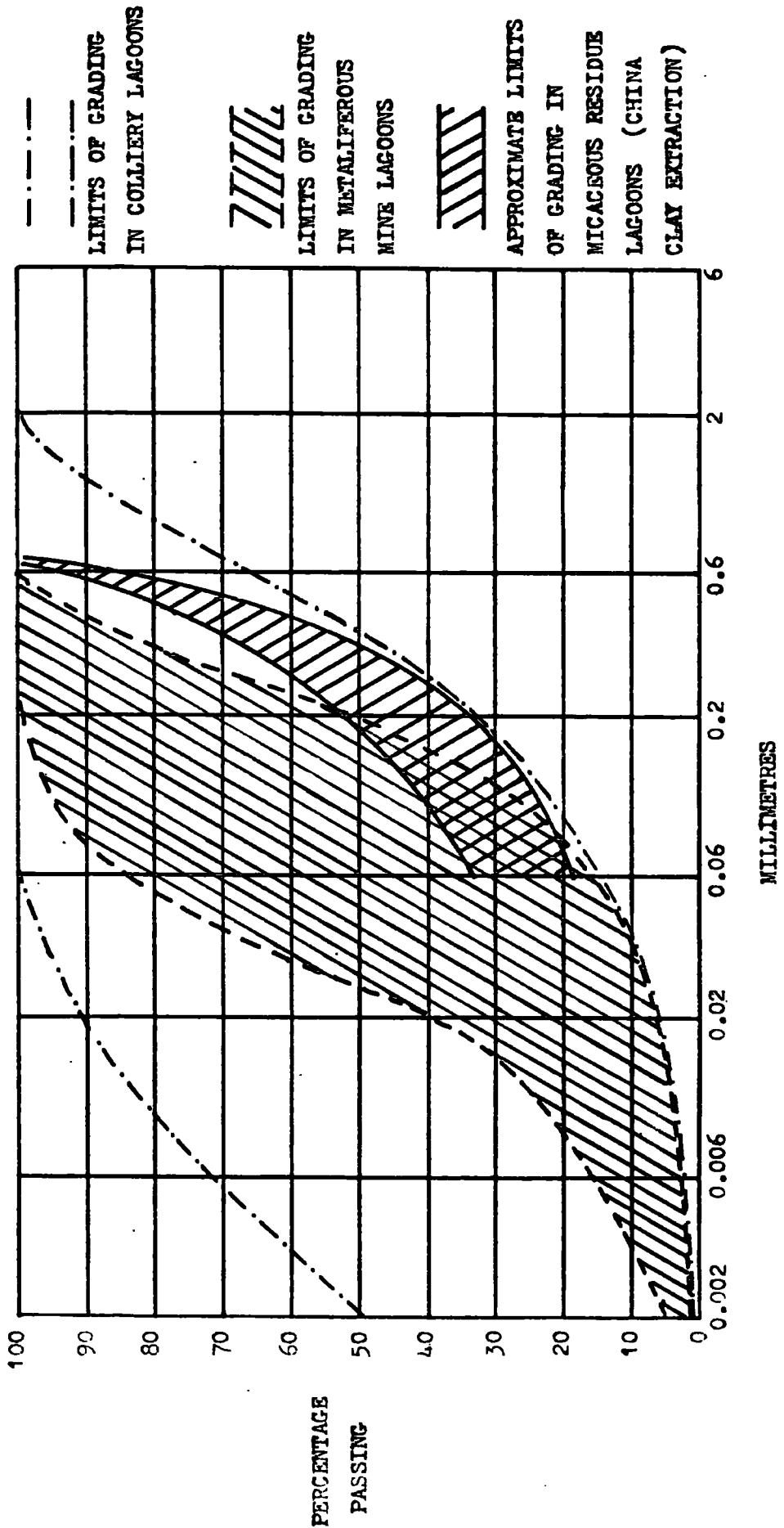


FIGURE 4.2

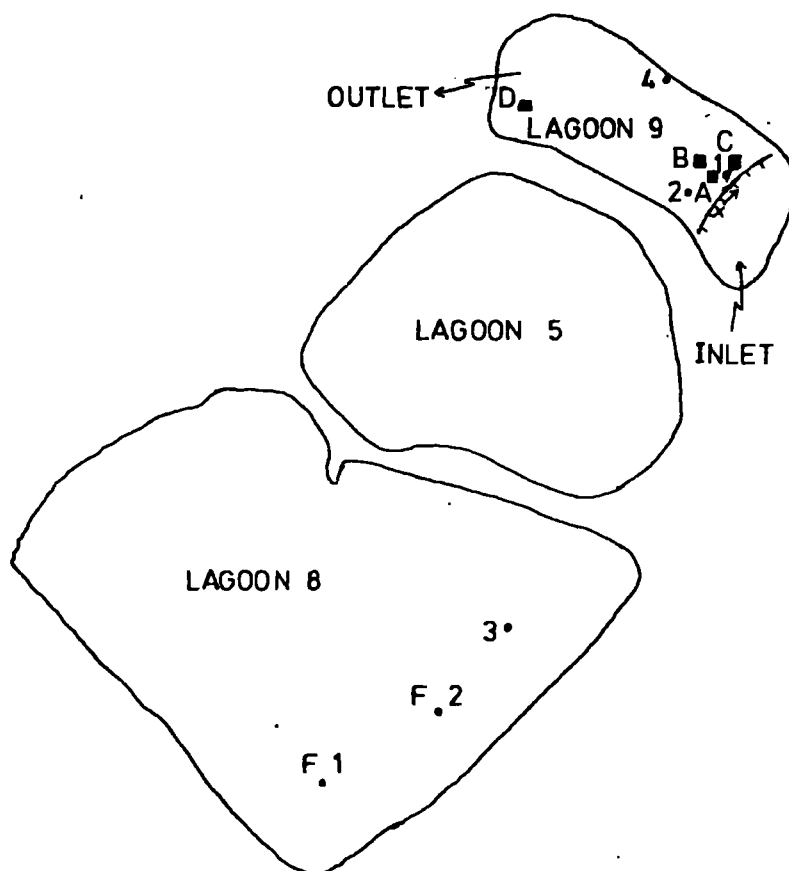
COMPARISON OF GRADING OF MATERIALS IN SEVERAL DIFFERENT TYPES OF LAGOONS



CADEBY KEY PLAN

FIGURE 4.3

- × VERTICAL TRAVERSE
- DIRECTION OF HORIZONTAL VANE TRAVERSES
- U100's (1-3 DOUBLE U100's)
- A-D BLOCK SAMPLES
- F1, F2 WIMPEY VANE POSITIONS

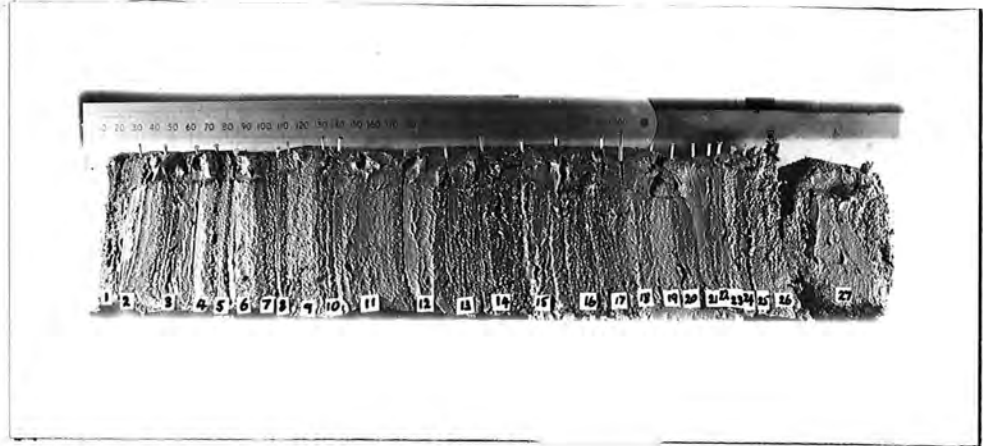


SCALE 1/2500

FIGURE 4.4

CADEBY LAGOON 8, U100 SAMPLE NUMBER 3

(a)



(b)

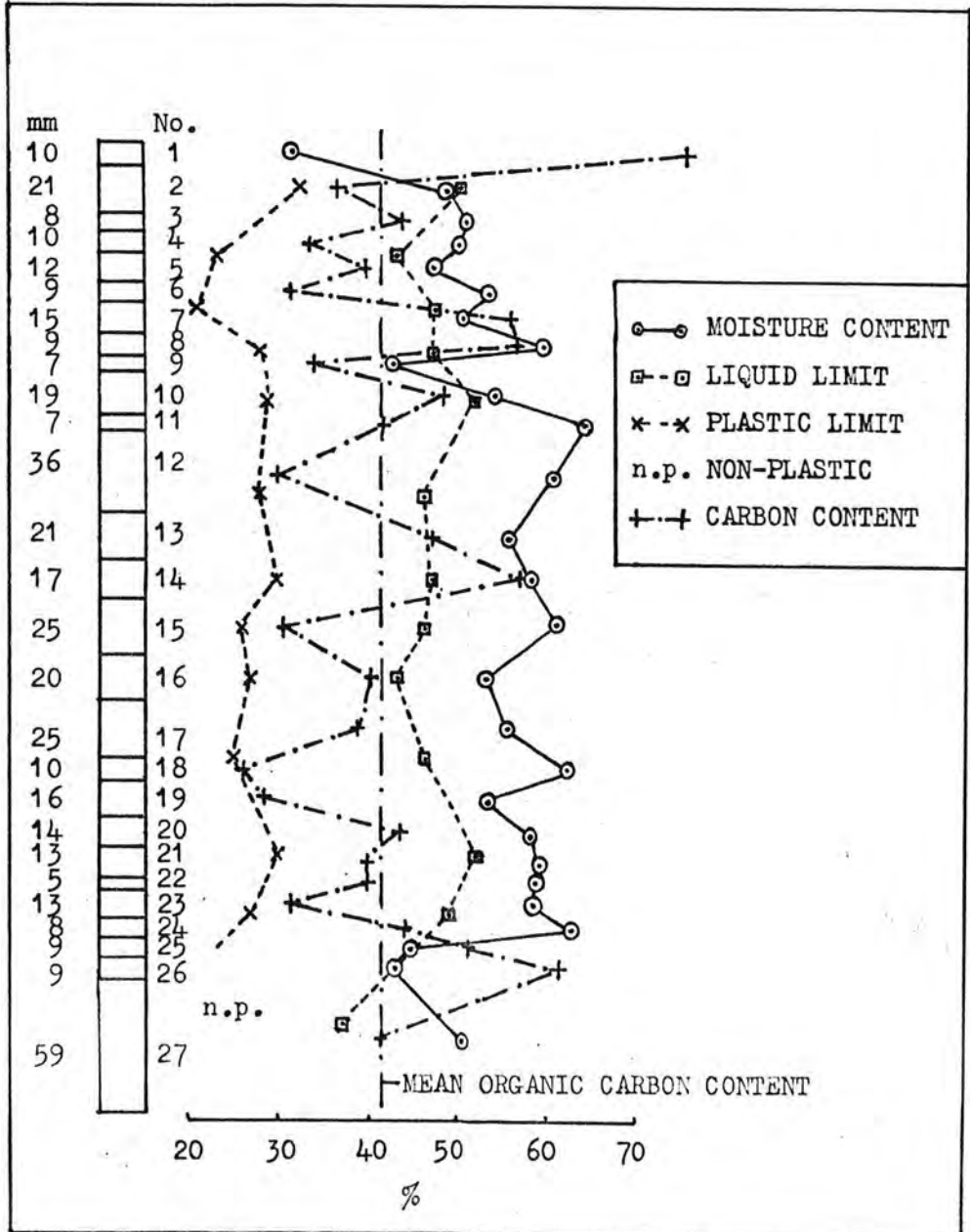


FIGURE 4.5

GRADING CURVES OF SAMPLES FROM CADEBY LAGOON 9

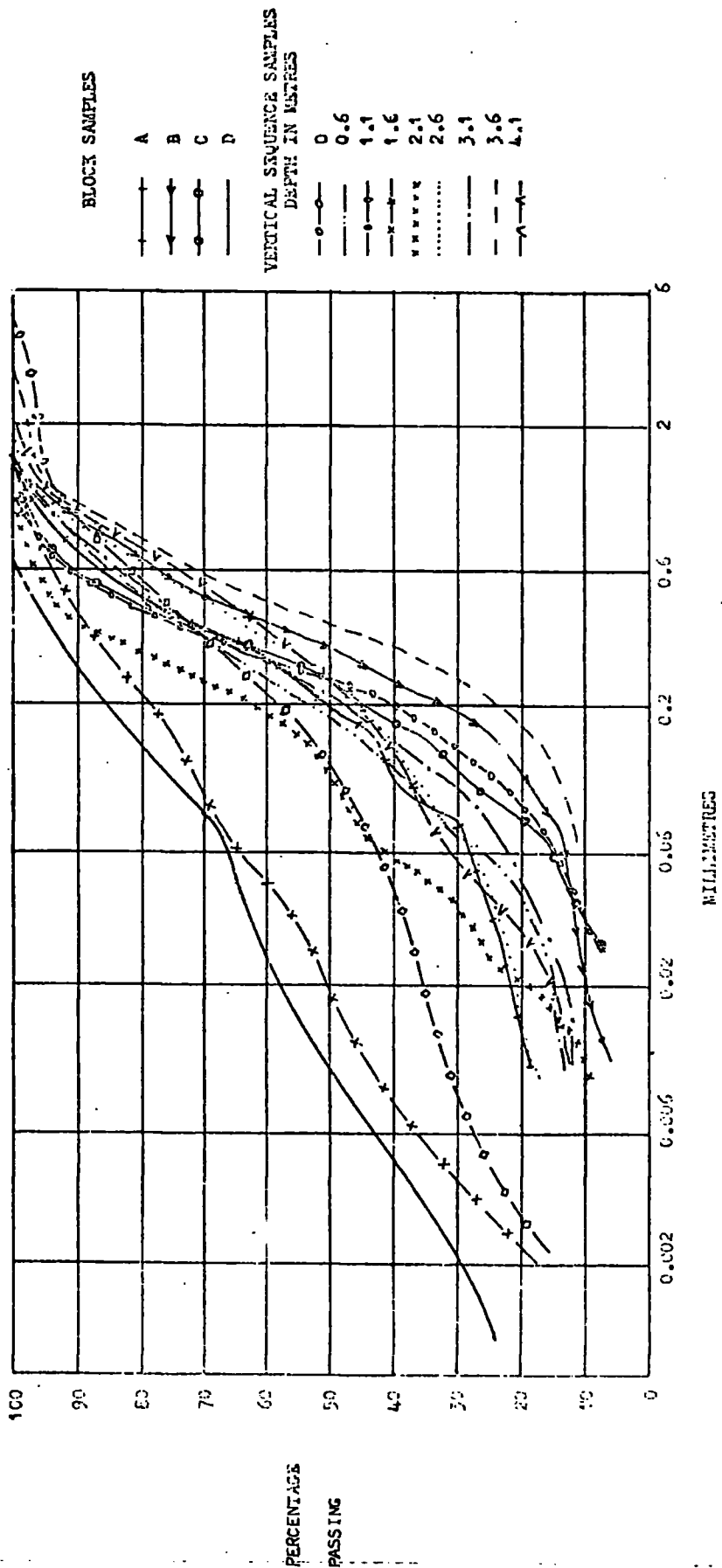


FIGURE 4.6
CADEBY LAGOON 9

RELATIONSHIP BETWEEN SPECIFIC GRAVITY AND ORGANIC
CARBON CONTENT

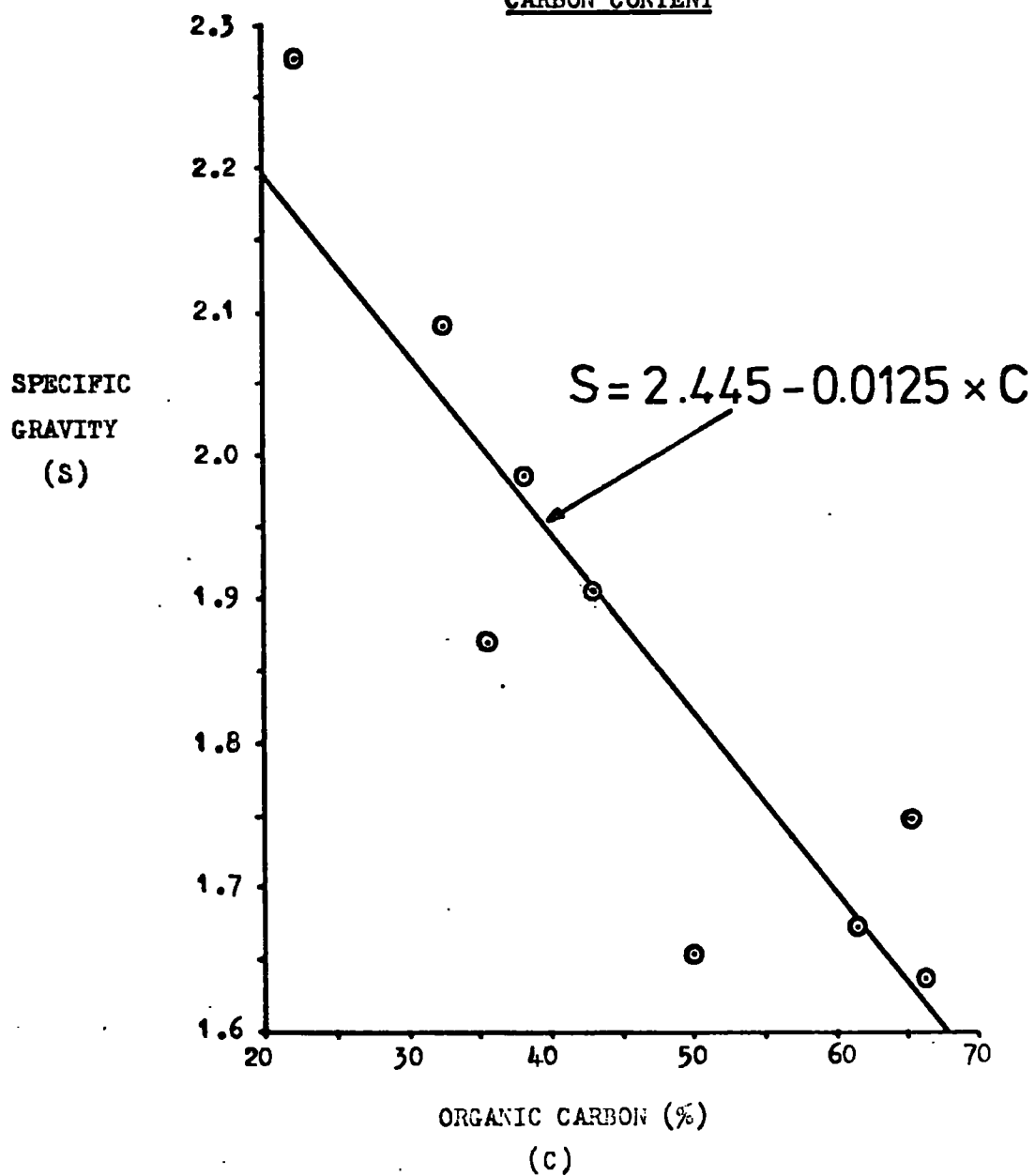


FIGURE 4.7 CADEBY LAGOON 9

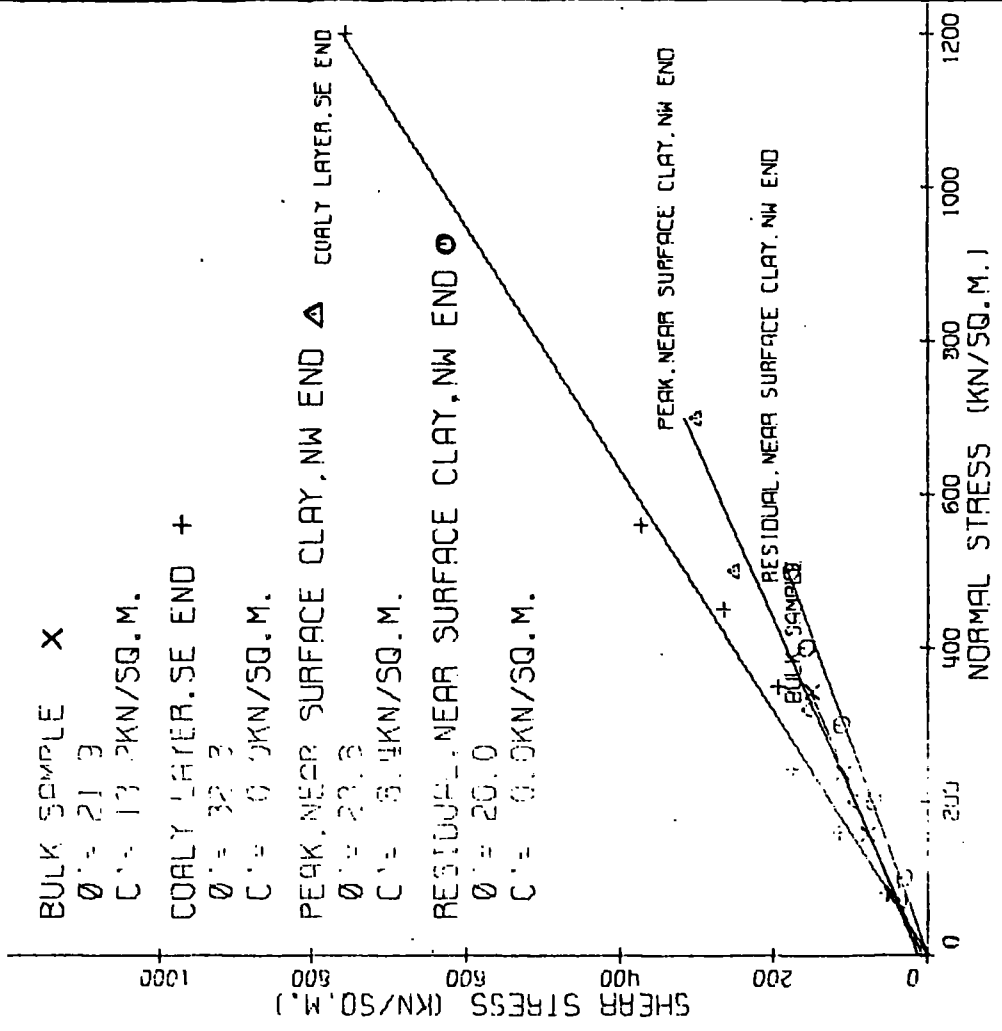
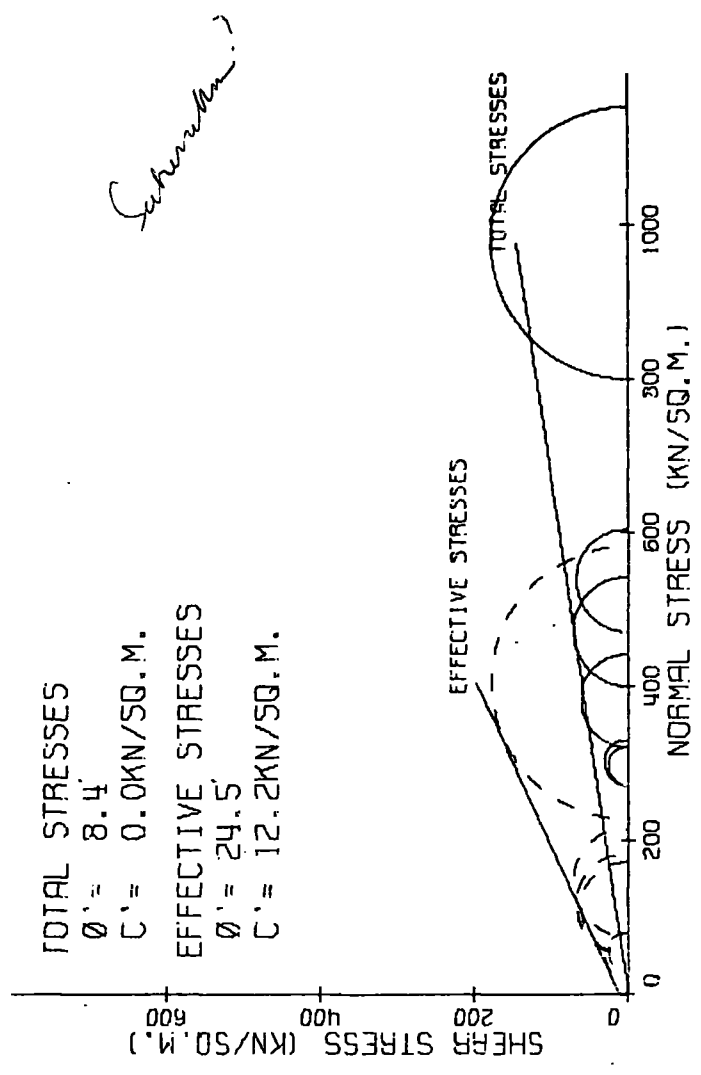
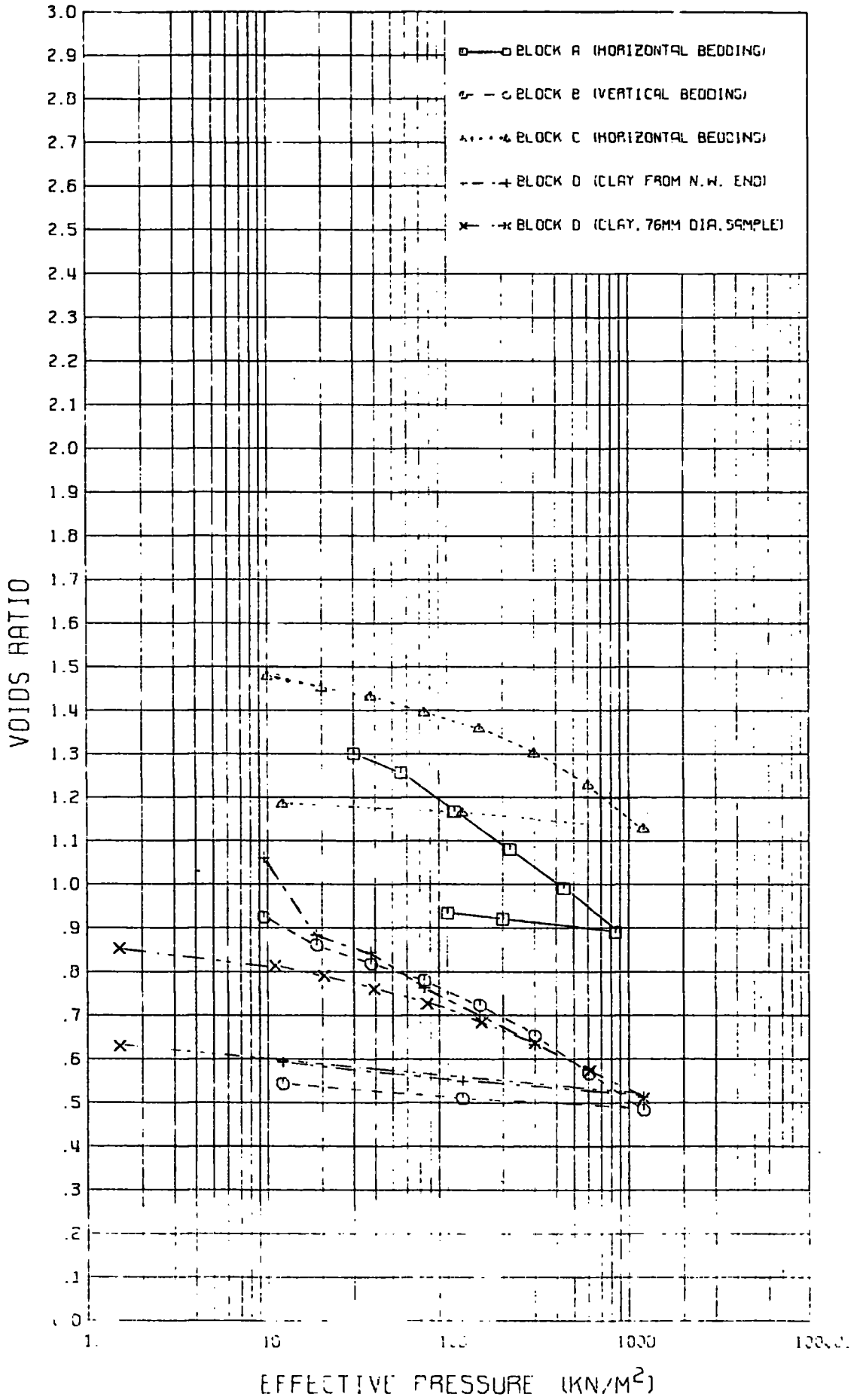


FIGURE 4.8 CADEBY LAGOON 8
(DATA, WIMPEY, 1974)



CADEBY LAGOON 9

FIGURE 4.9



CADEBY LAGOON 9

FIGURE 4.10

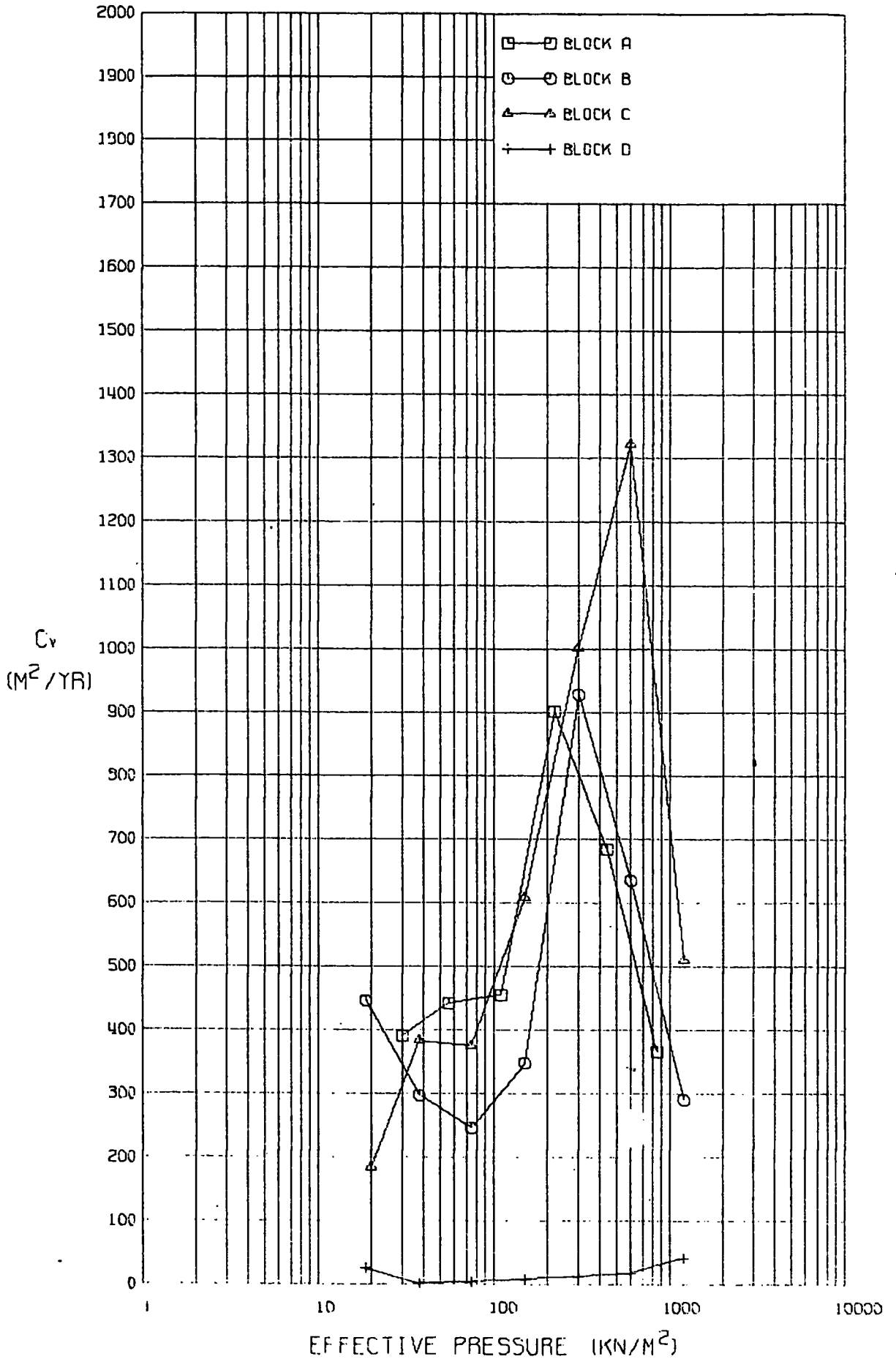
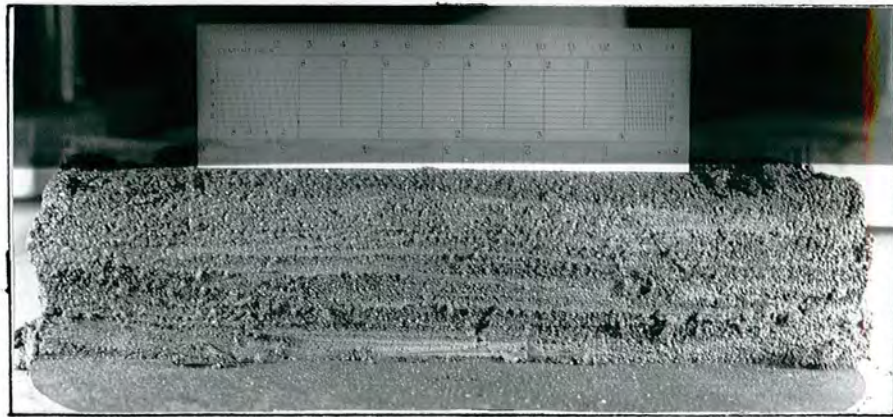


FIGURE 4.11

CADEBY LAGOON 9, 254mm DIAMETER
ROWE CELL SAMPLES

(a) Block B, vertically orientated bedding



(b) Block C, horizontally orientated bedding

FIGURE 4.12

CADEBY LAGOON 9, EXCAVATED FACE



CADEBY LAGOON 8 WIMPEY (1974)

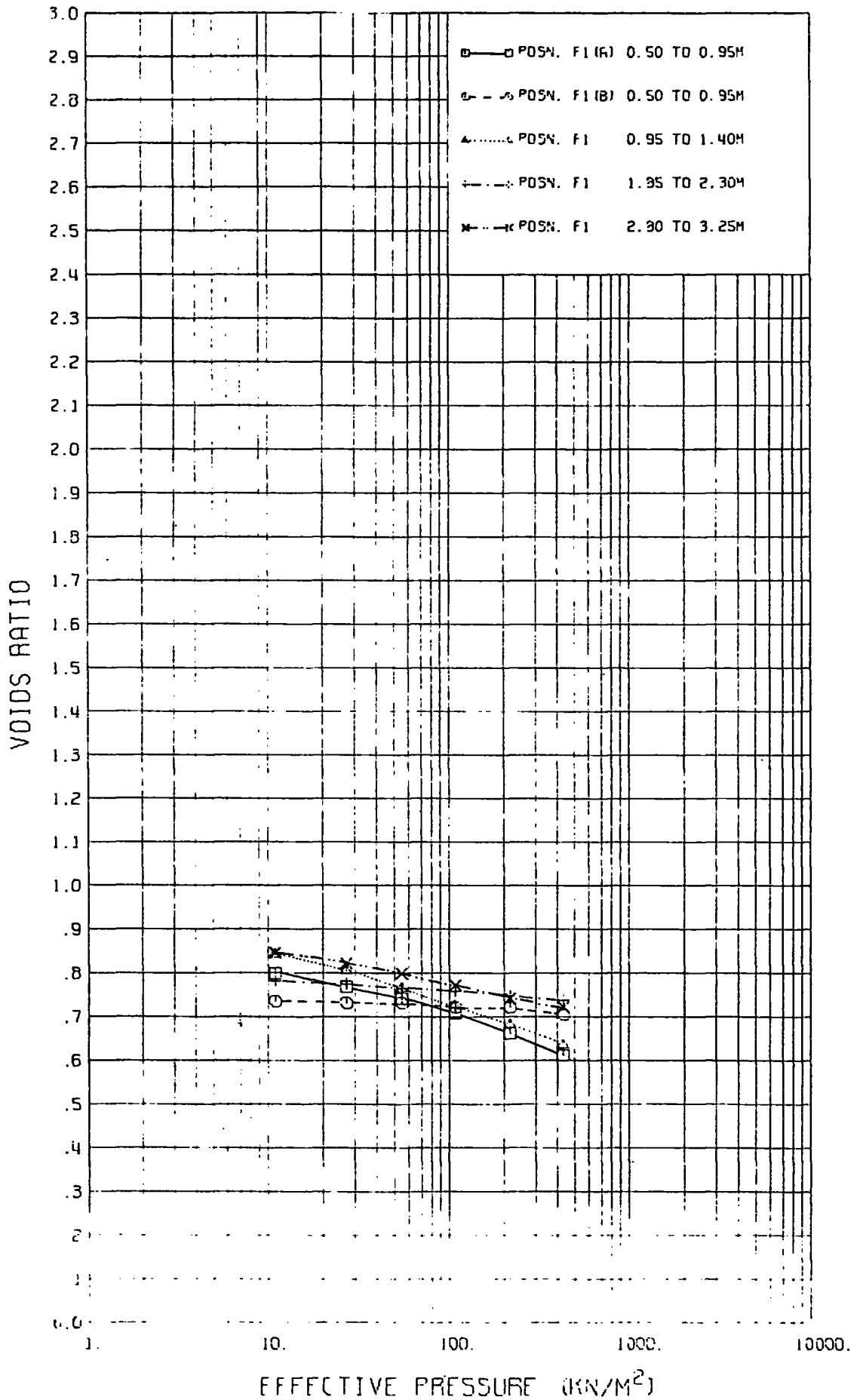


FIGURE 4.14

CADEBY LAGOON 9, U100 SAMPLE NUMBER 4 FROM LAGOON - EMBANKMENT
INTERFACE

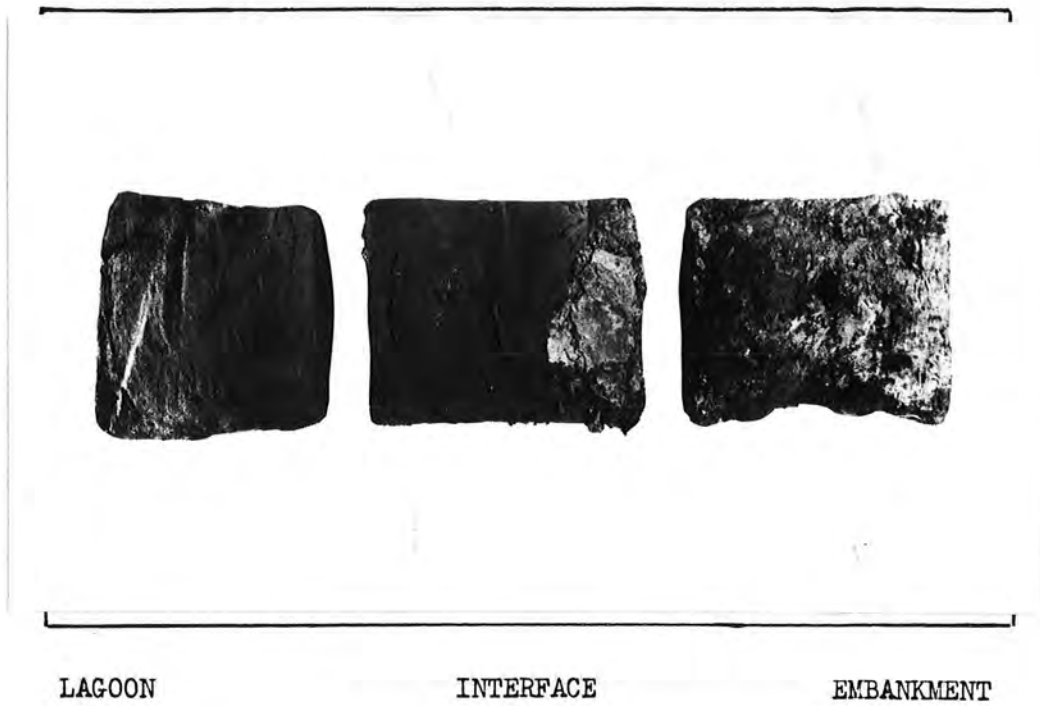


FIGURE 4.15

GRADING CURVES OF SUB-SAMPLES FROM U100 SAMPLE NUMBER 4 IN CADEBY
LAGOON 9

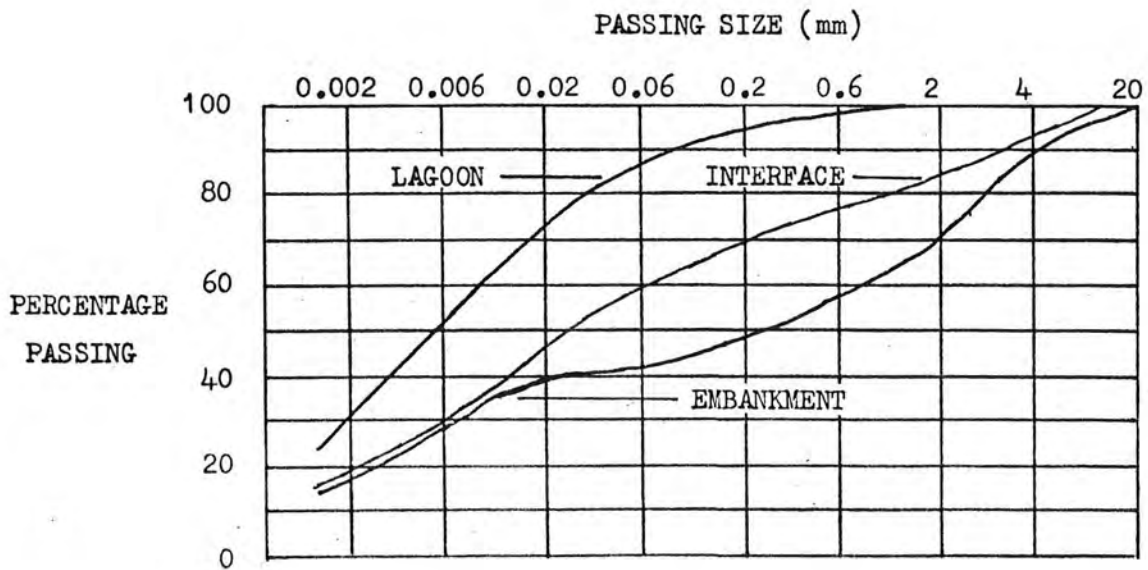
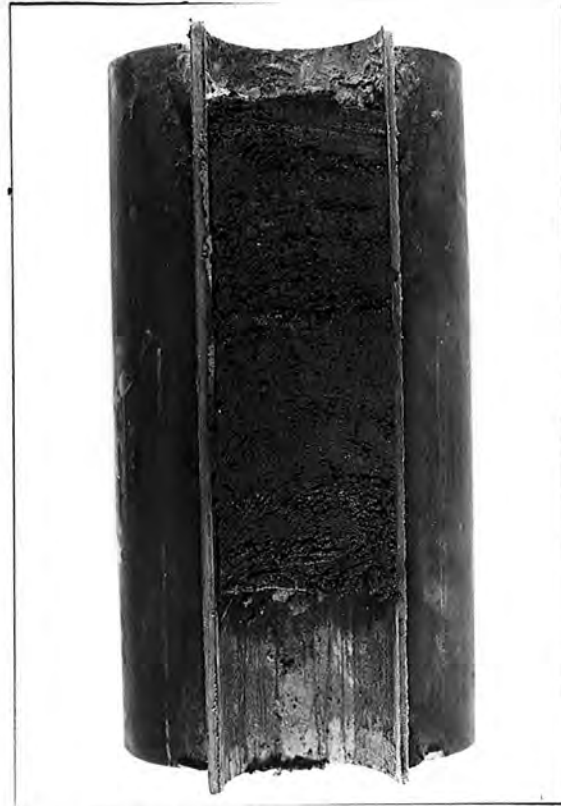


FIGURE 4.16

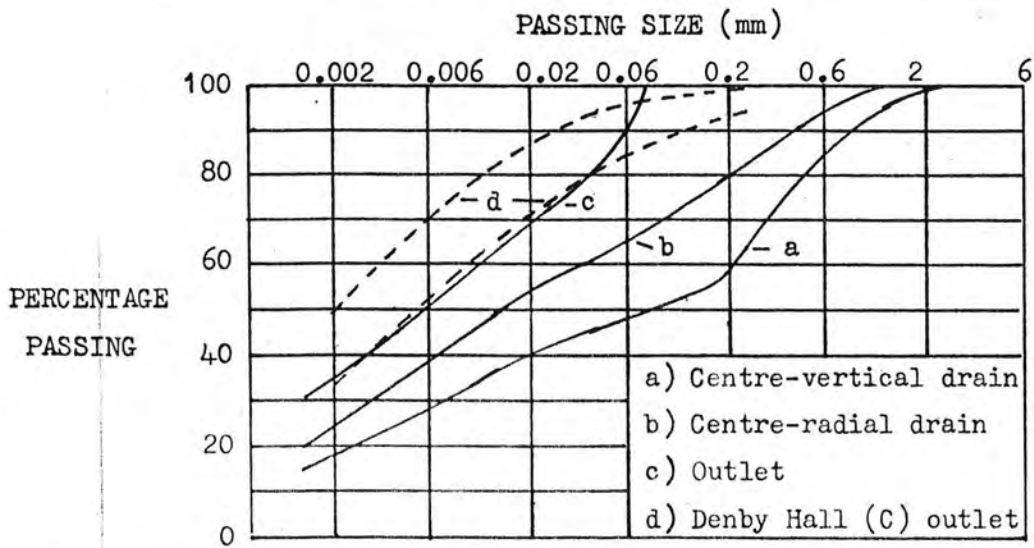
CENTRAL SAMPLE, GEDLING LAGOON 12



(Sample width is 76 mm)

FIGURE 4.17

GRADING CURVES FOR SAMPLES FROM GEDLING LAGOON 12



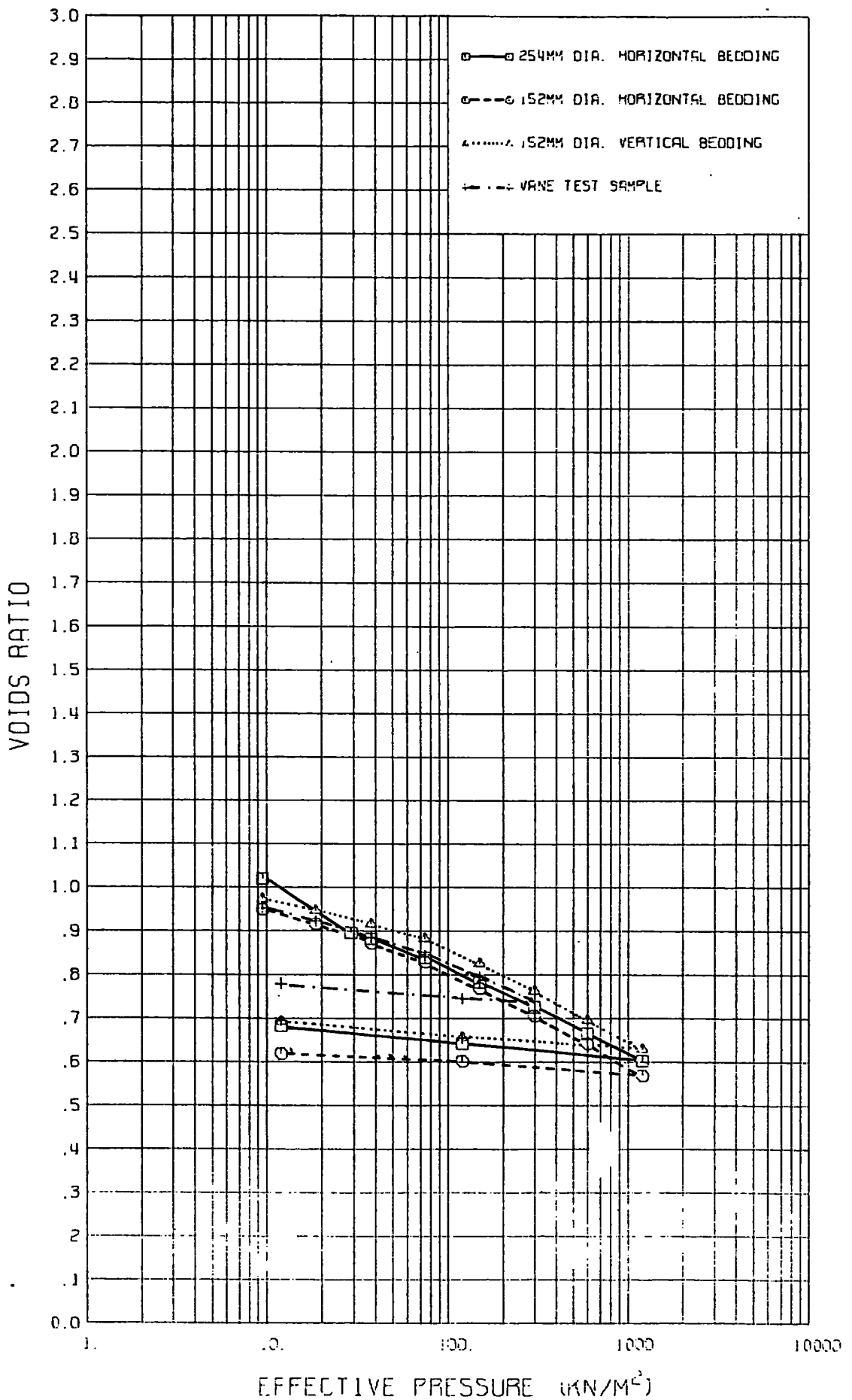
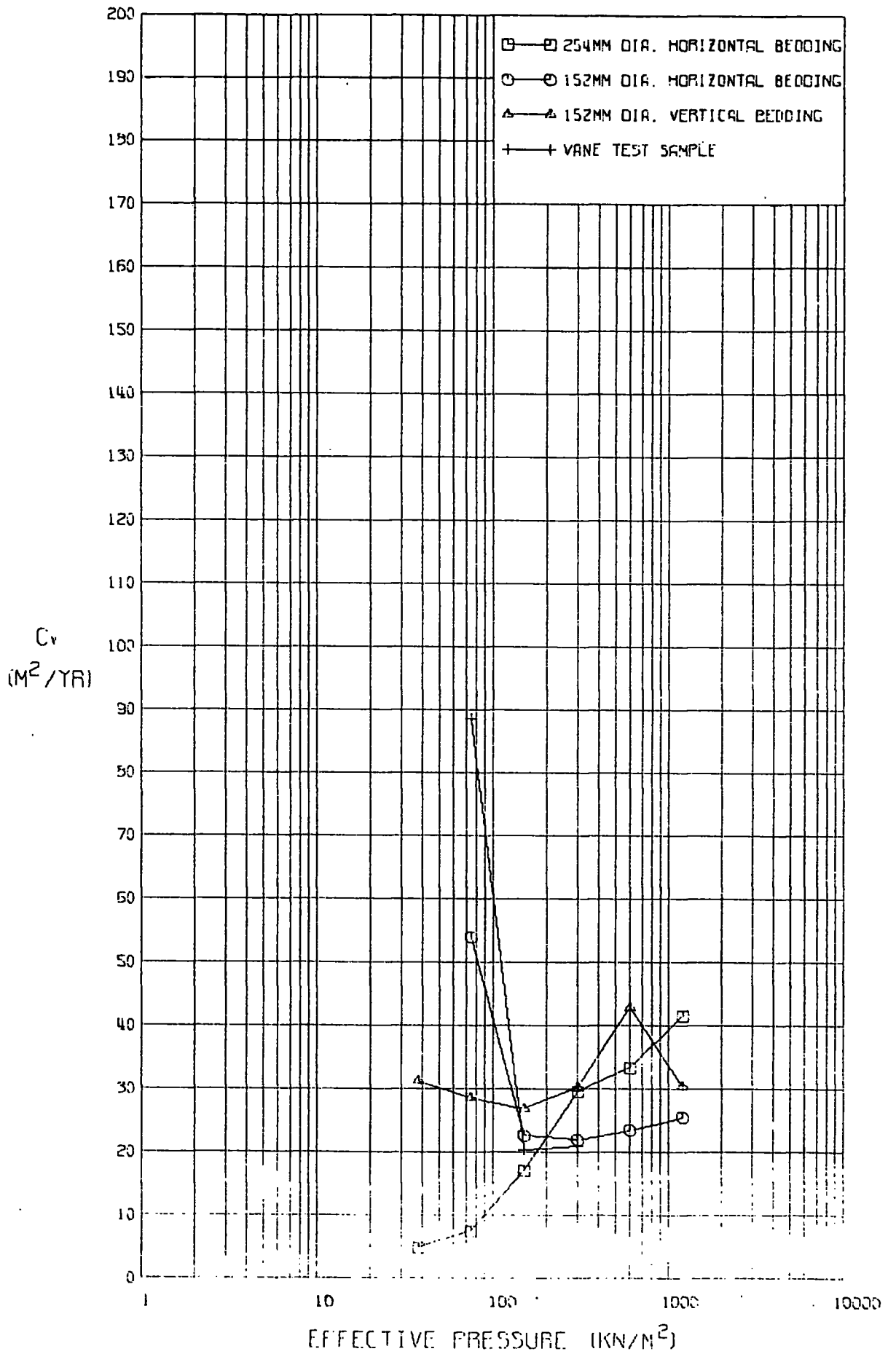
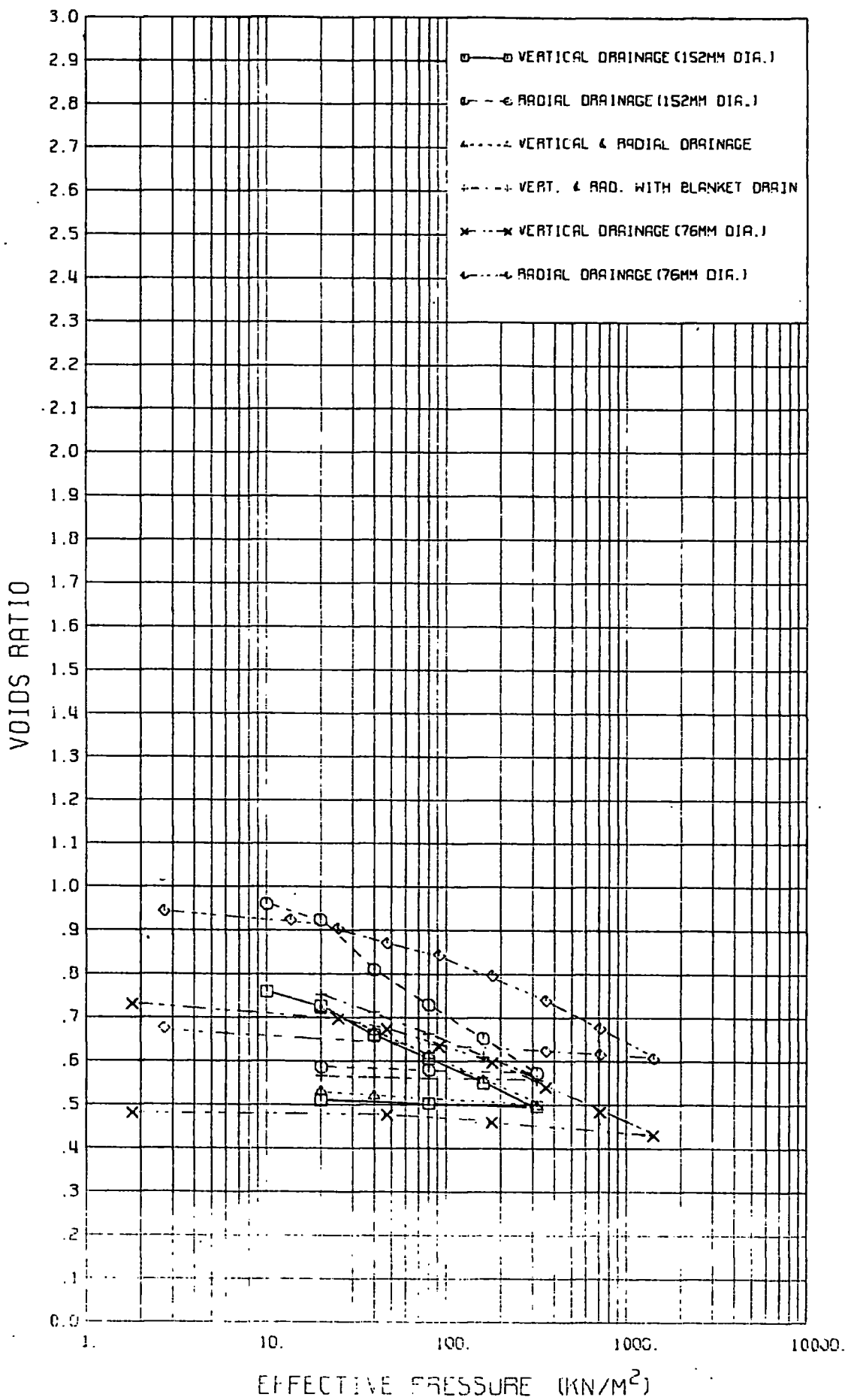


FIGURE 4.19

GEDLING LAGOON 12 (OUTLET)



GEDLING LAGOON 12 (CENTRAL) FIGURE 4.20



GEDLING LAGOON 12 (CENTRE) FIGURE 4.21

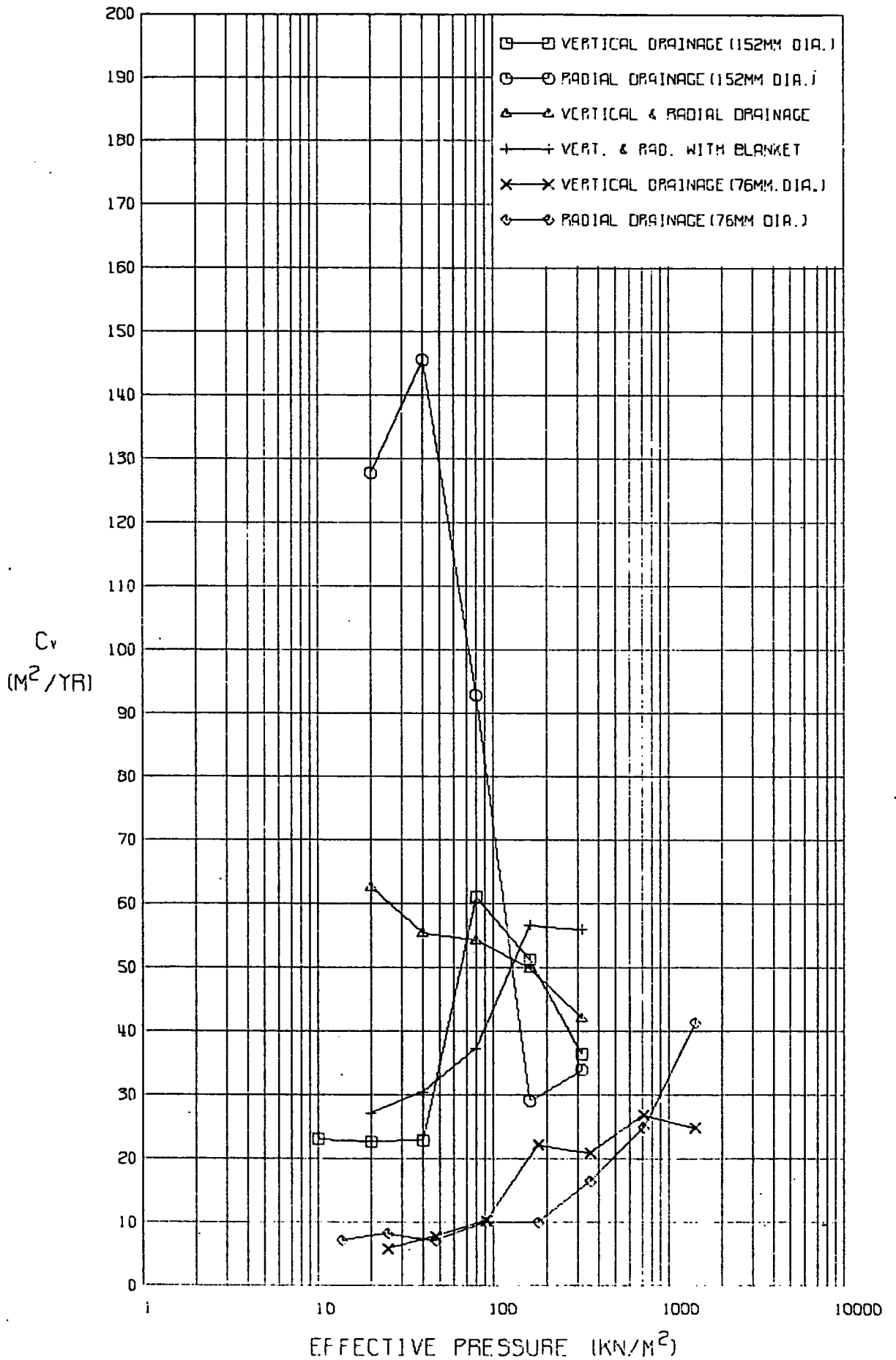


FIGURE 4.22
KELLINGLEY PRESSED TAILINGS

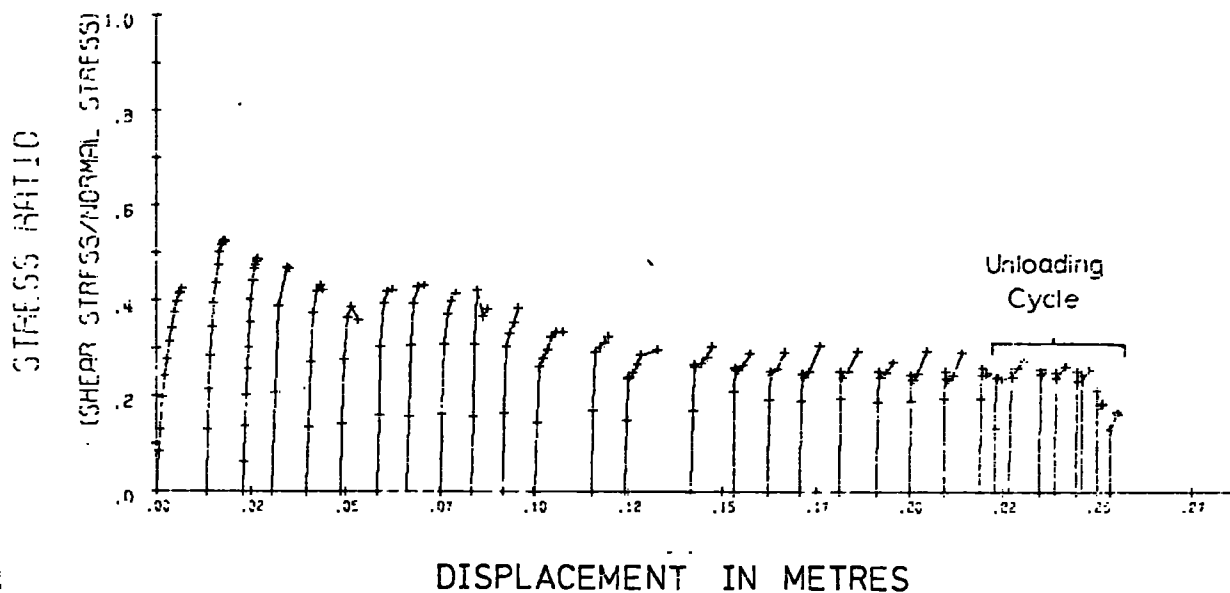


FIGURE 4.23
KELLINGLEY PRESSED TAILINGS

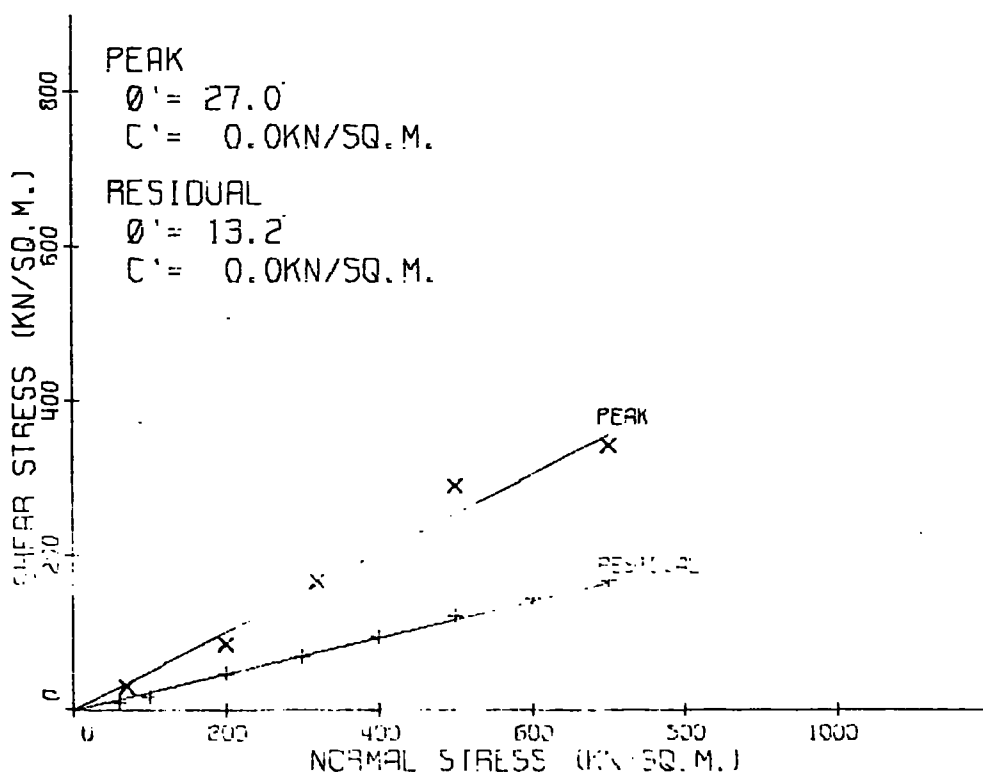


FIGURE 4.24
SEDIMENTING APPARATUS

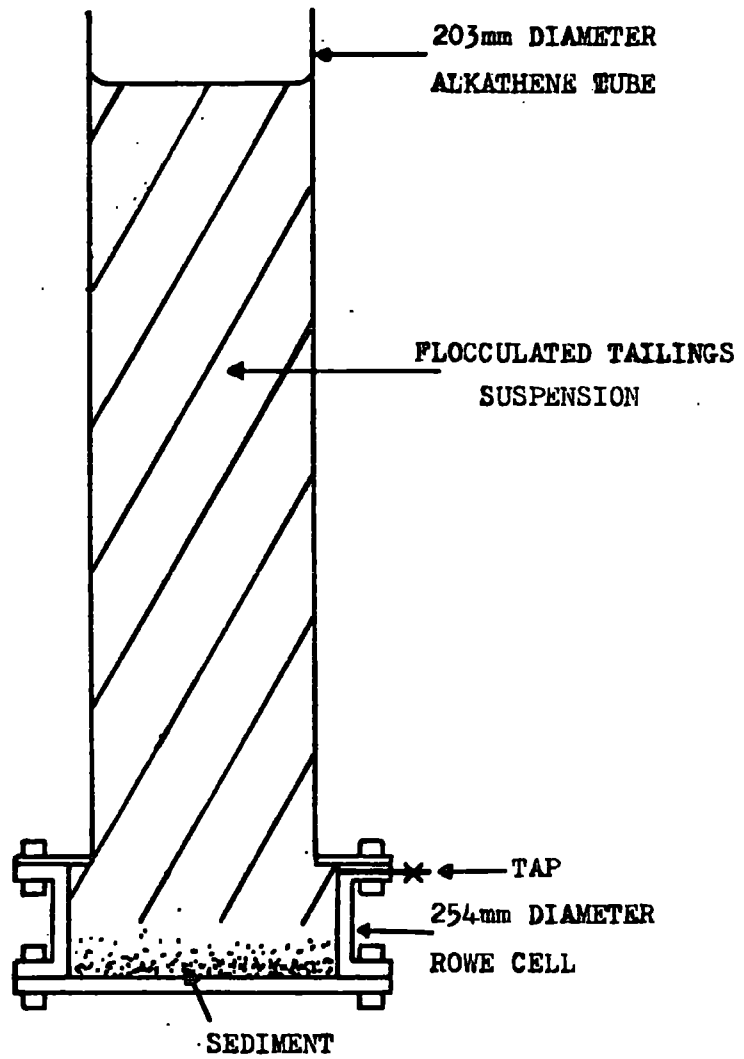
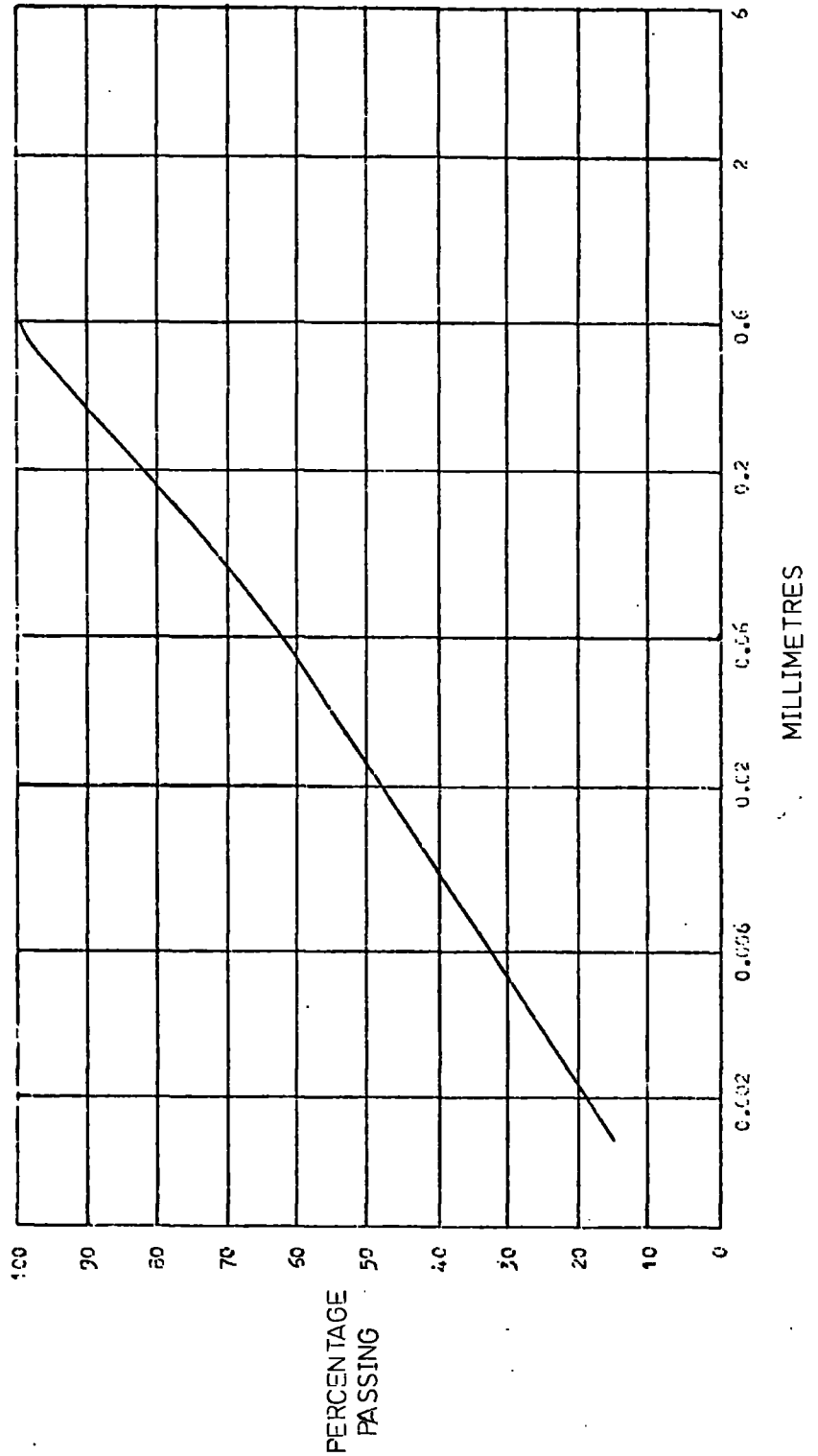


FIGURE 4.25

GRADING CURVE FOR MANVERS TAILINGS



MANVERS TAILINGS

FIGURE 4.26

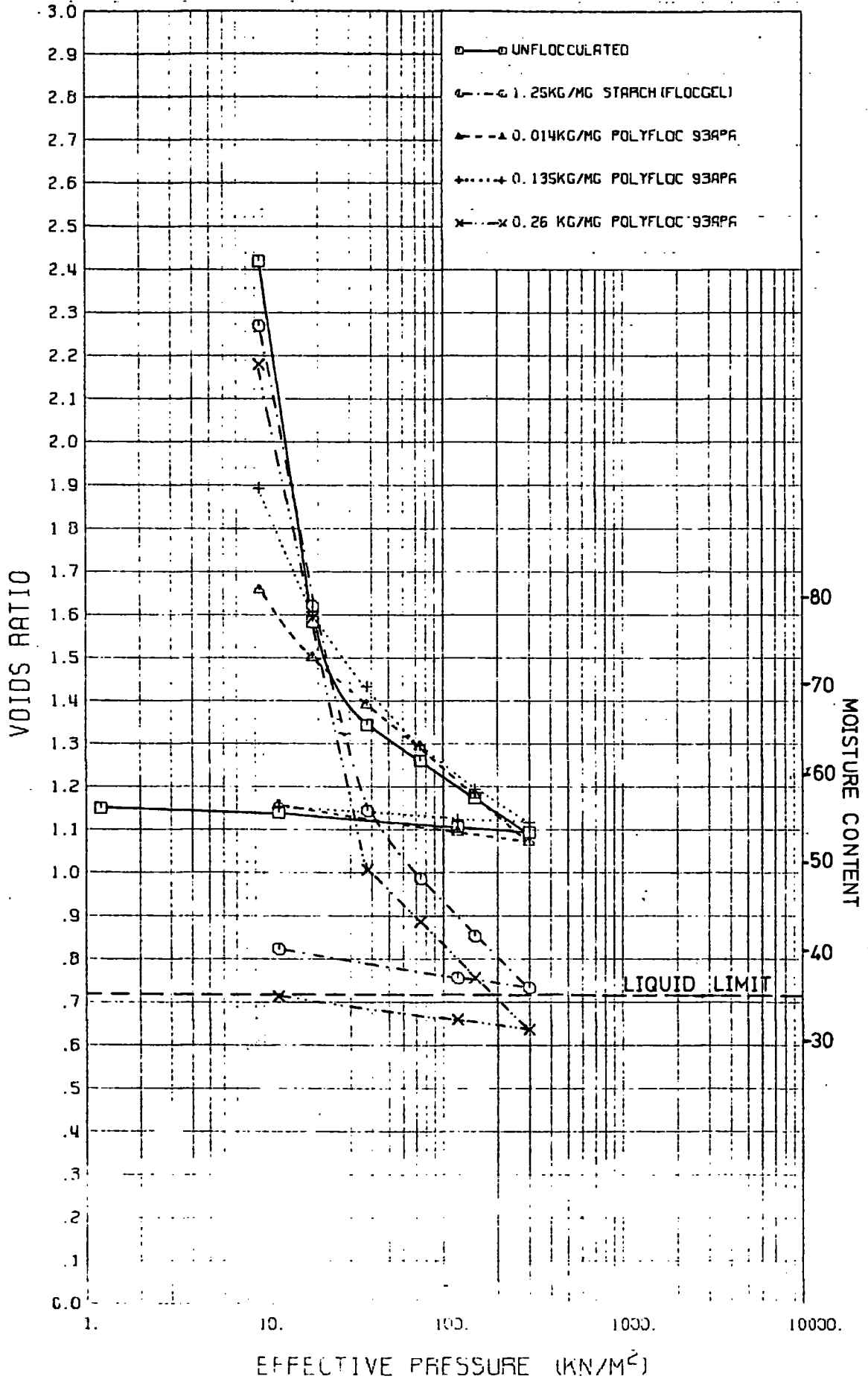


Fig 4.26

FIGURE 4.27

MANVERS TAILINGS, PASSING 72MICRONS. COMPARISON BETWEEN GRADING
OF TOP & BOTTOM OF SAMPLES AT VARIOUS FLOCCULANT CONCENTRATIONS

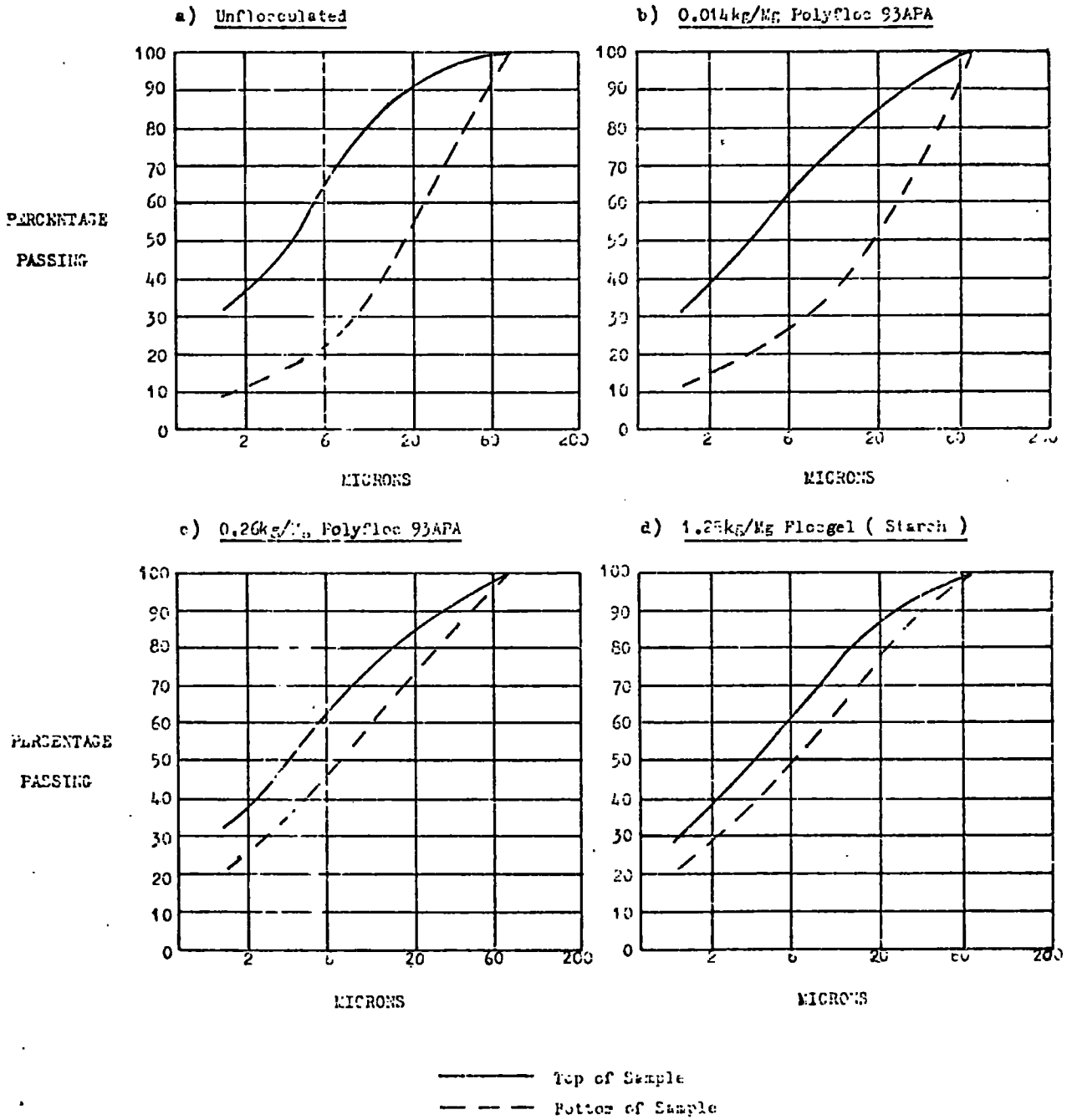
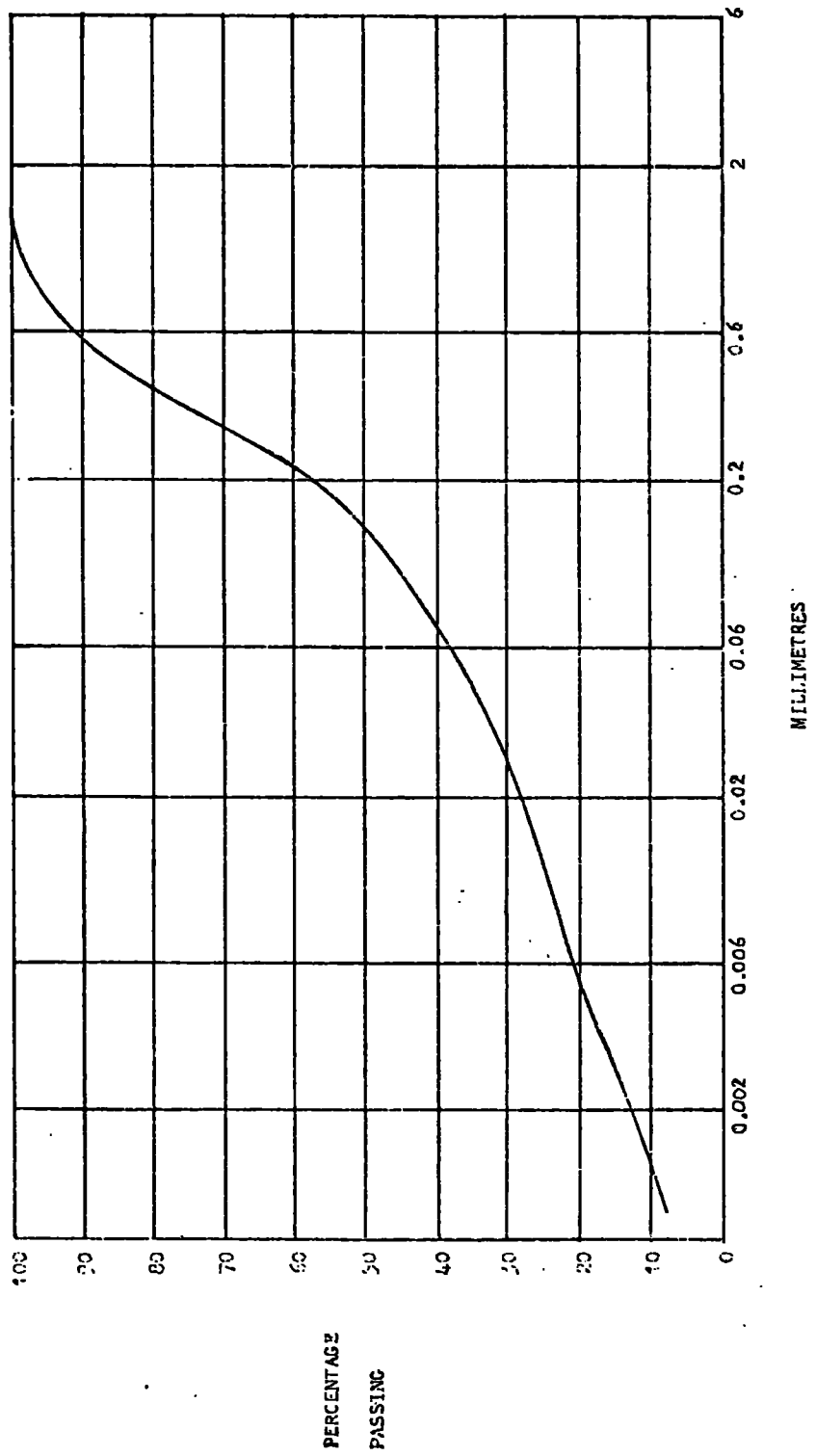


FIGURE 4.28

GRADING CURVE FOR MORRISON BUSTY TAILINGS



MORRISON BUSTY TAILINGS

FIGURE 4.29

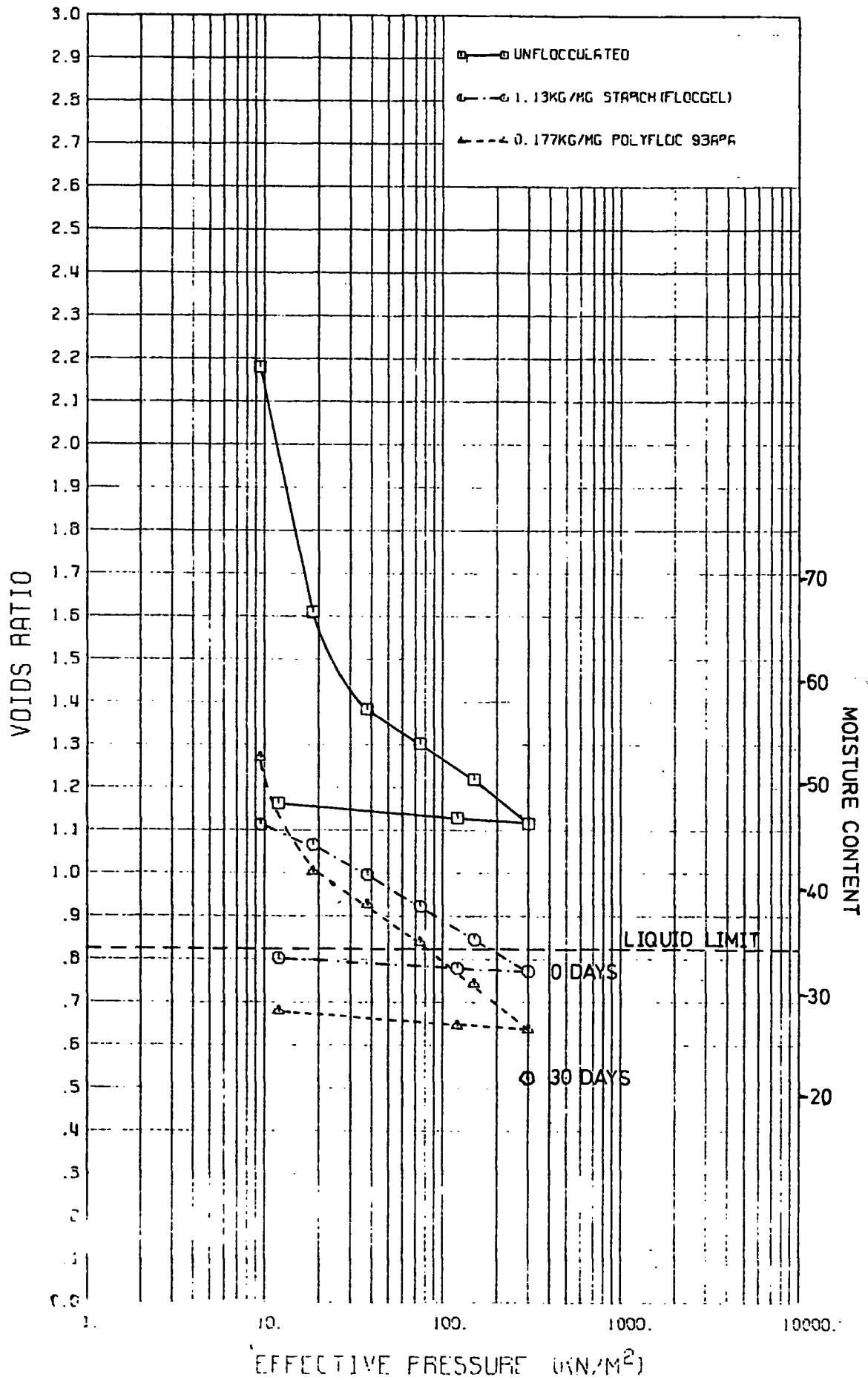
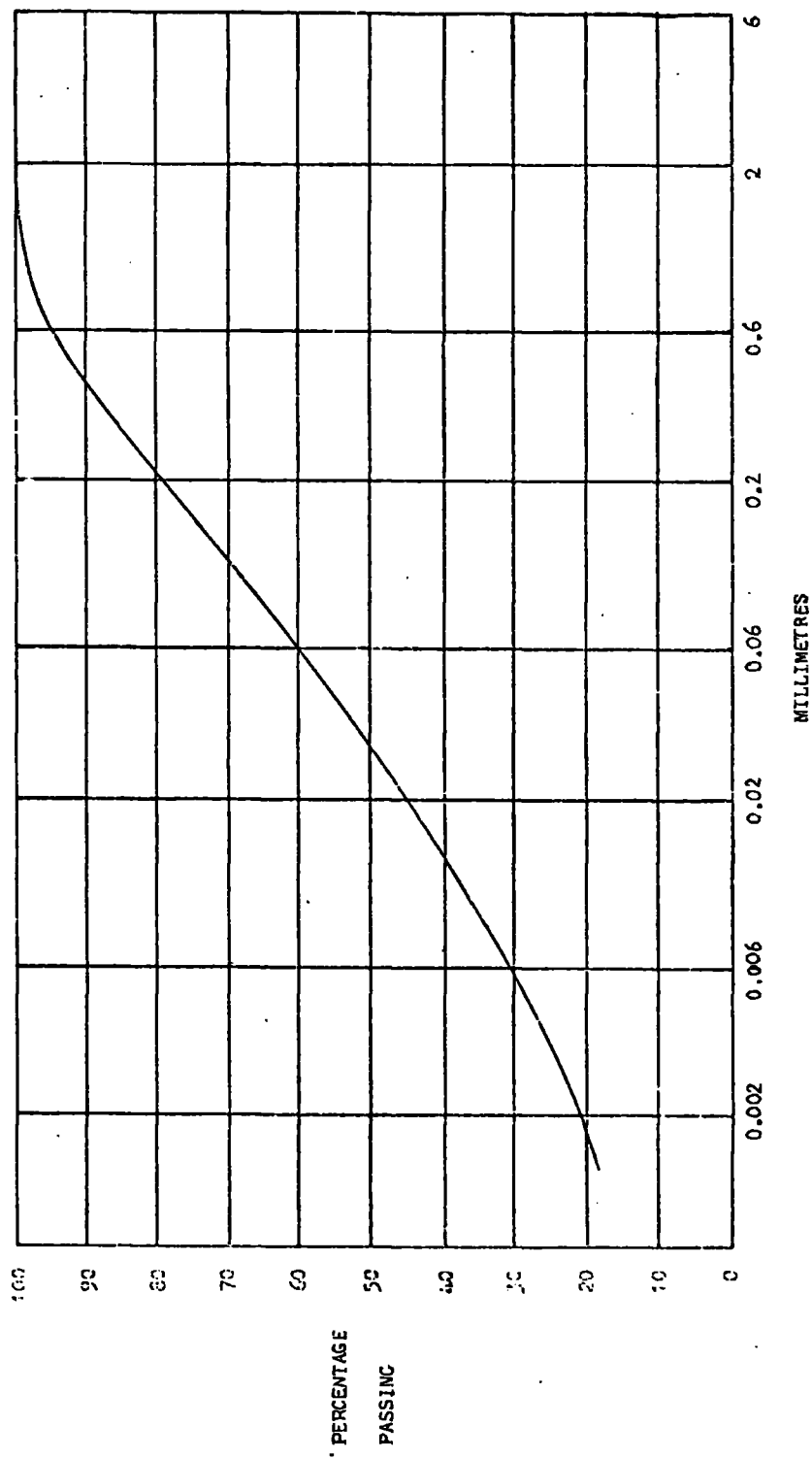


FIGURE 4.30

GRADING CURVE FOR GEDLING TAILINGS



GEDLING TAILINGS

FIGURE 4.31

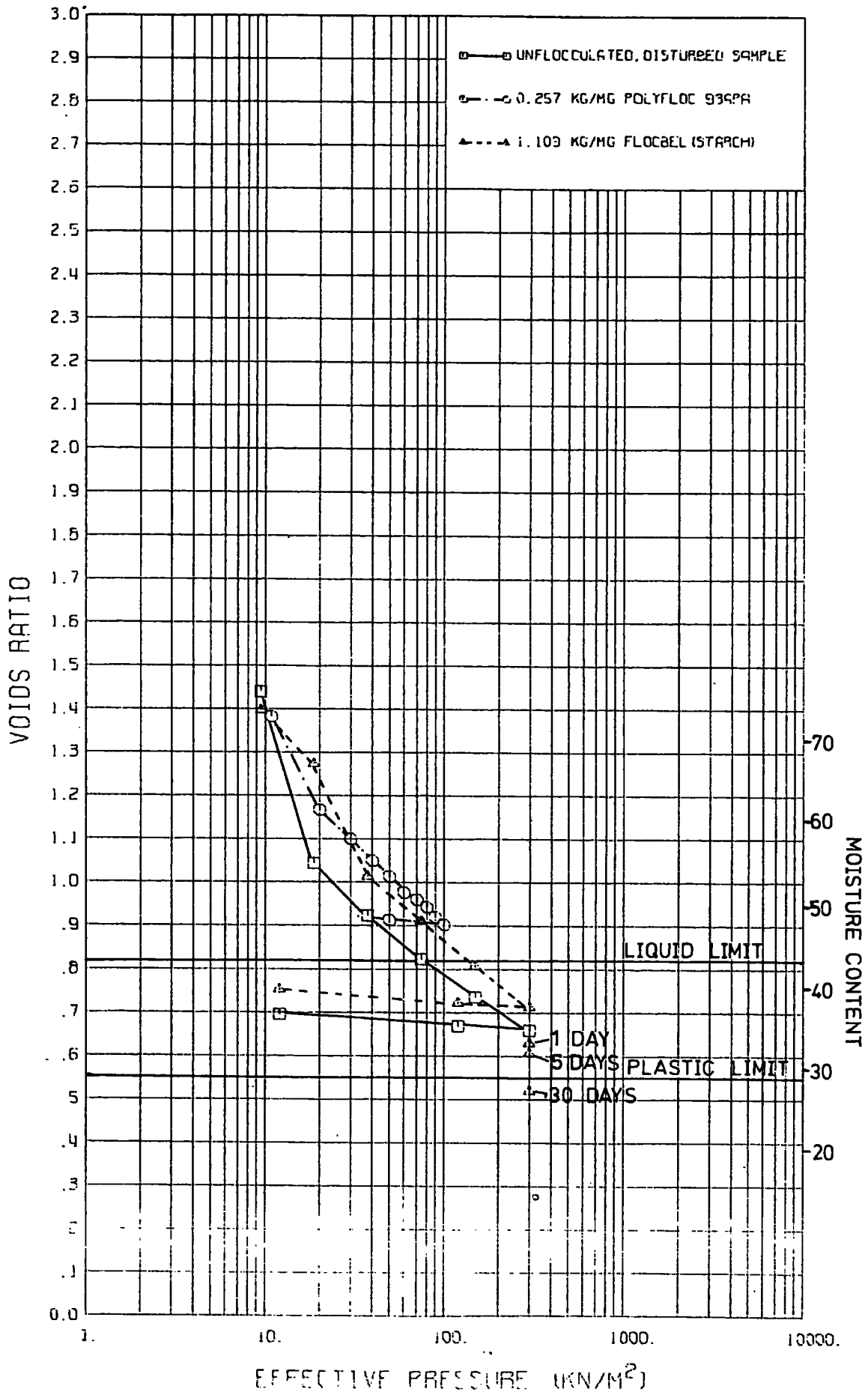
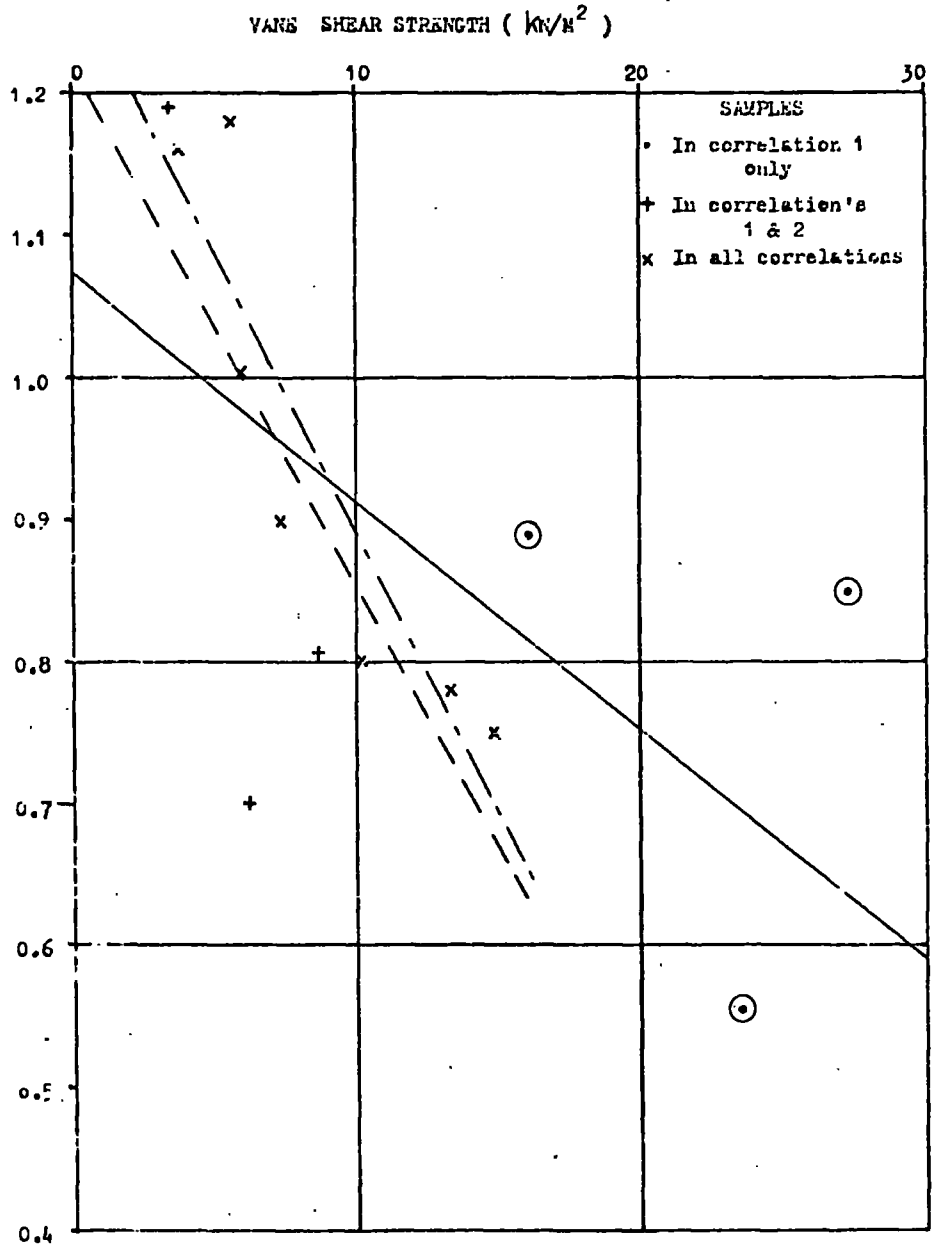


FIGURE 4.32

GRAPH OF VANE SHEAR STRENGTH AGAINST VOIDS RATIO FOR SLURRY/TAILINGS SAMPLES



LINEs FITTED BY REDUCED MAJOR AXIS STATISTICAL TECHNIQUE

- To all data points
- - - - - To data points in correlation 2
- · - · - To data points in correlation 3

FIGURE 4.33

(MODIFIED FROM FIGURE 28.12 IN LAMBE & WHITMAN, 1969)

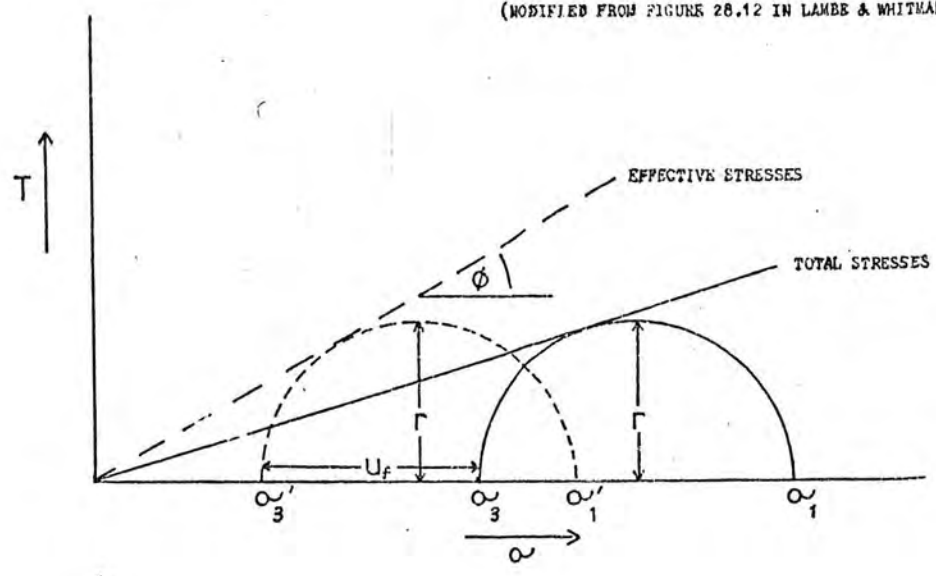
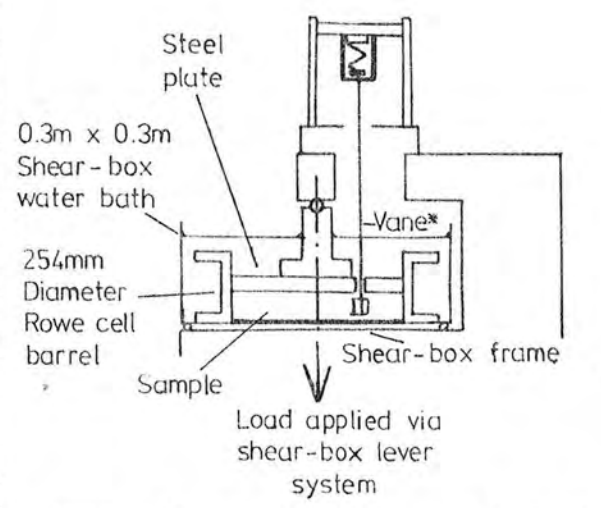


FIGURE 4.34
APPARATUS FOR STATIC LOADING OF A
SAMPLE INCORPORATING A VANE TEST



* Vane not present during normal storage under static load

FIGURE 4.35

MANVERS TAILINGS, COMPARISON OF SHEAR STRENGTH MEASUREMENTS

REDUCED MAJOR AXIS
 STATISTICAL FITS
 ——— SHEAR-BOX
 - - - VANE-PEAK
 - . - VANE-REMOULDED

Cu/P RELATIONSHIP LINES
 --- C / P = 0.3
 - . - C / P = f(PI)

SYMBOLS
 ⊙ SHEAR-BOX
 × VANE-PEAK
 + VANE-REMOULDED

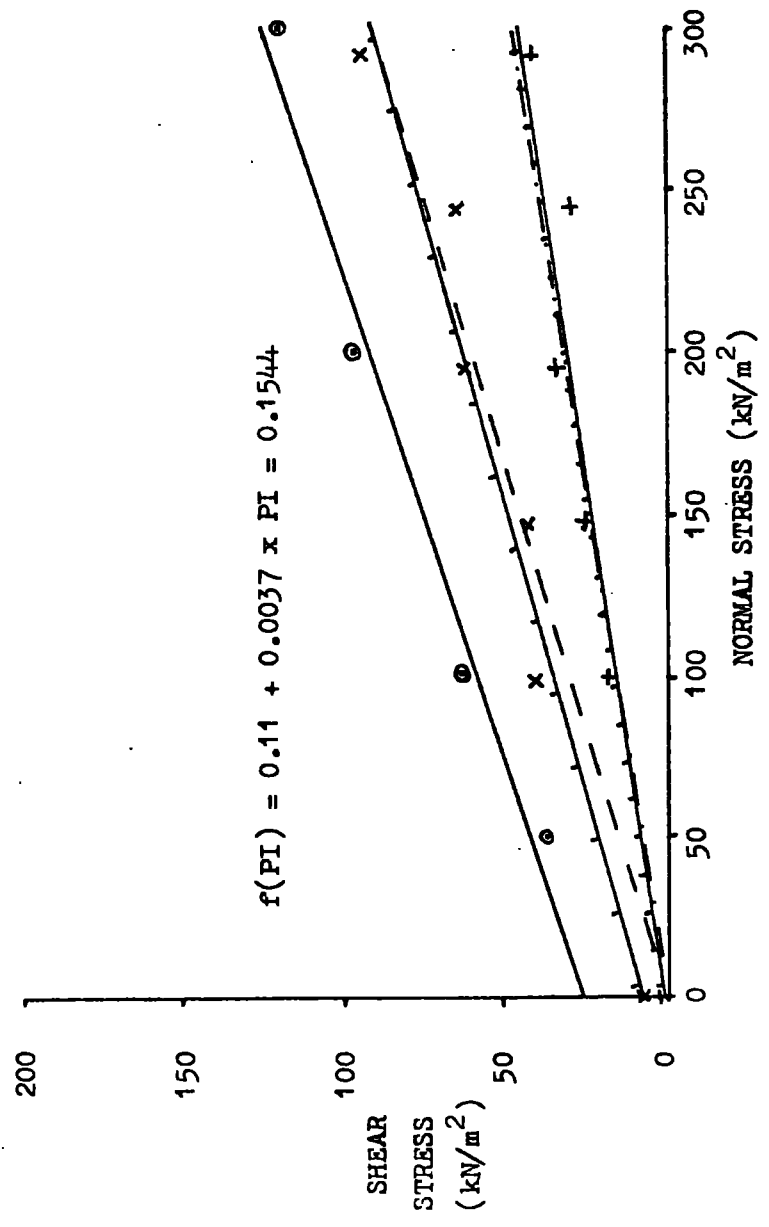


FIGURE 4.36

GEDLING TAILINGS, COMPARISON OF SHEAR STRENGTH MESUREMENTS

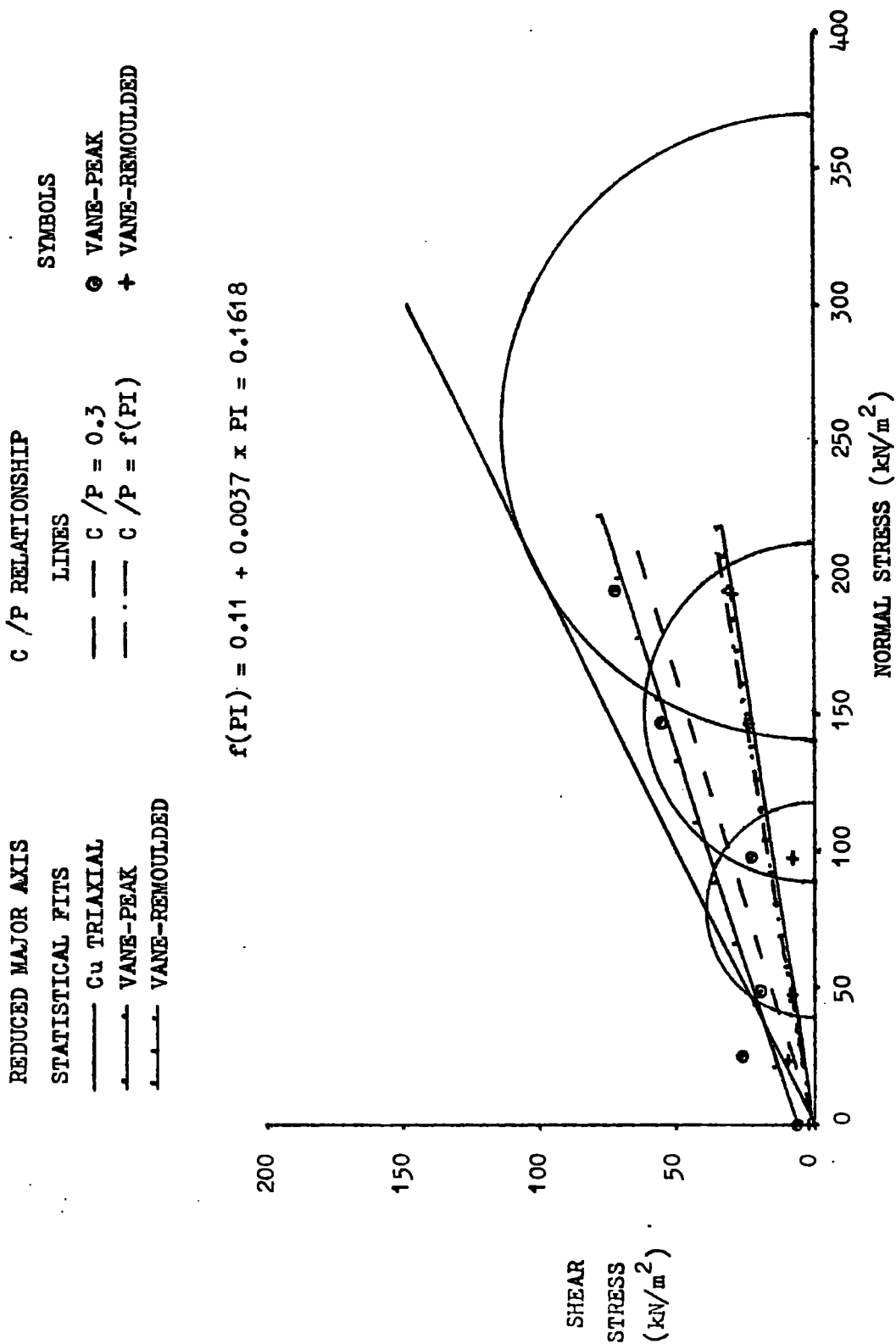


FIGURE 4.37

FAILURE ENVELOPES OF OVERCONSOLIDATED CLAYS (ADAPTED FROM LAMBE & WHITMAN, 1969)

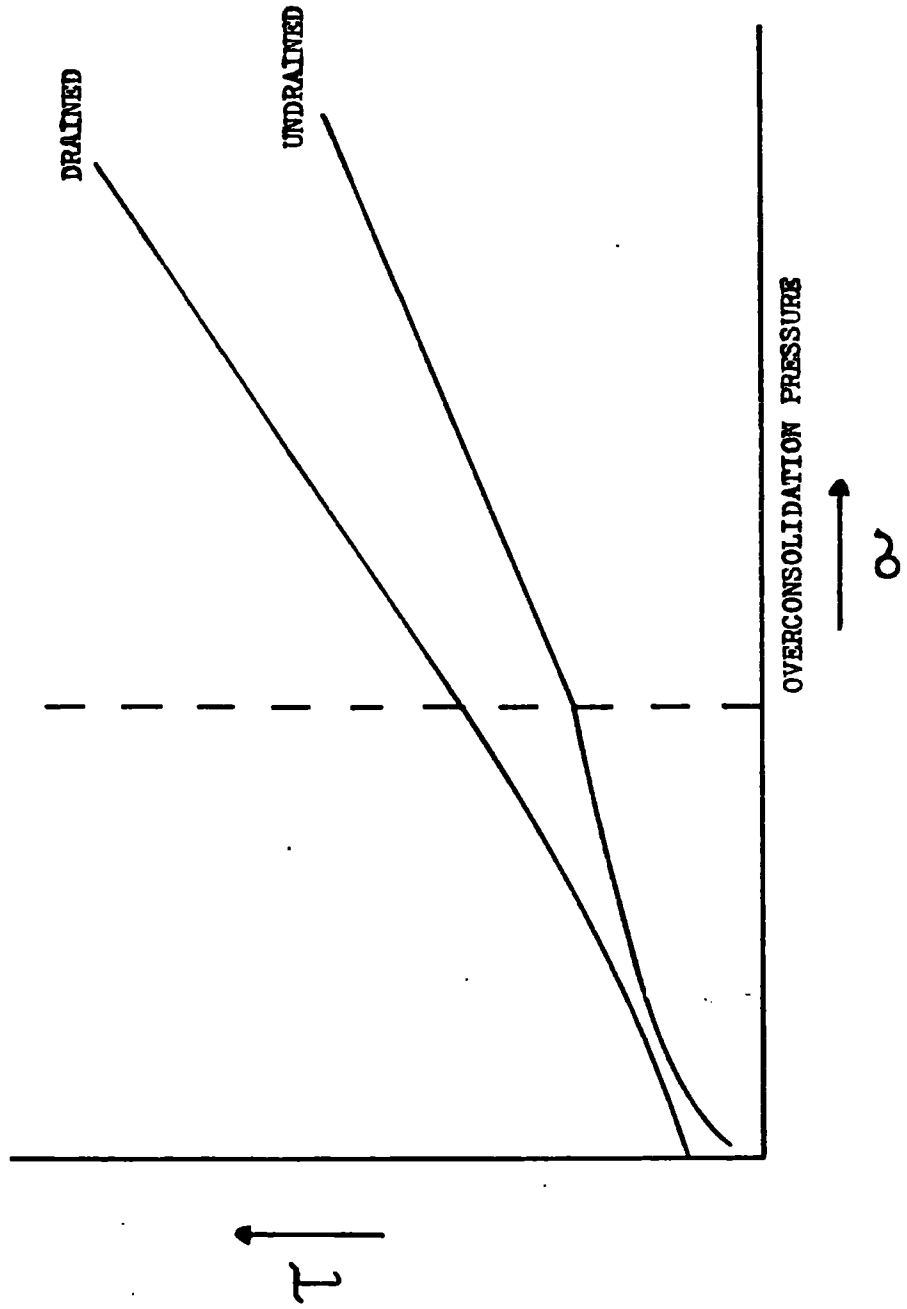
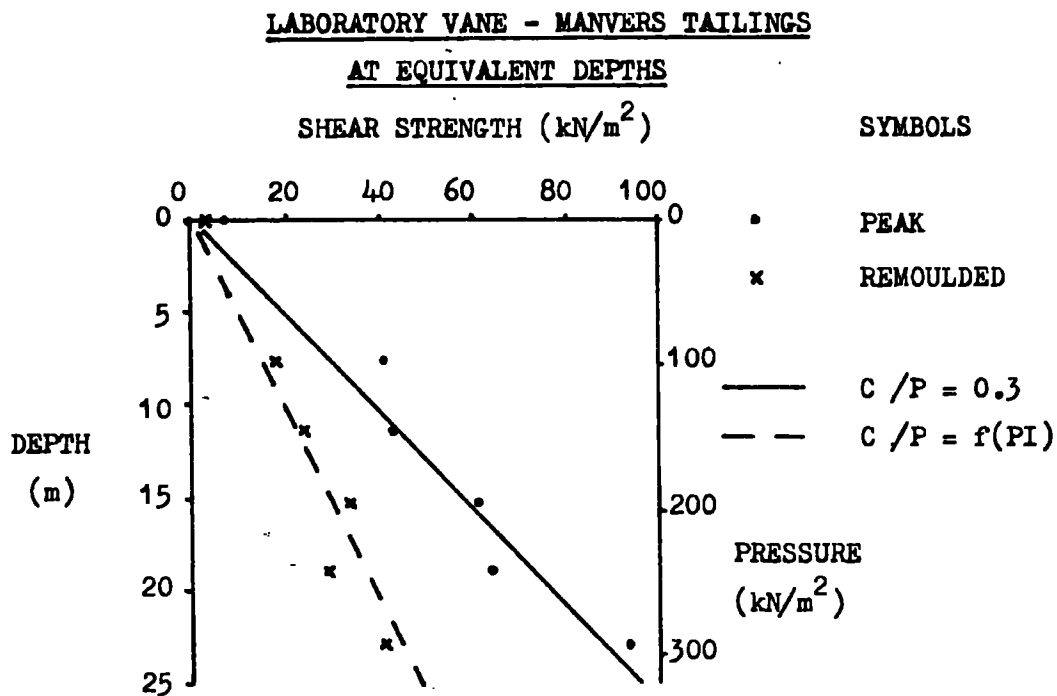
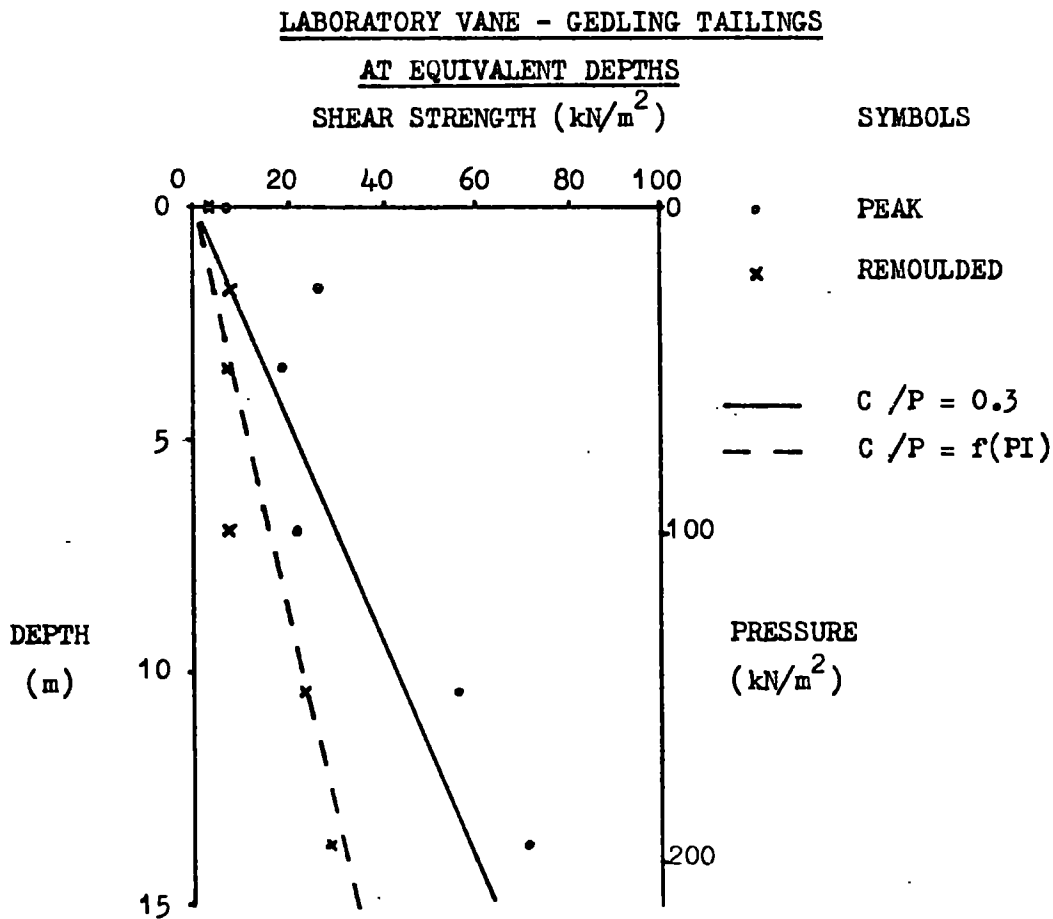


FIGURE 4.38



N.B. Depth calculated on a total stress basis, using a bulk density of 1.31 Mg/m^3 .

FIGURE 4.39



N.B. Depth calculated on a total stress basis, using a bulk density of 1.45 Mg/m^3 .

FIGURE 4.40

FIELD VANE - GEDLING EAST TIP LAGOON, INLET END

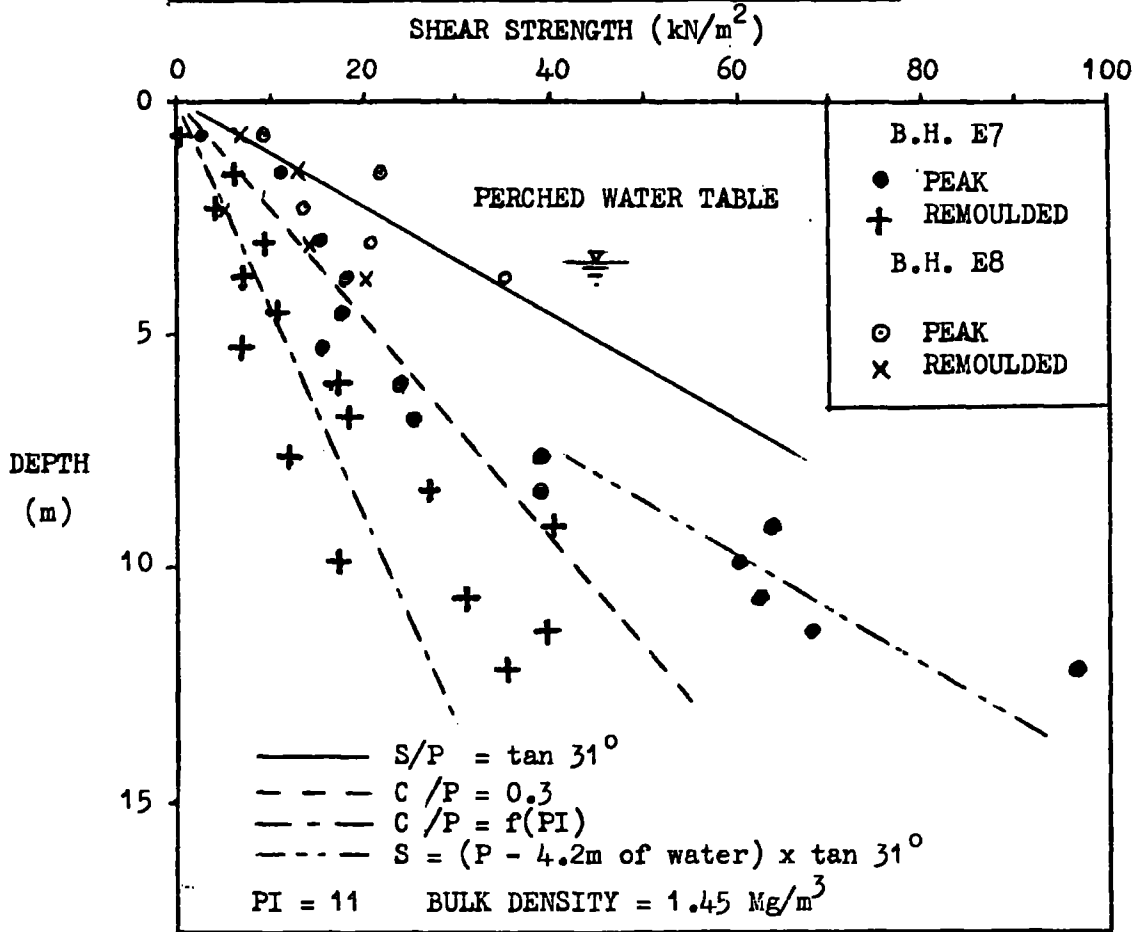


FIGURE 4.41

FIELD VANE - GEDLING EAST TIP LAGOON, OUTLET END

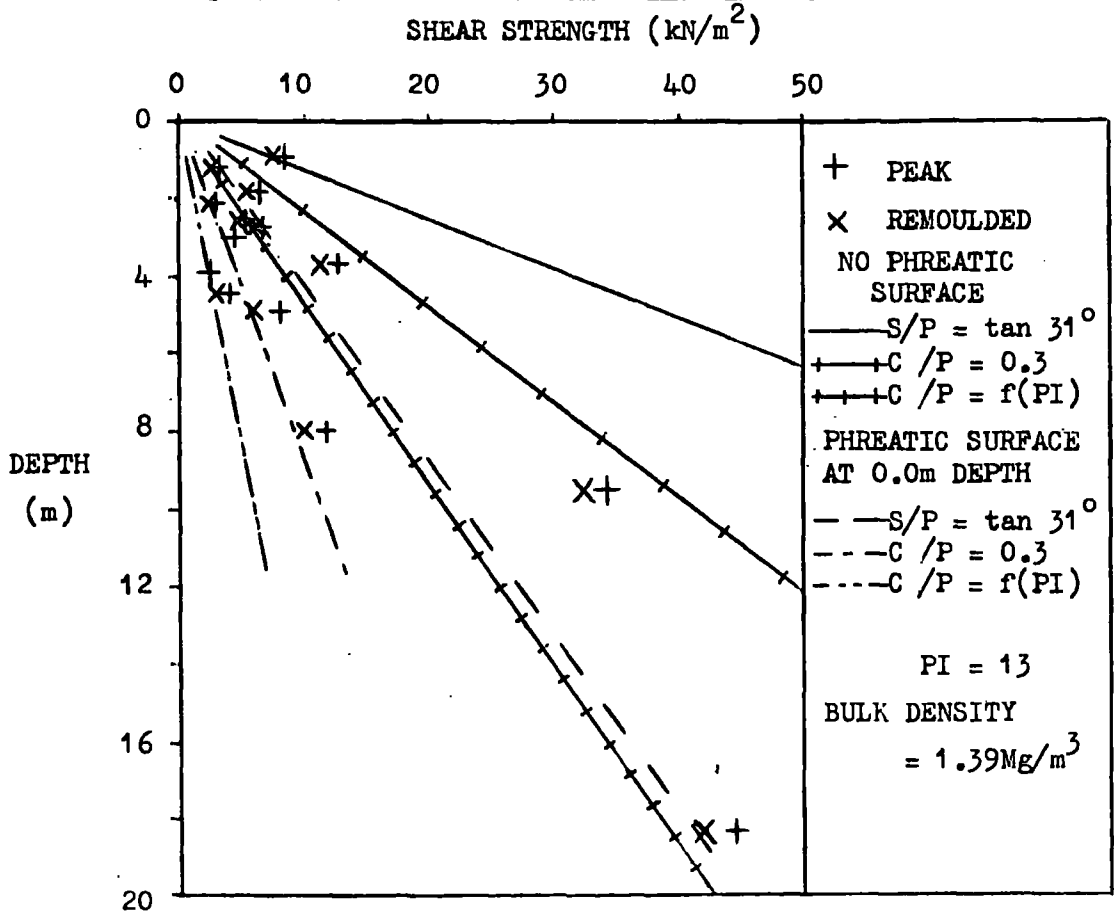


FIGURE 4.43

FIELD VANE - BLIDWORTH LAGOON, OUTLET

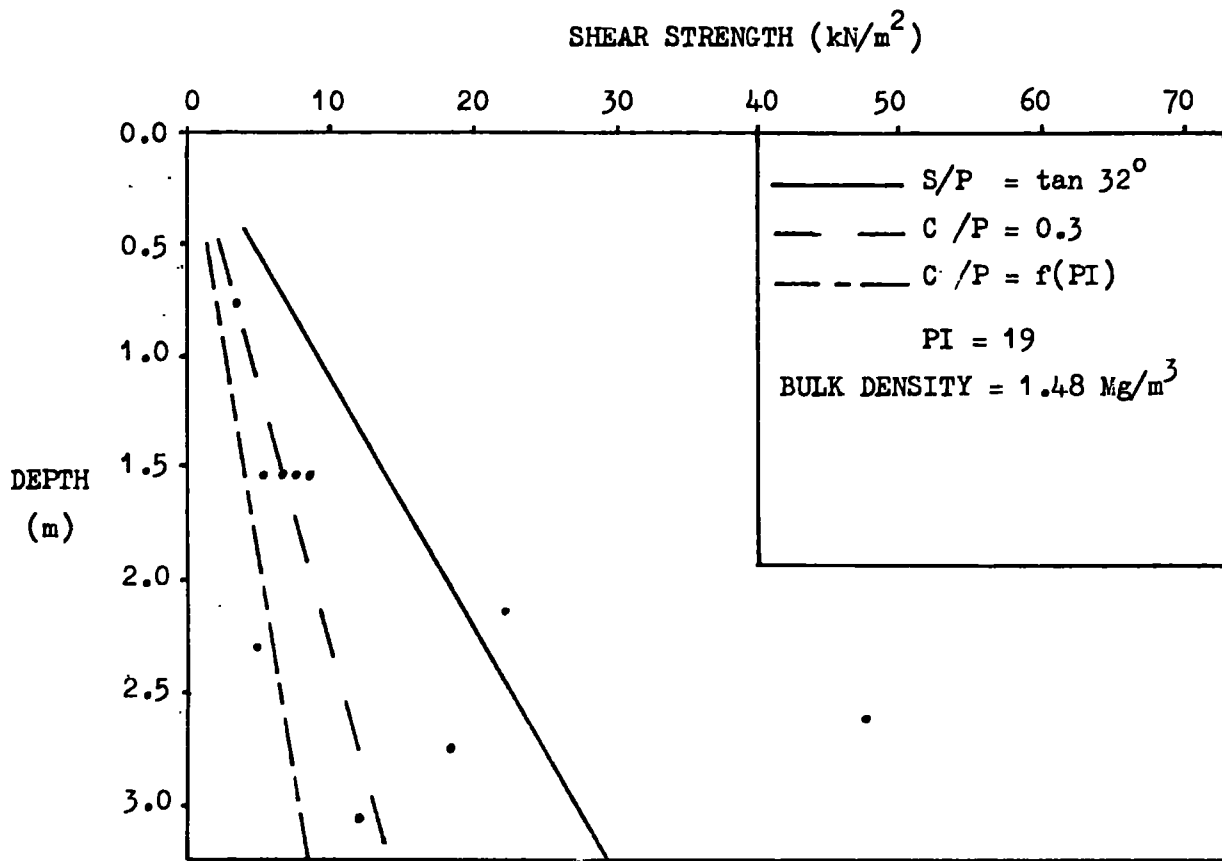


FIGURE 4.44

FIELD VANE - KINNEIL LAGOON 22/2S, OUTLET

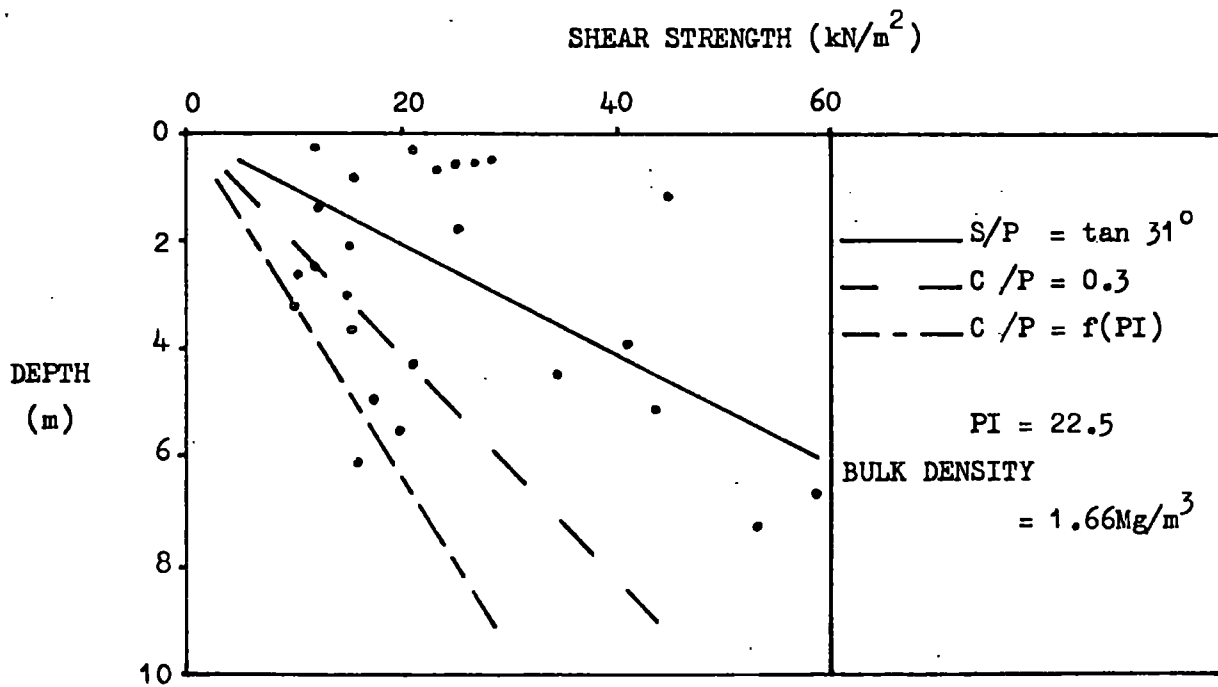
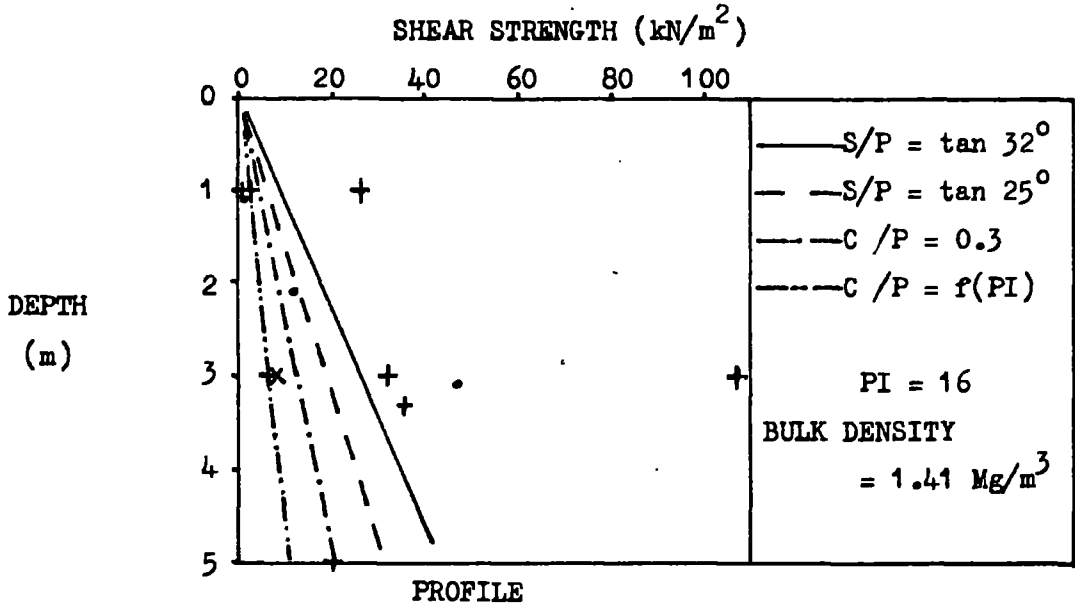


FIGURE 4.47

FIELD VANE - CADEBY LAGOON 9



- HAND VANE - IN EXCAVATED FACE
- + F10, F11, F12, F13 - NEAR EXCAVATED FACE
- x F14 - CENTRE OF LAGOON

FIGURE 4.48

FIELD VANE - CADEBY LAGOON 8

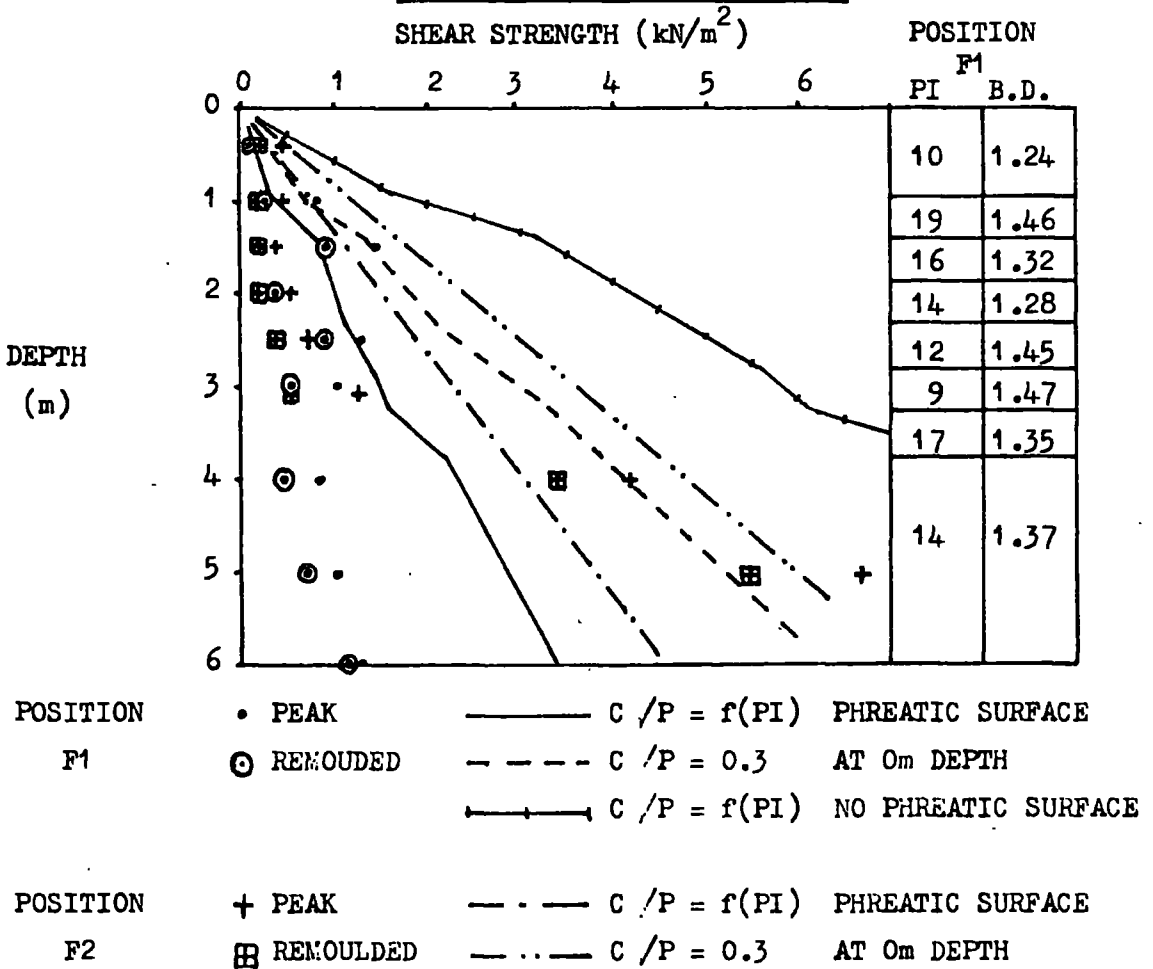
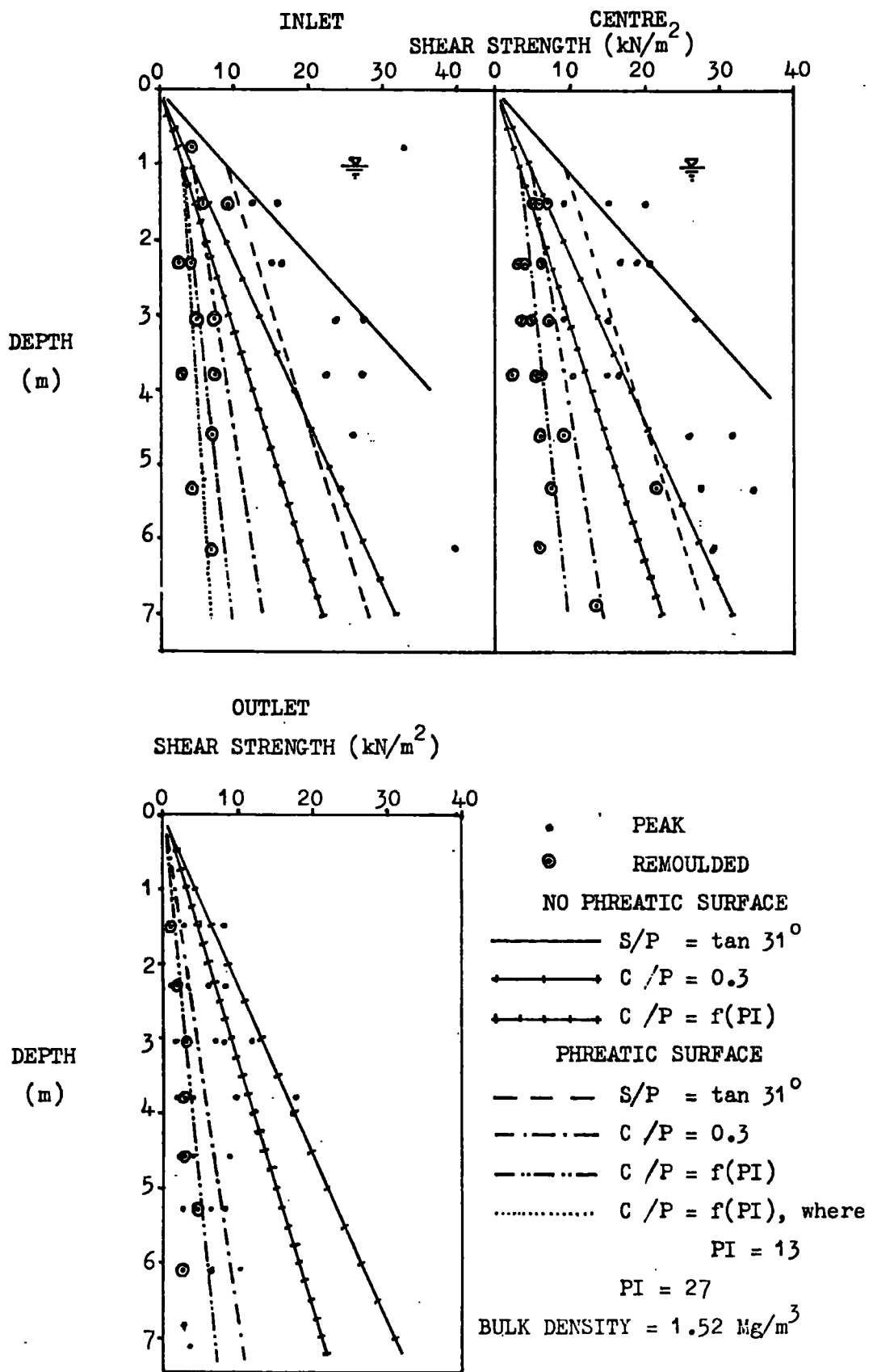


FIGURE 4.49

FIELD VANE - DENBY HALL LAGOON C



CHAPTER 5

CASE HISTORY STUDIES OF THE STABILITY OF SHALE EMBANKMENTS

5.1 Introduction

During the progress of the laboratory work, it was evident that the effects of weathering and curvature of Mohr failure envelopes should be evaluated by slope stability analysis of real situations.

5.1.2. Methods of analysis

Before proceeding further however, a choice of analytical techniques had to be made. The usual methods are those of limit equilibrium analysis. In these, the equilibrium of a potential sliding mass is determined by considering the ratio of the potential restraining to the disturbing forces acting on the mass. In the case of c, ϕ soils, these methods all make an assumption regarding the degree of mobilization of c and $\tan \phi$.

The ratio of strength to stress gives the Factor of Safety (F), whose reliability depends on two factors: a) the measurement of shear strength and b) the computation of shear stress. Hence, it is not sensible to use a method of computing shear stress which is more accurate than the measurement of shear strength. Indeed, it can give a false sense of accuracy.

The three usual methods of analysis are all based on the method of slices (Figure 5.1a) in which the mass is divided into slices, and the total forces acting on it are calculated by summing the forces acting on the slices. They also assume that shear strength (τ) is given by the expression:

$$\tau = c' + \sigma' \tan \phi' \dots\dots\dots(1)$$

where σ' is the effective normal stress

5.1.2.1. Fellenius (Swedish Circle) analysis

In this method (Fellenius, 1936), the opposing inter-slice forces are assumed to have a resultant acting parallel to the

base of the slice. The failure plane is also assumed to be an arc of a circle.

Hence, for one slice, the disturbing forces, D_i are given by $D_i = dW_i \sin \alpha_i \dots\dots\dots(2)$ (Fig. 5.1)

and the resisting forces, S_i are given by

$$S_i = C'_i dL_i + (dW_i \cos \alpha_i - u_i dL_i) \tan \phi'_i \dots(3)$$
 (Fig. 5.1)

Hence the factor of safety, F , is given by

$$F = \frac{\sum_{i=1}^n C'_i dL_i + (dW_i \cos \alpha_i - u_i dL_i) \tan \phi'_i}{\sum_{i=1}^n dW_i \sin \alpha_i} \dots\dots\dots(4)$$

The assumptions made in this method are incorrect, and give rise to errors, which can be very large (up to 60%) when the change in α is large, or when ϕ' is large (Whitman and Bailey, 1967). However, the errors are all on the safe side, the calculations are simple and do not require iteration to produce a value of F .

5.1.2.2. Simplified Bishop Method

In this method (Bishop, 1955, Janbu et al 1956), the failure surface is still assumed to be a circular arc, but the resultant of the interslice forces is assumed to act in a horizontal direction.

The disturbing forces are the same as for the Fellenius method, i.e.

$$D_i = dW_i \sin \alpha_i \dots\dots\dots(2)$$

but the resisting forces now become:

$$S_i = \frac{[C'_i dx_i + (dW_i - u_i dx_i) \tan \phi'_i]}{\cos \alpha_i \left[1 + \frac{\tan \alpha_i \tan \phi'_i}{F} \right]} \dots\dots(5)$$

Hence

$$F = \frac{\sum_{i=1}^n \frac{[C'_i dx_i + (dW_i - u_i dx_i) \tan \phi'_i]}{\cos \alpha_i \left[1 + \frac{\tan \alpha_i \tan \phi'_i}{F} \right]}}{\sum_{i=1}^n dW_i \sin \alpha_i} \dots\dots\dots(6)$$

To solve this expression requires iteration to find the least value of F . The assumptions made can lead to errors up to 8 per cent on the safe side (i.e. values of F some 8% less than the true value), but this is generally acceptable. A more rigorous method is available (Bishop, 1955) in which the total interslice forces are taken into account. However, this requires considerably more calculation and is not generally considered worthwhile, especially as the assumption of a circular slip plane is not necessarily valid.

5.1.2.3. Janbu analysis

In this method (Janbu, 1954, 1973) any shape of failure surface may be considered. In the generalized procedure, the resultant of the interslice forces can act along any line.

Considering the equilibrium of one slice (Figure 5.1b)

$$dW_i + dT_i = dS_i \sin \alpha_i + dN_i \cos \alpha_i \quad \dots\dots\dots (7)$$

$$dE_i = -dS_i \cos \alpha_i + dN_i \sin \alpha_i \quad \dots\dots\dots (8)$$

For equilibrium of the whole mass:

$$\sum_{i=1}^n (dS_i \sin \alpha_i + dN_i \cos \alpha_i) = \sum_{i=1}^n dW_i \text{ i.e. } \sum_{i=1}^n T_i = 0 \dots\dots (9)$$

$$\sum_{i=1}^n (-dS_i \cos \alpha_i + dN_i \sin \alpha_i) = -Q \text{ i.e. } \sum_{i=1}^n dE_i + Q = 0 \dots\dots (10)$$

(where Q is a horizontal force acting at the top of the failure surface, i.e. from a water filled crack).

From (7) and (8)

$$dS_i = (dW_i + dT_i) \sin \alpha_i - dE_i \cos \alpha_i \quad \dots\dots\dots (11)$$

Hence from equation (10)

$$\sum_{i=1}^n \frac{dS_i}{\cos \alpha_i} = Q + \sum_{i=1}^n (dW_i + dT_i) \tan \alpha_i$$

$$\therefore \sum_{i=1}^n \frac{S_i dx_i}{\cos^2 \alpha_i} = Q + \sum_{i=1}^n (dW_i + dT_i) \tan \alpha_i \dots\dots (12)$$

where $S_i = \frac{dS_i}{dL_i}$ and $dx_i =$ width of slice

$$\text{Now, } S_i = \frac{C'_i + \left(\frac{dN_i}{dL_i} - u_i\right) \tan \phi'_i}{F} \dots\dots\dots(13)$$

and, from (7)

$$dN_i = \frac{dW_i + dT_i - dS_i \sin \alpha_i}{\cos \alpha_i} \dots\dots\dots(14)$$

Therefore,

$$S_i = \frac{C'_i + (p_i + t_i - u_i) \tan \phi'_i}{F \left(1 + \frac{\tan \alpha_i \tan \phi'_i}{F}\right)} \dots\dots\dots(15)$$

where $p_i = \frac{dW_i}{dx_i}$, $t_i = \frac{dT_i}{dx_i}$

Inserting (15) in (12) and solving for F,

$$F = \frac{\sum_{i=1}^n \frac{(C'_i + (P_i + t_i - u_i) \tan \phi'_i) dx_i}{\cos^2 \alpha_i (1 + \tan \alpha_i \tan \phi'_i / F)}}{Q + \sum_{i=1}^n (P_i + t_i) \tan \alpha_i dx_i} \dots\dots\dots(16)$$

From moment equilibrium for the slice,

$$dE_i (P_i + t_i) dx_i \tan \alpha_i - S_i dx_i (1 + \tan^2 \alpha_i) \dots\dots\dots(17)$$

$$\text{and } T_i = -E_i \tan \alpha_{t_i} + h_{t_i} \frac{dE_i}{dx_i} \dots\dots\dots(18)$$

where h_t is the height at which the line of thrust intersects the slice (Janbu, 1973). From this, the value of t can be calculated.

To be completely rigorous , the Factor of Safety using several different lines of thrust should be calculated. However, the value of F varies only slightly when this line is based on reasonable positioning (Morgenstern and Price, 1965). Hence

one can draw it to pass through the lower third of the slices without the accuracy being impaired.

5.1.2.4. Morgenstern and Price

There is also another, rigorous method, that of Morgenstern and Price (1965) in which both the Factor of Safety and the internal force distribution have to be found by iteration. It is generally considered to give the most accurate results. However, for the reasons given in Section 5.1.2. it was not used in this work.

5.1.3. Modification of equations to accommodate curved Mohr envelopes

To accommodate the curved shear stress function employed in Chapter 3, certain modifications need to be made to the equations for resolving the Factor of Safety. As the shear strength equation only affects the restraining forces, the denominators of the Factor of Safety equations (i.e. the driving forces) will remain the same.

Consider the shear stress equation

$$\tau = m (\sigma')^z \quad \dots\dots\dots(19)$$

At any normal pressure, p , the corresponding shear stress, s , on the Mohr envelope can be defined by an angle, ϕ'_p , where

$$\tan \phi'_p = \frac{s}{p} \quad \dots\dots\dots(20)$$

From equation (19), (Fig 5.2)

$$s = mp'^z$$

$$\therefore \tan \phi'_p = mp^{(z-1)} \quad \dots\dots\dots(21)$$

Now, provided that the slice is thin enough, the part of the failure envelope corresponding to the stress regime at the slice base can be approximated by a straight line drawn from the origin at an angle of ϕ'_p to the horizontal.

Thus, in the stability equation, $\tan \phi'$ may be replaced by $m_p (z-1)$. Making this substitution, the equations become:-

1) Janbu

$$F = \frac{\sum_{i=1}^n \frac{m_i (p_i + t_i - u_i)^{z_i} dx}{\cos^2 \alpha_i (1 + \tan \alpha_i m_i (p_i + t_i - u_i)^{(z_i-1)})}}{Q + \sum_{i=1}^n (p_i + t_i) \tan \alpha_i dx} \dots(22)$$

2) Bishop

$$F = \frac{\sum_{i=1}^n \frac{m_i (p_i - u_i)^{z_i} dx_i}{\cos \alpha_i (1 + \tan \alpha_i m_i (p_i - u_i)^{(z_i-1)})}}{\sum_{i=1}^n p_i \sin \alpha_i dx_i} \dots(24)$$

3) Fellenius

$$F = \frac{\sum_{i=1}^n \frac{(W_i \cos \alpha_i - u_i d(i)) m_i (p_i - u_i)^{(z_i-1)}}{\sum_{i=1}^n p_i \sin \alpha_i dx_i}}$$

It will be realized that the substitutions made are only correct for a slice with uniform pressure on its base (i.e. one which is a parallelogram). In the methods of slices an assumption is made that the mass of the slice acts at the centre of the slice. This is also only true when the slice is a parallelogram. It follows that slices should be as narrow as possible when the shape is greatly distorted from a parallelogram. The number and thickness of slices will be considered further in Section 5.2.2.

5.2. The slope stability program

5.2.1. Aims of the program

To carry out the analyses a computer program (Appendix A) was written in PL/1 for use on the NUMAC IBM 370 computer. The aim of the program was to be as general as possible, but it

was required to cover the following points:-

- 1) To analyse a multi-layered slope section, with a phreatic surface, whilst taking into account any number of failure surfaces.
- 2) Non-circular surfaces to be analysed by the Janbu (1973) method.
- 3) Circular-arc surfaces to be analysed by the Janbu (1972) Bishop (1955) and/or Fellenius (1936) methods.
- 4) A Bishop self-seeking grid of circular-arc failure surfaces which can be tangential to any material layer in the slope or to any straight line.
- 5) The possibility of the slope being partly submerged.
- 6) The facility for individual layers in the slope to contain areas in which excess pore pressures are developed.
- 7) Isotropic or anisotropic strength parameters, based on linear or curved Mohr envelopes should be accommodated.

5.2.2. Methods used in the program

In a stability analysis using a method of slices, the potential sliding mass is itself divided up into slices. The forces acting on each slice are then calculated and summed to give the stability of the slope. To comply with the assumptions, the slice must not contravene the following points:-

- a) Its sides must be vertical
- b) Its base must be linear
- c) Its base must be all in the same material
- d) Its base must not intersect the phreatic surface.

The program divides up the sliding mass into slices in four steps which ensure these points are observed.

The first step is to define slice boundaries using all the points on the failure surface. This ensures a linear base for all slices (Figure 5.3a). The intersection points between the failure surface and the inter-material layer boundaries, and between the failure surface and the phreatic surface are then calculated. These points then define further slice boundaries (Figure 5.3b). The third step is to interpolate more slice boundaries where the slices are too wide. When considering the width of slices, there are several points to bear in mind. The first is that computing time increases with the number of slices used. However, accuracy improves by increasing the number of slices. Nonetheless, there is a point at which the increase in accuracy is negligible (Spencer 1967) and there is no point in attaining an accuracy which is greater than is justified by the data. Finally, the computer cannot store numbers of magnitude less than 10^{-68} , or to a greater accuracy than fifteen significant figures. This produces an ultimate limit on the thinness of slices, but in practice the other considerations impose a limit of far greater width to the slices.

In Section 5.1.3. it was shown that the assumptions made' in methods of slices were most inaccurate when the shape of the slices was greatly distorted from that of a parallelogram. Therefore, to attain accuracy with the least number of slices, it is desirable that slices be at their minimum width at positions where they are most distorted from the ideal shape. Now, if the slices are of trapezoidal shape, this situation will arise when the vertical slice sides are greatly different in length. This fact has been exploited in the system of subdividing slices. Firstly, all points defining the ground surface, between the extremities of the failure surface, are

used to define further slice boundaries. This ensures all slices are trapezoidal (Figure 5.3c). The difference in length of the vertical sides of each slice is then calculated. Where this is greater than the permissible amount, the slice is subdivided sufficiently to ensure that all the sub-slices do conform (Figure 5.3d). The maximum difference in length of vertical sides is taken as one tenth of the maximum vertical deviation of the failure surface from a line joining the first and last points of the failure surface. This value was decided upon after experimenting with the program to find the point at which the relationship between number of slices versus factor of safety attains a constant value of F (see Figure 5.4).

Figures 5.4 and 5.5 illustrate some interesting points which arose during the experimentation with slice numbers. It can be seen that, with curved envelopes, fewer slices are necessary when using a method which limits the slice side height differences, rather than limiting the slice width. However, with linear failure envelopes there is no change in Factor of Safety, greater than 0.01, due to a mere increase in slice numbers (Figure 5.4). With linear failure envelopes, it is the number of points on the failure surface which controls the *sensitivity* of the Factor of Safety (Figure 5.5). This shows that the errors produced by the assumption that the weight of a slice acts at its centre must be negligible, since this is the error that would be reduced by sub-dividing slices when the failure envelope is linear.* However, from Figure 5.5, it follows that the changes in the angle of the base of the slice

* When the failure envelope is curved, in addition to this error, the errors made in the approximation of the shear strength are also reduced by sub-dividing slices (See Section 5.1.3). This is why the accuracy improves on slice sub-division with curved failure envelopes.

are important, and that at least fifteen points on a failure surface are desirable. As a result of these relations discussed above, the program was modified to allow slices to be sub-divided only when their bases were in material with a curved failure envelope. This provides the shortest computing time for a given accuracy. The actual number of points on a failure surface is under the control of the programmer.

Spencer (1967) concluded that sensitivity increased to a limiting point with an increase in slice numbers. However, he increased the number of slices by increasing the number of points on a (circular) failure surface. Thus his results are in accordance with those found here. At comparable accuracy in F (i.e. 0.01), the number of slices required by him (16), is very similar to the number of points on the failure surface found to be necessary in the current work.

While the points on a non-circular failure surface are read in as data, those for circular arc surfaces have to be calculated from the coordinates of the centre of the circle and its radius. The equation of a circle is of the form:

$$(x - a)^2 + (y - b)^2 = R^2$$

where a = x co-ordinate of centre

b = y co-ordinate of centre

R = Radius of circle.

In a slope stability analysis the arc required is always in the lower semicircle. Thus the points at which the circle cuts the top layer surface (i.e. the extremities of the sliding mass) can easily be found by solving simultaneous equations. The circular arc may then be sub-divided into as many points as desired knowing the co-ordinates of the end points, the x co-ordinates of the failure surface can be found by sub-division

of the horizontal distance between the end points. The y co-ordinates are then calculated from the equation given above, the smaller of the two values which are produced being the one required.

Having acquired the slice boundary data, the next step is to calculate dW , du , dx , $\tan\alpha$ and, for the Janbu analysis, $\tan\alpha_t$ (see Figure 5.1). $\tan\alpha$ and dx are simple to calculate. $\tan\alpha$ is the gradient of the slice base, which is already known, since it is the same as that for the portion of the failure surface that the slice is on, whilst dx is the slice width. $\tan\alpha_t$ is the gradient of the line of thrust, which is taken to pass through points which are one third the height of the slice from its base. The weight of the slice is found by summing the product of area and density of each layer occurring in the slice. The area of each layer is found by summing the area between the top surface of a layer and the x axis and then subtracting the area between the top of the layer below (or the base of the slice) and the x axis. The hydrostatic pressure due to the phreatic surface can be found in a similar manner, the density of water being taken as 1 Mg/m^3 . Excess pore pressures, if present, are calculated from the pore water pressure gradient within the layer in which the base of the slice is located.

From a knowledge of the layer in which the slice base is located, it is possible to pick the relevant shear strength parameters, and to define on which basis they are derived (i.e. curved or linear). In the case of anisotropic material, the shear strength parameters pertaining to the horizontal stratification are presumed to act whenever the slice base is inclined at an angle between plus or minus ten degrees from the horizontal. These parameters can then be combined with the values for weight, water pressure and base gradient to compute the restraining and

disturbing forces due to the slice. In the case of the Janbu and Bishop methods of analysis, the former can only be approximate as F is unknown. In fact, the expression $\cos^{(2)}\alpha \left(1 + \frac{\tan\alpha \tan\phi'}{F}\right)$ is taken as unity (Janbu, 1954) for the initial approximation. The restraining and disturbing forces are then summed. For a Fellenius analysis, the factor of safety, F , can be obtained directly from these, but for the Bishop and Janbu methods an iterative process is required. The value of F which is obtained initially is fed into the equations and used to obtain a value for $\cos^{(2)}\alpha \left(1 + \frac{\tan\alpha \tan\phi'}{F}\right)$ which enables a new value for F to be calculated. This is continued until the last two values of F obtained close to within 0.005 of each other. For a Bishop analysis this value is then reported, to two decimal places as the factor of safety. For a Janbu analysis, it is used to calculate an initial approximation for the side forces (Janbu, 1973). Using these side force values, another iteration is performed to procure a new value of F . This is then used to modify the side force values, and the iterative process continued. Iteration ceases when the difference in F before and after side force modification attains a value of 0.005. This value is then reported.

The iterative process sometimes fails to converge (i.e. the last two values of F are never closer than 0.005). This usually occurs when the factor of safety is high or when a failure surface of complex shape is employed. To prevent iteration continuing ad infinitum in these circumstances, a maximum of 30 iterations is imposed. If this number is exceeded, calculation for that failure surface will cease, and a message is printed, giving the last two values of F .

An example of the program's operation, along with its method of use will be found in Appendix A.

5.3. Gedling Spoil Heaps -overtipping of lagoon deposits - weak spoil on strong foundations

5.3.1. Introduction

In 1968, a major extension and heightening of existing spoil heaps at Gedling colliery was proposed. This involves overtipping five lagoons, and the construction of new lagoons in the tip complex. A site investigation was carried out by Wimpey Central Laboratories Ltd. The results of this investigation showed that based on the properties of the materials then in the heaps, the extended heaps would be stable.

In Chapter 2.2 and 4.2.2. physical parameters for some materials being disposed of in the period 1973 - 1975 have been reported. It was noted that the spoil was weaker than the pre-1968 material. It was therefore decided to re-assess the stability of the heaps using these current parameters, and also to employ curved Mohr envelopes.

5.3.2. Description of site

5.3.2.1. General

Gedling colliery is situated 5km north east of Nottingham (Figure 1.1) in the bottom of a tributary valley of the River Trent. The two spoil heaps (West and East) are built on the northern side of this valley. The site plan (Figure 5.6) shows that the tips are actually founded on the site of three small valleys.

The solid geology at the site consists of Permo-Triassic rocks of Keuper facies. Two formations are present, the Waterstones (flaggy silt-stones and sand-stones with shale partings) overlain by Keuper Marl (red mudstones with occasional sandstones). These beds dip in an east-south-easterly direction at 1 to 5 degrees. The boundary between the two formations occurs under

the spoil heaps (Figure 5.6 and Geological Survey 1 inch sheet No. 126). The investigation by Messrs Wimpey showed the presence of thin layers of alluvial material in the small valleys mentioned above.

5.3.2.2. The West tip

The West tip originally consisted of several small heaps deposited by aerial ropeway, Maclane tippler and railway waggons. The spoil in the south western area of the tip ignited, and this part now comprises a considerable quantity of burnt material. A valley between these small heaps was dammed and used as a tailings/slurry lagoon. While in operation, its bund was gradually raised. Its extent was variable, its superficial location being altered by the continuously growing tips around it. By 1969 this lagoon was not in use, and nearly all of it was overtipped. Overtipping is now complete (see Figure 5.7 and Sections D-D, E-E Figures 5.11 and 5.12). Since 1969, some new lagoons have been built on the northern side of the tip (Figure 5.7). These too are now not used. The proposed extension will increase the height of the tip from 115m to 125m A.O.D., while the toe height is 65m A.O.D.

Water was noticed to be seeping from the burnt material in the western part of the tip.

5.3.2.3. The East tip

The East tip was originally built from material transported by aerial ropeway and then redeposited by scrapers. It impounded a large lagoon on its northern side. These lagoons have now been overtipped and a new pair are being constructed over them (Figure 5.7). The height of this eastern tip will be raised from 90 to 115m A.O.D., its toe height being 55 - 60 m A.O.D. The small side valley which it completely fills may well have had springs

emerging in its floor.

5.3.3.1. Slope stability analysis

Five sections were chosen for analysis viz:- A-A (Figure 5.8), B-B (Figure 5.9), C-C (Figure 5.10), D-D (Figure 5.11) and E-E (Figure 5.12). These sections, whose position is shown on the site plan (Figure 5.7), cover the most critical positions, namely the steepest proposed sections on East and West tips (B-B and E-E respectively), the infilled valley under the eastern tip (A-A) the position at which the old lagoon in the West tip approaches closest to the tip face (D-D) and a section in the present tip where excess pore pressures have developed (C-C). The results of the analysis are listed in Table 5.1 and discussed below.

5.3.3.2. Parameters used (Figure 5.13 and Table 5.2)

The parameters used for the new spoil are those derived during the current work, namely:-

$$\begin{aligned} c' &= 22.9 \text{ kN/m}^2 && \text{) where a linear Mohr envelope is} \\ & && \text{)} \\ \phi' &= 23.4^\circ && \text{) used} \\ m &= 1.096 && \text{) where a curved Mohr envelope} \\ & && \text{)} \\ z &= 0.871 && \text{) is used} \end{aligned}$$

A bulk density of 2.012 Mg/m^3 was assigned, this being the density of an undisturbed sample from the tip.

The old tip materials were assigned parameters determined by Messrs Wimpey, viz:-

$$\begin{aligned} c' &= 7.18 \text{ kN/m}^2 && \text{) for linear Mohr} \\ & && \text{)} \\ \phi_1 &= 27.5^\circ && \text{) envelopes} \\ m &= 0.874 && \text{) for curved Mohr} \\ & && \text{)} \\ z &= 0.920 && \text{) envelopes} \end{aligned}$$

with a bulk density of 1.922 Mg/m^3 .

TABLE 5.1
FACTORS OF SAFETY PERTAINING TO STABILITY
ANALYSES AT GEDLING

SECTION		Location of Failure Surface	Factor of Safety (F)
A - A	a	Critical surface (passes through weathered crust)	1.48
	b	Minimum F surface passing through alluvium	1.56
	c	Minimum F surface in new discard only (i.e. not passing through weathered crust)	1.59
B - B	a	Critical surface for whole face as originally proposed	1.35
	b	Critical surface for short, steep sections on original proposed section	1.17
	c	As (b) but with a weathered crust	1.47
	d	Critical surface for smoothed profile	1.44
	e	Surface through old lagoon	2.83
	f	As (f) but with lagoon liquefied	1.56
	g	Surface (a) with linear c' , ϕ' parameters	1.42
	h	Surface (b) with linear c' , ϕ_1 parameters	1.56
	i	Surface (a) with ϕ'_e parameter	1.02
C - C		Critical surface	2.04
D - D	a	Critical surface through weathered spoil	1.45
	b	Surface passing through postulated residual area and weathered spoil	2.01
	c	Critical surface assuming lagoon liquefied	0.43

Cont'd....

TABLE 5.1 (Continued)

Section	Location of Failure Surface	Factor of Safety (F)
E - E	a Critical surface (passes through weathered crust)	1.63
	b Surface passing through postulated residual area	2.22
	c Surface passing through old lagoon, assuming this to be liquefied.	1.41

TABLE 5.2

PARAMETERS EMPLOYED FOR GEDLING STABILITY ANALYSES

Material	Shear Strength Parameters		Bulk density (Mg/m ³)
New spoil	c' (kN/m ²)	∅'	2.012
	22.9	23.4	
	m	z	
	1.096	0.871	
		∅' _e	
		27.2	
Old spoil	c' (kN/m ²)	∅'	1.922
	7.18	27.5	
	m	z	
	0.874	0.920	
Weathered spoil	c' (kN/m ²)	∅'	1.9
	33.9	16.9	
Old Lagoon	0	31.0	1.7
Alluvium	8.62	31.0	2.051

For the weathered crusts, the parameters for weathered material (Chapter 2.2) are employed:-

$$c' = 33.9 \text{ kN/m}^2$$

$$\phi' = 16.9^\circ$$

while the bulk density was assumed to be 1.9 Mg/m^3

Old lagoon deposits are given the parameters reported by

Messrs Wimpey (1968), these are:-

$$c' = 0$$

$$\phi' = 31.0^\circ$$

$$\text{Bulk density} = 1.7 \text{ Mg/m}^3$$

(This density is that of consolidated deposits).

The alluvial materials in the valleys have also been assigned the parameters determined from Messrs Wimpeys investigation.

$$c' = 8.62 \text{ kN/m}^2$$

$$\phi' = 31.0^\circ$$

$$\text{Bulk density} = 2.051 \text{ Mg/m}^3$$

5.3.3.3. Section A-A (Figure 5.8)

5.3.3.3.1. Factor of Safety

This section is drawn along the line of one of the infilled valleys under the East Tip. A study of the shear strengths of the materials involved (Figure 5.13) shows that the alluvium on the valley floor is stronger than any materials in the tip itself. As it is reported as a sandy silt it is unlikely to develop excess pore pressures. It should not, therefore, adversely affect the tip's stability. This is indeed found to be the case. The minimum factor of safety of any circle drawn tangential to the base of the alluvium is 1.56, whereas the minimum for the tip is 1.48, on a surface tangential to its base. This being so, the presence of alluvium has been ignored in all the other sections. It will be seen that all these minima are

controlled by the postulated zone of weathering on the old tip. For failure surfaces in the new discard, the minimum is 1.59. Hence the presence of a weak, weathered zone in the spoil heap can produce a drop in the factor of safety of 0.11, if as in this case, the weathered surface approaches the toe of the tip.

5.3.3.3.2. Effect of changes in parameters m and z

The sensitivity of the factor of safety to variations in the curved Mohr failure envelope parameters m and z was tested using this section. A circle shown as a dashed line on Figure 5.8, which passes through new discard only, was chosen. The effect of varying the parameters m and z is shown in Figures 5.14 and 5.15.

It can be seen that there is a positive correlation between the Factor of Safety (F) and z and between F and m . A change of 0.01 in z results in a change of 0.085 in F , whereas a change of 0.01 in m only gives a corresponding change of 0.015. Now as the Factor of Safety is found to ± 0.005 , (i.e. a possible range of 0.01) it follows that the z parameter can vary by up to 0.0012 before a change in F will result. Similarly m may vary by up to 0.0067 before a change in F occurs. It follows from this that neither need to be quoted to more than three decimal places.

5.3.3.4. Section B-B (Figure 5.9)

5.3.3.4.1. Factor of Safety

This section is drawn where the old lagoon in the East tip is closest to the toe of the slope in the area of the steepest proposed final profile. In this case the critical failure surfaces are shallow (13 metres maximum depth). A Factor of Safety of 1.35 exists for the main slope, but for the short

steep sections on it, the Factor of Safety is 1.17. Whilst this is less than the specified value of 1.25 customarily required by the National Coal Board for non-critical areas, the slip plane is shallow, and it can be concluded that most of the material affected will weather and develop cohesion, thus improving the Factor of Safety. From Figure 5.13 it will be observed that weathered spoil is in fact stronger than unweathered spoil in the effective normal stress range up to 100 kN/m^2 (accommodated by the potential failure under consideration), due to its developed cohesion. When a weathered crust of 3 metres depth is assumed over the surface of the new tip, the Factor of Safety increases to 1.47 which is acceptable. Thus the stability of the face would only give cause for concern over the first six months after construction.

The low Factors of Safety on this face can also be increased at the construction time by smoothing out the steps in the profile, or by emplacing stronger material only in this section (e.g. run-of-mine dirt). By employing the profile shown by the dotted line in Figure 5.9, the Factor of Safety increases to 1.44 and the volume of spoil marginally increases. It is understood (Mr. A.R. Bacon, personal communication) that this last named option is to be employed.

Under effective stress conditions, with full dissipation of pore water pressures, the presence of the lagoon is not detrimental to the stability. This is because, under these conditions, the lagoon sediments are stronger than the tip materials (Figure 5.13). The Factor of Safety for a slip surface passing through the lagoon is in fact 2.83. Even when the lagoon is assumed to liquefy completely and possess zero

strength, the Factor of Safety is still 1.56. It is too deeply buried within the coarse discard of the spoil heap to have any serious effect upon overall stability. The same argument applies to the weathered crust of the old tip.

5.3.3.4.2. Comparison of different evaluations of shear strength parameters

This being the most critical cross-section, the linear Mohr envelope and the ϕ'_e fit were also used in the analysis in order to test their effects (Figure 5.16). Using the linear envelope, the Factor of Safety is increased to 1.42 and the shallow slip surface which had a Factor of Safety of 1.17 using a curved envelope now has a Factor of Safety of 1.56. This increase is due to the effect of cohesion which greatly enhances the apparent stability of a shallow slip surface (N.B. the effect of weathering, mentioned above). It is in these circumstances that a linear envelope may seriously overestimate the value of the Factor of Safety.

The ϕ'_e approach (McKechnie, Thomson and Rodin, 1972) was described in Chapter 3.1. It was not developed for stability criteria, and as will be seen it is not very realistic when employed for such a purpose. The ϕ'_e value of new Gedling spoil is 27.2° . Using this, the Factor of Safety for Section B-B is only 1.02. This is a severe underestimate and is a result of the shear strength defined by the ϕ'_e line, being much lower than the actual shear strength for all shallow slip planes (Figure 5.16). As Gedling spoil has a markedly curved envelope, the disparity is great in this case.

5.3.3.5. Section C-C (Figure 5.10)

During construction an area of very high pore pressure has developed in the south eastern corner of the East Tip.

Pore pressures of over 30 metres of water (i.e. higher than the height of the tip at the present time) have been measured under the crest of the tip (see Figure 5.10). These pore pressures have gradually dissipated over the past two years, because construction has been stopped in this area. It was decided to carry out a stability analysis of the steepest section affected, to ascertain whether stability had, in fact, been jeopardized.

As can be seen in Figure 5.10, the area of very high pore pressures is deeply buried, being 20 metres below the crest of the tip. No excess pore pressures are developed in the large toe area. This geometry is found to be stable, the lowest Factor of Safety being 2.03. The analysis suggests that high pore pressures in tips are not a cause for concern provided that they are only generated at depth beneath the crestal section of the tip. High pore pressures near the toe would be considerably more dangerous.

5.3.3.6. Section D-D (Figure 5.11)

This section is drawn across the West Tip, where the old lagoon is closest to the toe. This lagoon was formed some time before 1941 by damming a valley between the heaps in this area. The dam was gradually raised when necessary by tipping over its upstream face, which produces a "fir tree" profile (Figure 5.17). The downstream extent of the lagoon materials was not determined during Messrs Wimpeys investigation, and the extent has been estimated by projecting a line from the two known points on the downstream face of the lagoon.

Examination of the cross section (Figure 5.11) shows that the lagoon boundary furthest from the toe is steep. Now, the

lagoon deposits will be very compressible, while the coarse discard will not. In that part of the tip which lies above 84 metres A.O.D., i.e. above the level of the lagoon, there will be relative movement between that part which is founded on lagoon sediments and that which is not. This movement will take place above the lagoon boundary, and will thus be concentrated into a small area.

It is possible to calculate the settlement of compressible deposits using the relation:-

$$dH = \frac{H (e_o - e_1)}{(1 + e_o)} \quad (\text{Terzaghi and Peck, 1967})$$

where H = thickness of deposit

e_o = initial voids ratio

e_1 = voids ratio at full pressure

There are, however, no consolidation data for this lagoon. Data obtained for new lagoons on the West tip during the course of this research had to be employed instead. Taking the worst conditions, the outlet sample materials pressure-voids ratio relationship was used (Figure 4.18). The thickness of spoil over the lagoon will reach 30.8m and the depth of slurry/tailings at this point is 17.5m. With a density of 2 Mg/m^3 for the spoil, a pressure of 600 kN/m^2 will be exerted on the lagoon materials. With an initial voids ratio of 1.19 (Table 4.11) and a value of 0.65 at 600 kN/m^2 (Figure 4.18), the settlement would be 4.3 metres. Gedling spoil drops to a residual shear strength after a displacement of two metres (Figure 2.14). It is quite possible that a zone of coarse discard in the vicinity of the lagoon banks may be subject to shear displacements such that it falls to a residual strength (see Figure 5.11).

Similar displacements must affect the lagoon deposits. There is, however, no information on either the residual strength, or the shear displacement required to attain it, for Gedling Tailings. The bulk sample of Cadeby tailings (Chapter 4.2.1.) showed no fall-off in strength with displacement, and present day Gedling tailings do resemble Cadeby chemically (Table 4.3). They may therefore exhibit a similar behaviour.

Potential failure surfaces drawn through the area of residual strength show no signs of instability, the Factors of Safety being greater than 2.0 (surfaces (2) and (3), Figure 5.11). Thus, whether or not there is a small area of low strength in the lagoon at the bank furthest from the toe is immaterial.

Before leaving the subject of potential failure areas in the spoil it is pertinent to consider the possibility of bearing capacity failures during the construction of the tip over the lagoon.

The problem of the bearing capacity of clays when overlain by embankments has been analysed by Raymond (1967), and his solution has been utilized here. A major problem in calculating the bearing capacity of the lagoon in the West tip is the lack of undrained shear strength data. Vane test results from the outlet of the old East tip lagoon have had to be employed instead. A desiccated crust of 1m thickness has also been assumed, this being the thickness of crust in the old East Tip lagoon (Figure 4.41).

According to Raymond (1967), the minimum Factor of Safety, F , against localized failure* of an embankment is $\frac{5.5 c_m}{q}$

* With soils in which undrained shear strength increases with depth, such as lagoons, the Factor of Safety against general failure is larger than that against localized failure.

where:-

C_m = minimum undrained shear strength

q_e = equivalent value of intensity of loading

In the present case, C_m is equal to 3 kN/m² (Figure 4.41). For a value of F of 2, q_e is therefore 8.25 kN/m². This basic value should be modified slightly to allow for the spread of the load through the desiccated crust. As this crust is thin, however, this modification (which would increase the value of q_e) has been ignored.

The value q_e is related to the embankment by the relation:

$$q_e = \frac{4e^2 + 4b \cdot e + b^2}{3e^2 + 3b \cdot e + b^2} \cdot \frac{3}{4} \gamma h$$

where

b = width of side slope of embankment

e = distance of shoulder from backscarp of failure

γ = bulk density of embankment material

h = height of embankment.

The most likely failure is when $e = 0$ (Raymond 1967).

Therefore,

$$q_e = \frac{3}{4} \gamma h$$

Now, the bulk density of compacted Gedling spoil is approximately 2 Mg/m³. Therefore,

$$\frac{h \times 2 \times 3}{4} = \frac{8.25}{9.81}$$

∴ h = 0.56m

With a Factor of Safety of unity, this value would be doubled, to approximately 1m. However, the possibility still arises that bearing capacity failures, at least of limited extent, occurred during the overtipping of the lagoon. Whether they would seriously weaken the coarse discard, is however, doubtful.

The failure surfaces due to bearing capacity failures will be virtually vertical in the coarse discard, and hence nearly perpendicular to any failure surface involving the main tip. Furthermore, at the low pressures (0-100 kN/m²) operative in the spoil at the time of a bearing capacity failure, shear strength reduction is reduced (Chapter 3.3.1.). The possible existence of a zone of bearing capacity type failures above the lagoon has therefore been ignored in the analyses.

Turning to the stability of the final profile, it has already been mentioned that failure surfaces through the end of the lagoon remote from the toe have Factors of Safety greater than 2. In fact, under effective stress conditions, with full dissipation of pore pressures, the most critical surface passes through the zone of weathered spoil in the old tip. It has a Factor of Safety of 1.45, which is acceptable.

Since the lagoon sediments are fine-grained, full dissipation of pore pressures may not be achieved until some time after construction has been completed. In order to evaluate the necessity for calculating probable pore pressures, the Factor of Safety assuming zero strength for the lagoon deposits was calculated. This was 0.43, indicating that an attempt had to be made to evaluate pore pressures in the lagoon.

Pore pressures are usually calculated by using Skempton's A and B pore pressure parameter relationship, customarily calculated from consolidated-undrained triaxial tests with pore pressure measurement. As this type of test has not been performed on the Gedling lagoon deposits, another approach had to be used.

It is possible to calculate pore pressure distributions

from the coefficient of consolidation. The method, which is outlined in Lambe and Whitman, (1969) considers the pore pressure in a consolidating layer, viz:

$$u_e = u_o \frac{4}{\pi} \sum_{n=0}^{\infty} \frac{1}{(2N+1)} \left\{ \frac{\sin (2N+1) \pi Z}{2H} \right\} e^{-(2N+1)^2 \pi^2 T/4} \dots\dots\dots(25)$$

where $T = \frac{c_v t}{H}$

H = thickness of consolidating layer per drainage surface

z = depth within the consolidating layer at which the pore pressure is required

t = time since start of consolidation

u_e = pore pressure after time t

u_o = initial pore pressure

N is an interger of the series 0,1,2,3.....

The initial pore pressure is taken as being equal to the initial load. This will be the case when the material is fully saturated*.

The expression above is derived from Terzaghi's consolidation equation viz:

$$c_v \frac{\delta^2 u_e}{\delta z^2} = \frac{\delta u_e}{\delta t} - \frac{\delta \sigma_v}{\delta t} \dots\dots\dots(26)$$

where σ_v = total stress.

If total stress is assumed constant with time, i.e. $\frac{\delta \sigma_v}{\delta t} = 0$ and if the substitution $T = \frac{c_v t}{H}$ and $Z = \frac{z}{H}$ are made, this equation becomes

$$\frac{\delta^2 u_e}{\delta Z^2} = \frac{\delta u_e}{\delta T} \dots\dots\dots(27)$$

* When the material is not fully saturated, the pore pressure developed will be less than the initial load.

If uniaxial drainage is assumed, the following conditions apply:

Initial condition at $t = 0$

$$u_e = u_o \text{ for } 0 \leq Z \leq 2$$

Boundary condition at all t

$$u_e = 0 \text{ for } Z = 0 \text{ and } Z = 2$$

The solution of the differential equation has been assessed (e.g. Taylor, 1948) and is:

$$u_e = \sum_{N=0}^{\infty} \frac{u_o}{(2N+1)} \left(\sin \frac{\pi}{2} Z (2N+1) \right) e^{- \left(\frac{\pi}{2} (2N+1) \right)^2 T} \dots\dots\dots(28)$$

If Z is now replaced by $\frac{Z}{H}$, the equation, number (25) is achieved.

Using this equation (25), it is possible to calculate the pore pressure in a layer of clay, the load on which has been periodically increased. The pore pressure due to a load increment can be calculated after the time, t , which has elapsed since it was emplaced to the time when the last load was emplaced. The pore pressures due to all such load increments are summed, and added to that due to the final load increment to give the calculated pore pressure. Since the calculation depends upon c_v , and this parameter is generally underestimated in consolidation tests (Chapter 4.2.1.9), it follows that the pore pressure calculated will be an overestimate of the actual pore pressure.

While the calculations can be performed by hand, it is quicker to computerize them. This has been accomplished using the short program in Appendix C. It should be noted that the term $\sum_{N=0}^{\infty} \frac{1}{(2N+1)} \left(\sin \frac{(2N+1)}{2H} \pi Z \right) e^{- (2N+1)^2 \pi^2 T/4}$ is a converging series. As N increases the individual terms become smaller until they finally become insignificant. They are ignored once they are less than 10^{-5} .

Where a load is applied in stages, and excess pore-pressures are able to dissipate with time, it will be appreciated that the degree of pore pressure build up will depend upon the rate at which the load is applied. A series of estimates of pore pressure have been calculated, assuming differing rates of loading.

The value of the Factor of Safety was then calculated for each pore-pressure distribution. The loading rate at which it surpassed the permissible value could then be taken as the safe construction rate.

In order to calculate the pore pressure distributions, some assumptions have had to be made about the lagoon and its properties. Firstly, the c_v is assumed to be $30.4 \text{ m}^2/\text{yr}$. This is the average value for the outlet sample from Lagoon 12 on the Western tip. This sample being one of the finest grained lagoon samples, the c_v of the old lagoon is unlikely to be lower than this value. Secondly the lagoon materials are assumed to have double drainage.

This assumes that the old spoil on top of the lagoon and the rock upon which the lagoon stands are free draining. The old spoil was not heavily compacted, and the foundation rocks are the Waterstones, so that this assumption is probably valid.

The pore pressure distributions are calculated at five locations which are marked on Figure 5.11.

Two different lift heights were employed, 5 and 2.5 metres. 5 metres is the thickest lift allowed by the National Coal Board. The pore pressure distributions which yield a critical Factor of Safety near to the minimum acceptable value of 1.25 are given in Table 5.3.

It can be seen that, with 5m lifts, even with a four year period between lifts, the Factor of Safety is still only 1.24, i.e. just below the acceptable level. With 2.5m lifts, the Factor of Safety reaches an acceptable value of 1.29 with only 4.5 months between lifts. The faster construction rate which is possible with the thinner lifts is due to the lower initial pore pressure produced by the latter (10.06 metres of water for 5m lifts, 5.03 metres of water for 2.5m lifts). The critical failure surface, which is the same for all the critical pore pressure distributions, is shown by a dashed line on Figure 5.11. It can be seen that it passes through the part of the lagoon beneath the downstream bank. Hence, it is in this area that pore pressures must be controlled. It is obviously desirable for a line of piezometers to be installed in the lagoon sediments, although if only 2.5 metre lifts are employed, no serious trouble should arise provided that lifts are employed at intervals greater than 4.5 months.

5.3.3.7. Section E-E (Figure 5.12)

This section is drawn in the area of steepest profile where an arm of the old lagoon occurs (Figure 5.7). Using similar arguments to those in the previous section the maximum differential settlement was calculated. In this case it was 2.2 metres, again sufficient to reduce the shear strength of Gedling spoil to its residual shear strength.

As in Section D-D, the potential residual area does not produce any apparent instability, Factors of Safety for slip surfaces passing through it being greater than 2.2. The minimum Factor of Safety, 1.63, is again on a surface passing through the weathered zone of the old tip.

If the lagoon were assumed to liquefy due to seismicity

TABLE 5.3

CALCULATED PORE PRESSURES AT 5 LOCATIONS IN WEST TIP LAGOON
FOR DIFFERENT LOADING RATES

Location (Fig.5.11)	Pore Pressure in metres of water					Loading Rate	Critical Factor of Safety
	D*						
	0.333	0.667	1.0	1.333	1.667		
A	10.07	10.08	10.09	10.08	10.07	One 5m lift per year	1.17
B	12.54	14.36	15.02	14.36	12.54		
C	12.62	14.50	15.18	14.50	12.62		
D	12.36	14.05	14.67	14.05	12.36		
E	11.96	13.34	13.85	13.34	11.96		
A	10.06	10.06	10.06	10.06	10.06	One 5m lift per 4 yrs	1.24
B	10.38	10.63	10.71	10.63	10.38		
C	10.34	10.55	10.63	10.55	10.34		
D	10.26	10.40	10.46	10.40	10.26		
E	10.19	10.28	10.32	10.28	10.19		
A	6.71	7.94	8.38	7.94	6.71	One 2.5m lift per 3 mths	1.24
B	13.96	19.64	21.44	19.64	13.96		
C	14.68	20.98	23.02	20.98	14.68		
D	15.63	22.78	25.19	22.78	15.63		
E	15.12	22.04	24.41	22.04	15.12		
A	5.88	6.50	6.72	6.50	5.88	One 2.5m lift per 4.5 mths	1.29
B	12.03	16.83	18.47	16.83	12.03		
C	12.37	17.47	19.23	17.47	12.37		
D	12.55	17.85	18.72	17.85	12.55		
E	11.91	16.80	18.54	16.80	11.91		

TABLE 5.3 (Continued)

Location (Fig.5.11)	Pore Pressure in metres of water					Loading Rate	Critical Factor of Safety
	D*						
A	5.49	5.82	5.95	5.82	5.49	One	1.33
B	10.58	14.67	16.08	14.67	10.58	2.5m	
C	10.79	14.90	16.37	14.90	10.79	lift	
D	10.62	14.64	16.09	14.64	10.62	per 6	
E	10.01	13.61	14.91	13.61	10.01	mths	

* $D = \frac{\text{Depth in consolidating layer from its top surface}}{\text{Thickness of the consolidating layer per drainage surface}}$

or sudden loading (e.g. conventional rotational failure) its shear strength could be assumed to be negligible. Even under these circumstances the Factor of Safety does not drop below 1.41 (on surface (3) Figure 5.12). This being so, no attempt was made to assess pore water pressures in the lagoon, as was appropriate in the case of Section D-D.

5.4. Gale Common pulverized fuel ash lagoon,

A shale embankment on weak foundations.

5.4.1. Introduction

The lagoons at Gale Common, near Knottingley, Yorkshire (Grid Ref. SE 535217) provide for the disposal of some 1 million tonnes of pulverized fuel ash (P.F.A.) per annum from the Eggborough and Ferrybridge coal fired power stations. The disposal site lies approximately between the two power stations so that the P.F.A. is pumped by pipeline as a slurry over distances of about 7.2km (Ferrybridge) and 4.8km (Eggborough) (Figure 5.18).

The scheme, which was started in 1964, has reached the stage shown in Figure 5.19. It consists of the two main lagoons A and B of 21.3 hectares combined areal extent, and the two emergency lagoons, C and D, of 20 hectares areal extent. There are two experimental lagoons (E and F) on the north east side of lagoon D. Ultimately the lagoons and containing embankments will form a landscaped hill over 47m in height, and further lagoons are planned to the south of the site.

Pumped P.F.A. slurry is either processed in the vacuum filtration plant at the site to produce conditioned P.F.A. for embankment construction purposes, or if the solids concentration is too low, it is pumped directly into the main lagoons A or B. The principal embankments are of composite

construction with colliery shale from Kellingley Colliery (some 2 km to the NW) mainly in the upstream section and conditioned P.F.A. forming the downstream section as illustrated in Figure 5.20. The southern embankment to date is entirely of colliery shale.

The compacted embankments are being constructed according to conventional engineering principles, and in order to control seepages through the structure a chimney drain is incorporated behind the upstream shoulder, and this is linked to a system of finger drains which terminate in a rock toe surrounding the main lagoons (see Figures 5.19 and 5.20).

After the inception of the scheme, it became apparent that the quantities of conditioned and untreated P.F.A. were such that it would be necessary to investigate the possibility of increasing lagoon capacity, without increasing the amounts of construction materials involved. A complete review of the design was therefore instigated, including additional site investigation and laboratory testing, to increase the understanding of the geology and engineering properties of the complex foundation sediments which have an important bearing on the stability of the embankments and upon settlement behaviour. In addition, sampling and laboratory testing of the construction materials were put in hand during the 1974 field investigation in order to optimise design parameters (see Taylor, Barton, Mitchell and Cobb, 1976). A further potentially complicating factor that has had to be considered is underground coal-mining. The 1.5m thick Beeston seam is being worked at about 700m beneath the site from Kellingley Colliery. Insofar as the main lagoons A and B are concerned, a panel (Beestons 72's) was anticipated to produce a maximum subsidence of 240mm (National Coal Board, 1975, Walton, 1974). The panel

shown in Figure 5.19 was temporarily discontinued early in 1973, however, because of faulting difficulties and hence a greatly reduced maximum subsidence could be anticipated (circa.25mm). In fact, the average subsidence recorded in the vicinity of the main lagoons over the 17 months following the temporary discontinuation of the panel is only 7.6mm. Three markers situated on the line of the outfall culvert however, (Figure 5.19, Lagoon A) have shown downward movements of up to 54 mm. Part of this subsidence can undoubtedly be attributed to settlement of the compacted fill and foundation sediments. The present subsidence is consequently of smaller magnitude than originally predicted, but renewed working of the panel is expected to result in further movements.

The factors affecting the stability of the southern embankment of Lagoon B which is built of colliery spoil will be the primary concern of this Section.

5.4.2. Foundation materials

5.4.2.1. Geological setting

As the foundation materials are weak in comparison to the construction materials (Figure 5.21), the geological setting will be considered in detail.

The sketch map (Figure 5.22), (Wilson, 1948) shows that Gale Common lies well to the south of the limit of Devensian (Newer Drift') Tills in the Vale of York. It is also outside the Devensian maximum ice limit recently postulated for the region by Gaunt (1976). It does, however, lie within the area formerly occupied by Lake Humber in Devensian times. Much of the 25-Foot Drift (Warp and Lacustrine clay of the older survey sheets) of the Vale of York, which is present beneath Gale Common, was deposited in the later, low-level phase of this lake.

The basic geology of the Gale Common site is illustrated

TABLE 5.4
GALE COMMON DEPOSITS

DEPOSIT	THICKNESS	ORIGIN ⁽¹⁾	AGE ⁽¹⁾
6 Peat	0-0.6 m ⁽²⁾	Small blanket bog occupying minor hollow; possibly a subsidence feature, following solution of underlying Permian evaporites	Flandrian
5 Upper sand of 25-foot Drift	0-2.9 m ⁽²⁾	Largely fossil levees of post-Lake Humber proto-rivers; lower lacustrine, due to proximity of Lake margin	Devensian, older than 10,700 radio-carbon years
4 (a) Upper "clay" of 25-foot Drift	1.0-1.6 m ⁽³⁾	Lacustrine, formed in low-level phase of Lake Humber	Devensian, older than 11,100, but probably not older than about 22,000 radio-carbon years
(b) Lower "clay" Drift	0.3-1.3 m ⁽³⁾ (a plus b up to 7.5 m ⁽²⁾)		
3 Lower sand of 25-foot Drift	0-3.5 m	Probably largely lacustrine	
2 Gravel and sand with some intercalated silty clay beds	1.8-5.5 m	Probably fluvial	Either (a) Devensian, but prior to initiation of Lake Humber in Late Devensian time, or (b) Ipswichian
1 Bedrock (Bunter Sandstone/Permian Upper Marl*)			

(1) Based on Gaunt et al, 1971, Gaunt et al, 1972, Gaunt, 1974, Gaunt et al, 1974.

(2) From drillers' logs 1963 site investigation

(3) From trial trenches 1974 field investigations

* Revised nomenclature in view of diachronism

TABLE 5.5
SIMPLIFIED LOGS OF TRENCHES: 25-FOOT DRIFT DEPOSITS

Thickness of beds	TRENCH A		TRENCH B		TRENCH D	
	1.6m + upper 'clay'	Mottled brown/grey silty clay, slightly fissured; tree roots	1.3m+ Mottled brown/grey fissured clay with occasional rootlets	1.0m+ Mottled brown/grey silty, sandy clay		
0.5m lower 'clay'	Dark brown laminated clay	0.6m Dark brown silty clay with "leafy" laminations 0.3m Dark brown laminated clay with silty laminations	1.1m Mottled dark brown/grey; slightly fissured laminated clay			
Lower sand	*light brown silty fine sand	* Red/brown silty fine sand	* Brown poorly graded medium to fine sand			

Continued.....

TABLE 5.5 Cont'd.
 SIMPLIFIED LOGS OF TRENCHES: 25-FOOT DRIFT DEPOSITS

TRENCH C		TRENCH E	
0.2m	Clay slurry	1.0m Upper sand	Brown medium sand
0.8m lower 'clay'	Dark brown very silty laminated clay with amorphous peak and lenses of red/brown silty fine sand	0.9m Upper 'clay'	Mottled brown/grey sandy clay
0.5m lower 'clay'	Dark brown silty clay, organic near base	0.1m	Brown/green medium to fine sand
1.0m lower sand	Red/brown silty fine sand grading to grey silty v. fine sand	0.3m lower 'clay'	Purple/brown clay
0.6m	Grey sandy silt * Red/brown silty fine sand with light brown clay laminae		*Brown fine sand with clay laminae

* logged remotely from auger cuttings

in Figure 5.23 and details of the sub-divided sediments both in terms of lithology and chronology are given in Table 5.4. Apart from the thin blanket bog horizon (peat) at the top of the succession and possibly the gravel and sand bed which immediately overlies Bunter Sandstones or Permian Upper Marl, the remaining horizons comprise 25-Foot drift deposits of undoubted Devensian age.

With respect to the upper sandy bed of the 25 Foot Drift (horizon 5 in Table 5.4) the drillers' logs imply that it is not entirely remnant levee material of the post - Lake Humber proto-rivers. Sandy and silty intercalations in the underlying upper section of the Lake Humber clays tend to highlight the fact that Gale Common was very close to the shore-line during the low-level phase of the lake. There is also some evidence to suggest that the lake may have emptied rather rapidly. Both visual observations from the trial trenches referred to in Table 5.5 and mineralogical variations suggest that entrainment of coarser grained material during this latter phase might well have been partly responsible for the upper clay being coarser grained and disturbed over much of the site.

Significant variations in lithology, bed thickness and the geotechnical properties of the pro-glacial lacustrine sediments can be attributed to the close proximity of the Lake Humber shoreline as shown in Figure 5.22.

The 25-Foot Drift succession of upper sand, clay and lower sand which are defined on the cross sections in Figure 5.24 is compatible with other localities such as Ingham, nr Goole (Gaunt et al 1974), but the underlying gravels at Gale Common cannot easily be correlated with neighbouring deposits. Mr. G.D. Gaunt (Pers. comm) identified ventifacts on top of the

gravels when they were exposed in the aquaduct trench which crosses the site (see Figure 5.19). This fact, together with the obvious westerly derivation of the pebbles leads him to suspect that the gravels are fluvial deposits, either of Ipswichian interglacial age, and so equivalent to the Older River Gravel on the I.G.S. Doncaster (88) sheets, or of Devension age but formed prior to the initiation of Lake Humber in Late Devension times (Gaunt, 1974). In the absence of material from the 1963 boreholes it can only be concluded that the gravels are almost certainly fluvial in origin and that they pre-date the Lake Humber sediments.

5.4.2.2. Field Investigation

During 1963, the initial site investigation entailed the sinking of some 24 shell and auger boreholes, supplemented by 28 shallower auger holes. The locations of these boreholes with respect to the current construction area are shown in Figure 5.19. Within the proposed confines of Lagoons A and B a further 47 shallow probe holes were sunk after construction commenced.

During 1974 the detailed re-examination of the site included an in-depth study of the geology and the properties of the clay horizon of the 25-Foot Drift. In the first instance grab samples were taken by machine from 5 pits (preliminary foundation pits 1P to 5P, Figure 5.19) in order to ascertain its variation in thickness, its fundamental properties, and its relationship with the underlying sandy horizon. Furthermore, these pits provided an insight into ground water conditions, so that an efficient pumping scheme could be achieved when the 5 sampling trenches, A to E, were excavated. The trenches, up to 10.5m long, were excavated progressively as benches in order to retrieve

0.3m³ undisturbed pillar samples for laboratory testing.

Additionally U100's were pressed into the clay by the excavator bucket to provide a more complete profile of the clay for re-examination. Pillar samples of P.F.A. (trenches 1PFA - 3PFA, Figure 5.19) and excavated colliery spoil samples from different embankment locations and stockpiles provided sufficient material for optimisation of shear strength data to be used in the design review. In addition to the usual site control tests of fill materials a complementary programme of in situ density tests (sand replacement method) was put in hand. These extra density tests were related to sampling locations, and in the case of the colliery spoil provided a laboratory compaction level for the triaxial and shear-box tests. The results relating to the colliery spoil have been discussed earlier in this work (Chapter 2.3).

5.4.2.3. Nature of the sediments

Correlation of the succession listed in Table 5.4 was confirmed by some 10 cross-sections, a typical example being section A-B (Figure 5.24a). At one location (Boreholes 9 and 50, Figure 5.19) a large slump structure or clay infilled channel coincides with the downstream perimeter of the western part of the southern embankment of Lagoon B. The log of borehole 50 gives the clay as being soft to firm, whilst the clay, sandwiched within the gravel of Borehole 9 is recorded as being firm to stiff, and laminated. It may be that the structure represents a pre-Lake Humber channel of laminated clay that was subsequently eroded and infilled with weaker non-laminated clay during Lake Humber sedimentation. That this structure coincides with a faulted Permian Upper Marl/Bunter sandstone contact may, or may not, be significant. The cross-sections indicated that

both faulted and unfaulted sub-drift contacts of marl and sandstone have invariably been subject to erosion.

The channel-like feature in Figure 5.24b does not occur on any of the other cross-sections, implying a restricted size for the structure. Assuming that the structure is a buried channel, and that because of its probable east-west orientation it might cut the southern embankment at another location, a differential settlement of the order of 1.1m could be involved using most likely m_v values from oedometer tests, details of which are given in Table 5.7. If the most unfavourable values of m_v are employed, the differential settlement would be 2.2m. The actual rate of differential settlement would be small, however, some 77mm per year at worst. This is because of the slow construction rate of 3.3m in 2 years. It should be remembered, however, that there is no evidence that this channel-like feature actually underlies the embankment.

Average values of Standard and Cone Penetration Tests from the initial boreholes given in Table 5.6 suggest that the gravels underlying the 25-Foot Drift deposits have a relative density verging on dense, whilst the overlying more sandy and silty beds are generally very much looser. Piping in the boreholes could well mean that the values recorded are somewhat pessimistic. In terms of shear strength, the earlier laboratory tests show that the ϕ' values of the finer-grained granular sediments are in the range $\phi' = 30^\circ$ to 37° .

S.P.T. values together with sample descriptions show that the bedrock is commonly weathered to depths of up to 2.25m. Borehole 13 (see Figure 5.24b) is unusual in that N values of only 21 to 36 occur to a depth of 7.5m below rockhead. The bedrock strata dip south-easterly at a few degrees. They

TABLE 5.6
GALE COMMON PENETRATION TESTS

	No Tests	Average N Value uncorrected	General order of relative density/consistency
Upper sand	16	11	medium dense
Silty clay	4	11	stiff
Lower sand	18	12	medium dense
Gravel (with sand)	57	29	medium dense
Bunter Sandstone	22	13-50+	General indications of weathered state
Permian Upper Marl	12	21-50+	

Relative density of sand N = 4-10 loose

(Terzaghi & Peck, 1967) =10-30 medium dense

=30-50 dense

50+very dense

TABEL 5.7

RANGE OF CONSOLIDATION PARAMETERS

(average for $\sigma_v = 0$ to 1255.5 kN/m²)

Clay Type	Natural Moisture Content %	LL%	PL%	c_v m ² /yr	m_v m ² /MN	k(calculated) m/s
Upper generally mottled	21.6-36.3	48-57	25-27	15-20	0.20-0.26	1.8×10^{-9} - 9.5×10^{-10}
Upper mottled (Trench E)	25.4	34	21	51	0.34	4.7×10^{-9}
Upper (laminated- inter- mediate)	26.7-27.4	52-53	26	6-9	0.15-0.45	2.2×10^{-10} - 9.8×10^{-10}
Lower laminated	31.8-36.7	66-77	28-29	3-4	0.35-0.62	3.6×10^{-10} - 9.0×10^{-10}
Lower (Trench E)	25.1	44	23	12	0.25	7.6×10^{-10}

are cut by an east-west fault with a southerly throw to the south of the present site. This fault lies slightly to the south of the conjectured position shown for it on the published geological sheets.

5.4.2.4. Description and classification of the 25Foot Drift clay

Considerable variation in the grain size composition of the 25 foot Drift clay horizon is evident from the cross-sections. The simplified logs of the sample trenches (Table 5.5) provide further evidence of this variation. Visually, the most striking change is the upper part of the clay being mottled and possessing more silt and sand than the lower part.

This upper part, which is generally mottled brown/grey also shows signs of disturbance, caused partly by rootlets. The mottling is probably a weathering phenomenon, it extending down into the laminated, lower, section in places (e.g. Trench D, Table 5.5).

The clay succession can be divided into two general divisions on colour and macro-structure and these are illustrated in Figure 5.25. The upper, disturbed, mottled brown/grey clay is seen in Specimen 1, while the stratified dark brown clay, laminated by silt dustings is shown by Specimen 3.

Within the upper mottled section, however, some of the clay retains a vestige of a laminated structure (Specimen 2, Figure 5.25) and the consolidation parameters given in Table 5.10 are intermediate between those of the more typical laminated clay and the mottled clay. The influx of silty sediment and subsequent sediment redistribution followed by weathering was clearly not a uniform process.

The lower division of the clay is not uniform, either

In the south-western part of the site it is less well stratified, as shown by Trenches C and E (Table 5.5).

Tree roots were common in a number of the pits and trenches, the largest seen being of 50mm diameter. Examination of the samples showed that rootlets were abundant, penetrating both upper and lower clay horizons. These tend to give near-vertical drainage paths in the sediments. In addition, near-vertical discontinuities (fissures) were by no means uncommon in the trial trenches, suggesting that desiccation was prevalent at some period post-Lake Humber times.

Considering the wide variation in the nature of the argillaceous sediments it is pertinent that they fall within the medium to high plasticity range on the Casagrande Plasticity Chart in Figure 5.26, displaying a linear relationship parallel to the 'A' line. This is symptomatic of soils from the same stratum (Terzaghi and Peak, 1967). In general terms the 25-Foot Drift clay may be regarded as the same stratum, but perhaps more importantly, the mineral components are similar in type (Taylor et al, 1976).

5.4.2.5. Consolidation characteristics of the clay

The log pressure-voids ratio curves illustrated in Figure 5.27 were obtained from oedometer tests on a selection of samples from the 25-Foot Drift clay. The curves all display a convex-upwards shape, which is symptomatic of an overconsolidated deposit. The calculated pre-consolidation pressures cannot, however, be easily reconciled with field evidence. For example, that calculated for the Trench B 'leafy' clay is some 78.5 kN/m^2 , implying some 5.5m of overlying sediment has been subsequently eroded. The upper sand on the site attains a maximum thickness

of 2.9m and the consensus of geological and geomorphological evidence in this part of Yorkshire is against there having been any overlying sediments. Thus the overconsolidated appearance of the curves is probably a result of desiccation, as suggested by the fissures recorded in the trial trenches. The vegetation which was established presumably assisted with the desiccation.

Average values for consolidation parameters are given in Table 5.7. In terms of c_v values, the upper part of the upper mottled clay has considerably higher values than the remainder of the 25-Foot Drift clay. The lowest values come from the lower laminated clay. However, in the non-laminated lower clay of Trench E, the values of c_v are similar to those in the lower part of the upper mottled section.

5.4.2.6. Shear strength parameters of the clay horizon

A wide range of shear strength parameters were obtained in 1964 and one of the aims of the later investigations was to interpret these results on a spatial and depth basis.

Anisotropy in ϕ' is commonly quite small, even in clays with a high degree of clay mineral orientation. A variation of about 3° is common. In contrast, considerable anisotropy can be encountered in studies of clay-shales (e.g. 12° for the Oxford Clay, Parry, 1972). The overconsolidated laminated Gale Common materials shown in Table 5.11 also have quite a marked anisotropy, particularly when comparing the triaxial test results with shear-box specimens in which the laminations were aligned parallel to the plane of shear. The effect may be influenced to a certain extent by the presence of near-vertical rootlets in the triaxial samples. These rootlets could be more

easily excluded from the shear-box specimens. It must be admitted that because of differences in stress regimes during testing, comparisons between shear-box and triaxial results may be invalid. However, Leach (1973), using a small 60m x 60m shear-box also found a marked anisotropy in ϕ' in an over-consolidated Late Devensian laminated lake clay from Hebburn-upon-Tyne. For a suite of 9 samples tested at varying angles to the plane of shear, the shear strength parameters ranged from $c' = 14$ to 31.1 kN/m^2 , $\phi' = 14.8 - 23.8$ degrees, a somewhat greater anisotropy in ϕ' than for the Gale Common laminated clays.

It is noticeable that the non-laminated lower clay from Trench E (Table 5.8) shows little anisotropy.

It is also stronger than the lower clay from other locations, having a strength similar to the upper, mottled, clay.

Turning to the effective shear strength parameters from the earlier investigation, these show close similarity to those from the later investigation. Their variation is probably also due to the anisotropy of the laminated clay layer, rather than changes in strength with location or depth. Large-scale distortions of laminations in lake clays do occur (see Legget, 1962, Figure 4.3) and they may therefore become orientated in the plane of potential triaxial shear when sampled. Alternatively the lamination reorientation may be a result of disturbance during dynamic sampling with driven U100's.

5.4.3. Stability analyses

5.4.3.1. Sections analyzed

The stability analyses undertaken by the writer are primarily concerned with the evaluation of shear strength parameters determined during the course of the present work. Analyses

TABLE 5.8
EFFECTIVE SHEAR STRENGTH PARAMETERS

Clay Type	c' kN/m ²	ϕ' degrees (statistical fit)	Type of Test
Upper, generally mottled	6.1	25.5	Drained triaxial with back-saturation
Lower laminated	17.7-33.7	19.6-22	Drained triaxial with back-saturation
Lower laminated	10.0-16.1	14.5-15.2	Drained shear-box, laminations horizontal
Lower laminated	23.7	19.0	Drained shear-box laminations 90° to horizontal
Lower, Trench E	31.2	25.1	Drained triaxial with back-saturation
Lower, Trench E	13.9	24.8	Drained shear-box, bedding horizontal

for the scheme itself have been conducted by the Consulting Engineers (Messrs. Rendal Palmer and Tritton) on behalf of the Central Electricity Generating Board. This being the case the present analyses concern only the southern embankment which is intended to be constructed entirely of colliery shale from Kellingley Colliery. Analyses relating to embankments constructed in P.F.A. are outside the scope of this thesis.

Two sections have been analyzed, one of the original proposed profile, and one of a new possible profile proposed by the Consulting Engineers (Figures 5.28 and 5.29). The field investigation showed that the nature of the clay varies under the site of the southern embankment. To the east, weak, anisotropic laminated clay is present. This changes to stronger, purple silty clay in the west. The cross-sections are therefore located in the eastern part of the southern embankment.

5.4.3.2. Parameters used in stability analyses

The parameters employed in the stability analyses are shown in Table 5.9. Those for the embankment are the curved Mohr envelope parameters found in the current work. They are:-

$$m = 1.324$$

$$z = 0.890$$

The average bulk density, 1.89 Mg/m^3 was determined from six sand replacement tests carried out in the southern embankment (see Chapter 2.3.5).

The parameters for the lower laminated clay have been used to represent the entire 25-Foot Drift clay division for simplicity. The values are those derived from the 1973-74 site investigation, while Messrs Wimpey's 1963 site investigation provided the values for the sands.

For the hydraulically placed P.F.A. slurry in the lagoon, an undrained shear strength was adopted. Messrs Wimpey's 1963 site investigation also included vane shear strength profiles from P.F.A. lagoons at High Marnam. The strength was uniform with depth, averaging 10 kN/m^2 . P.F.A. being somewhat silty, the strength is likely to be greater than this (re- Chapter 4.4). This being so, this value (which was the only information for P.F.A. slurry in the area) can be safely adopted.

5.4.3.3. Pore pressure development during construction

Because of the low rate of construction of only 3.3m in every two years, excess pore pressures are unlikely to be a problem.

For the foundation clays, an analysis was conducted using the consolidation data to calculate the excess pore pressure. The method was similar to that used for the Gedling problem (Section 5.3.3.6.), i.e. that outlined in Lambe and Whitman (1969). From the trench logs (Table 5.5), the greatest thickness of clay is some 2.2m. Applying to this a c_v value of $3.5 \text{ m}^2/\text{yr}$, i.e. that pertaining to the lower, laminated, clay (Table 5.7) and which must be a pessimistic estimate for the clay as a whole, as the c_v 's of the upper, mottled, section are higher, the pore pressure calculated by the pore pressure program (Appendix C) showed that the pore pressure developed by each lift would dissipate before the next lift was emplaced. The problem therefore becomes one of predicting the pore pressure developed after each lift. As each lift takes 6 months to emplace, a figure equal to the extra load generated by the lift is clearly not appropriate. The individual layers in a lift

are of 0.3m thickness, placed on average one per 2.6 weeks. Employing these figures in the program (Appendix C), a pore pressure at the end of construction of 2.2m of water was obtained. A line of piezometers located under the western embankment, (Figure 5.19) give results, (Figure 5.30) compatible with these calculated results. The somewhat high levels shown by two piezometers located beneath the lagoon are believed to be due to poor sealing.

Turning to the embankment, the pore pressures cannot be easily computed, owing to the complex geometry of the situation. It will be noticed from Figure 5.29, that there is no part of the proposed final profile which is further than 15m from a drainage surface. Using this fact, it is possible to make a crude estimate of possible pore pressures by calculating the pore pressure at the centre of a 30m thick layer undergoing drainage at two opposite boundaries. A consolidation test was performed upon a compacted specimen of the passing 19 mm fraction of Kellingley spoil. This yielded an average c_v value of $860 \text{ m}^2/\text{yr}$ over the pressure range 10-600 kN/m^2 . Using this value in the pore pressure program (Appendix C), a similar result to that obtained for the foundation clays is found, namely that pore pressures generated by one lift dissipate before the next is emplaced. A similar assumption to that used above for the foundation clays was employed to calculate the pore pressure after the emplacement of one lift, i.e. eleven 0.3m layers emplaced every 2.6 weeks. This resulted in a maximum possible value for the pore pressure in the centre of the embankment of 1.8 metres of water. It should be noted that this dissipates very rapidly being less than 18mm of water after 6 months.

TABLE 5.9
PARAMETERS USED IN GALE COMMON STABILITY ANALYSES

Material	Shear strength parameters		Bulk Density (Mg/m ³)
	m	z	
Kellingley Colliery Shale.	1.324	0.890	1.89
Laminated clay across laminations	$c' \text{ (kN/m}^2\text{)}$ 33.6	ϕ' 21.9	1.80
Laminated clay parallel to laminations	16.1	15.1	
Sand	0	37.0	2.06
Hydraulically placed P.F.A.	10	0	1.60

5.4.3.4. Original Section (Figure 5.28)

The stability of the original proposed section has been considered by the writer to see what the stability situation is in the light of the test data determined for colliery discards. The critical failure surfaces will occur in two positions. The first is the downstream face of the embankment and concerns the ability of the embankment to stand on the soft foundations, and the second concerns the ability of the embankment to resist sliding on the weak laminated clays due to the force produced by the P.F.A. slurry in the lagoon.

As can be seen from Figure 5.28 the Factors of Safety are high, implying that the embankment is perfectly stable. It is noticeable that the laminated clay, with its low shear strength parallel to its laminations controls the position of the critical surfaces.

5.4.3.5. New Section (Figure 5.29)

Comparison of the proposed new section with the old, (Figure 5.20) shows that the downstream face has been flattened slightly, resulting in a general loss in the mass of the embankment. These alterations could be expected to (a) increase the stability of the actual embankment (b) decrease the ability of the embankment to resist the pressure from the lagoon. As Figure 5.29 shows, these expectations are justified, the Factor of Safety of the embankment increasing from 1.84 to 1.92 whilst that of a surface such as (1) decreases from 1.75 to 1.68. However, the embankment is still perfectly stable.

During the 1973-74 site investigation, it was noted that the P.F.A. slurry liquefied extremely easily. This being the case, and as mining has recently been resumed under the site

(January 1976), with the possibility that subsidence movements might provide sufficient ground motion to liquefy the P.F.A. slurry, further analyses have been carried out assuming liquefied P.F.A. in the lagoon. In this case, the Factor of Safety is 1.53, showing that the new section is capable of withstanding the worst conditions likely to occur.

At this point it is pertinent to consider what effect a change in the embankment material might produce. It will be remembered from Chapter 2.3 that Kellingley spoil is extremely coaly - 26 per cent organic carbon. What would happen if the Kellingley washery were to be improved? The shear strength of the material would fall (Taylor, 1974b) and the bulk density would increase, the density of coal being less than that of shale. The reduction in shear strength would affect the downstream stability of the embankment, but because this section has such a large margin of safety, it is unlikely to affect it drastically. Using parameters giving a fall in ϕ'_e of 5° , a reduction predicted for a fall-off in organic carbon of 15 per cent (see Figure 5, Taylor, 1974b) - the Factor of Safety is still 1.8.

When the case of the embankment being pushed bodily on its foundations by the pressure of lagoon deposits is considered, it is clear that the increase in mass produced by the increase in bulk density will increase the Factor of Safety. Thus there is no apparent cause for alarm over changes in the nature of the material from the colliery.

5.5. Conclusions

From the stability analyses carried out in connection with the Gedling spoil heap, it has been found that the presence of

a weathered layer on old tips is detrimental to their stability when they are heightened assuming that a corresponding increase in toe area is not included in the design. This should be borne in mind when tips constructed of easily degradable materials such as seatearths (i.e. similar to Gedling) are to be extended. Weak, weathered zones could also occur upon parts of the tip during construction, where, for any reason, construction is halted for periods of 6 months or more (Section C-C, Figure 5.7, for example). When such occurrences arise it would be advisable to assess the stability allowing for consideration of the weak layer in the analysis.

The weathered crust when developed can, however, improve the stability of the superficial zone of the final spoil heap. This is due to the development of cohesive forces between the clay particles liberated by physical degradation from the shale particles.

Lagoons will only cause stability problems when they are not free draining and are close to the toe of the spoil heap. Drainage will depend upon the site. "Fir -tree" banked lagoons have the worst geometry, in that slurry/tailings will occur near to the toe of the slope. As both the analyses on Gedling and Gale Common showed, where sufficiently large embankments with large toe areas are present in front of the lagoon sediments, the state of the latter will not cause the overall stability to be critically affected. Thus, where lagoons of unknown properties exist, the safest method of overtipping would be to build a large compacted toe to support the existing embankment.

The use of c' , ϕ' parameters for material, the Mohr failure envelope of which is in reality curved, can give rise

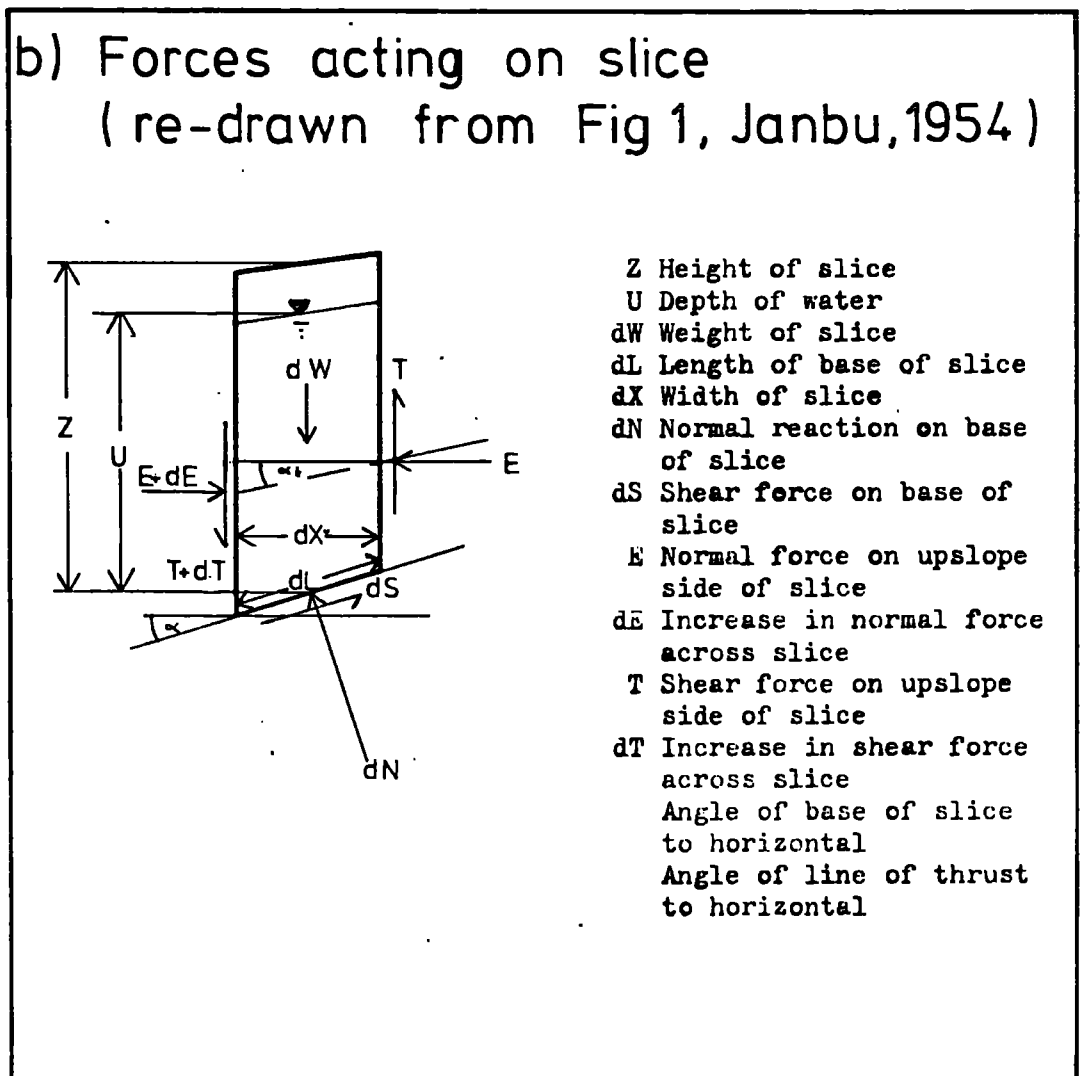
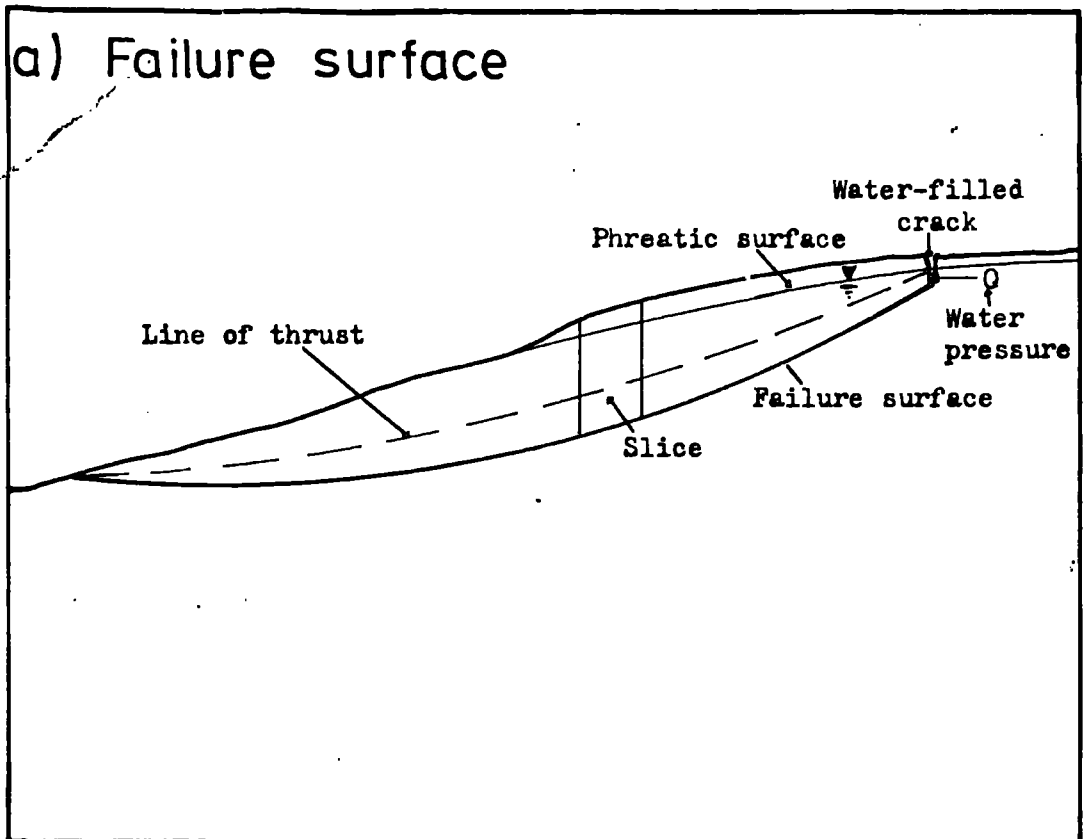
to overestimates of values of the Factor of Safety of a slope. This is especially marked for shallow slip surfaces, where, the normal stress being fairly small, the cohesion parameter provides a large proportion of the apparent shear strength.

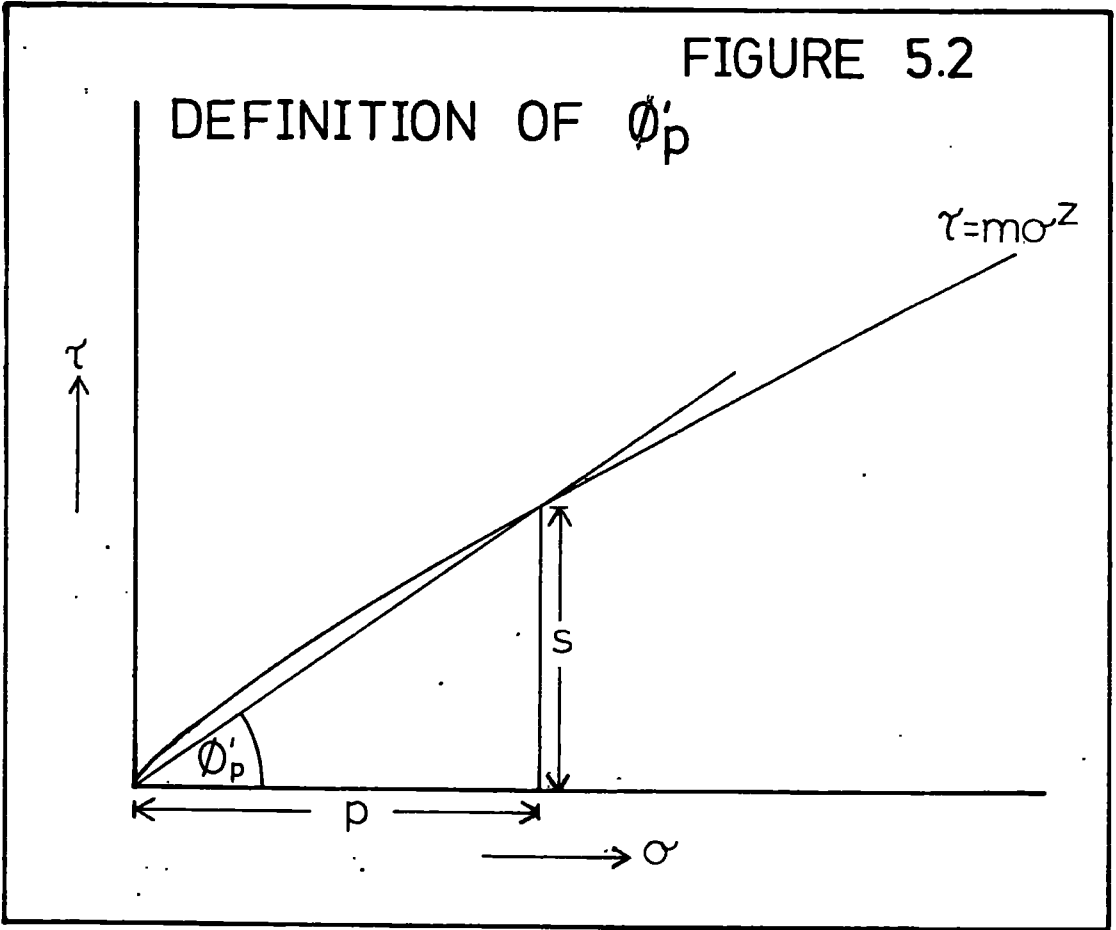
In contrast, an alternative method of fitting straight line parameters to curved envelopes, i.e. using the ϕ'_e value, severely underestimates the Factor of Safety.

This, whilst being a safe method from the design point of view, will give rise to wasteful use of available tipping areas, slopes being flatter than they need to be. While the use of a curved envelope increases the amount of computer time needed*, and thus the cost of the analysis, the ϕ'_e method will result in greater expenditure on land than is necessary. The economics of using a curved envelope fit will thus depend on the cost of computer time compared to the cost of land at the tipping site.

* A curved fit uses approximately 1.5 times more computer time than a linear fit in stability calculations.

FIGURE 5.1





DIVISION OF SLOPE INTO SLICES

FIGURE 5.3

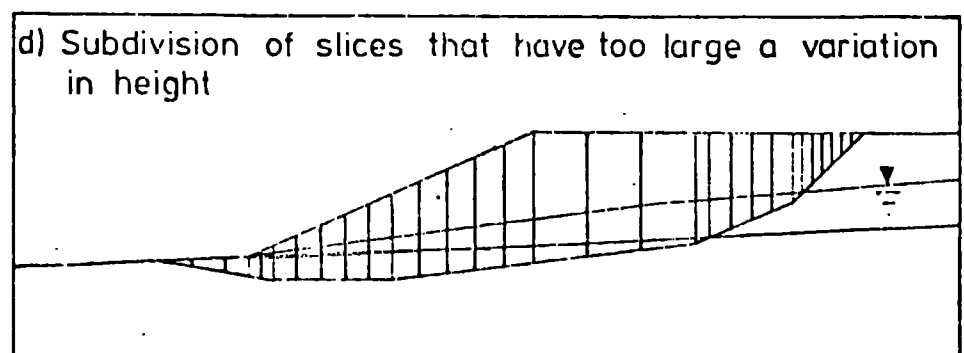
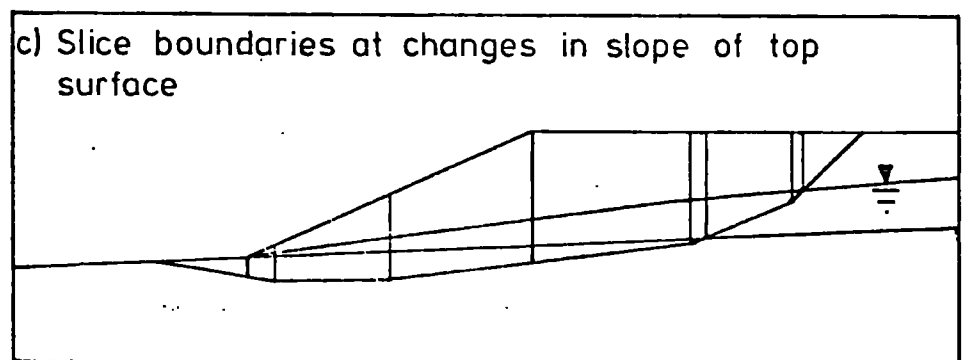
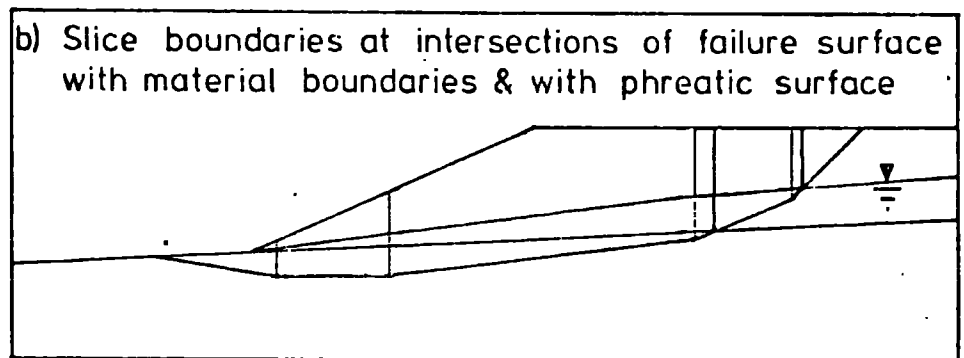
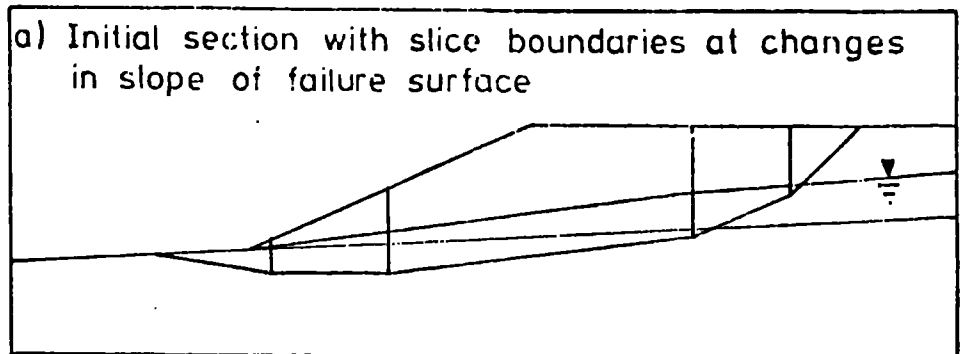


FIGURE 5.4

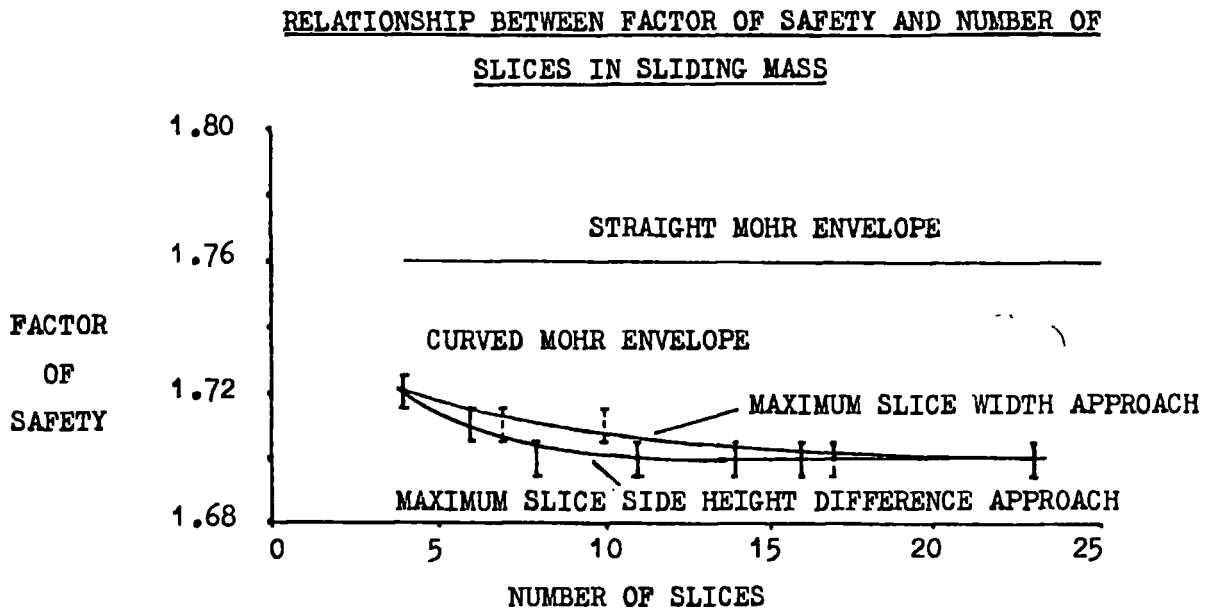


FIGURE 5.5

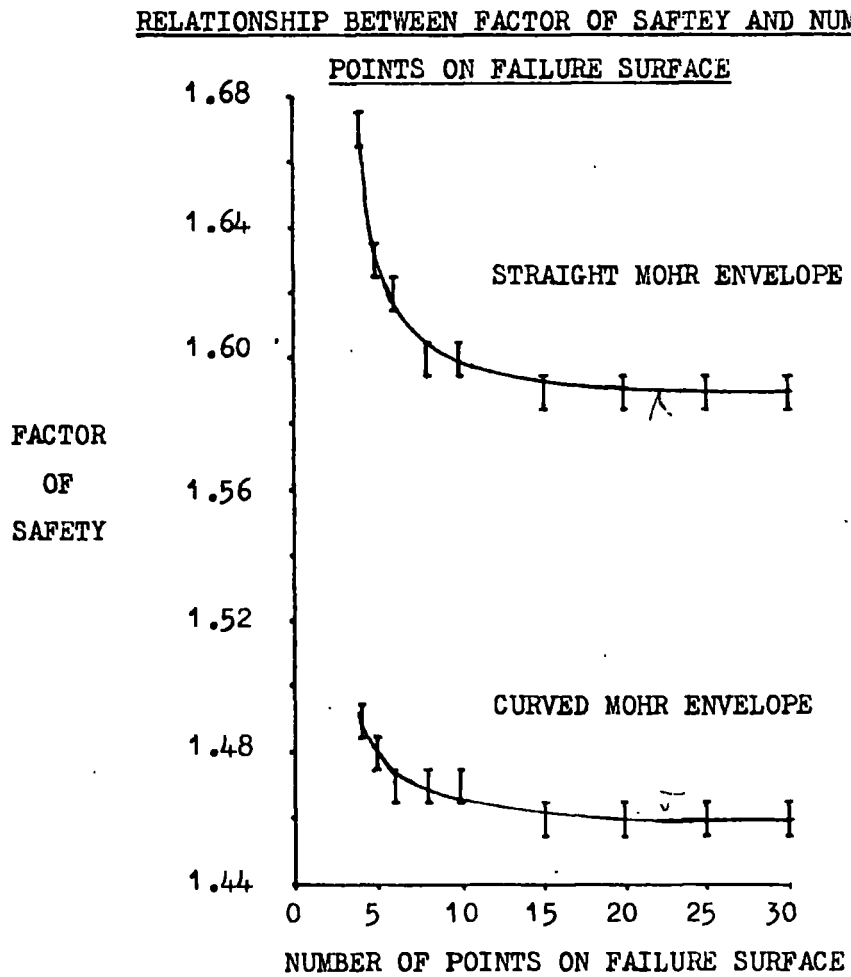


FIGURE 5.6

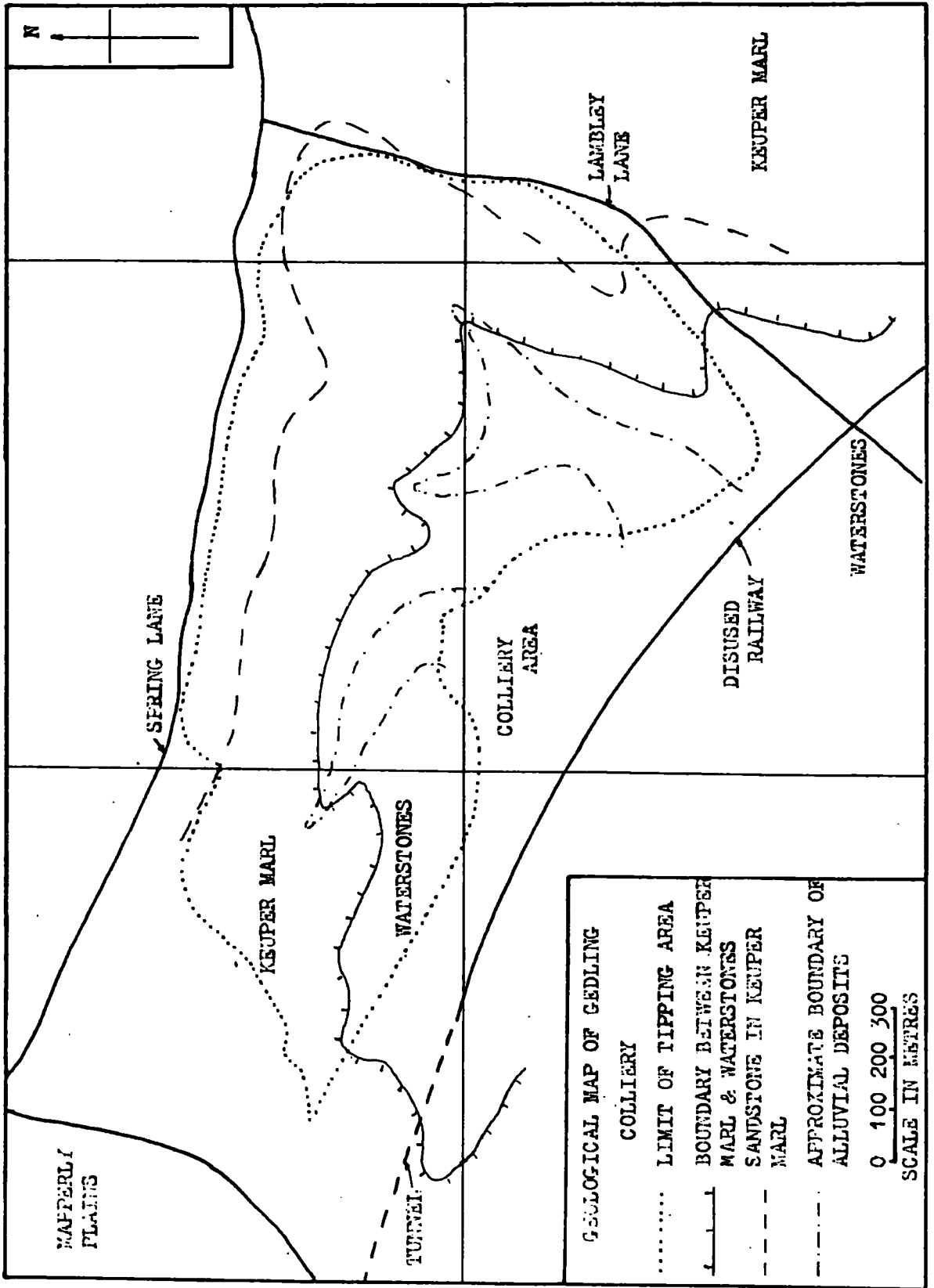


FIGURE 5.7

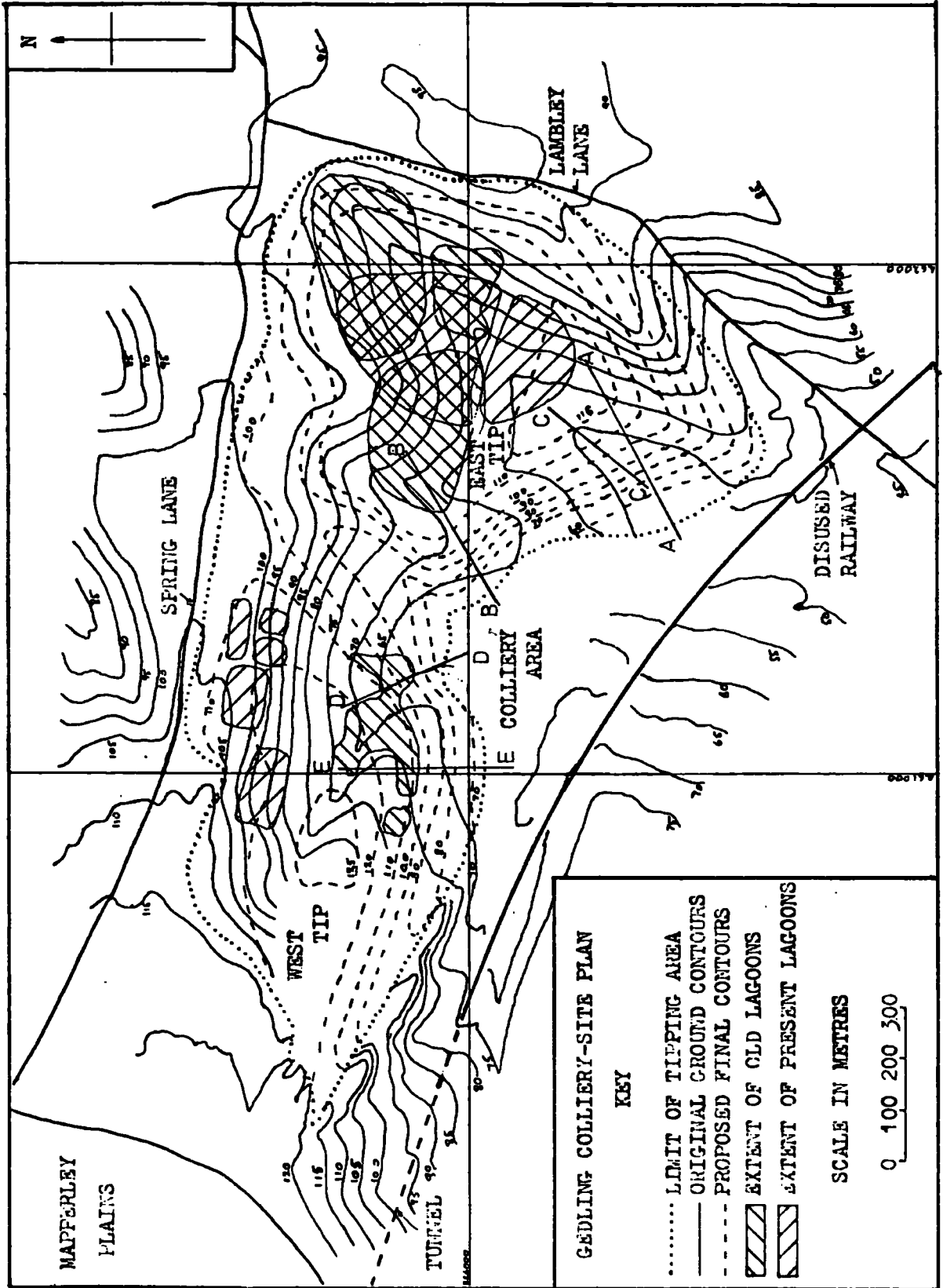


FIGURE 5.8

GEDLING EAST TIP, SECTION A - A

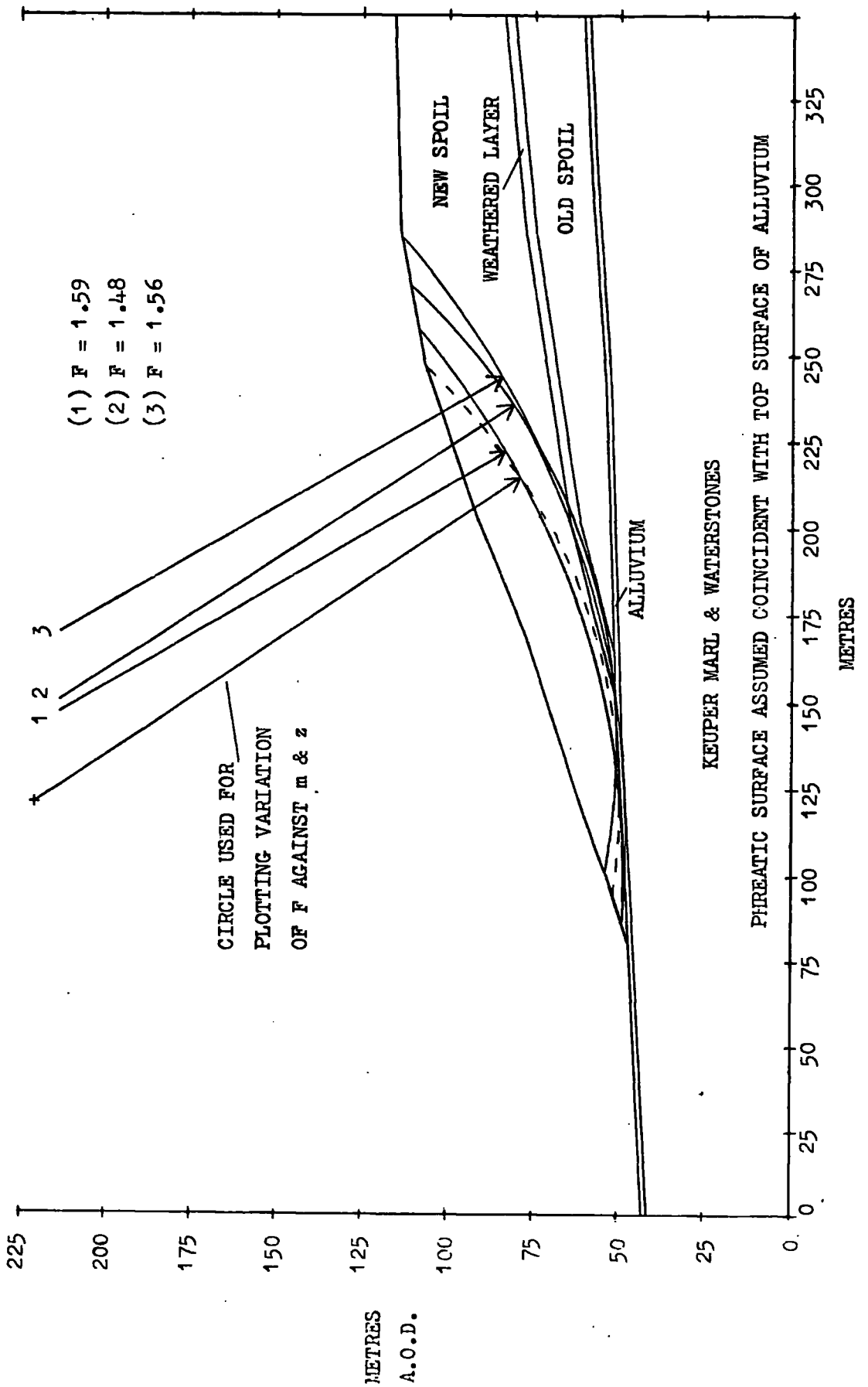


FIGURE 5.9

GEDLING EAST TIP, SECTION B-B

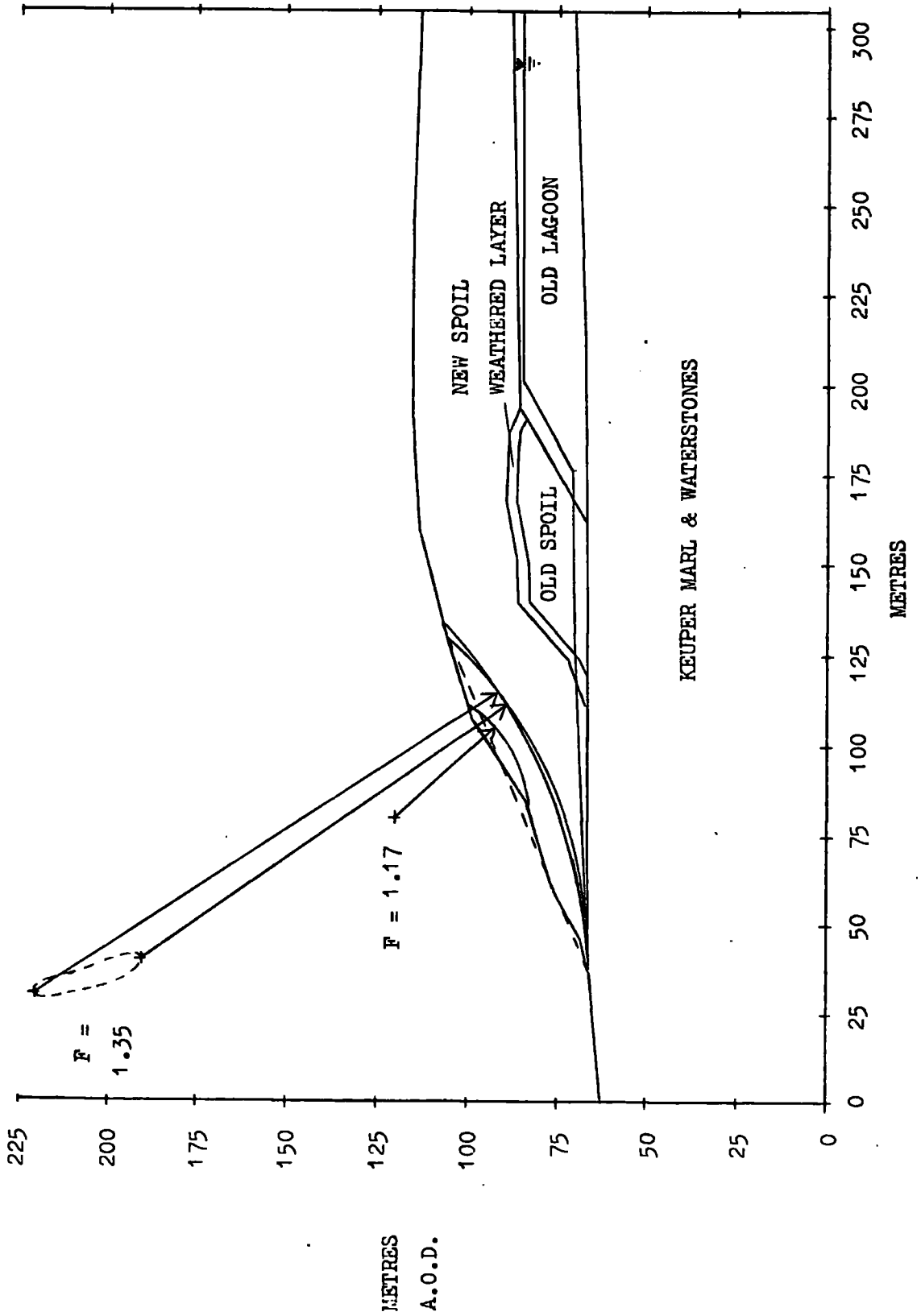


FIGURE 5.10

GEDLING EAST TIP, SECTION C-C

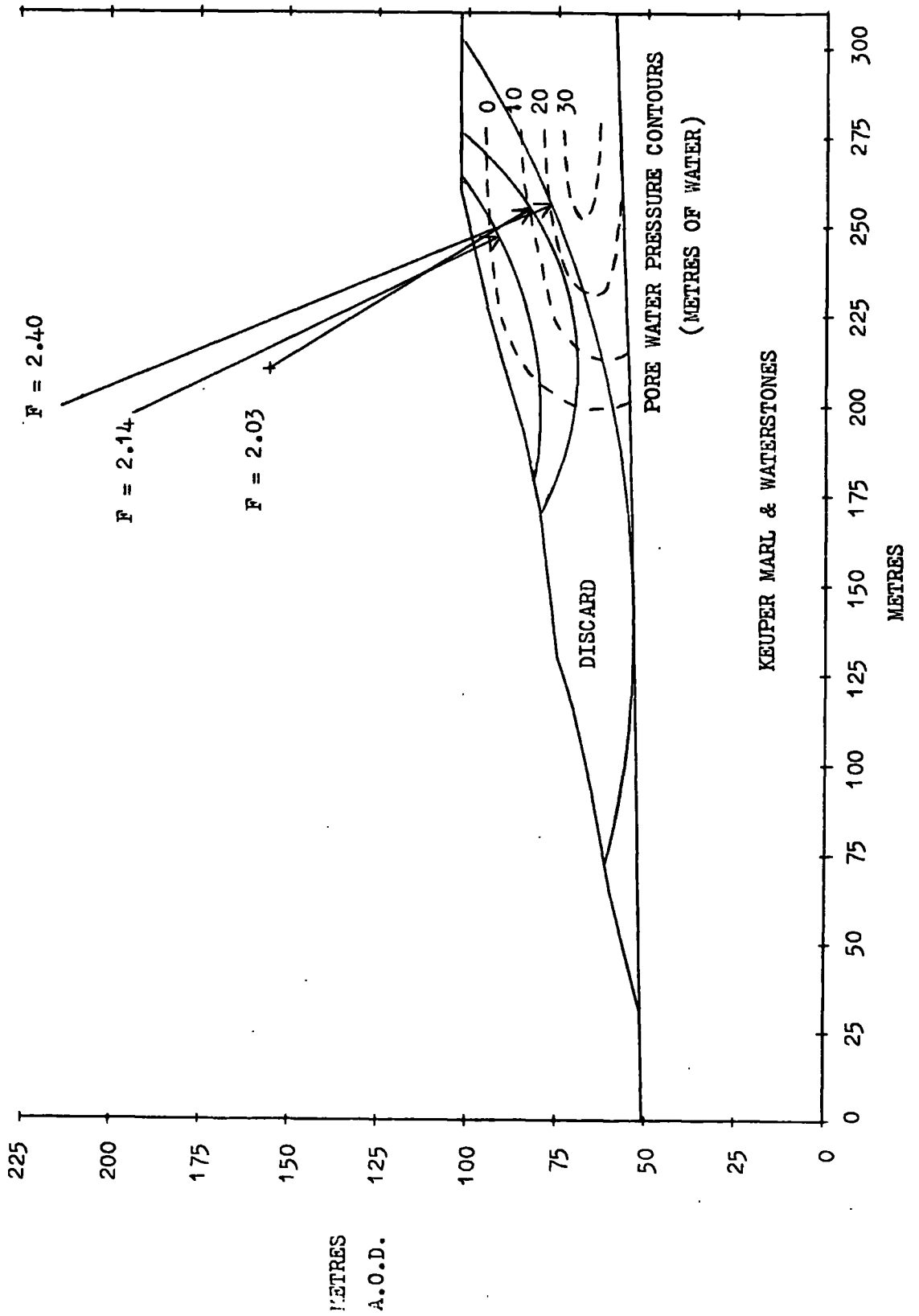


FIGURE 5.11

GEDLING WEST TIP, SECTION D-D

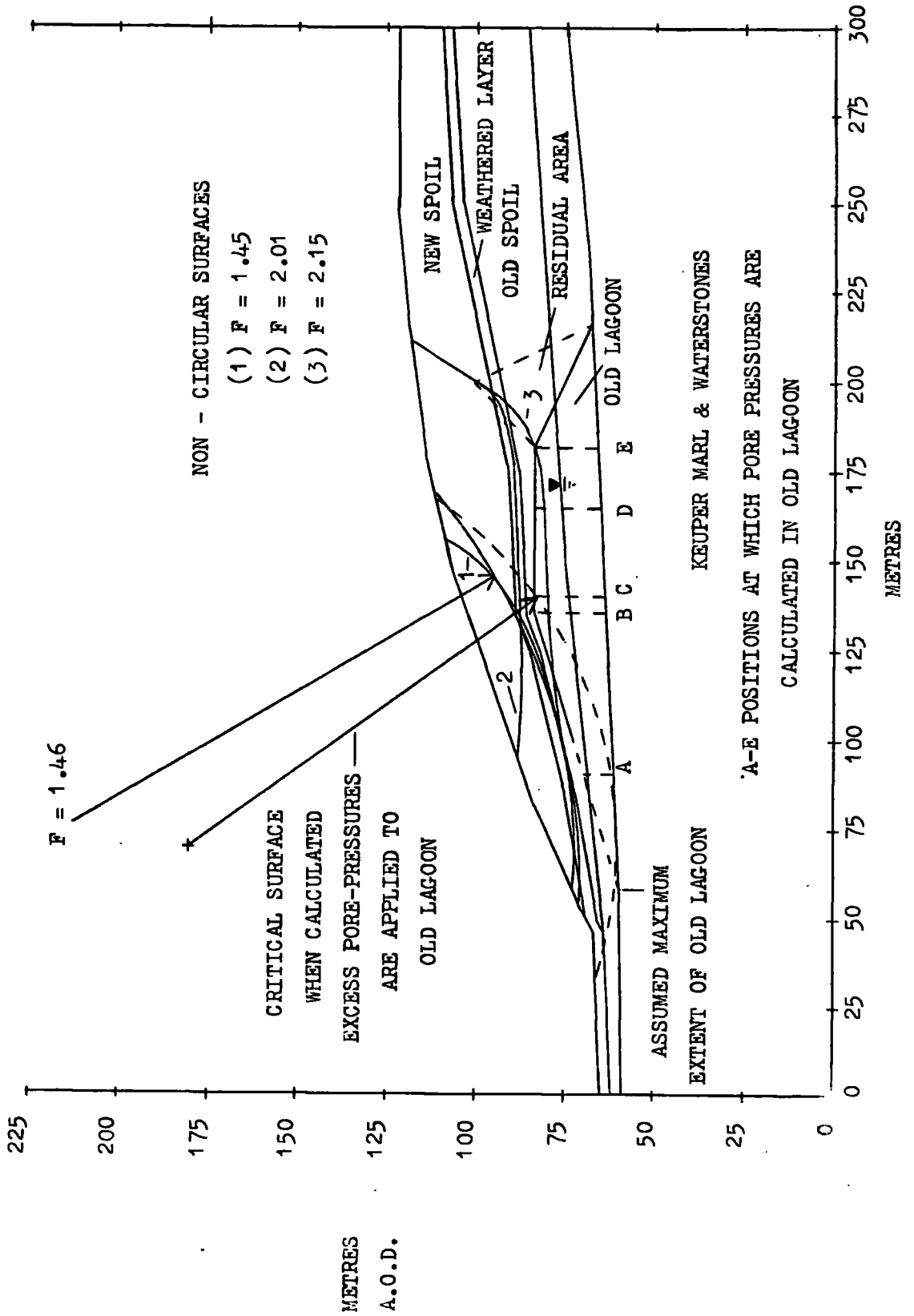


FIGURE 5.12

GEDLING WEST TIP, SECTION E-E

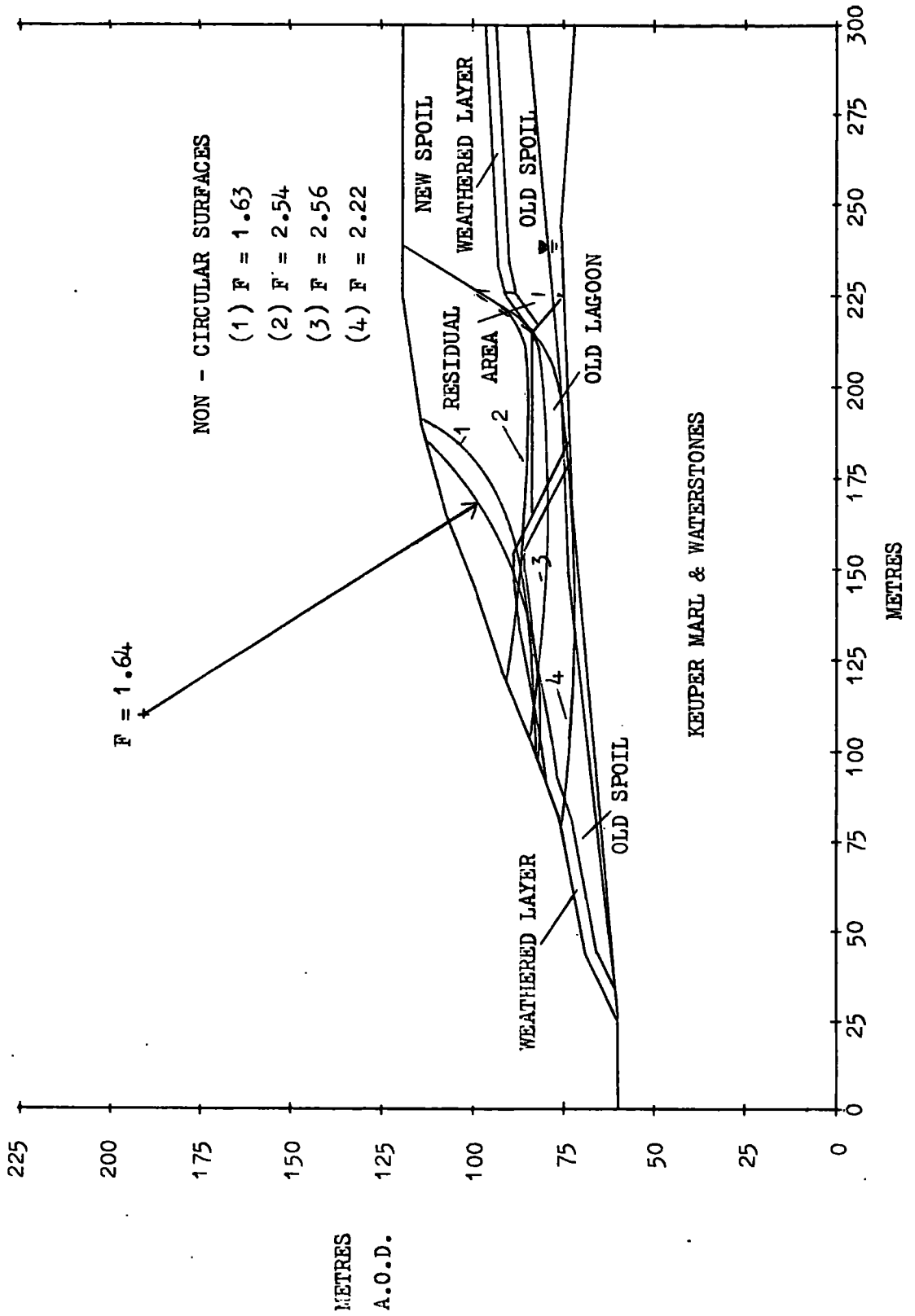
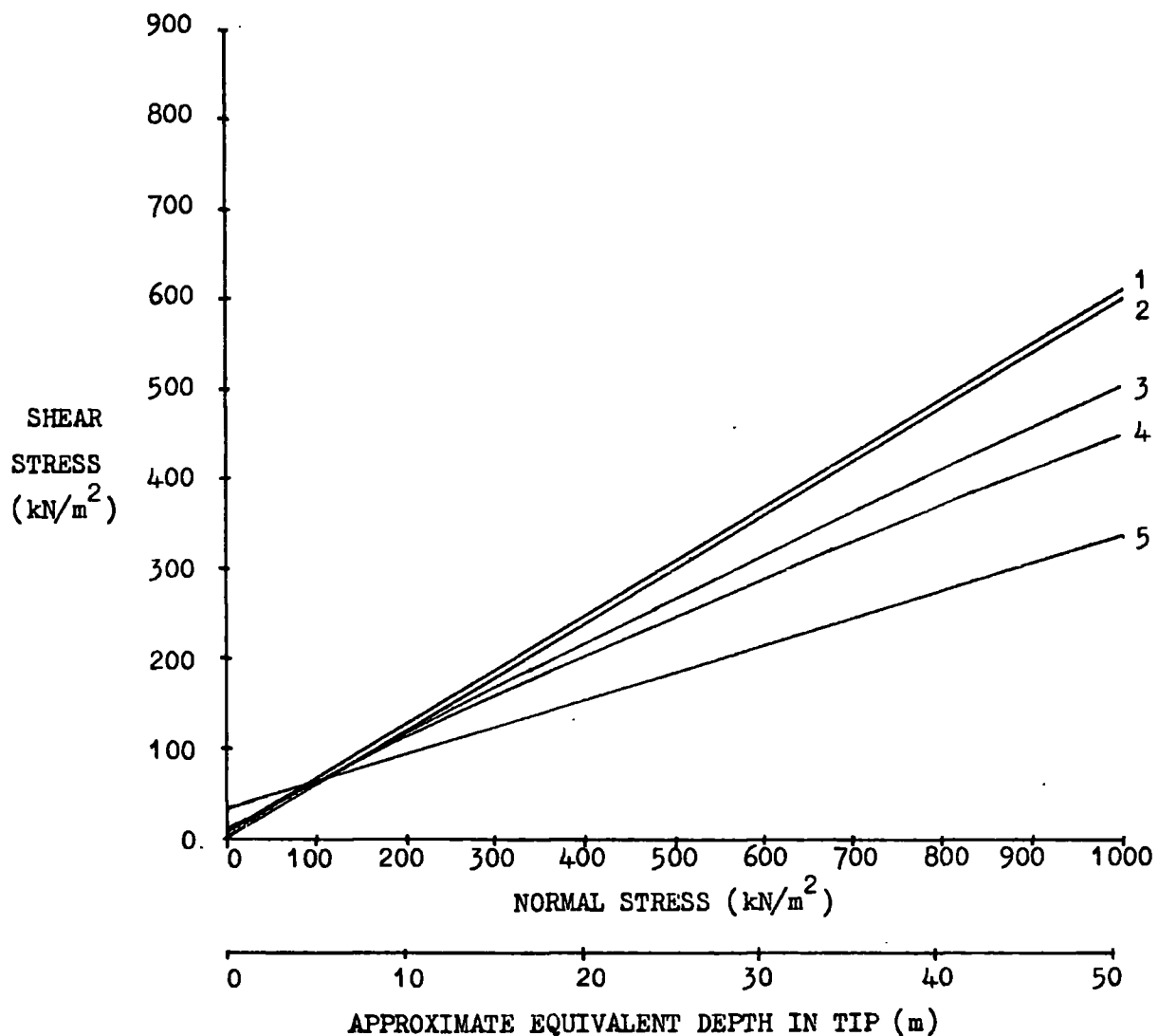


FIGURE 5.13

COMPARISON OF SHEAR STRENGTHS OF MATERIALS AT GEDLING

- (1) ALLUVIUM $\phi' = 31.0^\circ$ $c' = 8.6 \text{ kN/m}^2$
 (2) LAGOON $\phi' = 31.0^\circ$ $c' = 0.0 \text{ kN/m}^2$
 (3) OLD SPOIL $m = 0.874$ $z = 0.920$
 (4) NEW SPOIL $m = 1.096$ $z = 0.871$
 (5) WEATHERED SPOIL
 $\phi' = 16.9^\circ$ $c' = 33.9 \text{ kN/m}^2$

FIGURE 5.14

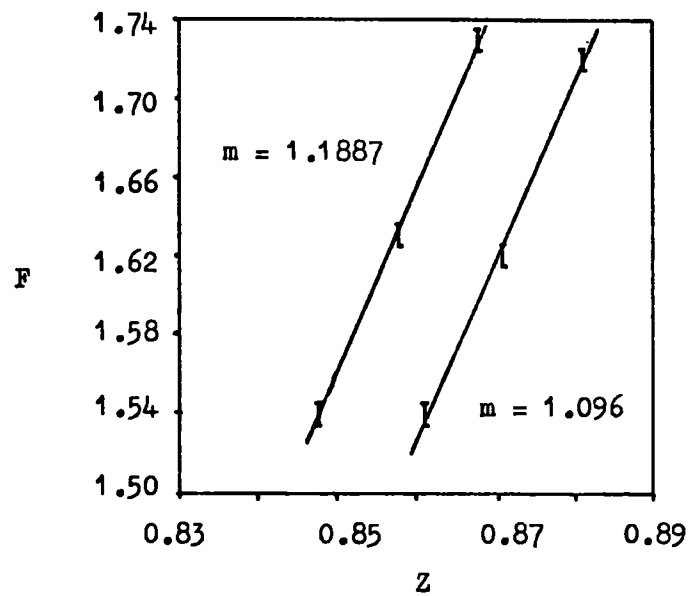
VARIATION OF FACTOR OF SAFETY (F) WITH Z

FIGURE 5.15

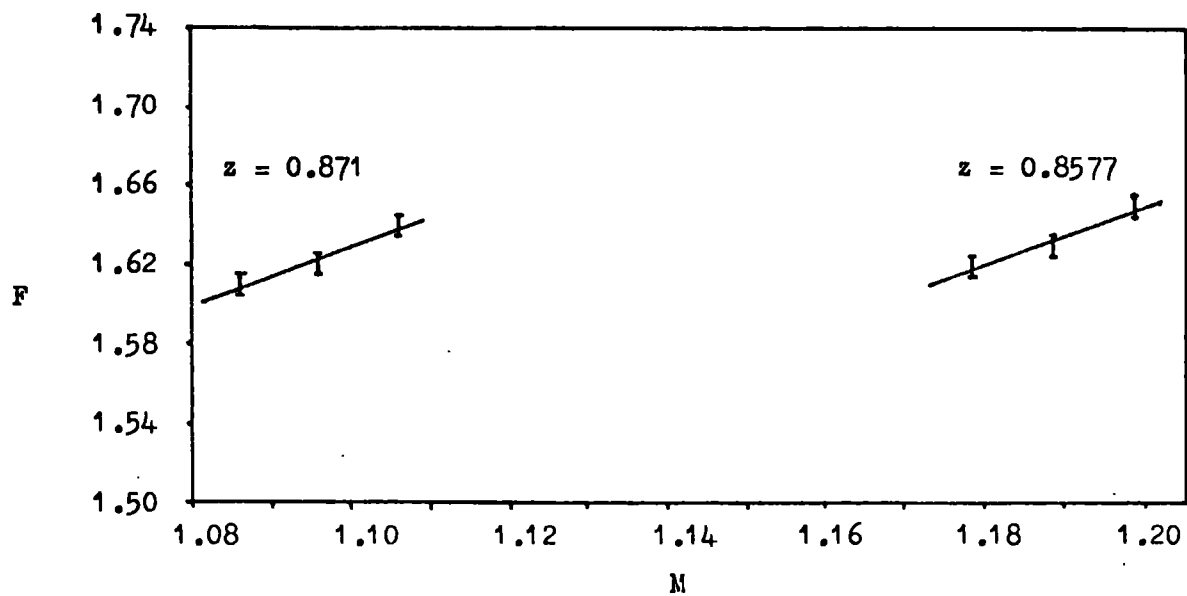
VARIATION OF FACTOR OF SAFETY (F) WITH M

FIGURE 5.16

COMPARISON OF SHEAR STRENGTH PARAMETERS OF NEW GEDLING SPOIL

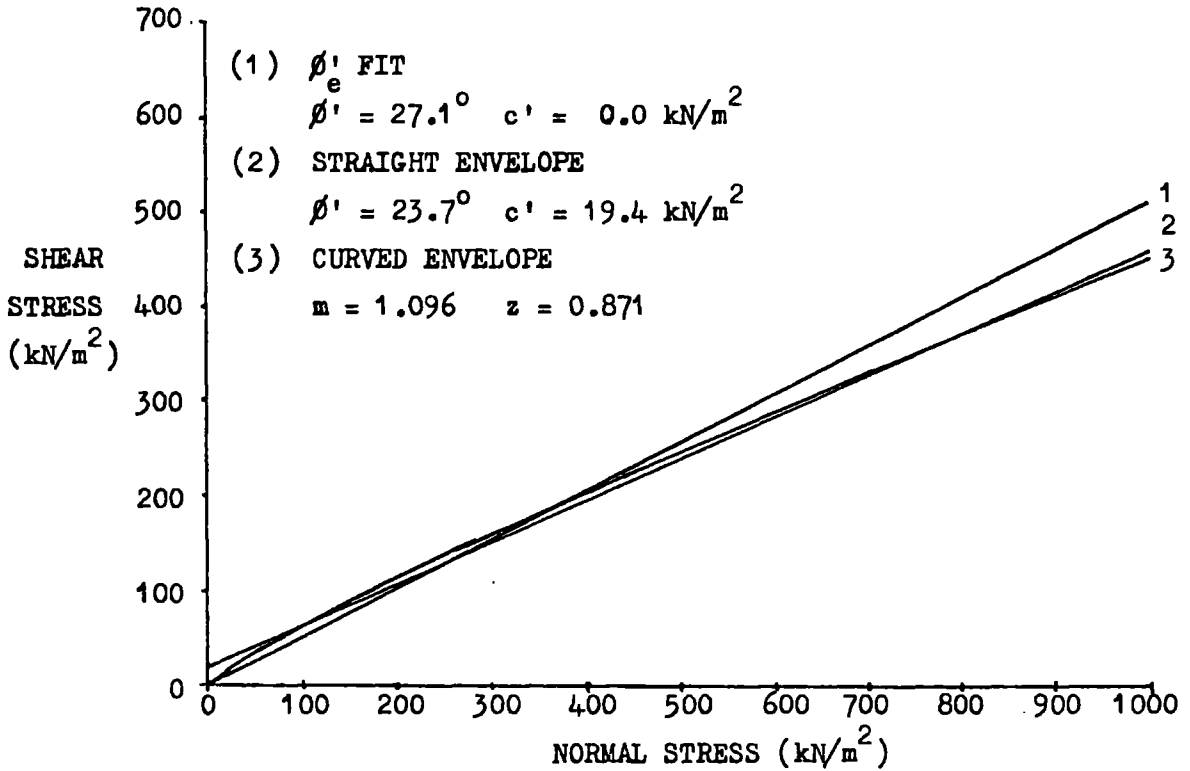


FIGURE 5.17

'FIR TREE' PROFILE EMBANKMENT

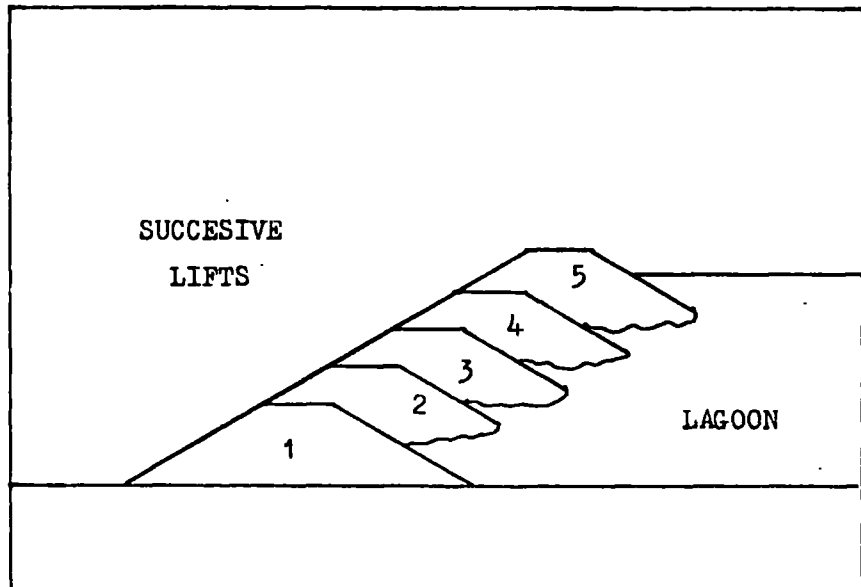


FIGURE 5.18

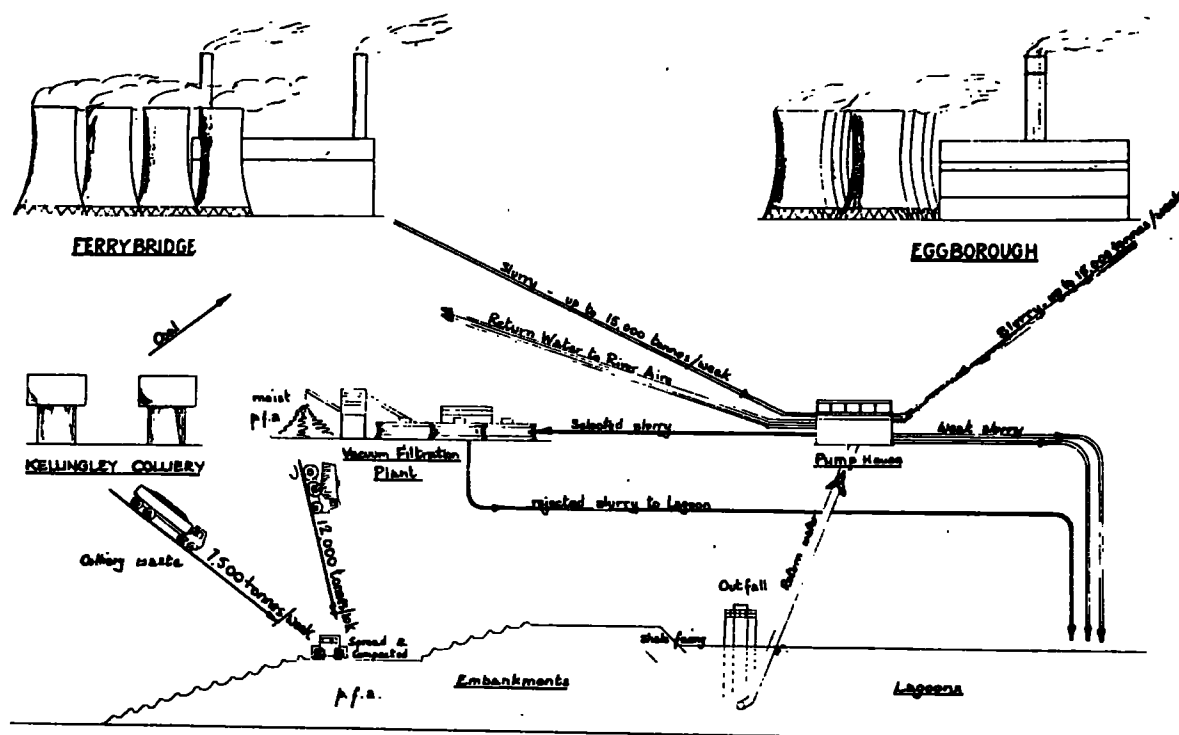
GALE COMMON OPERATION

FIGURE 5.19

GALE COMMON SITE PLAN

(FIGURE 1, TAYLOR et al, 1976)

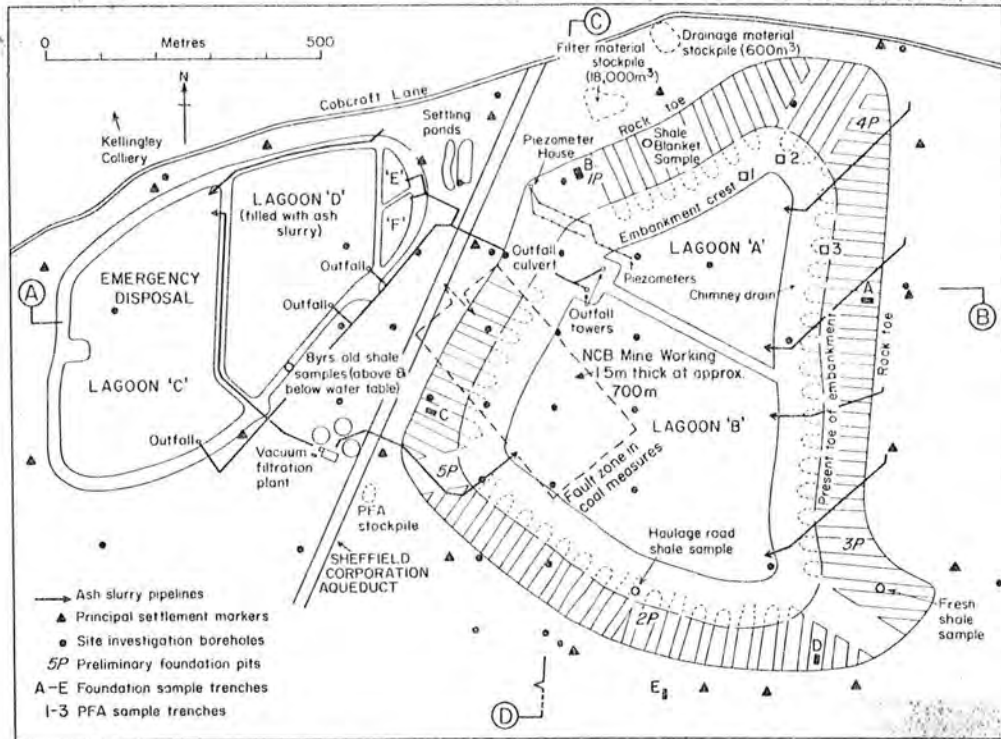


FIGURE 5.20

GALE COMMON, MAIN EMBANKMENT

(FIGURE 2, TAYLOR et al, 1976)

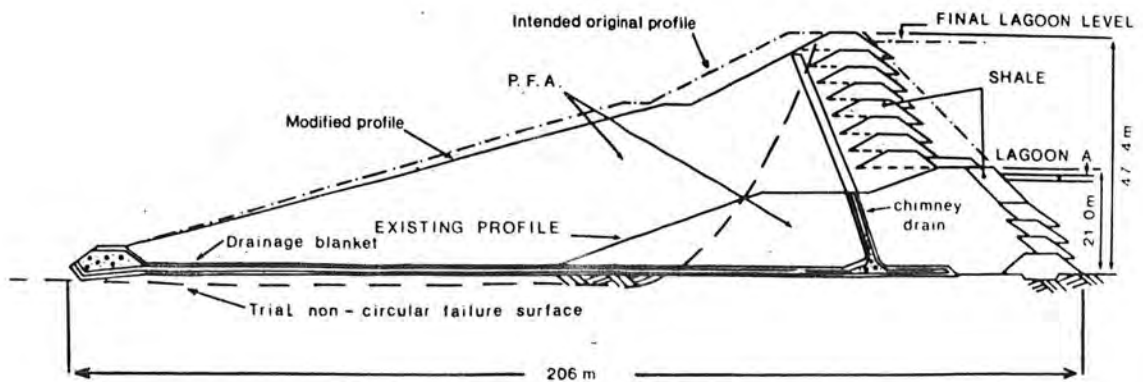
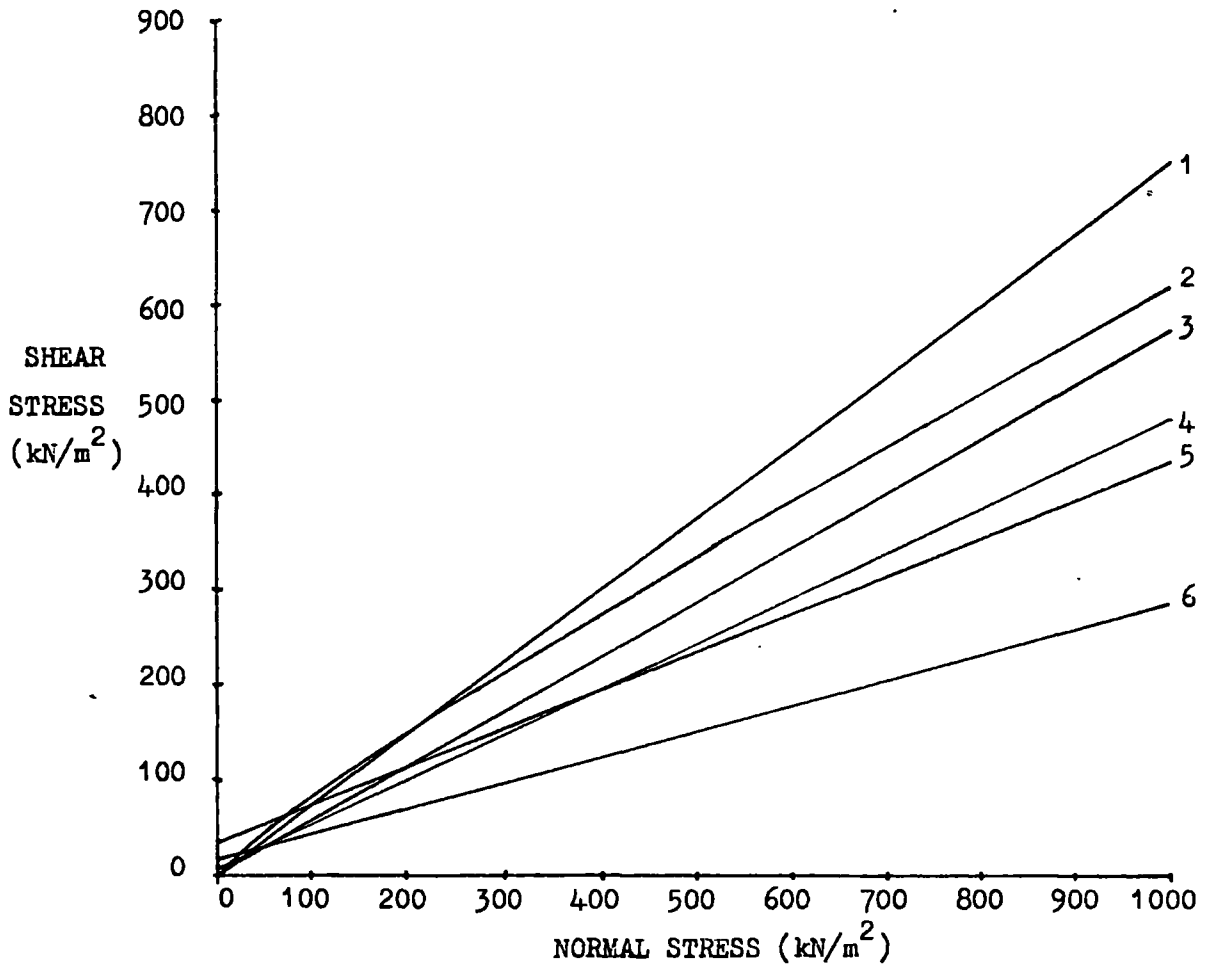


FIGURE 5.21

COMPARISON OF SHEAR STRENGTHS OF MATERIALS AT GALE COMMON

- (1) SAND $\phi' = 37.0^\circ$ $c' = 0.0 \text{ kN/m}^2$
 (2) KELLINGLEY SPOIL $m = 1.324$ $z = 0.890$
 (3) CONDITIONED P.F.A. $\phi' = 30.0^\circ$ $c' = 0.0 \text{ kN/m}^2$
 (4) MOTTLED CLAY $\phi' = 25.5^\circ$ $c' = 6.0 \text{ kN/m}^2$
 (5) LAMINATED CLAY - ACROSS LAMINATIONS
 $\phi' = 21.9^\circ$ $c' = 33.6 \text{ kN/m}^2$
 (6) LAMINATED CLAY - PARALLEL TO LAMINATIONS
 $\phi' = 15.1^\circ$ $c' = 16.1 \text{ kN/m}^2$

FIGURE 5.22

GEOLOGICAL SKETCH MAP OF LAKE HUMBER

(FIGURE 3a, TAYLOR et al, 1976)

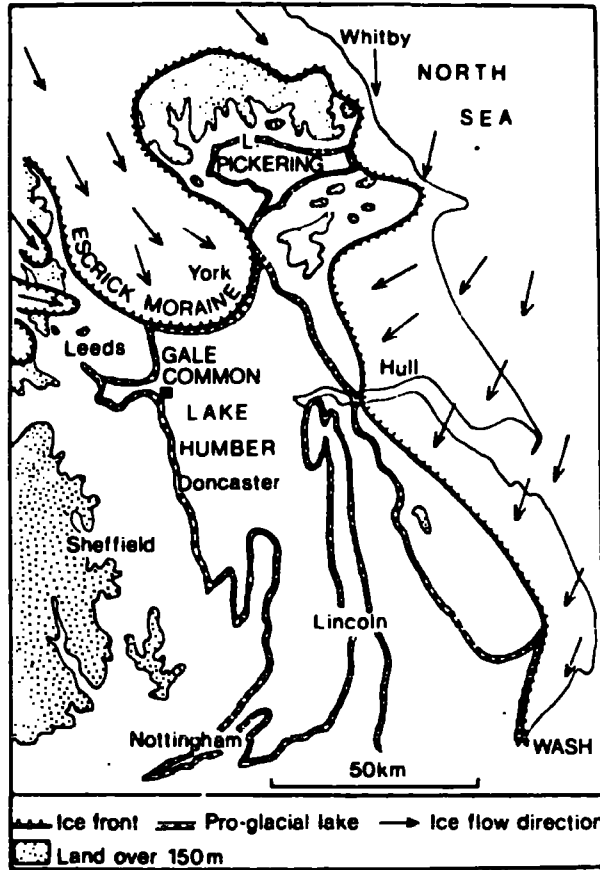


FIGURE 5.23

GENERAL GEOLOGY OF GALE COMMON AREA

(FIGURE 3b, TAYLOR et al, 1976)

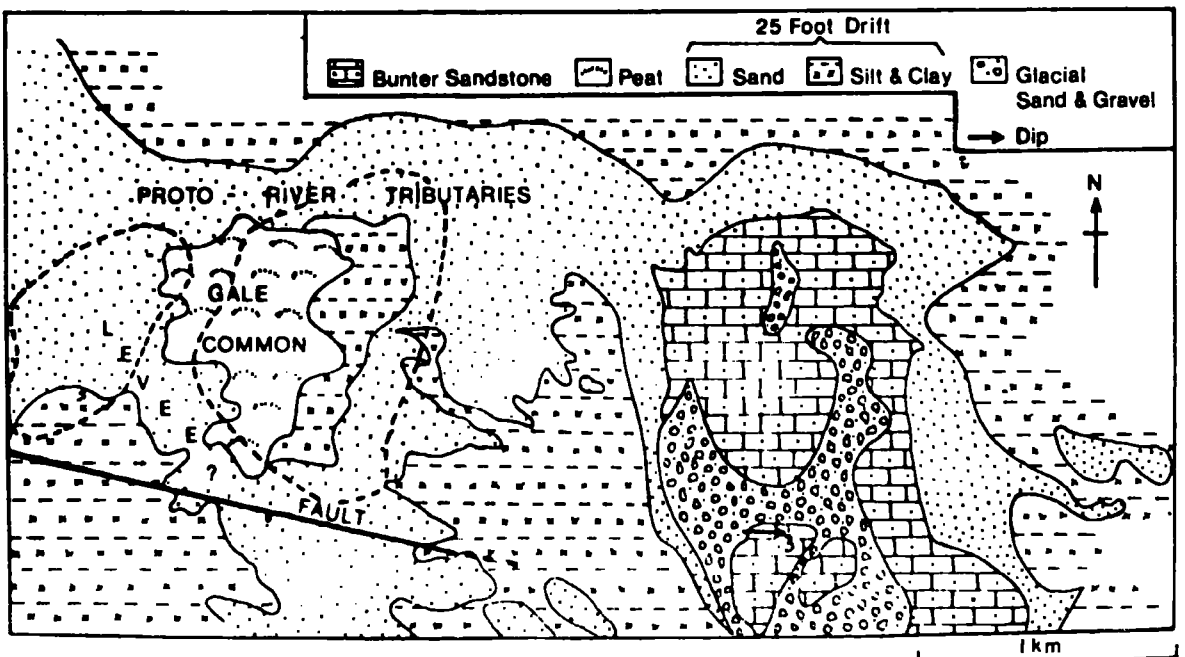


FIGURE 5.24

GALE COMMON DRIFT AND BEDROCK PROFILE

(FIGURE 4, TAYLOR et al, 1976)

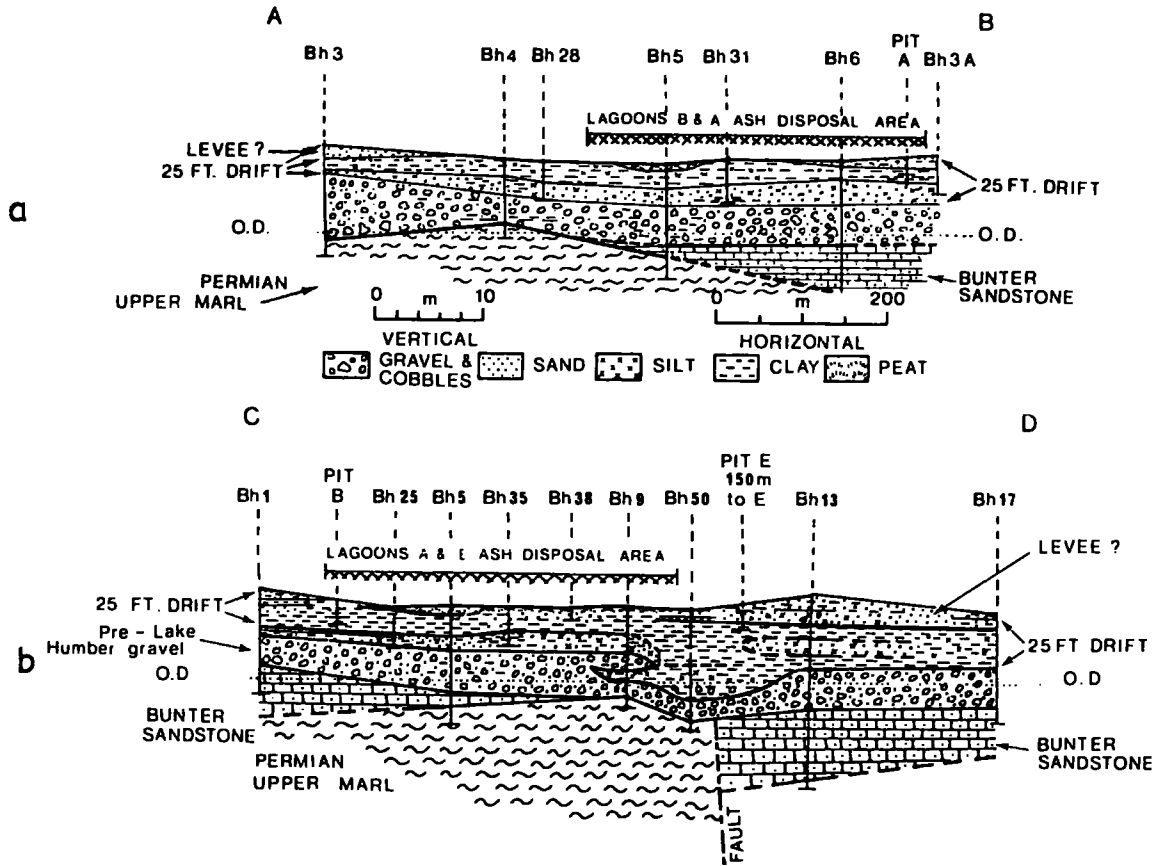


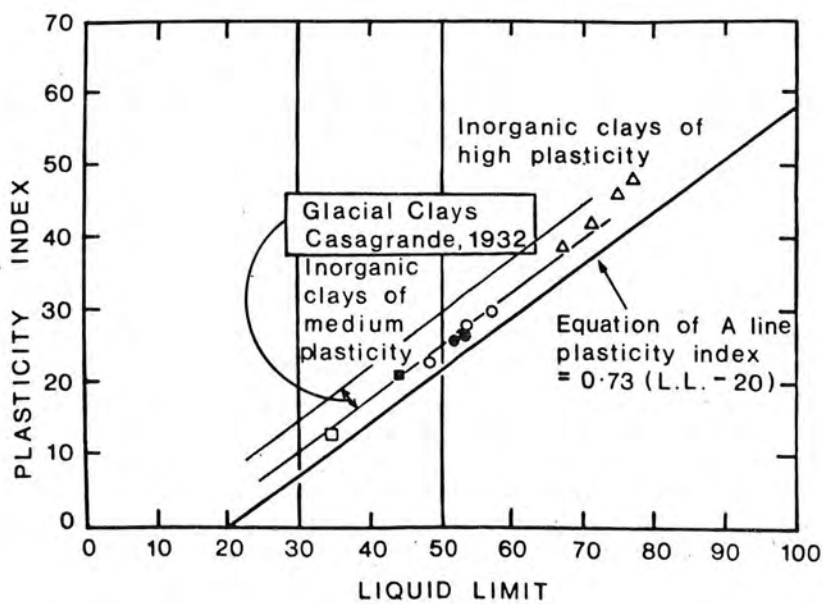
FIGURE 5.25

GALE COMMON UPPER CLAYS
 (FIGURE 5a, TAYLOR et al, 1976)



FIGURE 5.26

GALE COMMON UPPER CLAYS PLASTICITY PROPERTIES
 (FIGURE 6, TAYLOR et al, 1976)



25-Foot Drift Clay

- 1 Δ Laminated clay (lower clay)
- 2 \bullet Intermediate between 1 and 3
- 3 \circ Brown grey mottled clay (upper clay)
- 4 \square Brown grey mottled clay, Trench E (upper clay)
- 5 \blacksquare Purple brown clay Trench E (lower clay)

FIGURE 5.27

GALE COMMON, EFFECTIVE PRESSURE - VOIDS RATIO

(FIGURE 8, TAYLOR et al, 1976)

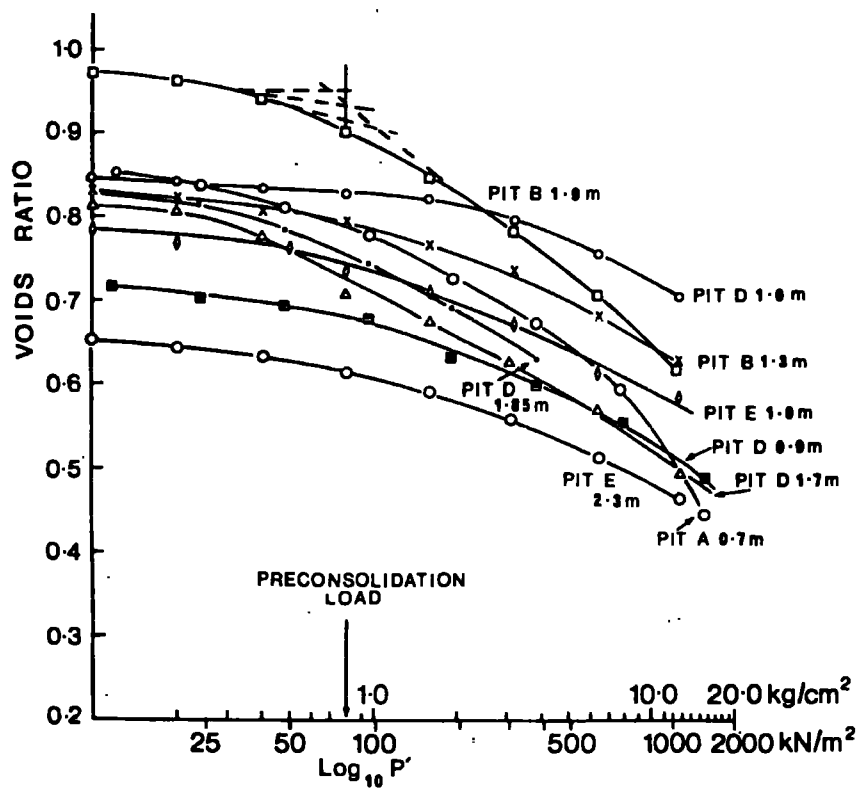


FIGURE 5.28

GALE COMMON, SOUTH EMBANKMENT TO LAGOON B, ORIGINAL SECTION

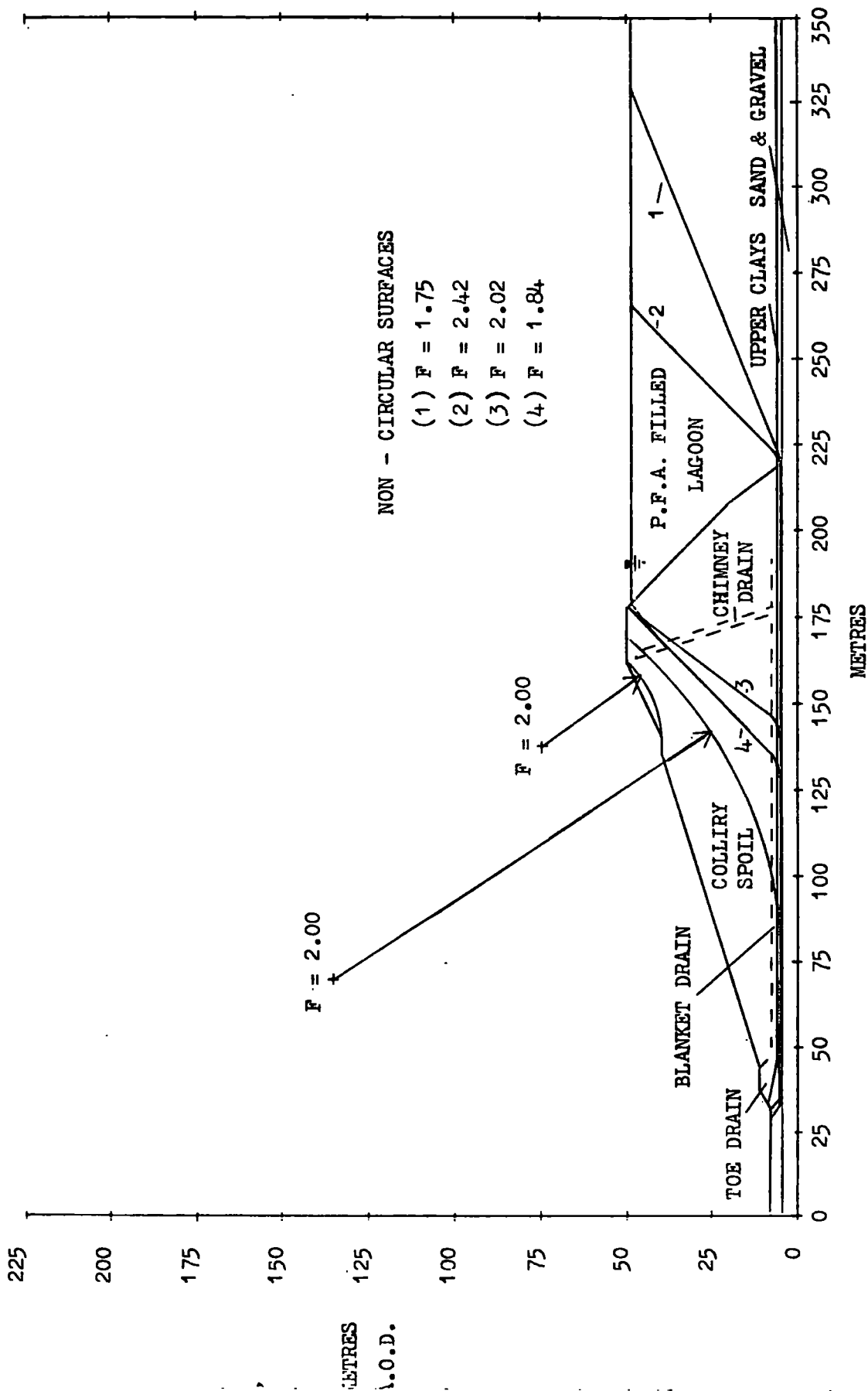


FIGURE 5.29

GALE COMMON, SOUTH EMBANKMENT TO LAGOON B, PROPOSED NEW SECTION

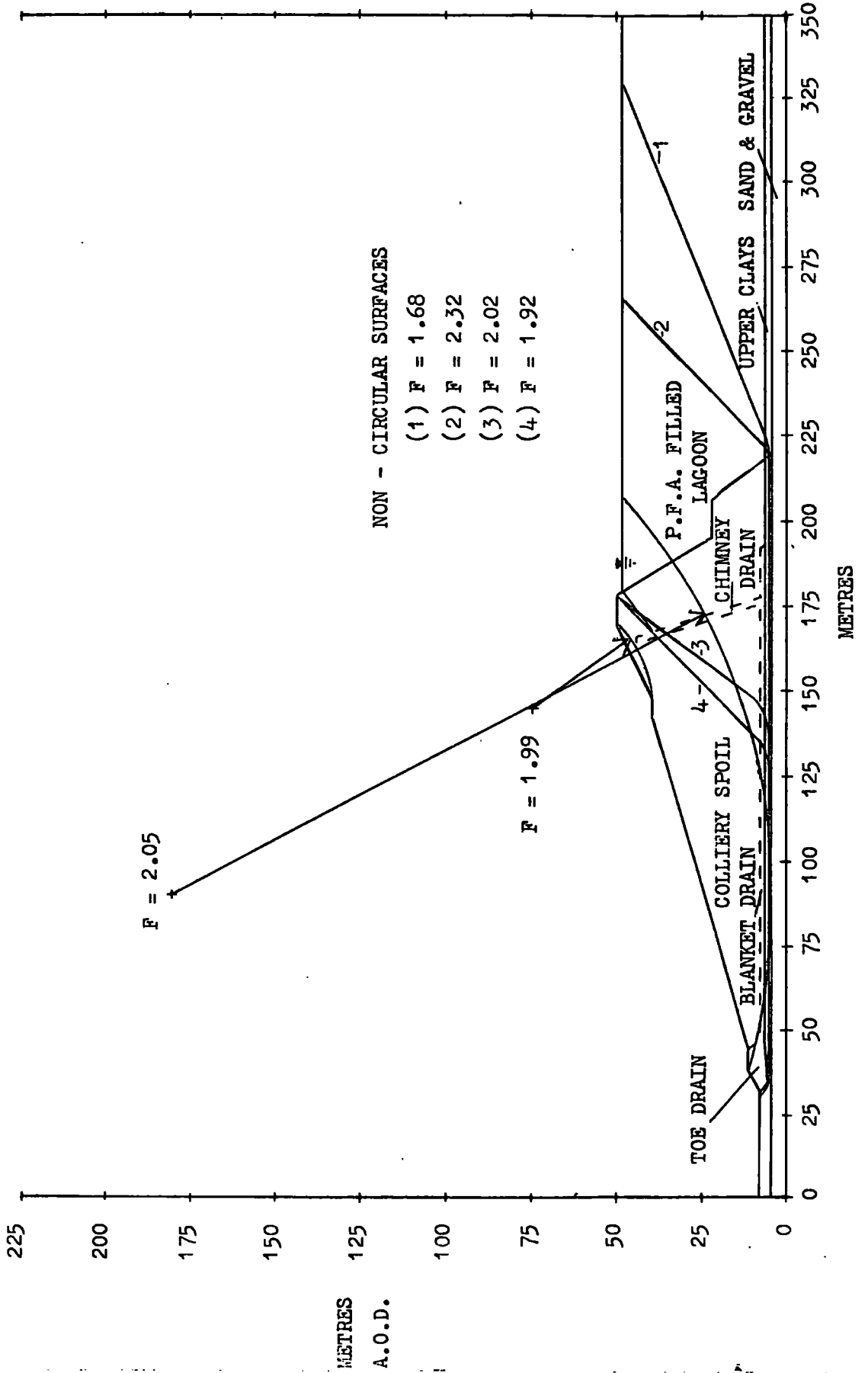
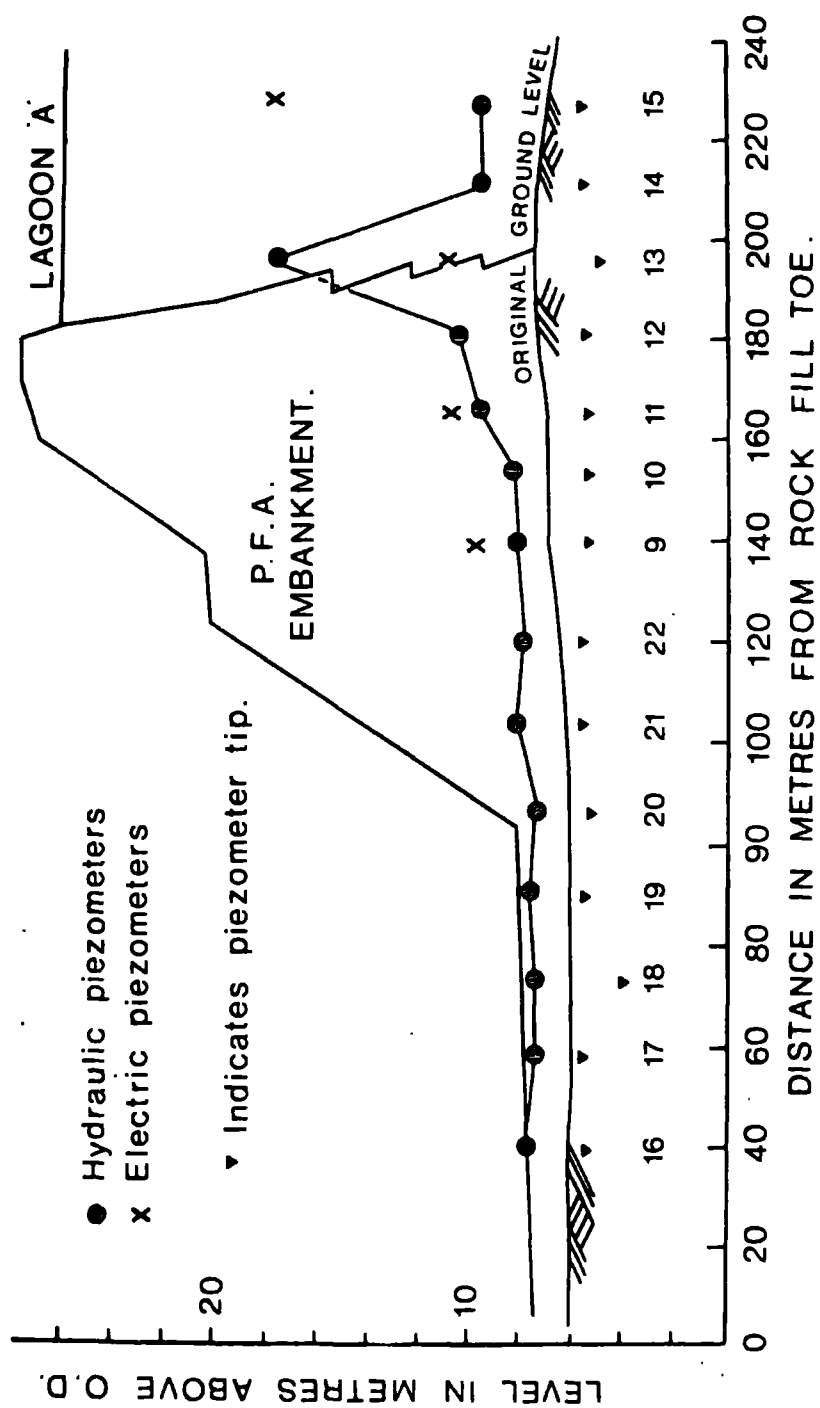


FIGURE 5.30

GALE COMMON PEIZOMETRIC LEVELS, AUGUST, 1975

(FIGURE 8, TAYLOR et al, 1976)



CHAPTER 6

GENERAL SUMMARY AND CONCLUSIONS

The conclusions reached during the course of this work will now be reviewed with special emphasis on their effects on slope stability.

The presence of a positive cohesion parameter has considerable influence upon the Factor of Safety of a slope. The fact that colliery spoils show a statistically significant* overall value of cohesion, needs, therefore, to be carefully considered. The cohesion value has two possible explanations; either colliery spoils actually possess cohesion, or they have curved failure envelopes. It is not possible, statistically, to reject either of these hypotheses, there being no test which is applicable for the present case in which the amount of curvature is small. It is, however, possible to show that specially prepared samples of colliery spoil show statistically significant cohesion values. As these samples were of coarse sand size, and loosely placed (e.g. Table 3.3) it is very unlikely that they did actually possess cohesion. Hence colliery spoil materials can show curved failure envelopes and it is reasonable to suppose that cohesion values of most other colliery spoils are, in fact, a reflection of curved failure envelopes.

When considered spoil by spoil, it became apparent that curvature is associated mainly with spoils of rank 400 to 901. Spoils with higher ranks are without significant cohesion, and the failure envelope can be taken as linear, at least in the pressure range 0 to 1,000 kN/m² which would be expected in a spoil heap.

* 99.0 per cent probability that $c' > 0$ (see Table 3.1).

The curved failure envelope of spoils is approximated reasonably well by an expression of the form:

$$\tau = m (\sigma')^z$$

where m and z are constants. Average values for English and Welsh spoils are given in Table 6.1, and illustrated in Figures 6.1 and 6.2.

The slope stability equations can be easily modified to accept this curved failure envelope (Chapter 5.1.3). Analysis of the East Tip at Gedling Colliery shows that, for shallow failure surfaces a linear c' , ϕ' envelope overestimates the Factor of Safety by 0.39, (some 33 per cent) when compared to values obtained for a curved envelope. For deeper surfaces, the linear envelope gives values approaching closer to those derived from curved envelopes, the error being only 5 per cent for a toe failure surface.

As curved envelopes require more computing time than do straight ones, an analysis using curved envelopes will be more expensive. It is thus not sensible to use them when not necessary, i.e. where the potential failure surface is deep seated. An example of this is the analysis of the South Embankment at Gale Common, where the critical surface is controlled by the underlying weak laminated clay. Use of a curved envelope for the embankment material as in the analysis performed in the current work would not be justified economically. In contrast, the analysis of Gedling East tip using a curved envelope revealed shallow slip surfaces with Factors of Safety below the requisite value of 1.25 which were undetectable when linear c' , ϕ' parameters were used.

Whilst cohesion may not be a real parameter for coarse

TABLE 6.1
AVERAGE PARAMETERS OF ENGLISH AND WELSH SOILS

	English			Welsh		
	Mean	99.5% < than	99.5% > than	Mean	99.5% < than	99.5% > than
Straight envelope						
ϕ'	29.7°	30.9°	28.5°	34.7°	35.9°	33.5°
c' (kN/m ²)	23.9	36.6	11.2	15.8	30.9	0.7
Curved envelope						
m	1.202	1.458	0.990	1.204	1.503	0.965
z	0.895	0.929	0.862	0.919	0.881	0.956

discard in general, there is reason to believe that the undisturbed surficial skin of a seatearth-rich tip such as Gedling can develop cohesion. The spoil is subject to intense physical disintegration, although remaining mineralogically unaltered, which results in its angle of shearing resistance being considerably reduced. When considered in terms of a linear envelope, the value of ϕ' of the weathered crust of Gedling tip is some 6.5 degrees less than that of the body of the tip. While, due to its cohesion, this weathered material when at the surface, may be stronger than the unweathered material, when buried to any depth by later spoil, it will form a zone of weakness in the tip. Such a buried weathered zone in Gedling East tip lowers the Factor of Safety by 0.11, a reduction of some 7 per cent (Table 5.1). Against this argument, the point must be made that the Factor of Safety against shallow failures can be increased by the presence of a weathered crust. For Section B-B in Gedling East tip (Table 5.1), a weathered crust increases the value of F by 0.3, a 26 per cent rise.

Spoils without high seatearth contents do not break down so readily upon exposure. When compacted; they are resistant for a period of at least 6 years, only minimal mineralogical weathering (limonite staining) occurring^r in this time. When unsaturated and uncompacted, however, it shows considerable alteration, both physically and mineralogically, over an 8 year period. This behaviour was noted with Kellingley spoil, of rank 502 and 702. Similar behaviour was noted by Kennard et al (1967) for Namurian shale fill at Balderhead and Burnhope over a 30 year period. This fill came from strata in the northern Pennines which are associated with high rank coals (100 to 200;

Jones and Cooper, 1970). Hence, this behaviour would appear to be fairly general for 'shale' spoils. It is apparent, therefore, that for modern, compacted low seatearth content tips there will be no stability problem caused by weathered layers.

This difference in behaviour between high and low seatearth content tips can be attributed to the nature of seatearths. They tend to contain numerous slickensided discontinuities which make them prone to physical disintegration. In comparative tests upon South Wales Coalfield shale types, seatearths weathered much more rapidly than did other shale types (Lawrence, 1972). Their behaviour on tips is thus not unexpected.

Whether or not fine discard in a lagoon will cause a stability problem will depend upon the geometry of the lagoon bank. Banks of large cross section and downstream construction, such as Gedling East tip and Gale Common are stable even if the lagoon behind them liquefies. With upstream construction methods and the resulting small embankment cross section, stability upon overtipping becomes dependent on the behaviour of the lagoon sediments (e.g. Gedling West tip lagoon, Chapter 5.3.3.6.). Slowly consolidating sediments will impose a maximum safe rate of construction due to the slow dissipation of the excess pore water pressures that are induced by loading.

The rate of consolidation varies markedly across a lagoon. Near the inlet it is high, with values of c_v of 200 to $1,000 \text{ m}^2/\text{yr}$. These drop to between 2 to $10 \text{ m}^2/\text{yr}$ as the outlet is approached. This variation is due to the change in grain size from coarse to fine across the lagoon. In terms of stability, it is desirable that the free draining coarser material which is associated with the inlet should be allowed to settle adjacent to the weakest

part of the containing embankment. This assumes, of course, that the embankment is itself free draining. That this may not be the case is illustrated by Cadeby Lagoon 9 where the embankment in the outlet half of the lagoon had a permeability of only 10^{-12} m/s, some six orders of magnitude less than the permeability of the lagoon sediments adjacent to the embankment. Proper filter protection of the embankment in the outlet area is probably required, as the low embankment permeability is most likely caused by fine material from the lagoon being carried into the embankment.

While considering this matter, it is worth pointing out that a permeable floor to a lagoon will also be an effective drain. In spite of their laminated structure, lagoon sediments show little, if any, anisotropy. This is probably due to small and large scale disturbances of the laminae which appears to be common. Anisotropy only shows itself, in fact, in the visually homogenous outlet material, where, at Gedling Lagoon 12 the horizontal permeability is some 25 per cent greater than the vertical permeability. This is not a very large difference, and is dwarfed by the 4,700 per cent increase in permeability occurring on passing from outlet to inlet. In terms of proportional lengths of drainage paths, even for a small lagoon the width (and hence the horizontal drainage path) is some five times as large as the depth (the vertical drainage path). For a typical lagoon, the ratio is nearer 12:1, and for some shallow lagoons can reach 20:1. These values are far greater than the ratio of horizontal to vertical permeability of the deposits, so the permeability of the lagoons floor is obviously an important factor in the drainage of the sediments.

While considering the permeability and coefficient of consolidation of lagoon sediments, it is worth noting that the type of flocculant employed does not have any economically consistent effect upon these parameters.

If current areas of high pore pressure can be located in a lagoon this can prove useful both in overtipping stability calculations and in excavation of the lagoon. Vane tests, where combined with measurements of plasticity index and bulk density, can be used to give some information on this subject. Provided that the lagoon deposits are normally consolidated, the shear strength measured by the vane should lie between two predictable values. The highest it should be is given by the relation:

$$\frac{s}{\bar{p}} = \tan \phi'$$

where s = shear strength

\bar{p} = effective pressure.

If this value is exceeded, then overconsolidation, which will normally have been caused by desiccation, may be suspected. The lowest value should be that predicted by Skempton's (1957) relation for clays, namely:

$$\frac{c}{\bar{p}} = 0.11 + 0.0037 \text{ PI}$$

where c = shear strength

\bar{p} = effective pressure

PI = plasticity index

A lower value than this is indicative of underconsolidation, and consequently points to an area of high pore water pressures.

While there is considerable variation in the rate of consolidation across a lagoon, the total amount of consolidation,

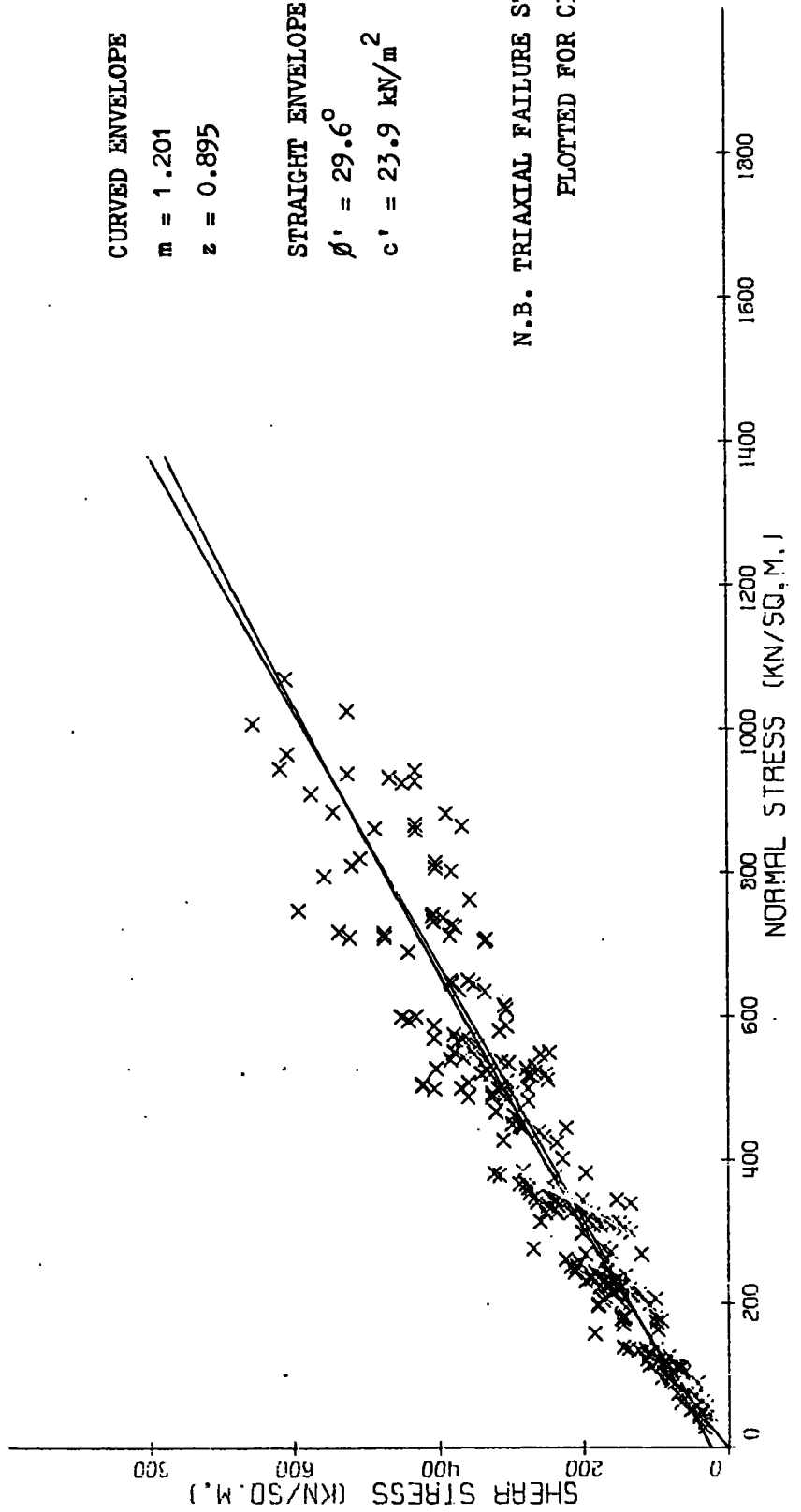
as shown by the coefficient of volume compressibility (m_v), stays relatively uniform. This indicates that the raised beach at the inlet end of a lagoon (Figure 4.1) is a primary depositional feature, and not a result of differential settlement.

When overtipping is resorted to, differential settlement will occur between the part of the new tip founded on the lagoon sediments and the part of the tip founded on coarse spoil. Differential settlements of over 4 metres can be associated with overtipping by 30 metres of spoil. This amount of displacement is sufficient to reduce the shear strength of some spoils (e.g. Gedling or Birch Coppice) to a residual value. Analysis shows, however, that such a situation is unlikely to cause critical stability problems, when the potential weak zone is deeply buried in the mass of the tip.

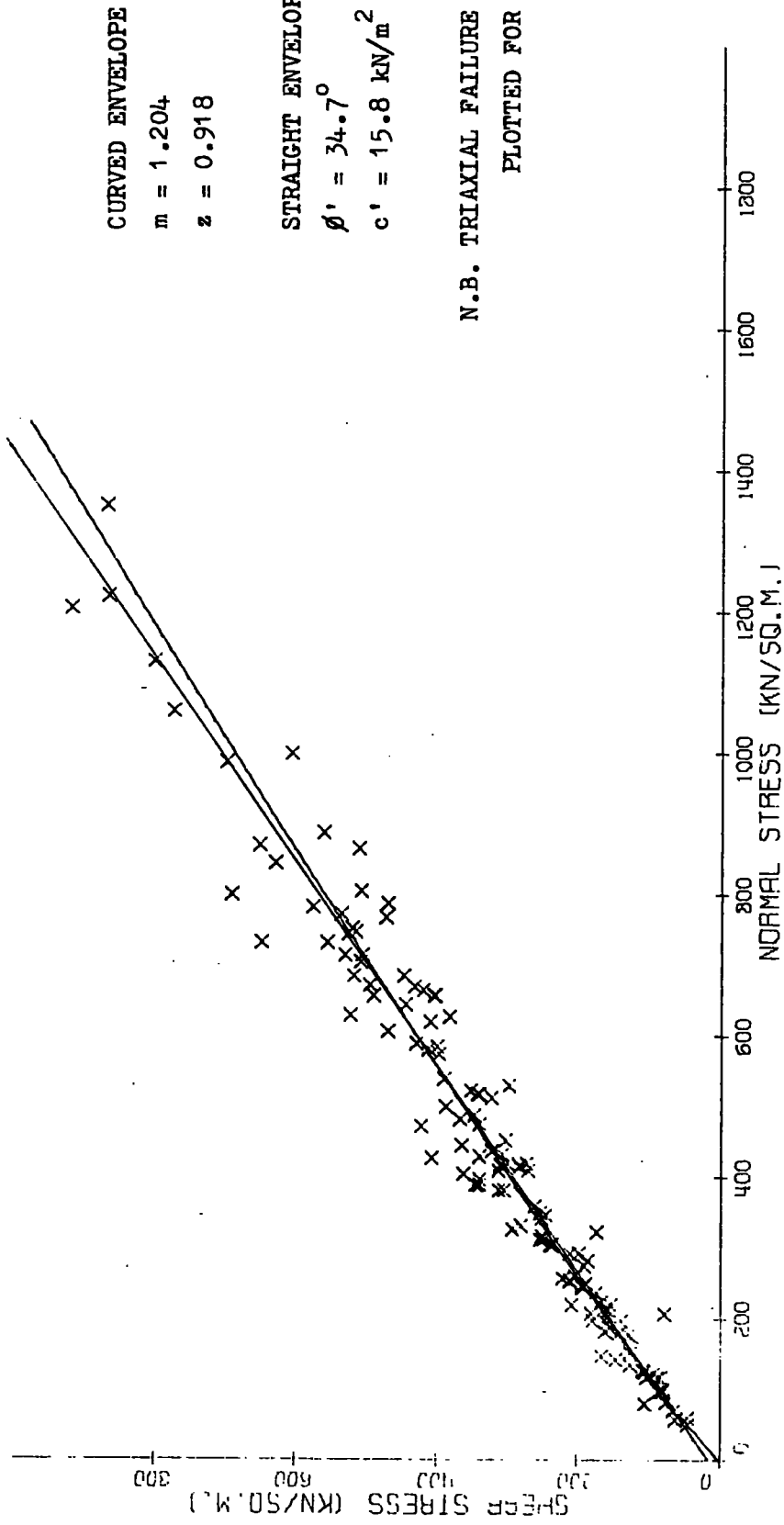
While the displacement due to differential settlement may reduce the shear strength of spoil to a residual value, it is unlikely that the displacements associated with bearing capacity type failures during the initial overtipping stages will cause a similar reduction, even though the displacements involved may be similar. This is due to the accelerated rate of particle breakdown (and hence shorter displacement to residual) associated with the higher pressures found in the body of a tip. Apart from this, factors affecting residual shear strength are not well known. There are two areas which might repay further research: the controls on the ultimate residual shear strength and the shape of the residual shear strength envelope. A ring shear apparatus would be necessary for the latter investigation. With the reversing shear-box, the loss of sample makes it impossible to determine residual shear strength at constant

normal stresses below 300 - 400 kN/m². The ring shear-box does not suffer from sample loss to the same degree (Bishop et al, 1971) and should thus be able to reach the true residual shear strength, even if large displacements are required.

ENGLISH COLLIERIES FIGURE 6.1



WELSH COLLIERIES FIGURE 6.2



CURVED ENVELOPE
 $m = 1.204$
 $z = 0.918$

STRAIGHT ENVELOPE
 $\phi' = 34.7^\circ$
 $c' = 15.8 \text{ kN/m}^2$

N.B. TRIAXIAL FAILURE STRESS POINTS
PLOTTED FOR CLARITY

BIBLIOGRAPHY

- AGARWAL, K.B. (1967)
- "The influence of size and orientation of sample on undrained strength of London Clay," Ph. D. thesis, Imperial College
- ALLEN, D.W. (1973)
- "The effect of coal content on two colliery spoils of extreme rank," M.Sc thesis, University of Durham.
- BARRABE, L. and FEYS, R. (1965)
- "Geologie du Charbon et des bassins houilliers," Masson and Cie, pp 117 - 123.
- BISHOP, A.W. (1955)
- "The use of the slip circle in the stability analysis of slopes," Geotechnique, Vol. 5, No. 1, pp 7 - 17.
- BISHOP, A.W. (1967)
- "Progressive failure - with special reference to the mechanism causing it," Panel discussion, Proc. Geotech. Conf. Oslo, Vol.2, pp 142 - 150.
- BISHOP, A.W. (1973)
- "The stability of tips and spoil heaps," Q.J. Engng. Geol, Vol. 6, pp 335 - 376.
- BISHOP, A.W. and HENKEL, D.J. (1962)
- "The measurement of soil properties in the triaxial test," 2nd Edition, 281pp, Edward Arnold, London.
- BISHOP, A.W. HUTCHINSON, J.N. PENMAN, A.D.M. and EVANS, H.E. (1969)
- "Geotechnical investigation into the causes and circumstances of the disaster of 21st October 1966," A Selection of Technical Reports submitted to the Aberfan Tribunal, Item 1, ppl - 80 Welsh Office, H.M.S.O. London.

- BISHOP, A.W. GREEN, G.E. GARGA, V.K. ANDRESEN, A. and BROWN, J.D. (1971)
- "A new ring shear apparatus and its application to the measurement of residual strength," *Geotechnique*, Vol. 21, No. 4, pp273 - 328.
- BLIGHT, G.E. (1968)
- "A note on field vane testing of silty soils," *Canadian Geotechnical Journal*, Vol. 5, No. 3, pp142 - 149.
- BORLAND, V.M. (1971)
- "Reservoir sedimentation," *River Mechanics* Vol. 2, Ch. 29, H.W. Shen (Ed. and Publ.) Colorado.
- BUSCH, R.A. BACKER, R.R. and ATKINS, L.A. (1974)
- "Physical property data on coal waste embankment materials," U.S. Bureau of Mines, RI7964, Washington.
- BUSCH, R.A. BACKER, R.R. ATKINS, L.A. and KEALY, C.D. (1975)
- "Physical property data on fine coal refuse," U.S. Bureau of Mines, RI8062, Washington.
- CARR, J. (1947/48)
- "A particular treatment of spoil bank fires in the South Derbyshire coalfield," *Trans. Inst. Min. Engrs.* Vol. 107, pp169 - 184.
- CHINA CLAY ASSOCIATION (1971)
- "China Clay Association, Technical handbook," St. Austell.
- COLEMAN, J.H. and GAGLIANO, S.M. (1965)
- "Sedimentary structures: Mississippi River deltaic plain," *Primary sedimentary Structures and their Hydrodynamic Interpretation*, Soc. of Econ. Paleontologists and Mineralogists Special Publ. No. 12, pp130 - 172.
- COLLINS, R.J. (1976)
- "A method for measuring the mineralogical variation of spoils from British collieries," *Clay Minerals*, Vol. 11, pp31 - 50.

FELLENIIUS, W. (1936)

"Calculation of stability of earth dams," Transactions, 2nd Congress on Large Dams, Washington D.C. Vol. 4, pp445 - 462, U.S. Government Printing Office, Washington D.C.

FISHER, R.A. and YATES, F. (1948)

"Statistical tables for Biological, Agricultural and Medical research," Oliver and Boyd, Edinburgh, 112p.

GAUNT, G.D. (1974)

"A radiocarbon date relating to Lake Humber," Proc. Yorks, Geol. Soc. Vol. 40, pp195 - 197.

GAUNT, G.D. (1976)

"The Devensian maximum ice limit in the Vale of York," Proc. Yorks. Geol. Soc. Vol. 40, pp631 - 637.

GAUNT, G.D. JARVIS, R.A. and MATHEWS, B. (1971)

"The late Weichselian sequence in the Vale of York," Proc. Yorks. Geol. Soc. Vol. 38. pp281 - 284.

GAUNT, G.D. COOPE, G.R. OSBORNE, P.J. and FRANKS, J.W. (1972)

"An interglacial deposit near Austerfield, Southern Yorkshire," Rep. No. 72/4, Inst. Geol. Sci. 13pp.

GAUNT, G.D. BARTLEY, D.D. and HARLAND, R. (1974)

"Two interglacial deposits proved in boreholes in the southern part of the Vale of York and their bearing on contemporaneous sea levels," Bull. Geol. Surv. U.K. No. 48. pp1 - 23.

GEOTECHNICAL AND CONCRETE SERVICES LTD (1968)

"Denby Hall Colliery tip," Internal report to the National Coal Board, Ref. No. 1974, Sheffield.

SIR WILLIAM HALCROW AND PARTNERS (1972)

"Denby Hall spoil heap," Internal report to the National Coal Board, Ref. No. DH.1(11/026) London.

- HUGHES, J.H. and WINDLE, D. (1976)
 "Some geotechnical properties of mineral waste tailings lagoons,"
 Ground Engineering, Vol. 9, No. 1. pp23 - 28.
- JANBU, N. (1954)
 "Application of composite slip surfaces for stability analysis,"
 Proc. European Conf. on Stability of Earth Slopes, Stockholm,
 Vol. 3, pp43 - 49.
- JANBU, N. (1973)
 "Slope stability computations," Embankment Dam Engineering - Casagrande
 Volume, Hirschfeld and Poulos (Ed.), pp47 - 86, Wiley and Sons,
 New York.
- JANBU, N. BJERRUM, L. and KJAERNSLI, B. (1956)
 "Veiledning ved løsnig av funamenterings oppgaver (Soil mechanics
 applied to some Engineering problems)," Norwegian Geotechnical
 Institute, Publ. 16, Oslo.
- JONES, J.M. and COOPER, B.S. (1970)
 "Coal," in Geology of Durham County, G.A.L. Johnson (compiler),
 G. Hickling (Ed.), Transactions of the Natural History Society
 of Northumberland, Durham and Newcastle upon Tyne, Vol. 41,
 No. 1, pp43 - 65.
- JOWETT, A. and CHOPRA, V.K. (1974)
 "Experiments on tailings samples from Gedling Colliery," National
 Coal Board Research Project, unpublished report, University of
 Leeds.
- KENNARD, M.F. KNILL, J.L. and VAUGHAN, P.R. (1967)
 "The geotechnical properties and behaviour of Carboniferous shale
 at the Balderhead Dam," Q.J. Engng. Geol. Vol. 1, pp3 - 24.
- LAMBE, W.T. and WHITMAN, R.V. (1969)
 "Soil Mechanics," Wiley and Sons, New York, 553p.

LAWRENCE, J.A. (1972)

"Some properties of South Wales discards," Coll. Gaurd, Vol. 220, No. 6, pp 270 - 278.

LEACH, B. (1973)

"The effects of planar anisotropy on the consolidation and drained shear strength characteristics of a laminated clay," M.Sc. thesis, University of Durham.

LEGGET, R.F. (1962)

"Geology and Engineering," McGraw-Hill, New York, 883p.

MARSAL, R.J. (1973)

"Mechanical properties of rockfill," Embankment Dam Engineering - Casagrande Volume, Hirschfeld and Poulos (Ed.), pp109 - 200, Wiley and Sons, New York.

MCKECHNIE THOMSON, G. and RODIN, S. (1972)

"Colliery spoil tips - after Aberfan," Inst. of Civ. Engrs. Paper 7522, London.

MCKEE, E.D. REYNOLDS, M.A. and BAKER, C.H. Jr. (1962)

"Experiments on intraformational recumbent folds in cross-bedded sand," U.S. Geol. Surv. Prof. Paper 450-D, pp155 - 160.

MCWILLIAM, D.J. (1975)

"Compositional and shear strength characteristics of a spoil heap at Littleton colliery," Staffordshire, M.Sc. thesis, University of Durham.

MORGENSTERN, N.R. and PRICE, V.E. (1965)

"The analysis of the stability of general slip surfaces," Geotechnique, Vol. 15, No. 1, pp79 - 93.

MURRAY, R.T. and SIMONS, I.F. (1974)

"Embankments on soft foundations: settlement and stability study at Tickton in Yorkshire," Transport and Road Research Laboratory, TRRLR 643, Crowthorne.

NATIONAL COAL BOARD (1970)

"Technical handbook - spoil heaps and lagoons," 2nd. draft,
National Coal Board, London.

NATIONAL COAL BOARD (1972)

"Review of research on properties of spoil tip materials,"
Headquarters Research Report, Wimpey Laboratories Ltd. Hayes,
Middlesex.

NATIONAL COAL BOARD, (1975)

"Subsidence Engineers handbook," National Coal Board (Mining Dept.)
London.

PARRY, R.G.H. (1972)

"Some properties of heavily overconsolidated Oxford Clay at a site
near Bedford," Geotechnique, Vol. 22, pp485 - 507.

PETTIBONE, H.C. and KEALY, C.D. (1971)

"Engineering properties of mine tailings," J. of Soil Mech. and
Found. Div. Proc. ASCE, Vol. 97, SM9, pp1207 - 1255.

PRICE, N.J. (1966)

"Fault and Joint Development in Brittle and Semi - Brittle Rock,"
Pergamon Press, London.

RATSEY, J. (1973)

"Shear strength characteristics of certain colliery discards
with respect to coal rank," M.Sc. thesis, University of Durham.

RAYMOND, G.P. (1967)

"The bearing capacity of large footings and embankments on clays,"
Geotechnique, Vol. 17, No. 1, pp1 - 10.

RICHARDSON, H.L. (1951)

"Phase changes which occur on heating kaolin clays," in X-ray
identification and crystal structures of clay minerals, Min.
Soc. London.

ROWE, P.W. and BARDEN, L. (1966)

"A new consolidation cell," Geotechnique, Vol.16, pp162 - 170.

SKEMPTON, A.W. (1957)

Discussion: "The planning and design of the new Hong Kong airport," Proc. Inst. Civil Engrs. Vol. 7, pp305 - 307.

SPEARS, D.A. TAYLOR, R.K. and TILL, R. (1970)

"A mineralogical investigation of a spoil heap at Yorkshire Main Colliery," Q.J. Engng. Geol. Vol. 3, No. 4, pp239 - 252.

SPEARS, D.A. and TAYLOR, R.K. (1972)

"The influence of weathering on the compositions and engineering properties of in situ Coal Measures rocks," Int. J. Rock Mech. Min. Sci. Vol. 9, pp729 - 756.

SPENCER, E. (1967)

"A method of analysis of the stability of embankments assuming parallel inter-slice forces," Geotechnique, Vol. 17, No. 1. pp11 - 26.

TAYLOR, D.W. (1948)

"Fundamentals of Soil Mechanics," Wiley and Sons, New York.

TAYLOR, R.K.(1973a)

"Composition and geotechnical characteristics of a 100 - year- old colliery spoil heap," Trans. Instn. Min. Metall. Section A (Mining Industry), Vol. 82, ppA1 - 14, A145 - 147.

TAYLOR, R.K. (1973b)

Discussion: "Colliery spoil heaps after Aberfan," Proc. Instn. Civil Engrs. Vol. 55, pp677 - 712.

TAYLOR, R.K. (1974_a)

"Colliery spoil heap materials - time dependant changes," Grnd. Engrg. Vol. 7, No. 4, pp24 - 27.

TAYLOR, R.K. (1974_b)

"Influence of coal content on the peak shear strength of colliery shales," Geotechnique, Vol. 24, No. 4, pp683 - 688.

TAYLOR, R.K. (1975)

"English and Welsh colliery spoil heaps - mineralogical and mechanical interrelationships," Eng. Geol. Vol. 9, No. 1, pp39 - 52.

TAYLOR, R.K. and SPEARS, D.A. (1970)

"The breakdown of British Coal Measures Rocks," Int. J. Rock Mech. Min. Sci. Vol. 7, pp481 - 501.

TAYLOR, R.K. and SPEARS, D.A. (1972)

"The geotechnical characteristics of a spoil heap at Yorkshire Main Colliery," Q.J. Engng. Geol. Vol. 5, No. 3, pp243 - 263.

TAYLOR, R.K. BARTON, R. MITCHELL, J.E. and COBB, A.E. (1976)

"The engineering geology of Devensian deposits underlying PFA lagoons at Gale Common," Yorkshire, Q.J. Engng. Geol. Vol. 9, No. 3, pp195 - 216.

TERZAGHI, K. and PECK, R.B. (1967)

"Soil mechanics in engineering practice," 2nd ed. Wiley and Sons, New York.

WALTON, G. (1974)

"Notes on mining subsidence beneath Gale Common ash disposal works," unpub. report to Rendal Palmer and Tritton.

WHITMAN, R.V. and BAILEY, W.A. (1967)

"Use of computers for slope stability analyses," J. of Soil Mech. and Found. Div. ASCE, Vol. 93, SM4, pp455 - 498.

WIMPEY LABORATORIES LTD (1968)

"Proposed extension and heightening of East spoil heap at Gedling colliery nr. Nottingham," Internal report to the National Coal Board, L.R. S/6235, Hayes.

WIMPEY LABORATORIES LTD. (1969a)

"Proposed extension and heightening of West spoil heap at Gedling colliery nr. Nottingham," Internal report to the National Coal Board L.R. S/6235/1 Hayes.

WIMPEY LABORATORIES LTD (1969b)

"Stability of spoil heap at Denby Hall colliery, nr. Ripley, Derbyshire," Internal report to the National Coal Board, L.R. S/6646, Hayes.

WIMPEY LABORATORIES LTD (1974)

"Proposed extension of tipping site at Pastures Lane, Cadeby colliery, South Yorkshire," Internal report to the National Coal Board, L.R. S/10190, Hayes.

WILSON, V. (1948)

"East Yorkshire and Lincolnshire," Br. Reg. Geol. H.M.S.O. London.

APPENDIX A

SLOPE STABILITY PROGRAM

A.1 Program use

The slope to be analysed should be drawn up on graph paper and orientated such that the toe points towards the left (Figure A.1). A system of rectangular Cartesian coordinates are then drawn, with the x-axis horizontal, and the y-axis vertical. Coordinates should increase from left to right, and from bottom to top (Figure A.1).

The program requires all data to be in S.I. units (i.e. dimensions in metres, densities in Mg/m^3 , shear strength parameters in kN/m^2 and degrees).

The data is in free format (i.e. only the order is important) and the following is required (e.g. Table A.1):-

1) A title, which can be up to sixty characters, and must be enclosed in single parentheses.

2) The number of layers in the slope.

The data describing the layers follows. All coordinates are referred to the grid system drawn up).

3) The number of coordinate pairs describing the layer.

4) Layer description, again up to sixty characters enclosed in single parentheses. The first four characters are used to indicate special conditions in the layer, and the fifth should always remain blank. If the first four are left blank then the layer will be assumed to have a non-curved isotropic envelope. It will also be assumed that excess pore water pressures do not obtain. Where one or more of these assumptions is invalid, it is indicated in the following way:-

a) PP as the first two characters indicates excess pore water pressures.

TABLE A1
EXAMPLE -- INPUT

SECTION FROM P550 L=10
CHANGING RATE = HOMOGENEITY, BATCH
PLOT OF STRESS BASE 1776154 NEW NOV 17/76
IN THE MIDDLE OF THE DAY 14:55:08 ON THU NOV 17/76
SCHEMATIC
FILE NAME HAS BEEN CREATED.
SIZE = 24
DEPTH =
SLOPE =
SLOPE NUMBER
SLOPE = 87

EXAMPLE SECTION 3

3 * C SOIL BANK (WITH CURVED WOMP ENVELOPE)

9 0.5 20 12 30 12 1.12 0.65 2.0
5 * D LAKE FLOES CLAY (WITH POPE PRESSURE DEVELOPED)
0 0.5 9 6.5 14.2 4.5 0 0 2 0 20 2.1
4 * E LAMINATED CLAY (WITH ANISOTROPY)

0 4 12 5 15 7 30 8 10 16 12 18 2.3

0 0.7 9.4 5.7 19 8 30 0.75

0 0.67

0 7 * J

0 6.5 11 5.1 13 6.2 15 6.7 17 7.9 19 5.8 21.5 12

0 21 * K

0 14 20 14

0 21 * LGR

0 5 10 1 2

0 21 * MGR

0 7 8 0.5

0 10 5.5

END OF FILE

4500 SUPSTR+POLITH SCORPS=IX
PAPUTIC BEJINS

- b) A as the third character indicates an anisotropic Mohr failure envelope.
- c) C as the fourth character indicates a curved Mohr failure envelope.
- 5) a) The coordinate pairs(x,y) of the top surface of the layer are given in increasing values of x (if a value of x is smaller than its predecessor an error message is printed and execution stopped). The first and last values of x should be the same for all the layers, except where a layer "pinches out". In this case the point of divergence or convergence with the layer below is specified.
- b) If PP is specified, then the pore pressure at the x-coordinates of the layer should be given in metres of water in excess of hydrostatic.
- 6) The strength parameters are then described. For materials with curved Mohr envelopes, enter the parameters m and z, from the expression $\tau = m (\sigma')^z$. For materials with linear Mohr envelopes, enter c' and ϕ' , from the expression
- $$\tau = c' + \sigma' \tan \phi'.$$
- For anisotropic materials, two pairs of parameters are entered, those for the horizontal direction being designated first.
- 7) The bulk density is specified.
- (Steps 3-7 should be repeated until all the layers are described).
- 8) The number of coordinate pairs describing the phreatic surface is then given.
- 9) The coordinate pairs of the phreatic surface are specified in a similar manner to those of the layer surfaces. A similar

response will be obtained in case of error.

- 10) When a slope is partly submerged in water, this is indicated by 'WL' followed by the height of the water surface. If this is omitted a height of zero is assumed. (The above procedure completes the description of the slope, and the potential failure surfaces may now be entered).
- 11) For a Janbu analysis of a non-circular surface the following are required:-
 - a) The number of coordinate pairs describing the failure surface
 - b) The letter J in single parentheses
 - c) The coordinate pairs(x,y) of the failure surface in increasing values of x are then entered. If a tension crack is present behind the crest, then the penultimate point should be vertically beneath the ultimate point, and in the position which defines the bottom of the crack. For the best results, there should be at least fifteen points describing the failure surface.
- 12) For a single circular arc failure surface the following are required:-
 - a) The number of points into which the arc should be divided (preferably more than fifteen).
 - b) One of the following (in single parentheses) to prescribe the type of analysis performed:
 - i) B - Bishop analysis
 - ii) F - Fellenius analysis
 - iii) JBF - Janbu, Bishop and Fellenius analysis
 - iv) BF - Bishop and Fellenius analysis
 - c) Coordinates (x,y) of the centre of the circle
 - d) Radius of the circle.

- 13) For a Bishop analysis of a grid of circle centres, the data required are as follows:
- a) As (12(a))
 - b) The letters BGR in single parentheses
 - c) The coordinates of the bottom left hand corner of the grid, which is 15 x 15 points
 - d) The proposed increment between adjacent points of the grid square
 - e) The number of the layer in the slope to which the circles will be tangential (Note: if a number larger than the maximum number of layers is specified, then an error message is printed and the bottom layer is automatically substituted).
 - f) If (e) was zero, then the gradient and y-intercept of any line which is to be the common tangent of all the circles must be inserted.
- (Steps 11-13 may be repeated in any order, and any number of times). The program will terminate itself upon encountering the end of file indicator positioned at the end of the data file.

A.2 Program output (e.g. Table A2)

The data describing the slope are printed out in tabular form. For non-circular and single circular-arc failure surfaces, the program prints the surface particulars followed by the type of analysis. Two values of the Factor of Safety (F) are then printed, the first approximation and the final value. The number of iterations required to obtain this value is also printed.

For the grid, the program prints out the search square, with details of the line or layer to which its circles are tangential. The x and y coordinates of the circle centres are

TABLE A2

EXAMPLE OUTPUT FROM DATA IN TABLE A1

```

EXAMPLE SECTION
SLOPE BANK WITH CURVED MOHA ENVELOPE
M=1.12000000 Z=0.85000000 G= 2.100
POINTS
9.00 6.50 20.00 12.00 30.00 12.00
LAKE FLOOR (LAY WITH DEF PRESSURE DEVELOPED)
C= 0.00 PHI=20.0 G= 2.100
POINTS
0.00 6.50 9.00 6.50 14.20 6.50
Pore Pressures
0.00 0.00 2.00
LAMINATED (LAY WITH ANISOTROPY)
HORIZONTAL VERTICAL C= 2.200
C= 10.00 PHI=16.0 C= 12.00 PHI=19.0
POINTS
0.00 4.00 12.00 5.00 15.00 7.00 30.00 8.00
GROUND WATER POINTS
0.00 6.70 9.40 6.70 15.00 8.50 30.00 8.75
STANDING WATER LEVEL
6.70
FAILURE SURFACE POINTS
9.00 6.50 11.00 6.10 13.00 6.20 15.00 6.70 17.00 7.00 19.00 9.40
21.50 12.00
JANUS ANALYSIS
FACTOR OF SAFETY, 1ST APPROXIMATION 0.94
FACTOR OF SAFETY, 2 ITERATIONS 0.98
COORDINATES OF CENTRE OF CIRCLE
14.00 20.00
RADIUS
15.00
SLOPE ANALYSIS
FACTOR OF SAFETY, 1ST APPROXIMATION 1.49
FACTOR OF SAFETY, 2 ITERATIONS 1.49
    
```


TABLE A2 (Cont'd.)

GRID: FACTOR OF SAFETY ABOVE RADIUS OF CIRCLE BELOW
CIRCLES TANGENTIAL TO LINE Y = 0.0X + 5.5

Y-CO-0

15.0	1.57	1.74	1.13	1.07	0.58	0.53	0.50	1.22	1.15	1.18	1.22	1.25	1.31	1.37
	9.50	9.50	9.50	9.50	9.50	9.50	9.50	9.50	9.50	9.50	9.50	9.50	9.50	9.50
14.5	1.64	1.25	1.20	1.17	0.59	0.53	0.50	1.12	1.14	1.14	1.22	1.25	1.31	1.37
	9.50	9.50	9.00	9.00	9.00	9.00	9.00	9.00	9.00	9.00	9.00	9.00	9.00	9.00
14.0	1.72	1.40	1.19	1.03	0.99	0.93	0.88	1.01	1.10	1.19	1.22	1.25	1.31	1.38
	9.50	8.50	8.50	8.50	8.50	8.50	8.50	8.50	8.50	8.50	8.50	8.50	8.50	8.50
13.5	1.81	1.45	1.22	1.07	0.99	0.93	0.88	0.95	1.03	1.15	1.22	1.26	1.33	1.40
	9.00	8.00	8.00	8.00	8.00	8.00	8.00	8.00	8.00	8.00	8.00	8.00	8.00	8.00
13.0	1.85	1.51	1.25	1.09	0.98	0.93	0.88	0.95	1.03	1.14	1.20	1.24	1.28	1.41
	7.50	7.50	7.50	7.50	7.50	7.50	7.50	7.50	7.50	7.50	7.50	7.50	7.50	7.50
12.5	2.14	1.67	1.29	1.11	0.99	0.91	0.88	0.84	1.05	1.16	1.22	1.26	1.32	1.45
	7.00	7.00	7.00	7.00	7.00	7.00	7.00	7.00	7.00	7.00	7.00	7.00	7.00	7.00
12.0	2.35	1.67	1.21	1.13	1.00	0.91	0.86	0.82	1.01	1.13	1.24	1.29	1.36	1.51
	6.50	6.50	6.50	6.50	6.50	6.50	6.50	6.50	6.50	6.50	6.50	6.50	6.50	6.50
11.5	2.09	1.40	1.37	1.13	1.01	0.92	0.86	0.82	0.94	1.16	1.26	1.33	1.40	1.60
	6.00	6.00	6.00	6.00	6.00	6.00	6.00	6.00	6.00	6.00	6.00	6.00	6.00	6.00
11.0	3.21	1.95	1.45	1.17	1.00	0.92	0.86	0.83	0.91	1.15	1.26	1.36	1.46	1.71
	5.50	5.50	5.50	5.50	5.50	5.50	5.50	5.50	5.50	5.50	5.50	5.50	5.50	5.50
10.5	4.01	2.21	1.52	1.22	1.03	0.91	0.84	0.81	0.82	1.15	1.31	1.43	1.54	1.85
	5.00	5.00	5.00	5.00	5.00	5.00	5.00	5.00	5.00	5.00	5.00	5.00	5.00	5.00
10.0	5.51	2.59	1.57	1.25	1.05	0.93	0.86	0.82	0.81	1.05	1.36	1.53	1.70	2.09
	4.50	4.50	4.50	4.50	4.50	4.50	4.50	4.50	4.50	4.50	4.50	4.50	4.50	4.50
9.5	8.74	3.17	1.87	1.34	1.07	0.93	0.87	0.83	0.83	0.84	1.45	1.65	1.89	2.48
	4.00	4.00	4.00	4.00	4.00	4.00	4.00	4.00	4.00	4.00	4.00	4.00	4.00	4.00
9.0	14.90	4.26	2.16	1.47	1.13	0.96	0.87	0.84	0.85	0.89	1.57	1.93	2.27	2.68
	3.50	3.50	3.50	3.50	3.50	3.50	3.50	3.50	3.50	3.50	3.50	3.50	3.50	3.50
8.5	74.74	6.76	2.71	1.64	1.20	0.99	0.89	0.86	0.84	0.87	1.79	2.44	3.11	4.21
	3.00	3.00	3.00	3.00	3.00	3.00	3.00	3.00	3.00	3.00	3.00	3.00	3.00	3.00
8.0	33.74	15.40	3.77	1.97	1.35	1.08	0.87	0.85	1.00	1.14	1.94	4.12	7.10	14.27
	2.50	2.50	2.50	2.50	2.50	2.50	2.50	2.50	2.50	2.50	2.50	2.50	2.50	2.50

X-COOPD

EXECUTION TERMINATED

SSIGNOFF

printed on the bottom and left hand sides, respectively. The values of F found are printed in the relevant positions in the square, with the radii of the circles below them (see Table A.2). Contours of Factor of Safety may then be drawn (Figure A.1).

SLOPE STABILITY PROGRAM LISTING

SETUP: CLOA T=6 P=20
CHECK DATE = UNIFORMITY, BATCH
MESSAGE WAS: 17:35:17 TUE DEC 14/76
USER: GLOM SIGNED ON AT 10:05:26 ON WED DEC 15/76
SLOPE PROFILE

READY
READY PROFILE
NO. 1
SLOPE

SLOPE
SLOPE PROFILE

```

1 76 SLOPE STABILITY ANALYSIS
2 76 FRAMMENT SHOULD HAVE HIGHEST POINT OF FAILURE SURFACE
3 76 CAUGHT PAID SIDE
4 76 DATA TO BE ENTERED FROM LEFT TO RIGHT
5 76 6 LAYERS FROM TOP TO BOTTOM
6 76 DATA REQUIRE:-
7 76 TITLE(UP TO 60 CHARACTERS)
8 76 NO. OF LAYERS
9 76
10 76 NO. OF COORDINATE PAIRS FOR LAYER
11 76 LAYER DESCRIPTION(UP TO 60 CHAR)
12 76 LIST 5 CHAR SHOULD CONTAIN BLANKS OR
13 76 CHIPS SYMBOL PROPERTY
14 76 PP EXCESS PORE PRESSURE PRESENT
15 76 T ANISOTROPY
16 76 C CURVATURE OF WATER ENVELOPE
17 76 (SPARE)
18 76 COORDINATES OF TOP SURFACE OF LAYER,
19 76 (X,Y)WHERE DIVERGENT FROM LAYER BELOW
20 76 NO. LENSOID LAYERS SHOULD ALL HAVE
21 76 SAME INITIAL AND/OR FINAL X COORD
22 76 IF PP SPEC. THEN VALUES OF PORE
23 76 PRESSURES (IN % OF WATER IN EXCESS
24 76 OF HYDROSTATIC) AT X COORDS OF LAYER
25 76
26 76 IF C SPEC. THEN ENTER
27 76 W F Z FROM T=0 TO
28 76 IF A SPEC. THEN ENTER
29 76 C E PHI FOR HORIZONTAL DIRECTION
30 76 C F PHI FOR VERTICAL DIRECTION
31 76 ELSE ENTER
32 76 COHESION (C LAYER(KN/M**2))
33 76 PHI FOR LAYER(DEGREES)
34 76 DENSITY OF LAYER(KN/M**3)
35 76
36 76 NO. OF COORDINATE PAIRS FOR WATER
37 76 SURFACE
38 76 COORDINATES OF WATER SURFACE (X,Y)
39 76
40 76 STANDING WATER LEVEL ASSUMED ZERO
41 76 UNLESS SPECIFIED BY:
42 76 1. WATER LEVEL
43 76
44 76 FOR EACH FAILURE SURFACE:-
45 76 FOR IANBU ANALYSIS:-
46 76 IJ
47 76 NO. OF POINTS ON FAILURE SURFACE
48 76
49 76 COORDINATES OF FAILURE SURFACE
50 76

```

SLOPE STABILITY PROGRAM LISTING (Cont'd.)

```

70 IF CRACK EXISTS THEN DENUITIMATE //
71 POINT SLOPE OF VERTICALLY BENEATH //
72 ULTIMATE POINT, A(0) AT THE POSITION //
73 OF THE BOTTOM OF THE CRACK //
74 //
75 NO. OF SLICES IN CIRCLE //
76 TYPE OF ANALYSIS //
77 1) FOR BISHOP ANALYSIS //
78 2) FOR FELLNERS ANALYSIS //
79 3) FOR ALL THREE //
80 4) FOR ALIGN. & BELLETRUS //
81 COORDINATES OF CENTRE OF CIRCLE //
82 RADIUS OF CIRCLE (METRES) //
83 //
84 NO. OF SLICES PER CIRCLE //
85 XGR //
86 COORDINATE OF BOTTOM LEFT CORNER OF //
87 SEARCH SQUARE (WHICH IS 15*15 POINTS) //
88 INCREMENT OF CIRCLE CENTRE COORDINATES //
89 NO. OF THE LAYER THAT THE FAILURE //
90 CIRCLES ARE TO BE TANGENTIAL TO. //
91 IF 0 SPECIFIED, THEN INSERT GRADIENT & //
92 INTERCEPT OF TANGENT. //
93 //
94 //
95 //
96 //
97 //
98 //
99 //
100 //
101 //
102 //
103 //
104 //
105 //
106 //
107 //
108 //
109 //
110 //
111 //
112 //
113 //
114 //
115 //
116 //
117 //
118 //
119 //
120 //
121 //
122 //
123 //
124 //
125 //
126 //
127 //
128 //
129 //
130 //
131 //
132 //
133 //
134 //
135 //
136 //
137 //
138 //
139 //
140 //
141 //
142 //
143 //
144 //
145 //
146 //
147 //
148 //
149 //
150 //
151 //
152 //
153 //
154 //
155 //
156 //
157 //
158 //
159 //
160 //
161 //
162 //
163 //
164 //
165 //
166 //
167 //
168 //
169 //
170 //
171 //
172 //
173 //
174 //
175 //
176 //
177 //
178 //
179 //
180 //
181 //
182 //
183 //
184 //
185 //
186 //
187 //
188 //
189 //
190 //
191 //
192 //
193 //
194 //
195 //
196 //
197 //
198 //
199 //
200 //
201 //
202 //
203 //
204 //
205 //
206 //
207 //
208 //
209 //
210 //
211 //
212 //
213 //
214 //
215 //
216 //
217 //
218 //
219 //
220 //
221 //
222 //
223 //
224 //
225 //
226 //
227 //
228 //
229 //
230 //
231 //
232 //
233 //
234 //
235 //
236 //
237 //
238 //
239 //
240 //
241 //
242 //
243 //
244 //
245 //
246 //
247 //
248 //
249 //
250 //
251 //
252 //
253 //
254 //
255 //
256 //
257 //
258 //
259 //
260 //
261 //
262 //
263 //
264 //
265 //
266 //
267 //
268 //
269 //
270 //
271 //
272 //
273 //
274 //
275 //
276 //
277 //
278 //
279 //
280 //
281 //
282 //
283 //
284 //
285 //
286 //
287 //
288 //
289 //
290 //
291 //
292 //
293 //
294 //
295 //
296 //
297 //
298 //
299 //
300 //
301 //
302 //
303 //
304 //
305 //
306 //
307 //
308 //
309 //
310 //
311 //
312 //
313 //
314 //
315 //
316 //
317 //
318 //
319 //
320 //
321 //
322 //
323 //
324 //
325 //
326 //
327 //
328 //
329 //
330 //
331 //
332 //
333 //
334 //
335 //
336 //
337 //
338 //
339 //
340 //
341 //
342 //
343 //
344 //
345 //
346 //
347 //
348 //
349 //
350 //
351 //
352 //
353 //
354 //
355 //
356 //
357 //
358 //
359 //
360 //
361 //
362 //
363 //
364 //
365 //
366 //
367 //
368 //
369 //
370 //
371 //
372 //
373 //
374 //
375 //
376 //
377 //
378 //
379 //
380 //
381 //
382 //
383 //
384 //
385 //
386 //
387 //
388 //
389 //
390 //
391 //
392 //
393 //
394 //
395 //
396 //
397 //
398 //
399 //
400 //
401 //
402 //
403 //
404 //
405 //
406 //
407 //
408 //
409 //
410 //
411 //
412 //
413 //
414 //
415 //
416 //
417 //
418 //
419 //
420 //
421 //
422 //
423 //
424 //
425 //
426 //
427 //
428 //
429 //
430 //
431 //
432 //
433 //
434 //
435 //
436 //
437 //
438 //
439 //
440 //
441 //
442 //
443 //
444 //
445 //
446 //
447 //
448 //
449 //
450 //
451 //
452 //
453 //
454 //
455 //
456 //
457 //
458 //
459 //
460 //
461 //
462 //
463 //
464 //
465 //
466 //
467 //
468 //
469 //
470 //
471 //
472 //
473 //
474 //
475 //
476 //
477 //
478 //
479 //
480 //
481 //
482 //
483 //
484 //
485 //
486 //
487 //
488 //
489 //
490 //
491 //
492 //
493 //
494 //
495 //
496 //
497 //
498 //
499 //
500 //
501 //
502 //
503 //
504 //
505 //
506 //
507 //
508 //
509 //
510 //
511 //
512 //
513 //
514 //
515 //
516 //
517 //
518 //
519 //
520 //
521 //
522 //
523 //
524 //
525 //
526 //
527 //
528 //
529 //
530 //
531 //
532 //
533 //
534 //
535 //
536 //
537 //
538 //
539 //
540 //
541 //
542 //
543 //
544 //
545 //
546 //
547 //
548 //
549 //
550 //
551 //
552 //
553 //
554 //
555 //
556 //
557 //
558 //
559 //
560 //
561 //
562 //
563 //
564 //
565 //
566 //
567 //
568 //
569 //
570 //
571 //
572 //
573 //
574 //
575 //
576 //
577 //
578 //
579 //
580 //
581 //
582 //
583 //
584 //
585 //
586 //
587 //
588 //
589 //
590 //
591 //
592 //
593 //
594 //
595 //
596 //
597 //
598 //
599 //
600 //
601 //
602 //
603 //
604 //
605 //
606 //
607 //
608 //
609 //
610 //
611 //
612 //
613 //
614 //
615 //
616 //
617 //
618 //
619 //
620 //
621 //
622 //
623 //
624 //
625 //
626 //
627 //
628 //
629 //
630 //
631 //
632 //
633 //
634 //
635 //
636 //
637 //
638 //
639 //
640 //
641 //
642 //
643 //
644 //
645 //
646 //
647 //
648 //
649 //
650 //
651 //
652 //
653 //
654 //
655 //
656 //
657 //
658 //
659 //
660 //
661 //
662 //
663 //
664 //
665 //
666 //
667 //
668 //
669 //
670 //
671 //
672 //
673 //
674 //
675 //
676 //
677 //
678 //
679 //
680 //
681 //
682 //
683 //
684 //
685 //
686 //
687 //
688 //
689 //
690 //
691 //
692 //
693 //
694 //
695 //
696 //
697 //
698 //
699 //
700 //
701 //
702 //
703 //
704 //
705 //
706 //
707 //
708 //
709 //
710 //
711 //
712 //
713 //
714 //
715 //
716 //
717 //
718 //
719 //
720 //
721 //
722 //
723 //
724 //
725 //
726 //
727 //
728 //
729 //
730 //
731 //
732 //
733 //
734 //
735 //
736 //
737 //
738 //
739 //
740 //
741 //
742 //
743 //
744 //
745 //
746 //
747 //
748 //
749 //
750 //
751 //
752 //
753 //
754 //
755 //
756 //
757 //
758 //
759 //
760 //
761 //
762 //
763 //
764 //
765 //
766 //
767 //
768 //
769 //
770 //
771 //
772 //
773 //
774 //
775 //
776 //
777 //
778 //
779 //
780 //
781 //
782 //
783 //
784 //
785 //
786 //
787 //
788 //
789 //
790 //
791 //
792 //
793 //
794 //
795 //
796 //
797 //
798 //
799 //
800 //
801 //
802 //
803 //
804 //
805 //
806 //
807 //
808 //
809 //
810 //
811 //
812 //
813 //
814 //
815 //
816 //
817 //
818 //
819 //
820 //
821 //
822 //
823 //
824 //
825 //
826 //
827 //
828 //
829 //
830 //
831 //
832 //
833 //
834 //
835 //
836 //
837 //
838 //
839 //
840 //
841 //
842 //
843 //
844 //
845 //
846 //
847 //
848 //
849 //
850 //
851 //
852 //
853 //
854 //
855 //
856 //
857 //
858 //
859 //
860 //
861 //
862 //
863 //
864 //
865 //
866 //
867 //
868 //
869 //
870 //
871 //
872 //
873 //
874 //
875 //
876 //
877 //
878 //
879 //
880 //
881 //
882 //
883 //
884 //
885 //
886 //
887 //
888 //
889 //
890 //
891 //
892 //
893 //
894 //
895 //
896 //
897 //
898 //
899 //
900 //
901 //
902 //
903 //
904 //
905 //
906 //
907 //
908 //
909 //
910 //
911 //
912 //
913 //
914 //
915 //
916 //
917 //
918 //
919 //
920 //
921 //
922 //
923 //
924 //
925 //
926 //
927 //
928 //
929 //
930 //
931 //
932 //
933 //
934 //
935 //
936 //
937 //
938 //
939 //
940 //
941 //
942 //
943 //
944 //
945 //
946 //
947 //
948 //
949 //
950 //
951 //
952 //
953 //
954 //
955 //
956 //
957 //
958 //
959 //
960 //
961 //
962 //
963 //
964 //
965 //
966 //
967 //
968 //
969 //
970 //
971 //
972 //
973 //
974 //
975 //
976 //
977 //
978 //
979 //
980 //
981 //
982 //
983 //
984 //
985 //
986 //
987 //
988 //
989 //
990 //
991 //
992 //
993 //
994 //
995 //
996 //
997 //
998 //
999 //
1000 //

```

SLOPE STABILITY PROGRAM LISTING (Cont'd.)

```

110 TAP,
111 READ,
112 PAP;
113
114
115
116
117
118
119
120
121
122
123
124
125
126
127
128
129
130
131
132
133
134
135
136
137
138
139
140
141
142
143
144
145
146
147
148
149
150
151
152
153
154
155
156
157
158
159
160
161
162
163
164
165
166
167
168
169
170
171
172
173
174
175
176
177
178
179
180
181
182
183
184
185
186
187
188
189
190
191
192
193
194
195
196
197
198
199
200
201
202
203
204
205
206
207
208
209
210
211
212
213
214
215
216
217
218
219
220
221
222
223
224
225
226
227
228
229
230
231
232
233
234
235
236
237
238
239
240
241
242
243
244
245
246
247
248
249
250
251
252
253
254
255
256
257
258
259
260
261
262
263
264
265
266
267
268
269
270
271
272
273
274
275
276
277
278
279
280
281
282
283
284
285
286
287
288
289
290
291
292
293
294
295
296
297
298
299
300
301
302
303
304
305
306
307
308
309
310
311
312
313
314
315
316
317
318
319
320
321
322
323
324
325
326
327
328
329
330
331
332
333
334
335
336
337
338
339
340
341
342
343
344
345
346
347
348
349
350
351
352
353
354
355
356
357
358
359
360
361
362
363
364
365
366
367
368
369
370
371
372
373
374
375
376
377
378
379
380
381
382
383
384
385
386
387
388
389
390
391
392
393
394
395
396
397
398
399
400
401
402
403
404
405
406
407
408
409
410
411
412
413
414
415
416
417
418
419
420
421
422
423
424
425
426
427
428
429
430
431
432
433
434
435
436
437
438
439
440
441
442
443
444
445
446
447
448
449
450
451
452
453
454
455
456
457
458
459
460
461
462
463
464
465
466
467
468
469
470
471
472
473
474
475
476
477
478
479
480
481
482
483
484
485
486
487
488
489
490
491
492
493
494
495
496
497
498
499
500
501
502
503
504
505
506
507
508
509
510
511
512
513
514
515
516
517
518
519
520
521
522
523
524
525
526
527
528
529
530
531
532
533
534
535
536
537
538
539
540
541
542
543
544
545
546
547
548
549
550
551
552
553
554
555
556
557
558
559
560
561
562
563
564
565
566
567
568
569
570
571
572
573
574
575
576
577
578
579
580
581
582
583
584
585
586
587
588
589
590
591
592
593
594
595
596
597
598
599
600
601
602
603
604
605
606
607
608
609
610
611
612
613
614
615
616
617
618
619
620
621
622
623
624
625
626
627
628
629
630
631
632
633
634
635
636
637
638
639
640
641
642
643
644
645
646
647
648
649
650
651
652
653
654
655
656
657
658
659
660
661
662
663
664
665
666
667
668
669
670
671
672
673
674
675
676
677
678
679
680
681
682
683
684
685
686
687
688
689
690
691
692
693
694
695
696
697
698
699
700
701
702
703
704
705
706
707
708
709
710
711
712
713
714
715
716
717
718
719
720
721
722
723
724
725
726
727
728
729
730
731
732
733
734
735
736
737
738
739
740
741
742
743
744
745
746
747
748
749
750
751
752
753
754
755
756
757
758
759
760
761
762
763
764
765
766
767
768
769
770
771
772
773
774
775
776
777
778
779
780
781
782
783
784
785
786
787
788
789
790
791
792
793
794
795
796
797
798
799
800
801
802
803
804
805
806
807
808
809
810
811
812
813
814
815
816
817
818
819
820
821
822
823
824
825
826
827
828
829
830
831
832
833
834
835
836
837
838
839
840
841
842
843
844
845
846
847
848
849
850
851
852
853
854
855
856
857
858
859
860
861
862
863
864
865
866
867
868
869
870
871
872
873
874
875
876
877
878
879
880
881
882
883
884
885
886
887
888
889
890
891
892
893
894
895
896
897
898
899
900
901
902
903
904
905
906
907
908
909
910
911
912
913
914
915
916
917
918
919
920
921
922
923
924
925
926
927
928
929
930
931
932
933
934
935
936
937
938
939
940
941
942
943
944
945
946
947
948
949
950
951
952
953
954
955
956
957
958
959
960
961
962
963
964
965
966
967
968
969
970
971
972
973
974
975
976
977
978
979
980
981
982
983
984
985
986
987
988
989
990
991
992
993
994
995
996
997
998
999
1000

```

SLOPE STABILITY PROGRAM LISTING (Cont'd.)

```

170 DO I=AL TO 2 BY -1;
171   J=I-1;
172   IF TPNTS(I,1)<TPNTS(J,1,1) THEN DO;
173     DO K=1 TO NPT(I) WHILE(TPNTS(J,1,1)>TPNTS(I,K,1));
174     END;
175     IF TPNTS(J,1,1)=TPNTS(I,K,1) THEN TPNTS(J,1,2)=TPNTS(I,K,2);
176     ELSE TPNTS(J,1,2)=TPNTS(I,K,2)-(TPNTS(I,K,1)-TPNTS(J,1,1))
177       *(TPNTS(I,K,2)-TPNTS(I,(K-1),2))/
178       (TPNTS(I,K,1)-TPNTS(I,(K-1),1));
179   K=K-1;
180   DO L=NPT(I) TO 1 BY -1;
181     TPNTS(J,(L+K),1)=TPNTS(J,L,1);
182     TPNTS(J,(L+K),2)=TPNTS(J,L,2);
183     TPNT(J,(L+K))=TOP(J,L);
184   END;
185   NPT(J)=NPT(I)+K;
186   DO L=1 TO K;
187     TPNTS(J,L,1)=TPNTS(I,L,1);
188     TPNTS(J,L,2)=TPNTS(I,L,2);
189     TOP(J,L)=0;
190   END;
191   FN:
192   IF TPNTS(I,NPT(I),1)>TPNTS(J,NPT(J),1) THEN DO;
193     DO K=NPT(I) TO 1 BY -1
194       WHILE(TPNTS(J,NPT(J),1)<TPNTS(I,K,1));
195     END;
196     IF TPNTS(J,NPT(J),1)=TPNTS(I,K,1) THEN
197       TPNTS(J,NPT(J),2)=TPNTS(I,K,2);
198     ELSE TPNTS(J,NPT(J),2)=TPNTS(I,K,2)+
199       (TPNTS(I,(K+1),2)-TPNTS(I,K,2))
200       *(TPNTS(J,NPT(J),1)-TPNTS(I,K,1))
201       / (TPNTS(I,(K+1),1)-TPNTS(I,K,1));
202   K=K+1;
203   IF=NPT(I)+1;
204   DO L=K TO NPT(I);
205     TPNTS(J,(L+1),1)=TPNTS(I,L,1);
206     TPNTS(J,(L+1),2)=TPNTS(I,L,2);
207   IF=IF+1;
208   END;
209   NPT(J)=IF-1;
210   FN:
211   NP=NPT(I);
212   DO I=2 TO NL;
213     IF NP(I)>NP THEN NP=NPT(I);
214   END;
215   EXT: IF NEXP THEN NP=NF;
216   NP=NP+2;
217   NPL=NP-1;
218   ALLOCATE LAYER,
219     LT,
220     LINES;
221   DO I=1 TO NL;
222     PNTS(I,1)=6.0E40;
223     PNTS(I,2)=TPNTS(I,1,2);
224     FP(I,1)=0;
225     PC I=1 TO NP(I);
226     PNTS(I,(J+1),1)=TPNTS(I,J,1);
227     PNTS(I,(J+1),2)=TPNTS(I,J,2);
228     DP(I,(J+1))=TOP(I,J);
229   END;

```

SLOPE STABILITY PROGRAM LISTING (Cont'd.)

```

251      END;
252      IF NP(I+2) < NP THEN DO I=(NP(I)+2) TO NPL;
253      PNTS(I,J,1)=PNTS(I,(J-1),1)+10;
254      PNTS(I,J,2)=PNTS(I,(J-1),2);
255      PNTS(I,J)=0;
256      END;
257      PNTS(I,MP,1)=6.9540;
258      PNTS(I,MP,2)=PNTS(I,MP,1);
259      PNTS(I,MP)=0;
260      END;
261      WT(I,1)=4.0F40;
262      WT(I,2)=WT(I,1)+2;
263      DO I=1 TO NP;
264      WT((I+1),1)=WT(I,1);
265      WT((I+1),2)=WT(I,2);
266      END;
267      I=(NP+2)CMP T=FI; DO I=(I+2) TO NPL;
268      WT(I,1)=WT((I-1),1)+10;
269      WT(I,2)=WT((I-1),2);
270      END;
271      WT(NP,1)=6.0F40;
272      WT(NP,2)=WT(NP,1)+2;
273      FREE T=FI;
274      END;
275      DO CONVERGENCE BEGINS;
276      GET LIST(I);
277      PUT FOUT('STANDING WATER LEVEL',NL) (SKIP,4(20),X(1),F(7,2));
278      DO TO RES;
279      END;
280      RES=GET LIST(I);
281      DO I=1 TO NL;
282      DO J=1 TO NP;
283      Z(I,J)=(PNTS(I,(J+1),2)-PNTS(I,J,2))
284      / (PNTS(I,(J+1),1)-PNTS(I,J,1));
285      P(I,J)=PNTS(I,J,2)-Z(I,J)*PNTS(I,J,1);
286      END;
287      END;
288      DO I=1 TO NPL;
289      R(I,1)=WT(I,1)+2-A(NL,1)*WT(I,1);
290      R(I,2)=WT(I,2)+2-A(NL,2)*WT(I,1);
291      END;
292      CONTO=RES=Z-I;
293      IF A(1) < 0 THEN FLAG=(NL+2)*R(1);
294      IF A(2) < 0 THEN FLAG=(NL+2)*R(2);
295      ALLOCATE RES;
296      1 RES;
297      2 RES;
298      3 INT;
299      2 WT,2 XT,2 YT,2 NP,2 MT;
300      END;
301      DO CONVERGENCE SYSTEM;
302      GET LIST(TYPE);
303      P=VAL;
304      IF TYPE=1 THEN GO TO J=ARU;
305      PJ=SWIP(2);
306      IF TYPE=2 THEN DO;
307      P=VAL;
308      TYPE=J;
309      END;
310      ELSE IF TYPE=3 THEN DO;

```

SLOPE STABILITY PROGRAM LISTING (Cont'd).

```

200  N=NL+2;
201  TYPE='R';
202  END;
203  ALLOCATE FSOR,
204  RAC;
205  PAD=0,GETO;
206  FSOR(1,1)=IFLAG;
207  NAPI=0;
208  TYPE='R';
209  NX, NY=2;
210  GET LIST(XC, YC, CIRC, L1);
211  PUT EDIT('CIR: FACTOR OF SAFETY ARCV, RADIUS OF CIRCLE BELOW',
212  'CIRCLS TANGENTIAL TO')
213  (PAGE, X(10), A(50), SKIP, X(14), A(21));
214  DO I=2 TO 16;
215  FSOR(I,1)=XC+(I-2)*CINC;
216  FSO(I,1)=YC+(I-2)*CIAC;
217  END;
218  IF L=0 THEN GO;
219  GET LIST(AS, AX);
220  PUT EDIT('LINE Y =', AS, 'X +', AX)
221  (X(1), A(8), F(4,1), A(3), F(5,1));
222  DO I=2 TO 16;
223  DO J=2 TO 16;
224  RAC(I, J)=SORT((FSOR(I,1)+AS-FSOR(I, J)+AX)**2/(AS*AS+1));
225  END;
226  END;
227  ELSE GO;
228  PUT EDIT('TOP OF LAYER', L1(X(1), A(12), F(2)));
229  IF L=AL THEN GO;
230  PUT EDIT('LAYER', L) DOES NOT EXIST, REPLACED BY LAYER',
231  NL(X(2), A(5), F(3), A(36), F(3));
232  L=NL;
233  END;
234  DO I=2 TO 15;
235  DO J=2 TO 16;
236  DO K=1 TO MPL;
237  AX=(FSOR(I,1)+AL(K))*((FSOR(I, J)-R(I, K))/
238  (AL(K)+AL(K)+1));
239  IF X<PNTS(L, K, 1) THEN
240  R=SORT((FSOR(I,1)-PNTS(L, K, 1))**2+
241  (FSOR(I, J)-PNTS(L, K, 2))**2);
242  ELSE IF X>PNTS(L, K, 1) THEN
243  R=SORT((FSOR(I,1)+PNTS(L, K, 1))**2+
244  (FSOR(I, J)+PNTS(L, K, 2))**2);
245  ELSE R=SORT((FSOR(I,1)-AX)**2+
246  (FSOR(I, J)-AL(K)+AX+R(L, K))**2);
247  IF X<PNTS(L, J) THEN RAC(I, J)=R;
248  END;
249  END;
250  END;
251  END;
252  P=PAR(2, 2);
253  GO TO CORR;
254  END;
255  GET LIST(XC, YC, P);
256  PUT EDIT('COORDINATES OF CENTER OF CIRCLE, XC, YC, RADIUS, R)
257  (SKIP, X(10), A(31), SKIP, X(10), F(7, 2), X(1), F(7, 2),
258  340

```

40 SLOPE STABILITY PROGRAM LISTING (Cont'd.)

```

350 GR05:FLAG=0; SKIP,X(10),A(6),SKIP,X(10),F(7,2));
351 GO L=APL TO I BY -1;
352 FI=A(1,1)-A(1,1)*I;
353 FR=A(1,1)*R(1,1)-YC)-XC;
354 AS=XC*(YF+YF-R0)*R(1,1)+A(1,1)-2*YC*B(1,1);
355 IF FI*SSSEC=EQ THEN GO TO NCLDC;
356 AX=SQR(F0=FN-FI*AS);
357 L=1;
358 XI=(AX-FN)/FI;
359 IF XI<=PNTS(1,(I+1),1) & XI>PNTS(1,I,1) THEN GO TO LCC;
360 XT=L*2;
361 XI=(FN-AX)/FI;
362 IF XI<=PNTS(1,(I+1),1) & XI>PNTS(1,I,1) THEN GO TO LCC;
363 GO TO NCLDC;
364 LCC:IF FLAG=0 THEN DO;
365 F(1,1)=XI;
366 F(1,2)=A(1,1)*XI+R(1,1);
367 FLAG=1;
368 IF L=1 THEN GO TO XIT;
369 ELSE GO TO NCLDC;
370 END;
371 ELSE DO;
372 ES(XF,1)=XI;
373 F(SNF,2)=A(1,1)*XI+A(1,1);
374 IF ES(XF,1)<F(1,1) THEN DO;
375 XI=ES(XF,1);
376 F(SNF,1)=F(1,1);
377 F(1,1)=XI;
378 XI=F(SNF,2);
379 F(SNF,2)=F(1,2);
380 ES(1,2)=XI;
381 END;
382 SWAY=(ES(XF,1)-F(1,1))/NPL;
383 IF SWAY<1.0E-60 THEN DO;
384 FLAG=0;
385 GO TO NCLDC;
386 END;
387 DO J=2 TO NPL;
388 F(J,1)=F(1,1)+SWAY;
389 F(J,2)=F(1,2)+SWAY*(F(7,2)-X(1)+F(7,2)*X(2));
390 END;
391 GO TO Sloop;
392 END;
393 NCLC:END;
394 IF NVAL=0 THEN DO;
395 F(0,1)=X,NV1=9.9E40;
396 F(0,2)=0;
397 GO TO JWR;
398 END;
399 IF FLAG=0 THEN PUT EDIT(RACIOS TO SMALL') (SKIP,X(10),A(15));
400 PAGE INT,F,S,FL,LD;
401 GET LIST(=);
402 GO TO CONT;
403 JWR:PUT LIST(FS);
404 PUT EDIT(RACIOS SURFACE POINTS',FS);
405 (SKIP,2),A(22),SKIP,(NF)(X(1),F(7,2),X(1),F(7,2),X(2));
406 FSCW=DN I=2 TO NF;
407 IF F(1,1)<F(S(1,1)) THEN DO;
408 PUT EDIT('CORRECT',F(1,1),F(S(1,1)),F(S(1,1)),F(S(1,1))) INCORRECT);
409 END;

```

SLOPE STABILITY PROGRAM LISTING (cont'd.)

```

410      ISKPIA(E),F(9,2),X(1),A(9),F(9),X(1),A(12));
411      STOP;
412      END;
413      END ASCHK;
414
415      SURF:DO=0;
416      IF FS(INF,1)=FS(NF,1) THEN DO;
417          Q=1,QFO;
418          CPEF:DO I=1 TO NL;
419              DO J=NP TO 1 BY -1 WHILE(FS(NF,1)<PNTS(I,J,1));
420                  END;
421              IF (ALL(J)=FS(INF,1)+R(I,J))>FS(NF,2) THEN GO TO FOSSET;
422              ELSE LP(I)=J;
423              END CPEF;
424
425              FOSSET:I=I-1;
426              NT(I)=I;
427              NF=NFL;
428              *FL=NFL-1;
429              END;
430
431              ELSE DO;
432                  O=0,OFO;
433                  DO J=NP TO 1 BY -1 WHILE(FS(NF,1)<PNTS(I,J,1));
434                      END;
435                  LP(I)=J;
436                  FS(P,2)=A(I,J)=FS(NF,1)+R(I,J);
437                  IF NL=1 THEN NT(I)=1;
438                  ELSE DO I=2 TO NL;
439                      L=I;
440                      DO K=NP TO 1 BY -1 WHILE(FS(NF,1)<PNTS(I,K,1));
441                          END;
442                      FS(P,2)=A(I,J)=FS(NF,1)+R(I,J);
443                      IF FS(NF,1)=PNTS(I,K,1) & FS(NF,2)=PNTS(I,K,2) THEN
444                          IF ALL(V)=((FS(INF,2)-FS(NF-1,2))/(FS(NF,1)-FS(NF-1,1)))
445                          THEN P=0;
446                          *NT(I)=I-1;
447                          I=NL;
448                          END;
449                      ELSE I=I+1;
450                      END;
451                      *NT(I)=I;
452                      IF L=NL THEN I=I-1;
453                      END;
454
455                      DO J=NP TO 1 BY -1 WHILE(FS(1,1)<PNTS(1,J,1));
456                          END;
457                      FS(1,2)=A(1,J)=FS(1,1)+R(1,J);
458                      NS=NS;
459                      NT(NS)=Q;
460                      XT(NS)=FS(1,1);
461                      YT(NS)=FS(1,2);
462                      *NT(NS)=C;
463                      DO I=1 TO NPL;
464                          A(I)=((FS(I,1)+P)-FS(I,2))/(FS(I,1,1)-FS(I,1));
465                          P(I)=FS(I,2)-A(I)*FS(I,1);
466                          END;
467                      XT(I)=FS(I,1);
468                      YT(I)=FS(INF,2);
469                      *NT(I)=NPL;
470                      ON OVERFLOW XI=6.6E+70;

```

SLOPE STABILITY PROGRAM LISTING (Cont'd)

```

470  ON UNDERFLOW GOTO 0;
471  AX=PSINE,1)/1.0P5;
472  IF MI=1 THEN DO;
473  DO I=1 TO (NF-1);
474  NT(I)=1;
475  Y(I)=PS((NF-I+1),1);
476  Y(I)=PS((NF-I+1),2);
477  NT(I)=NF-I;
478  END;
479  FND;
480  ELSE DO;
481  DO I=NF1 TO 2 BY -1;
482  DO J=1 TO NL;
483  DO K=NP TO 1 BY -1 WHILE(PNTS(J,K,1)>FS(I,1));
484  FND;
485  L=J;
486  J=K;
487  IF (FS(I,1)=PNTS(L,K,1) & FS(I,2)=PNTS(L,K,2)) THEN
488  IF A(L,K-1)>AF(I-1) THEN L=L-1; ELSE;
489  ELSE IF A(L,K)+FS(I,1)+R(L,K)=FS(I,2) THEN
490  IF A(L,K)>AF(I-1) THEN L=L-1; ELSE;
491  ELSE IF A(L,K)+FS(I,1)+R(L,K)<FS(I,2) THEN L=L-1;
492  ELSE J=K;
493  IF L(L)=0 THEN P(L)=K;
494  FND;
495  K=K-1;
496  Y(I,K)=L;
497  X(I,K)=FS(I,1);
498  Y(I,K)=FS(I,2);
499  W(I,K)=1;
500  FND;
501  DO I=NF1 TO 1 BY -1;
502  DO J=2 TO NL;
503  DO K=NP TO 1 BY -1 WHILE(PNTS(J,K,1)>FS(I,1));
504  FND;
505  DO L=K TO 1 BY -1 WHILE(PNTS(J,L+1,1)>FS(I,1));
506  IF A(J,L)=AF(I) THEN DO;
507  X(I)=(P(J,L)-AF(I))/AF(I)-A(J,L,1);
508  Y(I)=FS(I,1) & X(I)<FS(I,1)+1
509  & X(I)<PNTS(J,L+1,1)+AX) & X(I)>(PNTS(J,L,1)-AX)
510  THEN DO;
511  IF L>P(J) THEN LP(J)=L;
512  DO K=NS TO 1 BY -1 WHILE(X(I)>X(I,K));
513  IF X(I)>X(I,K)+AX) | X(I)<X(I,K)-2*AX) THEN DO;
514  K=K+1;
515  DO I=NS TO K BY -1;
516  INT(I)=INT(I);
517  FND;
518  X(I)=X(I);
519  IF A(I,LP(J,L)) THEN Y(I,K)=X(I)+R(J,L,1);
520  ELSE Y(I,K)=X(I)+AF(I)+PF(I);
521  W(I)=1;
522  NT(K)=J; NS=NS+1;
523  END;
524  IF A(J,L)>AF(I) THEN IF(J-1)<Y(I,K) THEN NT(K)=J-1;
525  ELSE;
526  ELSE IF J>NT(K) THEN NT(K)=J; ELSE;
527  END;
528  END;
529  END;

```

SLOPE STABILITY PROGRAM LISTING (Cont'd.)

```

530      END:
531      END:
532      END:
533      END:
534      END:
535      END:
536      END:
537      END:
538      END:
539      END:
540      END:
541      END:
542      END:
543      END:
544      END:
545      END:
546      END:
547      END:
548      END:
549      END:
550      END:
551      END:
552      END:
553      END:
554      END:
555      END:
556      END:
557      END:
558      END:
559      END:
560      END:
561      END:
562      END:
563      END:
564      END:
565      END:
566      END:
567      END:
568      END:
569      END:
570      END:
571      END:
572      END:
573      END:
574      END:
575      END:
576      END:
577      END:
578      END:
579      END:
580      END:
581      END:
582      END:
583      END:
584      END:
585      END:
586      END:
587      END:
588      END:
589      END:
590      END:
591      END:
592      END:
593      END:
594      END:
595      END:
596      END:
597      END:
598      END:
599      END:
600      END:

```

SLOPE STABILITY PROGRAM LISTING (Cont'd)

```

600      END;
601      FND;
602      J=J+1;
603      ON OVERFLOW SYSTEM;
604      ON UNDERFLOW SYSTEM;
605      IF Q=1.0 THEN AS=(FS(NF+1,2)-FS(1,2))/(FS(NF+1,1))-FS(1,1);
606      ELSE AS=(FS(NF,2)-FS(1,2))/(FS(NF,1))-FS(1,1);
607      AX=FS(1,2)-AS*FS(1,1);
608      SMAX=0;
609      DO I=2 TO ML;
610          R=ZS*FS(I,1)*AX-FS(I,2);
611          IF R>SMAX THEN SMAX=R;
612      FND;
613      IF SMAX=0 THEN SMAX=1;
614      ELSE SMAX=SMAX/10;
615      IF Q=1.0 THEN AS=FS(NF+1,2)-FS(NF,2);
616      ELSE AS=0;
617      L=IP(1);
618      DO I=2 TO NS;
619          DO K=L TO I BY -1 WHILE(XT(I)<PNTS(I,K,1));
620              END;
621          IF I=NS THEN AX=0;
622          ELSE AX=(L,K)*XT(I,K,1)-YT(I);
623          IF COUNT(I-1)=1 THEN DO;
624              S(I)=CZ(I)/AS*(AX-AS)/SMAX;
625              AS=S+ NP(I)-1;
626          FND;
627          ELSE NP(I-1)=1;
628          ELSE NP(I-1)=1;
629          L=K;
630          AS=AX;
631      FND;
632      SMD;
633      ALLOCATE I 1SL,
634              2 "1/2 X,2 Y,2 M;
635      AS=NS-1;
636      I=1;
637      P(I)=MT(I);
638      X(I)=XY(I);
639      Y(I)=YT(I);
640      DO I=1 UP J;
641          I=I+1;
642          IF X(I)>1 THEN DO;
643              XI=(X(I)-XT(I+1))/MP(I);
644              DO I=2 TO NP(I);
645                  Y(I)=M(I-1);
646                  X(I)=X(I-1)-XI;
647                  Y(I)=X(I)*MP(I)+RF(MT(I));
648                  W(I)=MT(I);
649                  L=I+1;
650              FND;
651          FND;
652          Y(I)=MT(I+1);
653          Y(I)=XT(I+1);
654          Y(I)=YT(I+1);
655          X(I)=T(I+1);
656      FND;
657      DIFF TMT;
658      ALLOCATE SLICE;
659      YP;
660      IF "AKAL" THEN DO;

```


SLOPE STABILITY PROGRAM LISTING (Cont'd.)

```

710 GR=G(U);
711 END;
712 X=X(I)-X(I+1);
713 AX=0.5*(X+X(I+1));
714 P=P-GP+AV;
715 H=0;
716 N=0;
717 H=H+G*(X-Y(LP(N),1,1))*(Y(LNLI)+WT(LP(NLI),2));
718 Y(LNLI)=WT(LP(NLI),2);
719 X=X-Y(LP(NLI),1);
720 H(LNLI)=H(LNLI)+X;
721 GO TO WTP;
722 END;
723 END;
724 V=X(I+1)/A(LI)+LP(NLI)+H(LI+LP(NLI));
725 H(LI)=X(I+1)*(Y(LNLI)+V);
726 Y(LI)=V;
727 IF USAX THEN DO;
728   IF USAX THEN P=U-AS;
729   ELSE;
730     IF USAX THEN DO;
731       P=AX-WL*XD;
732       L=U-WL*XD;
733     END;
734   ELSE U=AX;
735 END;
736 END;
737 H(LI)=((Y(LI)-Y(LI+1))/3+Y(LI)-Y(LI+1))/XD;
738 WT(LI)=(X+Y(LI))/2;
739 P(LI)=(P-U)*P0/XP;
740 C(LI)=COS(ATAN(T(LI)));
741 CM UNDEFLOW ADD(LI)=0;
742 IF TYPE=L THEN DO;
743   C(LI)=C(LI)*C(LI);
744   P(LI)=P(LI)+C(LI);
745   END;
746 ELSE P(LI)=C(LI)*C(LI);
747 IF C(LI)=0 THEN DO;
748   T(LI)=TAN(T(LI));
749   IF TYPE=L THEN ADD(LI)=C(LI)*XD/P0+
750     (P-C(LI)*C(LI)-U)/C(LI);
751   ELSE ADD(LI)=(P-U)+C(LI)*XD/P0;
752   END;
753 ELSE IF P(LI)<0 THEN ADD(LI)=0;
754   ELSE DO;
755     AS=C(LI)*EXP(T(LI)-1)*LOG(P(LI));
756     IF TYPE=L THEN ADD(LI)=P+C(LI)-U/C(LI)*AS;
757     ELSE ADD(LI)=(P-U)*AS;
758   END;
759 CM UNDEFLOW SYSTEM;
760 SAF=SAF+ADD(LI);
761 C=SEC(P(LI));
762 END;
763 CM UNDEFLOW;
764 P=C*(V/LI+SQ);
765 IF TYPE=L THEN DO;
766   PUT FORTIFELLENTS ANALYSIS, FACTOR OF SAFETY, P0
767     (CRIP(T,A(LI),V(LI),P(LI),X(LI),E(LI)));
768   PUT ISL,SLICE,N;
769   GO TO END;

```

SLOPE STABILITY PROGRAM LISTING (Cont'd.)

```

770 FIC:
771 SAC=0:
772 DO I=1 TO NS:
773   IF FU(I)=0 THEN S/AO=S/AO+AD(I)/CSO(I)/(1+TA(I)*TP(I)/FO):
774   ELSE IF PU(I)<0 THEN:
775     SAC=SAC+AD(I)/CSO(I)/(1+TA(I)*C(I)*EXP((TP(I)-1)
776     *LOG(PU(I))/FO):
777   END:
778 FISSAO/(O+SAC):
779 IF TYPE=1 THEN IC=NAVAL=0 THEN:
780   ELSE PUT EDIT('RISKOP ANALYSIS',
781   'FACTOR OF SAFETY,1ST APPROXIMATION',FI)
782   (SKIP(2),A(15),SKIP,A(36),X(1),F(5,2)):
783 ELSE PUT EDIT('JANUJ ANALYSIS',
784 'FACTOR OF SAFETY,1ST APPROXIMATION',FI)
785 (SKIP(2),A(15),SKIP,A(36),X(1),F(5,2)):
786 DO L=2 TO 30:
787   J=L:
788   FO=FI:
789   SAC=0:
790   DO I=1 TO NS:
791     IF CU(I)=0 THEN AD(I)=AD(I)/CSO(I)/(1+TA(I)*TP(I)/FO):
792     ELSE IF PU(I)<0 THEN AC(I)=0:
793     ELSE AC(I)=AC(I)/CSO(I)/(1+TA(I)*C(I)*EXP((TP(I)-1)
794     *LOG(PU(I))/FO):
795     SAC=SAC+AC(I):
796   END:
797   FI=SAC/(O+SAC):
798   IF F(1*(FO-0.005) & FI)>(FO-0.005) THEN L=L+30:
799   END:
800 IF TYPE=1 THEN DO:
801   DO L=2 TO 70:
802     J=L:
803     FC=FI:
804     DF(I)=0:
805     DY(I)=PI(I)-AD(I)/FO:
806     DO I=2 TO NS:
807       DT(I)=PI(I)-AC(I)/FO:
808       DF(I)=DT(I)+DT(I-1)*HT(I)/(X(I)-1+X(I+1)):
809     END:
810     SDE=0:
811     XI=0:
812     DO I=1 TO NS:
813       SDE=SDE+DT(I):
814       XI=XI+Y(I)*SDE:
815       CT(I)=XI-XI:
816       IF CU(I)=1 THEN DT(I)=DT(I)/(X(I)-1+X(I+1)):
817       XI=XI:
818     END:
819     DO I=2 TO 30:
820       AS=FI:
821       SAC=SAC+C:
822       DO I=1 TO NS:
823         IF CU(I)=0 THEN DO:
824           DT(I)=(FO(I)+DT(I)+TP(I)/CSO(I)
825           /1+TA(I)*TP(I)/FI)
826           RT(I)=RO(I)+DT(I)*TA(I):
827         END:
828       ELSE DO:
829         AX=ARSIPU(I)+DT(I)*9.8071:

```


SLOPE STABILITY PROGRAM LISTING (Cont'd.)

```

898 XC=ESQR(2,11)
899 F=RAF(X,Y,VI)
900 IFLAG=ESOF(1,1)
901 ALLOCATE I(10),
902           Z(NT,2),VT(2),NO,2,MT:
903 NGL=NF-1:
904 GO TO GRNS:
905 END:
906
907 ELSE DO:
908 PUT EDIT('Y-COORD',(F5QR(1,J),F5QR(1,J)) DO I=2 TO 16),
909       ('X(1,J) DO I=2 TO 16) DO J=16 TO 2 BY -1),
910       (F5QR(1,1) DO I=2 TO 16), 'X-COORD'):
911 (LINE(4),A(7),
912  15(SKIP(2)),X(2),F(5,1),X(1),15(X(1),F(5,2)),SKIP,
913  X(8),15(F(5,2))),SKIP(2),X(7),15(X(1),F(5,1)),
914  X(3),A(7)):
915
916 END:
917 END:PRPF F5,F5,LP:
918 GET LISTOP1:
919 GO TO CCNT:
920 FIN:END:
921
922
923
924
925
926
927
928
929
930
931
932
933
934
935
936
937
938
939
940
941
942
943
944
945
946
947
948
949
950
951
952
953
954
955
956
957
958
959
960
961
962
963
964
965
966
967
968
969
970
971
972
973
974
975
976
977
978
979
980
981
982
983
984
985
986
987
988
989
990
991
992
993
994
995
996
997
998
999
1000

```

END OF FILE

VSIR:OFF

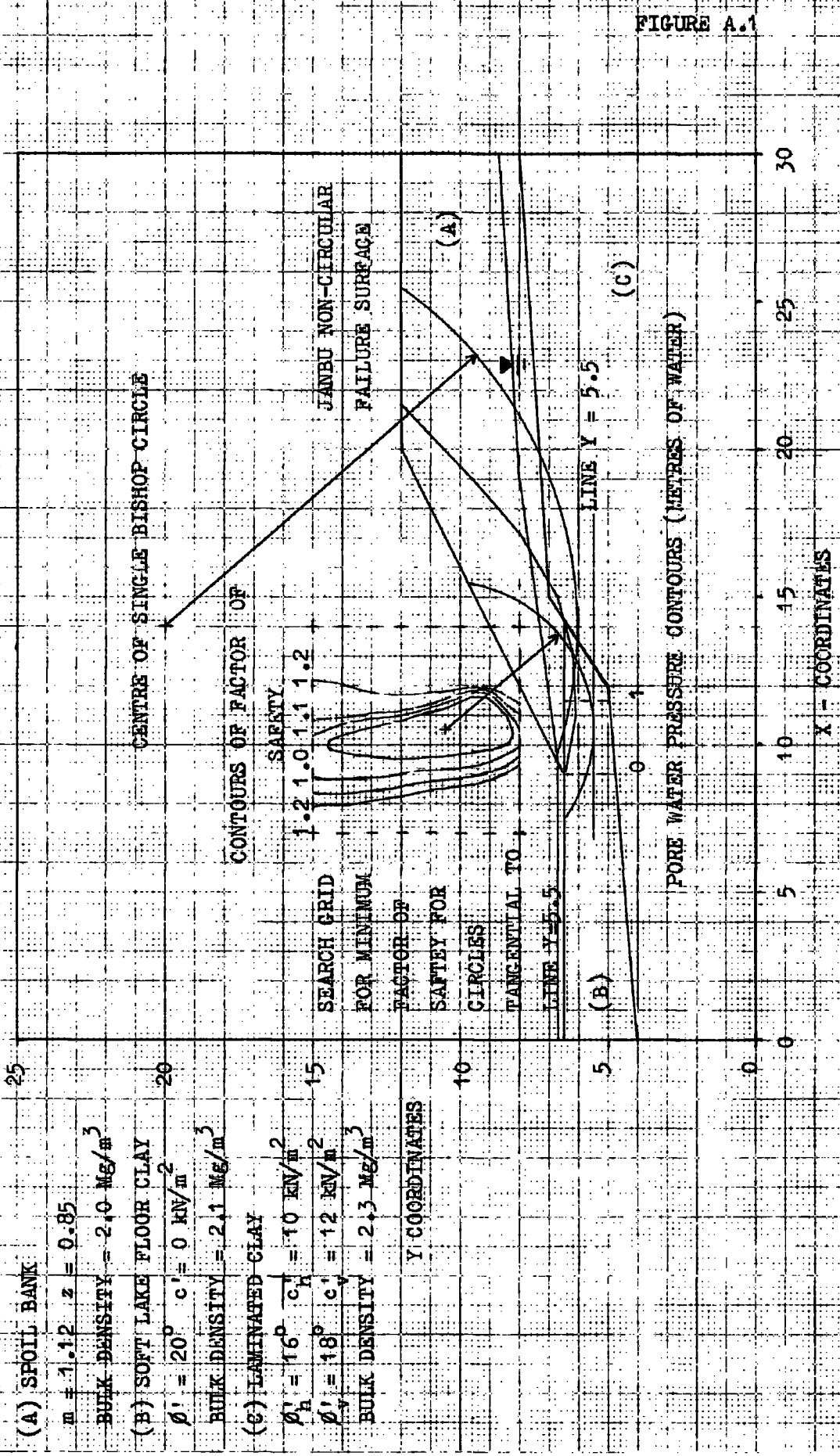


FIGURE A.1

APPENDIX B

REDUCED MAJOR AXIS PROGRAM

```

ESIGNON GLO6 T=2 P=20
CHARGING RATE = UNIVERSITY, BATCH
**LAST SIGNON WAS 11:04:50
USER "GLO6" SIGNED ON AT 11:17:53 ON WED DEC 15/76
GET PROFILE
READY.
EMPTY PROFILE
DONE.
ENUN
LUNNUM
LIST PROFILE
1 /* PROGRAMME FOR DRAWING BEST STRAIGHT LINE FIT TO
2 /* TRIAXIAL AND SHEAR BOX DATA
3 /*
4 /* DATA REQUIRED(TITLE(60),CHAR)
5 /* (MAKE LAST CHAR 'I' IF NON-A4 PLOT REQUIRED
6 /* NO. OF LINES TO BE DRAWN
7 /* MAX X AXIS LENGTH(IN MM/SQ.MM.)
8 /* MAX Y AXIS LENGTH(IN MM/SQ.MM.)
9 /*
10 /* IF CURVED FIT REQUIRED, 'CURVE'
11 /* TYPE('TRIAXIAL','TRIAX(PD)'
12 /* OR 'S-SHEAR BOX')
13 /* NO. DATA PAIRS FOR LINE
14 /* SUBTITLE(60 CHAR)
15 /*
16 /* DATA POINTS IN PAIRS
17 /* (S1,S3 FOR TRIAXIAL DATA
18 /* P, Q FOR MHON CIRCLE TOP POINT DATA
19 /* X, Y FOR SHEAR BOX DATA
20 /*
21 /*
22 /*
23 /*
24 /*
25 /*
26 /*
27 /*
28 /*
29 /*
30 /*
31 /*
32 /*
33 /*
34 /*
35 /*
36 /*
37 /*
38 /*
39 /*
40 /*
41 /*
42 /*
43 /*
44 /*
45 /*
46 /*
47 /*
48 /*
49 /*
IMPL:PROCEDURE OPTIONS(MAIN))
DECLARE TITLE CHAR(60),FILE DEFINED TITLE,
CHAR CHAR(60) VAR,PPAR DEFINED CHAR,
TYPE CHAR(9),
(C1,O,C,PHI,TPMI) FLOAT(16),
X(20),Y(20),PI FIXED(5,3),
P FIXED DECIMAL(4,1),
FN FIXED(4,1),
(K,L,KL)FIXED BINARY(31))
GET LIST(TITLE,N,A,S)
PUT EDIT(TITLE)(X(25),A(62))
L=4
IF SUBSTR(TITLE,60,1)='I' THEN S=0.008
ELSE DO
CALL PENUP(R,REW,0.25E0)
CALL PENDR(2,REW,P,MEW)
CALL PENOR(11,75E0,0,REW)
CALL PENDN(11,75E0,8.25E0)
CALL PENDR(2,REW,8.25E0)
IF A>1330 + B>600 THEN S=0.004 ELSE S=0.008
END
D=0.8/5
I=7
DI=9.64
DO E=0 TO A BY 0.1
P=SE
CHAR=CHAR(FN)

```

REDUCED MAJOR AXIS PROGRAM (Cont'd.)

```

50 CALL PSYMB(D1,0.04E0,-0.08E0,FPAR,0.0E0,K)
51 D1=01+0.07
52 END
53 O1=0.647
54 DO E=0 TO B BY D1
55 F=N*E
56 C=PAR=CHAR(FN)
57 CALL PSYMB(0.92E0,D1,-0.08E0,FPAR,90.0E0,K)
58 D1=01+0.07
59 END
60 C=PAR=NORMAL STRESS (KN/SQ.M)
61 A=AS*(-1)
62 D=17
63 KE=247
64 CALL PAXIS(1.9E0,1.0E0,FPAR,K,A,0.0E0,0.0E0,D,0.8E0)
65 C=PAR=ISMEAR STRESS (MN/SQ.M)
66 B=S*(-1)
67 K=237
68 CALL PAXIS(1.9E0,1.0E0,FPAR,K,0.90E0,0.0E0,D,0.8E0)
69 B=S*(-1)
70 C=PAR=IDCL 6617
71 K=07
72 CALL PSYMB(1.9E0,1.0E0,-0.2E0,FPAR,0.0E0,K)
73 D=0.127
74 K=007
75 CALL PSYMB(1.2E0,D,-0.2E0,FITL,0.0E0,K)
76 A=07
77 DO I=1 TO N1
78 IC=07
79 GET LIST(TYPE)
80 IF TYPE='CURVE' THEN DO
81 IC=17
82 GET LIST(TYPE,M,TITLE)
83 END
84 ELSE GET LIST(M,TITLE)
85 REG=HEGN7
86 DECLARE (PAR(M,2),LPAR(M,2)) FLOAT(16)
87 GET LIST(PAR)
88 PUT EDIT(TITLE,TYPE,EQUATION IS:1)
89 (SKIP(3),X(25),A(60),SKIP,X(20),A(9),SKIP(2),
90 X(26),A(12))
91 IF TYPE='TRIAX(P0)' T TYPE='TRIAXIAL' THEN DO
92 IF TYPE='TRIAXIAL' THEN DO
93 DO J=1 TO M
94 D=PAR(J,2)
95 PAR(J,2)=(PAR(J,1)+PAR(J,2))/27
96 PAR(J,1)=PAR(J,2)*D
97 END
98 END
99 IF IC=1 THEN DO
100 DO J=1 TO N1
101 G=PAR(J,1)+PAR(J,1)+PAR(J,2)+PAR(J,2)7
102 LPAR(J,2)=PAR(J,1)+PAR(J,2)+SQRT(D)/C7
103 LPAR(J,1)=LOG(PAR(J,1)+PAR(J,2)+LPAR(J,2)/PAR(J,1))7
104 LPAR(J,2)=LOG(LPAR(J,2))7
105 E=07
106 CALL LSTSU(M,LPAR,C,0,CCF,SEA,SEB,STC,STM)7
107 END
108 ELSE DO
109 CALL LSTSO(M,PAR,C,PHI,CCF,SEA,SEB,STC,STM)7
110

```

REDUCED MAJOR AXIS PROGRAM (Cont'd.)

```

112 TPPI=PHI/SORT(1-PPH*PHI)
111 PHI=ATAND(TPHI)
110 CEC/COSD(PHI)
109 END)
108 IF M>20 THEN DO)
107 ELSE LPAR=PAR)
106 K=1)
105 DO J=1 TO M)
104 DELPAR(J,1)*S+1)
103 E=LPAR(J,2)*S+1)
102 CALL PSYMB(D,E,-0.00E0,L,0.0E0,K)
101 END)
100 L=L-1)
99 IF L<0 THEN L=7)
98 END)
97 ELSE DO)
96 DO J=1 TO M)
95 D=PAR(J,1)*S+1)
94 E=PAR(J,2)*S)
93 CALL PCIRCL(D,1.0E0,1.0E2,0.0E0,E,A,0.0E0)
92 END)
91 A=AT0.1)
90 END)
89 ELSE IF TYPE='SHEAR BOX' THEN DO)
88 IF IC=1 THEN DO)
87 DO I=1 TO M)
86 LPAR(I,1)=LOG(PAR(I,1))
85 LPAR(I,2)=LOG(PAR(I,2))
84 END)
83 CALL LSTSO(M,LPAR,C,0,CCF,SEA,SEB,STC,STM)
82 END)
81 ELSE DO)
80 CALL LSTSO(M,PAR,C,TPHI,CCF,SEA,SEB,STC,STM)
79 PHI=ATAND(TPHI)
78 END)
77 K=1)
76 DO J=1 TO M)
75 D=PAR(J,1)*S+1)
74 E=PAR(J,2)*S+1)
73 CALL PSYMB(D,E,-0.00E0,L,0.0E0,K)
72 END)
71 L=L-1)
70 IF L<0 THEN L=7)
69 END)
68 ELSE DO)
67 PUT EDIT('ERROR: RUN',I,J,'TYPE SPECIFICATION INCORRECT')
66 (SKIP,X(10),A(10),F(2),X(1),A(2B))
65 GO TO END)
64 END)
63 D=PAR(1,1)
62 DO J=2 TO M)
61 IF PAR(J,1)>D1 THEN D1=PAR(J,1) ELSE)
60 END)
59 IF IC=1 THEN DO)
58 C1=EXP(C)
57 PUT EDIT('N',S1,C1,I*P NN/M=2,'CCF=1,CCF)
56 (SKIP(2),X(42),F(12,9),SKIP,X(26),A(2),
55 F(12,9),A(21),SKIP(2),X(26),A(4),F(8,6))
54 END)
53 END)
52 END)
51 END)
50 END)
49 END)
48 END)
47 END)
46 END)
45 END)
44 END)
43 END)
42 END)
41 END)
40 END)
39 END)
38 END)
37 END)
36 END)
35 END)
34 END)
33 END)
32 END)
31 END)
30 END)
29 END)
28 END)
27 END)
26 END)
25 END)
24 END)
23 END)
22 END)
21 END)
20 END)
19 END)
18 END)
17 END)
16 END)
15 END)
14 END)
13 END)
12 END)
11 END)
10 END)
9 END)
8 END)
7 END)
6 END)
5 END)
4 END)
3 END)
2 END)
1 END)

```

REDUCED MAJOR AXIS PROGRAM (Cont'd.)

```

178 PUT EDIT('STD,ERROR (M)=,SEA,ISTD,ERROR(Z)=,SER,
179 'STUDENT'S T (M)=,STC,ISTUDENT'S T (Z)=,STH)
172 (SKIP(2),X(16),A(14),F(8),X(8),A(14),F(10),B),
173 SKIP(2),X(14),A(16),F(9),X(5),A(16),F(9),B))
174 X(1)=1
175 Y(1)=1
176 K=1
177 E=1
178 DO I=1 TO 200 WHILE(DI>1+10)
179   K=K+1
180   E=E+12
181   X(K)=E*S+1
182   Y(K)=EXP(D+LOG(E)+C)*S+1
183   E=D
184   KL=1
185   CALL PLINE(X(1),Y(1),K,KL,0,0E0,0,0E0,0,0E0)
186   D=X(K)-0.05
187   E=Y(K)+0.05
188   K=64
189   CALL PSYMS(D,E,-0.0E0,FITLE,0,0E0,K)
190   E=I-J*0.7+1.4
191   CALL PSYMB(1.2E0,E,-0.12E0,FITLE,0,0E0,K)
192   E=I-0.4
193   X(1)=1.25 X(2)=1.31 X(3)=1.35 X(4)=1.39
194   X(5)=1.42 X(6)=1.46 X(7)=1.50
195   X(8)=1.54 X(9)=1.58 X(10)=1.62
196   Y(6),Y(8)=E*0.02
197   K=4
198   CALL PLINE(X(1),Y(1),K,KL,0,0E0,0,0E0,0,0E0)
199   CALL PLINE(X(5),Y(5),K,KL,0,0E0,0,0E0,0,0E0)
200   D=E*0.05 CALL PENUP(1.45E0,D) CALL PENON(1.53E0,D)
201   D=E*0.08 CALL PENUP(1.45E0,D) CALL PENON(1.53E0,D)
202   FI=ROUND(C1,3)
203   CMPARECHAR(FI)
204   K=8
205   CALL PSYMB(1.3E0,E,-0.12E0,FPAR,0,0E0,K)
206   X(1)=2.05 X(2)=2.81 X(3)=X(10),X(11)=2.77
207   X(4)=X(9)=2.73 X(5)=X(8)=2.69 X(6)=X(7)=2.65
208   Y(1),Y(4),Y(5)=E*0.12 Y(2),Y(3),Y(6),Y(11)=E*0.08
209   Y(7),Y(10)=E*0.04 Y(8),Y(9)=E
210   X=E*0.15
211   K=11
212   CALL PLINE(X(1),Y(1),K,KL,0,0E0,0,0E0,0,0E0)
213   E=E*0.12
214   FI=ROUND(0,3)
215   CMPARECHAR(FI)
216   K=6
217   CALL PSYMB(2.18E0,E,-0.12E0,FPAR,0,0E0,K)
218   END
219 ELSE DO:
220   PUT EDIT('S=PATANI,PHI,1,1,C,KN/M=2,1CCF=,CCF)
221   (SKIP(2),X(20),A(7),F(4),A(1),F(5),A(7),
222   SKIP(2),X(20),A(4),F(8),6))
223 PUT EDIT('STD,ERROR (C)=,SEA,ISTD,ERROR(M)=,SER,
224 'STUDENT'S T (C)=,STC,ISTUDENT'S T (M)=,STH)
225 (SKIP(2),X(16),A(14),F(8),X(8),A(14),F(10),B),
226 SKIP(2),X(14),A(16),F(9),X(5),A(16),F(9),B))
227 D=1
228 E=C*S+1
229 CALL PENUP(D,E)

```

REDUCED MAJOR AXIS PROGRAM (Cont'd.)

```

230 D=D1+S+1)
231 E=(D-1)*T*PHI+E)
232 IF E>(6+1) THEN 001
233 E=E+1)
234 D=(E-C+S-1)/T*PHI+1)
235 END)
236 CALL PENON(O,E)
237 D=D-0.05)
238 E=E+0.05)
239 K=0)
240 CALL PSYMB(O,E,-0.08E0,FITLE,0,0E0,K)
241 E=B-IJ=0.7+1.4)
242 CALL PSYMB(1,2E0,E,-0.12E0,FITLE,0,0E0,K)
243 E=E-0.2)
244 F=ROUND(PHI,1)
245 TYPE=CHAR(F)
246 C$PAR=I*10+1+SUBSTR(TYPE,3,5)
247 K=8)
248 CALL PSYMB(1,3E0,E,-0.12E0,FPAR,0,0E0,K)
249 C$PAR=I/1)
250 K=1)
251 CALL PSYMB(1,3E0,E,-0.12E0,FPAR,0,0E0,K)
252 KL=7)
253 K=3)
254 CALL PSYMB(2,1E0,E+0.11,-0.02E0,KL,0,0E0,K)
255 E=E-0.2)
256 F=ROUND(C,1)
257 TYPE=CHAR(F)
258 C$PAR=I*10+1+SUBSTR(TYPE,3,5)+I*KN/50,K,1)
259 K=16)
260 CALL PSYMB(1,3E0,E,-0.12E0,FPAK,0,0E0,K)
261 END)
262 END REGR)
263 END)END)
264
265 /* SUBROUTINE FOR FINDING BEST STRAIGHT LINE BY
266 /* REDUCED MAJOR AXIS METHOD
267 /* PARAMETERS=N-PASS NO. OF DATA PAIRS
268 /* PAR=ARRAY(*,2)-PASS DATA ARRAY
269 /* A=RECEIVES CONSTANT A IN Y=A+BX
270 /* B=RECEIVES CONSTANT B IN Y=A+BX
271 /* CCF=RECEIVES CORRELATION COEFFICIENT
272 /* SE=RECEIVES STD.ERROR OF A
273 /* SEB=RECEIVES STD.ERROR OF B
274 /* STA=RECEIVES STUDENT'S T OF A
275 /* STB=RECEIVES STUDENT'S T OF B
276 /*
277 /* EQUATIONS USED:R=(SQRT(H**2+G**2))-H)/2G
278 /* WHERE G=E(X)*E(Y)/N
279 /* H=E(X**2)-E(X)**2/N
280 /* CCF=G/SQRT((E(Y**2)-E(Y)**2/N)*
281 /* (E(X**2)-E(X)**2/N))
282 /*
283 /*
284 /* L$SYO=PROCEDURE(N,PAR,A,B,CCF,SEA,SEB,STA,STB)
285 /* DECLARE (PAR(*),A,B,XS,YS,XY,XSS,YSS,G,H)FLOAT(16)
286 /* XS=A)
287 /* YS=B)
288 /* XY=0)
289 /* XSS=0)

```

REDUCED MAJOR AXIS PROGRAM (Cont'd.)

```

290 YSS=BI
291 DO I=1 TO N;
292   XS=XS+PAR(I,1);
293   YS=YS+PAR(I,2);
294   XY=XY+PAR(I,1)*PAR(I,2);
295   XSS=XSS+PAR(I,1)**2;
296   YSS=YSS+PAR(I,2)**2;
297   END;
298   G=XY-XS*YS/N;
299   H=XSS-YSS-(XS**2-YS**2)/N;
300   B=(SQRT(H**2+4*G**2)-H)/(2*G);
301   A=YS/N+B*XS/N;
302   IF PAR(N,1)>10 & A<5 THEN DO;
303     A=0;
304     B=YS/XS;
305   END;
306   CCF=G/SQRT((YSS-YS*YS/N)*(XSS-XS*XS/N));
307   H=(1-CCF*CCF)/N;
308   SEH=B*SQRT(H);
309   SEAS=SQRT((YSS-YS*YS/N)*H*(XS*XS/N+(XSS-XS*XS/N)*1)/N);
310   STAA=SEA;
311   STB=H/SEB;
312   RETURN;
313   END;
314
315   CALL PLTEND;
316   END;
END OF FILE

```

```

&SIGNOFF

```

APPENDIX C

PORE PRESSURE CALCULATION PROGRAM

```

ESTIGNON GUC6 Y=2 P=28
CHARGING RATE = UNIVERSITY, BATCH
*LAST SIGNON *AS: 14:45115
USER "GUC6" SIGNED ON AT 15:03148 ON WED DEC 15/76
FSET PRCGFILE
READY
EMPTY PROFILE
DONE.
ENUNM
EDUNUM
ELIST PROFILE

```

```

1 /* PORE PRESSURE CALCULATION PROGRAMME
2 DATA REQUIRED:
3 1) TITLE(UP TO 68 CHARACTERS
4 2) THICKNESS OF CLAY(METRES)
5 3) NO. OF DRAINAGE PATHS
6 4) NO. OF DEPTHS IN CLAY AT WHICH P.P. IS REQUIRED
7 5) DEPTHS(METRES) IN CLAY AT WHICH P.P. REQUIRED
8 6) CV OF CLAY(M**2/YR)
9 7) THICKNESS OF FILL PLACED IN 1 LIFT(METRES)
10 8) DENSITY OF FILL(MG/M**3)
11 9) TIME BETWEEN LIFTS(YEARS)
12 10) NO. OF LIFTS
13 11) NO. OF ITEM (12) REQUIRED
14 12) TIMES(YEARS) AFTER LAST LIFT AT WHICH P.P. IS REQUIRED
15 13) IF MORE THAN 1 CLAY THICKNESS REQUIRED, REPEAT FROM ITEM(2) */
16 PORPRS:PROCEDURE OPTIONS(MAIN)
17 ON ENDFILE(SCARDS) GO TO FIN
18 DECLARE TITLE CHAR(68),
19 Z(NZ) CONTROLLED,UZ(NZ) CONTROLLED)
20 URATIO:PROCEDURE(ZR,TV)
21 SF=M
22 DO I=0 TO IWR
23 E=(I+2)*.3*.4159*U*.5)
24 ON UNDERFLOW F1=9.5320001)
25 F1=EXP(-1.1E*TV)*SIN(E*ZR)*2/E)
26 ON UNDERFLOW SYSTEM)
27 IF 44S(F1)EQ.000001 THEN RETURN(SF)
28 ELSE SF=SF*F1)
29 END)
30 END URATIO)
31 GET LIST(TITLE)
32 PUT EDIT(TITLE)(PAGE,4(68))
33 NE*TCIGET LIST(TC,ND,NZ))
34 ALLOCATE Z,UZ)
35 GET LIST(Z,CV,TL,DF,YL,N,NT))
36 MATC/NOI IF=0)
37 UO=TL-DF)
38 DO J=1 TO NZ)
39 ZV=Z(J)/N)
40 UZ(J)=UO)
41 DO K=1 TO (N-1))
42 YK*YL*CV/(M*M))
43 UZ(J)=UZ(J)+UO*URATIO(ZV,T))
44 END)
45 END)
46 PUT EDIT(THICKNESS OF CLAY LAYER,TC,NO, OF DRAINAGE PATHS,ND
47 ,CV OF CLAY,CV,THICKNESS OF FILL IN 1 LIFT,TL,
48 ,DENSITY OF FILL,DF,TIME BETWEEN LIFTS,YL,
49 ,NO. OF LIFTS,N,

```

VARIABLE
TITLE
TC
ND
NZ
Z(*)
CV
TL
DF
YL
N
NT
TA

PORE PRESSURE CALCULATION PROGRAM (Cont'd.)

```

50      PORE PRESSURE PLOT ON COMPLETION OF LAST LIFT)
51      (SKIP(2),A,X(7),F(7,3),SKIP,A,X(9),F(3,0),SKIP,A,X(19),
52      F(8,3),SKIP,A,X(3),F(7,3),SKIP,A,X(18),F(7,3),SKIP,A,
53      X(12),F(7,3),SKIP,A,X(18),F(3,0),SKIP(2),A)
54      PNT:PUT EDIT('DEPTH IN PORE PRESSURE',ICLAY(M) (M. OF WATER)),
55      (Z(J),UZ(J) DU J=1 TO NZ)
56      (SKIP(2),X(11),A,SKIP,X(12),A,(NZ)(SKIP,X(11),F(7,3),
57      X(7),F(9,5)))
58      IF IF=NT THEN GO TO NEWTC)
59      ELSE)
60      IF=IF*1)
61      GET LIST(TA)
62      DO J=1 TO NZ)
63      ZV=Z(J)/H)
64      UZ(J)=0)
65      DO K=1 TO N)
66      T=((K-1)*VL+TA)*CV/(H*M)
67      UZ(J)=UZ(J)+UO*URATIO(ZV,T)
68      END)
69      END)
70      PUT EDIT('PORE PRESSURE PLOT',TA, IYEARS AFTER LAST LIFT)
71      (SKIP(2),A,F(7,3),A)
72      GO TO PNT)
73      FIN:END)
END OF FILE

```

ESTGHOFF

